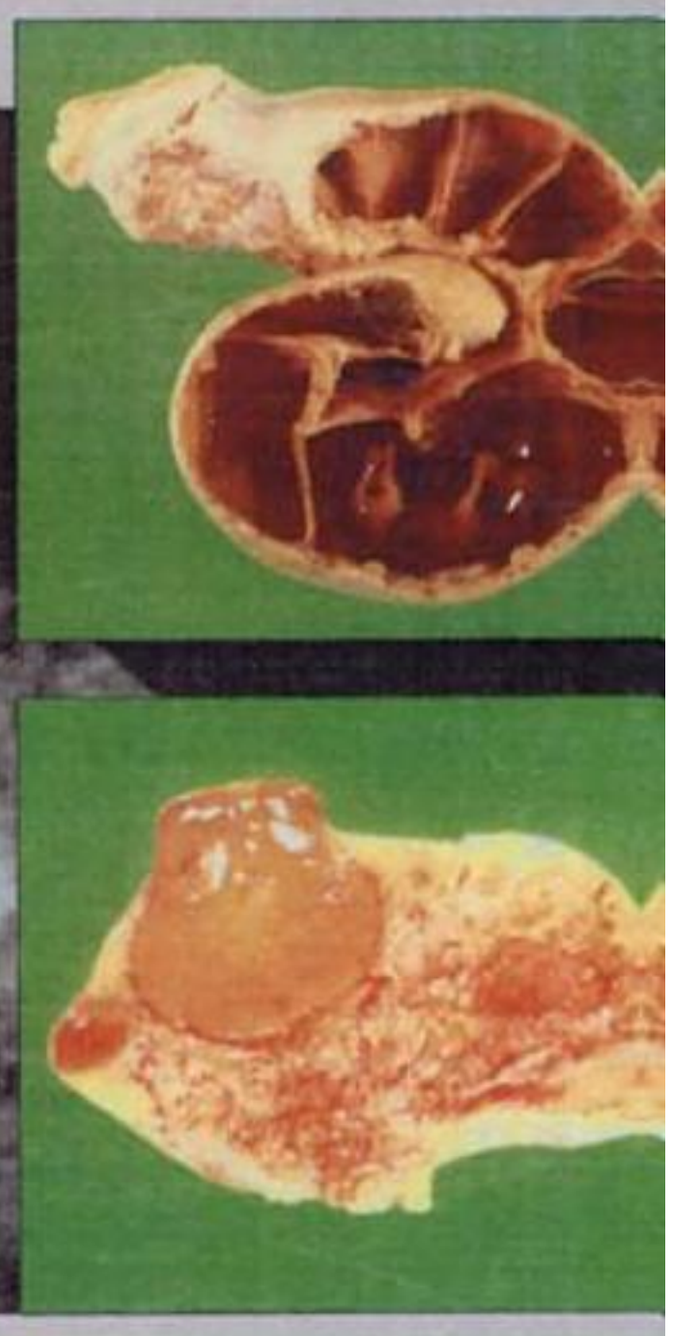
Wolfgang Kähn

Veterinary Reproductive Ultrasonography

Horse · Cattle · Sheep · Goat ·
Pig · Dog · Cat





English Translation and Revision
Dietrich Volkmann · Robert Kenney

vet

schlütersche

Avtorsko zaščiteno gradivo

Downloaded From Vet-eBooks.com

Wolfgang Kähn

VETERINARY REPRODUCTIVE ULTRASONOGRAPHY

Horse • Cattle
Sheep • Goat • Pig
Dog • Cat

This One
SCH9-9TN-BAWT
Avtorsko zaščiteno gradivo

Downloaded From Vet-eBooks.com

VETERINARY REPRODUCTIVE ULTRASONOGRAPHY

Horse • Cattle
Sheep • Goat • Pig
Dog • Cat

Dr Wolfgang Kähn

English Translation and Revision

Professor Dietrich Volkmann
College of Veterinary Medicine
Cornell University, USA

Professor Robert M Kenney
School of Veterinary Medicine
University of Pennsylvania, USA

schlütersche

Avtorsko zaščiteno gradivo

Downloaded From Vet-eBooks.com

Wolfgang Kähn, Dr. Dr. habil.
Professor
Clinic of Reproductive Medicine, Veterinary Faculty
University of Zürich, Switzerland

English Translation and Revision
Robert M Kenney, DVM, PhD
Professor
School of Veterinary Medicine
University of Pennsylvania, USA

Dietrich Volkmann, BVSc, MMed Vet (Gyn)
Associate Professor
College of Veterinary Medicine
Cornell University, USA

© 2004, Schlütersche Verlagsgesellschaft mbH & Co. KG, Hans-Böckler-Allee 7, 30173 Hannover
E-mail: info@schluetersche.de

Printed in Germany

ISBN 3-89993-005-3

Special edition. Reprint from 1994.

Bibliographic information published by Die Deutsche Bibliothek

Die Deutsche Bibliothek lists this publication in the Deutsche Nationalbibliografie; detailed bibliographic data are available in the Internet at http://dnb.ddb.de.

The author assumes no responsibility and makes no guarantee for the use of drugs listed in this book. The author / publisher shall not be held responsible for any damages that might be incurred by the recommended use of drugs or dosages contained within this textbook. In many cases controlled research concerning the use of a given drug in animals is lacking. This book makes no attempt to validate claims made by authors of reports for off-label use of drugs. Practitioners are urged to follow manufacturers´ recommendations for the use of any drug.

All rights reserved. The contents of this book both photographic and textual, may not be reproduced in any form, by print, photoprint, phototransparency, microfilm, video, video disc, microfiche, or any other means, nor may it be included in any computer retrieval system, without written permission from the publisher.

Any person who does any unauthorised act in relation to this publication may be liable to criminal prosecution and civil claims for damages.

Avtorsko zaščiteno gradivo

Downloaded From Vet-eBooks.com

Contents

Preface to first edition

Preface to current edition

1 Ultrasonography in the mare 11

1.1 Technique of ultrasonography in the mare 11

1.2 Ovarian structures in the mare 15

1.2.1 Follicles 15

1.2.1.1 Sonographic images of follicles 15

1.2.1.2 Development of preovulatory follicles 19

1.2.1.3 Transvaginal sonographic puncture of follicles 23

1.2.2 Corpora lutea 25

1.2.2.1 Sonographic images of corpora lutea 25

1.2.2.2 Development of corpora lutea during the estrous cycle and in early pregnancy 27

1.2.3 Anovulatory luteinized follicles 33

1.2.4 Follicular and ovarian hematomas 35

1.2.5 Ovarian tumors and cysts 37

1.3 Uterine structures in the mare 41

1.3.1 Non-pregnant uterus 41

1.3.2 Pregnant uterus 43

1.3.2.1 Day 9 to 13 of pregnancy 43

1.3.2.2 Day 14 to 20 of pregnancy 43

1.3.2.3 Day 21 to 40 of pregnancy 49

1.3.2.4 Day 41 to 60 of pregnancy 51

1.3.2.5 Twin pregnancy 53

1.3.2.6 Transvaginal sonographic puncture of the conceptus 57

1.3.3 Ultrasonography of the equine fetus 61

1.3.3.1 Imaging of fetal organs 61

1.3.3.1.1 Head, neck and spinal column 61

1.3.3.1.2 Thorax and heart 61

1.3.3.1.3 Abdomen and pelvic region 63

1.3.3.2 Accessibility of equine fetuses by transrectal sonography 65

1.3.3.3 Sonographic fetometry in horses 65

1.3.3.3.1 Eye and braincase 65

1.3.3.3.2 Ribs, trunk and stomach 67

1.3.4 Uterine pathology 69

1.3.4.1 Embryonic death 69

1.3.4.2 Abnormal pregnancy 71

1.3.4.3 Post partum uterus 71

1.3.4.4 Endometritis 75

1.3.4.5 Pyo-, muco- and urometra 77

1.3.4.6 Endometrial cysts 79

References to preface 80

References to chapter 1 80

2 Ultrasonography in the cow 83

2.1 Technique of ultrasonography in the cow 83

2.2 Ovarian structures in the cow 89

2.2.1 Follicles 89

2.2.1.1 Sonographic images of follicles 89

Downloaded From Vet-eBooks.com

2.2.1.2 Follicular development during the estrous cycle and in early pregnancy 93
2.2.1.3 Estrous follicles 95
2.2.2 Corpora lutea 95
2.2.2.1 Sonographic images of corpora lutea 95
2.2.2.2 Incidence and development of cystic and non-cystic corpora lutea during the estrous cycle and in early pregnancy 103
2.2.3 Ovarian cysts 107
2.2.4 Ovarian tumors 111
2.3 Uterine structures in the cow 113
2.3.1 Non-pregnant uterus 113
2.3.2 Pregnant uterus 119
2.3.2.1 Day 10 to 20 of pregnancy 119
2.3.2.2 Day 21 to 24 of pregnancy 121
2.3.2.3 Day 25 to 30 of pregnancy 123
2.3.2.4 Day 31 to 40 of pregnancy 127
2.3.2.5 Day 41 to 90 of pregnancy 129
2.3.2.6 2nd and 3rd trimester of pregnancy 133
2.3.2.7 Twin and multiple pregnancies 135
2.3.3 Uterine pathology 137
2.3.3.1 Embryonic death 137
2.3.3.2 Fetal mummification 137
2.3.3.3 Fetal maceration 137
2.3.3.4 Postpartum uterus 139
2.3.3.5 Endometritis 141
2.3.3.6 Pyometra 141
2.4 Ultrasonography of the bovine fetus 143
2.4.1 Imaging of fetal organs 143
2.4.1.1 Head 145
2.4.1.2 Spinal column 153
2.4.1.3 Neck 157
2.4.1.4 Thorax 157
2.4.1.5 Abdomen 159
2.4.1.6 Pelvis 163
2.4.1.7 Front limb 163
2.4.1.8 Hind limb 165
2.4.1.9 Umbilical cord, amnion and allantois 167
2.4.2 Sex determination in the bovine fetus 169
2.4.2.1 Scrotum, teats and genital tubercle 169
2.4.3 Accessibility of bovine fetuses for transrectal sonography and their intra-uterine presentations during pregnancy 173
2.4.3.1 Accessibility of fetal body parts 173
2.4.3.2 Fetal intra-uterine presentations 173
2.4.4 Sonographie fetometry in cattle 175
2.4.4.1 Eye and braincase 175
2.4.4.2 Heart frequency, crown-rump-length, diameters of stomach, trunk, scrotum and umbilical cord 177
2.4.4.3 Cervical, thoracic, lumbar, coccygeal vertebrae and ribs 179
2.4.4.4 Front and hind limbs 181
References to chapter 2 184

Downloaded From Vet-eBooks.com

3 Ultrasonography in sheep and goats 187
3.1 Technique of ultrasonography in sheep and goats 187
3.1.1 Transcutaneous sonography 187
3.1.2 Transrectal sonography 189
3.2 Ovarian structures in sheep and goats 191
3.2.1 Follicles and corpora lutea 191
3.3 Uterine structures in sheep and goats 195
3.3.1 Non-pregnant uterus 195
3.3.2 Pregnant uterus 197
3.3.2.1 Before Day 20 of pregnancy 197
3.3.2.2 Day 20 to 40 of pregnancy 197
3.3.2.3 Day 40 to 100 of pregnancy 201
3.3.2.4 Day 100 to 150 of pregnancy 205
3.3.2.5 Accuracy of sonographic pregnancy diagnosis 207
3.3.3 Uterine pathology 209
References to chapter 3 210

4 Ultrasonography in pigs 213
4.1 Technique of ultrasonography in pigs 213
4.1.1 Transcutaneous sonography 213
4.1.2 Transrectal sonography 213
4.2 Ovarian structures in pigs 215
4.2.1 Follicles and corpora lutea 215
4.2.2 Ovarian cysts 217
4.3 Uterine structures in pigs 219
4.3.1 Non-pregnant uterus 219
4.3.2 Pregnant uterus 219
4.3.2.1 Before Day 20 of pregnancy 219
4.3.2.2 Day 20 to 115 of pregnancy 219
4.3.2.3 Accuracy of sonographic pregnancy diagnosis 223
References to chapter 4 224

5 Ultrasonography in dogs and cats 227
5.1 Technique of ultrasonography in dogs and cats 227
5.2 Ovarian structures in dogs and cats 231
5.2.1 Ovarian tumors and cysts 231
5.3 Uterine structures in dogs and cats 233
5.3.1 Pregnant uterus 233
5.3.1.1 Before Day 20 of pregnancy 233
5.3.1.2 Day 20 to 30 of pregnancy 233
5.3.1.3 Day 31 to 50 of pregnancy 239
5.3.1.4 Day 51 to 65 of pregnancy 245
5.3.1.5 Obstetric diagnostics 245
5.3.1.6 Postpartum uterus 245
5.3.2 Uterine pathology 247
5.3.2.1 Embryonic death 247
5.3.2.2 Pyometra, endometritis, cystic glandular hyperplasia 249
References to chapter 5 252

Subject index 253

Downloaded From Vet-eBooks.com

Preface to first edition

In 1980 it was reported for the first time that the ultrasound imaging system - sonography or B-scan-real-time echography - permitted a reliable early pregnancy diagnosis in mares (Palmer and Driancourt). This report triggered a development during the course of which sonography became an important tool for the management of reproductive problems.

Since then sonography provided significant contributions to our better understanding of the early embryonic phase and has contributed significantly to new discoveries concerning the function of the uterus and ovaries (Chevalier and Palmer 1982, Ginther 1983, Ginther and Pierson 1984).

Veterinary sonography has gained significant value in the gynecological examination of mares. In contrast to traditional methods, ultrasonography permits a much earlier and more accurate diagnosis of pregnancy and provides relevant practical information about many other conditions of the genital tract (Simpson et al. 1982, Valon et al. 1982, Leidl and Kähn 1984, Kähn and Leidl 1987).

Today ultrasonography is applied in the reproductive and obstetrical examination of numerous other species. Initial publications have appeared on virtually all domestic species. It has been shown that sonography can be applied very successfully in the diagnostic work-up on the bovine uterus and ovary (Chaffaux et al. 1982, Pierson and Ginther 1984 a and b, Reeves et al. 1984, Kähn 1985, Taverne et al. 1985, White et al. 1985). In countries where sheep and goats are bred intensively, ultrasonography spread surprisingly rapidly as a means of diagnosing pregnancy and establishing fetal numbers (Tainturier et al. 1983 a and b, De Bois and Taverne 1984, Fowler and Wilkins 1984, White et al. 1984). In the pig ultrasonography is also very useful in diagnosing pregnancy (Inaba et al. 1983, Botero et al. 1984, Irie et al. 1984). In the bitch and queen it is used to diagnose pregnancy at a much earlier stage than is possible by any other method (Mailhac et al. 1980, Boulet 1982, Laiblin et al. 1982, Legrand et al. 1982). In obstetrical cases fetal viability can be determined allowing a more rational decision to be made when choosing between medical or surgical interventions. Also in other veterinary disciplines the application of ultrasonography is gaining more importance.

It is thus becoming apparent that ultrasound diagnostics in veterinary medicine may experience the same kind of development as it has in human medicine where it was first applied in gynecology at the end of the fifties (Donald et al. 1958) and since then has expanded into virtually all fields of diagnostics.

Although the technique currently only stands at the beginning of its development in veterinary medicine it is obvious that ultrasound imaging provides a valuable additional diagnostic technique in gynecological and obstetrical examinations. In the few years of its application this technique has already provided several new indications for diagnostic examinations in normal and pathological conditions of the genital tract of domestic animals. When compared to conventional methods the diagnostic accuracy has improved significantly, too.

The sonographic progress provided the stimulus for writing this book so as to illustrate the possibilities and limitations of the application of ultrasonography to the examination of the reproductive systems in horses, cattle, sheep, goats, pigs, dogs and cats.

I thank my teacher and mentor, Professor Dr. DDr. hc W. Leidl, for his support and creative guidance of my scientific studies over many years. His influence has been a significant factor in the development of this book.

I wish to thank the following people for kindly providing illustrations and contributions to this book: Dr. C. Bouabid, Dr. J. Fraunholz, Dr. B. Kähn, Dr. T. Pyczak and Dr. K. Will.

I acknowledge the work of the staff of Schlütersche in the production of this edition.

Kaufungen, June 1994

WOLFGANG KÄHN

Avtorsko zaščiteno gradivo

Downloaded From Vet-eBooks.com

Preface to current edition

In 1994, when the first edition of Veterinary Reproductive Ultrasonography was published, ultrasound imaging was considered to be just a supplementary diagnostic tool. The technique was not widely used at that time and was often only employed when more conventional diagnostic tools were considered to be inadequate. In the meantime, diagnostic medical sonography has advanced to being a basic tool used in a variety of physiological and pathological reproductive conditions in the horse, cow, small ruminants, pig, dog and cat. Ultrasound imaging has found its way into routine veterinary practise for early pregnancy recognition in domestic animals, for improved ovarian diagnosis, and for a better detection of pathological changes in the uterus.

The extensive implementation of diagnostic medical sonography brought with it a great need for specialist literature and as a consequence, the first edition of this book was quickly sold out. Both veterinary surgeons and students have frequently requested that it should be reprinted or a new edition published. Looking through the first edition, it could be recognised that the book's contents have remained up-to-date. Even though there has been an enormous increase in knowledge about reproductive processes during the more than two decades of ultrasound imaging, the pertinent basic scientific knowledge had already been included in the first edition, and this has retained its validity. Therefore, the publisher and author have mutually decided to reprint the first edition without changing any of its contents.

Zurich, December 2003 WOLFGANG KÄHN

Avtorsko zaščiteno gradivo

Downloaded From Vet-eBooks.com

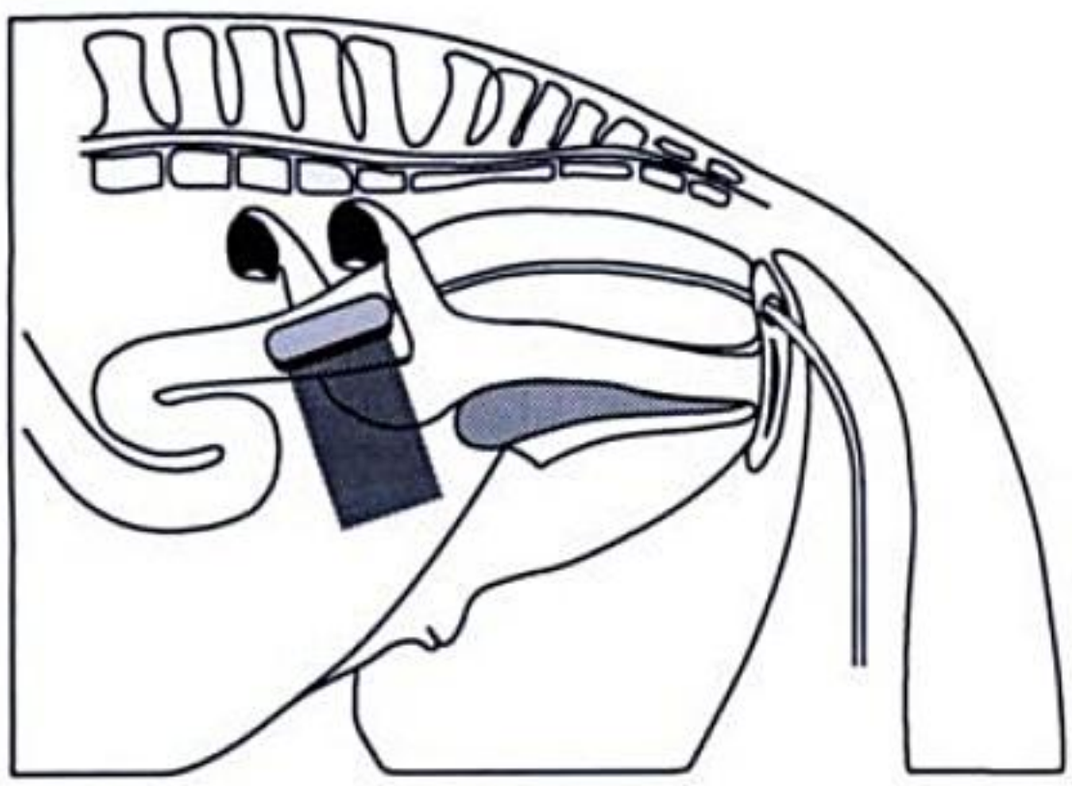


Fig. 1.1: Schematic presentation of the transrectal ultrasonography of the uterus and ovaries of a mare.

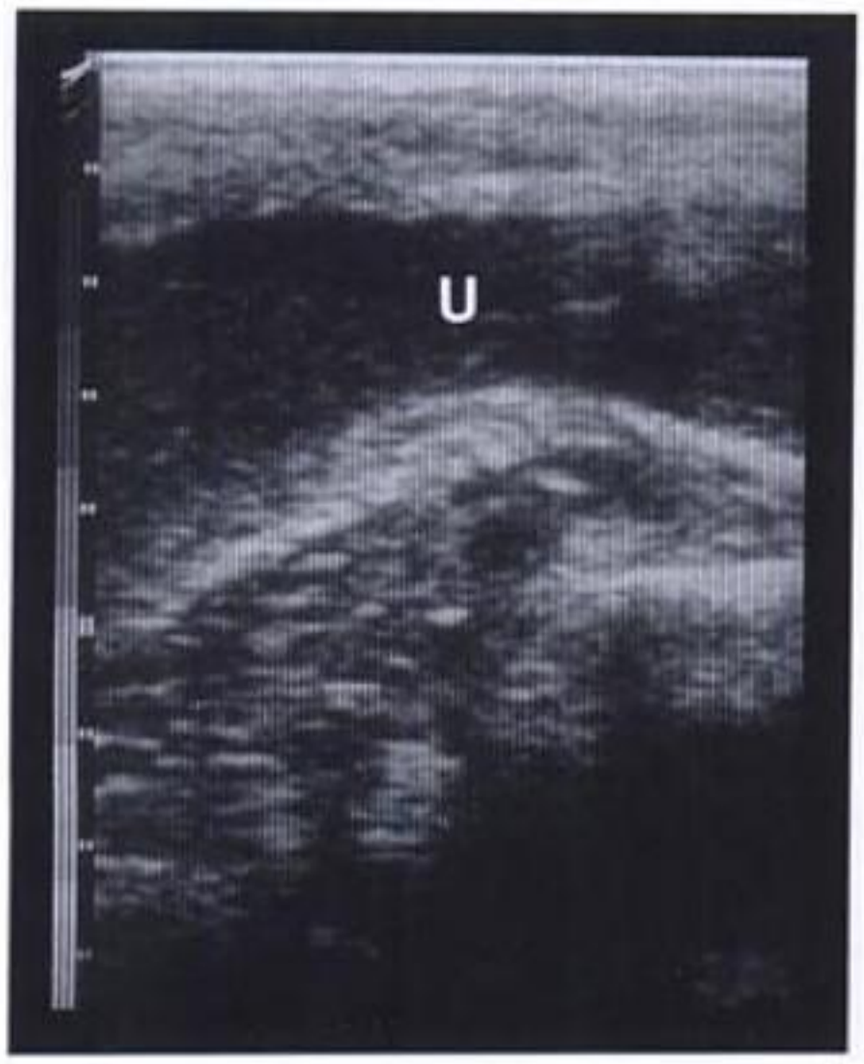


Fig. 1.2: Dorsoventral sagittal section through the neck of the urinary bladder (U) of a mare. The bladder lies on the hyperechoic pelvic floor widening as it extends cranially. The urine is slightly echoic. Ultrasonogram taken with a 5 MHz linear scanner[1].

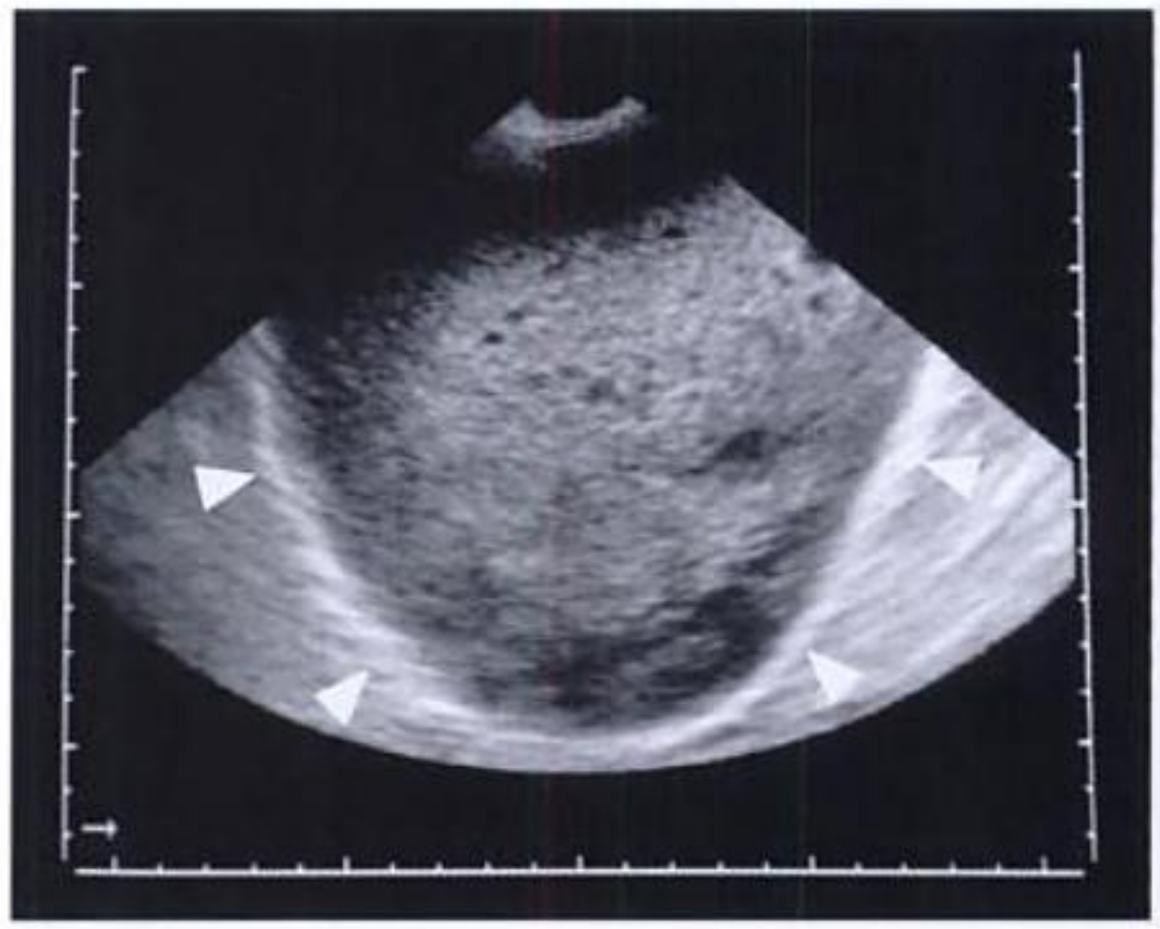


Fig. 1.3: Dorsoventral sagittal section through the body of the urinary bladder (arrows) of a mare. The urine is intensely echoic. Ultrasonogram taken with a 5 MHz sector scanner.

[1] Most ultrasonograms in this book were taken in vivo. Some photographs were made after scanning the excised organs in a waterbath and the legends marked accordingly.

Avtorsko zaščiteno gradivo

Downloaded From Vet-eBooks.com

1 Ultrasonography in the mare

1.1 Technique of ultrasonography in the mare

In mares the uterus and ovaries are examined by transrectal ultrasonography. For this purpose the ultrasound probe is introduced into the caudal rectum.

In order to keep the probe hygienic and to protect it from moisture it is preferable to pull a plastic sleeve over the probe. The space between the scanning window of the probe and the plastic sleeve must be filled with gel to exclude any air bubbles which cause undesirable reflections and thus affect the image quality. It is not necessary to apply any coupling gel between the plastic sleeve and the rectum, since he rectum's natural contractility and moist contents both provide favorable conditions for the exclusion of air between the probe's scanning surface and the rectal wall. Many veterinarians introduce the unprotected probe into the rectum.

The procedure of ultrasound examination of the uterus and ovaries is similar to that of a rectal examination (Fig. 1.1). Control and handling of the mare are also the same. Before the genital organs are scanned they are palpated in the usual manner thereby facilitating the speedy location of the organs and the correct positioning of the probe to ensure a swift and accurate examination. During the learning period of ultrasound examinations it is also helpful to compare the familiar palpable structures to the "new" images seen on the screen. This allows for the recognition and identification of the genital organs and their characteristic ultrasonic patterns.

Feces and fecal gas bubbles hinder the transmission of ultrasound waves. The absorption of sound waves by fecal matter lying between the probe's scanning window and the rectal wall will result in the appearance of black stripes in the depth of the image. The rectum must therefore be evacuated and the probe then introduced through the anus. The probe's scanning window is directed ventrally while it slides cranially along the rectal floor. During the examination the probe is covered dorsally by the examiner's hand and manipulated with the fingers. With increasing experience it is frequently possible to determine the position of organs and the probe's orientation inside the pelvis by recognizing typical images on the screen. It is usually not necessary to manually position the organs in preparation for an ultrasound examination.

The urinary bladder is the first ultrasonically striking organ encountered after passing the probe through the anus. The neck of the bladder widens over the cranial pelvic edge to join the body of the bladder (Fig. 1.2). The echogenicity of mares' urine can vary greatly. The ultrasonic image varies from almost anechoic to strongly echoic in the case of very viscous urine (Fig. 1.3). Turbulently moving reflexions can frequently be detected inside the bladder's fluid content.

Avtorsko zaščiteno gradivo

Downloaded From Vet-eBooks.com



Fig. 1.4: Transverse section through a uterine horn of a mare. The peritoneal borders are indicated by arrows. Analogous to the section represented by A in Fig. 1.5.

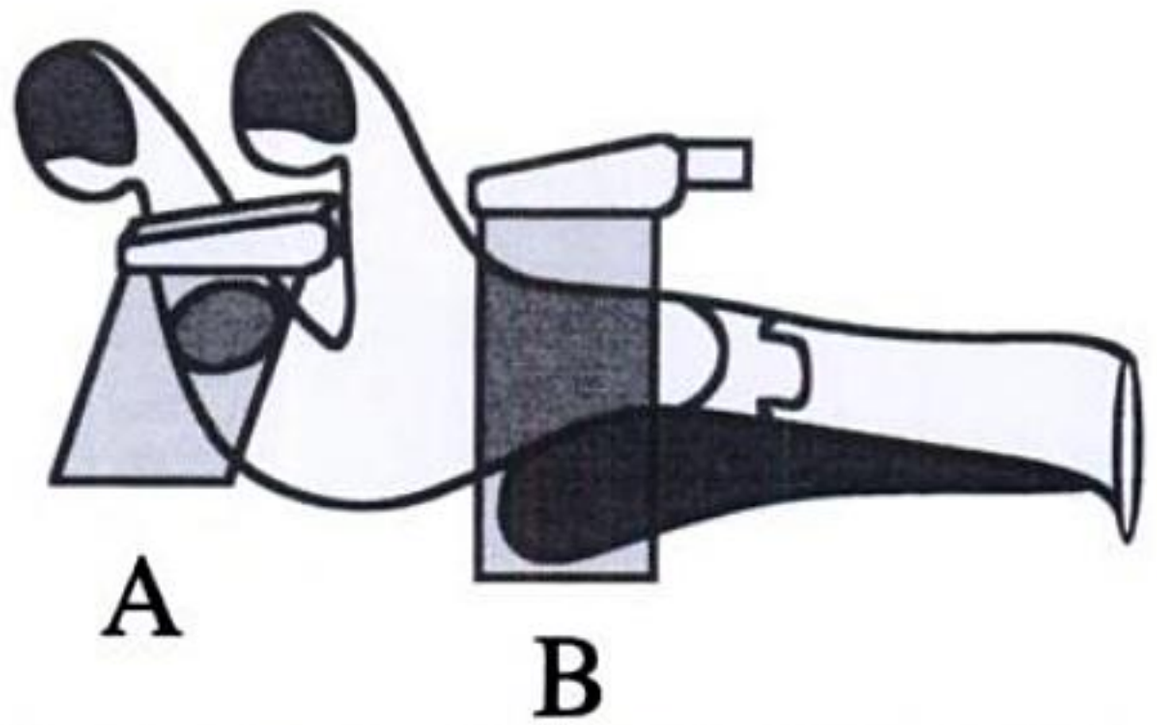


Fig. 1.5: Schematic presentation of a transverse section through a uterine horn (A) and a longitudinal section through the uterine body (B).

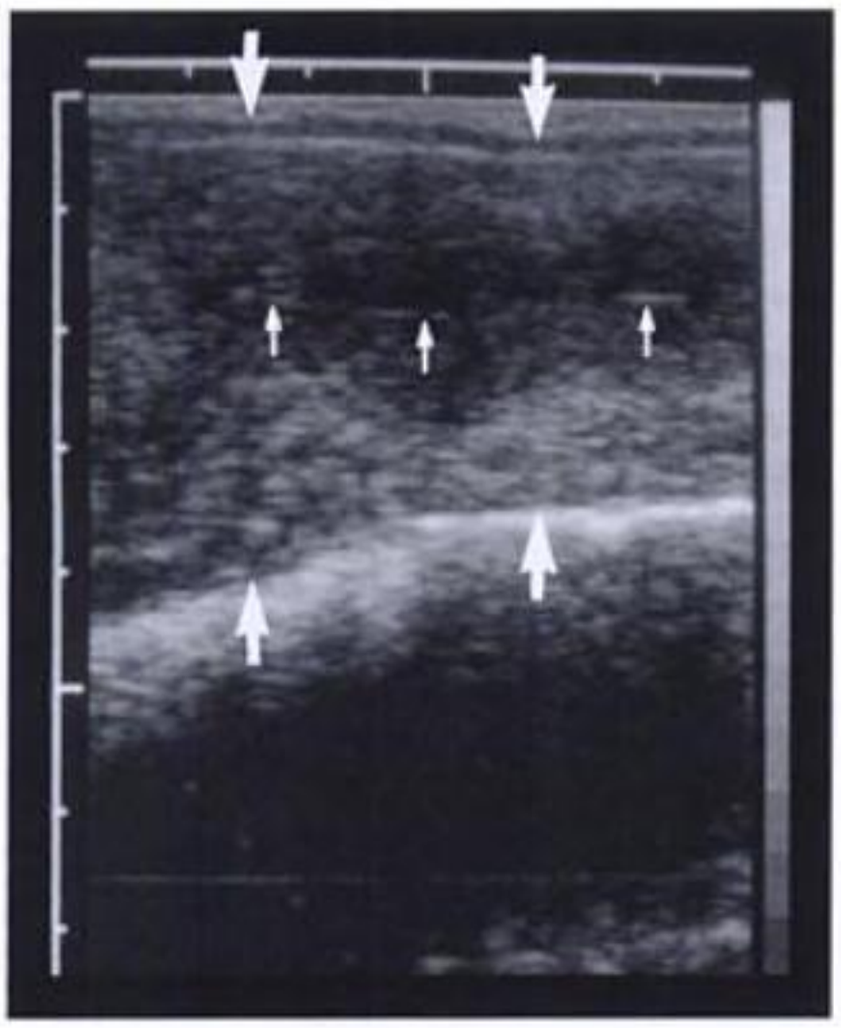


Fig. 1.6: Longitudinal section through the uterine body of a mare equivalent to the section illustrated by B in Fig. 1.5. The dorsal and ventral uterine borders are demarcated by large arrows. The opposing surfaces of the endometrium form an echoic line (small arrows).



Fig. 1.7: Transverse section through a uterine horn (arrows) of a nonpregnant mare. The uterus is positioned above 3 arched sacculations of the left dorsal colon. The difference in impedance between the intestinal wall and the feces cause total reflection of the ultrasound waves along the echoic sacculations of the colon.

Avtorsko zaščiteno gradivo

Downloaded From Vet-eBooks.com

After visualization of the urinary bladder the ultrasound probe is advanced cranially until the uterus appears on the screen. The probe is placed dorsally on the uterus at the level of the bifurcation. From here the ventrally directed probe is rotated laterally along the uterine horn until the ovary is visualized and then back to the opposite side to the second ovary. In this manner the uterine horns are scanned slice by slice. Each slice represents a sagittally oriented cross section through the uterine horn (Fig. 1.4 and 1.5). After the two horns the uterine body is imaged on the screen. Starting at the bifurcation the probe is withdrawn along the midline up to the level of the cervix. In the process one sees a sagittal longitudinal section of the uterine body (Fig. 1.5 and 1.6). During the course of an examination the probe should be moved rather slowly so as to ensure that the entire uterine tract as well as the ovaries and their functional structures can be assessed. It is important to be aware that only a minor rotation of the probe results in a significant shift of the scanning plane in the depth of the field. A 30 degree rotation of the probe results in a 5 cm movement of the scanning plane at a depth of 10 cm. Fast probe movements and motility of the targeted organs can be additive with the result that important features are passed too quickly or even missed.

Organs closely associated with the internal genitalia can be used as reference points to improve one's topographical orientation. Very echoic arches in the left abdomen, usually ventral to the left uterine horn, represent the sacculations of the left dorsal colon. The drastic change in impedance between the gut wall and the gas containing feces underneath it cause the total reflection of the ultrasound waves. The thin wall of the colon thus appears as a wavy structure of high echogenicity. The deeper areas are not reached by enough ultrasound waves and therefore remain almost totally dark. The bony pelvic floor also presents as a hyperechoic structure (Fig. 1.2). It is recognizable as anechoic line caudal and ventral to the uterus and the urinary bladder.

In addition to transrectal ultrasonography, transcutaneous ultrasonography can be applied in mares. The transcutaneous approach is less established for routine gynecological diagnostics than the transrectal method. One valuable indication is the visualization of the fetus and its uterine environment during the second and third trimesters of pregnancy (ADAMS-BRENDEMUEHL and PIPERS 1987). Since the hair on the abdominal wall prevents the penetration of the ultrasound waves, the mare's ventral abdominal hair must be thoroughly clipped very well before performing the ultrasound examination. The majority of mares tolerate the transcutaneous examination less well than the transrectal procedure.

Avtorsko zaščiteno gradivo

Downloaded From Vet-eBooks.com



Fig. 1.8: Schematic illustration of the ultrasonography of a fluid filled vesicle. A = oblique wave impact, b = perpendicular wave impact, c = tangential wave impact. D = hyperechoic distal wall, E = relative echo enhancement, S = shadow artifacts.

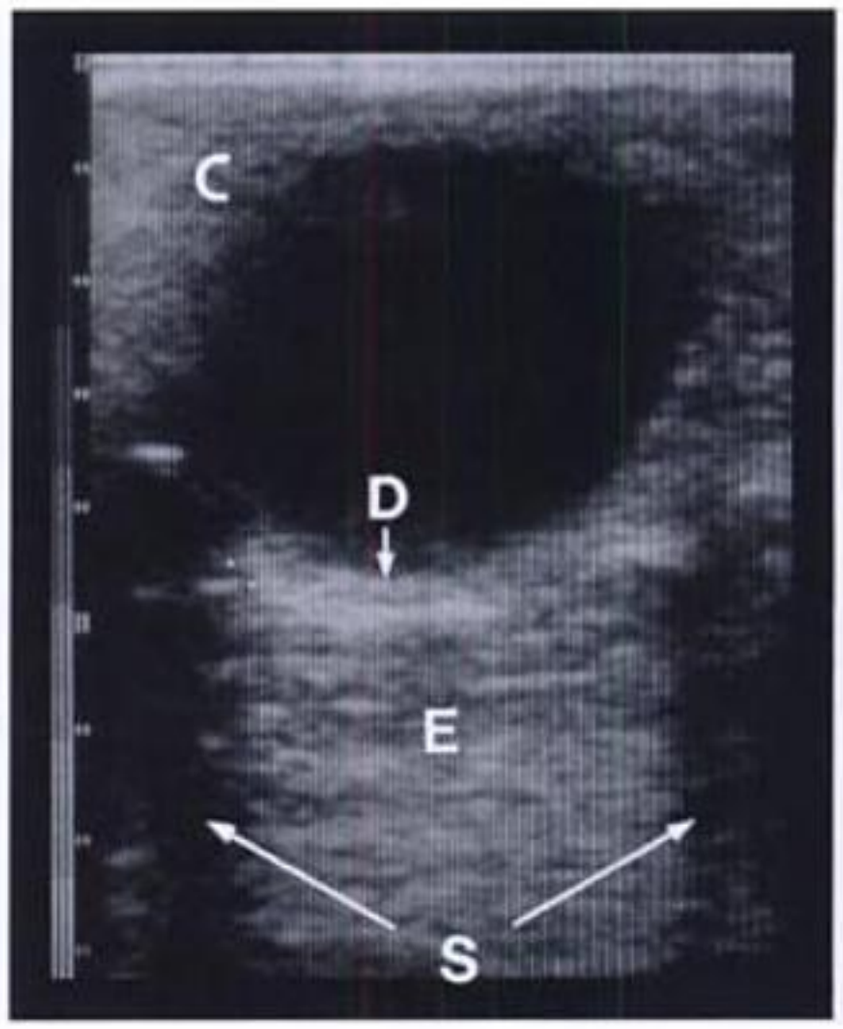


Fig. 1.9: Ultrasonogram of an estrous follicle in a mare analogous to the schematic representation shown in Fig 1.8. C = tangential wave entry. D = hyperechoic distal wall with specular reflection, E = relative echo enhancement, S = shadow artifacts.

Avtorsko zaščiteno gradivo

Downloaded From Vet-eBooks.com

1.2 Ovarian structures in the mare

1.2.1 Follicles

1.2.1.1 Sonographic images of follicles

The ultrasonic image of follicles exhibits features characteristic for fluid filled vesicles.

Some of the components of the image can be related to the presence of real morphological structures of the follicle (KÄHN and LEIDL 1987 b), while some ultrasonic image patterns typical for follicles are induced by physical phenomena when ultrasound waves impact onto vesicles and their fluid contents. They are thus seen as principal features which are referred to as artifacts. These image components which result from the interaction between ultrasound waves and fluid filled vesicles frequently do not reflect the presence of actual tissue components and should be viewed as artificial products. An understanding of their origin helps to avoid misinterpretations and permits proper conclusions about the nature of a vesicle.

When ultrasound waves impact vertically onto a smooth reflection surface, some waves are reflected back to the transducer and are depicted as an intense echo on the screen (Fig 1.8). The echogenicity is strongest where the ultrasound waves fall perpendicularly onto the front and back walls of the vesicle (Fig 1.9) which result in specular reflections. In the area where the ultrasound waves fall obliquely onto the follicle wall a smaller amount of the energy is reflected, the remainder being deflected away from the transducer and not received. At these sites the follicular wall is less echoic and thus darker. If the sound waves were to fall obliquely onto a perfectly level border surface they would all be deflected and no signals would be received (HASSLER 1984). Bordering layers in the body are, however, irregular and a varying number of sound waves are always reflected back to the transducer. Where the sound waves hit the follicular walls at a tangent, they are largely deflected (Fig 1.8 and 1.9) with hardly any echo signals reaching the probe from such sites. Very few sound waves continue to progress in a straight line from these sites into deeper tissues. The vast bulk of the ultrasound energy is deflected laterally from here. The result is that narrow, sometimes slightly widening, echo shadows form below such areas of tangential sound wave impact.

Amplified echoes or brighter images are seen behind larger fluid filled vesicles (Fig 1.8 and 1.9). Ultrasound is much less attenuated by fluid than by other body tissues. When sound waves penetrate larger fluid bodies they reach the deeper lying tissues with more energy and cast a much more intense echo than neighboring waves that followed a longer path through layers of tissue with more wave absorbency. Also on its path back towards the transducer the reflected ultrasound penetrating through fluid looses less energy and is absorbed to a lesser extent. This creates the impression of an echogenicity behind a fluid filled vesicle, the so called enhancement artifact. The width of the enhancement area is determined by the diameter of the fluid filled body. Laterally, the field of echo enhancement is usually demarcated by the narrow ultrasonic shadows which originate from where the sound waves impact tangentially onto the lateral walls of the fluid body.

Avtorsko zaščiteno gradivo

Downloaded From Vet-eBooks.com



Fig. 1.10: Ovary of an estrous mare with follicles of varying shapes. Four small round follicles and one large polygonal follicle of estrus can be distinguished.



Fig. 1.11: Ovarian follicles of a mare. A small follicle is indenting the wall of a larger estrous follicle.

Avtorsko zaščiteno gradivo

Downloaded From Vet-eBooks.com

The ultrasonic image of a follicle in cross section is seen as an anechoic area on the monitor. The latter can be delineated by a narrow brighter line which follows the outline of the follicle. The anechoic nature of the follicle is caused by the lack of reflection of sound waves as they travel through the relatively cell free, clear follicular fluid. Occasionally, and particularly in larger follicles, there will be clumps of reflexions visible close to the follicular wall. The shape of follicles varies from circular to oval to irregularly polygonal to nearly angular (Fig. 1.10). These variations in shape are the result of differences in pressure between neighboring follicles, corpora lutea or even the ovarian stroma itself (GINTHER and PIERSON 1984 a). When adjacent follicles are of equal pressure their adjoining walls are often completely straight. In contrast, small follicles of high inner pressure may clearly bulge into the lumen of larger, softer follicles (Fig. 1.11). When the ovary contains numerous small, tense follicles its ultrasound image may resemble a honeycomb.

The follicular wall is hyperechoic and thin. A narrow hyperechoic line is often visible where the ultrasound waves impact vertically onto the front and back walls of the follicle (Fig. 1.9 and 1.10). Laterally to this line the echogenicity is reduced along the obliquely oriented walls. The echo intensity in this area is comparable to that of moderately dense tissue and is hardly distinguishable from the surrounding stroma. In the region of tangential wave impact the follicular wall is usually not visible. These areas are frequently marked by the origins of the shadow artifacts that begin here and stretch into the depth of the image.

The echo enhancement of the tissues behind larger follicles is one of their typical features. The size of this enhancement area is correlated with the size of the follicle.

Using ultrasound at a frequency of 3.5 MHz one can relatively reliably detect follicles that are 6 to 8 mm in size, but with ultrasound at 5.0 MHz follicles of 3 to 5 mm are detectable with relative ease (PALMER and DRIANCOURT 1980, GINTHER and PIERSON 1984 b).

Avtorsko zaščiteno gradivo

Downloaded From Vet-eBooks.com

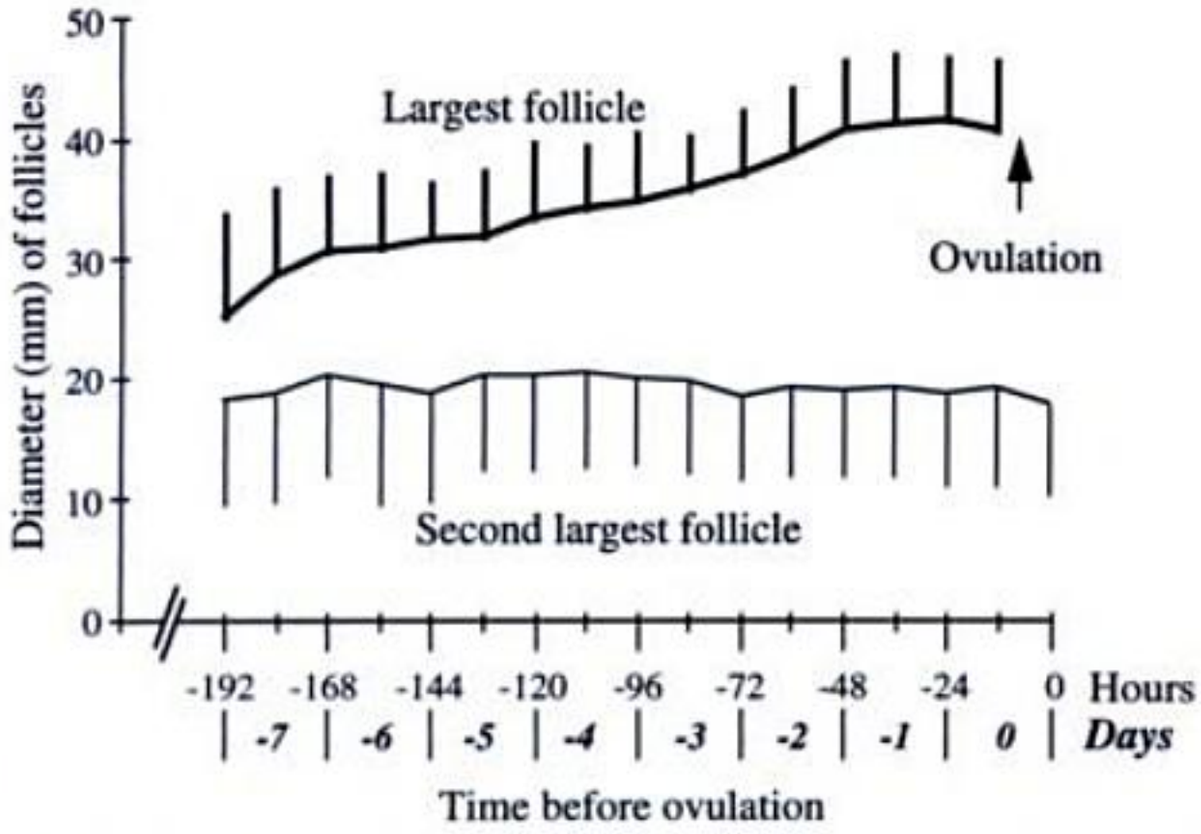


Fig. 1.12: Growth of the estrous follicle and the second largest follicle during the preovulatory period in mares (mean ± SD; adapted from WILL et al. 1988).

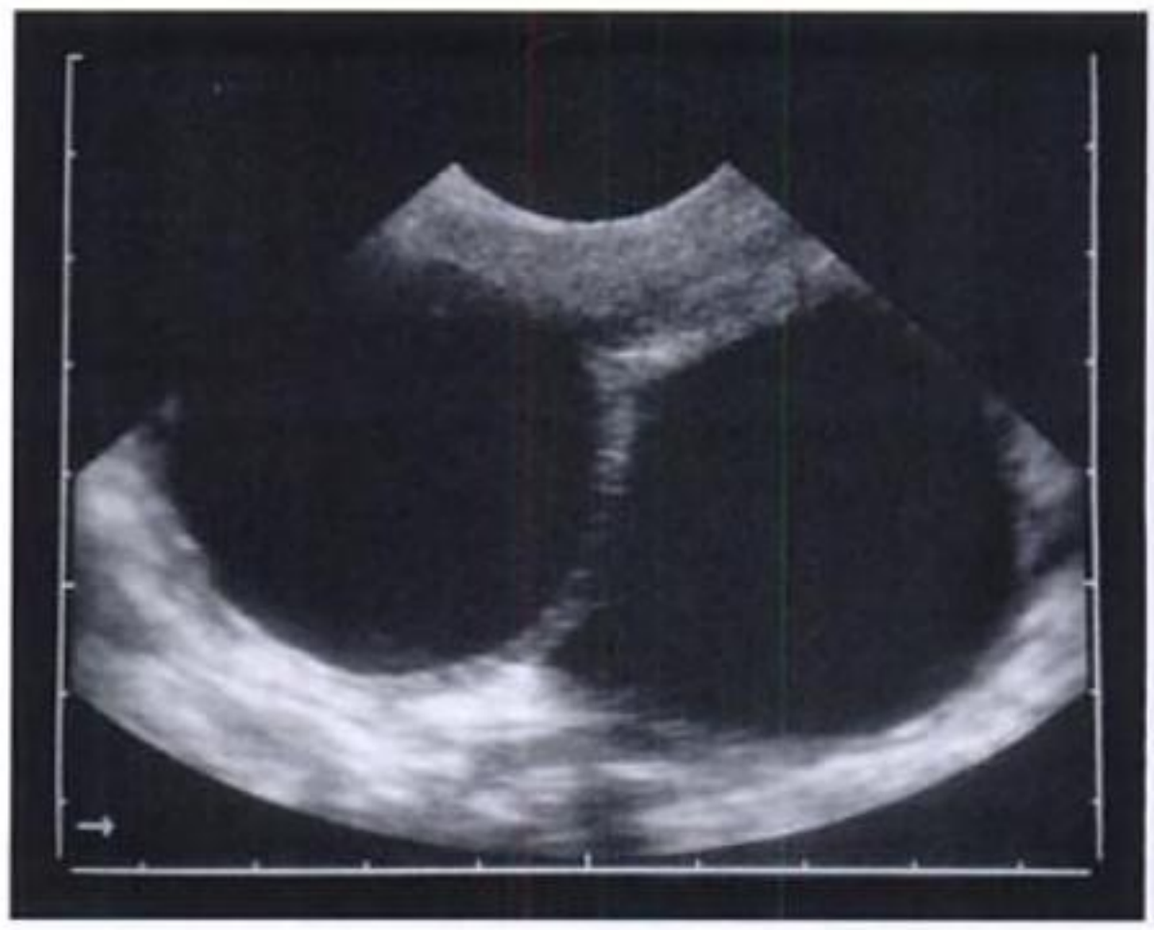


Fig. 1.13: Two estrous follicles in a mare shortly prior to double ovulation. Their diameters are between 35 and 37 mm.

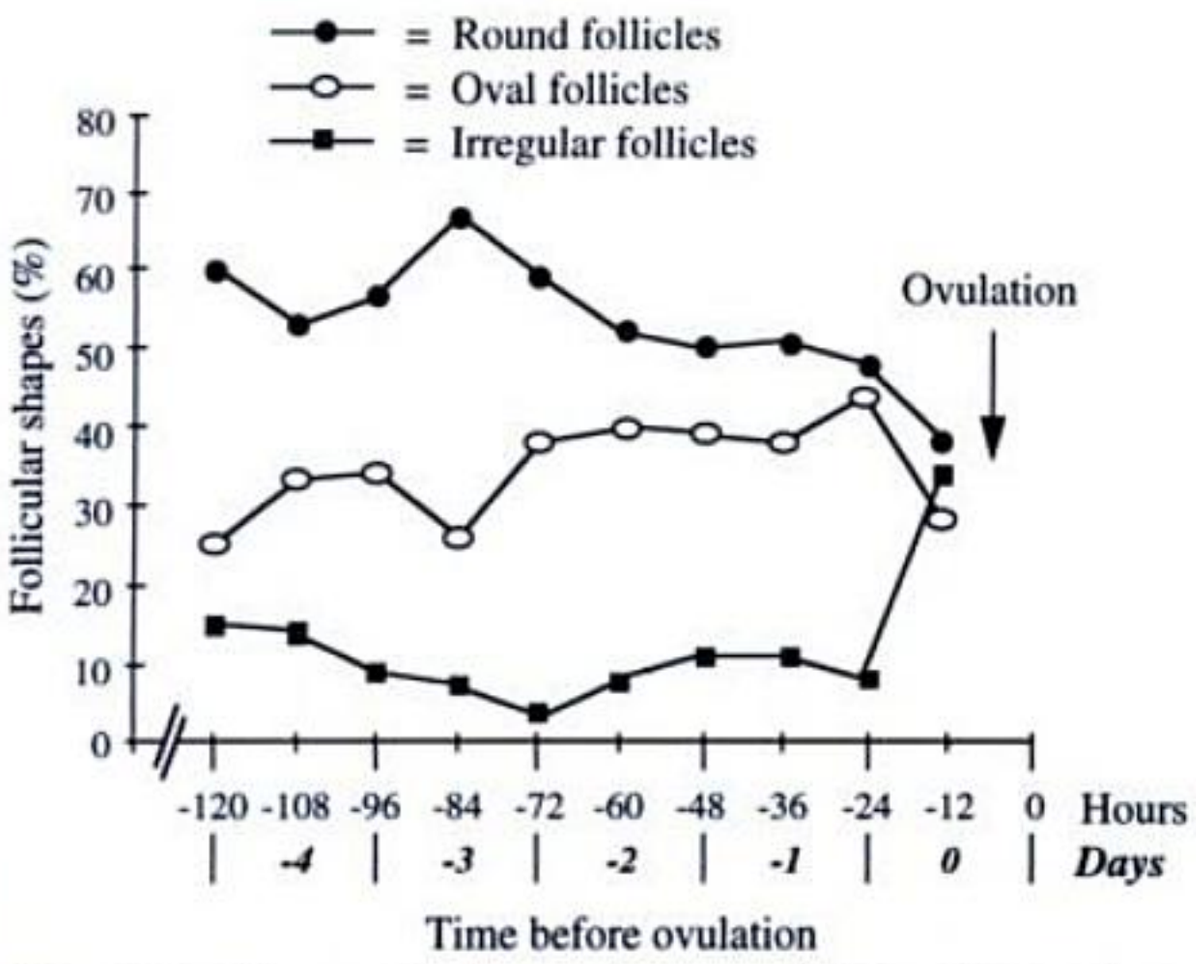


Fig. 1.14: Changes in shape of estrous follicles during the preovulatory period in mares (adapted from WILL et al. 1988).



Fig. 1.15: Irregularly shaped estrous follicle in a mare shortly before ovulation. Its largest diameter measures 53 mm (between markings).

Avtorsko zaščiteno gradivo

Downloaded From Vet-eBooks.com

1.2.1.2 Development of preovulatory follicles

Approximately 192 hours before ovulation (Day -7; Day of ovulation = Day 0 or Day 0 of the Cycle) dominant estrous follicles have a mean diameter of about 25 mm (Fig. 1.12). They then grow at 2 to 2.5 mm per day and reach their maximum diameter of 41 to 45 mm at 24 to 48 hours before ovulation (PIERSON and GINTHER 1985 b, WILL et al. 1988). In most cases no further growth occurs during the last 1 to 2 days before ovulation (PALMER and DRIANCOURT 1980). The diameter of the preovulatory follicle often remains static; sometimes even a reduction in the diameter can be measured on the day of ovulation.

At the time of ovulation of a single follicle it will usually have a diameter of 40 mm or more. Only occasionally will follicles be smaller at the time of ovulation. The upper limit of the size of normal ovulatory follicles lies between 55 and 58 mm.

When double ovulations occur the diameter of the preovulatory follicles may be smaller than those of single follicles (Fig. 1.13). In these cases ovulation of follicles with diameters of between 35 and 40 mm are not uncommon.

In many of the more mature preovulatory follicles one can see a change in shape during the days preceding ovulation (WILL et al. 1988). The majority of dominant follicles are distinctly round 3 or more days before ovulation (Fig. 1.14). During the days until ovulation the estrous follicle will change to a more oval or irregular shape (Fig. 1.15). On the day of ovulation only about one third of the estrous follicles will be round in shape.

Apart from the palpable feature of follicular consistency, the ultrasonic shape and size of a follicle can be utilized to help predict the time of an impending ovulation. Other parameters, such as the thickness of the follicular wall or the echogenicity of the follicular contents have been shown to be of little value. If the largest follicle shows an irregular shape, is at least 40 mm in size and has possibly been shown to have stopped growing for some time one should expect ovulation to occur very soon. Although sonography has contributed meaningfully to the prediction of the time of ovulation its value with regard to the accuracy of such predictions must not be overestimated. When manual criteria are combined with those of ultrasonography it is possible to correctly predict about one third of the ovulations that will occur during the next 0 to 12 hours (WILL et al. 1988).

Avtorsko zaščiteno gradivo

Downloaded From Vet-eBooks.com



Fig. 1.16: Collapsed follicle immediately after ovulation. The follicle still contains small amounts of residual fluid (between the crosses).

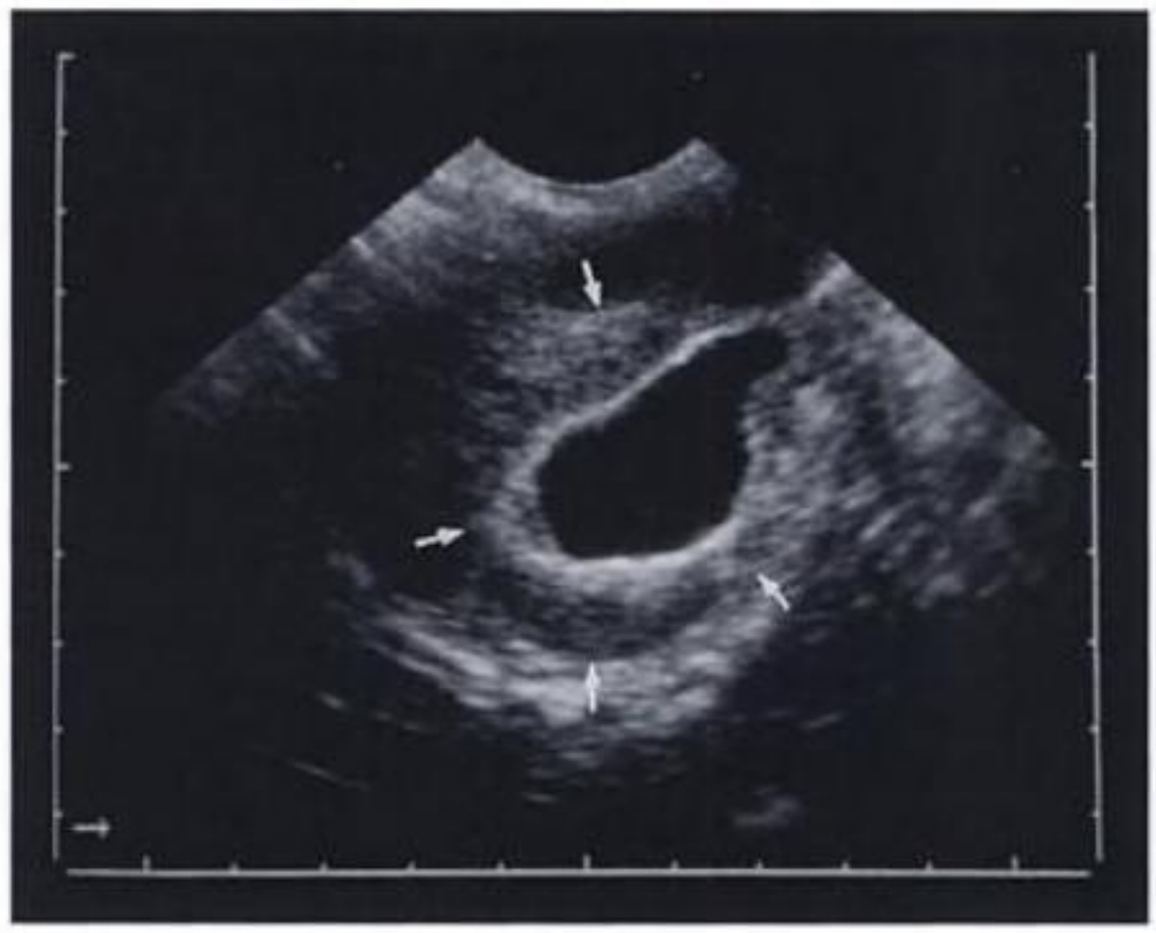


Fig. 1.17: Collapsed follicle on the day of ovulation showing a broad echoic seam (arrows) in the area of the original follicular wall. The center contains anechoic fluid.

Avtorsko zaščiteno gradivo

Downloaded From Vet-eBooks.com

An ovulation can be recognized ultrasonically when a follicle that was still present a short time ago cannot be found at a subsequent examination. Ovulation itself usually only takes seconds to minutes (CARNEVALE et al. 1988 b). The actual collapsing of the ovulating follicle can only be demonstrated by chance if the mare is examined very frequently (Fig. 1.16 and 1.17). The wall of the follicle appears to fold inwards, the follicular cavity is irregular in shape and sometimes contains small quantities of residual fluid. Whether the anechoic fluid in the lumen of the follicle consists of follicular fluid or blood, which accumulates inside the follicular lumen after ovulation, or a mixture of both, is unclear.

In many cases immediately after ovulation a large echogenicity is detectable near the collapsed follicular wall and may fill the entire area of the original follicle (see also Chapter 1.2.2.2).

Avtorsko zaščiteno gradivo

Downloaded From Vet-eBooks.com

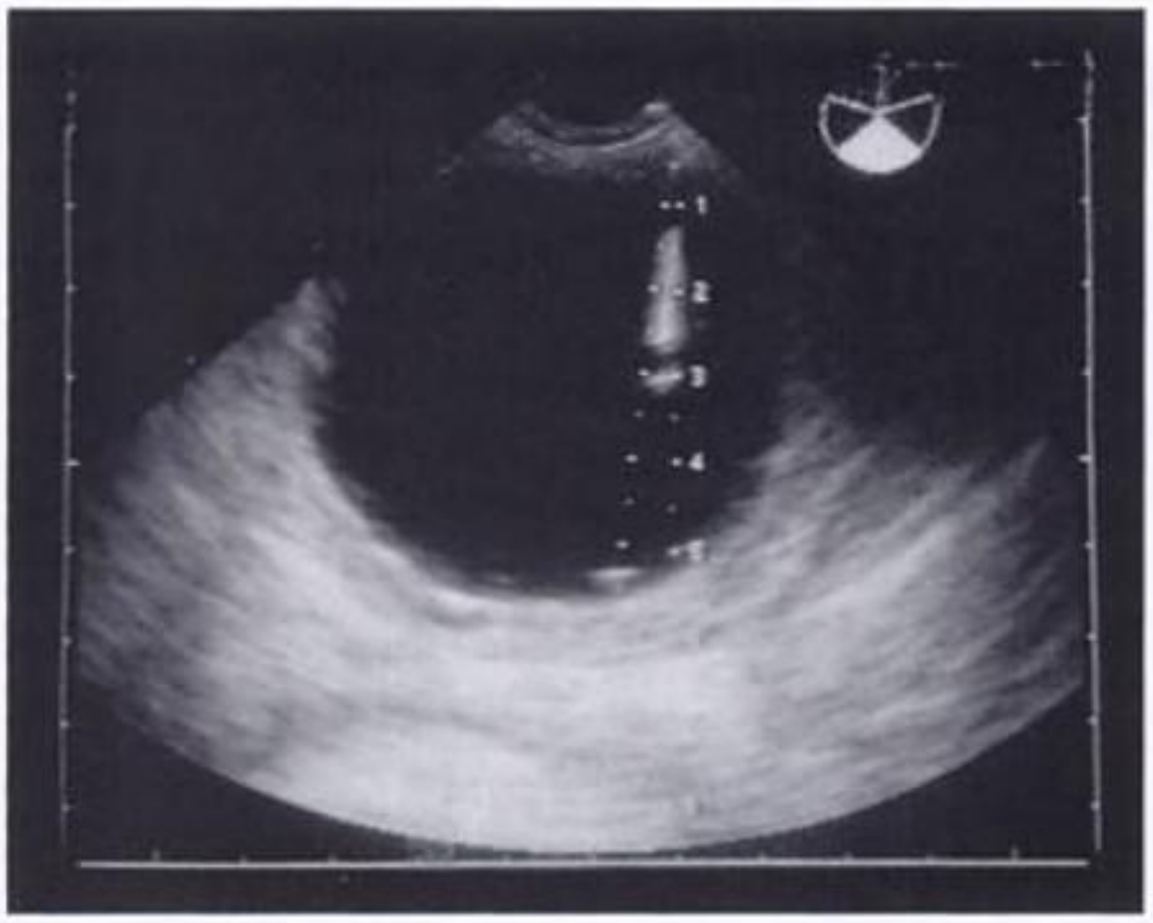


Fig. 1.18: Transvaginal sonographic puncture of an estrous follicle of a mare followed by the aspiration of the follicular fluid. The puncture needle can be seen between the two guiding lines and reaches approximately 3 cm into the follicular antrum.



Fig. 1.19: Ultrasonogram depicting the hemorrhage (between the dots) into a follicle 3 minutes after a puncture had been performed. The real time image clearly showed turbulences (arrow) inside the accumulated blood illustrating the inflow of more blood.

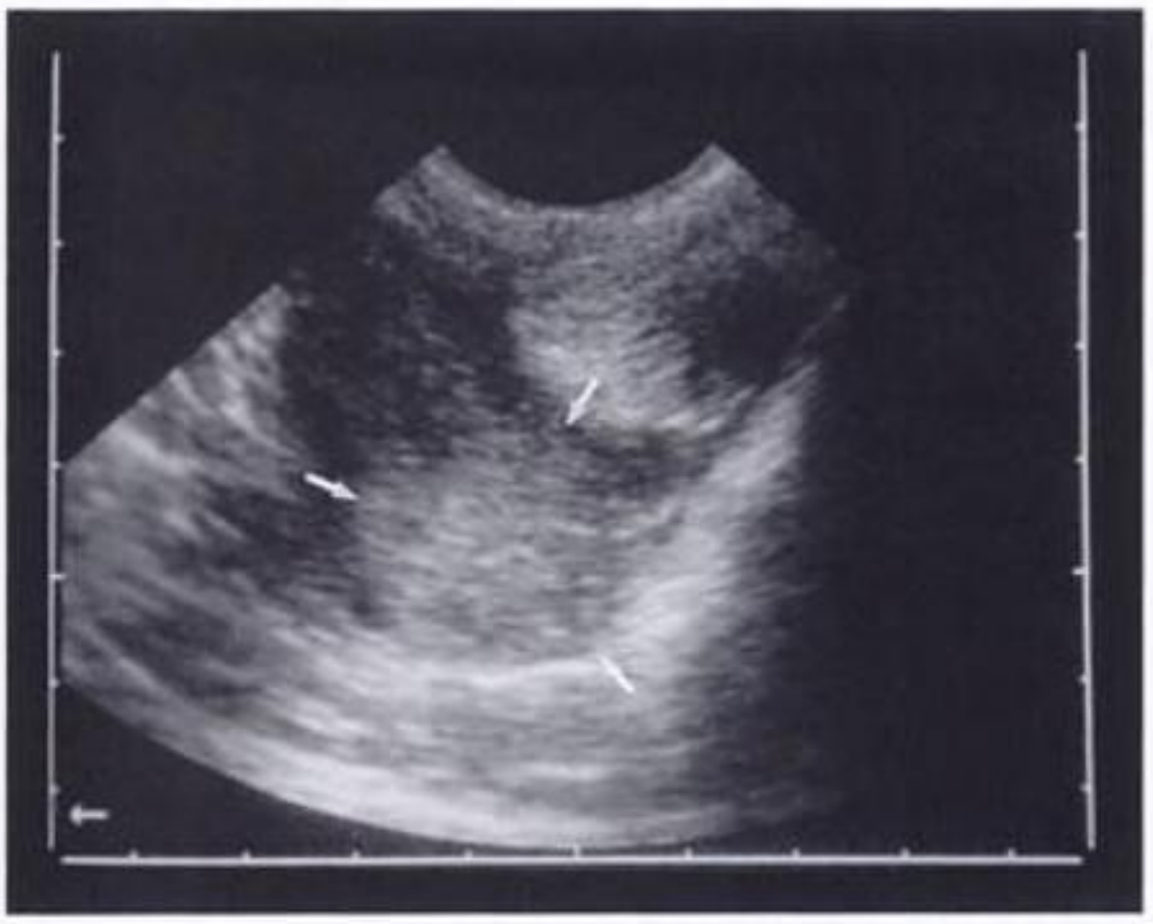


Fig. 1.20: Corpus luteum (arrows) which developed at the site of a follicle that had been punctured 4 days previously.

Avtorsko zaščiteno gradivo

Downloaded From Vet-eBooks.com

1.2.1.3 Transvaginal sonographic puncture of follicles

Transvaginal follicle punctures can be used to collect fluid from preovulatory follicles or to attempt the collection of oocytes. The same instrumentation that was designed for transvaginal conceptus punctures was applied for this purpose (see Chapter 1.3.2.6) using a similar technique. The automated puncture device, covered by a protective plastic sleeve, was introduced into the anterior vagina where it was gently pushed against the vaginal wall. Using a rectally introduced hand, the ovary was then brought towards the tip of the ultrasound probe. When it was evident on the monitor that the follicle was aligned in the direction of and for the correct depth of the puncture needle the automatic puncture device could be triggered (Fig. 1.18).

Using this technique it was possible to aspirate follicular fluid. Using a double barreled needle it was possible to continuously flush a follicle; with a single barreled needle follicles could be filled and the flushing fluid aspirated repeatedly.

Immediately after a follicle had been punctured it was evident that intrafollicular hemorrhage occurred (Fig. 1.19). Within only a few minutes the follicular cavity filled with blood which exhibited intensive echogenicity. Within this hemorrhage, turbulences, indicative of the streaming of blood into the follicle, were seen on the real-time ultrasound image. The extent of hemorrhage was similar to that seen at the site of the future corpus luteum after spontaneous ovulations (see Chapter 1.2.2.2). Thus far no disorders have been observed in mares after follicle puncture.

When the puncture site was examined ultrasonically during the next few days, the formation of a structure not unlike that of a corpus luteum could be observed (Fig. 1.20). A single puncture of a follicle shortly before its anticipated ovulation did not affect the development of a normal corpus luteum thereafter (CARNEVALE et al. 1988 a). In some mares whose follicles were punctured, lower plasma progesterone concentrations were measured during the first 3 to 5 days after puncture than in mares that ovulated without interference. This difference in progesterone secretion was, however, not evident after Day 8 of the cycle. Cycle length and the ensuing estrus of mares were not affected by follicle puncture.

Avtorsko zaščiteno gradivo

Downloaded From Vet-eBooks.com

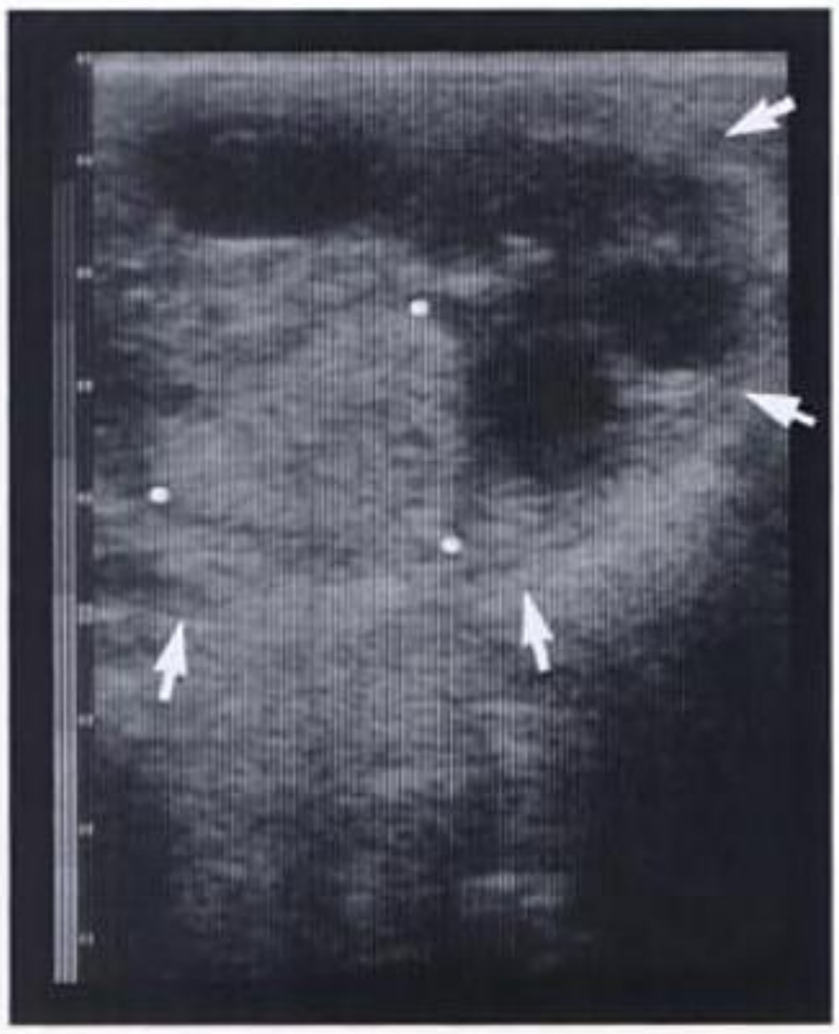


Fig. 1.21: Solid corpus luteum (dots) between several small follicles on the ovary (arrows) of a mare. A hypoechoic border zone separates the corpus luteum from the surrounding ovarian parenchyma.

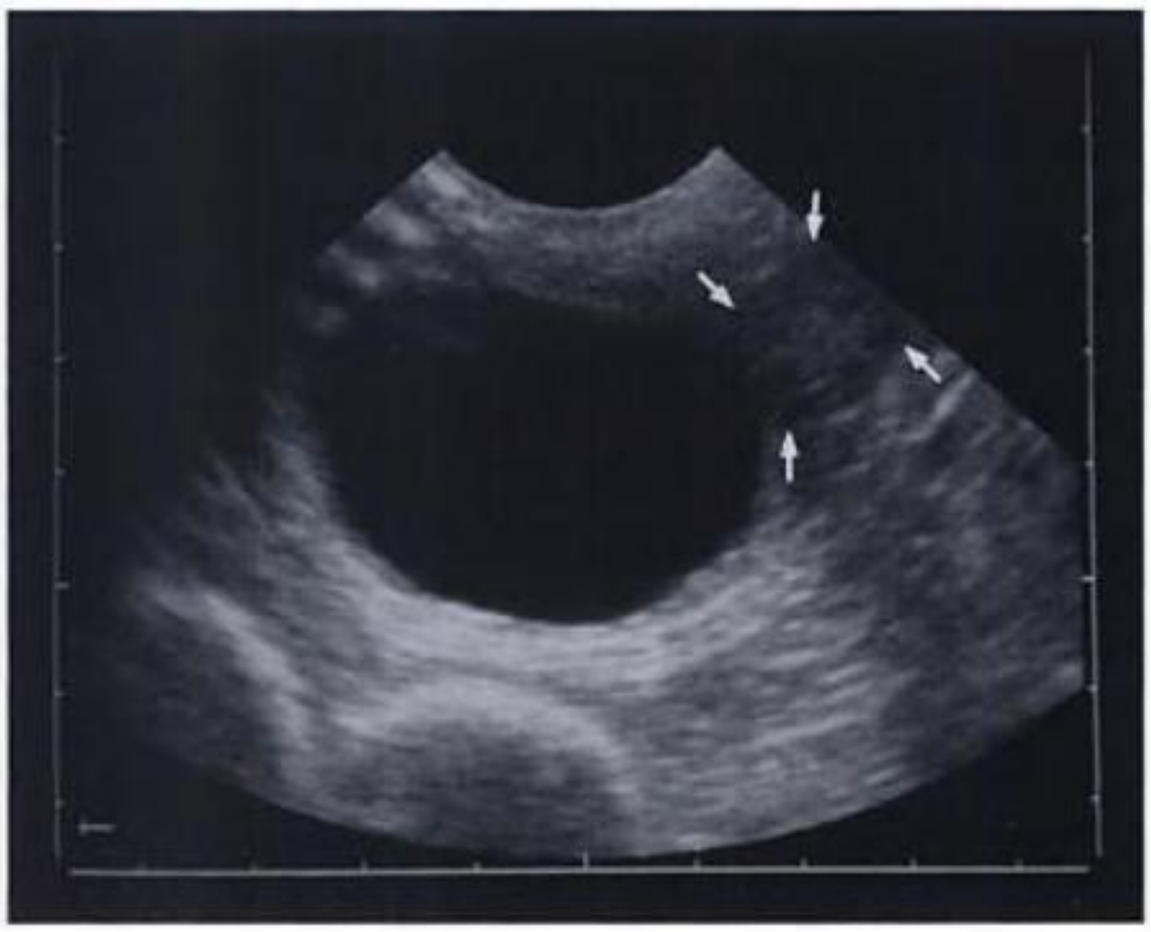


Fig. 1.22: Ultrasonogram of a regressing corpus luteum (arrows) next to an estrous follicle. Analogous to the sectioned ovary in Fig. 1.23. The inner diameter of the follicle is approximately 35 mm.



Fig. 1.23: Section through an ovary that was removed by ovariectomy from an estrous mare. A small remnant of hemorrhage is still visible in the center of the regressing corpus luteum (arrows). To the left of the corpus luteum lies the antrum of the estrous follicle.

Avtorsko zaščiteno gradivo

Downloaded From Vet-eBooks.com

1.2.2 Corpora lutea

1.2.2.1 Sonographic images of corpora lutea

Useful ultrasonic features in identifying a corpus luteum are its characteristic echogenicity, its size and shape, as well as a thin hypoechoic border zone which separates it from the surrounding ovarian parenchyma (Fig. 1.21). On ultrasound, luteal tissue shows up in varying gray tones which are typical of the reflections received from loose, moderately dense tissue. The surrounding ovarian parenchyma is more echogenic, due to its higher density and it contains many anechoic follicles. The shape of a corpus luteum is irregular in many cases, sometimes even cubical. It is often narrower near its center, resulting in a pear shape. Frequently, vesicles which lie adjacent to the corpus luteum are the cause of these indentations to the outline of the corpus luteum.

When 5 MHz scanners are used corpora lutea are relatively reliably detectable from their formation until middiestrus around Day 12 of the cycle (PIERSON and GINTHER 1985 a). Thereafter they become less distinct. At the time of luteolysis, approximately 14 to 16 days after ovulation, they are still detectable in many instances. Only rarely can the regressing corpus luteum be identified with certainty at the time of the following ovulation or even a few days later (GINTHER and PIERSON 1984 b). By this time it will have become significantly smaller (Fig. 1.22 and 1.23).

Avtorsko zaščiteno gradivo

Downloaded From Vet-eBooks.com

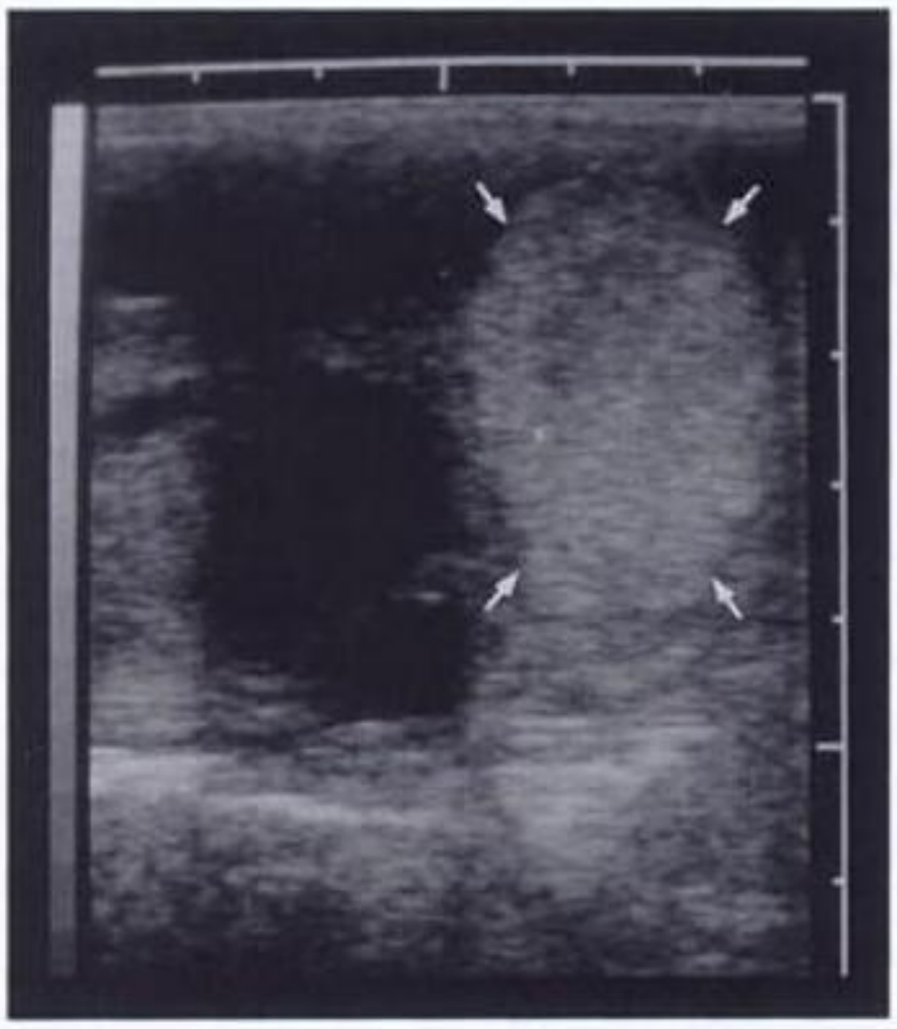


Fig. 1.24: Intense echogenicity (arrows) at the site of the estrous follicle one day after ovulation. The bright echogenicity is caused by the hemorrhage into the follicular antrum after ovulation.



Fig. 1.25: Sectioned ovary 3 days after ovulation showing a young corpus luteum in its center.

Avtorsko zaščiteno gradivo

Downloaded From Vet-eBooks.com

1.2.2.2 Development of corpora lutea during the estrous cycle and in early pregnancy

The site of the development of a corpus luteum can already be recognized by its intense ultrasonic echogenicity within the first 24 hours after ovulation (Fig. 1.24). In some cases this site can even be detected within minutes after ovulation (GINTHER and PIERSON 1984 a, KÄHN and LEIDL 1987 b). These intense reflections originate from the hemorrhage into the follicular lumen which occurs after ovulation (ALLEN et al. 1987). The development of such hyperechoic areas at the sites of former follicles can also be seen after iatrogenically induced hemorrhages during follicular punctures (see Chapter 1.2.1.3 and FIG. 1.19).

The hemorrhagic area of young corpora lutea remains very echoic for the first 3 to 4 days following ovulation (PALMER and DRIANCOURT 1980). This hyperechogenicity is only detectable for a short time after ovulation, because with the increasing proliferation of luteal cells in the area of the blood clot it becomes less echoic. This process of luteinization usually progresses so rapidly, that large areas of the blood clot are taken over by luteal tissue (Fig. 1.25).

Avtorsko zaščiteno gradivo

Downloaded From Vet-eBooks.com



Fig. 1.26: A solid corpus luteum (arrows) in a mare 8 days post ovulation. To its right is a follicle (between crosses) with a diameter of 24 mm.



Fig. 1.27: Hemorrhagic corpus luteum (arrows) of a mare 3 days post ovulation. The narrow, hyperechoic edge of luteal tissue surrounds the large, hypoechoic central area of the blood clot.



Fig. 1.28: Sectioned ovary of a mare containing a corpus hemorrhagicum. The luteinization progresses from the periphery towards the center of the blood clot.

Avtorsko zaščiteno gradivo

Downloaded From Vet-eBooks.com

Two kinds of corpora lutea can be distinguished during the diestrus in mares: Compact corpora lutea and hemorrhagic corpora lutea (PIERSON and GINTHER 1985 a). A solid corpus luteum develops in about half of all mares after ovulation while in the other half a corpus hemorrhagicum forms. No functional difference appears to exist between the two types of corpora lutea (TOWNSON et al. 1989). Both, progesterone concentrations and cyclic events, are the same in mares with a corpus luteum or a corpus hemorrhagicum. Knowledge of the typical appearance of a corpus luteum is, however, important for its correct ultrasonic identification.

Solid corpora lutea have a homogenous echogenicity and structure across their entire cross sectional surface when viewed by ultrasonography (Fig. 1.26). The entire compact corpus luteum seems to consist of tissue of equal echogenicity throughout. They retain the same echogenicity for the duration of diestrus.

The second form of corpora lutea, the corpus hemorrhagicum, consists of two distinct zones of differing appearance: A hyperechoic peripheral edge and a central, less echoic core area (Fig. 1.27). In the latter the echoes vary from hypoechoic to almost anechoic and not infrequently they form trabecular, web like patterns. These two zones of corpora hemorrhagica result from the echoic peripheral zone of luteinized tissue and the hypoechoic central zone of the blood clot, respectively (Fig. 1.28). The blood clot reflects ultrasound less strongly than the luteinized wall and is sometimes traversed by a network of fibrin.

After ovulation, the entire cross sections of almost all hemorrhagic corpora lutea are echoic (PIERSON and GINTHER 1985 a). Only after a few days can the hypoechoic central area be distinguished from the more echoic peripheral area. On the third day of the cycle often less than half of the cross sectional surface area of a corpus luteum consists of echoic luteinized tissue (Fig. 1.27). As the cycle progresses the echoic areas enlarge; by Day 9 of the cycle they make up about 70 %, by the end of the cycle usually 100 %, of the corpus luteum.

Avtorsko zaščiteno gradivo

Downloaded From Vet-eBooks.com



Fig. 1.29: Corpus luteum of pregnancy (arrows) in a mare on Day 17 of gestation. The corpus luteum is surrounded by several follicles.



Fig. 1.30: Two corpora lutea (arrows) on the ovary of a mare on Day 25 of gestation. Below the corpora lutea lies a follicle.

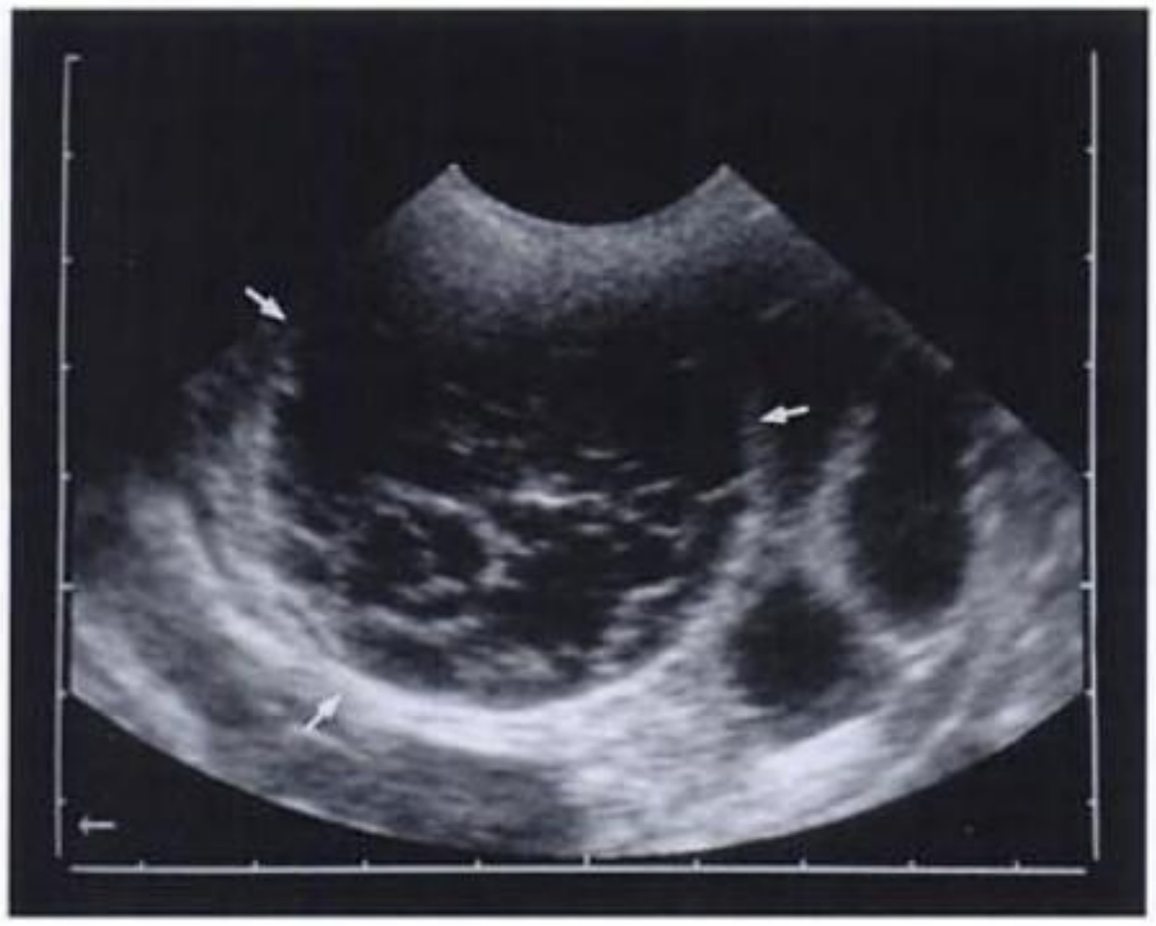


Fig. 1.31: Corpus hemorrhagicum (arrows) in a mare on Day 53 of gestation.



Fig. 1.32: Two corpora lutea (arrows) in a mare on Day 116 of gestation.

Avtorsko zaščiteno gradivo

Downloaded From Vet-eBooks.com

Once conception has occurred the primary corpus luteum of pregnancy remains detectable during the course of early gestation (Fig. 1.29). The same two forms of corpora lutea that are seen in diestrus can be found during the first two weeks of pregnancy. When the corpus luteum of pregnancy reaches a few weeks of age it usually has the same homogenous echogenicity as is typical of the solid corpus luteum of the cycle.

After a double ovulation has taken place, both corpora lutea can be depicted. Also in the case of an early twin pregnancy it is possible to depict both corpora lutea (Fig. 1.30).

Also the accessory corpora lutea of pregnancy which develop between Days 40 and 60 of gestation can be demonstrated by ultrasonography. Among these accessory corpora lutea of pregnancy are some that have the same appearance as the corpora hemorrhagica which occur during the nonpregnant cycle (Fig. 1.27). In the beginning these show a narrow peripheral edge which surrounds the trabecular hypoechoic central area (Fig. 1.31). During the further course of pregnancy the central, less echoic area becomes smaller while the hyperechoic luteinized wall grows thicker (Fig. 1.32).

Avtorsko zaščiteno gradivo

Downloaded From Vet-eBooks.com

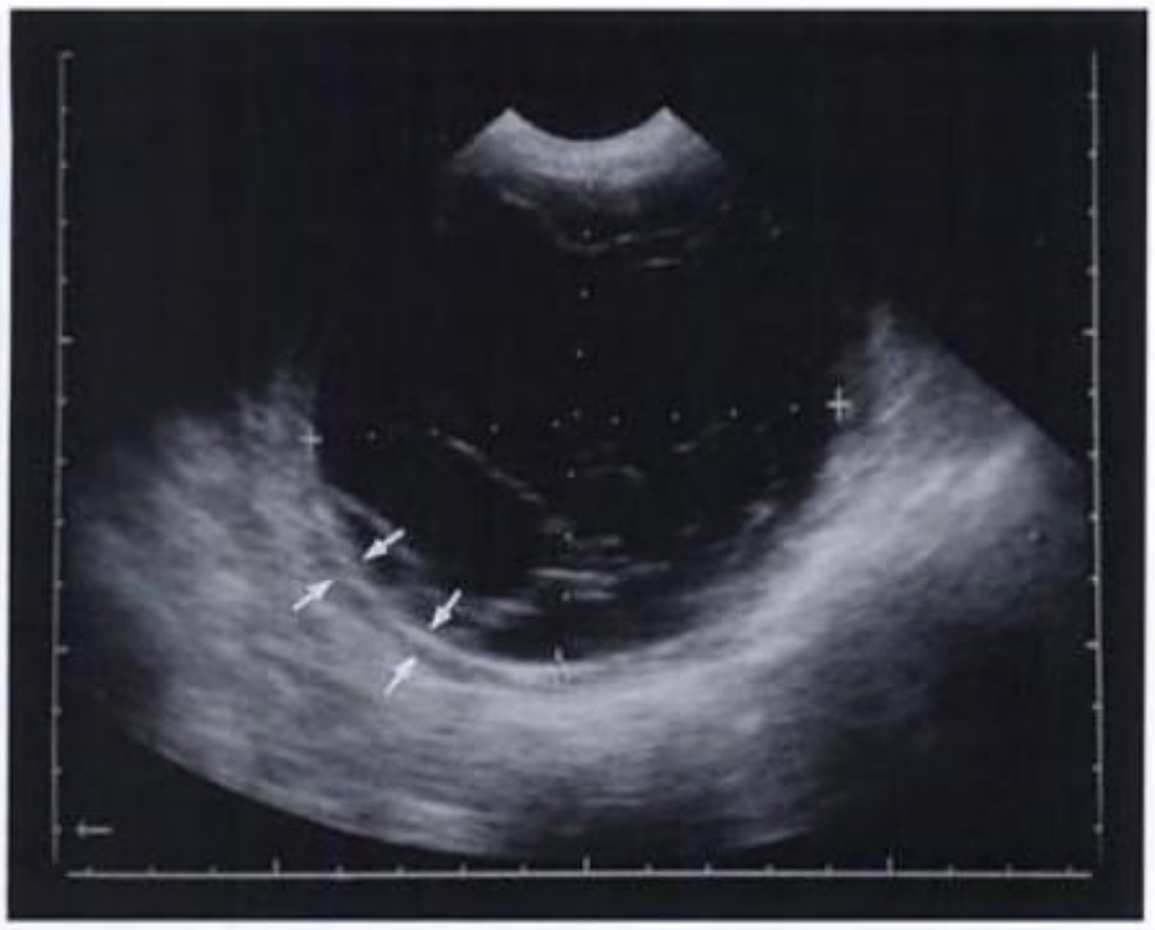


Fig. 1.33: Anovulatory, luteinizing follicle (between the crosses) with a network of internal echoes and a thin luteinized wall (arrows). The size of the follicle was 87 x 81 mm and the plasma progesterone concentration in the mare was 5.1 ng/ml.



Fig. 1.34: Anovulatory, luteinizing follicle (arrows) from Fig. 1.33 seven days later. The luteinized peripheral area surrounding the hypoechoic center has become substantially wider. The plasma progesterone concentration of the mare was 7.6 ng/ml.

Avtorsko zaščiteno gradivo

Downloaded From Vet-eBooks.com

1.2.3 Anovulatory luteinized follicles

Occasionally during an estrus a vesicle will develop into a dominant follicle, but will not ovulate. Such anovulatory follicles sometimes have the same size as that of normal, mature preovulatory follicles (WILL et al. 1988). Often they grow to larger diameters of 6 to 10 centimeters, and rarely even larger. Some of these anovulatory follicles seem to develop into hemorrhagic follicles, whereas others show clear signs of luteinization (SQUIRES et al. 1988, LEIDL and KÄHN 1989).

During estrus, the sonographic appearance of anovulatory follicles correlates well with that of normal follicles. In those follicles that will later develop signs of luteinization, reflections will appear with increasing frequency at a time shortly after ovulation would have normally taken place (Fig 1.33). These traverse the hypoechoic follicular lumen in the form of flocculation and/or networks of hyperechoic reflections. These echoes may originate from the bloody follicular contents such as occurs in hemorrhagic follicles or they may represent the onset of luteinization. At the time when the follicular contents starts to show this echogenicity the mare's behavioral estrus usually ends.

After the scattered inner echoes first become visible inside an anovulatory luteinizing follicle the narrow, hyperechoic wall will progressively become wider and wider (Fig. 1.34). The further development of these structures resemble that normally seen in hemorrhagic corpora lutea during the course of diestrus. The luteinized wall that surrounds the hemorrhagic center becomes wider while the central, hypoechoic area shrinks. Some of the anovulatory follicles therefore seem to luteinize to develop into structures similar to corpora lutea. This observation is supported by the plasma progesterone concentrations in these mares. In some individual cases it has been possible to demonstrate rising plasma progesterone concentrations at the time when the first hyperechoic foci appeared in the follicle. During the course of the development of the luteinized structure the plasma progesterone concentrations reached the expected levels and the ensuing estrus occurred at the normal time.

Similar pictures as have been described for anovulatory, luteinizing follicles during the estrous cycle could also be seen during early pregnancy (Fig. 1.31). At 40 to 50 days of gestation, at the time when the development of accessory corpora lutea can be expected, large vesicles which contained floccular echoes were found on the ovaries of mares. The lumina of these vesicles then filled up with tissue that showed the characteristic sonographic features of corpora lutea. It could thus be assumed that these structures were, in fact, accessory corpora lutea.

Avtorsko zaščiteno gradivo

Downloaded From Vet-eBooks.com



Fig. 1.35: Anovulatory follicular hematoma in a mare. Within the follicular lumen the snowy echogenicity caused by hemorrhage is evident.

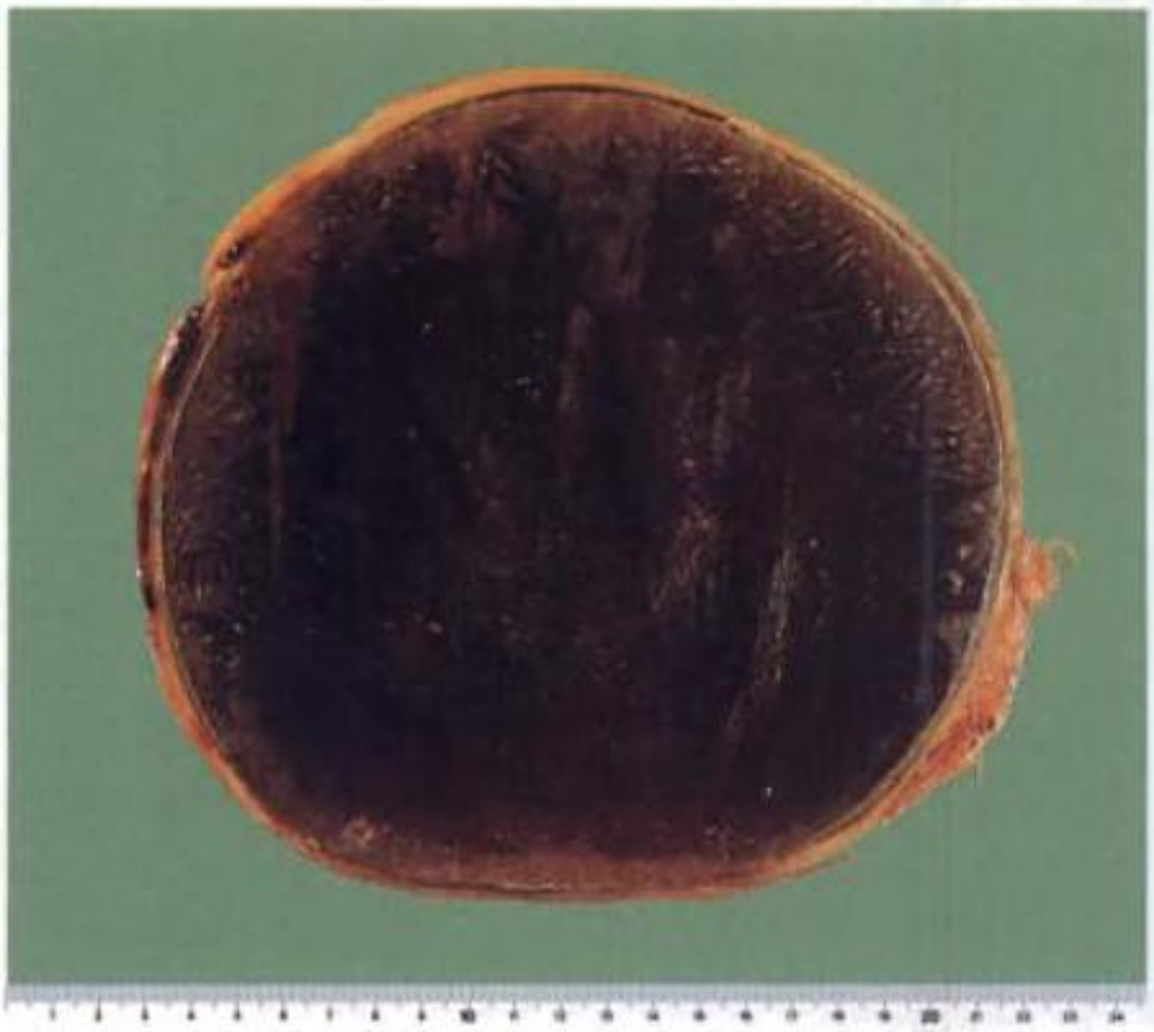


Fig. 1.36: Ovarian hematoma in a mare. The hematoma had a diameter of 20 cm and weighed 3.8 kg.

Avtorsko zaščiteno gradivo

Downloaded From Vet-eBooks.com

1.2.4 Follicular and ovarian hematomas

In addition to the luteinizing, anovulatory follicles described above, there are also anovulatory follicles which develop into hemorrhagic follicles or follicular hematomas (SQUIRES et al. 1988, LEIDL and KÄHN 1989). In the case of the anovulatory, hemorrhagic follicles the hemorrhage takes place by diapedesis into the follicular lumen. In this type of anovulatory follicle no ultrasonically apparent luteinization occurs in the follicular wall. When only the follicle fills with blood it is referred to as a hemorrhagic follicle or a follicular hematoma. Where the surrounding ovarian tissue is largely atrophic and the hematoma encompasses virtually the entire ovary it is called a ovarian hematoma.

Ultrasonically, follicular hematomas do not show a widening, hyperechoic edge indicative of progressive luteinization (Fig. 1.35). Instead, the wall of these anovulatory vesicle remains hyperechoic and thin and appears to remain unchanged for a long period of time, even beyond the end of a particular estrous period. The mesh of reflections that typically develops in the lumen of a luteinizing, anovulatory follicle fails to develop in this type of anovulatory follicle. In most follicular hematomas the initially hypoechoic lumen will only develop regularly scattered floccular reflections at a later stage. These can become more prominent as time passes. Only rarely will a few echoic lines become evident inside the follicular lumen. They are interpreted as being fibrin strands inside the hematoma as the latter is becoming more organized.

The diameters of anovulatory follicles which develop into follicular hematomas are occasionally only a little larger than those of mature preovulatory follicles. Follicular hematomas sometimes expand considerably even after the end of estrus.

In rare cases ovarian hematomas with a diameter of 20 cm and more and a weight of several kilograms are encountered (Fig. 1.36). On ultrasound such hematomas can appear as cystic structures with evenly scattered snow-like echoes in their lumina.

Avtorsko zaščiteno gradivo

Downloaded From Vet-eBooks.com

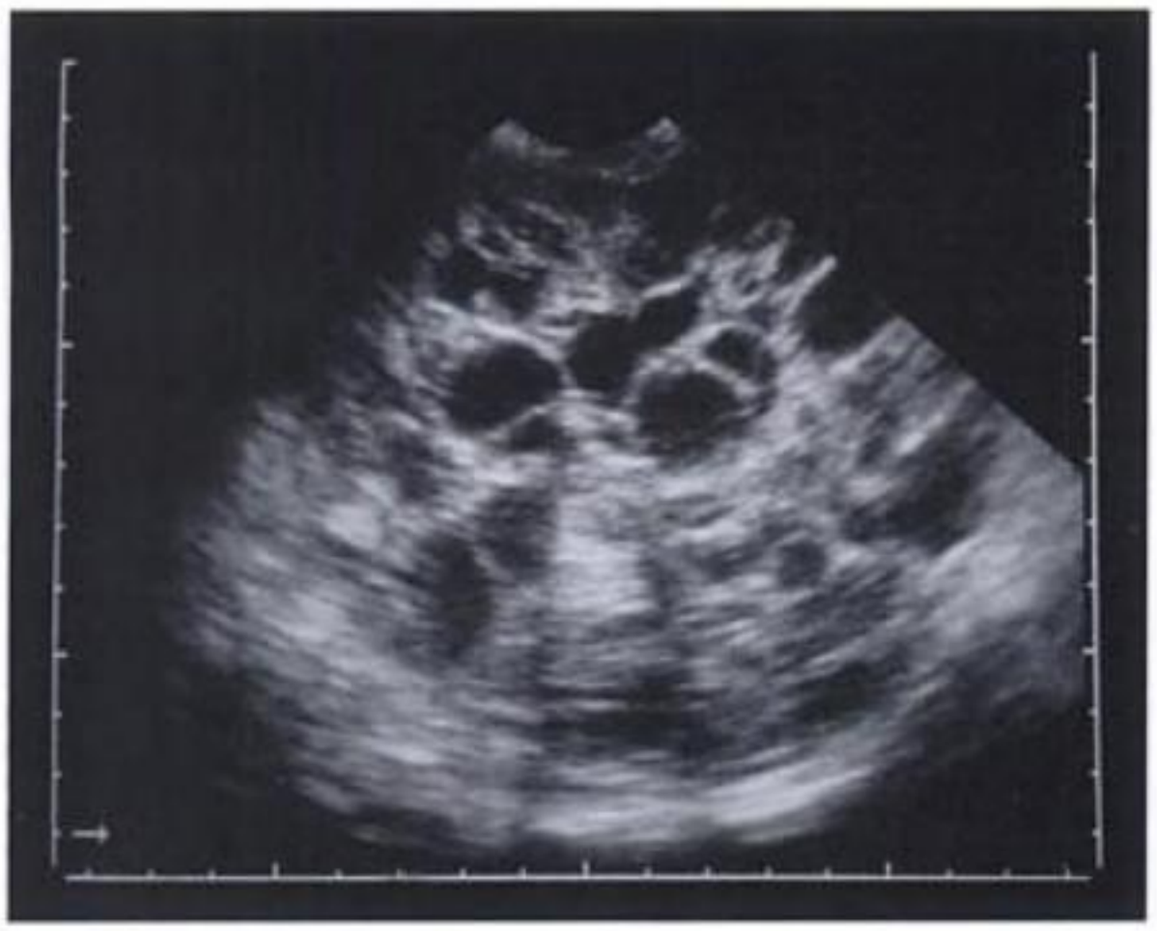


Fig. 1.37: Granulosa cell tumor in a mare. The tumor consists of numerous cystic structures.



Fig. 1.38: Sectioned ovary with the granulosa cell tumor from Fig. 1.37 after ovariectomy of the mare.

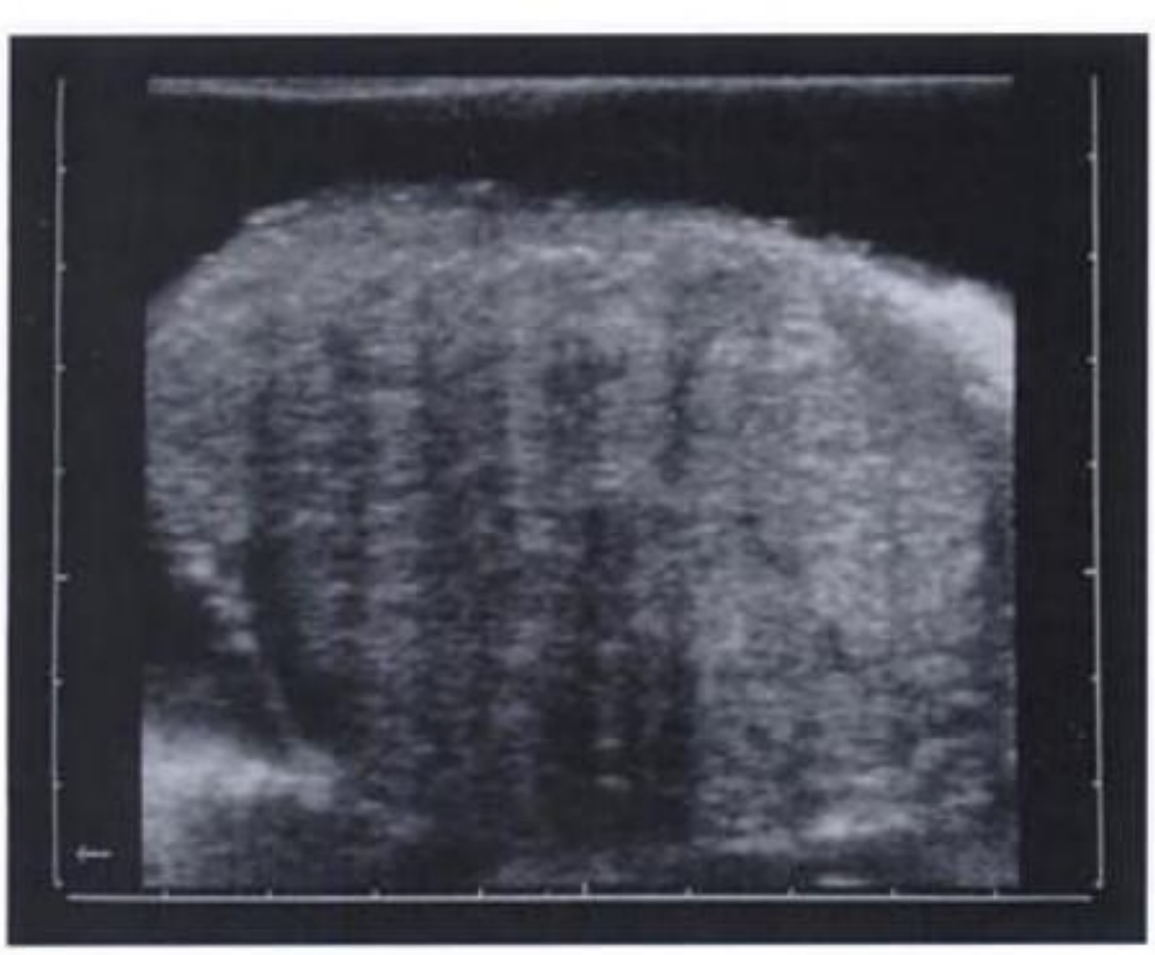


Fig. 1.39: Homogeneously echoic granulosa cell tumor. Narrow echo shadows originate from small foci of mineralization in the tumor tissue. Ultrasonogram taken in a waterbath.



Fig. 1.40: Sectioned ovary with granulosa cell tumor from Fig. 1.39. The cut surface has a solid, waxy appearance.

Avtorsko zaščiteno gradivo

Downloaded From Vet-eBooks.com

1.2.5 Ovarian tumors and cysts

The ultrasonic images of ovarian neoplasms can vary considerably. Among the most commonly encountered granulosa cell tumors the predominant form is characterized by a multicystic partitioning of the tumor (WHITE and ALLEN 1985, KÄHN and LEIDL 1987 b, LEIDL and KÄHN 1989). More vesicular structures can usually be counted in such tumors than would be expected in normal, intact ovaries. On a normal ovary 5 to 10 follicles with a diameter of more than 10 mm each will physiologically be found during an estrous cycle (PIERSON and GINTHER 1987). In cases of ultrasonically examined granulosa cell tumors and in excised specimens many more cystic structures were found. In single ovaries 50 to 60 cystic structures were identified.

The diameters of individual vesicles in granulosa cell tumors vary from a few millimeters to several centimeters. A normal ovary is characterized by the presence of many follicles of differing sizes in the same organ. It is rare to find more than 2 to 3 follicles with a diameter of 30 to 50 mm on a normal ovary, the majority of visible follicles ranging in size between 5 and 20 mm. The ultrasonic images of granulosa cell tumors usually differ from this pattern. Sometimes single, extremely large vesicles are seen within a tumor or the entire image of the tumor consists of numerous small, tightly packed vesicles (Fig. 1.37 and 1.38). On cross sectional image of GC tumors the proportion taken up by vesicular structures is mostly greater than that occupied by solid tumor tissue.

Apart from the multicystic granulosa cell tumors there are also those that are virtually solid on cross section (Fig. 1.39 and 1.40). Their ultrasonograms depict a relatively homogenous image free of hypoechoic vesicles. In some tumors there were areas of hyperechogenicity which were interpreted as areas of mineralized tumor tissue, which produced sound shadows beyond these foci.

Ovarian tumors consisting of a single large vesicle with moderately echoic contents have also been found. Their walls showed histopathological changes consistent with those seen in granulosa cell tumors.

The taking of accurate measurements of an ovary is an important application of ultrasonography during the examination of ovarian neoplasms. Measurements of the ovary taken at regular time intervals make it possible to calculate the growth rate of the tumor, and to confirm the diagnosis. In addition, knowledge of the ovary's exact size aid in the decision whether the ovariectomy should be performed by laparotomy or transvaginally.

Avtorsko zaščiteno gradivo

Downloaded From Vet-eBooks.com



Fig. 1.41: Ovarian cystadenoma in a mare. The ultrasonogram depicts numerous small, cystic structures.



Fig. 1.42: Sectioned ovary with cystadenoma from Fig. 1.41 after ovariectomy of the mare.

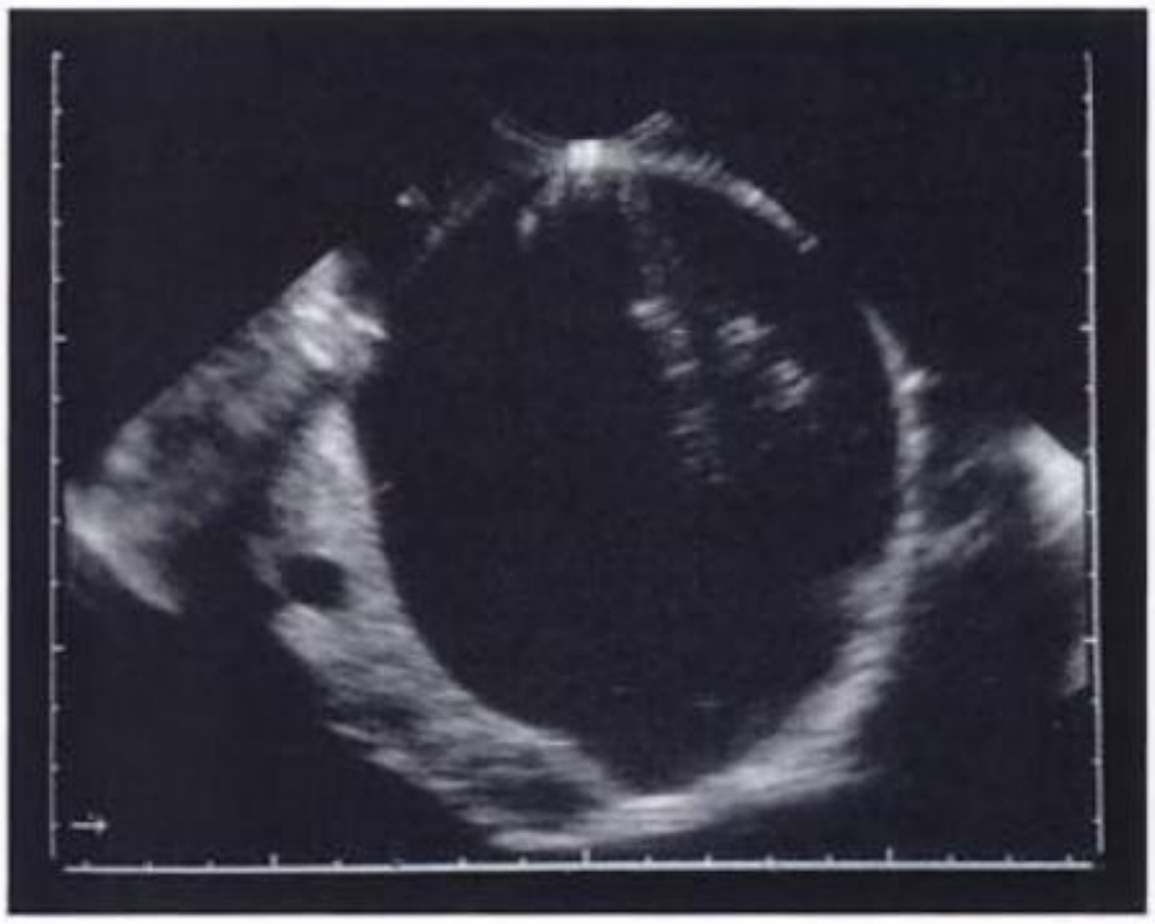


Fig. 1.43: Large ovarian cyst in a mare. The contents of the cyst were largely anechoic. Other cysts or follicles were not present. Ultrasonogram taken in a waterbath.



Fig. 1.44: Sectioned ovary from Fig. 1.43. The ovarian cyst measured approximately 12 cm in diameter.

Avtorsko zaščiteno gradivo

Downloaded From Vet-eBooks.com

Cystadenomas are much less frequently encountered ovarian neoplasms in the mare than granulosa cell tumors. In the cystadenomas examined ultrasonically thus far, the tumor tissue varied in echogenicity and contained numerous cystic structures (Fig. 1.41 and 1.42). The vesicles with hypoechoic contents measured only a few millimeters in diameter.

Ovarian cysts occur only very rarely in mares. The ultrasonic image of macrocystic ovarian degeneration features a few, very large cystic structures (LEIDL and KÄHN 1989). The cyst walls were echoic and remarkably thin (Fig. 1.43 to 1.46). The cysts were polygonal in cross sections. The ultrasonograms showed hardly any islands of ovarian parenchyma between the cystic structures. The diagnoses of macrocystic ovarian degeneration were based on histopathological examinations of the organ after ovariectomy.

Ultimately, it can be stated that the ultrasonic appearance of ovarian tumors and cysts can vary considerably. An accurate diagnosis of the ovarian changes, based on ultrasonography alone, is not possible in every case. In many instances, however, ultrasonography contributes meaningfully to the establishment of a correct therapeutic conclusion.



Fig. 1.45: Macrocystic ovarian degeneration in a mare. Multiple, thin walled cysts with anechoic contents are present on the ovary.

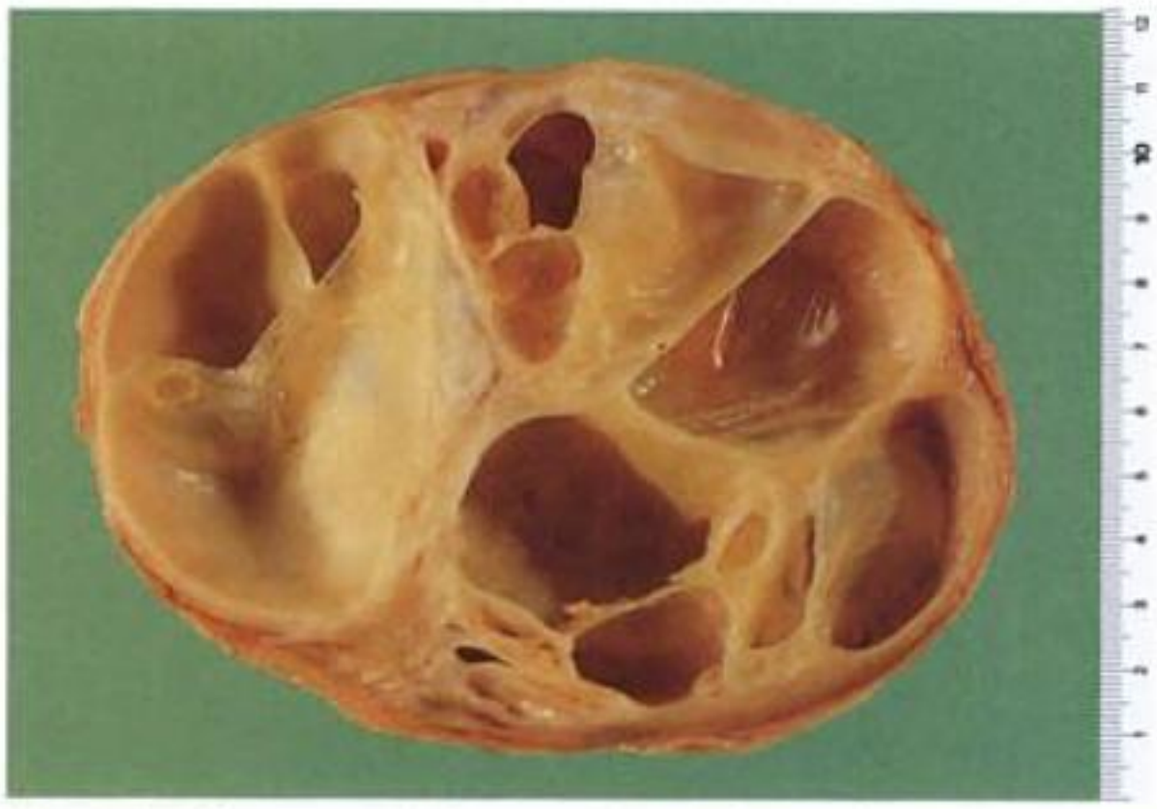


Fig. 1.46: Macrocystic degeneration and atrophy of the functional ovarian tissue in the sectioned ovary from Fig. 1.45.

Avtorsko zaščiteno gradivo

Downloaded From Vet-eBooks.com

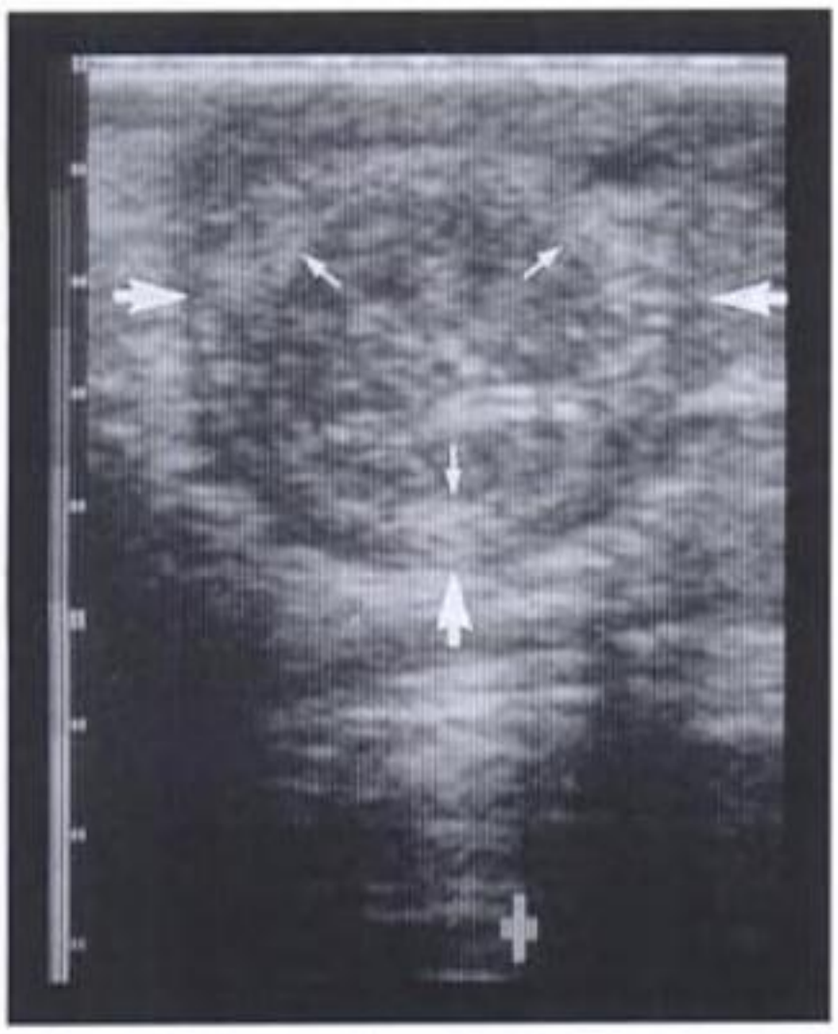


Fig. 1.47: Sagittal cross section through the uterine horn of a mare in diestrus. The hypoechoic peritoneal border (large arrows) and the transition from myometrium to endometrium (small arrows) can be seen.

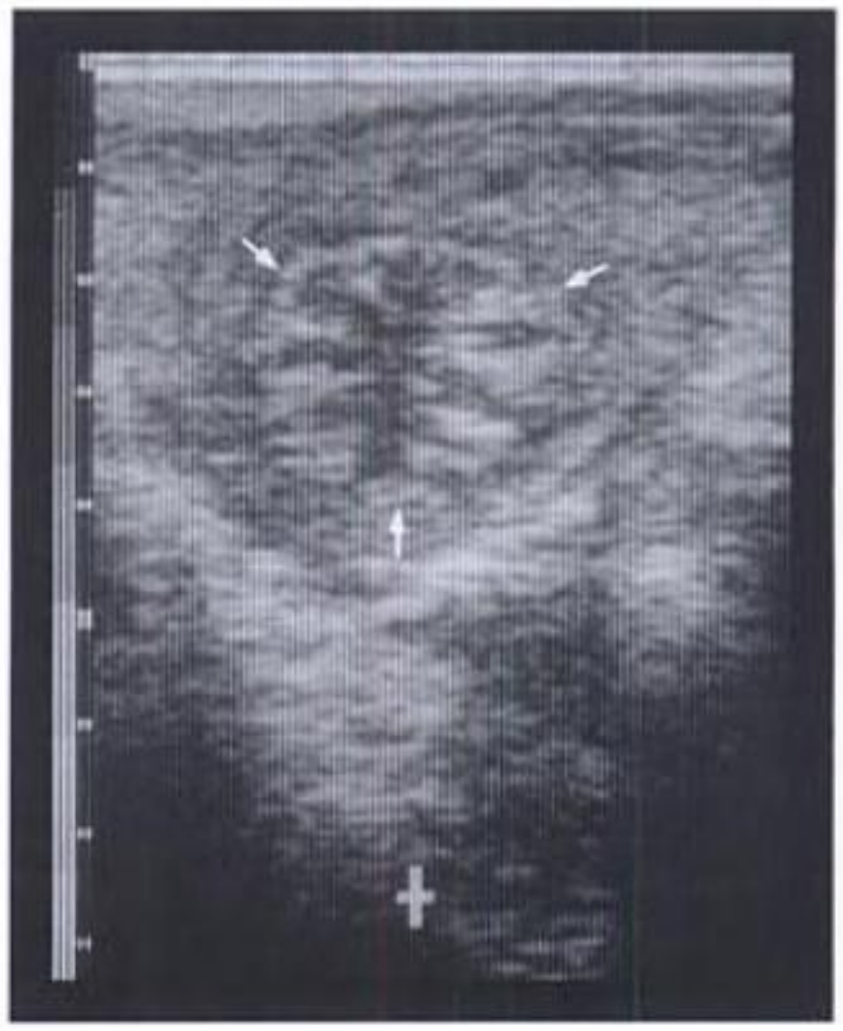


Fig. 1.48: Cross section through uterine horn during estrus. Due to the endometrial edema alternating areas of hypoechoic and more echoic tissues can be seen. This causes the typical spoke-wheel appearance of the uterine horn during estrus. Arrows indicate the transition from myo- to endometrium.



Fig. 1.49: Prominent spoke-wheel pattern of the uterus during estrus. Arrows indicate the peritoneal border of the uterus.

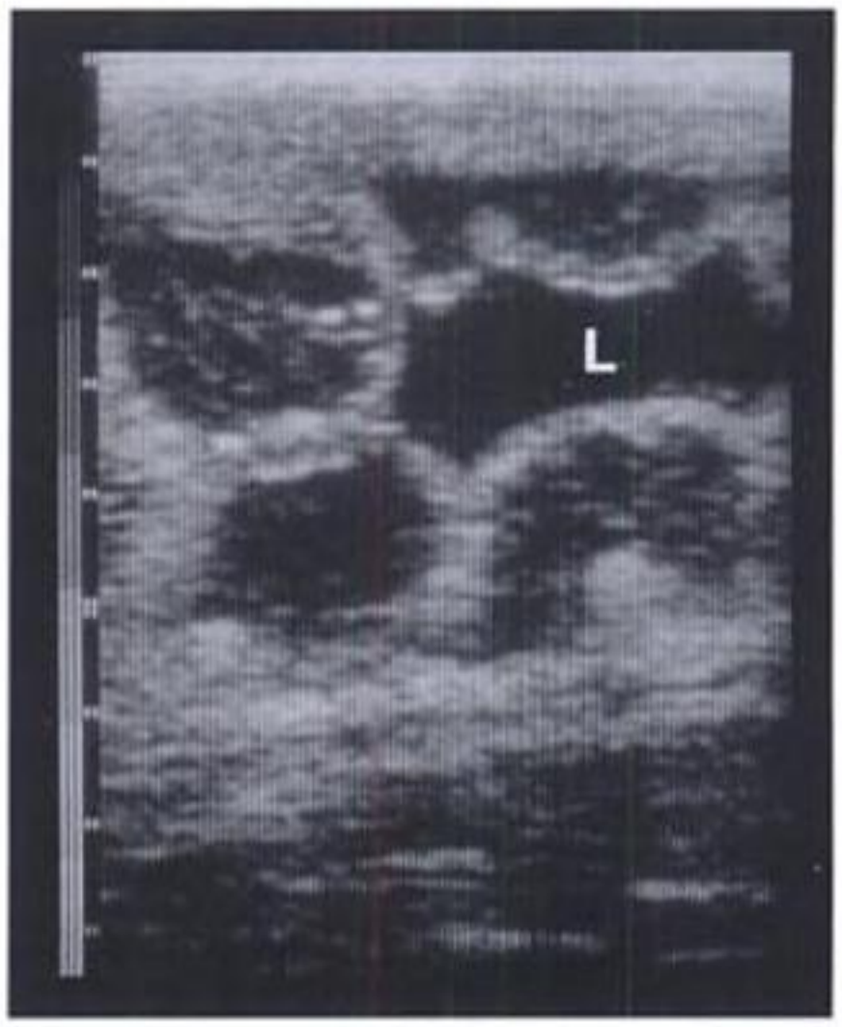


Fig. 1.50: Extensive edema of the endometrial folds during estrus. The endometrial folds with their echoic base, hypoechoic edematous central area and hyperechoic surface bulge into the uterine lumen (L) filled with secretions.

Avtorsko zaščiteno gradivo

Downloaded From Vet-eBooks.com

1.3 Uterine structures in the mare

1.3.1 Non-pregnant uterus

A sagittal cross section of a physiologic, nonpregnant uterine horn is sonographically seen as round to oval image (Fig. 1.47 to 1.49). The uterine wall appears as a gray structure of moderate echogenicity. The peritoneal border of the uterus can be seen as a thin, hypoechoic line. Concentrically positioned to this line, another line can occasionally be identified in the middle of the uterine wall (KÄHN and LEIDL 1985). This hypoechoic zone represents the transition from endometrium to myometrium (Fig. 1.47 and 1.48). In the center of the uterus a small area of high echogenicity can sometimes be found. It is caused by reflections from the echoic surface of opposing layers of the endometrium which lie in close apposition in the empty uterus and project as an echoic spot when seen in cross section or as anechoic line when viewed longitudinally (Fig 1.6).

The structure of the uterine wall is homogenous during anestrus and diestrus (Fig. 1.47). A distinct layering cannot be recognized. Around the time of estrus a clear distinction between areas of differing echogenicity can be observed in the transverse view of the uterus of many mares (Fig. 1.48 to 1.50).The ring like structure in the area between endo- and myometrium which lies concentrically oriented to the outer, peritoneal wall of the uterus is now very prominent. From this zone hypoechoic stripes run towards the center of the lumen where they meet to form a star (spoke-wheel) pattern. Hyperechoic segments lie between these areas of low echogenicity. This pattern is caused by the endometrial folds which bulge towards the center of the uterine lumen and consist of an echoic base, the hypoechoic, strongly edematous adluminal part and the hyperechoic luminal epithelium. This wagon wheel pattern of the uterus is typical of estrus and can clearly be seen in about 50% of all estrous mares (GINTHER and PIERSON 1984 c). It is associated with the estrogenisation during estrus and becomes apparent 6 to 10 days before ovulation (HAYES et al. 1985). The pattern is best developed about 1 to 4 days before ovulation and then gradually and progressively weakens until it disappears 2 to 6 days after ovulation.

Avtorsko zaščiteno gradivo

Downloaded From Vet-eBooks.com



Fig. 1.51: Uterus (arrows) of a mare immediately after mating. The uterine lumen contains hypoechoic semen which is speckled with floccular reflections.

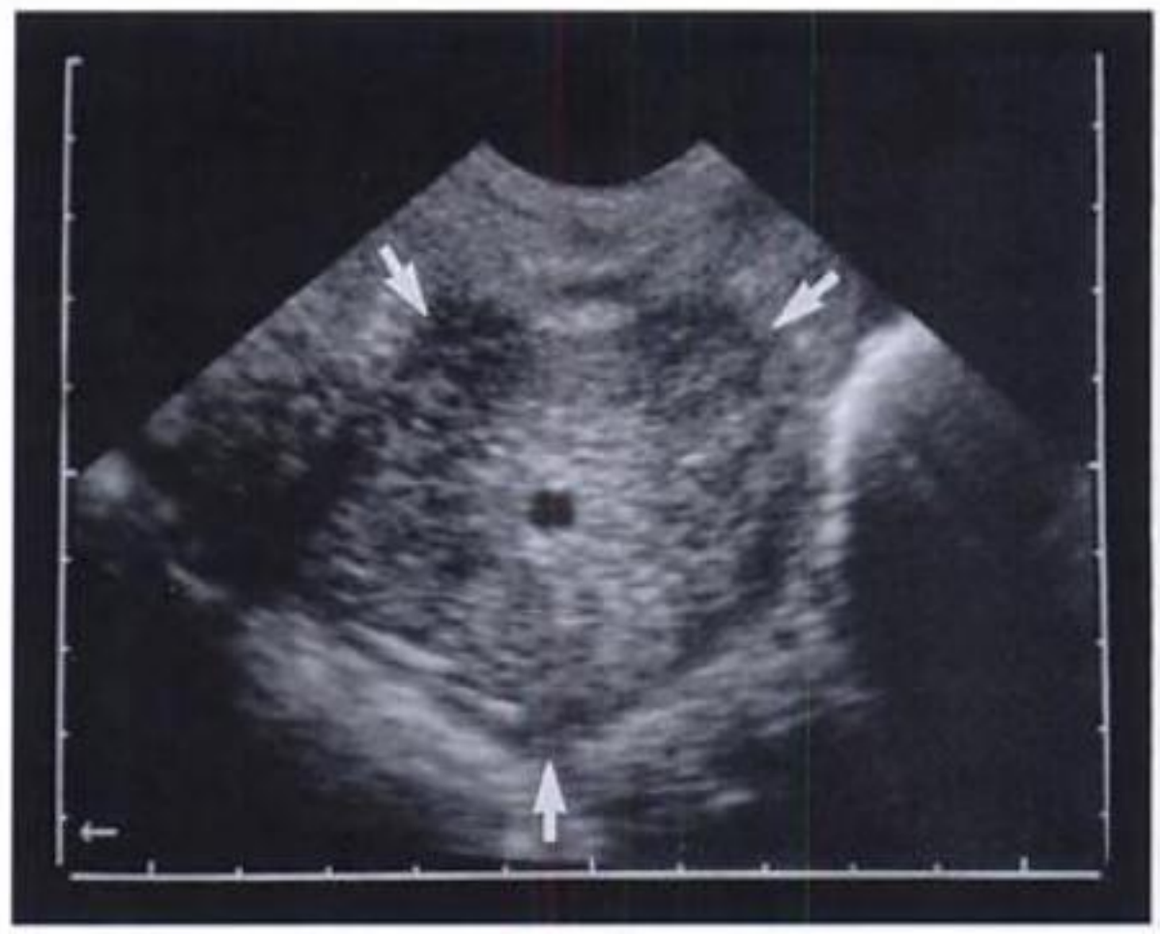


Fig. 1.52: Uterus on Day 9 of pregnancy (Day 0 = Day of ovulation). The anechoic, embryonic vesicle has a diameter of 4 to 5 mm and lies centrally in the horn (arrows).



Fig. 1.53: Conceptus on Day 11 of pregnancy. The anechoic embryonic vesicle shows the typical specular reflections where the sound waves impact vertically onto its front and back walls. Its diameter measures 9 mm.



Fig. 1.54: Conceptus on Day 14 of pregnancy. The spherical embryonic vesicle lies centrally in the uterine horn and measures 15 mm in diameter.

Avtorsko zaščiteno gradivo

Downloaded From Vet-eBooks.com

Larger fluid accumulations of a physiological origin will not be found in the nonpregnant uterus. Sonographically evident secretions in the lumen of the diestrous uterus can be seen as a indication of endometritis (ADAMS et al. 1987, SQUIRES et al. 1988). During estrus small amounts of free fluid may be seen as physiologic, but larger ones as pathologic (Fig. 1.50). Immediately after mating, the ejaculate can be seen in the uterine lumen (GINTHER and PIERSON 1984 c). Mares whose uterine lumina were initially closed, show fluid accumulations containing scattered echoes after service (Fig. 1.51).

The uterine cervix is depicted relatively poorly. Its ultrasonic image is more echoic during diestrus and pregnancy and is therefore easier to recognize than in estrus.

1.3.2 Pregnant uterus

1.3.2.1 Day 9 to 13 of pregnancy

The young conceptus first becomes visible when it forms a fluid filled vesicle, large enough to be recognized as a round, anechoic sphere on the ultrasound monitor (Fig. 1.52). Depending upon the quality of the scanner, this is first possible, with a variation of only a few days, between Days 9 and 13 of pregnancy (Day 0 = Day of ovulation or last day of service). When using high resolution ultrasonography with a frequency of 5 MHz, 3 to 5 mm large conceptuses can be detected as early as on Day 9 of gestation. On Day 10 the blastocyst measures 4 to 7 mm and will be detectable in as many as about 70% of the mares (GINTHER 1986). On the Day 11 it reaches 6 to 9 mm and will be visible in nearly all mares (Fig. 1.53 and 1.55). Around Day 12 the conceptus has a diameter of 10 to 12 mm and can now be detected even with scanners of lesser resolution using 3 to 3.5 MHz frequencies (GINTHER 1983 b).

1.3.2.2 Day 14 to 20 of pregnancy

By Day 14 the embryonic vesicle has a diameter of 14 to 19 mm (Fig. 1.54 and 1.55). The embryonic vesicle is now large enough to make accurate and reliable positive as well as negative diagnoses under field condition of general veterinary practice, provided 5 MHz ultrasonography is used (Kähn and Leidl 1984). Using ultrasound of lower frequency, this date may be postponed by a few days (CHEVALIER and PALMER 1982). The shape of the embryonic vesicle is spherical and the embryo proper is not yet visible.

Avtorsko zaščiteno gradivo

Downloaded From Vet-eBooks.com

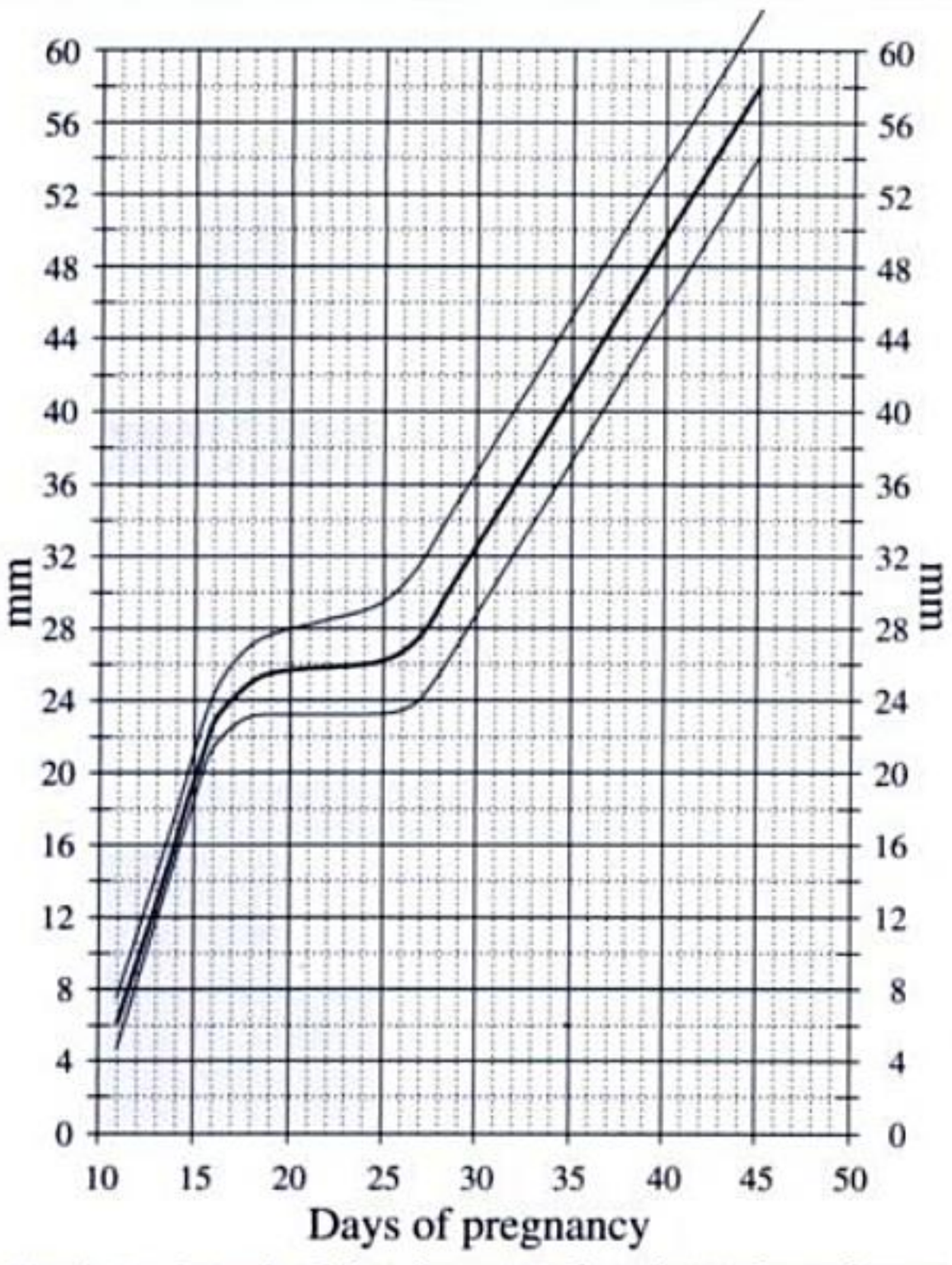


Fig. 1.55: Growth of the diameter of equine embryonic vesicles during early pregnancy (adapted from GINTHER 1986).

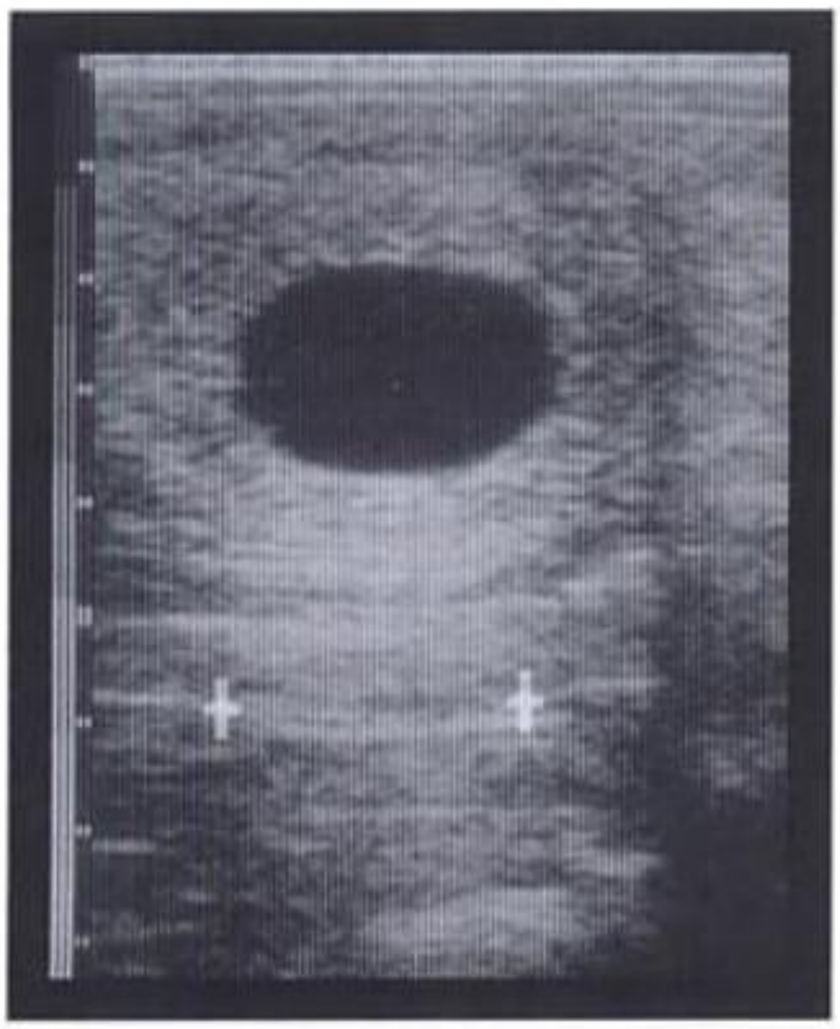


Fig. 1.56: Pregnancy on Day 16. The embryonic vesicle has an ovoid shape, measuring 26 x 20 mm. The largest diameter is marked by the 2 crosses below the vesicle.

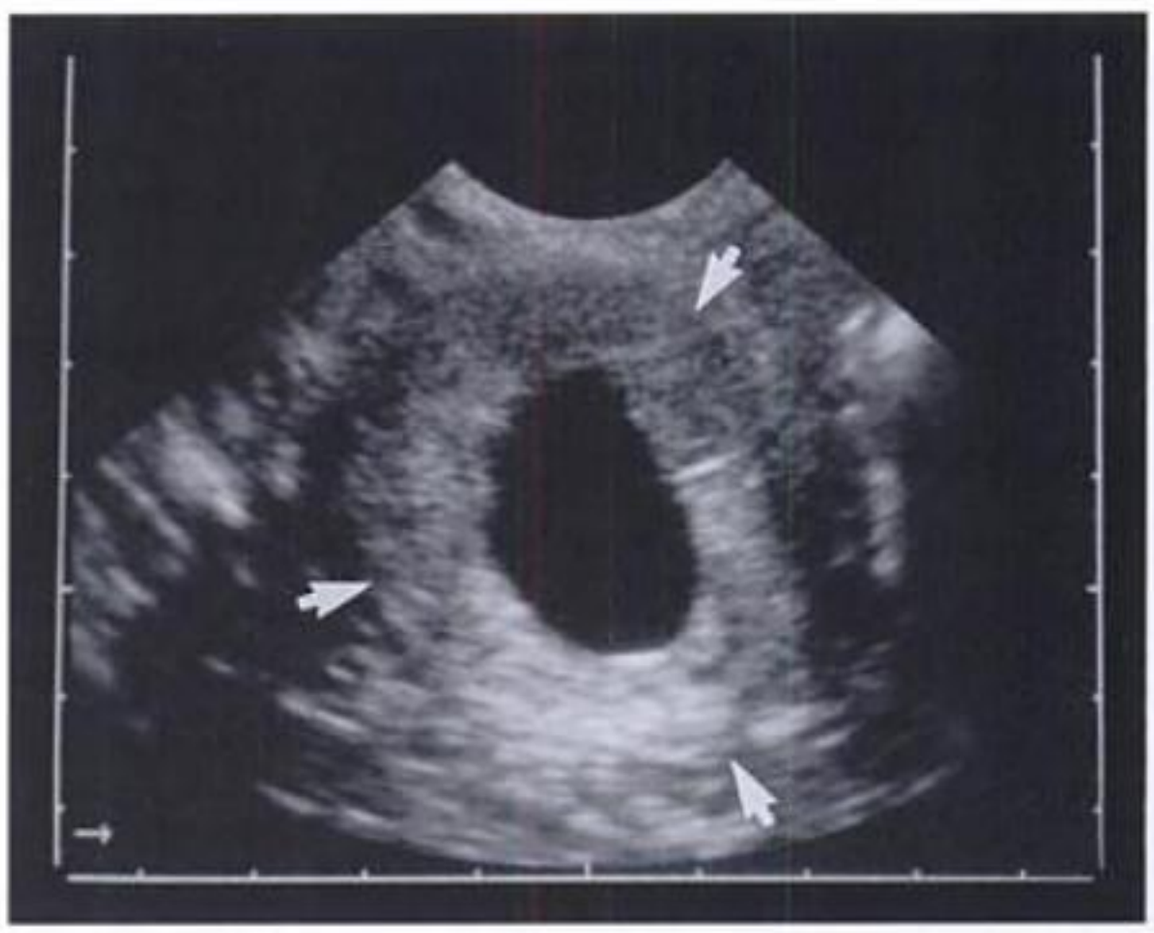


Fig. 1.57: Pregnancy on Day 18. The embryonic vesicle, located in the uterine horn (arrows), is pear shaped.

Avtorsko zaščiteno gradivo

Downloaded From Vet-eBooks.com

The embryonic vesicle grows at an average rate of 3 to 4 mm per day during the second week of gestation until the beginning of the third week to reach a diameter of 20 to 25 mm by Day 16 (Fig. 1.55). After this date the growth curve flattens considerably. The diameter of the conceptus appears to increase only marginally and seems to rest on a plateau between the 17th and 25th days of pregnancy (PALMER and DRIANCOURT 1980, VALON et al. 1982, GINTHER 1983 b). Breed related differences in the size of embryonic vesicles are negligible during the first three weeks of pregnancy. Even the growth curves of pony and large horse breed embryos are virtually identical (GINTHER 1986).

A remarkable phenomenon in the horse is its embryonic mobility which can be observed by ultrasonography from the time the conceptus first becomes visible until Day 17 of gestation (GINTHER 1983 a). The conceptus moves from one horn to the other, and through the uterine body several times every day and may be found in different positions within the uterus during successive examinations (GINTHER 1984a). This movement of the embryo can sometimes even be observed if a mare is scanned continuously for a number of minutes. The mobility is particularly strong from Day 11 to 14 and comes to a halt on Days 15 to 17. It has been shown through frequent examinations in 5 minute intervals that the embryo moved from one horn to the other or into the uterine body an average of 7 times within 2 hours during the period of maximal embryonic mobility between Days 11 and 14 (LEITH and GINTHER 1984). From Days 9 to 11 the embryo was found in the uterine body in 60 % of the cases, from Day 12 to 14 in 30 % of cases and thereafter only rarely. The positional changes of the conceptus appear to be caused by contractions of the uterine wall and can be controlled by the conceptus itself (GINTHER 1984 b, LEITH and GINTHER 1985). The careful sonographic examination of the corpus uteri during this stage of early pregnancy is of particular diagnostic importance. Due to its intense mobility the conceptus frequently lies in the uterine body. If only the uterine horns are scanned by ultrasound the further caudally positioned conceptus may remain undetected inside the uterine body. This is one of the most common reasons for not detecting or overlooking a conceptus or twin pregnancy. The intra-uterine positional changes of the equine conceptus can lead to, among other things, implantation not only in the horn ipsilateral to the ovulating ovary, but, in about half the cases, in the contralateral horn. Increases in uterine tone and size of the conceptus seem to be the cause for the cessation of conceptus mobility. The preferred site of implantation lies just next to the bifurcation in one of the uterine horns.

In the horse the early conceptus has a strictly spherical shape until Day 15 of gestation, thereafter first becoming ovoid until day 17 and, between Days 18 and 21 it is usually pear shaped, after which it assumes an irregular shape (Fig. 1.56 to 1.59).

From the time the conceptus is first detected until Day 18 the uterine wall is 10 to 15 mm thick. It becomes thinner over the next few weeks and ranges from 5 to 10 mm. Initially, the uterine wall is of uniform thickness around the entire conceptus (Fig. 1.52 and 1.54); from Day 18 to 20 on its thickness decreases, particularly ventrally to the conceptus (Fig. 1.58).

There are numerous criteria which can be used to differentiate the early embryonic vesicle from pathological conditions such as endometrial cysts, the secretions in cases of endometritis or embryonic death. At this stage the intact conceptus is a round spherical vesicle clearly visible and contrasted against the echoic uterine wall. There are no reflections inside the vesicle so that its fluid contents appear black. I f the probe is swept across the vesicle the increasing and decreasing diameter reveals the spherical shape of the conceptus. At the front and back sections of the conceptus, where the sound waves impact vertically onto the wall, a short hyperechoic line can be seen (CHEVALIER and PALMER 1982). These bright lines are the result of the specular reflections of the ultrasound waves from the wall of the tense embryonic vesicle and should not be misinterpreted as the embryonic disc (Fig. 1.53).

In veterinary practice there exists concern about the optimal time for early sonographic pregnancy detection. For several reasons the time from Days 15 to 18 can be considered most appropriate. At this stage it is no longer difficult to demonstrate the early embryonic vesicle. Not only are twin pregnancies easy to recognize at this time period but it is quite favorable for a timely intervention where indicated. In case of detection of non-pregnancy the ultrasound examination can be used to assess follicular development, because the following estrus should be imminent.

Once an early pregnancy has been diagnosed in a mare during the first few weeks of gestation, it is useful to reexamine the mare at about Day 30 of pregnancy so that a possible early embryonic death can be detected.

Avtorsko zaščiteno gradivo

Downloaded From Vet-eBooks.com



Fig. 1.58: Pregnancy on Day 20. The shape of the embryonic vesicle is triangular. The embryo (E) can be seen at the floor of the vesicle. Below the vesicle the uterine wall is relatively thin.



Fig. 1.59: Pregnancy on Day 21. The embryonic vesicle is irregular in shape. The embryo (E) lies on the floor of the vesicle.

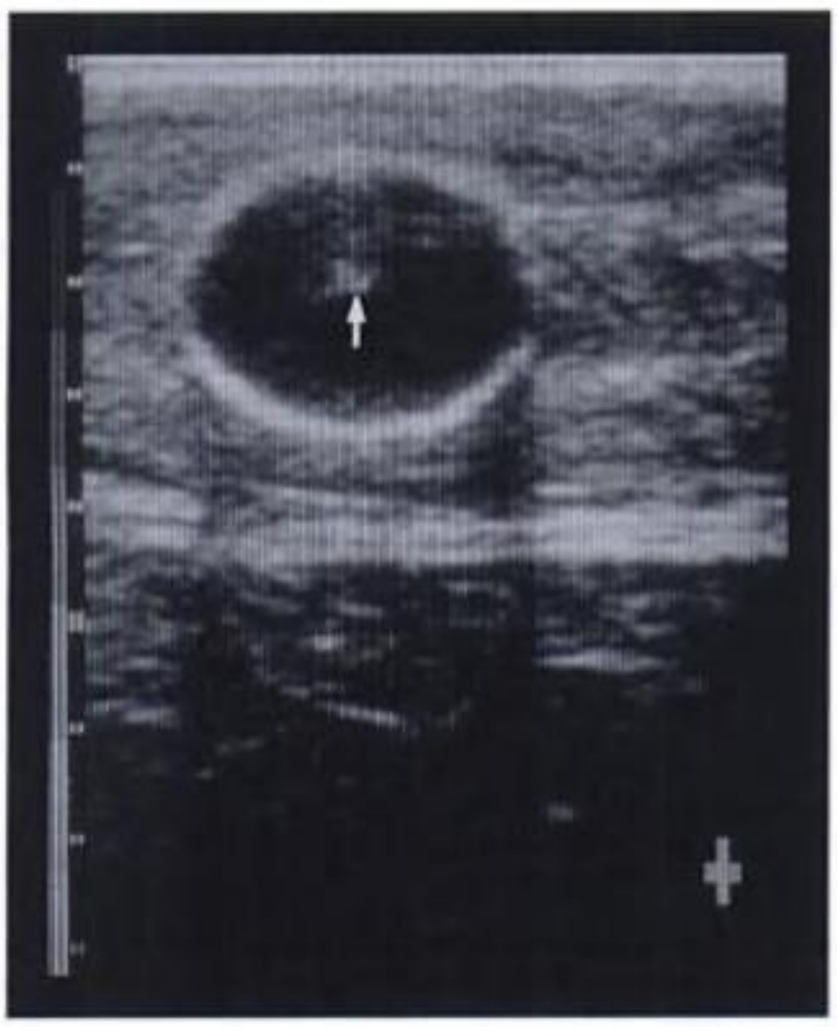


Fig. 1.60: Ultrasound image of the rubber balloon of a ballooned catheter within the uterus. In order to simulate an embryonic vesicle the balloon was filled with 20 ml water and then depicted by ultrasonography. The catheter (arrow) is shown in cross section at the center of the balloon.

Avtorsko zaščiteno gradivo

Downloaded From Vet-eBooks.com

By this time the majority of embryonic deaths will have taken place or will be in progress (GINTHER 1985, WOODS et al. 1985). The successful induction of another estrus is still possible and valuable time will not be wasted. Since embryonic deaths can also occur after Day 30 of gestation another examination is recommended between Days 50 and 60 so that all embryonic losses can be detected.

In the context of early pregnancy diagnoses, a training method for the detection of early pregnancies by ultrasonography should be mentioned. In the absence of a suitable training mare, a water filled rubber balloon can be introduced into the uterus to simulate an early pregnancy (Fig. 1.60). A ballooned catheter (e.g. Foley catheter) which is introduced through the cervix into the uterus is suitable for this purpose. Once the tip of the catheter is positioned inside a uterine horn the insufflation channel is used to fill the cuff with liquid making sure not to include any air in the fluid. In this manner the injection of 5 or 15 ml water into the cuff will result in a balloon diameter of 20 or 30 mm. These diameters would be equivalent to the sizes of an embryonic vesicle on Days 15 or Days 25 to 30. For training purposes a balloon introduced in this manner can now be sought using ultrasonography and then depicted on the monitor. Several features of the image of such a balloon are similar to those of an early conceptus. After the training examination the balloon can be emptied and removed without problems.

Avtorsko zaščiteno gradivo

Downloaded From Vet-eBooks.com

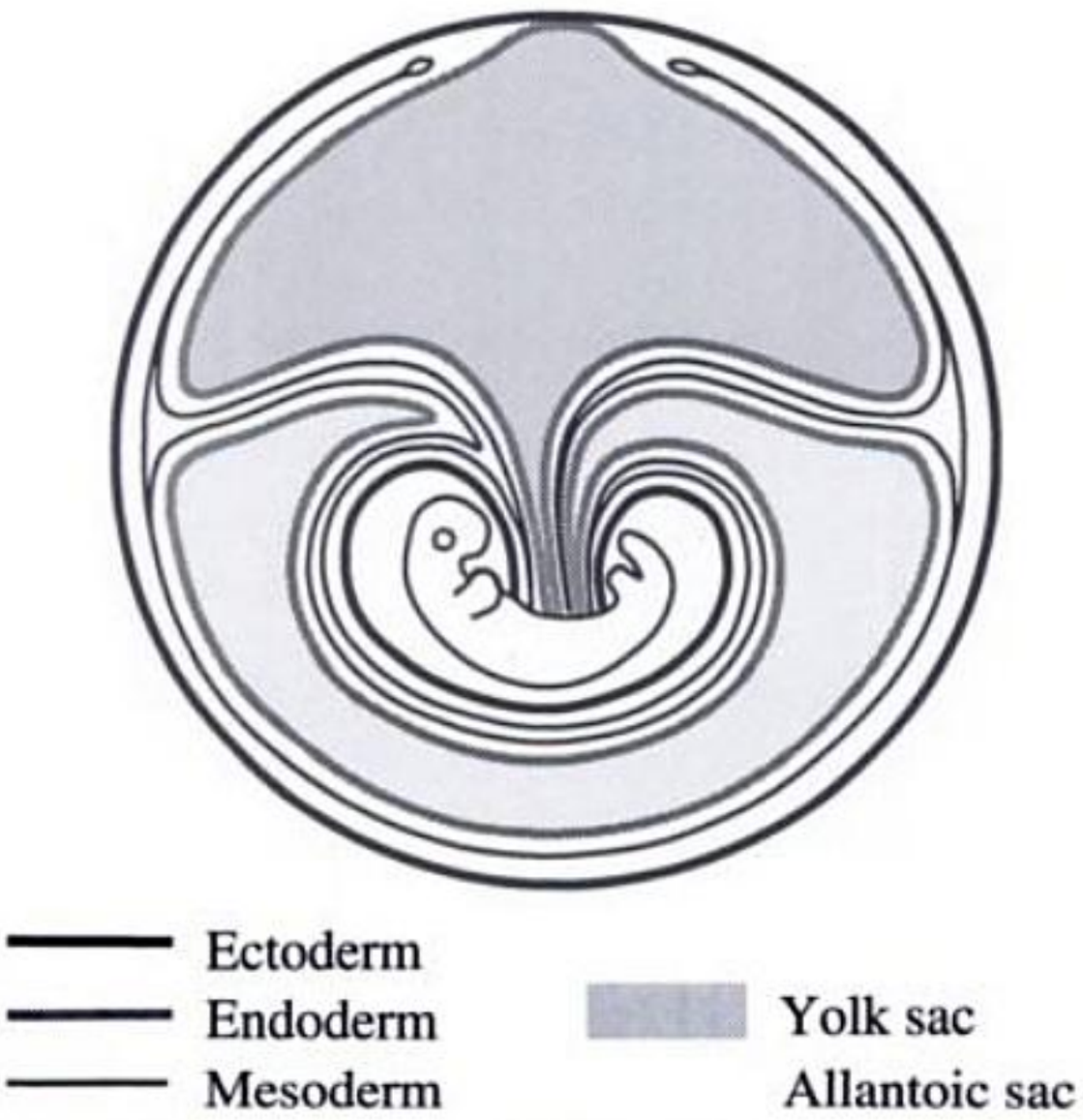


Fig. 1.61: Schematic presentation of a Day 30 embryonic vesicle in the horse. Due to shrinkage of the yolk sac and the filling of the allantois the embryo ascends from the floor and rises within the vesicle (adapted from GINTHER 1986).



Fig. 1.62: Pregnancy on Day 27. The "ascent" of the embryo (arrow) has begun. The ventrally positioned allantois starts to fill up.

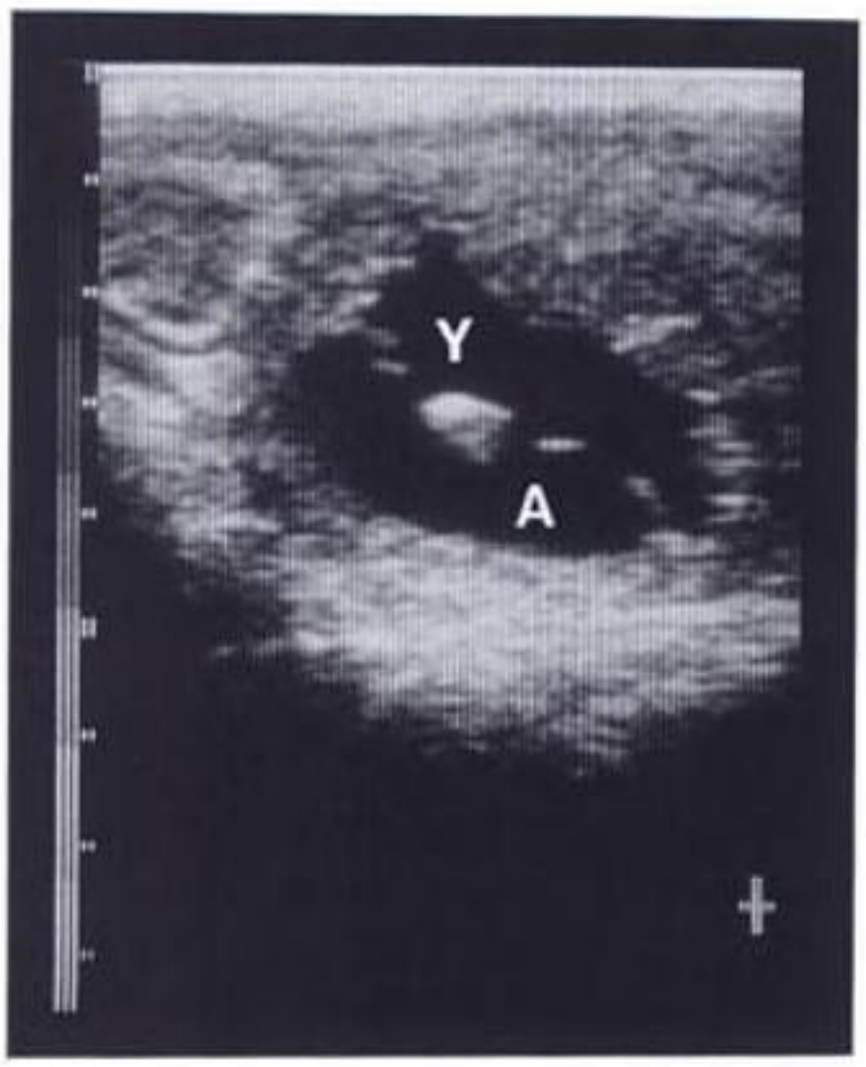


Fig. 1.63: Pregnancy on Day 29. The embryo is suspended in the center of the embryonic vesicle. The appositioned membranes of the yolk sac (Y) and the allantoic sac (A) form a hyperechoic structure which extends from the embryo towards the lateral walls of the vesicle (see also Fig. 1.62 to 1.67).



Fig. 1.64: Pregnancy on Day 30. The embryo is suspended in the upper portion of the vesicle.

Avtorsko zaščiteno gradivo

Downloaded From Vet-eBooks.com

1.3.2.3 Day 21 to 40 of pregnancy

On about Day 21 the embryo is detectable for the first time near the floor of the vesicle (GINTHER 1983 b, KÄHN and LEIDL 1984). It is initially visible as a hyperechoic spot on the floor of the embryonic vesicle and not yet separated from the endometrium (Fig. 1.58 and 1.59).

From Day 21 to 40 the embryo follows a characteristic ascent within its vesicle (VALON et al. 1982). Ventral to the embryo the allantois starts to fill up, lifting the embryo (Fig. 1.61 to 1.66). While the yolk sac above the embryo initially occupied the bulk of the early conceptus it now shrinks over the next few days. The ratio between the sizes of the two embryonic structures gradually moves in favor of the allantois until the yolk sac has virtually disappeared by Day 40. The embryo appears to be suspended by the hyperechoic membrane formed by allantois and yolk sac and floats inside the anechoic embryonic fluid. The majority of embryos commence their ascent between Days 22 and 25. On Day 27 they are still suspended in the bottom third of the vesicle (Fig 1.62), by Day 30 in the center (Fig. 1.63) and by Day 33 in the top third of the vesicle (Fig. 1.64 and 1.65).

On Day 25 the embryo is about 5 mm long (GINTHER 1986). It grows by about 1 mm per day to reach 12 mm by Day 30, 17 mm by Day 35 and 22 mm by about Day 40.

The embryos heart beat can be detected around day 26 which is only a few days after the embryo can be first detected. The heart beat is an important criterion for the assessment of embryonic viability and for the exclusion of a pathological pregnancy.

After the suspended growth period of the conceptus from Day 19 until Day 25 there is a renewed growth (Fig. 1.55). The growth rate until Day 50 of gestation is about 2 mm per day. From the fourth week of gestation a difference in the growth rate between fetuses of different breeds becomes evident; hence the diameter of the embryonic vesicle of heavy draught horses between Days 20 and 40 of gestation will be 1 to 4 mm larger than that observed in lighter horse breeds (CHEVALIER and PALMER 1982).

Avtorsko zaščiteno gradivo

Downloaded From Vet-eBooks.com

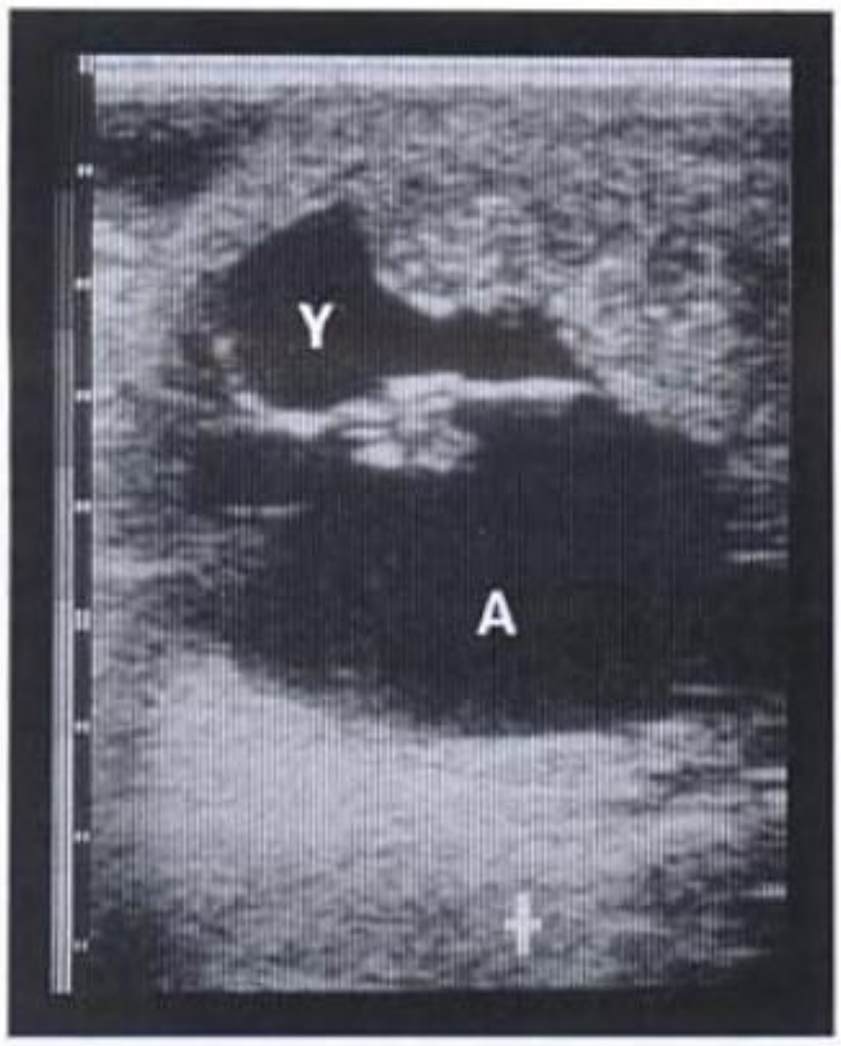


Fig. 1.65: Pregnancy on Day 32. The embryo floats in the upper third of the embryonic vesicle. The yolk sac (Y) has receded considerably. The allantoic sac (A) is expanding.



Fig. 1.66: Pregnancy on Day 35. The embryo is suspended very high in the embryonic vesicle. The yolk sac has almost disappeared.



Fig. 1.67: Pregnancy on Day 40. The embryo (arrow) descends back towards the floor of the vesicle while it hangs from the umbilical cord which still shows remnants of the yolk sac.



Fig. 1.68: Pregnancy on Day 37. The embryonic vesicle is disoriented. The allantoic sac (A) lies at the top and the yolk sac (Y) at the bottom. In this mare the "ascent" of the embryo within its vesicle was from the top to the bottom.

Avtorsko zaščiteno gradivo

Downloaded From Vet-eBooks.com

1.3.2.4 Day 41 to 60 of pregnancy

Around Day 40 the embryo reaches its highest position within the embryonic vesicle (Fig. 1.66 and 1.67). From here it gradually sinks, suspended by its umbilical cord, back down to the floor of the vesicle (KÄHN and LEIDL 1984). After this time movements of the fetus can be observed frequently (ALLEN and GODDARD 1984).

The umbilical cord normally attaches to the dorsal pole of the allantochorion. Very rarely it attaches laterally or ventrally. Cases have been observed where the yolk sac was positioned ventrally and the allantois dorsally to the embryo leading to an embryonic migration from top to bottom within the vesicle (Fig. 1.68). It is assumed that this kind of disorientation of the embryo is a sequel to an earlier twin conception (GINTHER 1984c). In singleton pregnancies there seems to be a mechanism which ensures that the conceptus is oriented with the embryonic disc at its ventral aspect at the time of fixation between Days 16 and 20. This also leads to the embryo rising from ventral to dorsal during its ascent between Days 20 and 40 and to the attachment of the umbilicus to the dorsal aspect of the allantochorion. This process sometimes appears to be disturbed in twin pregnancies when the two vesicles interfere with one another's orientation within the uterus.

The fetus has a crown rump length of 25 mm on Day 45 of gestation (Fig. 1.69) and grows to a length of 40 mm by Day 60. The placental vesicle reaches a diameter of 6 cm between Days 45 and 50. Subsequently it exceeds the scanning width of the 5 MHz scanner and can only be depicted in sections (Fig. 1.70). From Day 50 to 60 a penetration depth of 10 cm is also inadequate to show the vesicle in its entirety.

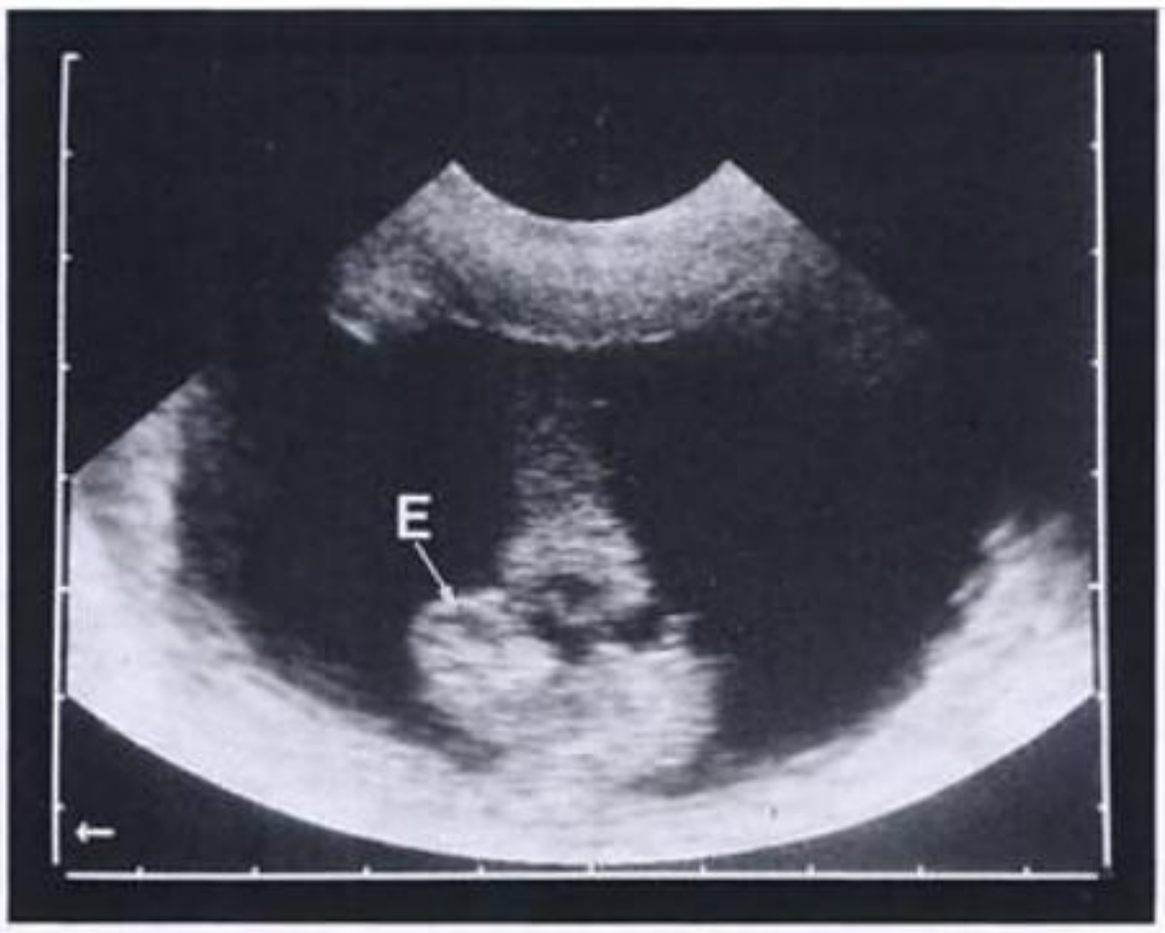


Fig. 1.69: Pregnancy on Day 46. The fetus lies on its back on the floor of the vesicle. Its crown rump length measures 33 mm. The head with the eyes (E) lies to the left.



Fig. 1.70: Pregnancy on Day 54. The diameter of the conceptus exceeds the scanning width of the ultrasound probe. The head (H) of the fetus lies to the left. The umbilical cord runs towards 3 o'clock out of the picture.

Avtorsko zaščiteno gradivo

Downloaded From Vet-eBooks.com

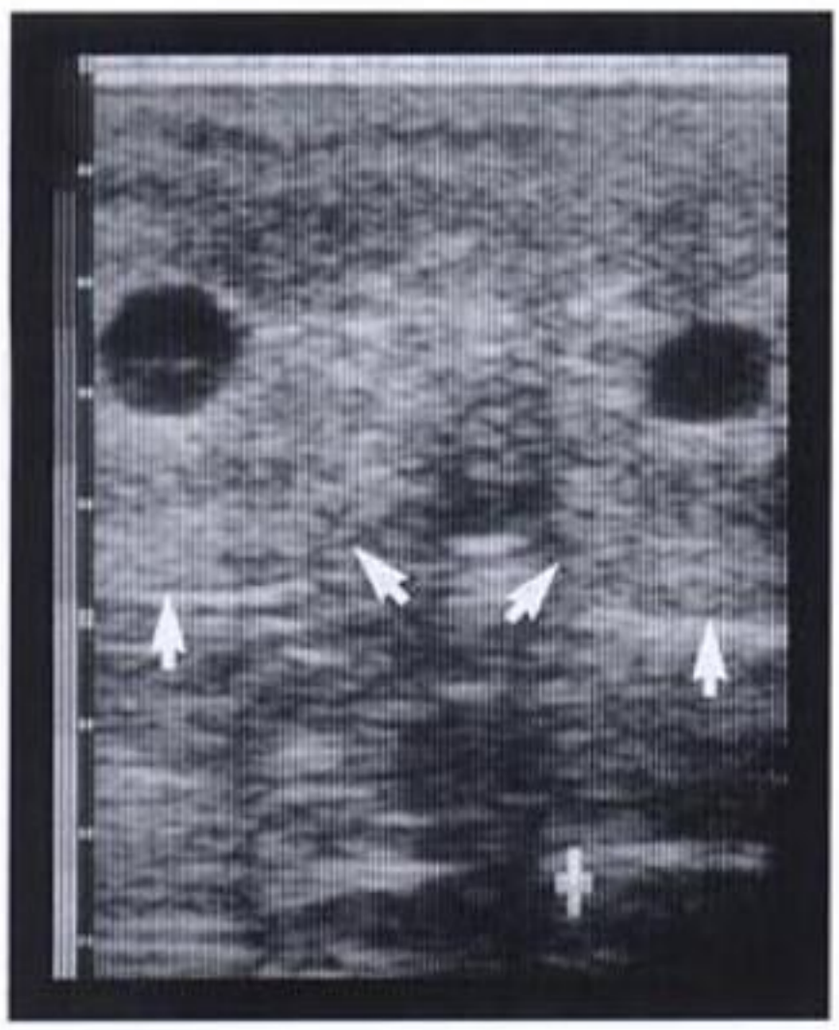


Fig. 1.71: Twin pregnancy on Day 13. The two vesicles are bilateral, one in each horn (arrows).

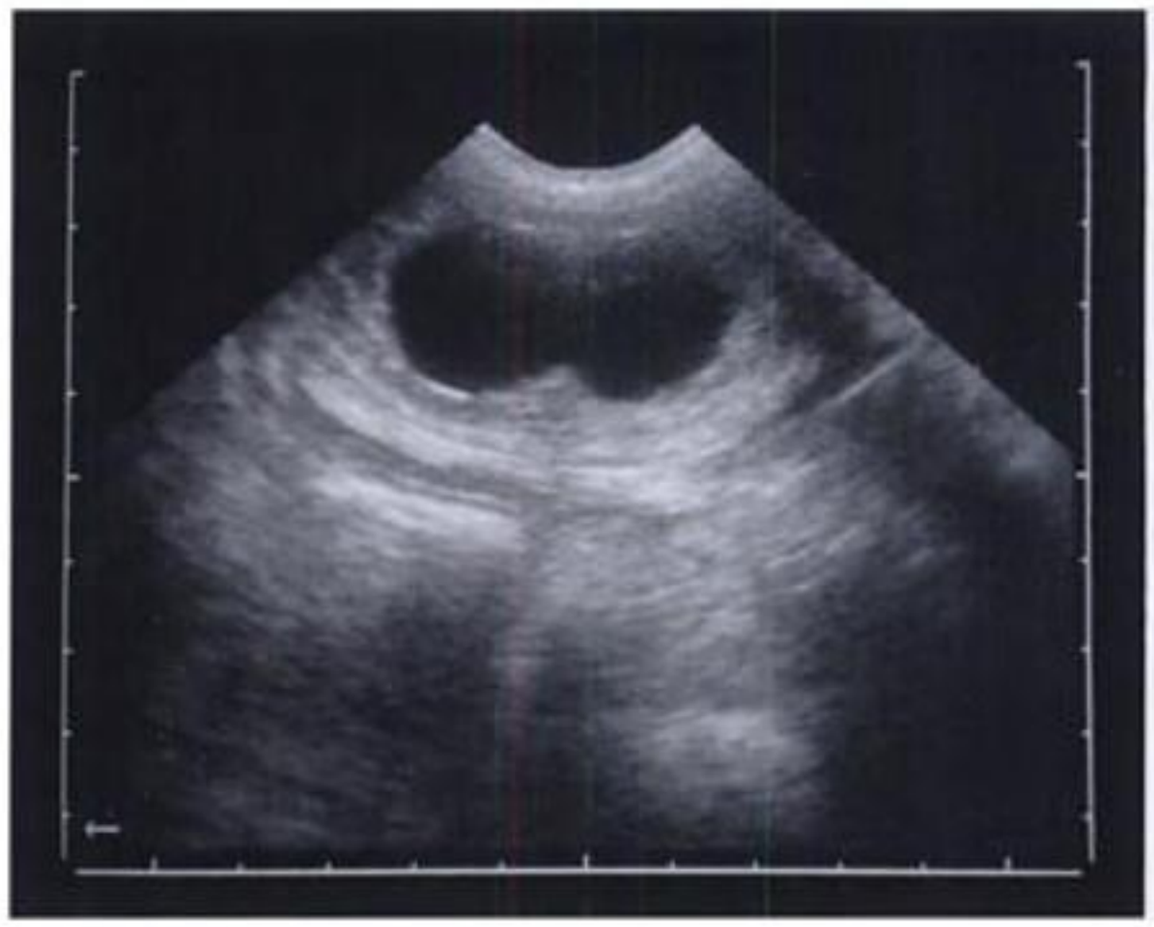


Fig. 1.72: Twin pregnancy on Day 16. The two vesicles are unilateral and close together.



Fig. 1.73: Twin pregnancy on Day 14. Only one embryonic vesicle seems to be visible. In relation to the last service date this vesicle is too large. The opposing walls of the two vesicles are hidden from view.



Fig. 1.74: Single pregnancy on Day 22. Due to the unfavorable positioning of the ultrasound probe the common membrane of allantois and yolk sac (arrow) is depicted without the embryo. A misinterpretation as a twin pregnancy is possible.

Avtorsko zaščiteno gradivo

Downloaded From Vet-eBooks.com

1.3.2.5 Twin pregnancy

An important indication for the use of ultrasonography is the timely diagnosis of a twin pregnancy. The frequency with which twin pregnancies are diagnosed depends on the time of the examination as well as the breed of the horse involved. It has been reported that the incidence of twin pregnancies diagnosed between Days 13 and 21 is 15 % in pregnant Thoroughbred mares and only 6 % in pregnant Standardbred mares (BOWMAN 1986). If the examination is performed later and Warmbloods and draught horses are included, this percentage may drop to 1 to 3 % (CHEVALIER and PALMER 1982). The detection of twins during the early stage of gestation requires a very carefully executed ultrasonographic examination of the uterus. The diagnosis is possible with relative ease between Days 12 and 16 (Fig. 1.71).Bilaterally positioned twin conceptuses are not difficult to recognize, provided the examination is carried out conscientiously (MERKT et al. 1983). Difficulties are encountered in cases of ipsilateral twin pregnancies where both conceptuses lie close together in the same horn (Fig. 1.72 to 1.74).

Many factors can contribute to the failure of recognizing a twin pregnancy. When two embryonic vesicles lie close together the positioning of the scanning probe may make it impossible to see the thin, echoic membrane formed by the two closely appositioned sets of vesicle walls (Fig. 1.73). The presence of twins should be suspected when an embryonic vesicle is too large for its age as determined by the last service date of the mare. If the first examination is performed after Day 20 the ascent of the embryo with the development of its characteristic septum across the middle of the vesicle will have already started. This membrane which is formed jointly by allantois and yolk sac can lead to the misinterpretation of a singleton embryo as a twin (Fig. 1.74). Equally, a twin with closely appositioned membranes of the two vesicles which are misinterpreted as being the allantois yolk sac membrane of a singleton is possible. The hyperechoic line formed by the apposition of two chorionic membranes usually runs straight and in a vertical direction, whereas the allantois yolk sac membrane commonly lies horizontally (SIMPSON et al. 1982). A very significant source of error is the examiner being satisfied with the detection of one embryonic vesicle and neglects to examine the remaining sections of the uterus for another vesicle. During the phase of embryonic mobility until Day 16 of gestation the embryos frequently lie in the uterine body where they are easily overlooked. At the time when a singleton embryo is detected on Day 14 or 15, another embryo from a second, asynchronous ovulation days later may still be too small to be found by ultrasonography. Since asynchronous double ovulations with a time interval of 48 to 96 hours between ovulations can still lead to the conception of a twin pregnancy, the younger of the two embryonic vesicles will be 2 to 4 days less advanced than the older and thereby have a diameter smaller than can be detected by ultrasound (GINTHER 1986). Endometrial cysts may also lead to a faulty diagnosis of a twin pregnancy (SIMPSON et al. 1982).

Avtorsko zaščiteno gradivo

Downloaded From Vet-eBooks.com

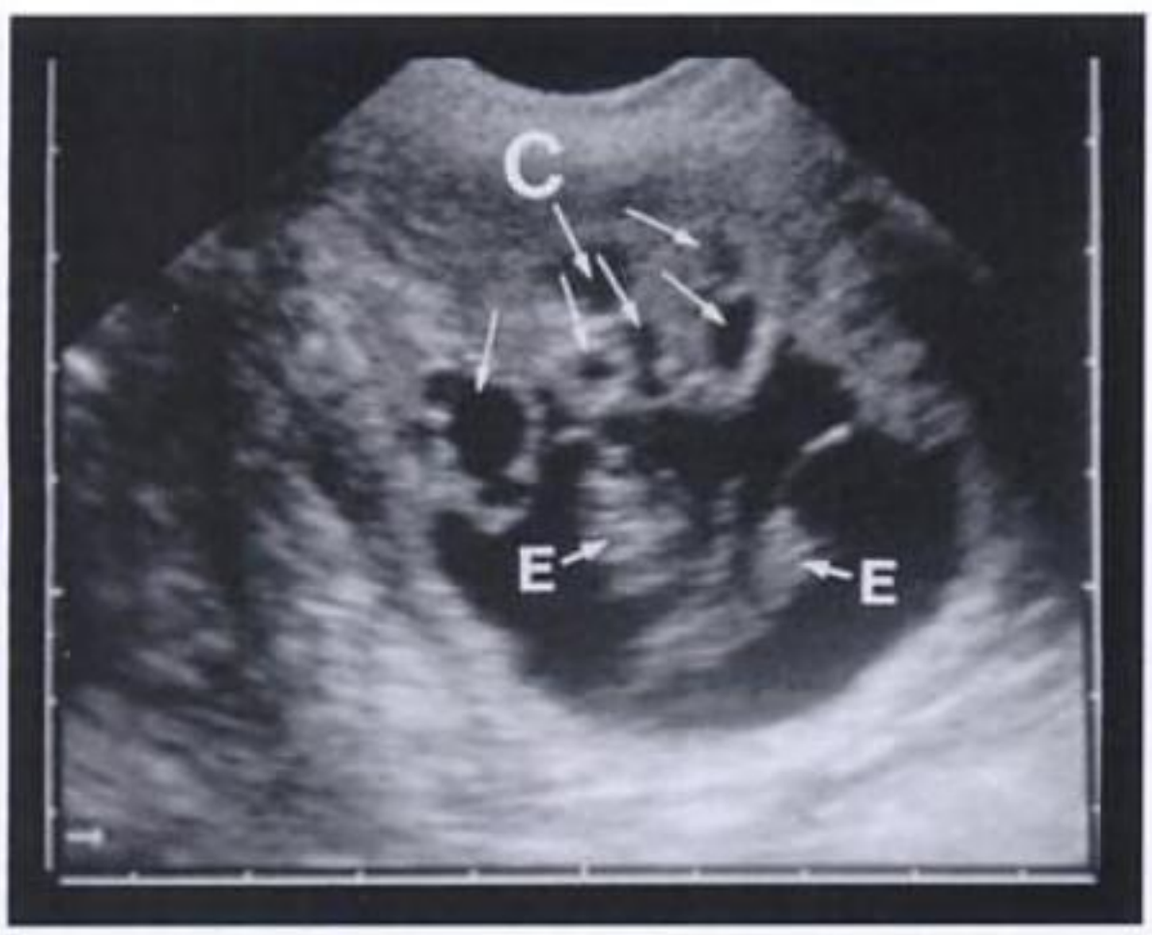


Fig. 1.75: Twin pregnancy on Day 28. Dorsally, a cluster of multiple endometrial cysts (C) can be seen. They can generate difficulties in diagnosing a twin pregnancy. To ensure an accurate diagnosis the two embryos (E) with the beating heart in each should be depicted.



Fig. 1.76: Twin pregnancy on Day 37. The two embryonic vesicles appear to be fused. Two embryos are visible.

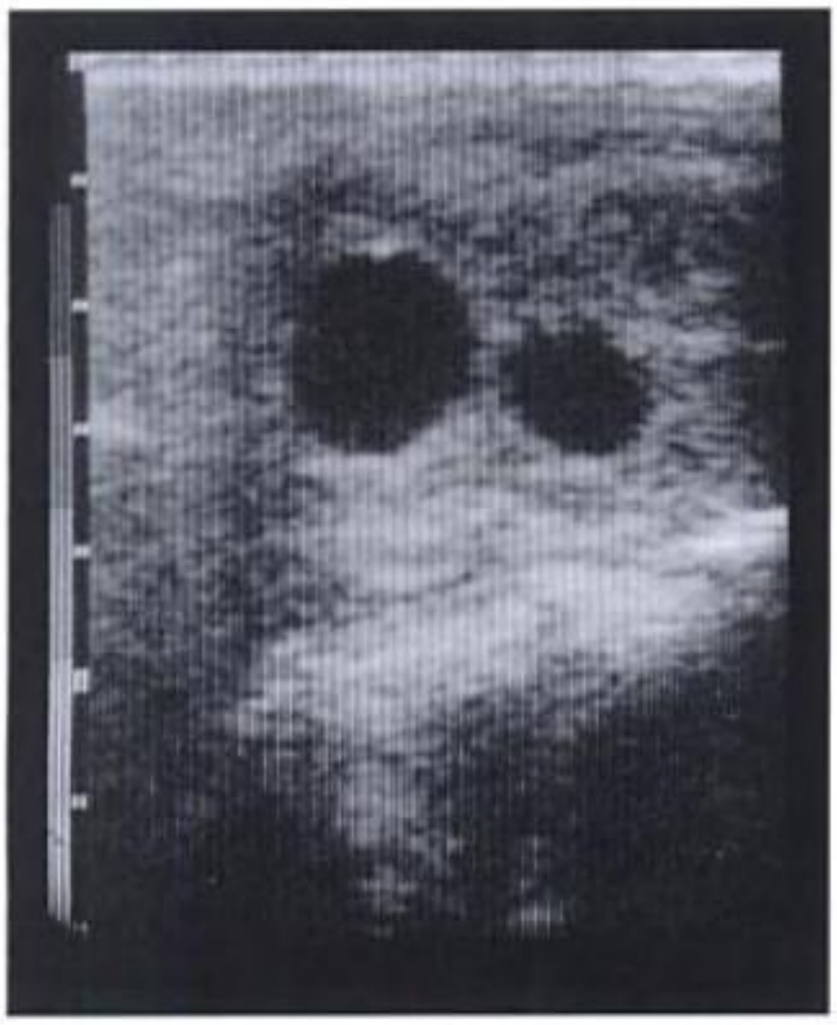


Fig. 1.77: Twin pregnancy on Day 15. The vesicle on the left has the appropriate size in relation to the service date, whereas the one on the right is too small.

Avtorsko zaščiteno gradivo

Downloaded From Vet-eBooks.com

There are mares with multiple endometrial cysts which can make the search and detection of twin vesicles in the uterus particularly difficult (Fig. 1.75). Occasionally it is difficult to find the membrane that divides the two vesicles of a twin pregnancy (Fig. 1.76). Where uncertainty exits the final decision should be postponed until the time when the detection of two heart beats can be expected.

The individual embryonic vesicles of a normal twin pregnancy often show the same growth rate as that seen in singleton pregnancies (GINTHER 1984 b, PIPERS et al. 1984).

In spite of that the sizes of individual vesicles in cases of twin pregnancies can differ (Fig. 1.77). This may indicate that the smaller member of a twin is retarded and is in the process of undergoing an embryonic death. However, in cases where twin vesicles of unequal size are detected the categorical conclusion that the smaller embryo must be dying, will often prove wrong. Asynchronous double ovulations with an interval of 48 to 96 hours between ovulations can lead to twin pregnancies. The two conceptuses will show differences in their stages of development, but can both continue to persist and grow into the fetal stage of pregnancy.

In unilaterally fixed adjacent twins an embryonic mortality is likely between Days 17 and 29 (GINTHER 1984 c). Prior to this, during the phase of mobility, resorptions are rare and after this until Day 45 only few mortalities will occur. The resorption of one member of a twin is more likely than that of both. Bilaterally fixed twins continue to develop in the majority of cases and lead to abortion during the advanced stages of pregnancy.

The following approach is recommended for veterinary practice: Where twins of clearly differing sizes are diagnosed until Day 16 of gestation, the possibility of a spontaneous resorption should be considered. Intervention may be postponed until 2 to 3 days later when it is evident from the follow-up examination that both embryos have continued to develop since the previous examination. Where twins are found before Day 16 and both vesicles appear to be intact it is useful to attempt the reduction of the pregnancy to a singleton pregnancy by manually crushing of either of the two vesicles. Since both vesicles are still mobile at this stage, repeated examinations can be performed until the two vesicles are found to be far enough apart so that the one can be crushed without harming the second one. If a bilaterally fixed twin pregnancy is first detected after Day 16 an intervention is indicated, because it is likely that both embryos will persist. Since a spontaneous resorption is more likely in unilaterally fixed twins after Day 16 an intervention can be postponed for some time.

Once a twin pregnancy has been reduced by crushing of one vesicle the successful elimination of the one and the further development of the other vesicle should be monitored ultrasonically. Where an embryo has been eliminated by crushing it before Day 20 the survival chance for the second conceptus is good, but in later cases one must expect the second embryo to die (BOWMAN 1986).

Avtorsko zaščiteno gradivo

Downloaded From Vet-eBooks.com



Fig. 1.78: Twin pregnancy on Day 39. The two embryonic vesicles lie next to each other and are visible on the same ultrasonogram.

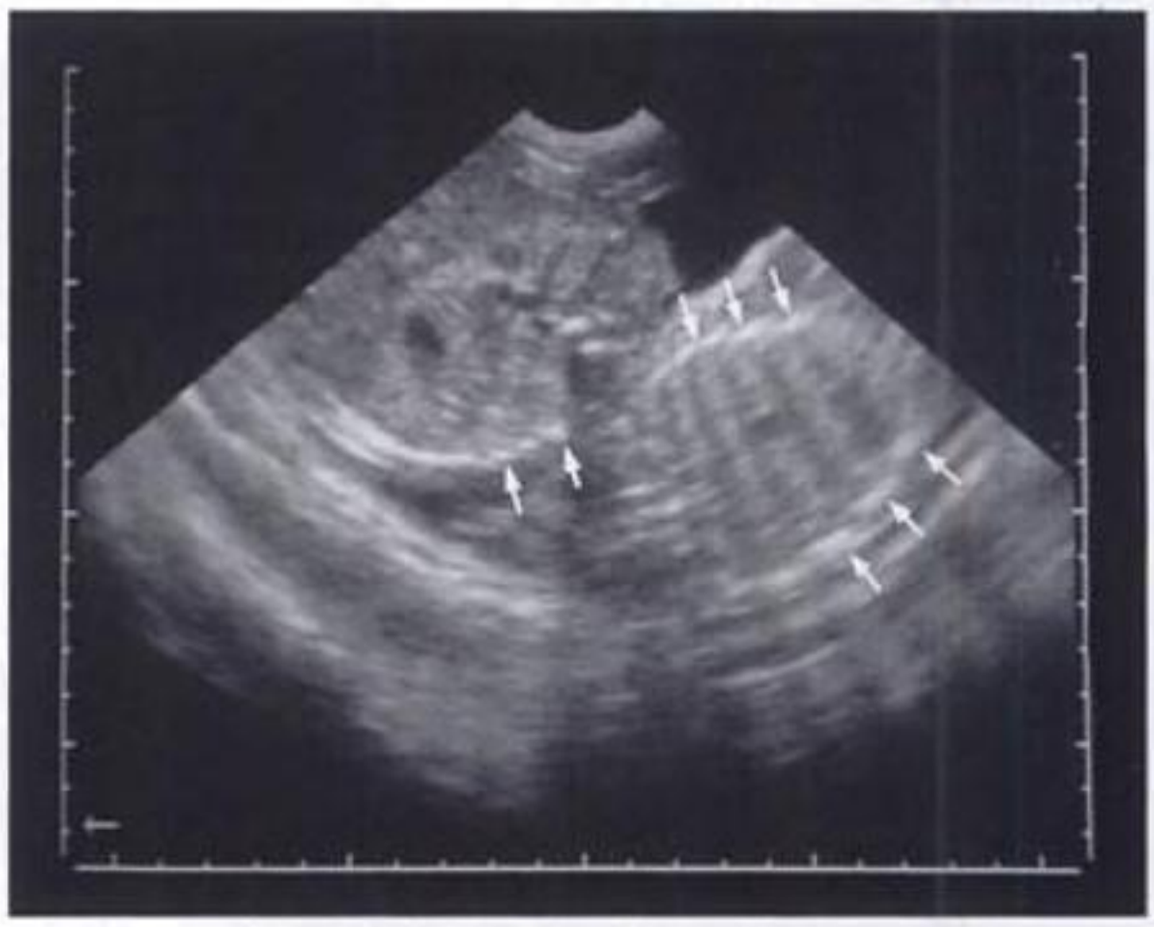


Fig. 1.79: Twin pregnancy on Day 129. The trunks of two fetuses lie next to each other. The echoes produced by the cross sections of the ribs (arrows) of both fetuses can be seen.



Fig. 1.80: Instrumentation for transvaginal sonography, including the automated puncture device (LABOTECT, Göttingen, Germany). Devices for adjustment and triggering of the automated puncture are situated on the left aspect of the handle. The scanning head (arrow) of the vaginal probe (SIEMENS, Erlangen, Germany) is pushed up to the cranial vaginal wall. Above the tube for the probe is the channel with the puncture needle.

Avtorsko zaščiteno gradivo

Downloaded From Vet-eBooks.com

From Day 40 even in unilateral twin pregnancies the two fetuses may be so far apart that it may be difficult to capture both on a single ultrasound image (Fig. 1.78).

In advanced gestation (2nd and 3rd trimesters) it is difficult to diagnose twin pregnancies by transrectal ultrasonography. Sometimes it is possible to see two fetuses (Fig. 1.79). Where this is possible the existence of a twin pregnancy can be confirmed. Should only one fetus be detectable making a diagnosis of a confirmed singleton should be approached with caution.

1.3.2.6 Transvaginal sonographic puncture of the conceptus

Since the manual reduction of a twin pregnancy is usually not successful after Day 20 to 25, the possibility of eliminating one conceptus by controlled puncture was considered. It appeared promising to puncture one conceptus under visual control of a vaginally introduced ultrasound probe.

For this purpose a pistol-like instrument was designed. The barrel of the instrument accommodates the ultrasound probe and on the handle is a trigger for the automated puncture device (Fig. 1.80). The handle of the vaginal sector probe is fixed within the tip of the barrel. A spring mechanism is used to drive the puncturing needle and an adjusting screw is used to set the depth to which the needle can be shot beyond the tip of the probe. The depth and direction of the puncture can be determined aiming with two puncture guide lines on the ultrasound monitor (Fig. 1.82). The total length of the instrument is about 80 cm.

The punctures are performed after the vestibulum and vagina are prepared aseptically and the mare is sedated. For the sake of sterility the instrumentation is covered in a sterile plastic sleeve. The tube of the instrument with the attached puncturing device is introduced into the vagina in the same manner as a tubular speculum. It is pushed against the anterior vaginal wall and one hand introduced into the rectum to hold the uterus caudally and fix it against the ultrasound probe. Once the image of the conceptus is aligned with the puncture direction of the needle the trigger mechanism is activated. The plastic sleeve is penetrated by the puncture needle when the trigger is pulled. It is possible to aspirate fetal fluid through the needle.

Avtorsko zaščiteno gradivo

Downloaded From Vet-eBooks.com

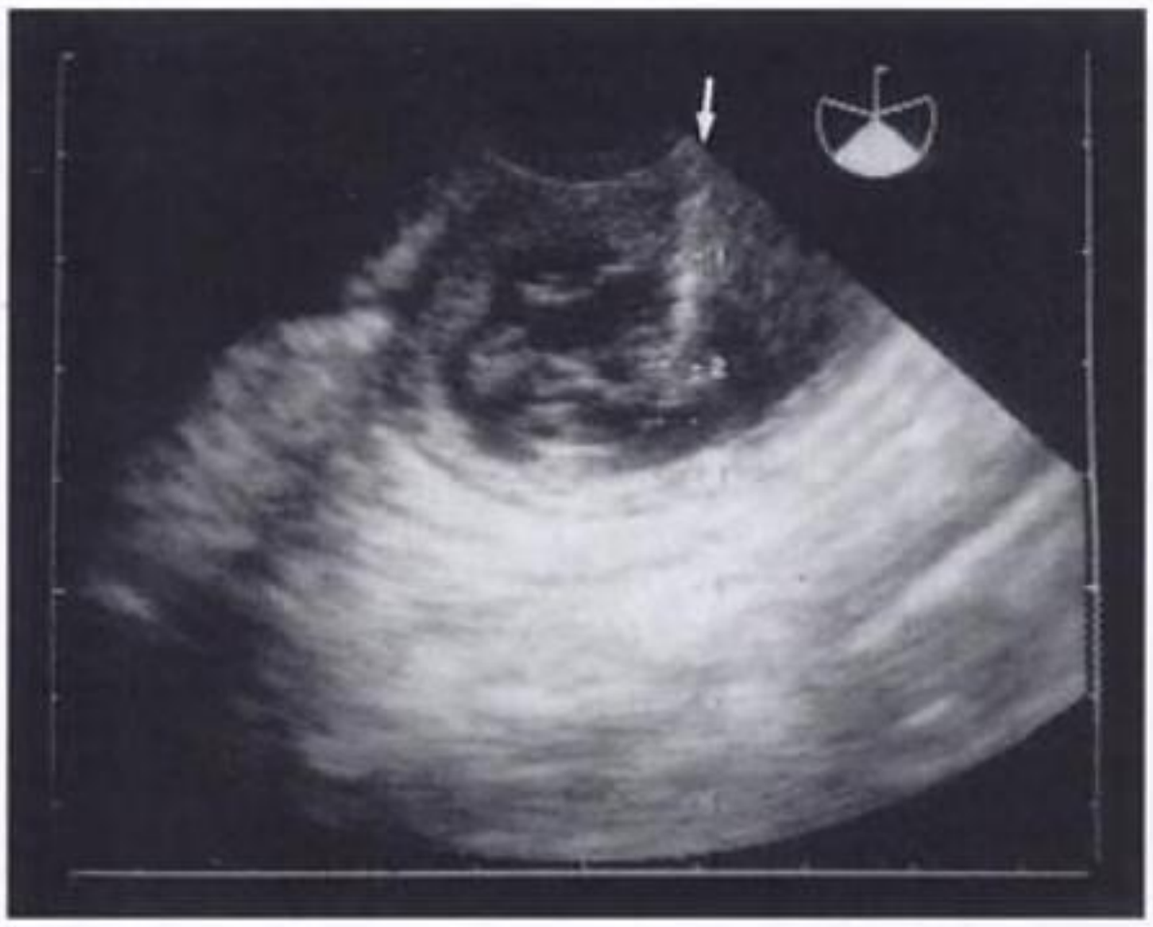


Fig. 1.81: Transvaginal puncture of an embryonic vesicle on Day 29 of gestation. The puncture needle (arrow) has penetrated about 2 cm into the vesicle. Within the conceptus the detaching embryonic membranes can be seen. The conceptus was subsequently resorbed.



Fig. 1.82: Transvaginal puncture of a conceptus on Day 50 of gestation. The puncture needle lies between the two guide lines. A transverse section through the fetus can be seen in the upper left of the vesicle. The conceptus was subsequently resorbed.

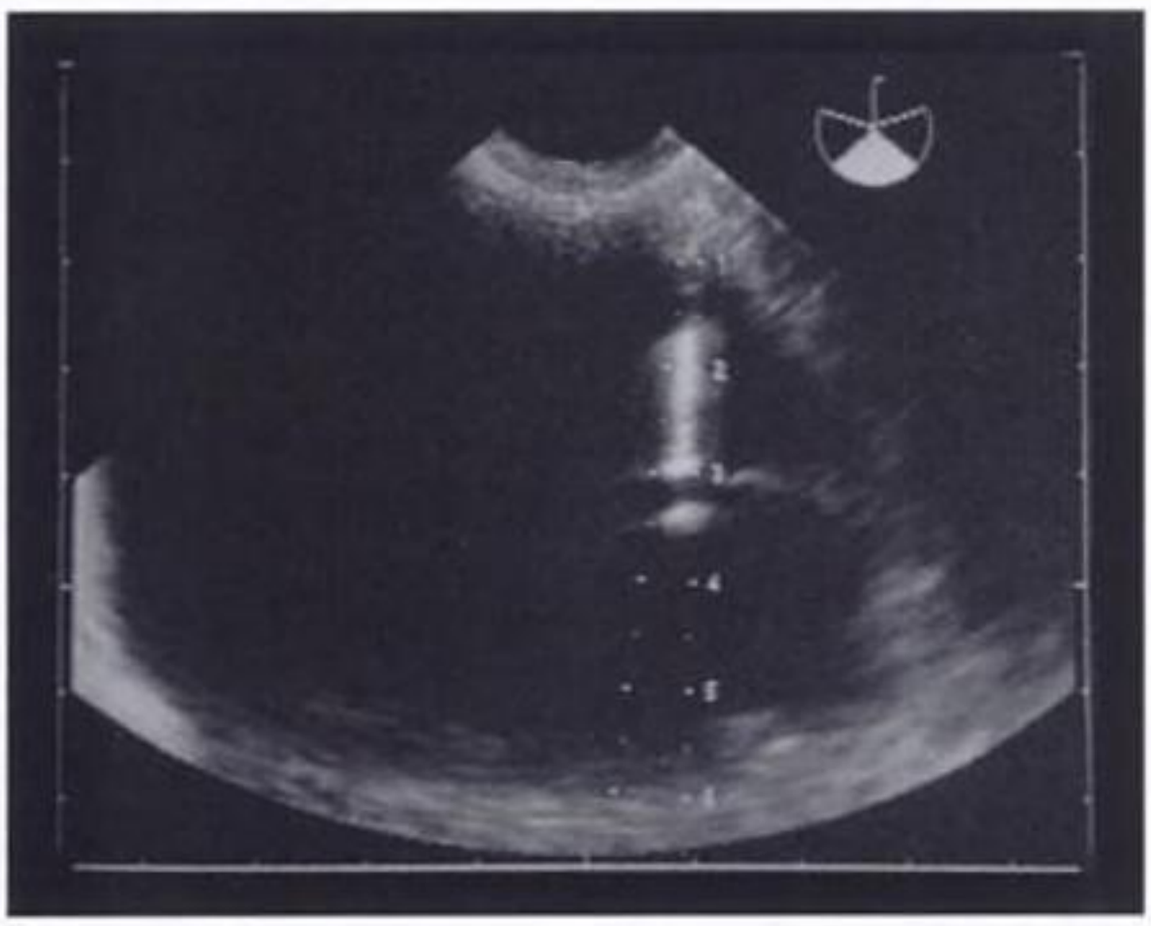


Fig. 1.83: Transvaginal puncture of a conceptus on Day 54 of gestation. The puncture needle runs between the two guide lines to a depth of 3 cm. The pregnancy continued to develop after the puncture.

Avtorsko zaščiteno gradivo

Downloaded From Vet-eBooks.com

Experiences with transvaginal punctures of conceptuses in the horse are still limited. In the punctures performed thus far one could usually observe a change in the typical features of the embryo or fetus immediately following penetration of the vesicle by the puncture needle (Fig. 1.81 and 1.82). Within the vesicle echoes reminiscent of floating parts of membranes became evident. These were assumed to have been freed placental membranes. Immediately after the puncture the embryo changed its position, coming to rest on the floor of the vesicle.

To date six punctures on singleton pregnancies have been performed between Days 19 and 75 with the aim of aspirating small quantities of placental fluid. In 4 pregnancies which were performed between Days 19 and 50 the conceptus died after the puncture. One conceptus which had been punctured on Day 54, and from which 7 ml allantoic fluid had been collected, continued to develop (Fig. 1.83). This pregnancy was purposefully interrupted on Day 75 by the collection of a large volume of fetal fluid.

Only one conceptus was punctured in each of two twin pregnancies on Days 29 and 44 of gestation, respectively. The remaining member of the twin pregnancy was intended to persist and develop as a singleton pregnancy. In both cases, however, both conceptuses died. In all cases the death of the conceptus was apparent within days of the puncture. Usually, a heart beat could not be detected by ultrasonography on the day following the puncture.

Avtorsko zaščiteno gradivo

Downloaded From Vet-eBooks.com



Fig. 1.84: Transrectal image of the eye and braincase of a fetus on Day 151 of gestation. In the anterior aspect of the eye the caudal wall of the lens (arrows) is depicted.

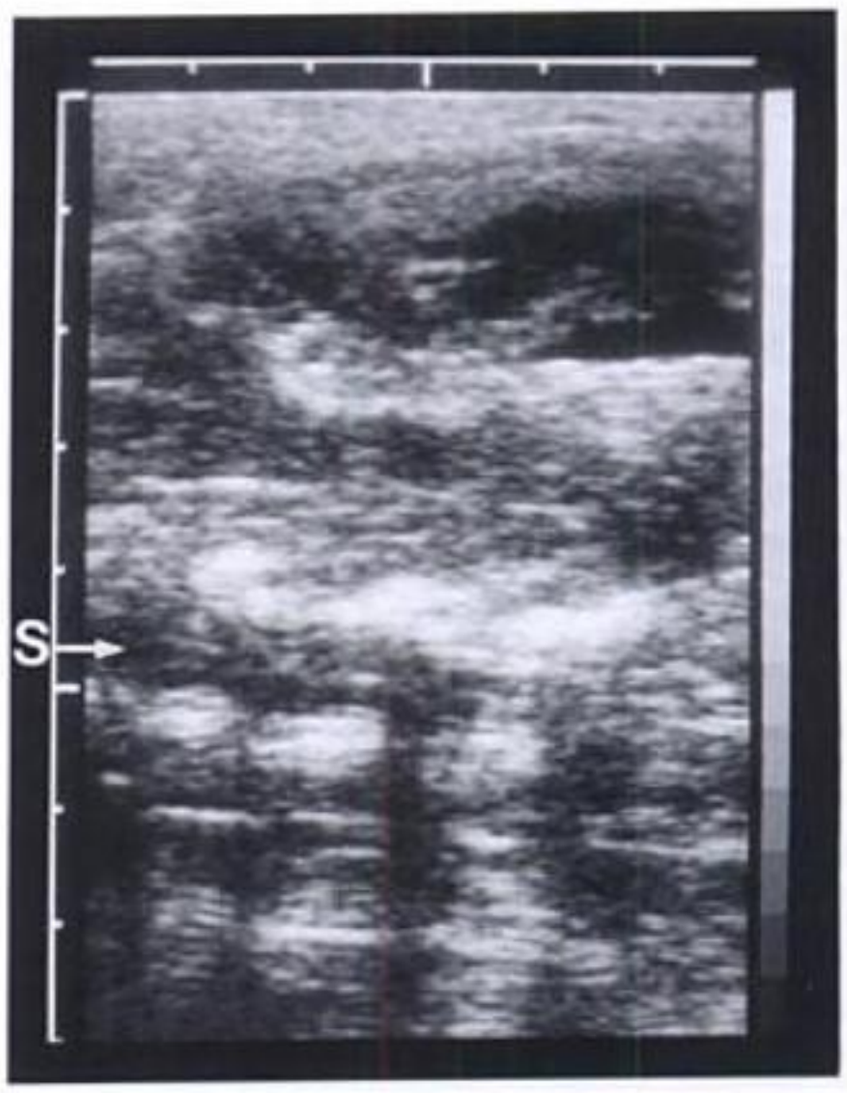


Fig. 1.85: Longitudinal section through the neck of a fetus on Day 154 of pregnancy. The arches and bodies of three vertebrae delineate the spinal canal (S). Behind them shadow artifacts extend into the depth of the image.

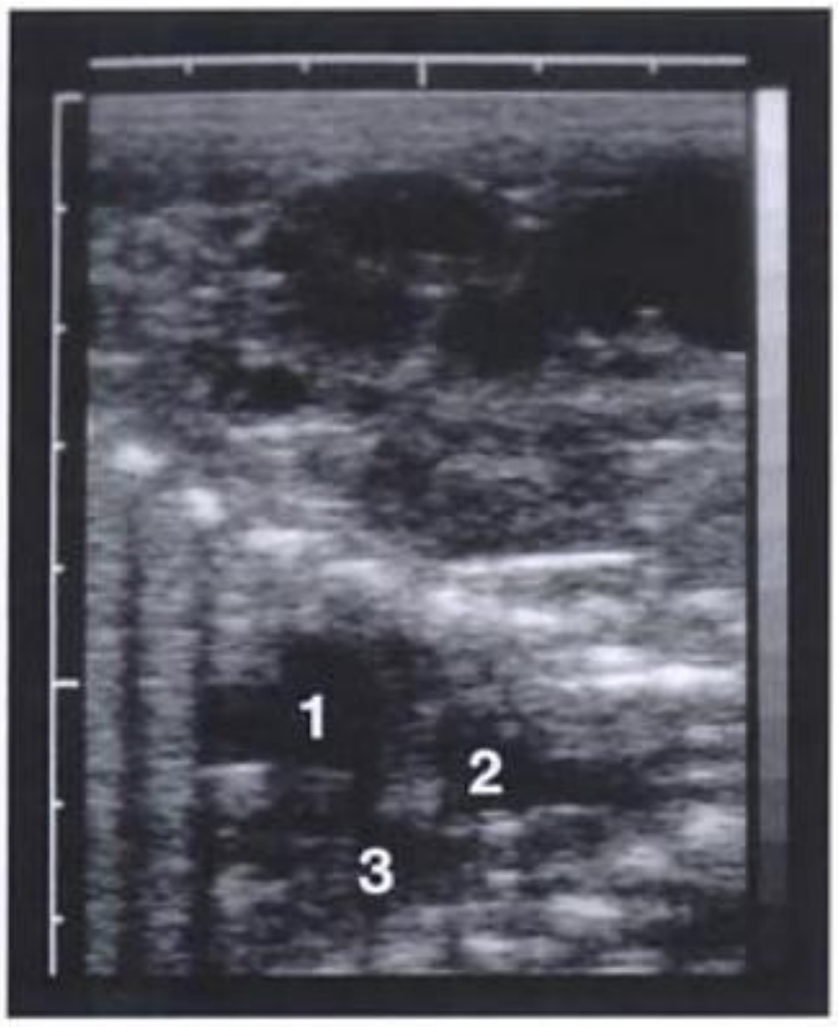


Fig. 1.86: Horizontal section through the thorax of a fetus on Day 134 of gestation. The echoes formed by the cross sections through the ribs of both halves of the chest run in two lines towards each other. Between the two lines three cardiac chambers (1, 2, 3) are visible.

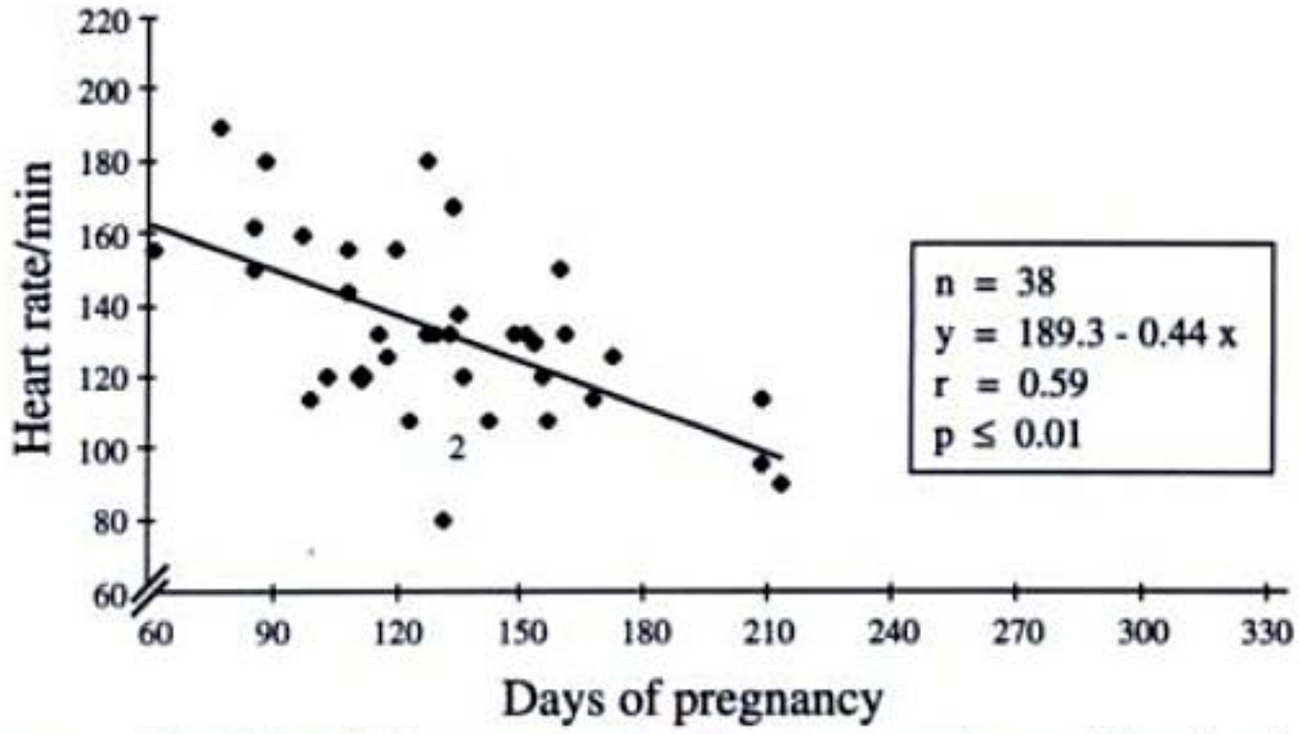


Fig. 1.87: The heart rate of equine fetuses (Thoroughbred and Standardbred) during pregnancy (adapted from KÄHN and LEIDL 1987 a).

Avtorsko zaščiteno gradivo

Downloaded From Vet-eBooks.com

1.3.3 Ultrasonography of the equine fetus

After Day 60 of pregnancy, significance of transrectal ultrasonography for merely diagnosing pregnancies in the horse decreases. At this stage the emphasis of the value of the ultrasound examination shifts towards fetal diagnostics. Through sonographic observation of the fetus in utero, the depiction of its body parts and organs as well as taking fetal measurements - the so called fetometry -, fetal development can be monitored and assessed (KÄHN and LEIDL 1987 a). Important conclusions for abnormal pregnancies can be made in this manner. Sizes determined by fetometry can be used to assess gestational age in cases were uncertainty exists about the exact service date. Transcutaneous ultrasonography through the dam's ventral abdominal wall may prove useful in some cases in order to visualize the fetus (ADAMS-BRENDEMUEHL and PIPERS 1987).

1.3.3.1 Imaging of fetal organs

The ultrasonic appearance of the various organs of equine fetuses generally resembles that of bovine fetuses (See Chapter 2.4.1). In the latter species the ultrasonography of the fetus has been well studied. Below follows a description of particularly characteristic ultrasonic images of equine fetuses.

1.3.3.1.1 Head, neck and spinal column

Prominent structures on the head of the equine fetus are the eye and the cranial cavity (Fig. 1.84). The vitreous body of the eye is anechoic and surrounded by the hyperechoic orbit. In the anterior portion of the eye ball Arch shaped structures become visible. The two convex lines that lie opposite one another represent the front and back wall of the lens.

The roof of the scull and the basal portion of the brain cavity form a hyperechoic, oval outline that is a few millimeters thick (Fig. 1.84). The oval outline of the brain cavity can be depicted until about the 8th month of gestation. After that the ossification of the bones of the cranium has progressed so far that only the bony parts in proximity of the transducer can be imaged.

The most apparent structure in the neck is the cervical spine (Fig. 1.85). The ossification centers of the vertebral bodies and arches produce disc like echoes. Due to the absorption of the sound waves, ultrasonic shadows are seen beyond the vertebrae.

When the probe is positioned favorably the spine can also be detected by ultrasonography in the thoracic, lumbar, sacral and even coccygeal regions. Usually the typical double row of hyperechoic discs is apparent. Only the tail vertebrae produce a single row of solid echoes.

1.3.3.1.2 Thorax and heart

The conically tapering images of the two halves of the chest cavity are obvious in the thoracic region (Fig. 1.86). Similar to the vertebrae, the cross sectional images of the ribs produce echoic circles. Ultrasonic shadows lie behind the ribs that produce them.

The heart will be evident in the apex of the thorax (Fig. 1.86).The echoic wall of the heart surrounds the hypoechoic lumina of the ventricles and atria which are separated from one another by bright valves and septa. The action of the heart can be demonstrated quite impressively if the probe is oriented properly.

The basal heart rate of equine fetuses is 150 to 190 beats per minute in the 3rd month of gestation and decreases slowly as pregnancy progresses (Fig. 1.87). In Month 7 the basal heart rate will vary from 100 to 110, and near term 60 to 80 beats per minute (COLLES and PARKES 1978, PIPERS and ADAMS-BRENDEMUEHL 1984, MATSUI et al. 1985, ADAMS-BRENDEMUEHL and PIPERS 1987). Generally, however, the heart rate is rather variable and can rise well above the basal values during short periods of observation.

Avtorsko zaščiteno gradivo

Downloaded From Vet-eBooks.com



Fig. 1.88: Transverse section through the trunk of a fetus on Day 148 of pregnancy. At the bottom lies the stomach (S), at the top lies the coarsely granular, moderately echoic liver (L), and between them runs the caudal caval vein to the right of which is a cross section of a vertebra with a ultrasonic shadow originating below it.



Fig. 1.89: Cross section through the umbilical cord with the two lumina of the umbilical arteries and that of the umbilical vein in a fetus on Day 185 of gestation.

Avtorsko zaščiteno gradivo

Downloaded From Vet-eBooks.com

1.3.3.1.3 Abdomen and pelvic region

The abdominal organ easiest to depict by ultrasonography is the stomach (Fig. 1.88). It fills a hypoechoic oval area in the background of the last few ribs and shows the typical features of an equine stomach, namely the dorsal cul-de-sac and the ventral body.

Next to the stomach lies the coarsely granular, moderately echoic liver which is passed by the black cords of the large abdominal blood vessels (Fig. 1.88).

Under optimal conditions it may be possible to determine the sex of equine fetuses by means of ultrasonography (CURRAN and GINTHER 1989). For this purpose the location of the genital tubercle between the hind legs must be determined. The embryonic genital bud differentiates into penis and prepuce in the male fetus and into clitoris and vulva in the female fetus. During fetal development the genital tubercle migrates from its origin between the hind legs cranially towards the umbilicus in the male and caudally towards the tail in the female. By determining its position from about Day 60 of gestation the sex of the fetus can be diagnosed. In both sexes the genital tubercle consists of a bilobular, hyperechoic structure. The optimal time for transrectal ultrasonographic sex determination in equine fetuses appears to lie between Days 60 and 70 of gestation. The sex determination is possible at later stages too, but then the more cranioventral position and the larger size of the fetus may make the optimal depiction of the caudal body region difficult and not possible in every examination.

In contrast to the situation in bovine fetuses (see Chapter 2.4.2), it has not been possible to determine the sex of equine fetuses by sonographic imaging of the scrotum (PIPERS and ADAMS-BRENDEMUEHL 1984). One reason for this is that the testes descend much later into the scrotum in the equine fetus than in the bovine fetus. Therefore, the depiction of the scrotum and testes cannot be used to differentiate between the sexes of equine fetuses.

Occasionally, the umbilical cord which floats around within the placental fluids can be seen (Fig. 1.89). A transverse section through the umbilical cord shows the typical arrangement of two umbilical arteries and one vein in the equine fetus.

Avtorsko zaščiteno gradivo

Downloaded From Vet-eBooks.com

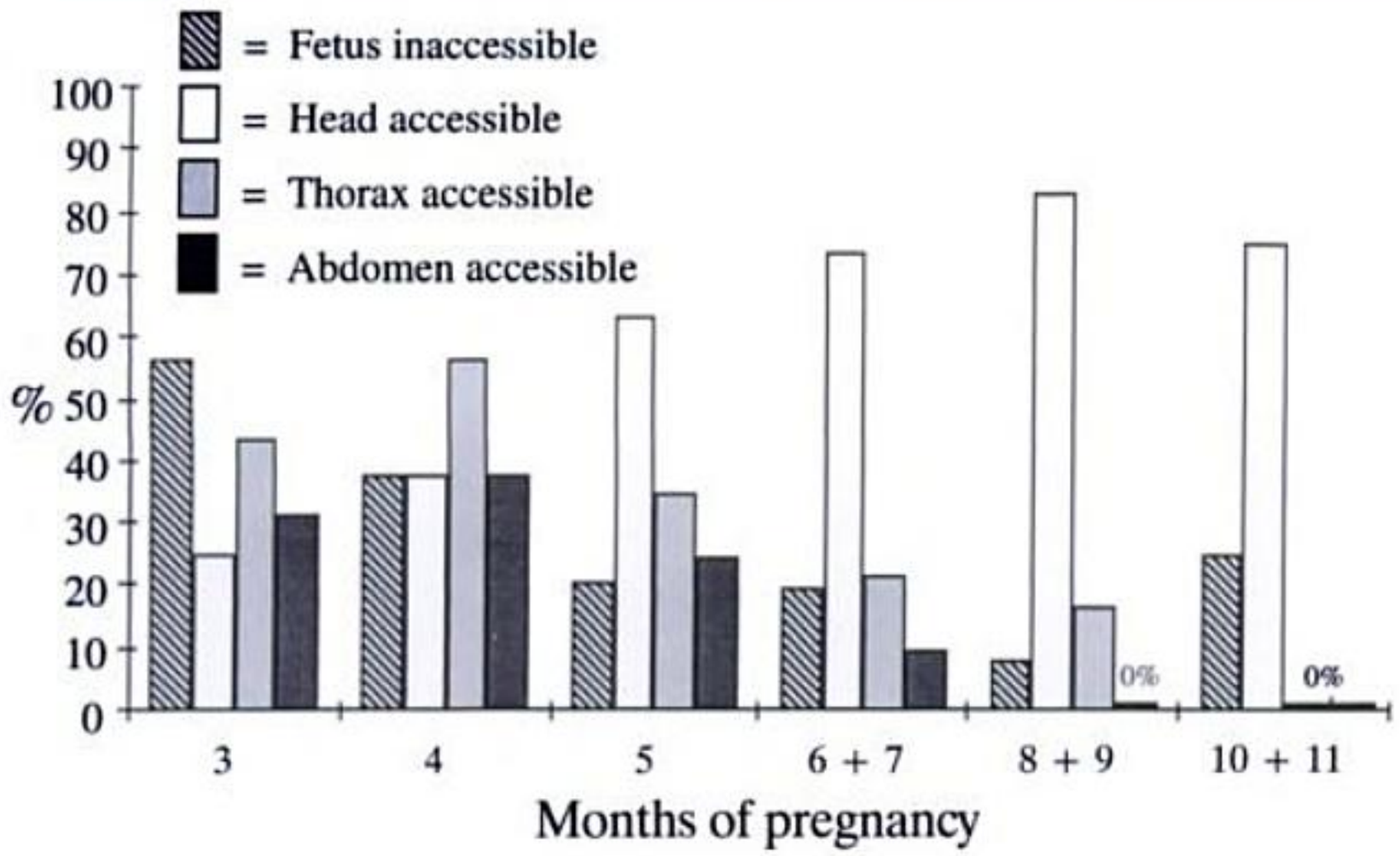


Fig. 1.90: The frequency with which the head, thorax and abdomen of equine fetuses (Thoroughbred and Standardbred) were accessible by transrectal sonography during pregnancy (adapted from KÄHN and LEIDL 1987 a).

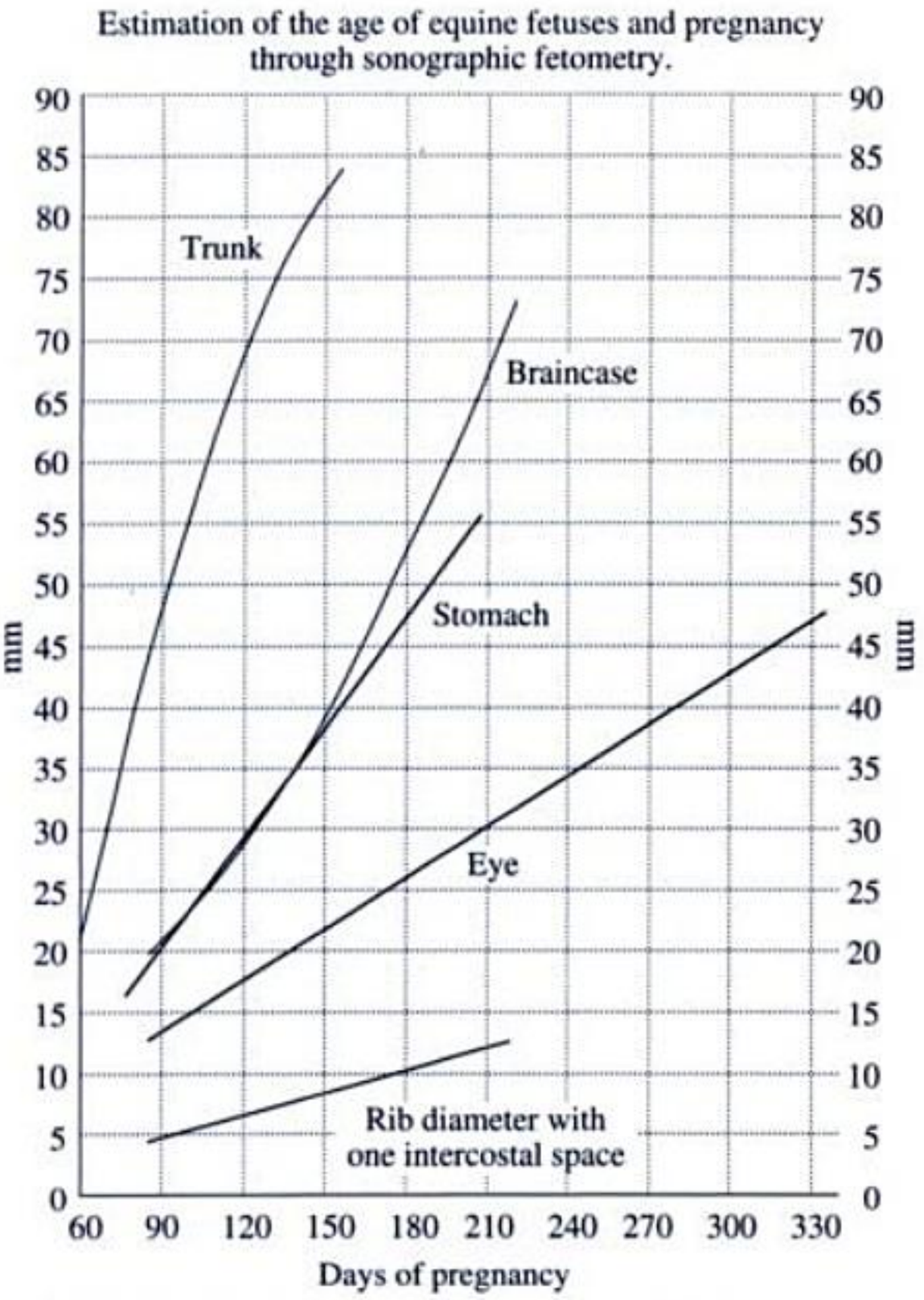


Fig. 1.91: Growth (regressions) of the largest diameters of the trunk, braincase, stomach, eye and one rib cross section with one intercostal space in equine fetuses (Thoroughbred and Standardbred) during pregnancy (adapted from KÄHN and LEIDL 1987 a).



Fig. 1.92: Example of taking measurements of the diameters of eye and braincase in a fetus on Day 159 of pregnancy.

Avtorsko zaščiteno gradivo

Downloaded From Vet-eBooks.com

1.3.3.2 Accessibility of equine fetuses by transrectal sonography

During one study involving 162 Thoroughbred and Trotter mares which were 3 to 11 months pregnant it was possible to reach the fetus by transrectal sonography at all stages of gestation (KÄHN and LEIDL 1987 a). For these examinations a 5 MHz linear ultrasound probe with a penetration depth of 10 cm was used. The technical difficulties associated with the ultrasonic examination of equine fetuses very much depend on the stage of gestation. In about one half of the mares examined between Days 80 and 100 of gestation the fetuses lay outside the range of the ultrasound waves (Fig. 1.90). At this stage the relatively small fetus had often descended cranioventrally into the uterus bulging far beyond the pelvic brim. In this position it was too far away to be detectable by the ultrasound waves. From the 4th month it became increasingly easier to reach some parts of the fetus so that only 10 to 20 % of all fetuses between the 5th and 11th months of gestation remained beyond reach.

The availability of individual fetal body parts for ultrasonic examination also depends heavily on the stage of gestation. The head will move closer to the maternal pelvis as pregnancy progresses and was visible in 74 to 83 % of all 6 to 11 month old fetuses in the above mentioned study (Fig. 1.90). In contrast, the thorax, abdomen and pelvis generally move ever further away. The chest and abdominal regions were accessible in 25 to 50 % of fetuses during the 3rd, 4th and 5th months and only in isolated cases thereafter.

The above mentioned results reflect tendencies and can be improved significantly through the development of better ultrasound technology. With improved technology equine fetuses and their body parts will then become even more available for sonographic examinations. It has also been demonstrated that the shortcomings of transrectal sonography could be compensated for in many cases by the transcutaneous application of the ultrasound probe (O'GRADY et al. 1981, PIPERS and ADAMS-BRENDEMUEHL 1984). By applying the probe in the area between the maternal udder and navel fetal structures in the proximity of the abdominal wall can be visualized from the outside during the 2nd and 3rd trimesters of gestation. Using this technique the trunk of the fetus remains accessible until birth.

1.3.3.3 Sonographic fetometry in horses

Through fetometry, ultrasonography offers the possibility of determining fetal age and to assess the development of the fetus and pregnancy (KÄHN and LEIDL 1987 a). The best approach for measuring a fetus depends on the approximately suspected stage of pregnancy. In principal it is expected that the combination of measurements from as many parameters as possible will result in the most accurate estimation. Until Month 6 the diameter of the trunk and the size of any additionally accessible organs should be determined. From the 6th month especially the head should be fetometrically evaluated. On the procedures for fetometry see also Chapter 2.4.4.

1.3.3.3.1 Eye and braincase

The eye is the fetal organ which is most frequently available for fetometrical assessment during the entire course of gestation (Fig. 1.90 and 1.92). The largest diameter of the eye increases approximately in a linear fashion as pregnancy progresses (Fig. 1.91).

The expansion of the inner diameter of the cranial cavity increases very rapidly (Fig. 1.91 and 1.92) and is well correlated with the stage of pregnancy. The braincase can only be measured until the 8th month of gestation, because thereafter the sound waves are too attenuated by the cranial bones and the imaging field of conventional scanners is too small to allow the cranium to be depicted in toto.

Avtorsko zaščiteno gradivo

Downloaded From Vet-eBooks.com

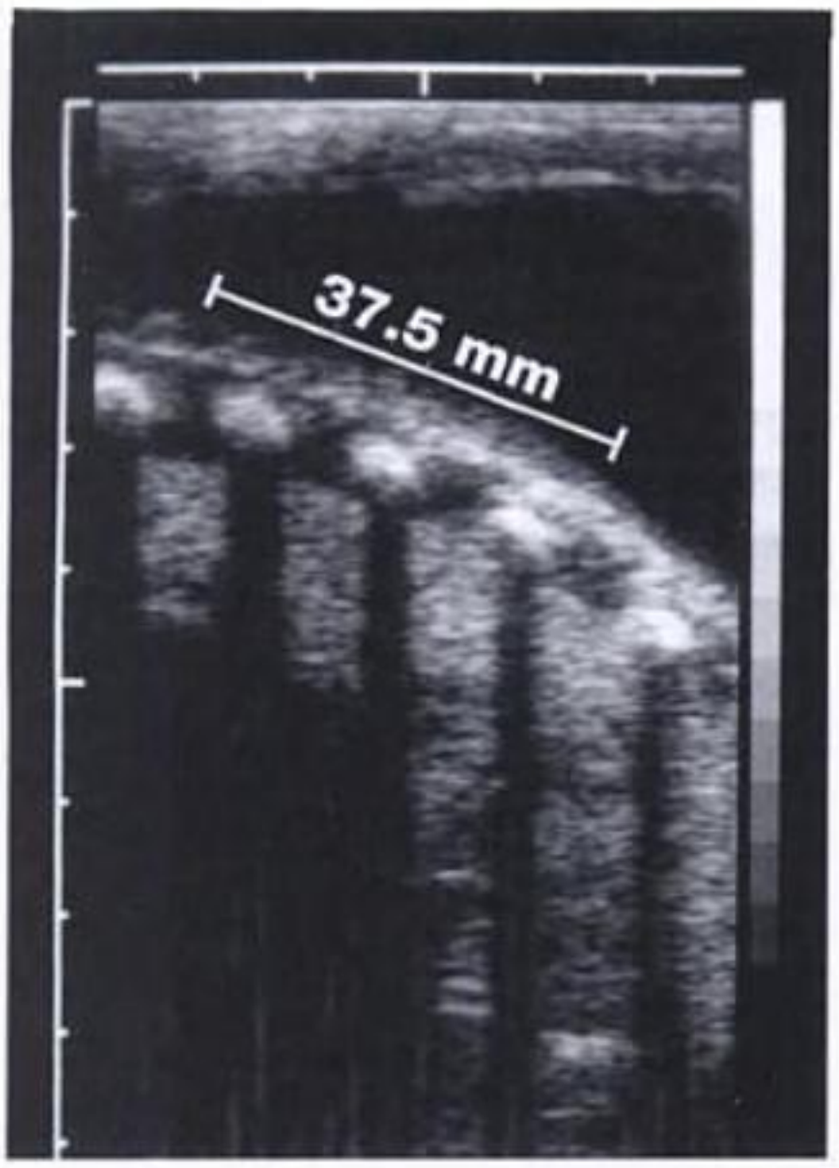


Fig. 1.93: Example of taking measurements of 3 rib cross sections with their corresponding intercostal spaces in a fetus on Day 188 of pregnancy. The length of one rib cross section with its corresponding intercostal space is 12.5 mm (37.5 divided by 3).



Fig. 1.94: Example of measuring the diameter of the trunk of a fetus on Day 88 of gestation.

Avtorsko zaščiteno gradivo

Downloaded From Vet-eBooks.com

1.3.3.3.2 Ribs, trunk and stomach

In order to determine the increase in the size of the transverse sections through the ribs, one must obtain a horizontal sonographic plane through the chest thereby making it will be possible to count the number of ribs and intercostal spaces per unit length (Fig. 1.93). In order to reduce the errors in measurements to a minimum, several ribs and their intercostal spaces (3 to 5) should be used for this assessment. The distance between the edges on the same side of the cross sections of two distant ribs is determined. When this distance is divided by the number of rib cross sections included, the result will be the length of one rib cross section with its adjoining intercostal space.

The size of the stomach can be measured by orientating the ultrasound probe to show the image with the greatest length of the stomach. Now the largest inner diameter of the hypoechoic lumen of the stomach can be measured.

The largest diameter of the trunk is determined at the level of the stomach and liver. The direct distance between the opposing body walls on a sonographic plane that is vertically oriented to the trunk is measured (Fig. 1.94). On average, the diameter of the trunk grows from 25 mm on Day 60 to 80 to 100 mm on about Day 150 (Fig. 1.91). During the Month 6 the size of the trunk exceeds the penetration depth of the ultrasound probe and can no longer be used for fetometrical purposes. Until the 5th month of gestation there is normally very little variation in the trunk diameter of different fetuses, making this a reliable parameter for the assessment of fetal development.

Avtorsko zaščiteno gradivo

Downloaded From Vet-eBooks.com

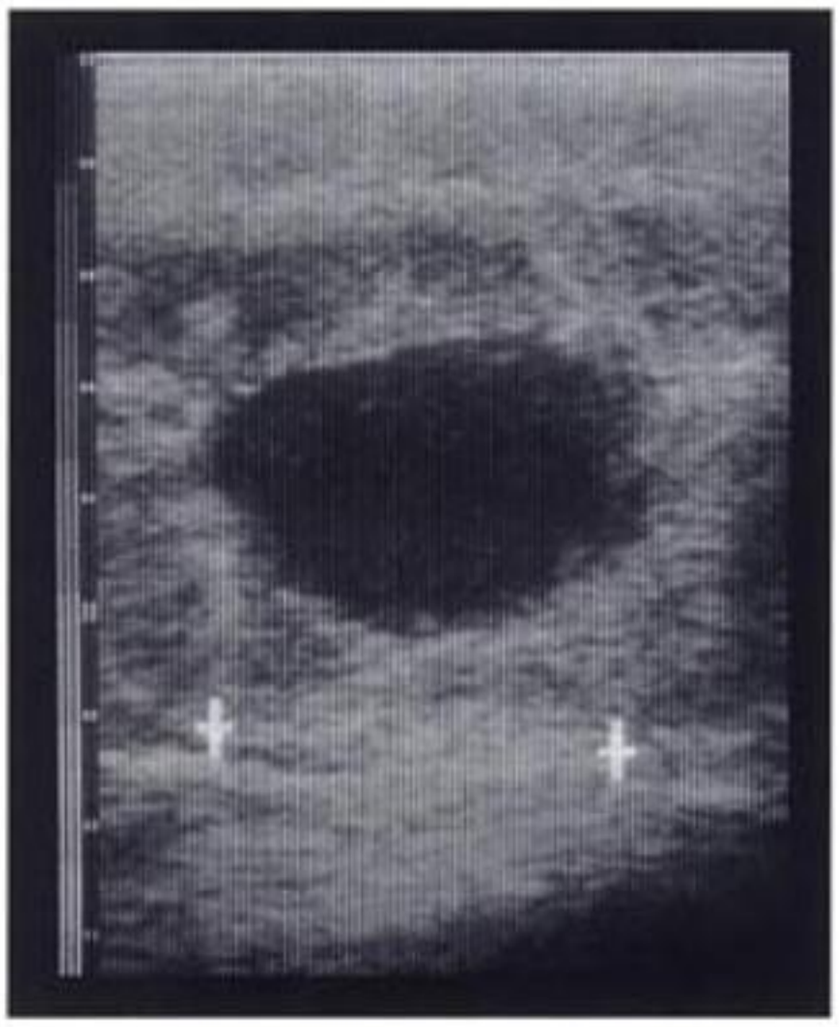


Fig. 1.95: Onset of embryonic mortality on Day 17 of gestation. Signs of abnormality are the increased echogenicity of the embryonic fluid as well as the vagueness of the interface between the embryonic vesicle and the uterine wall. Four days later the conceptus was largely resorbed.



Fig. 1.96: Abnormal pregnancy on Day 27. The embryo still exhibited heart beats. Signs of the impending embryonic death were the irregular outline of the embryonic vesicle and the smaller than expected size of the vesicle when compared to the last service date.



Fig. 1.97: Abnormal pregnancy from Fig. 1.96 on Day 33. The embryo had continued to grow and still had a beating heart. Signs of embryonic mortality are the uncharacteristic orientation and disorganization of the placental membranes (arrow), the echoes visible inside the fluid and the small size and flat shape of the vesicle.

Avtorsko zaščiteno gradivo

Downloaded From Vet-eBooks.com

1.3.4 Uterine pathology

1.3.4.1 Embryonic death

In the horse embryonic death occurs in 4 to 15% of all pregnancies between Days 10 and 50 (CHEVALIER and PALMER 1982, SIMPSON et al. 1982, VALON et al. 1982, SQUIRES et al. 1988).

There are numerous ultrasonic signs that can be used to predict an impending embryonic mortality. In principle, all findings that indicate a deviation from the normal should be interpreted as suspicious. Certain features are, however, more characteristic and occur quite regularly.

An important feature indicating the viability of a conceptus is the anechoic nature of the placental fluid. In the case of a resorption slight to moderate reflections will appear relatively soon within the fluid of the embryonic vesicle (Fig. 1.95). They are a sign of the increasing cellular content of the embryonic fluid and of the disorganization of the placental membranes.

The interface between the embryonic vesicle and its surrounding endometrium is smooth in the case of intact pregnancies. When this line becomes wavy it may serve as an indication that an embryonic death is imminent (Fig. 1.96). Occasionally, the interface appears tortuous in which case the resorption will have already progressed somewhat. The reason for this is the lack of inner tension in the vesicle which is caused by cessation of embryonic fluid production and by its increased resorption. The endometrial folds are no longer stretched smooth by the conceptus , but rather protrude into it (SQUIRES et al. 1988).

In the case of a disrupted pregnancy the loss of the embryonic vesicle's tension is associated with a loss of its typical shape. In the intact pregnancy the conceptus remains strictly spherical until Day 15 of gestation. If the embryonic vesicle assumes any other shape before this day it should be suspected to die. During later stages a change of shape can no longer be used as a reliable indicator since physiological changes in shape occur subsequently. In some cases of embryonic mortality a disorganization of the embryonic membranes have been observed (Fig. 1.97). Deviations from the typical arrangement of the allantoic yolk sac membrane occur in some cases of embryonic death during the ascending phase of the embryo (GINTHER et al. 1985).

The lack of a heart beat is the most reliable sign for embryonic death. Shortly before death a bradycardia can be seen in some embryos. In the intact embryo the heart rate is usually above 150 beats per minute.

Another indication that an embryonic death might be in progress is the inadequate size of the vesicle (small-for-date) due to the subnormal volume of embryonic fluid (GINTHER et al. 1985). An embryonic resorption occurring during the first 3 weeks of gestation usually runs a rapid course. It only takes a few days from noticing the first signs of a disorder until the embryonic vesicle has disappeared. After the 3rd week some resorptions run a protracted course (Fig. 1.96 and 1.97). In mares that loose their embryo at a later stage, a preceding subnormal vesicular size portends impending death. The involved embryonic structures sometimes continue to grow for several days and rarely for a few weeks (DARENIUS et al. 1988) yet do not obtain a normal growth rate and eventually die.

Avtorsko zaščiteno gradivo

Downloaded From Vet-eBooks.com

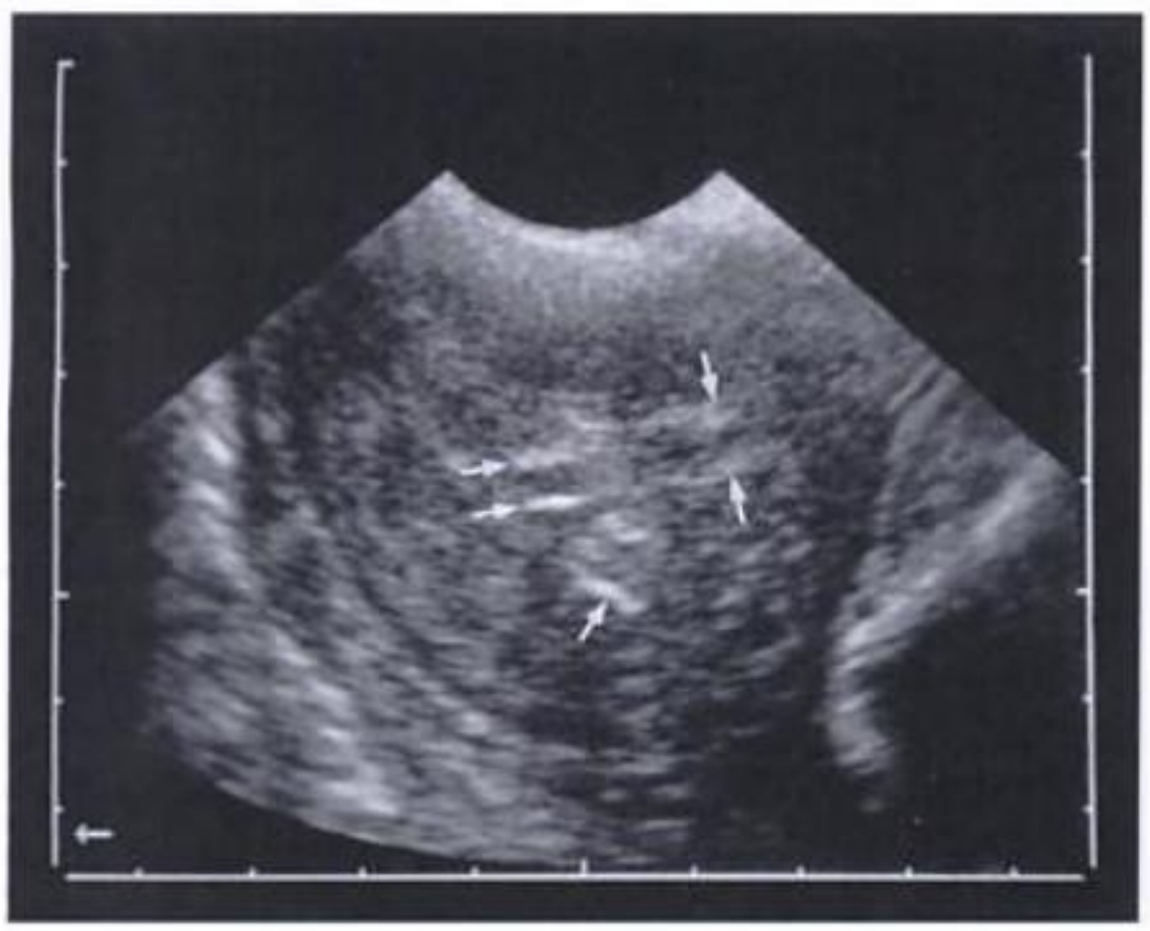


Fig. 1.98: Uterus 4 days after the death of the fetus on about Day 70 of pregnancy. At this time the fetal fluids had largely disappeared. Hyperechoic fetal remnants (arrows) were still detectable by ultrasonography for another 2 weeks.

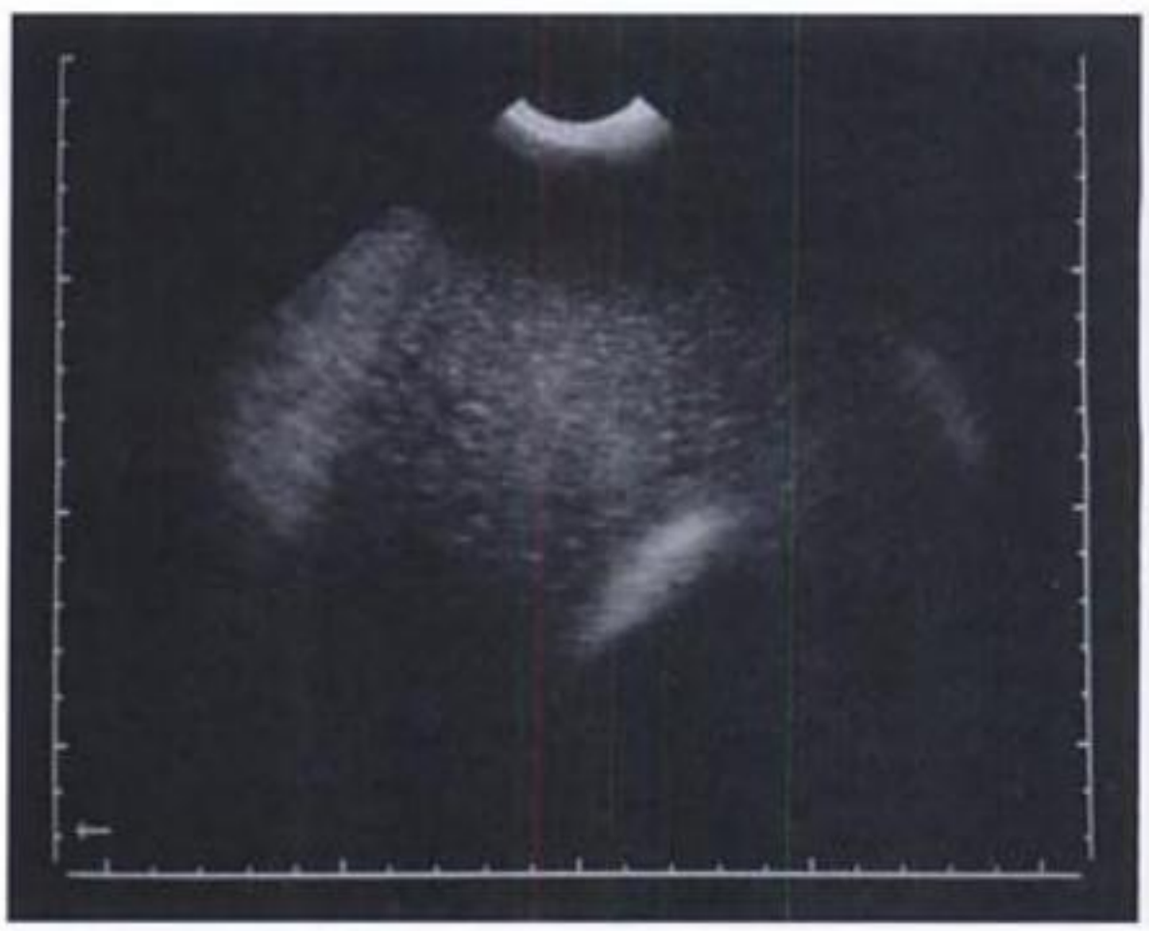


Fig. 1.99: Hydrops of the placental membranes in a mare at day 230 of gestation. The excessive accumulation of fluid can be seen to extend beyond the maximal penetration depth of the sound waves. The fetus could not be detected by transrectal ultrasonography.

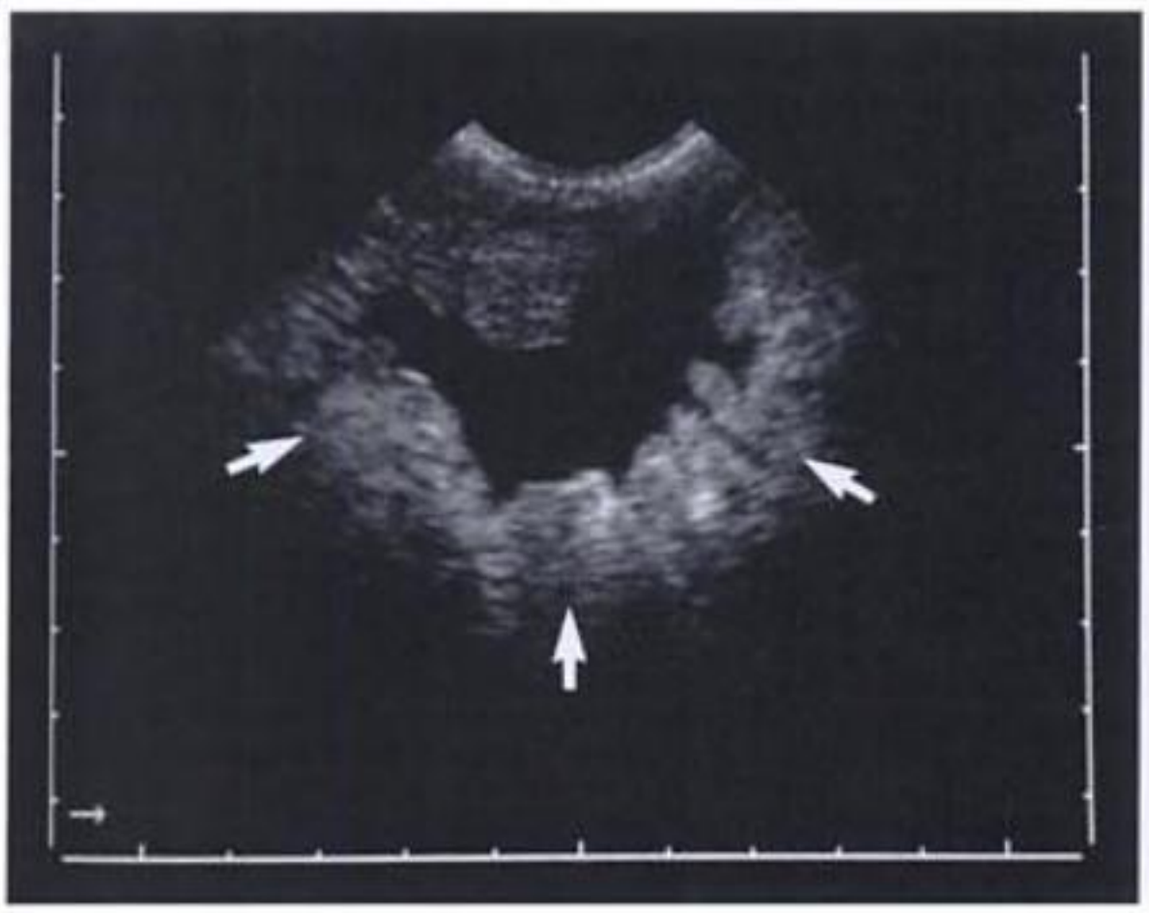


Fig. 1.100: Uterus (arrows) of a mare with a normal postpartum period 84 hours (3.5 days) after parturition. Within the uterus the anechoic lochial secretion expanding over a few centimeters can be seen.

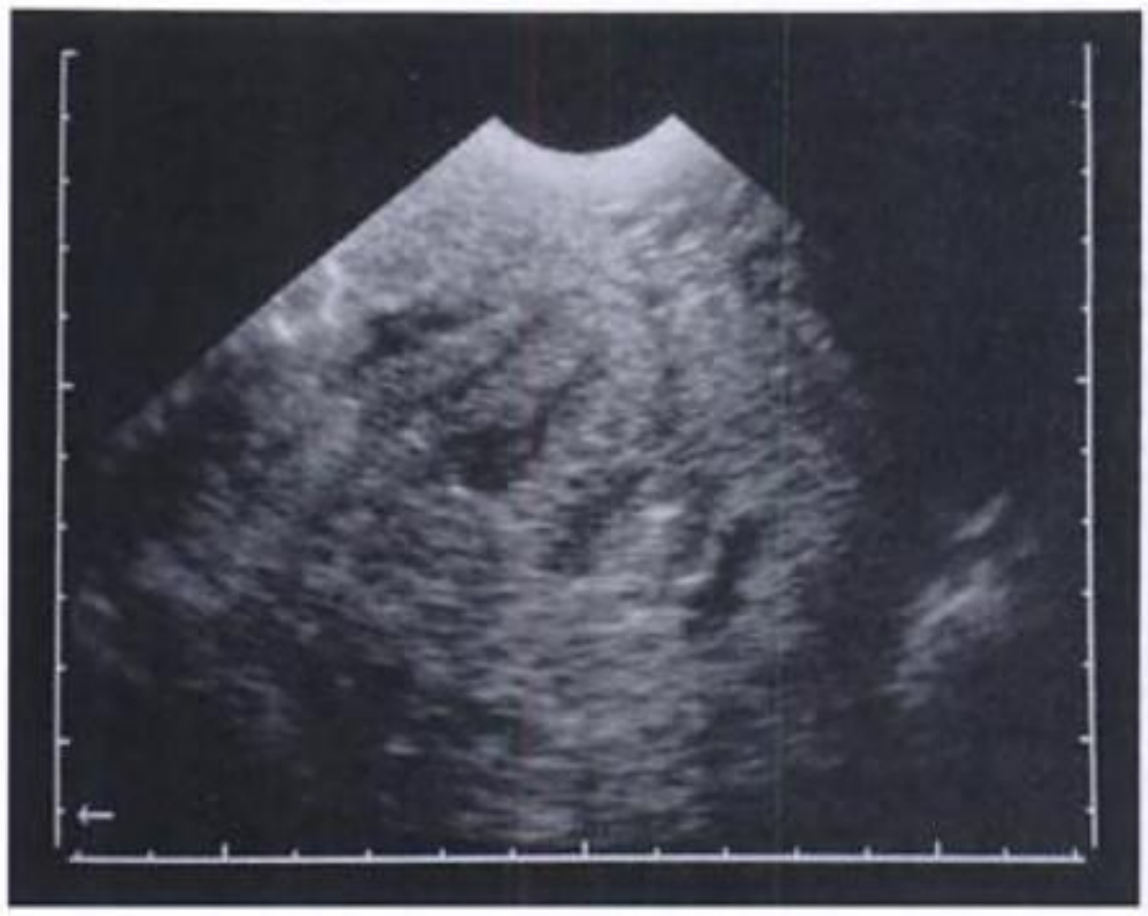


Fig. 1.101: Normal involution of the uterus in a mare 15 hours post partum. The uterine lumen is largely closed. A small amount of hypoechoic fluid is visible between the endometrial folds.

Avtorsko zaščiteno gradivo

Downloaded From Vet-eBooks.com

1.3.4.2 Abnormal pregnancy

There can be many signs of abnormal events during advanced pregnancy. The shape and size of the fetal sac can no longer be assessed, because it has become too large. Ultrasound examinations at this stage concentrate on the fetus (see also Chapter 1.3.3). In cases of imminent abortion it has been noted that the fetus had a heart rate beyond the outer limits observed in intact pregnancies.

Often the fetus is not immediately expelled after it has died. A steady decline in the amount of placental fluid can be observed by ultrasonography in such cases. The sonoanatomy of the fetus also changes. Many structures that can be seen in live fetuses become less clear (Fig. 1.98). Parenchymatous organs in particular, which undergo rapid postmortem changes and are normally traversed by a rich supply of blood vessels change their typical appearance (STAUDACH 1986). The hypoechoic appearance of blood vessels changes to look like the surrounding tissues, because of intravascular coagulation of blood. Soft tissues may loose their typical structure and look much less differentiated. Ossified bone segments retain their echogenicity and will therefore remain visible for a much longer period of time. Even once the placental fluids have totally disappeared fetal echoes can usually be found for several more weeks (GINTHER et al. 1985).

In hydrallantois and hydramnion cases the most obvious finding is the extensive amount of fluid in the uterus. There is an excessive accumulation of placental fluids between the uterine wall and the fetus. In some instances this is so extensive that it exceeds the scanning depth of 20 to 30 cm of low frequency ultrasound (Fig. 1. 99) and the fetus can not be reached transrectally. During transcutaneous examination it might be detectable in the vicinity of the maternal navel.

1.3.4.3 Post partum uterus

During the first few days of the post partum period the uterus of most mares contains some lochial secretions. The depth of the fluid accumulation can reach several centimeters, even in normal postpartum mares (Fig. 1.100). It sometimes happens that on the basis of an ultrasound examination a uterus is found to be free of fluid during the first few days after parturition (Fig. 1.101); not infrequently, however, lochial fluid may be found in the same uterus during a follow-up examination 1 to 2 days later (MCKINNON et al. 1988). The proportion of mares that do not have any fluid left in their uterine lumina increases significantly after Day 7 postpartum. At the time of foal heat only 25 % of mares have lochial secretions in their uterus. In the case of an abnormal postpartum period with the retention of lochia the resultant fluid accumulation in the uterus can be strikingly extensive and many centimeters deep (Fig.

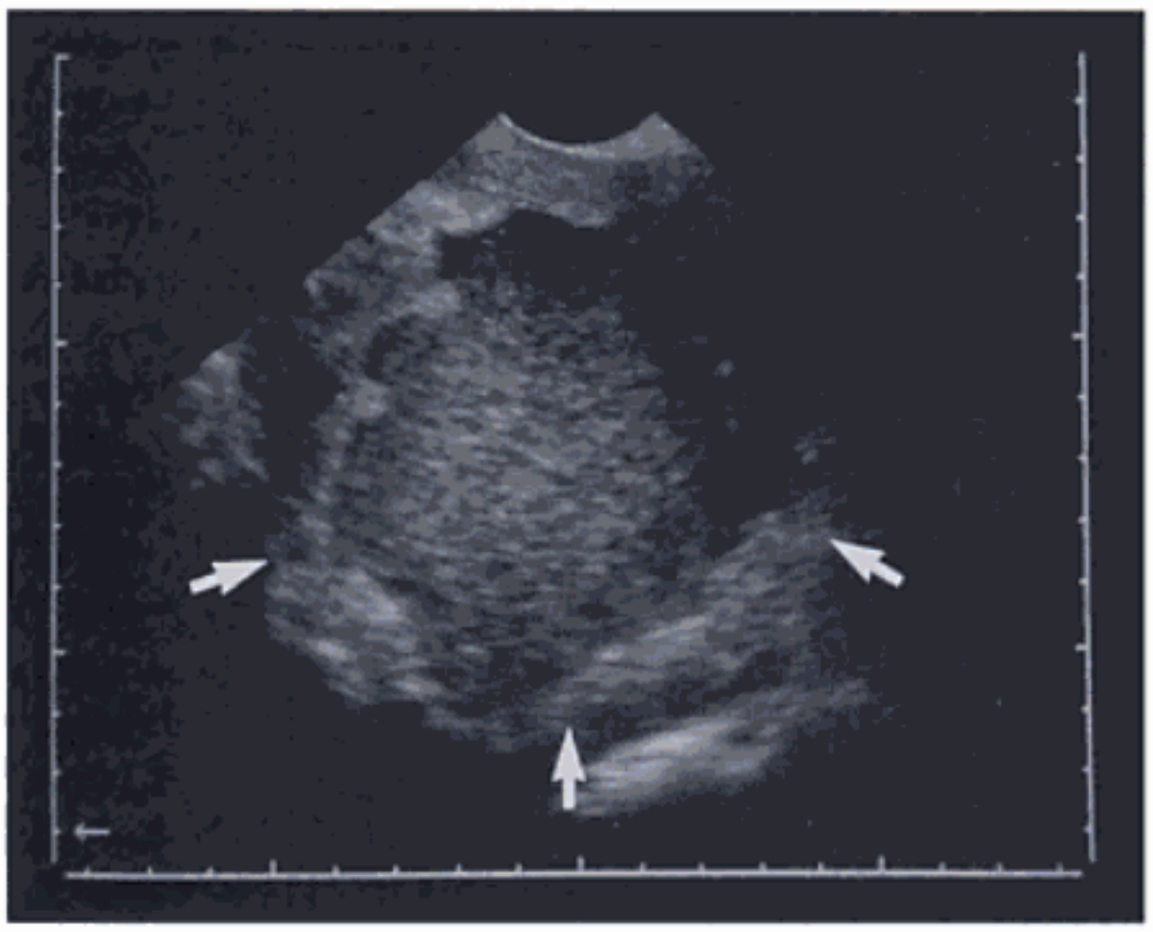


Fig. 1.102: Lochiometra in a mare 4.5 days postpartum. The fluid pool in the uterus (arrows) extends many centimeters deep. The same day 1.5 l of fluid were drained from this uterus.

Avtorsko zaščiteno gradivo

Downloaded From Vet-eBooks.com

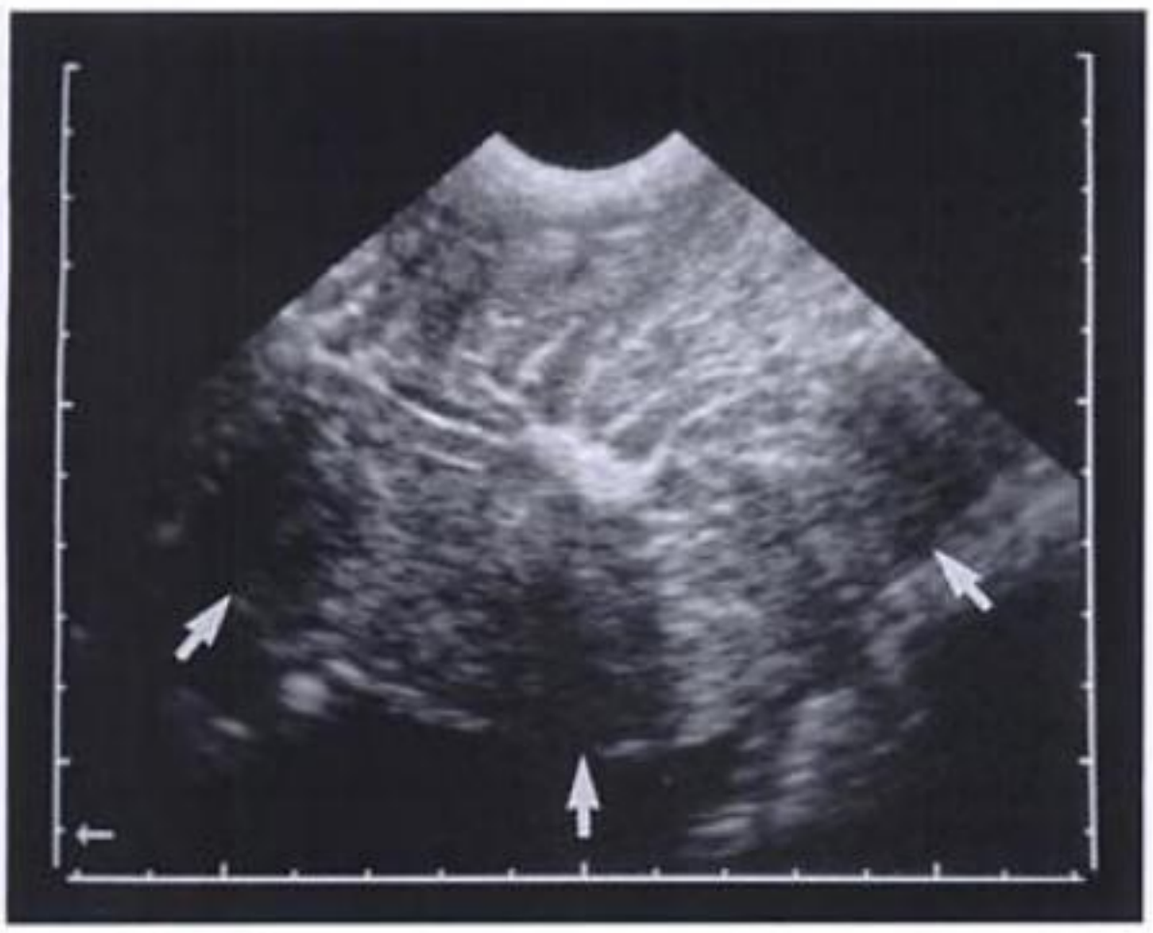


Fig. 1.103: Postpartum uterus (arrows) 3 days after parturition. There is hyperechoic lochial fluid in the uterine lumen. The hyperechoic structures branch out over the surfaces of the endometrial folds.

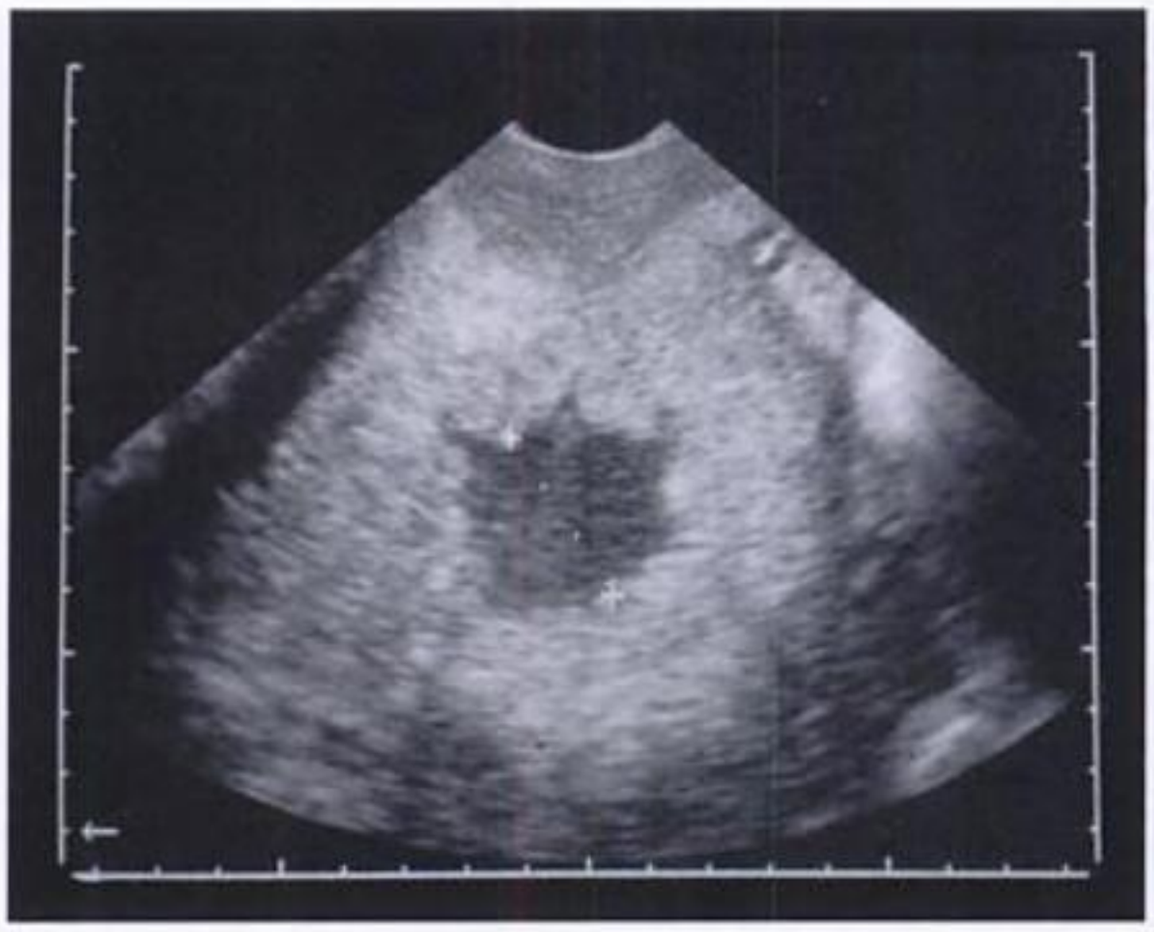


Fig. 1.104: Conspicuous accumulation of hyperechoic secretions (between the crosses) in a uterus with abnormal involution in a mare 8 days postpartum. Matings during foal heat and the next heat did not result in a pregnancy.

Avtorsko zaščiteno gradivo

Downloaded From Vet-eBooks.com

1.102). The echogenicity of lochia slowly decreases over the first few weeks of the postpartum period. Immediately after parturition the tissue components and inflammatory products contained in lochial secretions cause the latter to contain floccular echoes. These reflections can become very intensive in cases of viscous, purulent lochia. Sometimes the luminal epithelium also produces hyperechoic reflections (Fig. 1.103). The superficial layer of the uterine wall forms a narrow 1 to 2 mm, very hypoechoic seam which lines the uterine lumen and spreads between the endometrial folds.

Only few of the puerperal mares which have secretions in their uteri during foal heat at the time of mating conceive (Fig. 1.104). In contrast, mares that have a solid uterine image at the same time have a much better prognosis (McKINNON et al. 1988). In terms of practical stud management this means that only mares which do not show any ultrasonic evidence of intra-uterine fluid should be bred at foal heat.

Avtorsko zaščiteno gradivo

Downloaded From Vet-eBooks.com

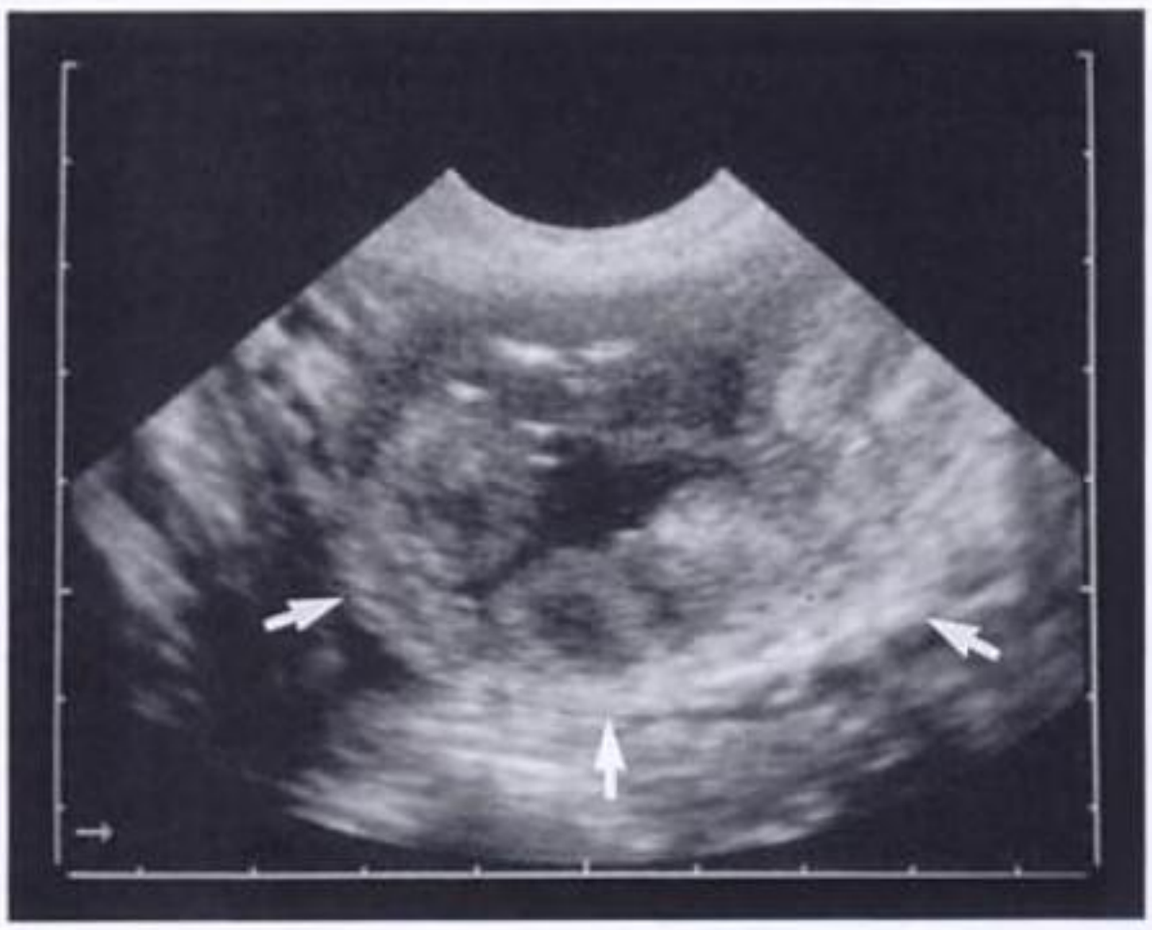


Fig. 1.105: Transverse section through the uterine horn (arrows) of a mare with chronic endometritis. The lumen contains a moderate amount of exudate.



Fig. 1.106: Uterus of a mare with large accumulation of exudate as a result of a chronic endometritis. The endometrial folds bulge into the lumen.



Fig. 1.107: Uterus (arrows) with an inflammatory secretion as a result of a chronic endometritis. The increased cellular content of the exudate causes floccular echoes.

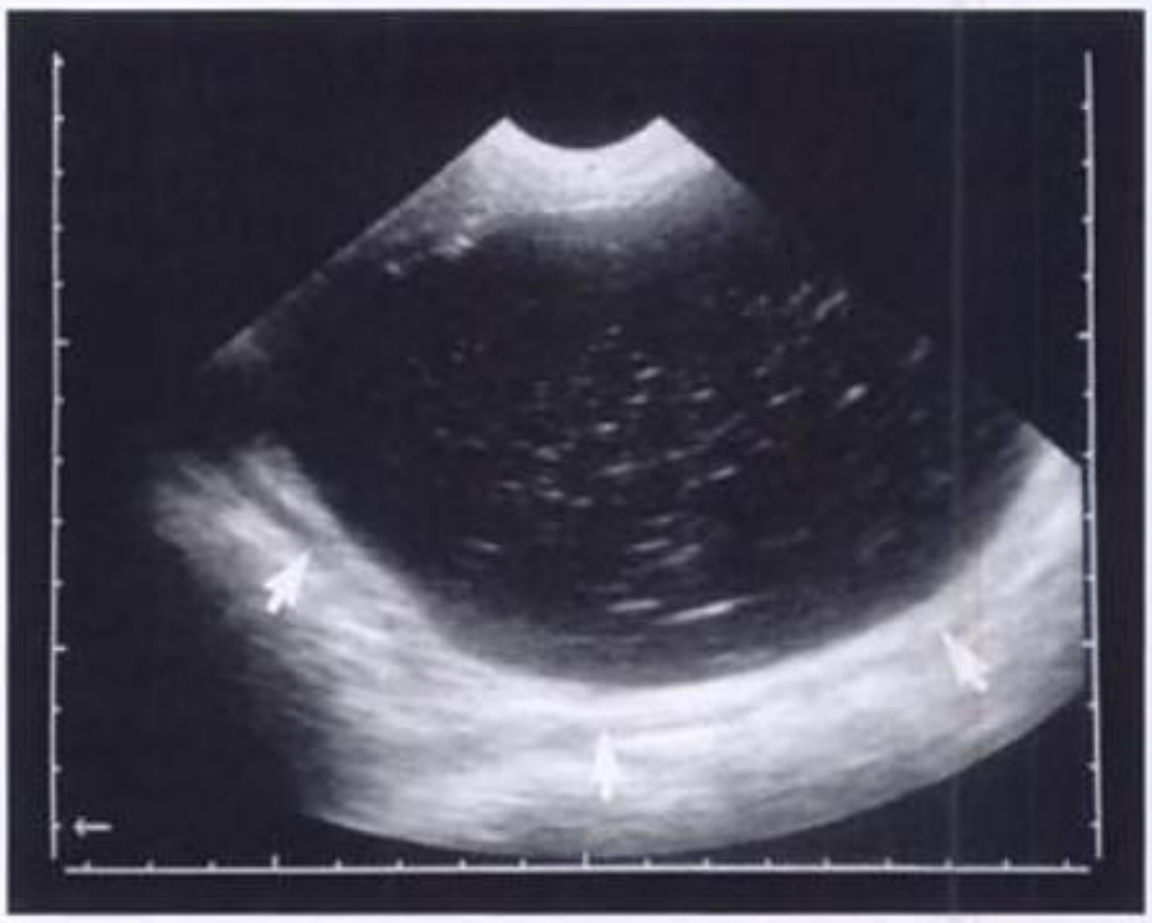


Fig. 1.108: Uterus (arrows) of a mare after the instillation of 1 l physiological saline solution for flushing. The air bubbles in the flushing solution produce intense floccular echoes.

Avtorsko zaščiteno gradivo

Downloaded From Vet-eBooks.com

1.3.4.4 Endometritis

Accumulations of fluid inside the uterine lumen are very typical of mares suffering from chronic endometritis. The amount of fluid in cases of uterine infections varies from mare to mare (Fig. 1.105 to 1.107). The amount of the secretions in the same mare can also vary from day to day. This is dependent on the stage of the cycle. Fluid accumulations found during estrus may be physiologic, but may also be an early indication of endometritis in many cases (ADAMS et al. 1987). Whenever fluid secretions are found in the uterus during diestrus they should be regarded as abnormal. Sometimes the secretions are concentrated in a particular area of the uterus and at other times they can be detected along the entire uterine lumen.

The outline of the fluid accumulations in endometritis cases is typically stellate shaped (LEIDL and KÄHN 1984) in a transverse section of a fluid filled uterine horn in which the endometrial folds bulge into the uterine lumen (Fig. 1.106). The interface between the secretion and the surrounding uterine wall is wavy. Quite frequently the 6 to 8 endometrial folds that are normally present in the uterus of a mare can be seen. The fluid distention of the uterus causes fluid to also penetrate in between the longitudinal folds, separating them from one another whereas in the absence of any fluid they normally lie in tight apposition.

The stellate shaped appearance of the sonographic cross section of a free intra-uterine fluid accumulation in cases of endometritis cannot be seen in fluid accumulations of other origins such as in intact pregnancies or with endometrial cysts. Due to the inner tension of the placental membranes or endometrial cysts these form relatively tightly filled vesicles which stretch the folds of the endometrium to form smooth lines. The interface between the uterine contents and the endometrium thus forms a smooth line. In rare individual cases a stellate shaped protrusion of the endometrial folds into the placental membranes can be found even in intact pregnancies. The cases thus far identified all occurred in older, multiparous mares. The irregular interface between the embryonic fluid and the surrounding uterine wall appears to be a consistent finding in all cases of embryonic death.

A typical feature of the uterine secretion in the case of endometritis is the increased echogenicity of the fluid. Clear fluids usually produce an anechoic, black image on ultrasonography. In contrast, the secretions of endometritis mares always contain echoes of varying intensity. Depending on the degree of change these can vary from occasional floccular echoic spots to echo patterns that can be more echoic than the surrounding uterine wall. Small air bubbles inside fluid accumulations can also produce floccular reflections. These are particularly evident after uterine infusions or flushes (Fig. 1. 108).

From a differential diagnosis point of view it should be pointed out that amniotic fluid can also be echoic during the 2nd and 3rd trimesters of gestation. Due to the increase in cellular components it is first floccular and later the amniotic fluid will have snowy reflections. This also applies to the allantoic fluid during the last trimester of pregnancy. The sonographic differentiation between the secretion of an endometritis and other fluid types in the uterus such as placental fluid or that contained in endometrial cysts, must be undertaken in conjunction with the assessment of other criteria. Important criteria in this regard are the echogenicity of the fluid, its intra-uterine position and its shape. The most suitable time for the ultrasonic diagnosis of an endometritis appears to be during the mid to late diestrous period (ADAMS et al. 1987). At this stage of the cycle, pathologic fluid secretions seem to be most prominent and can still be differentiated from the possibly physiologic secretions that may appear during estrus.

Avtorsko zaščiteno gradivo

Downloaded From Vet-eBooks.com

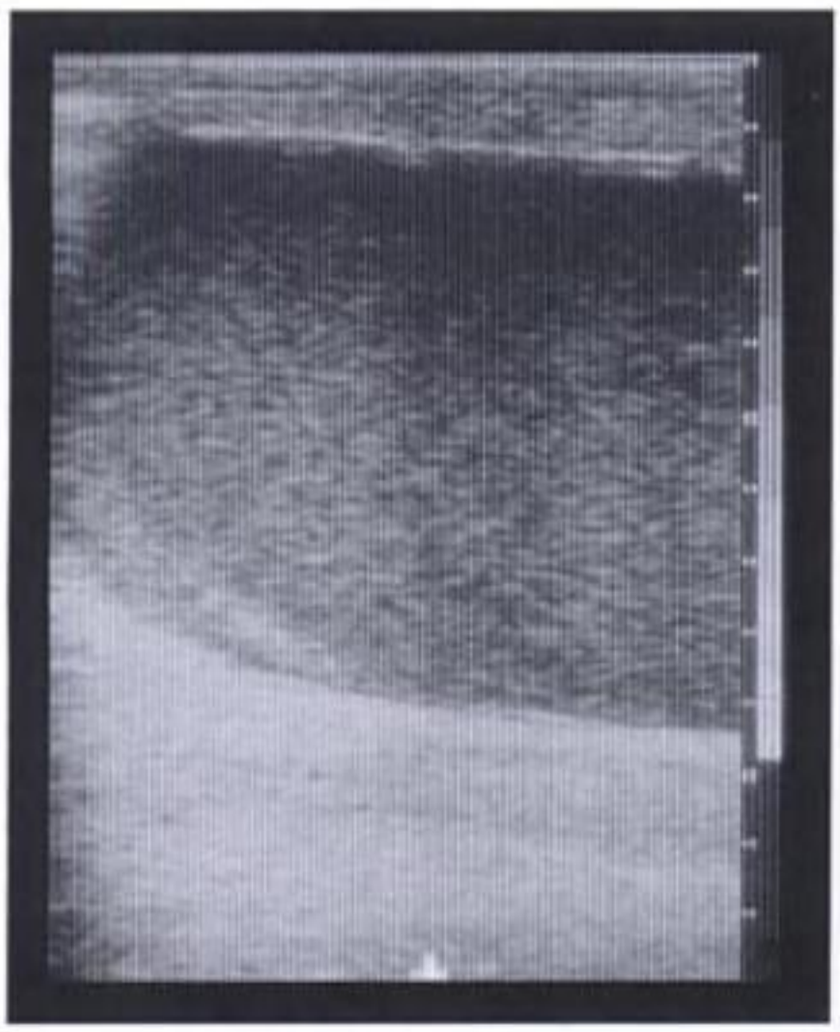


Fig. 1.109: Pyometra in a mare. The uterus is severely distended by a large amount of fluid. Due to the large number of leukocyte the purulent exudate contains very snowy reflections.

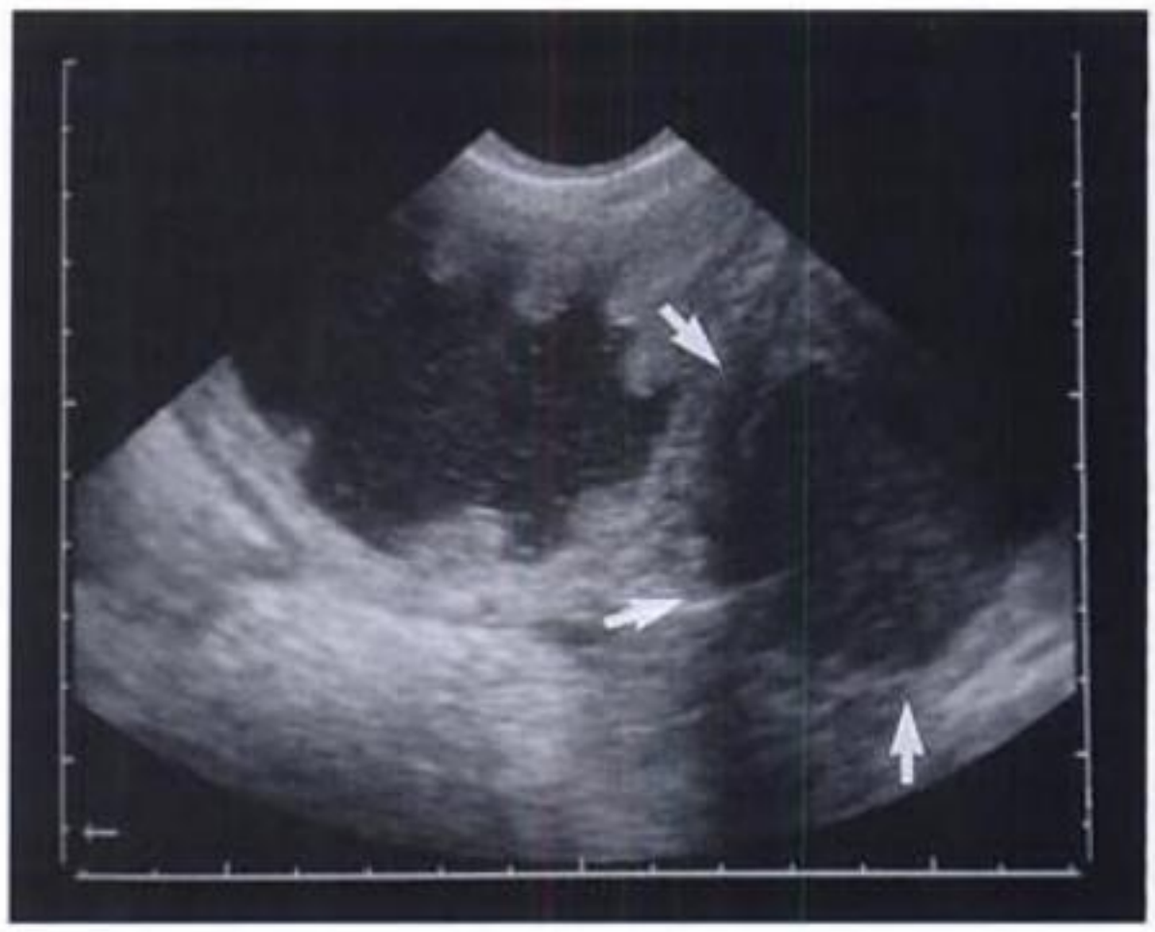


Fig. 1.110: Uterus and urinary bladder (arrows) of a mare suffering from severe endometritis. The uterus, with its endometrial folds bulging into the lumen, lies cranial to the urinary bladder.

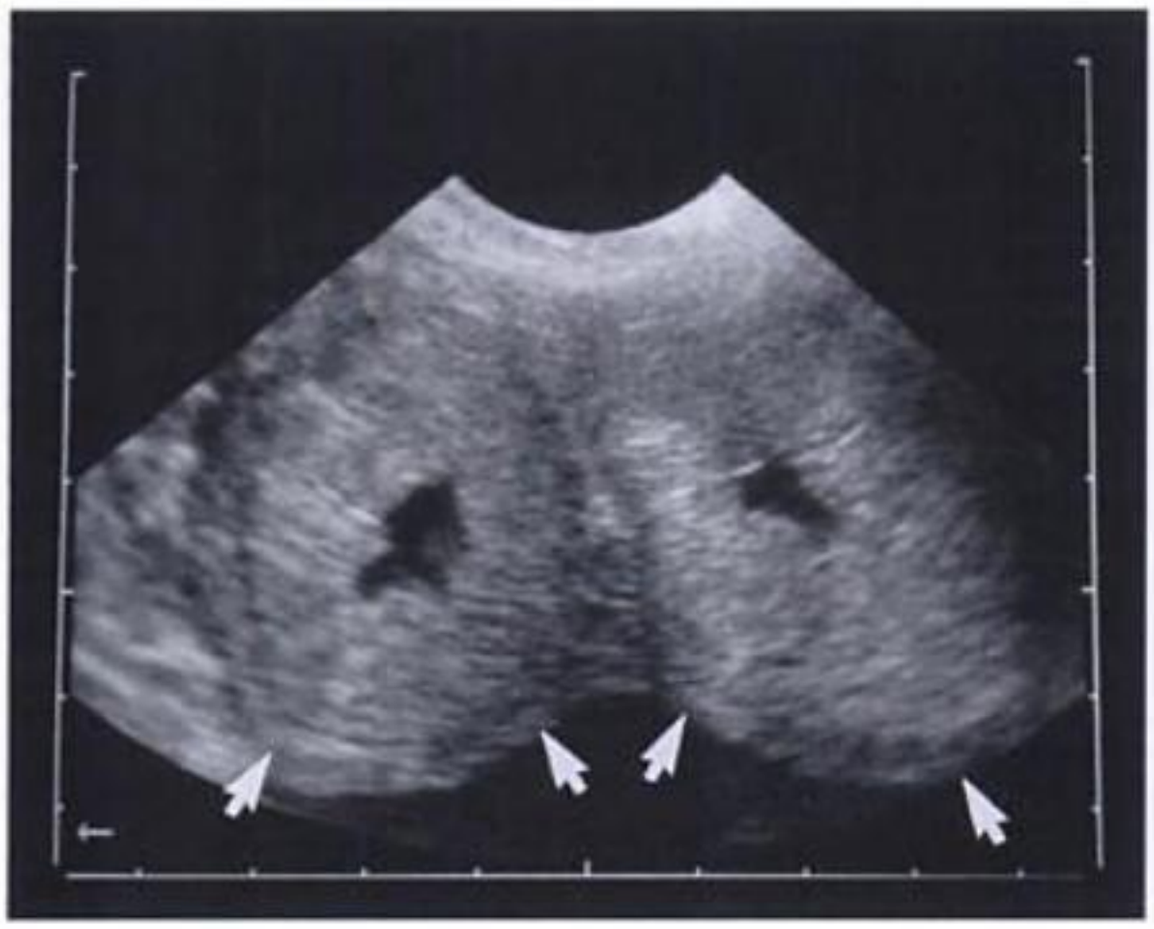


Fig. 1.111: Transverse section of both uterine horns (arrows) of a mare suffering from mucometra. The hypoechoic secretion is surrounded by the thickened uterine wall. A persistent hymen in this 2 year old mare caused the retention of fluid in her uterus and vagina.

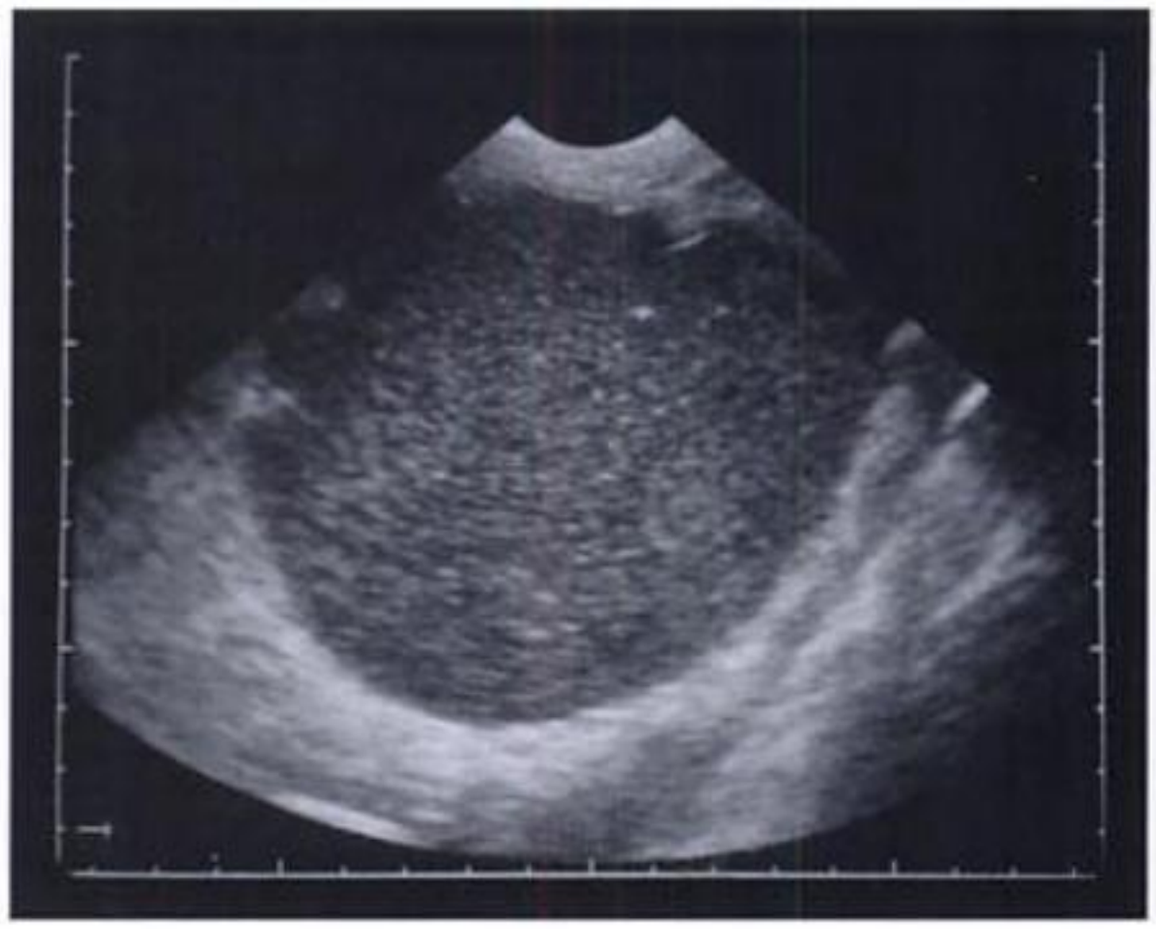


Fig. 1.112: Urometra in a mare. The uterus extends cranially. The intra-uterine fluid contains snowy reflections such as can be also typical for equine urine.

Avtorsko zaščiteno gradivo

Downloaded From Vet-eBooks.com

1.3.4.5 Pyo-, muco- and urometra

Pyometra represents a particularly severe form of endometritis. Its ultrasonic image features an extreme dilatation of the uterus (Fig. 1.109). Through this the endometrial folds are stretched and the interface between the uterine contents and the wall is smooth. Within the secretions of pyometra there are usually intensive reflections which increase in density ventrally. This is caused by the sedimentation of increased amounts of cellular components as well as the increasing consistency of the pyometra fluid in the uterus.

The ultrasound image of the urinary bladder can look much like that of a pyometra (Fig. 1.110). Due to the high viscosity of equine urine the luminal contents of the urinary bladder show an echo pattern with intensive reflections which can be confused with that seen in a pyometra. The appearance of the bladder can also be confused with a slightly cranially dilated uterus. Since this can lead to misinterpretations, a pyometra should only be diagnosed if two completely separate, closely opposed hollow organs can be demonstrated. It is important to depict the entire bladder wall without any interruption so as to ensure that there is no connection to the more cranially positioned hollow organ.

If difficulties are experienced in differentiating between a pyometra and a pregnant uterus efforts should be made to find floating segments of the amniotic membrane or other fetal structures such as the umbilical cord or parts of the fetus itself.

The ultrasonic diagnoses of muco- and urometra are based on similar criteria as are used for a pyometra. Mucometra is occasionally diagnosed in mares with an imperforate hymen. Most commonly the diagnosis is made in young fillies. After the onset of ovarian and uterine cyclic activity during puberty, the usual outflow of secretions from the genital tract is prevented by the persistent hymen. This then leads to the accumulation of the mucous secretions in the vagina and uterus. Apart from typical clinical signs, such as the protrusion of the hymen from the vulva or the rectally palpable enlargement of the uterus, the retained fluid can also be demonstrated sonographically in several sections of the uterus (Fig. 1.111).

Anatomical changes of the genitalia, such as the cranioventral displacement of vagina and uterus in the presence of an open cervix, can cause urine to flow cranially into the uterus and establish a urometra. Ultrasonically such a uterus appears fluid-filled and widely dilated (Fig. 1.112). The characteristic echogenicity of equine urine often also leads to floccular reflections in the uterine contents as in cases of urometra.

Avtorsko zaščiteno gradivo

Downloaded From Vet-eBooks.com

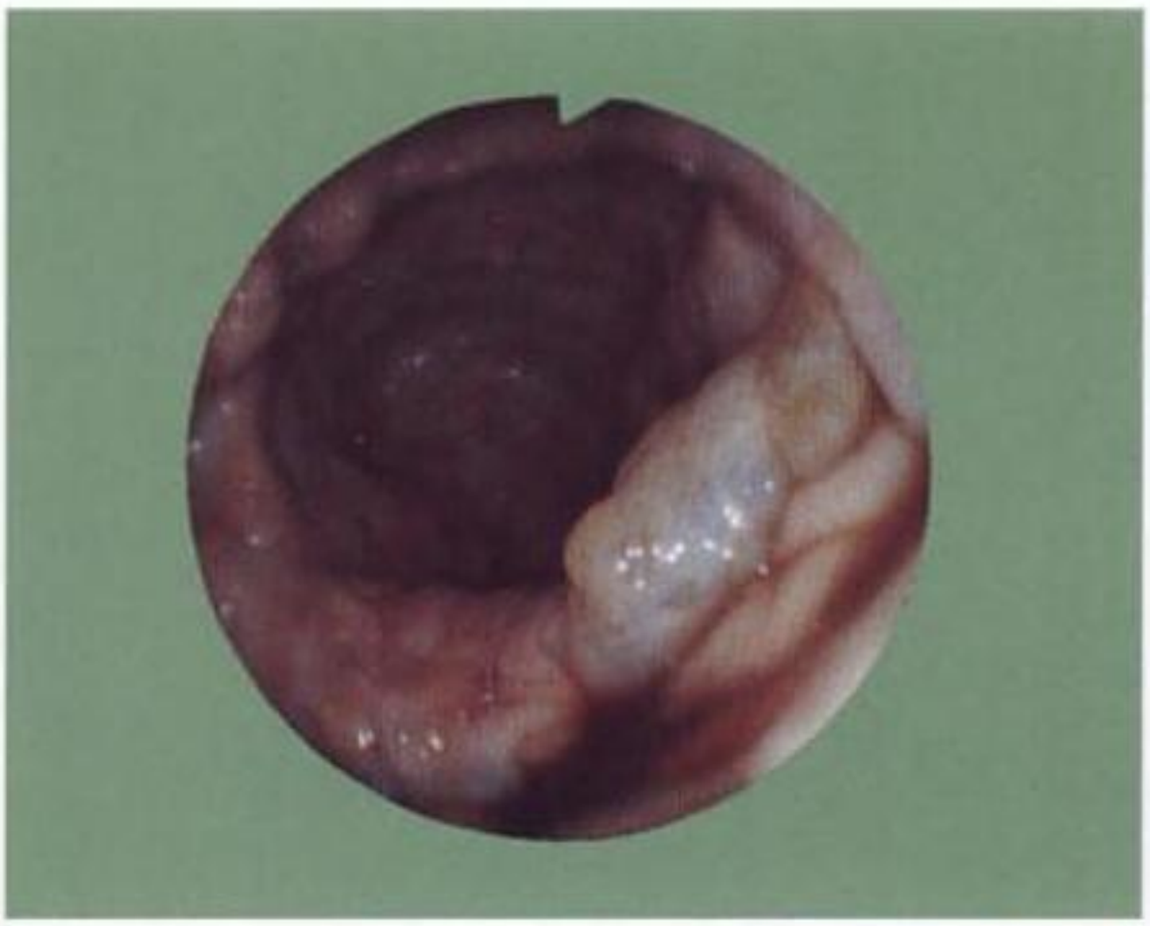


Fig. 1.113: Endoscopic view of a multilocular endometrial cyst in the uterine horn of a mare. In front of the cyst is some free fluid, indicating that the mare also has an endometritis.

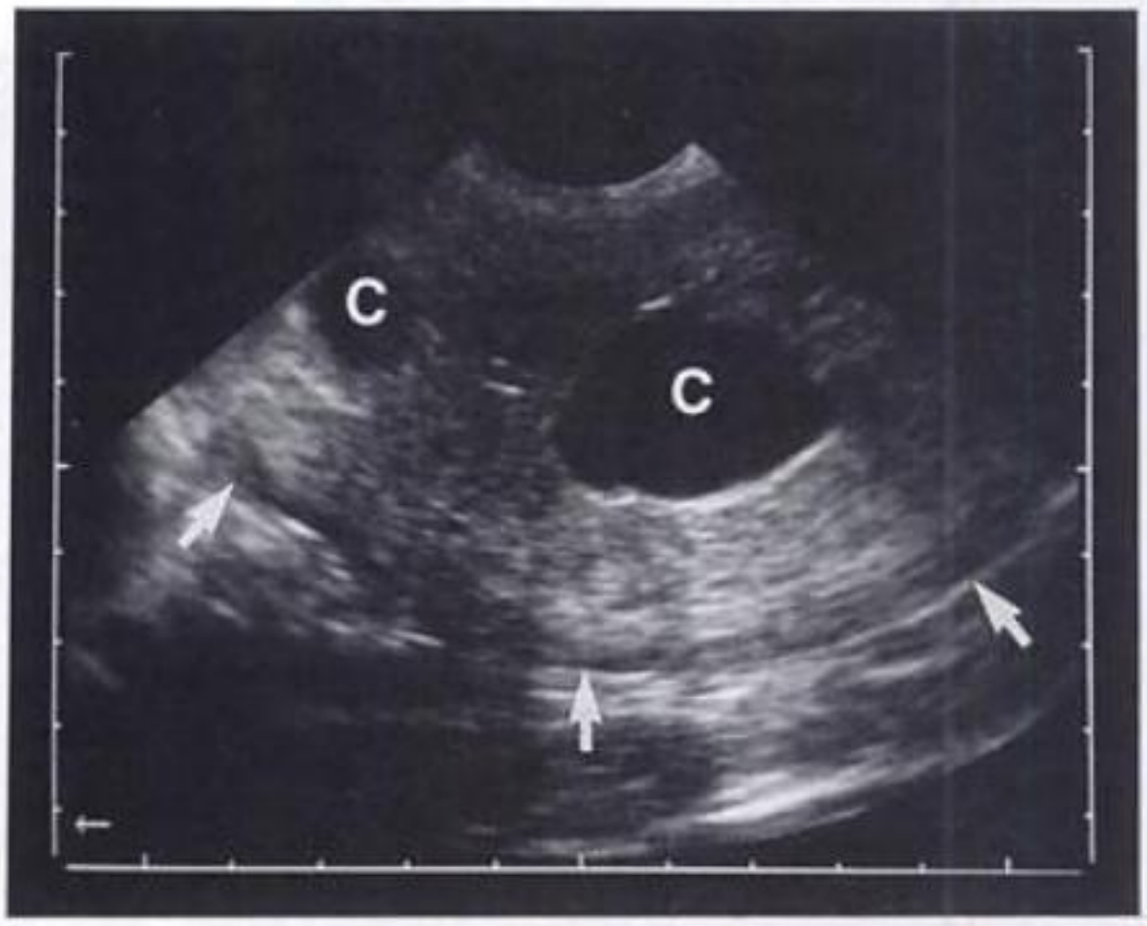


Fig. 1.114: Two endometrial cysts (C) within the uterus (arrows) of a mare. Both cysts produce an image which could be confused with an embryonic vesicle during an ultrasound examination.



Fig. 1.115: Large endometrial cysts with multiple septa in the uterus of a mare. The cysts were opened using a biopsy punch and the mare conceived three weeks later.

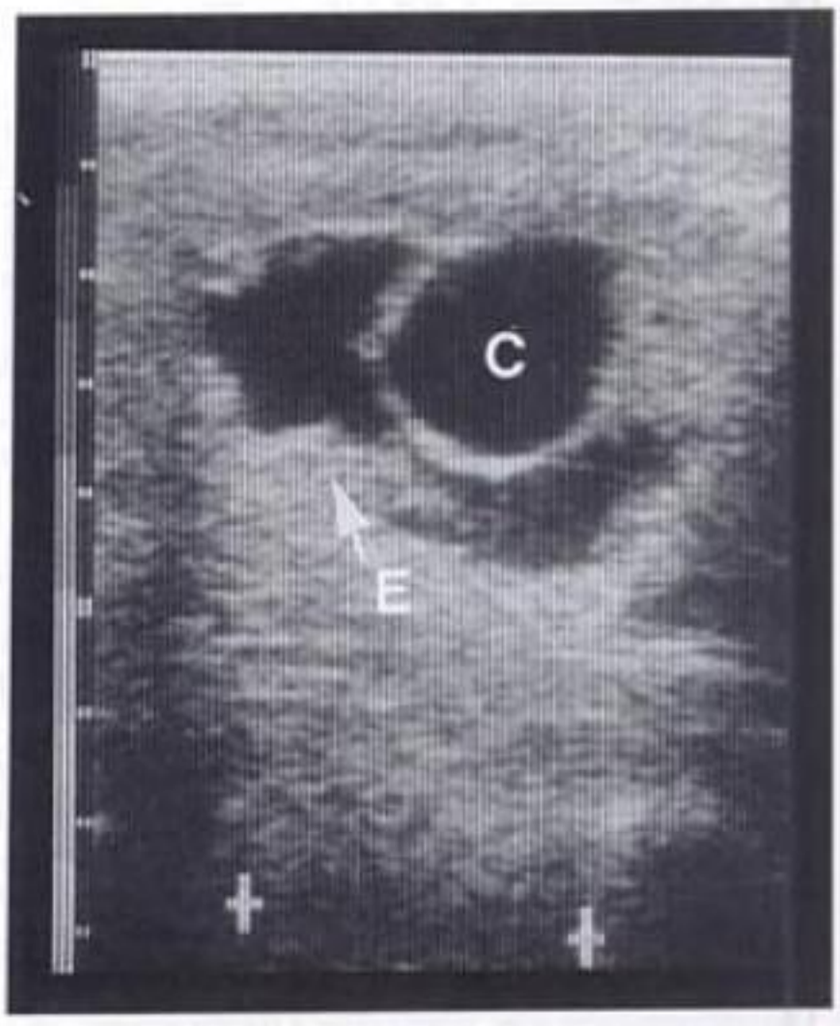


Fig. 1.116: Endometrial cyst (C) and conceptus on Day 29 of pregnancy. The cyst bulges into the embryonic vesicle containing the embryo (E). The pregnancy continued to develop uneventfully.

Avtorsko zaščiteno gradivo

Downloaded From Vet-eBooks.com

1.3.4.6 Endometrial cysts

Endometrial cysts are typically found in mares over 10 years of age (KENNEY and GANJAM 1975, KASPAR et al. 1987, LEIDL et al. 1987). In this age group cysts can be found in 20 to 25 % of all mares. The cysts can be of lymphatic or glandular origin. Endometrial cysts can be single or multiple (Fig. 1.113 and 1.114). They can occur in both, the uterine body and the uterine horns. It seems possible that the cysts can affect the fertility of the mare. They do not, however, present an absolute obstacle to the establishment of a pregnancy, because many pregnancies have been seen to develop quite normally in the presence of endometrial cysts (Fig. 1.116). In isolated cases, where the cysts are particularly large or numerous, they appear to cause embryonic maldevelopment by interfering with the normal implantation process of the embryo (ADAMS et al. 1987).

Ultrasonically, cysts look like fluid filled vesicles with a shape that can vary from spherical to long and oval. Their lumen can consist of a single cavity or can be divided into several cavities (Fig 1.115). The outer walls and possible inner septa of endometrial cysts possess the same echogenicity as that of the uterine wall. The front and back walls of the cysts which are oriented vertically to sound waves can show intensive, specular reflections. The cyst fluid, which is lymphatic fluid, is anechoic and looks virtually black on ultrasonography. The size of these cysts can vary from a few millimeters to several centimeters.

Some cysts ranging in size from 10 to 30 mm can at times be difficult to distinguish from Day 10 to Day 25 pregnancies (CHEVALIER and PALMER 1982, SIMPSON et al. 1982, LEIDL et al. 1987). From Week 4 of pregnancy the differentiation is easier, because the embryo exhibits a beating heart (Fig. 1.116). Even at this stage confusion can arise when there are twin embryonic vesicles or simultaneously occurring cysts and a conceptus.

Paying particular attention to the recognition of their typical, specific features makes the distinction between a conceptus and a cyst easier. A spherical shape, a diameter consistent with the last reported service date and a central position in the uterine lumen are all symptoms favoring the diagnosis of a conceptus. Mobility of the vesicle or the detectable presence of a heart beat inside the embryo will both confirm a pregnancy. The mobility of the embryo is usually evident until Day 15 or 16 and can be observed in most cases by scanning the vesicle for a few minutes (LEITH and GINTHER 1985).

Indications of a cyst include an irregular or oval shape, the presence of several compartments within their lumen, or their multiple occurrence in the uterus. Vesicles that lie eccentrically or intramurally in the uterus should also be viewed as cysts. Further indications that a detected vesicle may be a cyst include a discrepancy between the observed and the expected diameter (based on the last service date) of the vesicle or its failure to grow in size as demonstrated by repeated examinations at intervals of a few days.

If there is still doubt about the identity of a vesicle, other parameters than those established by ultrasonography must be relied on. These include the assessment by rectal palpation of uterine and cervical tone as well as the site and shape of a possible bulge in the uterus as well as progesterone determination. If even this cannot provide clarity, a repeated examination after a few days is indicated. If the mare is pregnant there will be a detectable increase in the size of the embryonic vesicle by the time of the next examination.

In order to avoid later confusion in differentiating between cysts and embryonic vesicles it has been found useful to look for the presence of cysts during a breeding soundness examination which is performed at the beginning of the breeding season, well before the mare is bred for the first time. During this examination the presence, locality, number and size of all endometrial cysts should be recorded. Should a new vesicle of the appropriate size appear during the first 3 weeks after service it would be most likely to be an embryo. Endometrial cysts grow much slower than embryos and they tend to remain sonographically unchanged for much longer than embryos.

Avtorsko zaščiteno gradivo

Downloaded From Vet-eBooks.com

References to preface

BOTERO, O., F. MARTINAT-BOTTÉ et F. CHEVALIER (1984): Diagnostic précoce de gestation par échographie d'ultrasons. Journeés Rech. Porcine en France 16, 181–188.

BOULET, D. (1982): Application de l'échographie au diagnostic de gestation chez la chienne Braque de Weimar. Bull. Acad. vét. Fr. 55, 229–232.

CHAFFAUX, S., F. VALON et J. MARTINEZ (1982): Evolution de l'image échographique du produit de conception chez la vache. Bull. Acad. vét. Fr. 55, 213–221.

CHEVALIER, F. and E. PALMER (1982): Ultrasonic echography in the mare. J. Reprod. Fert., Suppl. 32, 423–430.

DE BOIS, C. H. W. en M. A. M. TAVERNE (1984): Drachtigheidsonderzoek bij het schaap D. M. V. twee-dimensionele echografie. Vlaams diergeneesk. Tijdschr. 53, 240–252.

DONALD, I., J. MACVICAR and T. G. BROWN (1958): Investigation of abdominal masses by pulsed ultrasound. Lancet 1, 118–1191.

FOWLER, D. G. and J. F. WILKINS (1984): Diagnosis of pregnancy and number of foetuses in sheep by real-time ultrasonic imaging. I. Effects of number of foetuses, stage of gestation, operator and breed of ewe on accuracy of diagnosis. Livestock Production Science 11, 437–450.

GINTHER, O. J. (1983): Fixation and orientation of the early equine conceptus. Theriogenology 19, 619–623.

GINTHER, O. J. and R. A. PIERSON (1984): Ultrasonic anatomy of equine ovaries. Theriogenology 21, 471–483.

INABA, T., Y. NAKAZIMA, N. MATSUI and T. IMORI (1983): Early pregnancy diagnosis in sows by ultrasonic linear electronic scanning. Theriogenology 20, 97–101.

IRIE, M., K. OHMOTO and S. KUMAGA (1984): Diagnosis of pregnancy in pigs by real time ultrasonic B-mode scan. Jap. J. zootech. Sci. 55, 381–388.

KÄHN, W. (1985): Zur Trächtigkeitsdiagnose beim Rind mittels Ultraschall. Tierärztl. Umsch. 40, 472–477.

KÄHN, W. und W. LEIDL (1987): Echographische Befunde an Ovarien von Stuten. Tierärztl. Umsch. 42, 257–266.

LAIBLIN, C., S. SCHMIDT und J. W. DUDENHAUSEN (1982): Erste Erfahrungen mit dem ADR-Real-Time-Scanner zur Trächtigkeitsdiagnose bei Schaf, Schwein, Hund und Katze. Berl. Münch. tierärztl. Wschr. 95, 473–476.

LEGRAND, J. J., B. CARLIER, I. BERTRAND et P. F. VIARD (1982): Images échographiques de l'anatomie abdominale des carnivores domestiques. Bull. Acad. vét. Fr. 55, 223–228.

LEIDL. W. and W. KÄHN (1984): Differentialdiagnostische Befunde bei der Frühträchtigkeitsuntersuchung von Stuten mit dem Ultraschallverfahren (Echographie). Vlaams diergeneesk. Tijdschr. 53, 170–179.

MAILHAC, J. M., S. CHAFFAUX, J. J. LEGRAND, B. CARLIER et F. HEITZ (1980): Diagnostic de la gestation chez la chatte: utilisation de l'échographie. Recl. Méd. vét. Éc. Alfort 156, 899–907.

PALMER, E. and M. A. DRIANCOURT (1980): Use of ultrasonic echography in equine gynecology. Theriogenology 13, 203–216.

PIERSON, R. A. and O. J. GINTHER (1984a): Ultrasonography for detection of pregnancy and study of embryonic development in heifers. Theriogenology 22, 225–233.

PIERSON, R. A. and O. J. GINTHER (1984b): Ultrasonography of the bovine ovary. Theriogenology 21, 495–504.

REEVES, J. J., N. W. RANTANEN and M. HAUSER (1984): Transrectal real-time ultrasound scanning of the cow reproductive tract. Theriogenology 21, 485–494.

SIMPSON, D. J., R. E. S. GREENWOOD, S. W. RICKETTS, P. D. ROSSDALE, M. SANDERSON and W. R. ALLEN (1982): Use of ultrasound echography for early diagnosis of single and twin pregnancy in the mare. J. Reprod. Fert., Suppl. 32, 431–439.

TAINTURIER, D., L. LIJOUR, M. CHAARI, K. W. SARDJANA et B. DENIS (1983a): Diagnostic de la gestation chez la brebis par échotomographie. Revue Méd. vét. 134, 523–526.

TAINTURIER, D., L. LIJOUR, M. CHAARI, K. W. SARDJANA et LE NET (1983b): Diagnostic de la gestation chez la chèvre par échotomographie. Revue Méd. vét. 134, 597–599.

TAVERNE, M. A. M., O. SZENCI, J. SZÉTAG and A. PIROS (1985): Pregnancy diagnosis in cows with linear-array real-time ultrasound scanning: a preliminary note. The Veterinary Quarterly 7, 264–270.

VALON, F., F. SEGARD et St. CHAFFAUX (1982): Échotomographie en temps réel de l'utérus chez la jument. Bull. Acad. vét. Fr. 55, 187–211.

WHITE, I. R., A. J. F. RUSSEL and D. G. FOWLER (1984): Real-time ultrasonic scanning in the diagnosis of pregnancy and the determination of fetal numbers in sheep. Vet. Rec. 115, 140–143.

WHITE, I. R., A. J. F. RUSSEL, I. A. WRIGHT and T. K. WHYTE (1985): Real-time ultrasonic scanning in the diagnosis of pregnancy and the estimation of gestational age in cattle. Vet. Rec. 117, 5–8.

References to chapter 1

ADAMS, G. P., J. P. KASTELIC, D. R. BERGFELT and O. J. GINTHER (1987): Effect of uterine inflammation and ultrasonically-detected uterine phathology on fertility in the mare. J. Reprod. Fert., Suppl. 35, 445–454.

ADAMS-BRENDEMUEHL, C. and F. S. PIPERS (1987): Antepartum evaluations of the equine fetus. J. Reprod. Fert., Suppl. 35, 565–573.

ALLEN, W. E. and P. J. GODDARD (1984): Serial investigations of early pregnancy in pony mares using real time ultrasound scanning. Equine vet. J. 16, 509–514.

ALLEN, W. E., P. E. ARBEID, K. KOOROS and J. F. PYCOCK (1987): Ultrasonic appearance of the equine corpus haemorrhagicum. Vet. Rec. 121, 422–423.

BOWMAN, T. (1986): Ultrasonic diagnosis and management of early twins in the mare. Proc. Am. Ass. Equine Practnr. 32, 35–43.

CARNEVALE, E. M., A. O. MCKINNON and E. L. SQUIRES (1988 a): Effect of preovulatory follicular fluid aspiration upon luteal function in the mare. Theriogenology 29, 231.

CARNEVALE, E. M., A. O. MCKINNON and E. L. SQUIRES (1988 b): Ultrasonic characteristics of the preovulatory follicle directly proceeding and during ovulation in the mare. Theriogenology 29, 232.

CHEVALIER, F. and E. PALMER (1982): Ultrasonic echography in the mare. J. Reprod. Fert., Suppl. 32, 423–430.

COLLES, C. M. and R. D. PARKES (1978): Foetal electrocardiography in the mare. Equine vet. J. 10, 32–37.

CURRAN, S. and O. J. GINTHER (1989): Ultrasonic diagnosis of equine fetal sex by location of the genital tubercle. J. Equine vet. Sci. 9, 77–83.

DARENIUS, K., H. KINDAHL and A. MADEJ (1988): Clinical and endocrine studies in mares with known history of repeated conceptus losses. Theriogenology 29, 1215–1232.

GINTHER, O. J. (1983 a): Mobility of the early equine conceptus. Theriogenology 19, 603–611.

GINTHER, O. J. (1983 b): Fixation and orientation of the early equine conceptus. Theriogenology 19, 613–623.

Avtorsko zaščiteno gradivo

Downloaded From Vet-eBooks.com

GINTHER, O. J. (1984 a): Intrauterine movement of the early conceptus in barren and postpartum mares. Theriogenology 21, 633–644.
GINTHER, O. J. (1984 b): Mobility of twin embryonic vesicles in mares. Theriogenology 22, 83–95.
GINTHER, O. J. (1984 c): Postfixation embryo reduction in unilateral and bilateral twins in mares. Theriogenology 22, 213–223.
GINTHER, O. J. (1986): Ultrasonic imaging and reproductive events in the mare. Verlag Equiservices, Cross Plains, Wisconsin, USA.
GINTHER, O. J. and R. A. PIERSON (1984 a): Ultrasonic evaluation of the reproductive tract of the mare: ovaries. J. Equine vet. Sci. 4, 11–16.
GINTHER, O. J. and R. A. PIERSON (1984 b): Ultrasonic anatomy of equine ovaries. Theriogenology 21, 471–483.
GINTHER, O. J. and R. A. PIERSON (1984 c): Ultrasonic anatomy and pathology of the equine uterus. Theriogenology 21, 505–516.
GINTHER, O. J., D. R. BERGFELT, G. S. LEITH and S. T. SCRABA (1985): Embryonic loss in mares: incidence and ultrasonic morphology. Theriogenology 24, 73–86.
HASSLER, D. (1984): Physik und Technik der Ultraschall-Diagnostik. In: Die Ultraschalldiagnostik in der Schwangerschaft. Hrsg.: H.-J. Holländer. Verlag Urban & Schwarzenberg. München, Wien, Balitmore.
HAYES, K. E. N., R. A. PIERSON, S. T. SCRABA and O. J. GINTHER (1985): Effects of estrous cycle and season on ultrasonic uterine anatomy in mares. Theriogenology 24, 465–477.
KÄHN, W. und W. LEIDL (1984): Die Ultraschalldiagnostik (Echographie) in der gynäkologischen Untersuchung der Stute. Tierärztl. Prax. 12, 203–210.
KÄHN, W. und W. LEIDL (1985): Sonographische Befunde am Uterus von Stuten mit Ultraschall bei einer Frequenz von 5 Megahertz (MHz). Pferdeheilkunde 1, 239–246.
KÄHN, W. und W. LEIDL (1987 a): Die Ultraschall-Biometrie von Pferdefeten in utero und die sonographische Darstellung ihrer Organe. Dtsch. tierärztl. Wschr. 94, 509–515.
KÄHN, W. und W. LEIDL (1987 b): Echographische Befunde an Ovarien von Stuten. Tierärztl. Umsch. 42, 257–266.
KASPAR, B., W. KÄHN, C. LAGING und W. LEIDL (1987): Endometriumzysten bei Stuten. Teil 1. Post-mortem-Untersuchungen: Vorkommen und Morphologie. Tierärztl. Prax. 15, 161–166.
KENNEY, R. M. and V. K. GANJAM (1975): Selected pathological changes of the mare uterus and ovary. J. Reprod. Fert., Suppl. 23, 335–339.
LEIDL, W. und W. KÄHN (1984): Differentialdiagnostische Befunde bei der Frühträchtigkeitsuntersuchung von Stuten mit dem Ultraschallverfahren (Echographie). Vlaams diergeneesk. Tijdschr. 53, 170–179.
LEIDL, W. and W. KÄHN (1989): Ultrasonic characteristics of pathological conditions of the equine uterus and ovaries. In: Diagnostic Ultrasound and Animal Reproduction. Current Topics in Veterinary Medicine and Animal Science 51, 21–35. Eds.: M. A. M. Taverne and A. H. Willemse. Verlag Kluwers Academic Publishers. Dordrecht, Boston, London.
LEIDL, W., B. KASPAR und W. KÄHN (1987): Endometriumzysten bei Stuten. Teil 2. Klinische Untersuchungen: Vorkommen und Bedeutung. Tierärztl. Prax. 15, 281–289.
LEITH, G. S. and O. J. GINTHER (1984): Characterization of intrauterine mobility of the early equine conceptus. Theriogenology 22, 401–408.
LEITH, G. S. and O. J. GINTHER (1985): Mobility of the conceptus and uterine contractions in the mare. Theriogenology 24, 701–711.
MATSUI, K., S. SUGANO and I. MASUYAMA (1985): Changes in the fetal heart rate of Thoroughbred horse through the gestation. Jap. J. vet. Sci. 47, 597–601.
MCKINNON, A. O., E. L. SQUIRES, L. A. HARRISON, E. L. BLACH and R. K. SHIDELER (1988): Ultrasonographic studies on the reproductive tract of mares after parturition: Effect of involution and uterine fluid on pregnancy rates in mares with normal and delayed first postpartum ovulatory cycles. J. Am. vet. med. Ass. 192, 350–353.
MERKT, H., A.-R. GÜNZEL, W. ABEL und R. MATTOS (1983): Echographie – eine Ergänzung der gynäkologischen Untersuchungsmethoden zur Zyklus- und Trächtigkeitsdiagnostik beim Pferd. Dtsch. tierärztl. Wschr. 90, 225–230.
O'GRADY, J. P., C. H. YEAGER, L. FINDLETON, J. BROWN and G. ESRA (1981): In utero visualization of the fetal horse by ultrasonic scanning. Equine Pract. 3, 45–49.
PALMER, E. and M. A. DRIANCOURT (1980): Use of ultrasonic echography in equine gynecology. Theriogenology 13, 203–216.
PIERSON, R. A. and O. J. GINTHER (1985 a): Ultrasonic evaluation of the corpus luteum of the mare. Theriogenology 23, 795–806.
PIERSON, R. A. and O. J. GINTHER (1985 b): Ultrasonic evaluation of the preovulatory follicle in the mare. Theriogenology 24, 359–368.
PIERSON, R. A. and O. J. GINTHER (1987): Follicular population dynamics during the estrous cycle of the mare. Anim. Reprod. Sci. 14, 219–231.
PIPERS, F. S. and C. S. ADAMS-BRENDEMUEHL (1984): Techniques and applications of transabdominal ultrasonography in the pregnant mare. J. Am vet. med. Ass. 185, 766–771.
PIPERS, F. S., W. ZENT, R. HOLDER and A. ASBURY (1984): Ultrasonography as an adjunct to pregnancy assessments in the mare. J. Am vet. med. Ass. 184, 328–334.
SIMPSON, D. J., R. E. S. GREENWOOD, S. W. RICKETTS, P. D. ROSSDALE, M. SANDERSON and W. R. ALLEN (1982): Use of ultrasound echography for early diagnosis of single and twin pregnancy in the mare. J. Reprod. Fert., Suppl. 32, 431–439.
SQUIRES, E. L., A. O. MCKINNON and R. K. SHIDELER (1988): Use of ultrasonography in reproductive management of mares. Theriogenology 29, 55–70.
STAUDACH, A. (1986): Fetale Anatomie im Ultraschall, Springer Verlag, Berlin, Heidelberg, New York, London, Paris, Tokyo.
TOWNSON, D. H., R. A. PIERSON and O. J. GINTHER (1989): Characterization of plasma progesterone concentrations for two distinct luteal morphologies in mares. Theriogenology 32, 197–204.
VALON, F., F. SEGARD et St. CHAFFAUX (1982): Échotomographie en temps réel de l'utérus chez la jument. Bull. Acad. vét. Fr. 55, 187–211.
WHITE, R. A. S. and W. R. ALLEN (1985): Use of ultrasound echography for the differential diagnosis of a granulosa cell tumour in a mare. Equine vet. J. 17, 401–402.
WILL, K., W. KÄHN und W. LEIDL (1988): Sonographische Untersuchungen über die präovulatorische Follikelentwicklung bei der Stute. Dtsch. tierärztl. Wschr. 95, 362–365.
WOODS, G. L., C. B. BAKER, R. B. HILLMAN and D. H. SCHLAFER (1985): Recent studies relating to early embryonic death in the mare. Equine vet. J., Suppl. 3, 104–107.

Avtorsko zaščiteno gradivo
Downloaded From Vet-eBooks.com

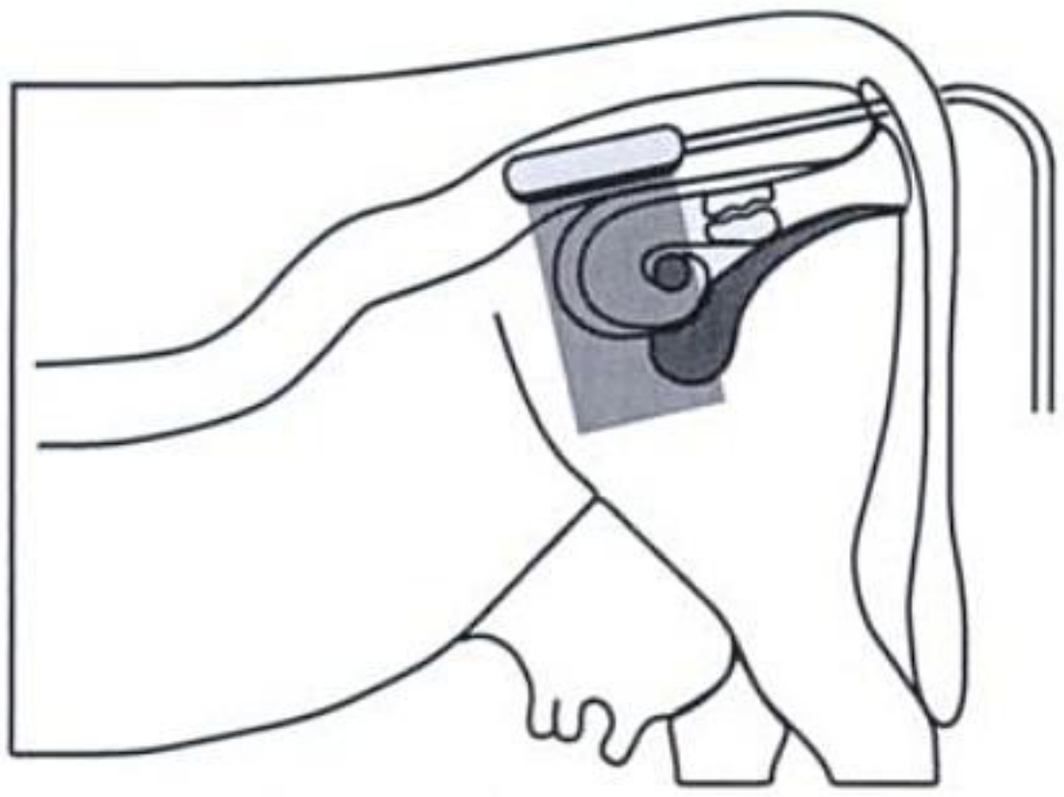


Fig. 2.1: Schematic presentation of an ultrasound examination of the internal genital tract of a cow, using a linear scanner. The ultrasound probe lies longitudinally inside the rectum, just dorsal to the uterine horn.



Fig. 2.2: Sagittal section through a non-pregnant uterus analogous to the examination plane in Fig. 2.1. The larger curvature of the uterus is demarcated by arrows.



Fig. 2.3: Schematic presentation of an ultrasound examination of the internal genital tract of a cow, using a sector scanner. Cranial view of the pelvic canal. The transversely oriented ultrasound plane produces a cross section of the uterus (1) and urinary bladder (2).

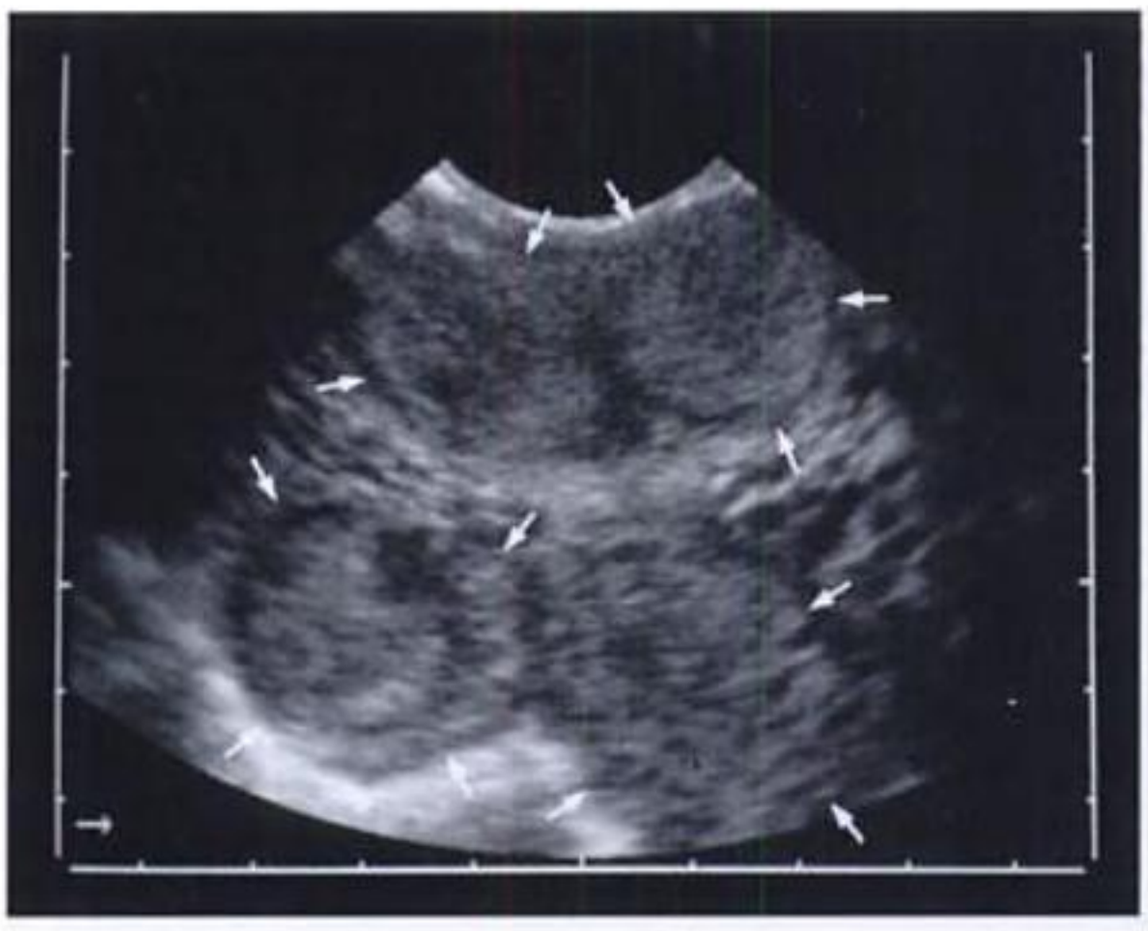


Fig. 2.4: Transverse section through a non-pregnant uterus analogous to the scanning plane in Fig. 2.3 and 2.63. The 4 transverse sections through the uterine horns are demarcated by arrows.

Avtorsko zaščiteno gradivo

Downloaded From Vet-eBooks.com

2 Ultrasonography in the cow

2.1 Technique of ultrasonography in the cow

The ultrasonographic examination of uterus and ovaries in cows is performed by transrectal sonography. The technical aspects of the procedure are largely the same as those applied in the mare (see Chapter 1.1). In the cow, too, the examination is performed in a way similar to that of the rectal palpation (Fig. 2.1 to 2.4). After the rectum has been evacuated and the internal genitalia have been palpated in the usual manner, the hand-held ultrasound probe is introduced through the anus and then advanced cranially along the rectal floor.

Generally, all commonly available ultrasound scanners (linear, sector and convex) can be used for transrectal sonography in cattle. The only condition for their use is that one must be able to manipulate the chosen ultrasound probes inside the rectum without causing damage. Experience has shown that the use of linear probes holds advantages over the other types when organs in the near field are examined. Examples of such situations are when the probe is held close to an ovary or very closely above the uterus. It is difficult, however, to turn a linear probe away from the longitudinal axis and hold it more in a transverse plane of the animal. They are thus best suited to examine sections parallel to the longitudinal axis of the body (Fig. 2.2). In contrast, sector probes offer advantages when more distant areas, such as the fetus in advanced pregnancy, are to be examined. Provided it is suitably constructed, a sector probe can be turned far enough inside the rectum to allow transverse views through the uterus to be depicted (Fig. 2.4).

Avtorsko zaščiteno gradivo

Downloaded From Vet-eBooks.com

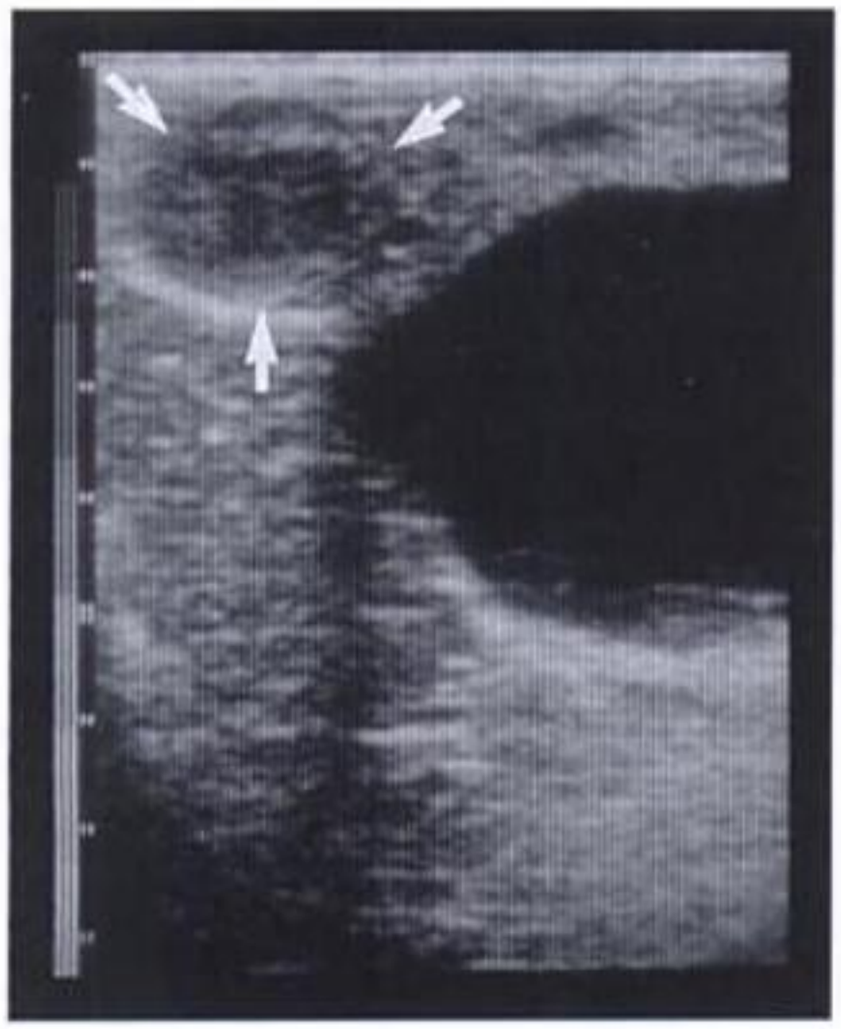


Fig. 2.5: Cranial half of the urinary bladder (fundus and body); above the fundus of the bladder is a mature corpus luteum (demarcated by arrows).

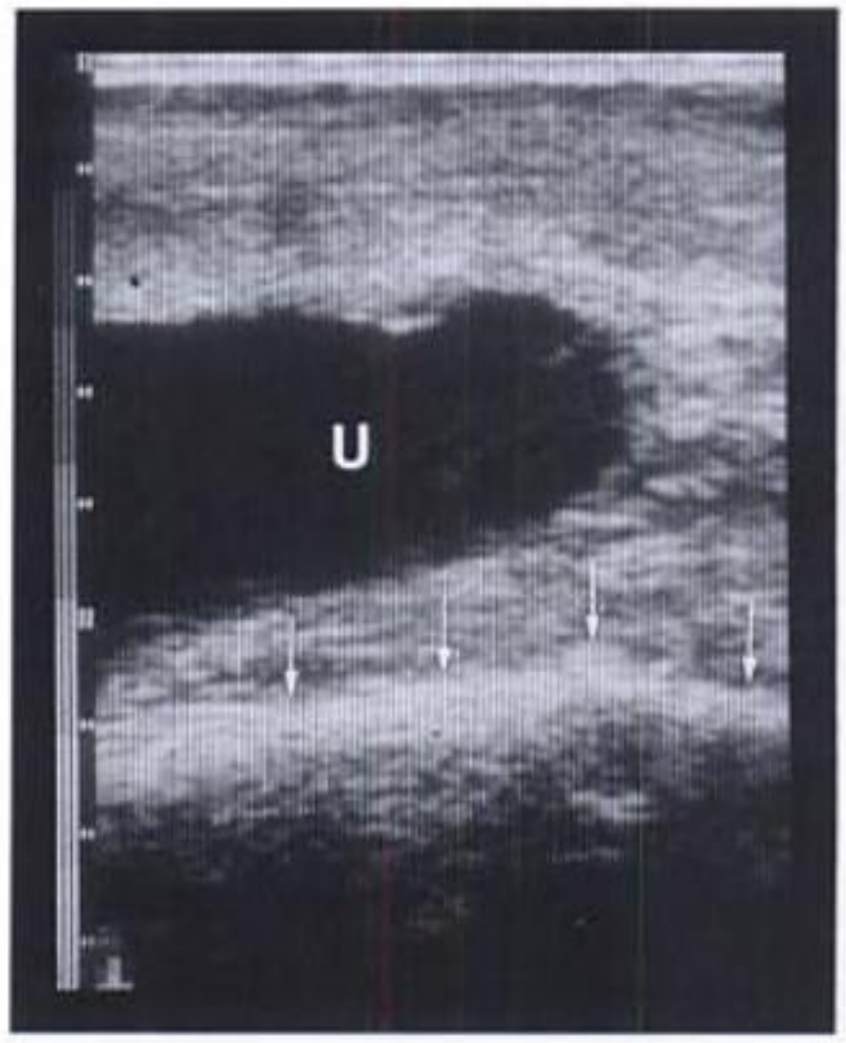


Fig. 2.6: Caudal half of the urinary bladder (U) with its neck (Cervix vesicae) and part of its body (Corpus vesicae). Ventral to the bladder lies the horizontally positioned, hyperechoic pelvic floor (arrows).



Fig. 2.7: Paramedian section through the pelvic floor (arrows); parallel to the initial echo, and stretching into the depth of the image, are a series of echoes which are caused by multiple reflections (reverberation artifacts) between the sound probe and the pelvic floor.

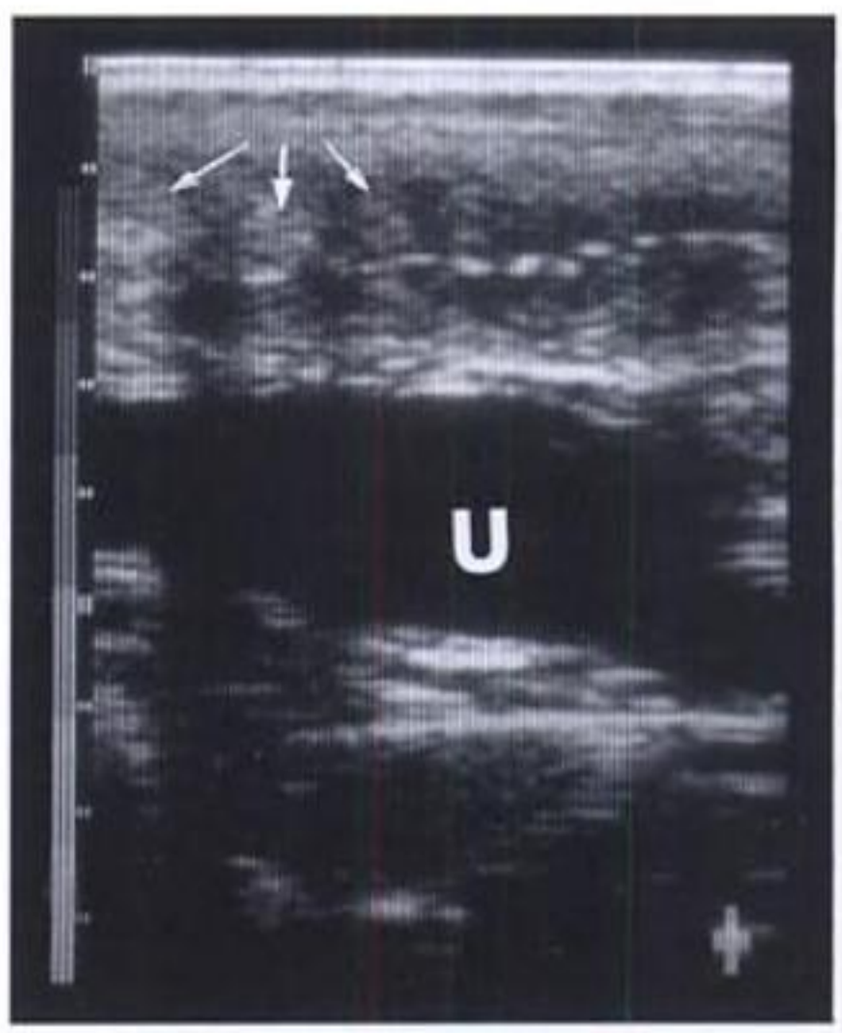


Fig. 2.8: Sagittal section through the uterine cervix; ventrally to the cervix lies the urinary bladder (U). Several cervical rings (arrows) can be recognized. In the center of the cervix is the horizontally positioned, bright linear echo of the cervical canal.

Avtorsko zaščiteno gradivo

Downloaded From Vet-eBooks.com

After passing through the anus the caudal structures in the pelvis, such as vestibulum and vagina, are only poorly recognizable. Moving further forward, the easily recognized neck of the urinary bladder will come into view (Fig. 2.6). It produces the typical image of a hollow organ containing hypoechoic fluid and expands cranioventrally to form the body of the bladder (Fig. 2.5). Ventral to the bladder, especially in the area of the neck of the bladder, the pelvic floor can be seen. Its bony components are evident as very bright, a few millimeter thick, structures. The floor of the pelvis formed by portions of the ischium and pubis, lies virtually horizontally in its cranial portion and rises slightly in a caudal direction (NICKEL et al. 1984). Deep to the echo of the pelvic floor one can often see further echoes which run parallel to it (Fig. 2.7). These are reverberation artifacts, created by the multiple reflections of sound waves between the hyperechoic bony surface and the ultrasound probe.

The cervix of the non-pregnant cow can be found at the level of the urinary bladder (Fig. 2.8). The cervical structures that can be identified include the cervical rings and a central, hyperechoic line which represents the cervical canal. Immediately cranial to the cervix, usually in the midline, appear the body and horns of the uterus. Occasionally, the uterus can also be found lateral to the urinary bladder. When the uterus has been recognized, the probe is positioned above the intercornual space. In the case of a linear array scanner with craniocaudal and dorsoventral sound beam the probe is swiveled from side to side to produce longitudinal images of the uterus (Fig. 2.2). When using a sector scanner, the operator can turn the beam through 90 degrees and thus change the scanning plane from longitudinal to transverse in relation to the body axis. In this manner transverse sections of the uterus can be obtained (Fig. 2.4).

After scanning the uterus, the probe can be rotated further laterally in order to visualize the ovaries. In their normal position they can usually be reached by the sound beam and any additional digital fixation or repositioning of the ovaries is not necessary. Care should be taken to allocate each identified ovary to the correct side. Since the exact scanning direction during an examination is not always clear to the operator and the both ovaries may be positioned rather close to one another it may happen that the ovary found first is allocated to the wrong side. Only after both ovaries can be identified in succession should they be appropriately allocated as belonging to either the left or right side.

Avtorsko zaščiteno gradivo

Downloaded From Vet-eBooks.com

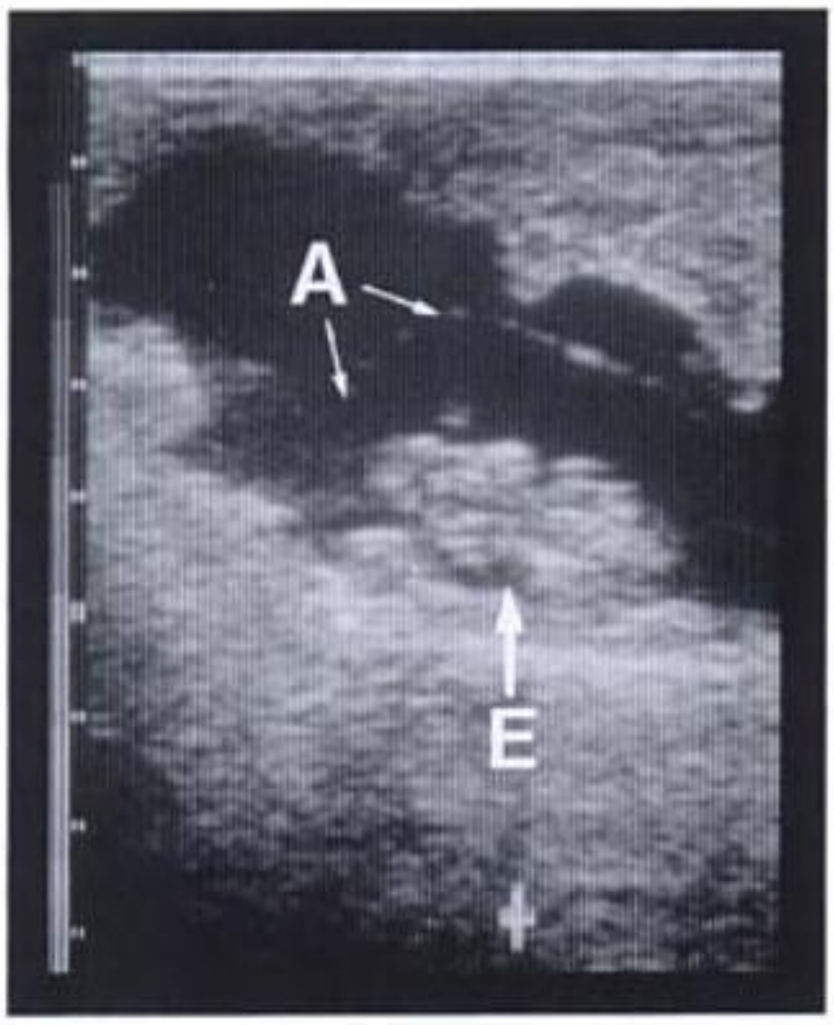


Fig. 2.9: Comparison of the image quality between lower and higher frequency ultrasound. Ultrasonogram of a conceptus on Day 45 of pregnancy at a frequency of 5.0 MHz. The embryo (E) lies on the floor of the uterus and is surrounded by its amnion (A).

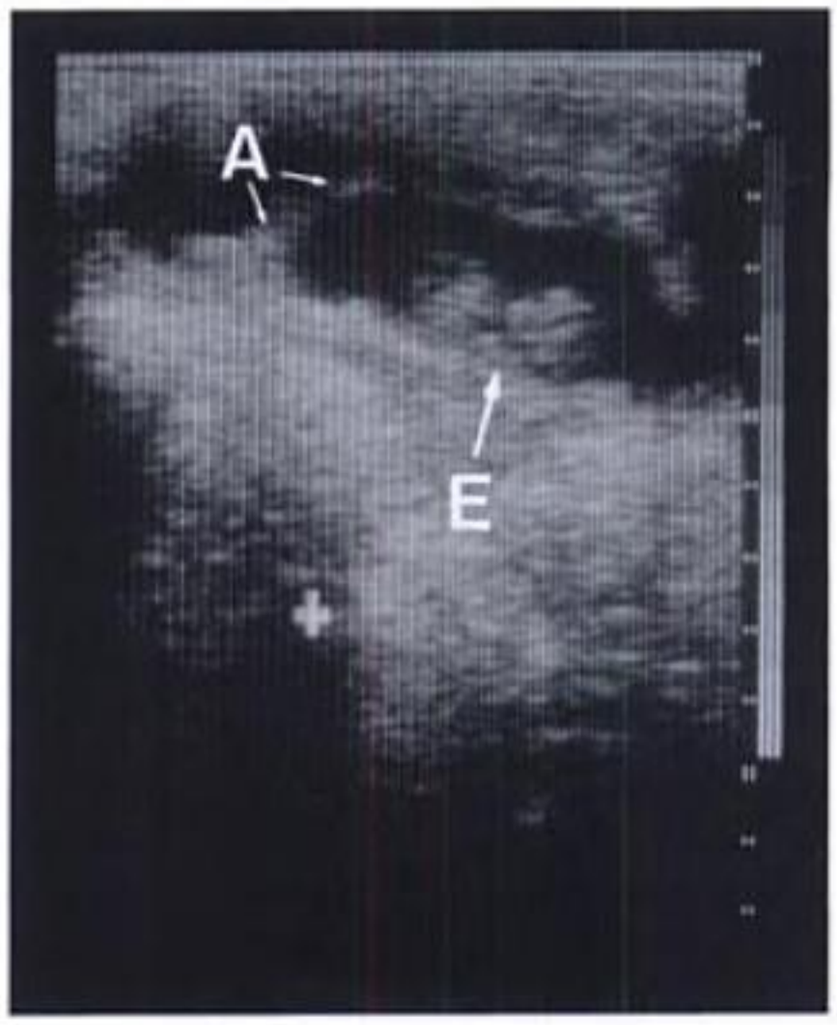


Fig. 2.10: The same pregnancy as in Fig. 2.9 imaged at a frequency of 3.5 MHz. Details are less well recognizable than at 5.0 MHz.

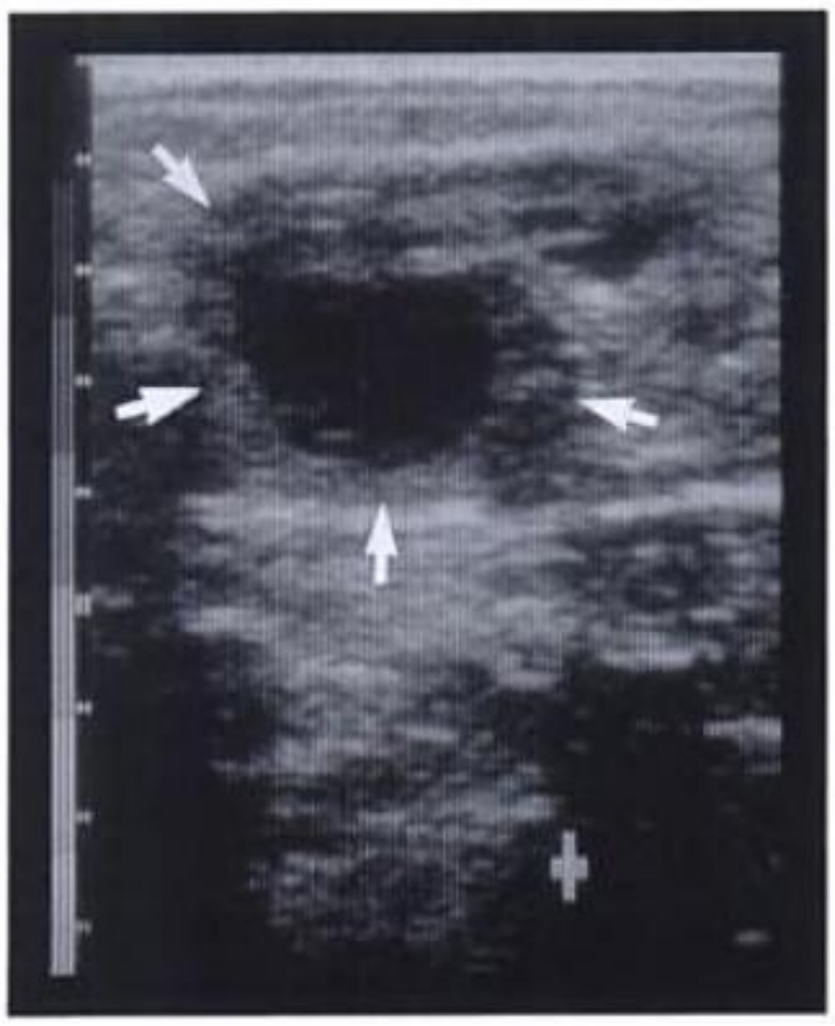


Fig. 2.11: Comparison of image quality between lower and higher frequency ultrasound. Ultrasonogram of a corpus luteum with a cavity imaged at a frequency of 5.0 MHz. The outline of the corpus luteum is indicated by arrows.

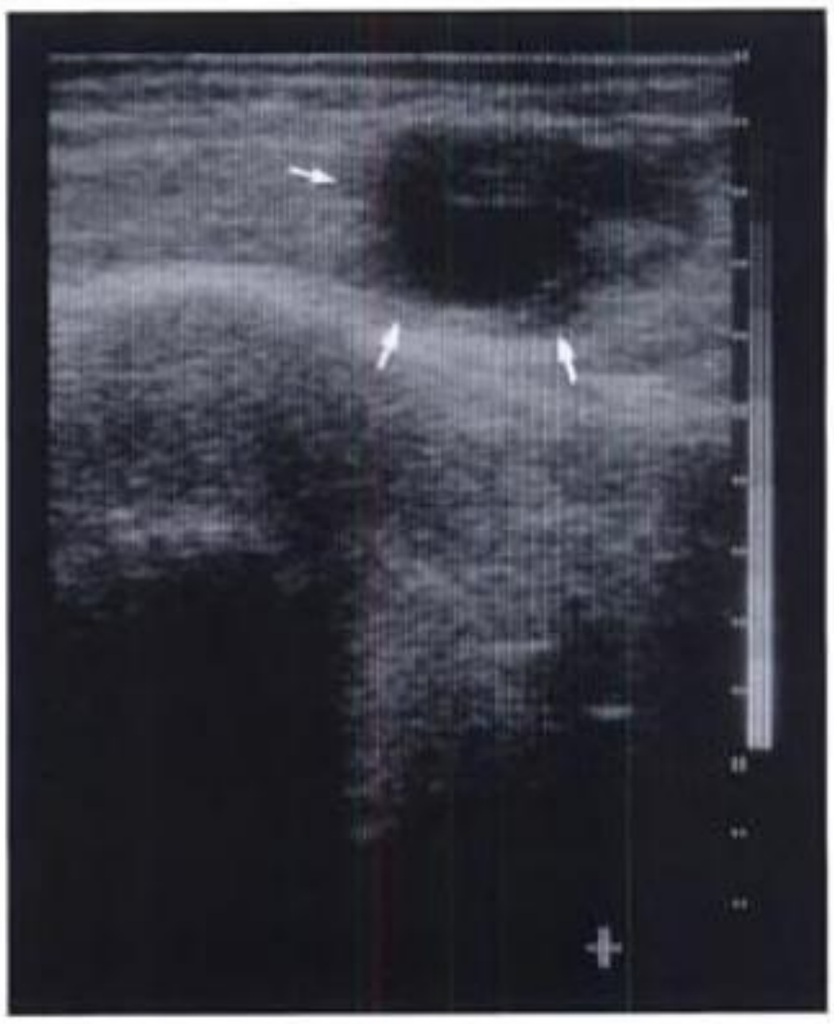


Fig. 2.12: The same corpus luteum as in Fig. 2.11 imaged at a frequency of 3.5 MHz. Size of the corpus luteum: 36.5 x 26 mm; size of its cavity: 25 x 18 mm.

Avtorsko zaščiteno gradivo

Downloaded From Vet-eBooks.com

When cow genitalia are examined sonographically the imaging of small structures, such as the embryo and its thin embryonic vesicle, intra-uterine fluid accumulations as well as follicles and corpora lutea, is of primary importance. The image quality generated by ultrasound at a frequency of 3 to 3.5 MHz is not adequate to reliably depict early embryonic structures or small functional structures on the ovaries (Fig. 2.9 to 2.12). For these, the use of sound waves of a higher frequency is essential. The resolution of ultrasound at a frequency of 5.0 MHz is high enough to identify vesicular structures with a diameter of 3 to 5 mm (DOBRINSKI and KREMER 1982). At the lower frequencies of 3 to 3.5 MHz vesicles of 6 to 8 mm can be seen. To further increase image quality 7.5 MHz ultrasonography can be used. Sound waves at this frequency provide a marginally better resolution than that obtained with 5 MHz.

The penetration depth of sound waves at 7.5 MHz is, however, only 4 to 5 cm (HASSLER 1984). For this reason the use of high frequency ultrasonography is restricted to the examination of structures that are extremely close to the probe. Sound waves at 5 MHz penetrate about 8 to 10 cm, thus allowing the examination of the ovaries and uterus during early gestation. Since ultrasound at 3.5 MHz penetrates 12 to 15 cm or deeper it can be very usefully applied in the later stages of gestation or in cows with pathologically enlarged genitalia.

Avtorsko zaščiteno gradivo

Downloaded From Vet-eBooks.com

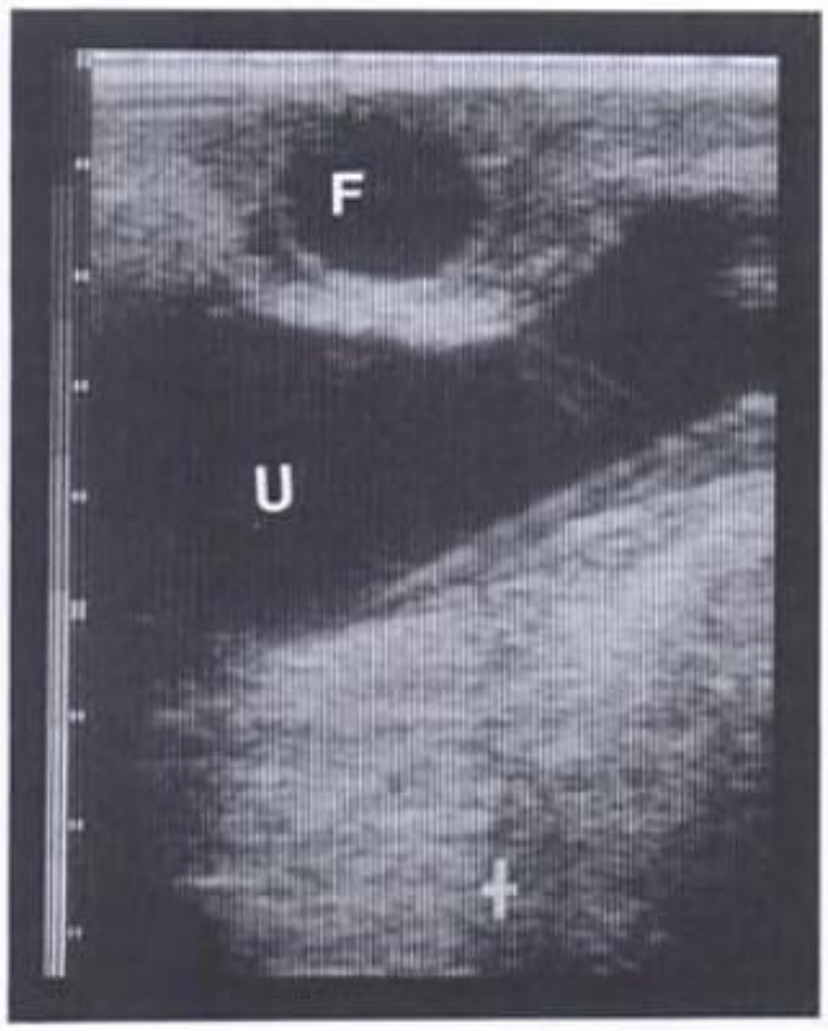


Fig. 2.13: Follicle (F) in a cow on the day of estrus. The diameter of the follicular antrum is 17 mm, the thickness of the follicular wall is 1 to 2 mm. Below the follicle lies the urinary bladder (U).



Fig. 2.14: Ovary (large arrows) with an estrus follicle on the day of ovulation. There is a echoic spot (small arrow) at the floor of the follicle. Ultrasonogram taken with a 5 MHz sector scanner.

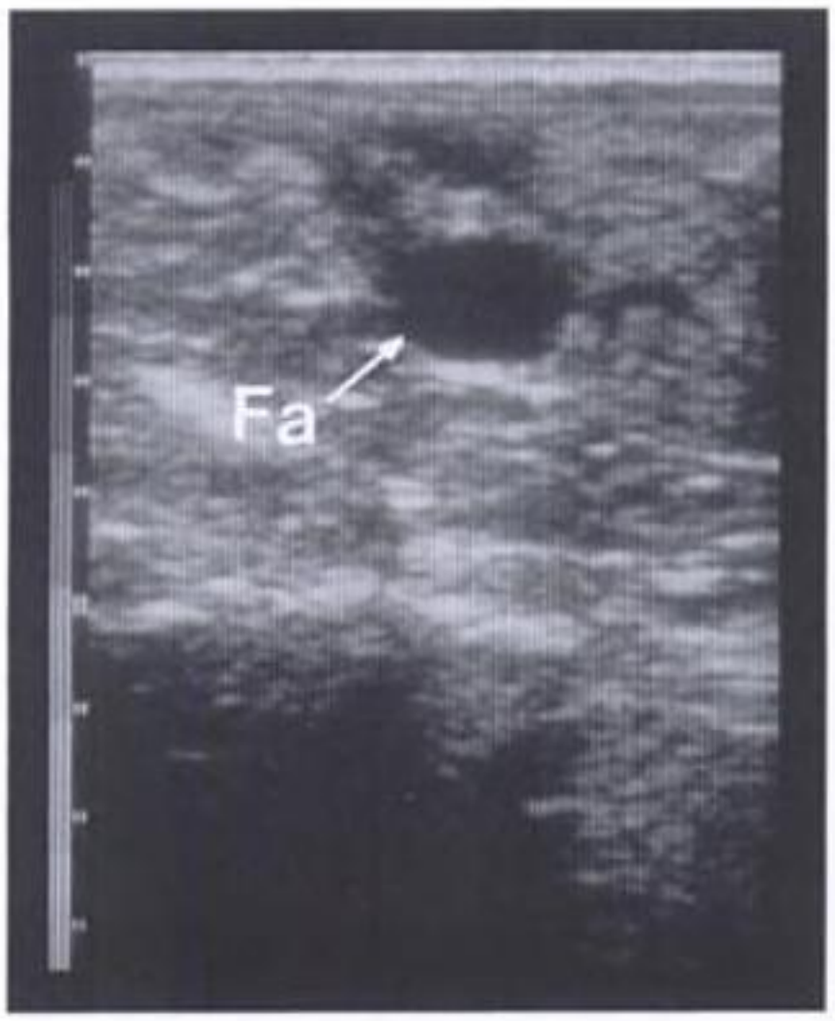


Fig. 2.15: Comparison of image quality between lower and higher frequency ultrasound. Ultrasonogram of an estrous follicle (Fa) at 5 MHz.

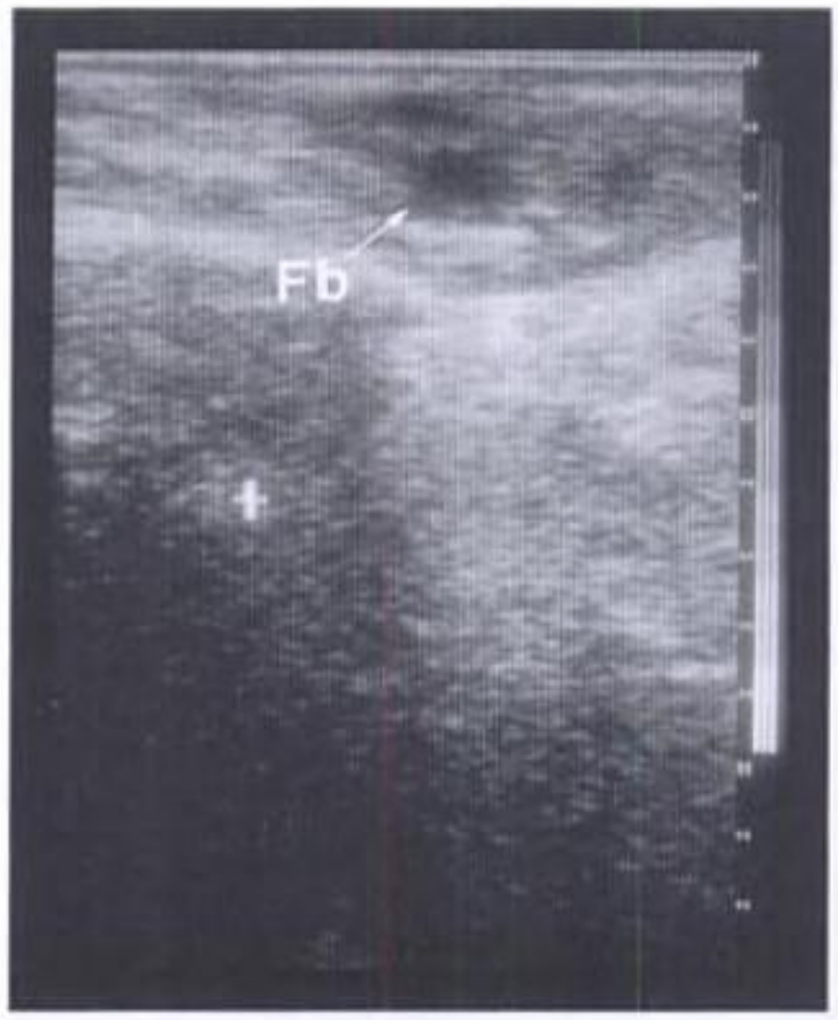


Fig. 2.16: The same follicle (Fb) as in Fig. 2.15 seen at 3.5 MHz. The diameter of the follicle is 16 mm.

Avtorsko zaščiteno gradivo

Downloaded From Vet-eBooks.com

2.2 Ovarian structures in the cow

2.2.1 Follicles

2.2.1.1 Sonographic images of follicles

The sonographic image of bovine ovarian follicles is characterized by the anechoic, circular area of the follicular lumen (Fig. 2.13 to 2.20). During real time scanning the spherical shape of the follicles can be demonstrated by moving the sound probe back and forth over the ovary. Their fluid content usually contains no reflections (PIERSON and GINTHER 1984 b, REEVES et al. 1984). Only in a few individual cases the lumina of follicles near ovulation will contain echoic spots close to the follicular wall (Fig. 2.14). Whether these spots possibly represent the cumulus oophorus or structures of a different kind is not clear yet. Where two vesicles are found to lie next to each other a dividing membrane, consisting of the appositioned follicular walls, can be detected. The wall of a follicle which is surrounded by the hyperechoic ovarian stroma can rarely be identified (Fig. 2.13 and 2.19). The thin follicular wall is occasionally separated from the ovarian parenchyma by a very narrow, hypoechoic line.

The shape of follicles is usually round (PIERSON and GINTHER 1984 b). The dividing walls of two neighbouring follicles of equal pressure often form a straight line. Smaller follicles often bulge into the lumen of a larger follicle.

The limit of resolution of 3.5 MHz ultrasound lies at 6 to 8 mm (PIERSON and GINTHER 1984 b) and cannot be used to reliably identify vesicular structures of less than 10 mm (Fig. 2.15 and 2.16). Low frequency ultrasound therefore only has very limited value for the precise examination of follicles on the ovary.

Avtorsko zaščiteno gradivo

Downloaded From Vet-eBooks.com



Fig. 2.17: Bovine ovary during metestrus. Several vesicles of varying sizes (from left to right: 4, 6, 8 and 11 mm). Arrows indicate the outline of the ovary.

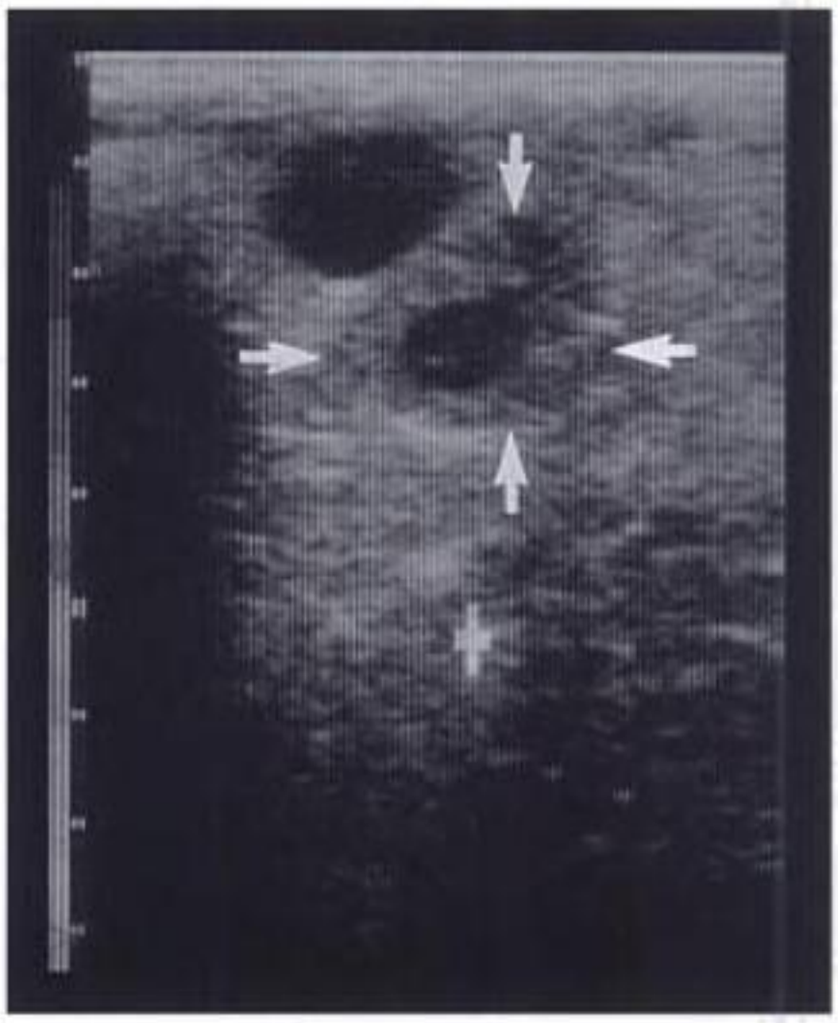


Fig. 2.18: Ovary containing a cystic corpus luteum (arrows) and a diestrous follicle 8 days after the last ovulation. The cavity of the corpus luteum is surrounded by a wall of luteal tissue. Dorsal and to the left of it is the diestrous follicle (inner diameter: 17 x 13 mm).



Fig. 2.19: Ovary with 4 developing follicles (1, 2, 3, 4) 5 days after the start of a superovulatory FSH treatment. The cow was given twice daily injections of FSH (6, 5, 4, 3 mg) for four days. The thin follicular wall surrounding the vesicles can be recognized in some of the follicles (No. 1 and 4).



Fig. 2.20: Multiple follicles on an ovary 9 days after the start of ECG induced superovulation. The cow received 3000 IU ECG 9 days earlier and 0.5 mg cloprostenol 7 days earlier.

Avtorsko zaščiteno gradivo

Downloaded From Vet-eBooks.com

Follicular vesicles with diameters of more than 10 mm can be easily detected using 5 MHz ultrasound (KÄHN and LEIDL 1986). The accurate recognition of vesicles with diameters of only a few millimeters depends mostly on the image quality generated by the scanner and on the experience of the operator. If the examination is conducted carefully, follicles in the size range of 5 to 10 mm can still be identified reasonably accurately (Fig. 2.17). Under less favorable conditions the differentiation between several small, neighbouring follicles may not be possible in every case.

When counting ovarian follicles by ultrasonography there is a tendency to count 10 to 30 % fewer follicles in the size order of 3 to 10 mm than are actually present. Vesicles with a diameter of less than 2 to 3 mm are too small to be detectable, even at the highest resolution of 5 MHz ultrasonography.

When carefully performed the ultrasonic determination of the inner diameters of follicles corresponds quite exactly to the real sizes of the follicular cavity (QUIRK et al. 1986). The total outer diameter of the same follicle, including its wall, is then 2 to 3 mm larger.

From a differential diagnostic point of view one must be able to separate the cavities of cystic corpora lutea from follicles (Fig. 2.18). The sonographic images of the cavities in cystic corpora lutea resemble those of follicles. In contrast to the anechoic follicular fluid, however, the anechoic fluid content of the corpus luteum cavity is surrounded by a moderately echoic wall of luteal tissue, which is a few millimeters thick.

Follicular development can also be monitored ultrasonically in hormone induced superovulation (Fig. 2.19 and 2.20). In this way the number of developing follicles can be assessed reasonably accurately and their ovulation with subsequent corpus luteum formation can be confirmed (DRIANCOURT et al. 1988). The ultrasound image of the individual FSH or ECG induced follicle is not different from that of a spontaneously developed follicle. Only the overall picture consisting of several, equally large vesicles is characteristic.

After ovulation has taken place, the ovulation depression, or any other sign of ovulation, cannot be detected. During early metestrus the echographic image of the ovary corresponds to that of an ovary without any significant functional structures. An ovulation can only be detected in a cow that was examined by ultrasound on the days preceding the ovulation. In such a case, the absence of a large vesicle, which had recently been present, indicates that an ovulation has occurred.

Avtorsko zaščiteno gradivo

Downloaded From Vet-eBooks.com

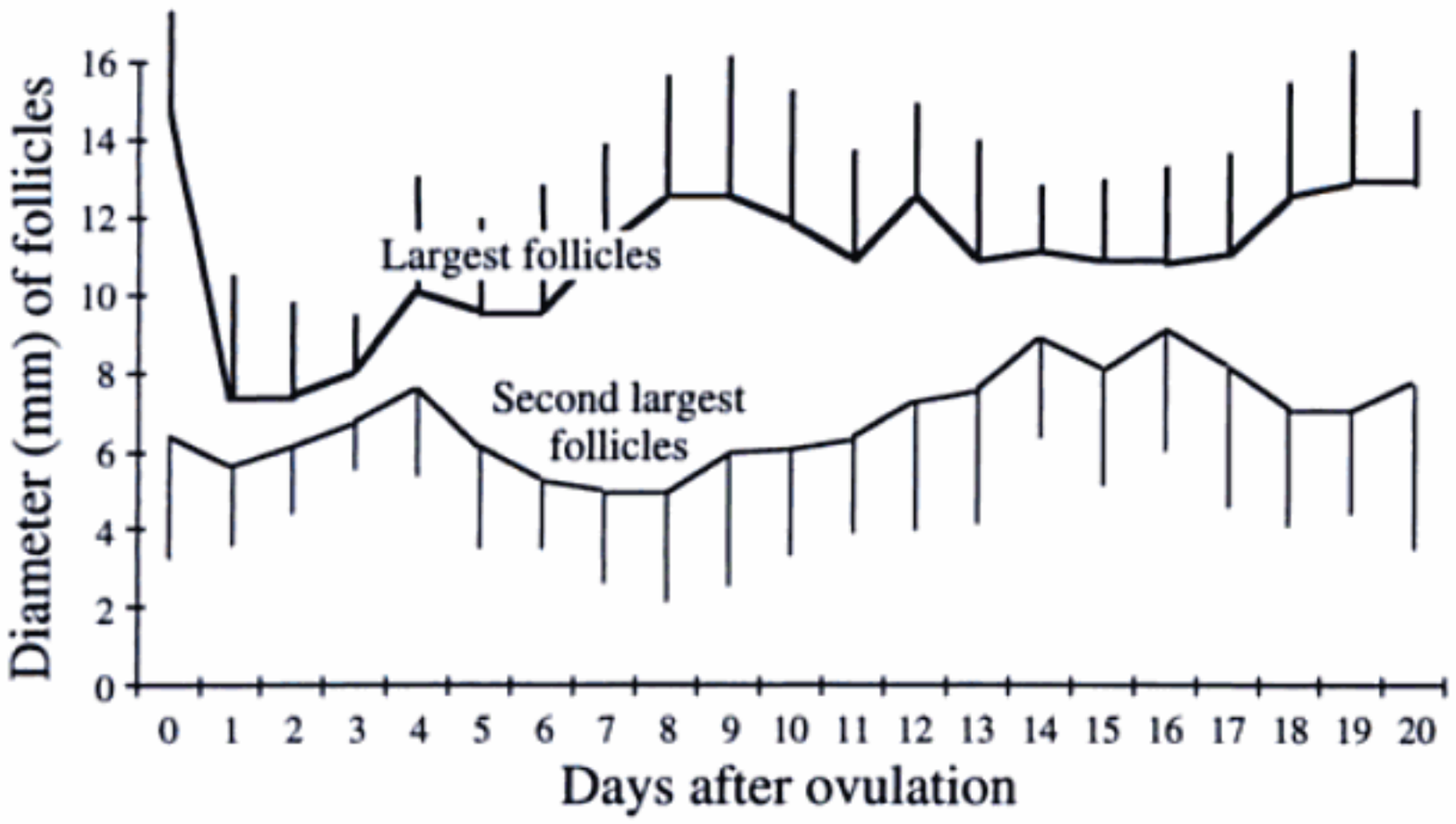


Fig. 2.21: The development of the diameters of the largest and second largest follicles in heifers during the estrous cycle (from KÄHN 1989 c).

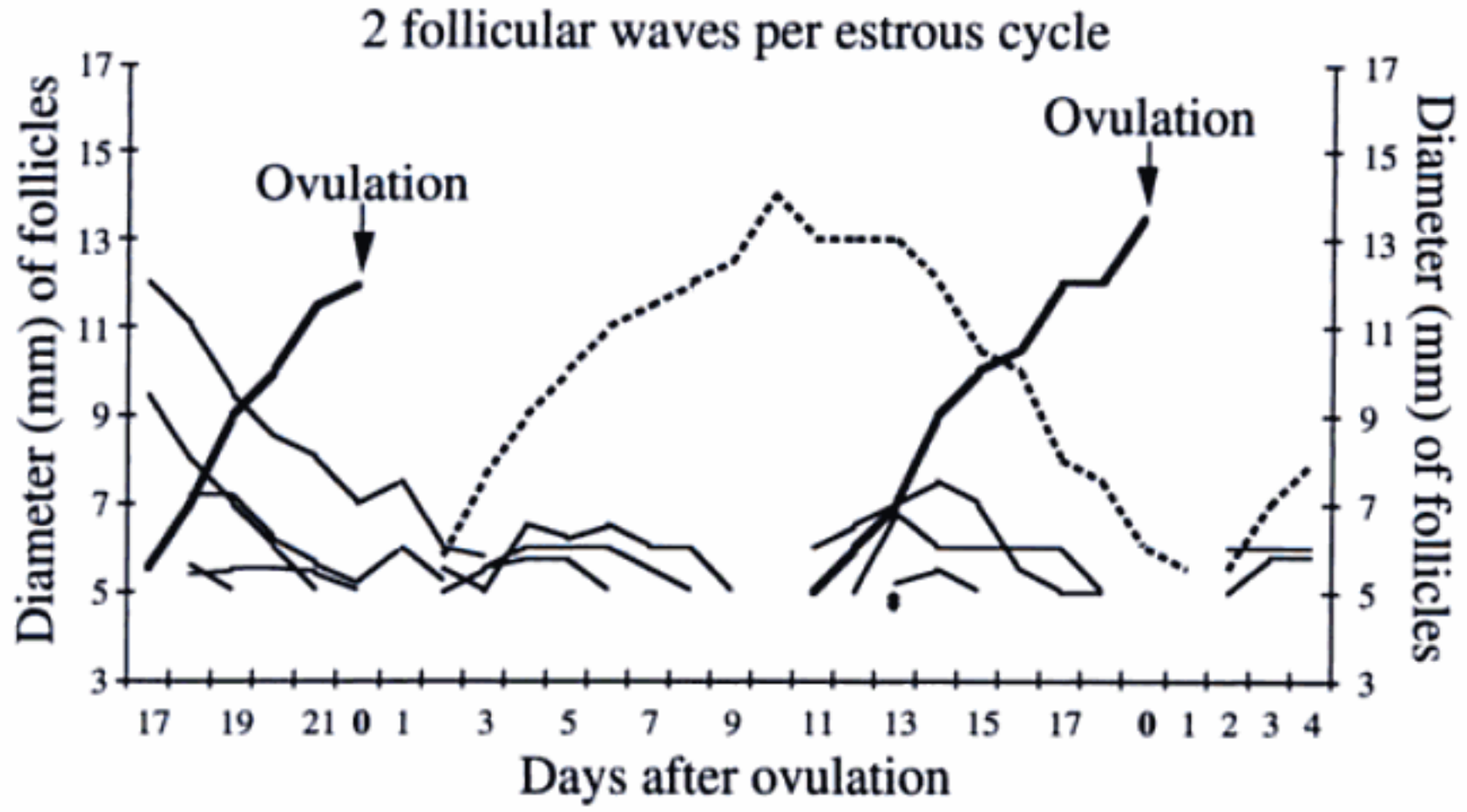


Fig. 2.22: The development of individual follicles in a heifer with two follicular waves during the estrous cycle (adapted from SIROIS and FORTUNE 1988).

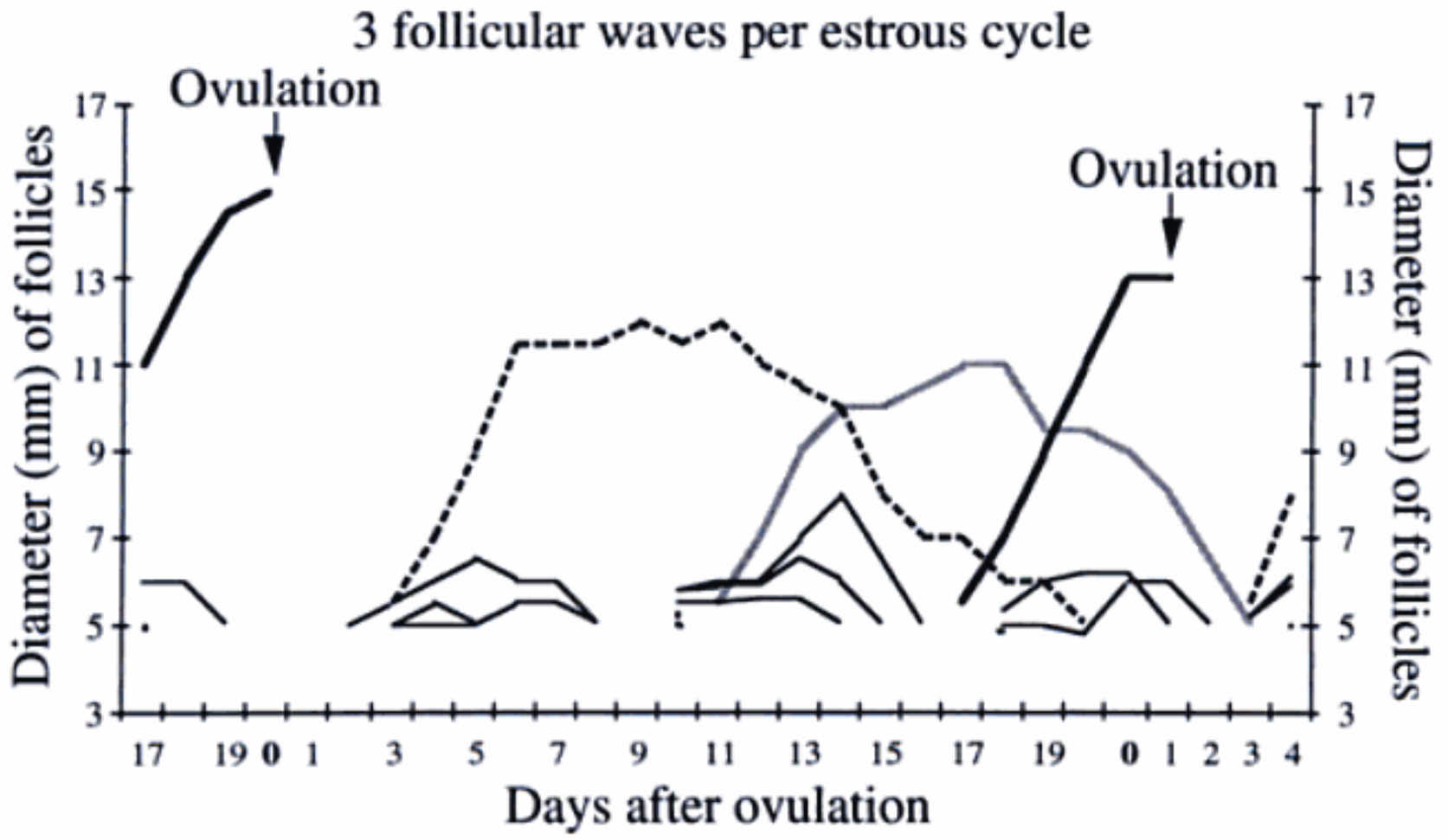


Fig. 2.23: The development of individual follicles in a heifer with three follicular waves during the estrous cycle (adapted from SIROIS and FORTUNE 1988).

Avtorsko zaščiteno gradivo

Downloaded From Vet-eBooks.com

2.2.1.2 Follicular development during the estrus cycle and in early pregnancy

Follicles grow on the ovaries at regular intervals of several days. The development of the largest follicle in each case is usually inversely correlated to the diameter of the second largest follicle and to the number of all other follicles (Fig. 2.21). During the first 3 days after an ovulation the largest follicle on a pair of ovaries usually only has a medium diameter of 5 to 8 mm. After that it develops rather rapidly to reach its maximum diameter of 12 to 14 mm between Days 7 and 10 and then becomes smaller again. While the dominant follicle grows, the second one becomes smaller, and visa versa. Also the number of the smaller, sonographically visible vesicles is inversely correlated to the development of the dominant follicle. The highest numbers of small follicles are found during the days following an ovulation, i.e. in metestrus (MATTON et al. 1981, PIERSON and GINTHER 1984 b, KÄHN 1989 c). When a diestrous follicle begins to develop thereafter, the number of smaller follicles rapidly declines. This contrasting pattern of the development of dominant and remaining follicles was found in cyclic as well as early pregnant heifers (PIERSON and GINTHER 1984 b and 1986).

The growth rate of the largest follicle from the time it becomes dominant until the day it reaches its maximum diameter is, on average, 1.5 to 2.5 mm per day (DRIANCOURT et al. 1988). This growth rate is the same for dominant follicles during the luteal phase, for estrous follicles during the last few days before ovulation and for those follicles that develop after induced superovulation.

Follicular growth in cattle occurs in wave like patterns. At the time of ovulation another vesicle is growing to develop into the dominant follicle, to grow further during metestrus and to reach its maximum diameter during the early luteal phase between Days 4 and 10 of the cycle. Shortly after this diestrous follicle has reached its maximum diameter, the second follicular wave starts and another dominant follicle develops. In the case of a 2-phase follicular cycle this one will terminate in ovulation (Fig. 2.22). Some cattle show a 2-phase, others a 3-phase pattern of development (IRELAND 1987, SIROIS and FORTUNE 1988, GINTHER et al. 1989 a). A follicular growth pattern where 4 dominant follicles develop in succession during a single cycle is a rarity. In 3-phase follicular development the second dominant follicle also regresses and a third follicle develops into the estrous follicle (Fig. 2.23). The time interval between the onset of growth of successive dominant follicles seems similar in 2- and 3-phasic cycles, namely 7 to 10 days (GINTHER et al. 1989 a). The total length of estrous cycles with 3 follicular waves is, on average, 2 to 3 days longer. A third wave of follicles is most commonly observed in heifers having a 2 to 3 day delay in the regression of their corpus luteum.

During the first few weeks of pregnancy this basic pattern of follicular growth, with its contrasts in the development between the dominant follicle on the one hand and the second largest follicle and the remainder of follicles on the other, persists (SCHNEEBELI 1984, PIERSON and GINTHER 1986). This wave-like succession of dominant follicles at intervals of 9 to 10 days can be observed during the first two months of gestation (GINTHER et al. 1989 b).

Except for the days during metestrus, there is usually a vesicle with a diameter of 10 or more millimeters present on one of the ovaries every day of the estrous cycle (CHOUDARY et al. 1968, IRELAND et al. 1979, STAIGMILLER and ENGLAND 1982). Most follicles have a diameter of less than 14 mm during met-, di- and proestrus. In a few cases, however, follicles with a diameter of 14 to 20 mm can be detected during diestrus or the first few weeks of pregnancy at the same time, the diameter of some estrous follicles can be smaller than 14 mm. It can be concluded that in veterinary practice the diameter of a follicle alone cannot be relied on to indicate the stage of the reproductive cycle of a cow.

Avtorsko zaščiteno gradivo

Downloaded From Vet-eBooks.com

Animals studied	Estrous follicles studied	Diameter of estrous follicles (mm) $\bar{x} \pm s$	smallest	largest
12 heifers in 51 cycles	54	14.7 ± 2.6	12.0	20.0
45 cows before AI	45	15.3 ± 2.9	10.0	20.0

Fig. 2.24: The internal diameters of estrous follicles in heifers and cows prior to AI (from KÄHN 1989 c).



Fig. 2.25: Ovary with a mature, compact corpus luteum. Compared to the surrounding ovarian parenchyma the corpus luteum (arrows) is less echoic. Ultrasonogram taken in a water bath.



Fig. 2.26: Cross section through the solid corpus luteum analogous to the sectional plane in Fig. 2.25.



Fig. 2.27: Corpus luteum (arrows) with central cavity. The echoic luteal wall of several millimeters thickness surrounds the anechoic cavity. Ultrasonogram taken in water bath.



Fig. 2.28: Cross section through the corpus luteum with cavity analogous to the sectional plane in Fig. 2.27.

Avtorsko zaščiteno gradivo

Downloaded From Vet-eBooks.com

2.2.1.3 Estrous follicles

The average diameter of the cavity of the estrous follicle at the time of standing heat is 15 mm (PIERSON and GINTHER 1984 b, KÄHN and LEIDL 1986). When its wall is included this means that a preovulatory follicle has a total size of 18 mm (QUIRK et al. 1986). The range of the inner diameter of estrous follicles on the day of standing estrus is 10 to 20 mm (Fig. 2.24). It is noteworthy that pregnancies can result from large follicles of 20 mm as well as from small follicles of 10 mm.

The daily increase in the size of the estrous follicle during the days preceding ovulation is 1.5 to 2.5 mm. Most estrous follicles that have been studied by ultrasonography reached their maximum size on the penultimate day before ovulation and did not grow larger during the 36 hours prior to ovulation.

2.2.2 Corpora lutea

2.2.2.1 Sonographic image of corpora lutea

Corpora lutea are recognized by their size and shape as well as their characteristic echographic appearance (PIERSON and GINTHER 1984 b, KÄHN and LEIDL 1986).

The sonographic section of luteal tissue appears as a roughly granular, gray-structured oval area on the monitor (Fig. 2.25 to 2.28). It can be delineated from the remaining ovarian tissue or other functional structures that may be on the ovary. The relatively hypoechogenicity of the active corpus luteum is in distinct contrast to the brighter gray of the ovarian parenchyma. The latter usually contains several vesicular structures of varying sizes, whereas the luteal tissue contains no fluid, except in the case where it developed a cavity during its development. The weak echogenicity of luteal tissue corresponds to reflections typically produced by loose, less dense, highly vascular soft tissues. The higher echogenicity of the ovarian stroma, in contrast, reflects its solid consistency and higher tissue density.

Corpora lutea with cavities, so called cystic corpora lutea, can also be diagnosed by ultrasonography (PIERSON and GINTHER 1984 b, REEVES et al. 1984, KÄHN and LEIDL 1986, KITO et al. 1986). In a corpus luteum with a cavity an echoic rim of tissue, a few millimeters thick, surrounds a central, anechoic fluid accumulation (Fig. 2.27). The echogenicity of the rim of tissue is the same as that of luteal tissue and thus corresponds to that of solid corpora lutea.

Avtorsko zaščiteno gradivo

Downloaded From Vet-eBooks.com



Fig. 2.29: A solid corpus luteum of the cycle (size: 28.5 x 18 mm) with a hyperechoic, central line. Ultrasonogram taken with a 7.5 MHz linear scanner.



Fig. 2.30: A corpus luteum of the cycle (arrows) 3 days after ovulation. Its size is 19 x 16 mm. At its center there is a cavity of 6.5 mm and to its left is a follicle of about 8 mm.



Fig. 2.31: A compact corpus luteum on Day 9 of the cycle. Length: 29 mm, width: 23.5 mm.

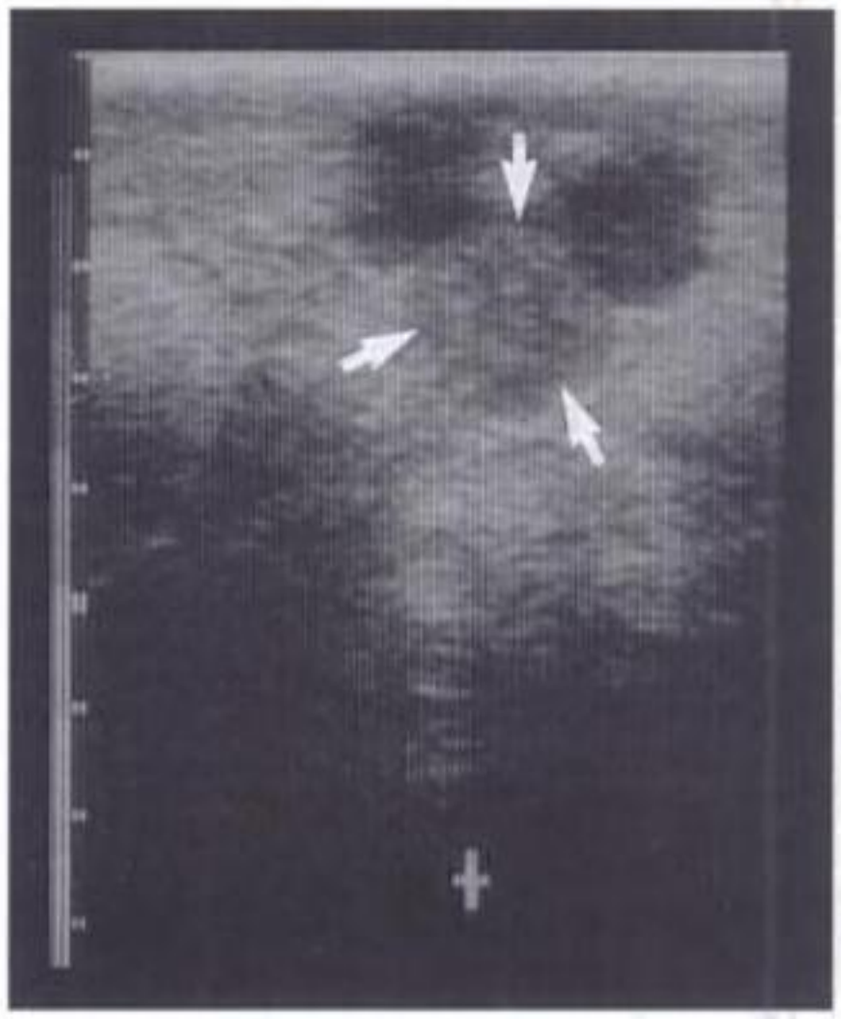


Fig. 2.32: Regressing corpus luteum (arrows) one day before the next estrus; length: 19.5 mm, width: 15.5 mm. Above the corpus luteum are two proestrous follicles (diameter about 14 mm).

Avtorsko zaščiteno gradivo

Downloaded From Vet-eBooks.com

Frequently, the cross section of a corpus luteum contains a narrow, hyperechoic zone in its center (Fig. 2.29 and 2.33). This site corresponds to a similar one that can be identified on the sectioned corpus luteum. It consists of branching connective tissue which, starting from the center, compartmentalizes the wavy, densely packed layers of luteinized tissue. A hyperechoic central zone can always be seen after the closure of a central cavity in a corpus luteum. This pattern can be found in corpora lutea of the cycle as well as those of pregnancy.

Immediately following ovulation the developing luteal tissue cannot yet be recognized. The young corpus luteum only becomes sonographically detectable 2 to 4 days post-ovulation (Fig. 2.30). Corpora lutea have a mean width of 14 mm and a mean length of between 18 and 21 mm when they first become detectable on the third day after ovulation (PIERSON and GINTHER 1984 b, KÄHN 1986).

They then grow 1 mm in width and 2 mm in length per day, and reach their maximum size of about 20 x 30 mm by Day 8 to 10 post ovulation (Fig. 2.31). After luteolysis has begun or PGF2a has been injected the largest diameter of the corpus luteum rapidly falls to below 23 mm (QUIRK et al. 1986). At a frequency of 5 MHz, corpora lutea are reliably detectable from their early development to the end of diestrus, and nearly all of them are still identifiable at the time of next ovulation (Fig. 2.32). In some cases they can still be identifiable as corpora albicans for several days after the onset of the next cycle.

Avtorsko zaščiteno gradivo

Downloaded From Vet-eBooks.com



Fig. 2.33: A solid corpus luteum of pregnancy (Size: 26 x 19.5 mm) with a hyperechoic line in its center. Day 21 of pregnancy.

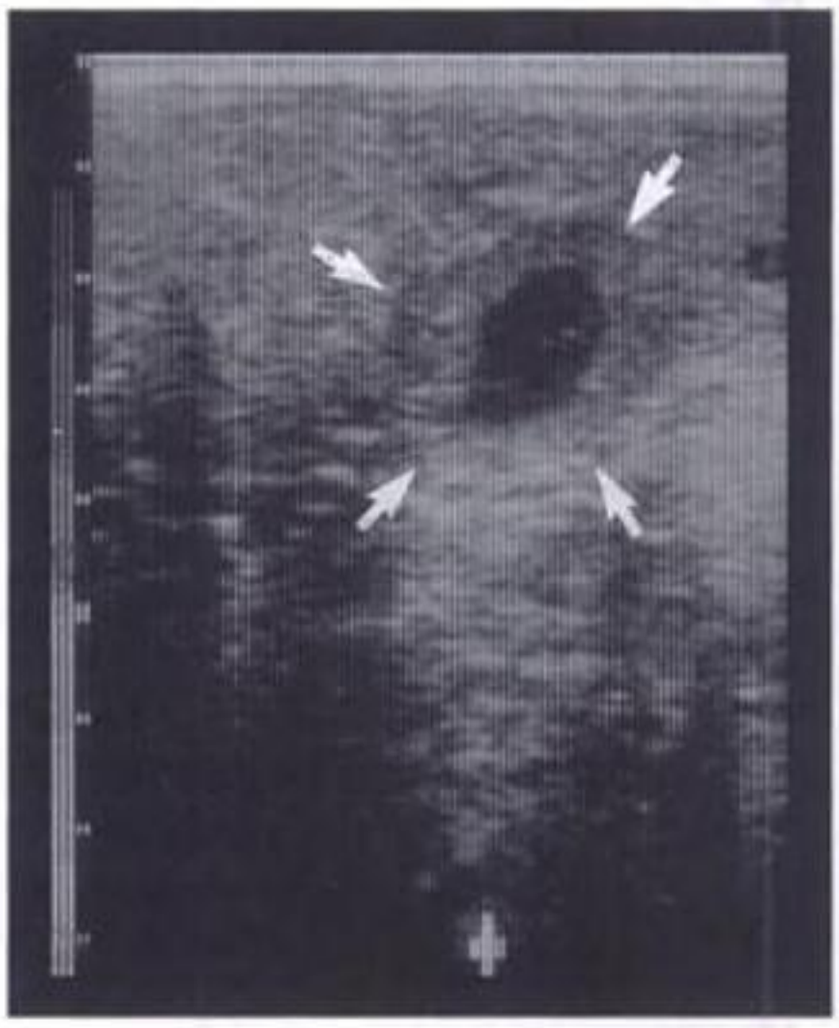


Fig. 2.34: Cystic corpus luteum (arrows) on Day 11 of the cycle. The corpus luteum measures 31 x 20 mm; the cavity measures 17 x 10.5 mm.



Fig. 2.35: Cystic corpus luteum (arrows) on Day 8 of the cycle. The cavity lies eccentrically and has an irregular outline.



Fig. 2.36: Cystic corpus luteum (arrows) on Day 11 of the cycle. The diameter of the cavity is 22 x 19 mm. The estrous cycle of the cow was 23 days long. Slight reflections can be seen within the fluid of the cavity.

Avtorsko zaščiteno gradivo

Downloaded From Vet-eBooks.com

Avtorsko zaščiteno gradivo

The gray scales of the corpora lutea of different ages vary very little and cannot be employed for diagnostic purposes. At the same time, corpora lutea of pregnancy cannot be distinguished on the basis of their echogenicity from those of the cycle (Fig. 2.33). The dimensions (length and width) of corpora lutea of pregnancy are much the same as those of corpora lutea of the cycle.

The cavities inside corpora lutea are usually oval, occasionally round and nearly always centrally positioned inside the gland (Fig. 2.34). Only in exceptional cases are they eccentrically positioned or have they an irregular shape (Fig. 2.35). The largest diameters of the cavities usually vary from a few millimeters to 1.5 cm. Rarely, they can reach 20 mm or more (Fig. 2.36).

The echogenicity of the cavities is similar to that of follicles. Slight reflections can occasionally be seen inside the cavity's fluid (Fig. 2.36).The luteinized wall is used to differentiate cystic corpora lutea from ovarian follicles. Whereas follicles are seen to lie embedded in the hyperechoic ovarian parenchyma, the cavity of the cystic corpus luteum is separated from the bright ovarian tissue by its slightly less echoic wall of luteal tissue.

Downloaded From Vet-eBooks.com

Avtorsko zaščiteno gradivo



Fig. 2.37: Corpus luteum of pregnancy with a central cavity (diameter 16 x 10 mm). This corpus luteum was found in a cow on Day 28 of gestation (see Fig. 2.38).

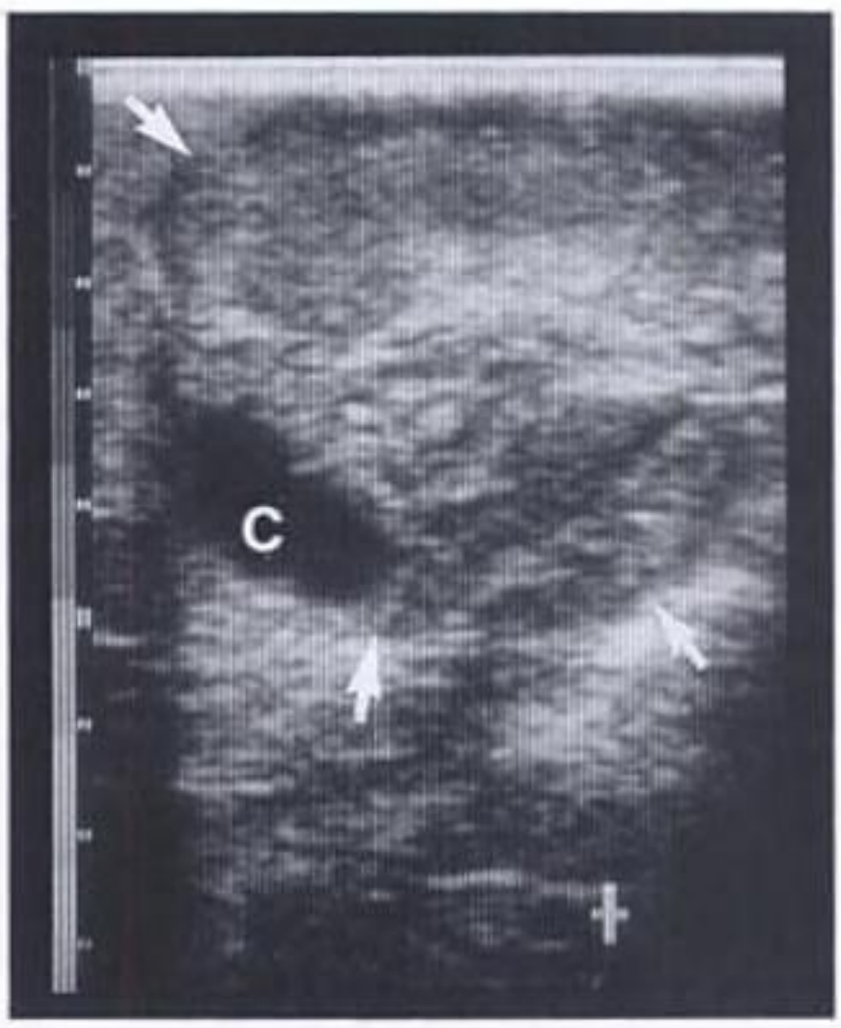


Fig. 2.38: Uterus (arrows) with a conceptus (C) on Day 28 with a simultaneously present cystic corpus luteum (see Fig. 2.37).



Fig. 2.39: Four non-cystic corpora lutea (1, 2, 3 and 4) on a single ovary after superovulation. Their length ranges from 24 to 25 mm; their width from 13 to 17 mm.



Fig. 2.40: A non-cystic and a cystic corpus luteum (left) on the ovary 6 days before the onset of the next cycle. The corpora lutea are indicated by arrows.

Downloaded From Vet-eBooks.com

Avtorsko zaščiteno gradivo

As during the estrous cycle, cystic corpora lutea can also be found during the first weeks of pregnancy (Fig. 2.37 and 2.38). After the third week of pregnancy they are seen infrequently. The fertility of animals with a cystic corpus luteum is the same as that of cows with the solid type of corpus luteum.

With the aid of ultrasonography the number of corpora lutea on an ovary can be determined quite accurately (DRIANCOURT et al. 1988). In this manner the success of a superovulation attempt can be assessed and the number of embryos that could possibly be harvested can be estimated. Where several corpora lutea lie closely together they are usually only separated by thin, hypoechoic tissue lines (Fig. 2.39). The bulk of the ovary then consists of the hypoechoic echo patterns which are typical for luteal tissue. The size and echogenicity encountered in multiple corpora lutea is not different from the picture observed in single luteal glands.

When multiple corpora lutea are present in a cow they can be of both, the compact and the cystic types (Fig. 2.40). Cases can be found in which only solid corpora lutea are present at the same time; sometimes the compact and cystic forms occur in adjacent corpora lutea and in other animals only the cystic forms can be visualized.

Downloaded From Vet-eBooks.com

Avtorsko zaščiteno gradivo

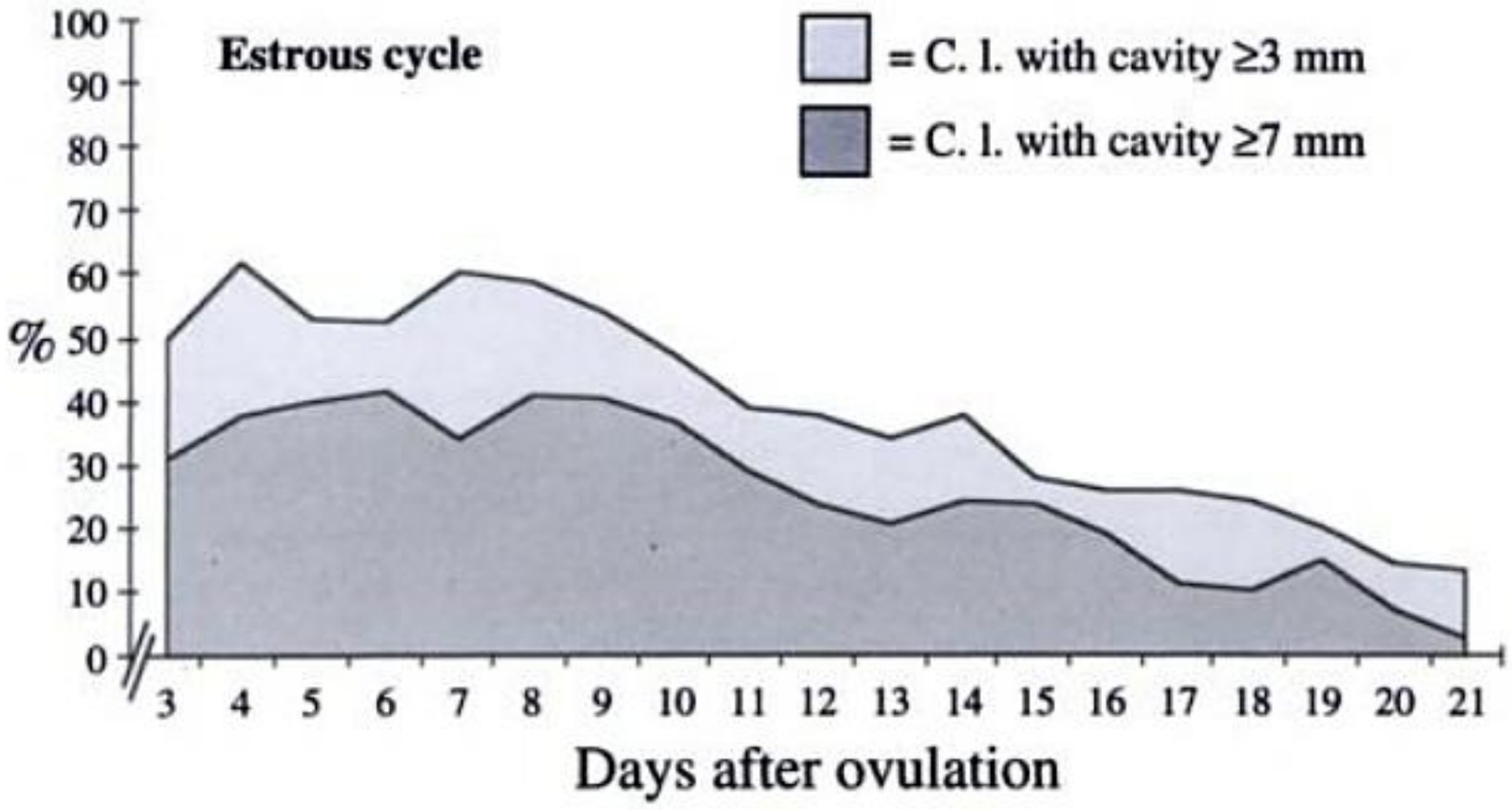


Fig. 2.41: The percentage of corpora lutea with a cavity (≥3 mm or ≥7 mm) during the estrous cycle in heifers (from KÄHN 1989 a).

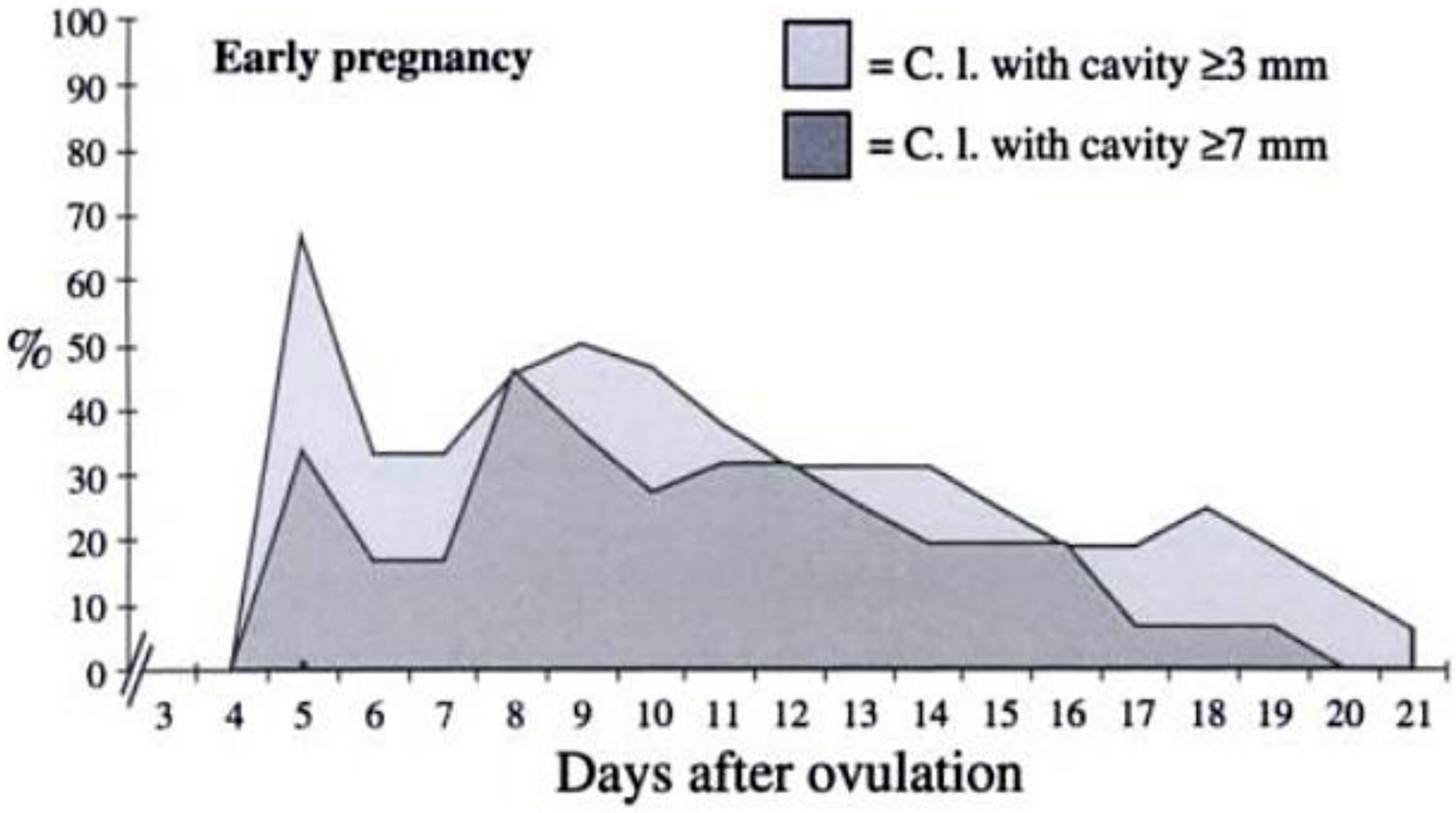


Fig. 2.42: The percentage of corpora lutea with a cavity (≥3 mm or ≥7 mm) during early pregnancy in heifers (from KÄHN 1989 a).

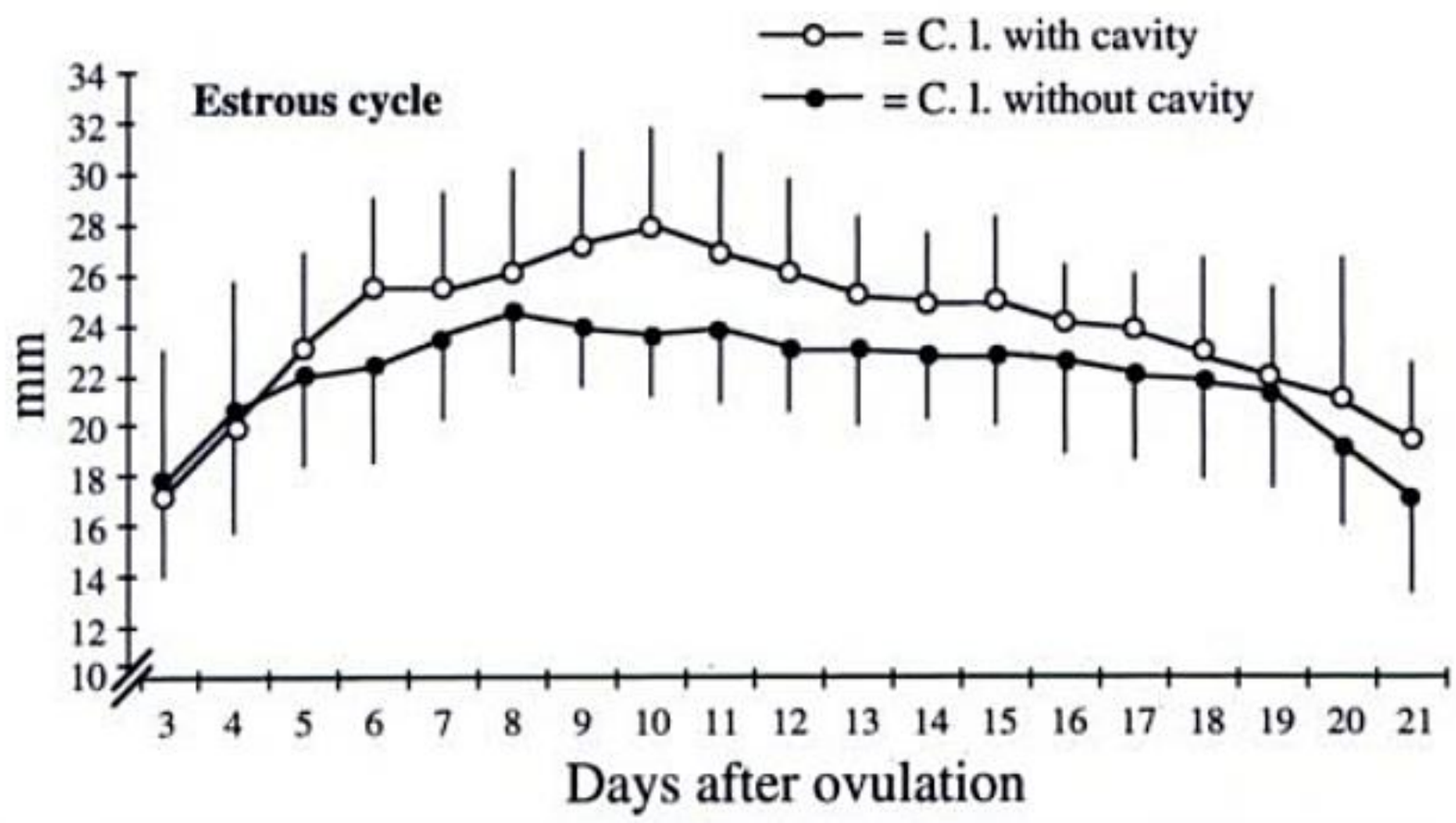


Fig. 2.43: The length of non-cystic and cystic corpora lutea during the estrous cycle in heifers (mean ± SD; from KÄHN 1989 a).

Downloaded From Vet-eBooks.com

2.2.2.2 Incidence and development of cystic and non-cystic corpora lutea during the estrous cycle and in early pregnancy

In cattle corpora lutea with or without a cavity occur during the cycle and early pregnancy. The non-cystic and cystic forms of corpora lutea can be seen as normal variations of luteal glands in cattle. Compact and cystic corpora lutea occur alternately in cattle. The type of the luteal gland had no effect on cycle length, endocrine pattern or fertility in cattle (KÄHN and LEIDL 1988, KÄHN 1989 a).

The incidence and the size of luteal glands, with or without a cavity, were studied in cattle during the cycle and in the first three weeks of pregnancy. It was shown that the cavity in cystic Cl reached its largest diameter between Days 8 and 10 of the cycle (KÄHN 1986). At this time cavities occurred most frequently and reached their largest size. Afterwards they decreased in incidence and size with time.

Until Day 10, one third to a half of all corpora lutea in normal cycles contained a sonographically detectable cavity (Fig. 2.41). After this day the incidence of cystic corpora lutea decreased by 3 to 4 % per day so that fewer than one third of all luteal glands contained cavities by day 13.

Non-cystic and cystic Cls could be found with equal frequency during normal cycles and in early pregnancy (Fig. 2.42). If cows with a cystic corpus luteum were less fertile than cows with compact luteal glands, the incidence of the former type should be lower in early pregnant cows. The observed ratios do not, however, support this hypothesis. In contrast, in pregnant cows cystic corpora lutea were found at least as frequently as during the cycle. This indicates that the pregnancy rates in cows with the two types of luteal glands are the same (KITO et al. 1986).

When cystic and non-cystic corpora lutea were first detected on Day 3 of the cycle they had a mean length of 17 mm (Fig. 2.43). Thereafter the increase in the length of the two types of corpora lutea differed, with the cystic type being longer than the compact type at all times. The cystic and compact types reached their maximum length of 28 and 24.5 mm on Day 8 and Day 10 of diestrus, respectively. They then slowly decreased in size. The length of cystic forms decreased faster than that of compact forms. From Day 6 to 17 of the cycle the cystic Cls were consistently 2 to 4 mm longer than their compact counterparts.

The cystic forms of luteal glands were also 1 to 3 mm longer than the compact forms from Day 9 until Day 21 of early gestation (Fig. 2.44). A comparison between luteal glands of the cycle and those of pregnancy revealed that both, compact and cystic corpora lutea were a little longer in pregnancy than during the cycle (KÄHN 1989 a). By Day 18 of the cycle and early pregnancy the sizes of compact corpora lutea varied between 22 and 24 mm, and between 24 and 26 mm, respectively.

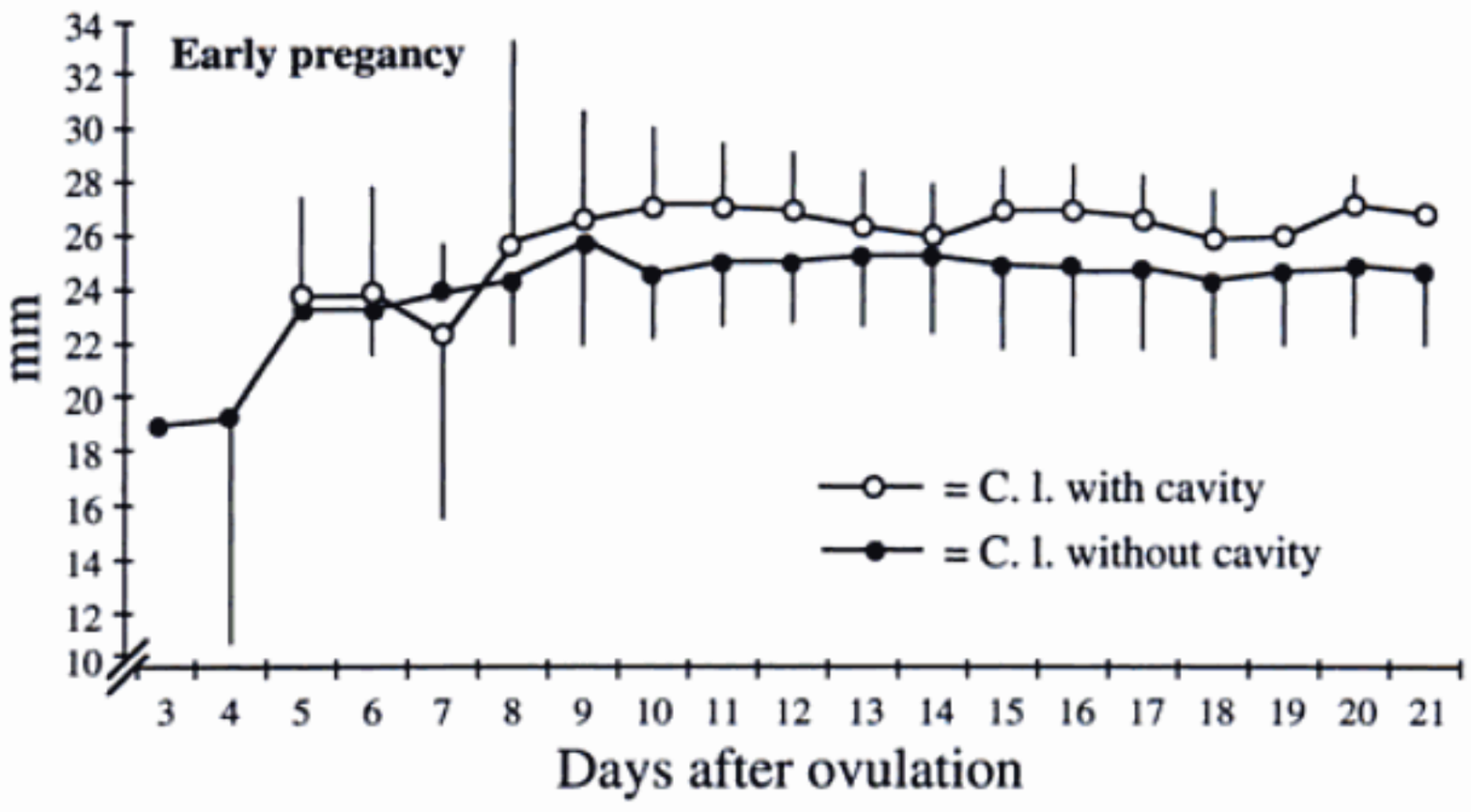


Fig. 2.44: The length of non-cystic and cystic corpora lutea during early pregnancy in heifers (mean ± SD; from KÄHN 1989 a).

Avtorsko zaščiteno gradivo

Downloaded From Vet-eBooks.com

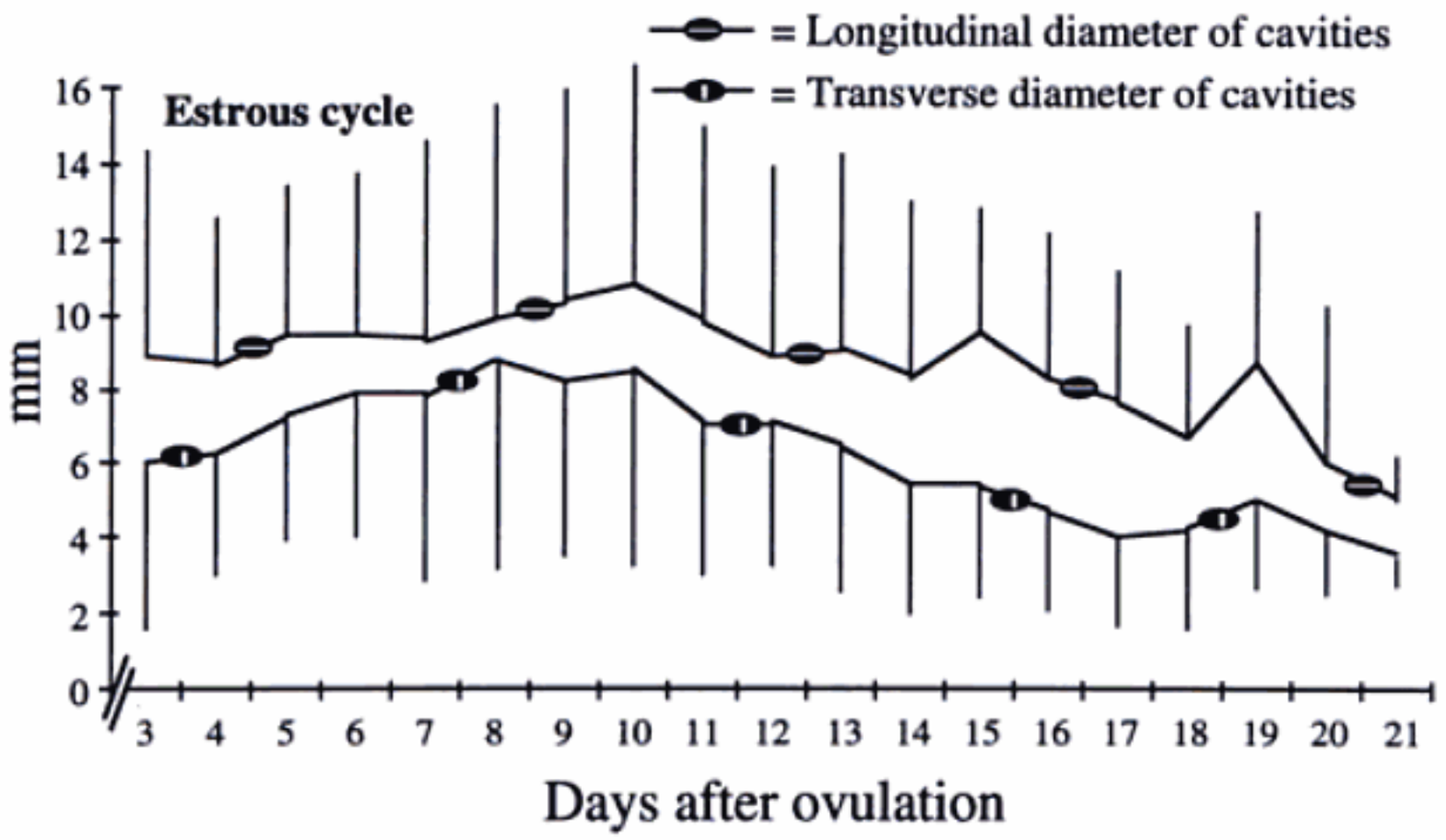


Fig. 2.45: The longitudinal and transverse diameters of the cavities in cystic corpora lutea during the estrous cycle in heifers (mean ± SD; from KÄHN 1989 a).

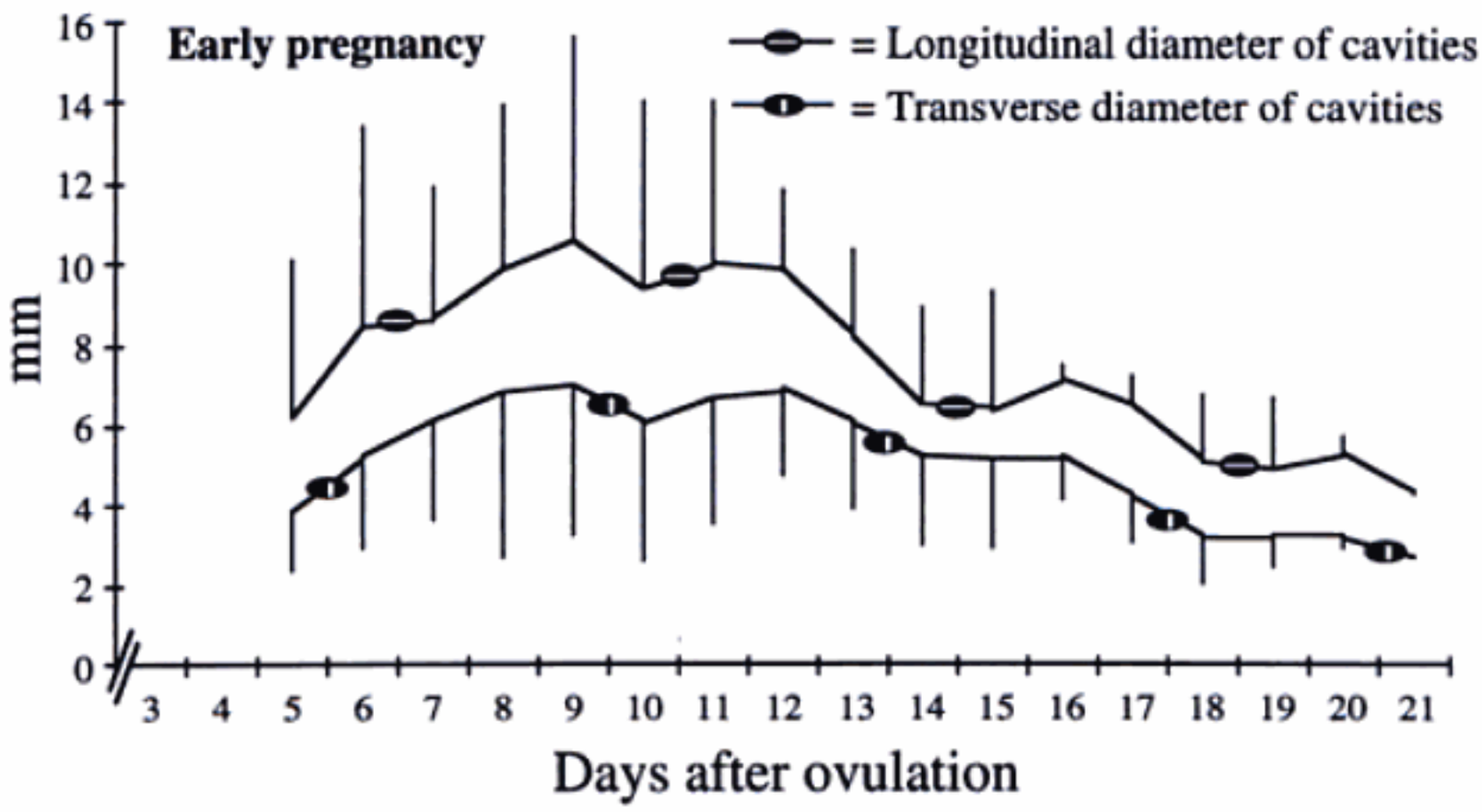


Fig. 2.46: The longitudinal and transverse diameters of the cavities in cystic corpora lutea during early pregnancy in heifers (mean ± SD; from KÄHN 1989 a).

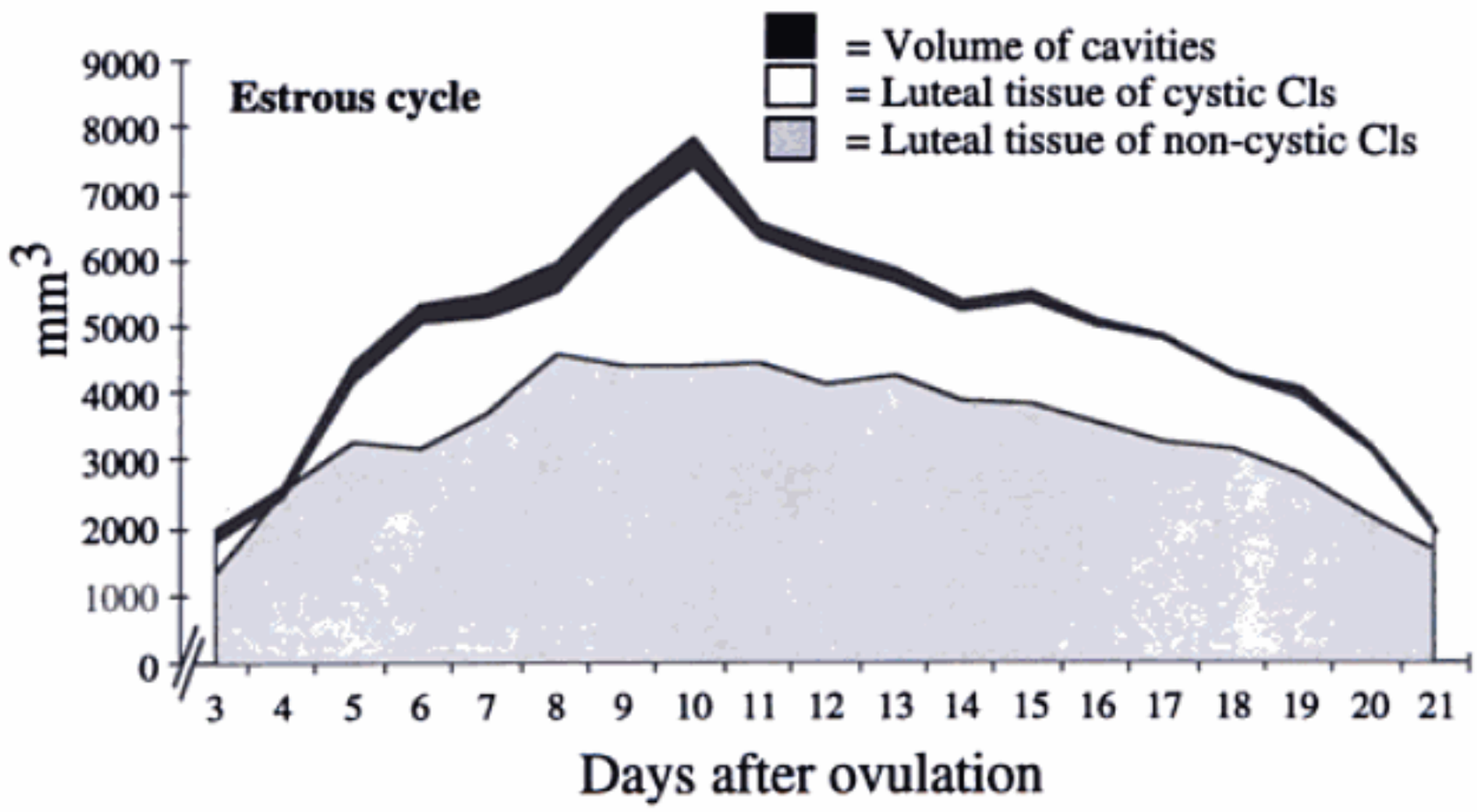


Fig. 2.47: The volumes of non-cystic and cystic corpora lutea and their cavities during the estrous cycle in heifers (mean; from KÄHN 1989 a).

Avtorsko zaščiteno gradivo

Downloaded From Vet-eBooks.com

The longitudinal diameters of the cavities of cyclic Cls and of Cls of pregnancy increased until about Day 10 post ovulation when they measured approximately 11 mm (Fig. 2.45 and 2.46). After that the longitudinal diameters of the cavities decreased by about 0.5 mm per day and measured only 5 mm at the time of the next estrus or on Day 21 of gestation.

Similar increases and decreases were recorded for the transverse diameters of the cavities of luteal glands of the cycle and of pregnancy. These were, however, consistently a few millimeters shorter than those of the longitudinal diameters. From these observations it is clear that the cavities in corpora lutea have a predominantly oval shape which largely follows the outer contours of the glands.

Since the cavities can reach a considerable size during the first 14 days post ovulation, it was suspected that cystic corpora lutea might contain less luteal tissue than their compact counterparts, and that they may thus secrete less progesterone.

The total volume of cystic and non-cystic luteal glands increased during the estrous cycle from a mean of 1984 mm^3 and 1329 mm^3 on the third day after ovulation to a mean of 6000 to 7000 mm^3 and 4000 mm^3, respectively, in the middle of diestrus around Day 8 to 13 of the cycle (Fig. 2.47). At the same time the cavities within the Cls grew from a mean of 170 to 400 mm^3. After subtracting the cavity's volume from the total volume of the cystic corpus luteum, it became surprisingly clear that the cystic glands contained more luteal tissue than compact glands. The difference in the amount of luteal tissue between the two forms varied from 1000 to 3000 mm3 in the period from the 6th to the 20th day of diestrus (OKUDA 1982).

A comparison of the development of luteal glands between those of normal diestrous and those of early pregnancy showed no significant differences. Overall, luteal glands of pregnancy were generally a little larger than those of normal diestrus. Similar to the observations during the cycle, it was also shown that during early gestation cystic corpora lutea contained more luteal tissue than compact ones (Fig. 2.48). Even in their development of cavities cystic corpora lutea of pregnancy and of normal diestrus did not differ markedly. They also grew to a mean size of 11 mm by Day 8 to 10 and then continuously became smaller (KITO et al. 1986). After Day 30 of gestation in cattle it is very rare to find a corpus luteum with a cavity, The disappearance of the cavities can be explained by the increase in thickness of the luteal walls of the Cls (LEIDL et al. 1983). Very few cystic corpora lutea are found in the fourth week of pregnancy.

Studies completed thus far on the endocrine status of cattle with either a cystic or a solid corpus luteum have shown no deficiency in the progesterone secretion of the luteal glands with cavities (KÄHN 1986, KITO et al. 1986). The mean plasma progesterone concentration over the entire cycle in cows with a cystic corpus luteum was maintained at the same level as that of cows with a compact gland. The adequacy of progesterone secretion by cystic luteal glands was also demonstrated by using hCG stimulation.

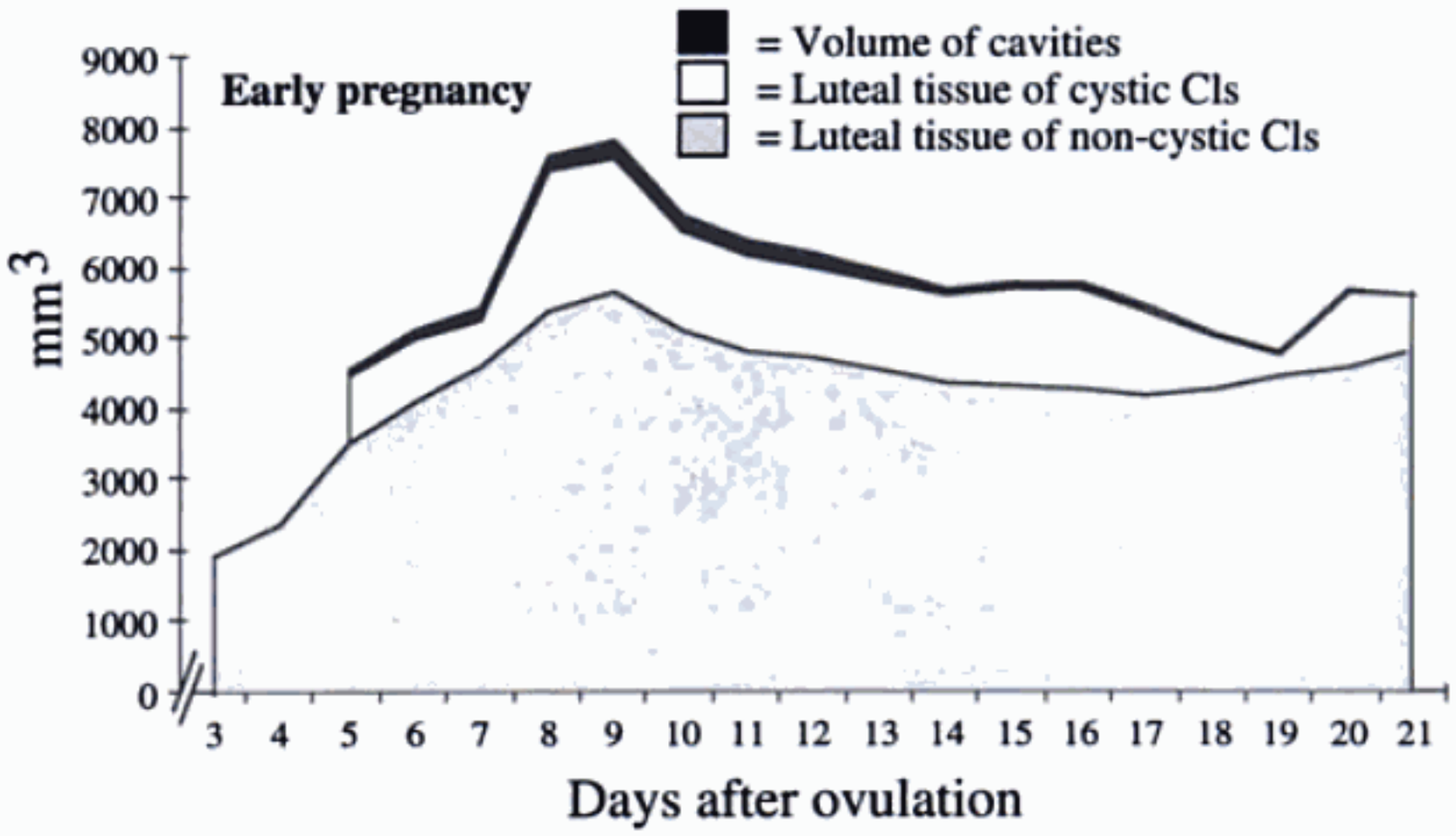


Fig. 2.48: The volumes of non-cystic and cystic corpora lutea and their cavities during early pregnancy in heifers (mean; from KÄHN 1989 a).

Downloaded From Vet-eBooks.com

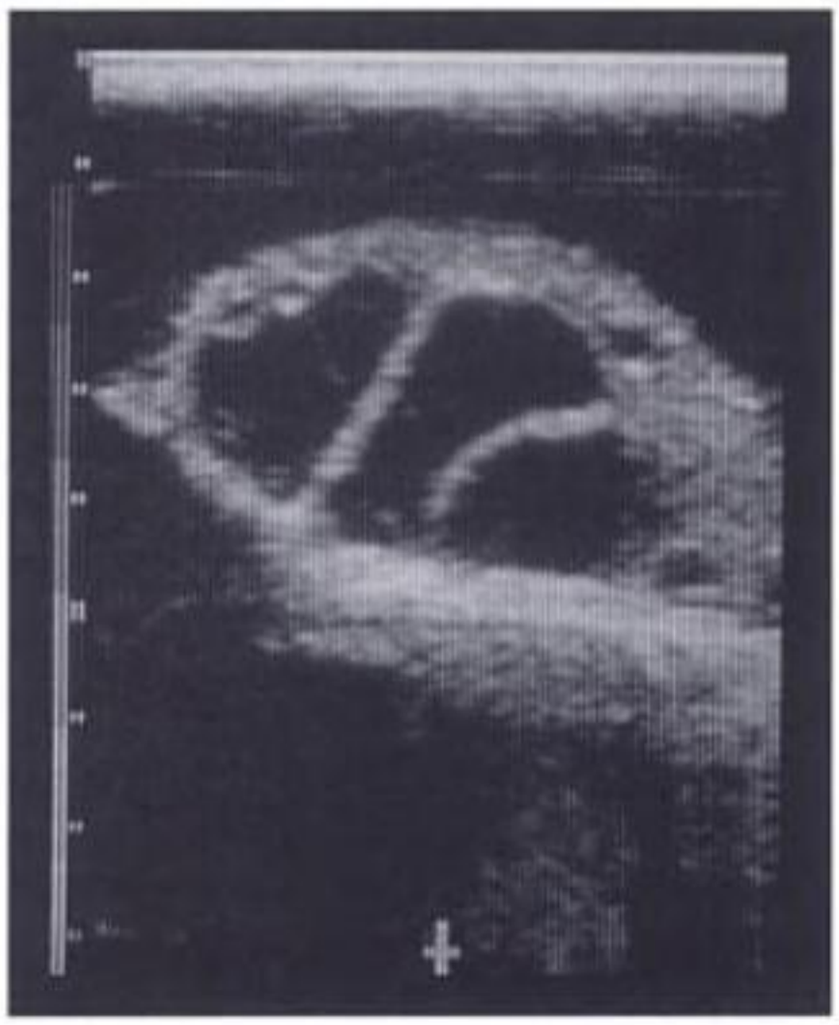


Fig. 2.49: Ovary containing three theca-follicular cysts. Two cysts share a straight dividing wall; on the right a smaller cyst bulges into the middle one. Ultrasonogram taken in a water-bath.



Fig. 2.50: Section through the same ovary analogous to the sectional plane in Fig. 2.49.



Fig. 2.51: Ovary containing a luteinized follicular cyst (arrows). The inner cavity shows a network of echoes. The wall measures several millimeters in thickness.



Fig. 2.52: Ovary containing a thecal follicular cyst. The diameter of the cyst is about 5 cm.

Avtorsko zaščiteno gradivo

Downloaded From Vet-eBooks.com

In some cases progesterone secretion of cystic luteal glands even exceeded the levels found in cows with compact corpora lutea. The tendency for higher plasma progesterone levels in cows with cystic luteal glands is likely explained by the fact that they have larger amounts of luteal tissue.

In conclusion, the studies completed thus far on the incidence, development and endocrine function of cystic corpora lutea of the cycle and of pregnancy, with cavity diameters ranging from a few millimeters to 2 centimeters, have no indication that they are endocrinologically dysfunctional. This conclusion is supported by the fact that the pregnancy rates of cattle with cystic corpora lutea are not decreased.

2.2.3 Ovarian cysts

In their sonographic appearance ovarian cysts resemble large follicles (Fig. 2.49 and 2.50). One distinguishing feature is their larger size. In the case of a luteinized follicular cyst its wall thickness can also assist in its identification. The sectional images of ovarian cysts are characterized by large anechoic areas. The dark fluid content of thecal follicular cysts hardly ever contains any reflections (Fig. 2.52). The lumina of luteinized cysts occasionally contain a network of echoes (Fig. 2.51).

Among the sonographically visible ovarian cysts two distinct forms can be recognized. The one form has such a thin wall that its structure cannot be assessed (Fig. 2.52). Most of these structures are likely to be thecal follicular cysts. The second kind are ovarian cysts with a thicker wall. The latter is a few millimeters thick and usually hypoechoic (Fig. 2.51). Its echogenicity is similar to that of luteal tissue. The adjacent ovarian tissue usually appears rather hyperechoic in comparison to the cyst wall. These vesicular structures are likely to fall into the category of luteinized follicular cysts. If thecal and luteinized follicular cysts appear in their very characteristic forms, i.e. with either a very thin or a very thick wall, respectively, their differentiation should present little difficulty. In the mixed or transitional forms it would, however be rather more difficult to reliably distinguish between the two types on their ultrasonic appearance alone.

Avtorsko zaščiteno gradivo

Downloaded From Vet-eBooks.com

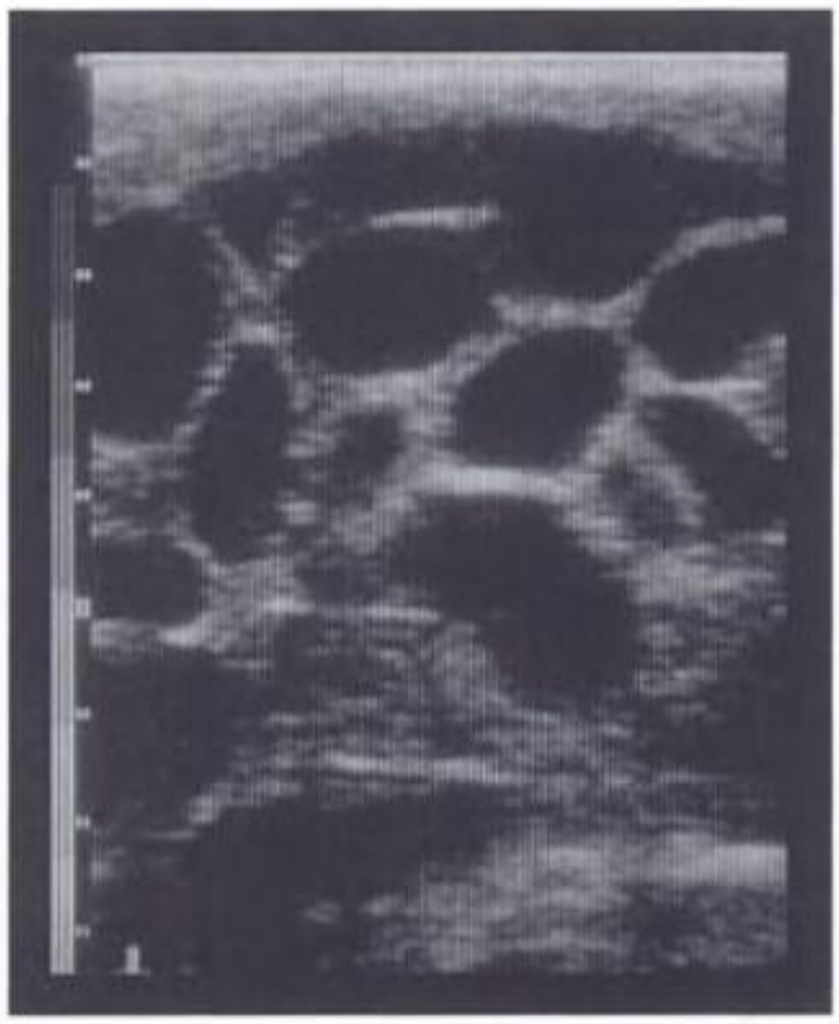


Fig. 2.53: Ovary containing multiple cysts after hormonal superovulation treatment of the cow. The cow had received daily treatments of FSH from Days 11 to 7 before and a single dose of PGF2α on Day 8 before this ultrasonogram was taken.

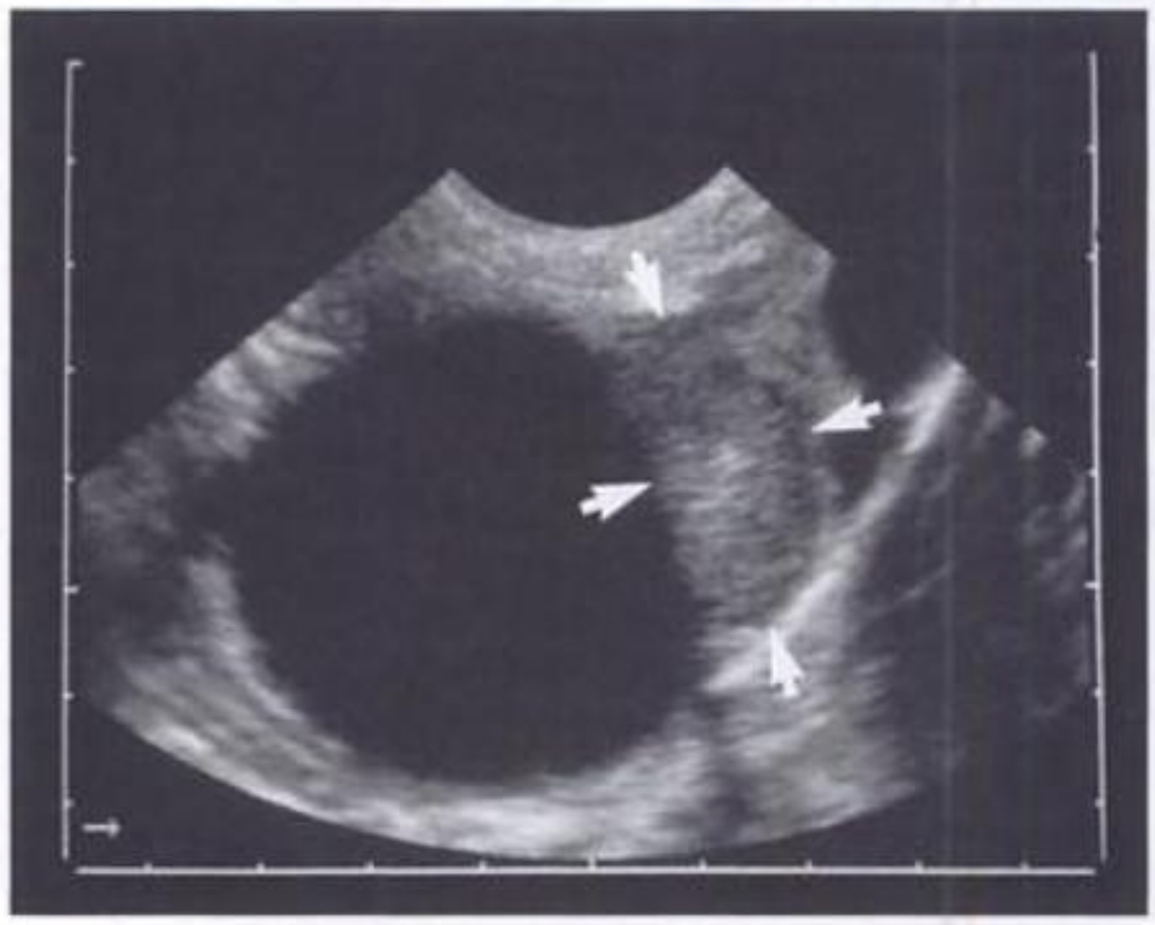


Fig. 2.54: Follicular cyst and corpus luteum of the cycle (arrows) on the ovary of a cow 13 days after she had been injected with GnRH (20 g Buserelin i.m.) for the treatment of ovarian cysts. Progesterone was elevated on the day of this ultrasound examination and the cow was treated with PGF2α. The insemination performed 4 days later resulted in a pregnancy.



Fig. 2.55: Follicular cyst in a cow on Day 59 of gestation (see Fig. 2.56).



Fig. 2.56: Pregnant uterus with fetus on Day 59 of pregnancy in a cow with an ovarian cyst (see Fig. 2.55). The fetal head (H) lies towards the right, the rump towards the left, and above the nose there is a front foot.

Avtorsko zaščiteno gradivo

Downloaded From Vet-eBooks.com

The shape of cysts ranges from round to oval to polygonal, sometimes even angular. When they occur as single structures on an ovary they are usually round. When more than one cyst appears on the same ovary their shapes are determined by the relative tensions inside adjacent cysts (Fig. 2.53). Their common, separating walls are often straight. Cysts with higher inner pressure will bulge into the lumen of cysts with lower pressure. Commonly, smaller vesicles bulge into larger cysts.

Not all follicular cysts that can be seen sonographically on ovaries of cows can be considered to have a pathological effect. Such cysts have been found during ultrasound examinations where a distinct corpus luteum of the cycle was present simultaneously (Fig. 2.54). In such cases the corpus luteum is usually the structure that determines cyclic events, which can be normal with pregnancies resulting from an involved estrus. Ovarian cysts can also be found in the presence of an intact pregnancy (Fig. 2.55 and 2.56). In single cases ovarian cysts have been detected as late as the third month of gestation.

As a result of their extensive fluid content and their resultant typical sonographic appearance ovarian cysts are easy to diagnose. Thecal follicular cysts are recognized by their thin, hyperechoic walls. Luteinized cysts can be diagnosed if they are more than 40 mm in diameter, their walls are thinner than 5 mm and they persist unchanged for a protracted period of time. The images of small luteinized cysts with thick walls can sometimes appear similar to those of large cystic corpora lutea (Fig. 2.51, 2.57 and 2.58). In the few cases where a structure with a particularly large inner cavity and a relatively thick wall are found it may not be possible to differentiate reliably between a cystic corpus luteum and a luteinized follicular cyst.

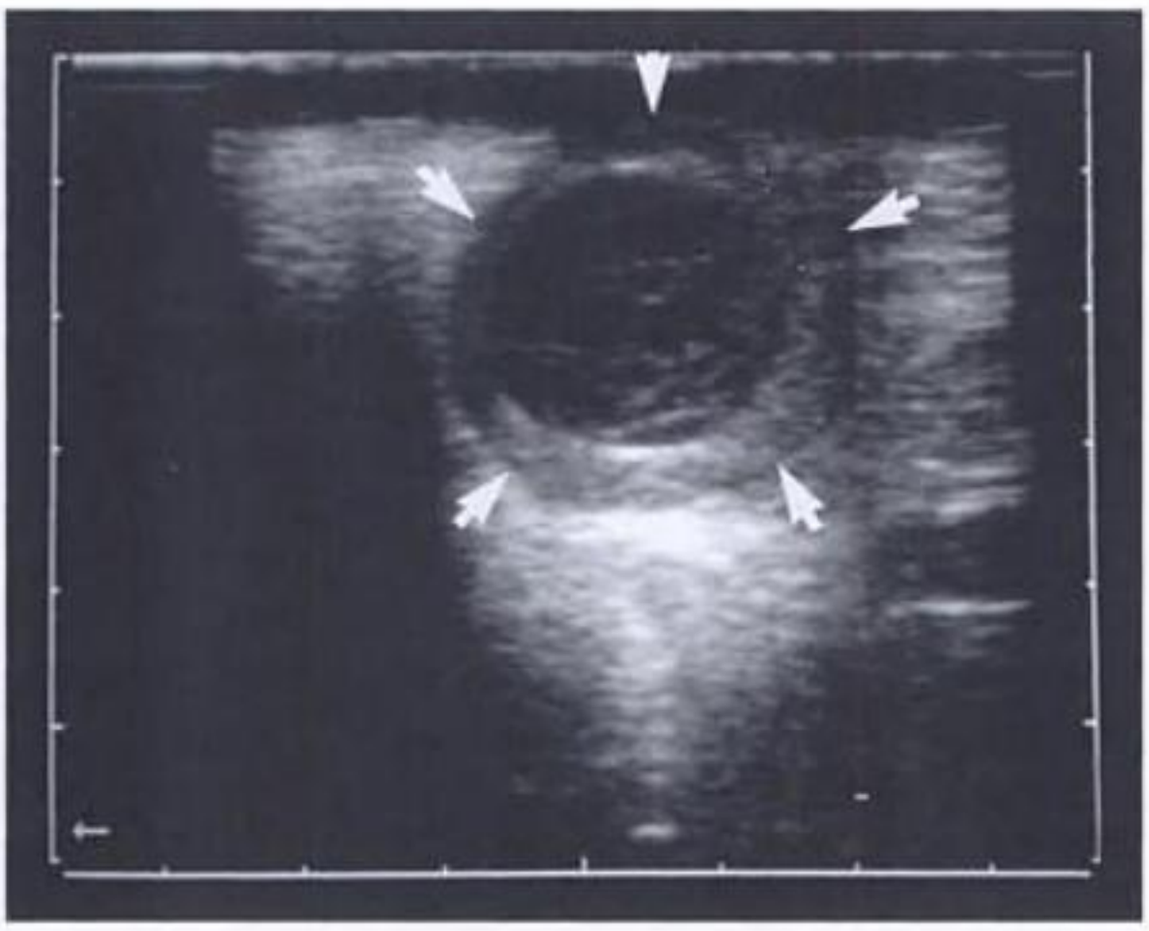


Fig. 2.57: Cystic corpus luteum (arrows) with a very large cavity 14 days after ovulation. The next estrus of this cow occurred at the normal time. Mild reflections are visible inside the lumen of the corpus luteum.



Fig. 2.58: Large cystic corpus luteum (between the crosses) 8 days after ovulation. The corpus luteum measures 36 x 27 mm and its cavity 13 x 9 mm.

Avtorsko zaščiteno gradivo

Downloaded From Vet-eBooks.com

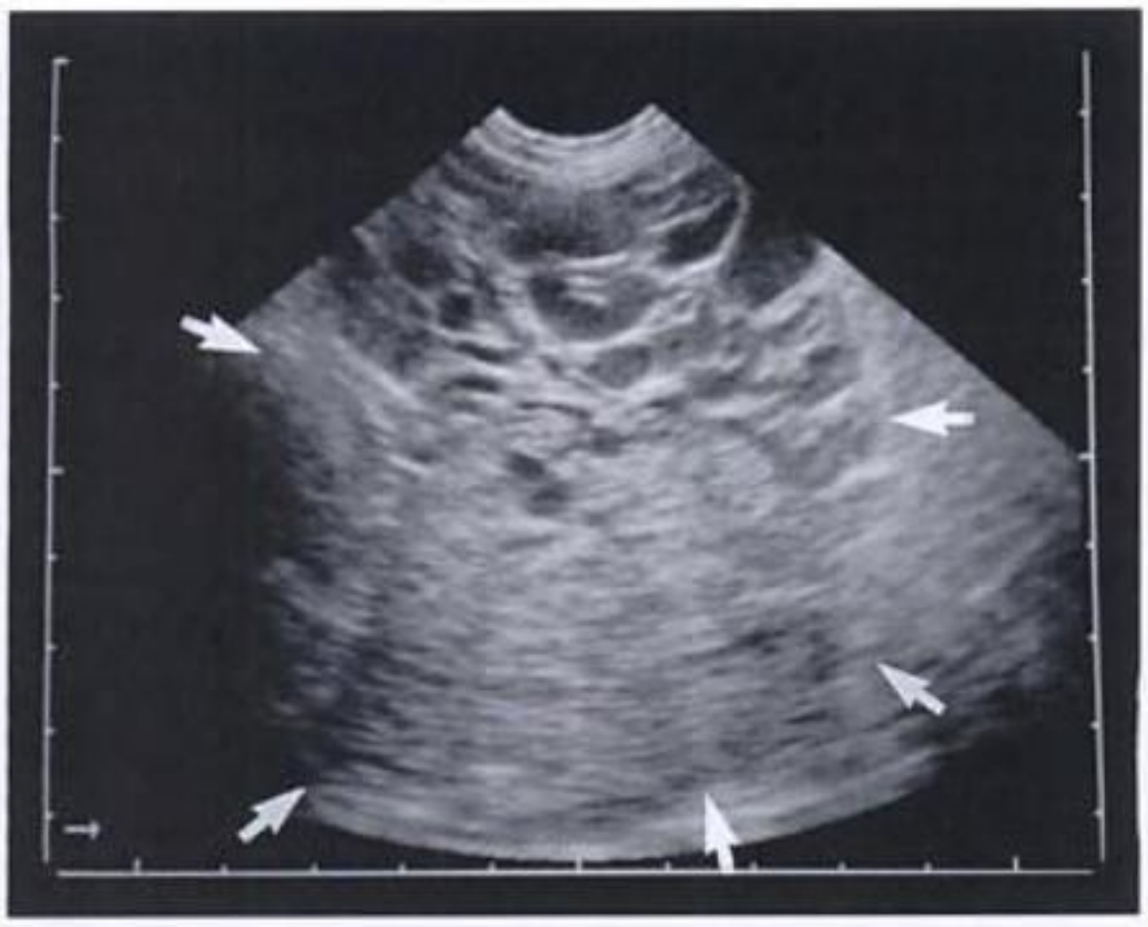


Fig. 2.59: Ovary with a granulosa cell tumor (arrows). During the last 3 weeks prior to ovariectomy, the cow had a plasma progesterone concentration of ‹ 1,0 ng/ml. There are numerous hypoechoic cross sections through blood vessels in the dorsal part of the tumor. The ventral part of the tumor shows the echogenicity typical of solid tissue.



Fig. 2.60: Cross section through the same ovarian tumor analogous to the examination plane as in Fig. 2.59.

Avtorsko zaščiteno gradivo

Downloaded From Vet-eBooks.com

2.2.4 Ovarian tumors

Ovarian tumors are rare in cattle. The case described here concerned a three and half year old cow. Nothing conspicuous was noticed about the cow during the first two months post partum. Once the cow showed estrus she was to be inseminated. When this was tried a structure twice as large as a child's head was palpated in the area of the left ovary. The right ovary was also enlarged. During an observation period of another 3 weeks the cow developed signs of nymphomania and repeated plasma hormone determinations revealed progesterone concentrations of less than 1.0 ng/ml.

The sonographic image of the tumor contained two distinct regions (Fig. 2.59). Hypoechoic transverse sections through numerous vessels were seen in the dorsal section of the tumor. The remainder of the tumor contained a coarsely granular echogenicity, producing an image of mixed tissue which was traversed by numerous cross sections of smaller vessels. The adjacent areas of brighter and less bright echoes reflected the compact nature of the tumor interspersed with islets of waxy tissue (Fig. 2.60). The outline of the tumor could be seen and measured.

Both ovaries were removed by ovariectomy. On pathological examination the left ovary was diagnosed to contain a soccer-ball-sized granulosa cell tumor with a few areas of hypervascularity. The right ovary also had changes consistent with a granulosa cell tumor.

The described ultrasonic picture of a granulosa cell tumor is not necessarily typical of this type of ovarian tumors in cattle. In this single case the tumor was very compact and its echoic sectional image was only interrupted by hypoechoic lumina of blood vessels. Other cases of granulosa cell tumors have been described as being more polycystic (Andresen et al. 1986). This type of granulosa cell tumor should then result in a sonographic image which is more commonly seen in cases of the same tumor in horses (WHITE and ALLEN 1985, KÄHN and LEIDL 1987). These often have a strong capsule of connective tissue underneath which lies a labyrinth containing numerous cystic structures (see chapter 1.2.5). The contents of the cysts may be serous or hemorrhagic and therefore generate an anechoic or moderately echoic image on ultrasound examination.

Avtorsko zaščiteno gradivo

Downloaded From Vet-eBooks.com



Fig. 2.61: Sagittal section through the non-pregnant uterus of a cow in diestrus. The large arrows indicate the greater curvature, the small arrows the lesser curvature.



Fig. 2.62: Sagittal section through a uterus during estrus. Two separate sections of the same uterine horn can be recognized. Fluid accumulations are visible inside the uterine lumen. Arrows demarcate the outer wall of the uterus. Ultrasonogram was produced with a sector scanner at 5 MHz.



Fig. 2.63: Schematic presentation of an ultrasound examination of the uterus in transverse direction using a sector scanner. The same scanning plane as in Fig. 2.64.

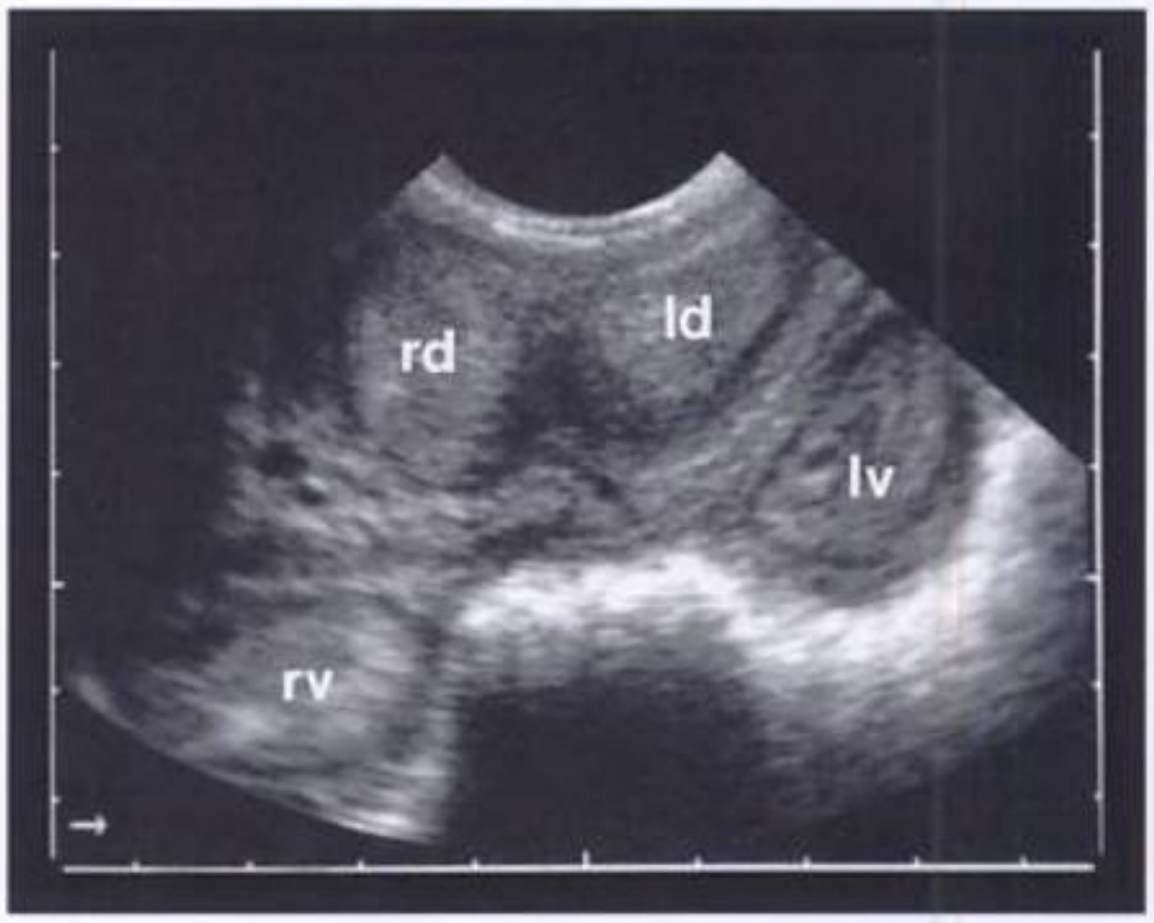


Fig. 2.64: Transverse section through the uterus on the day after ovulation. The transverse sections through the left dorsal (ld) and right dorsal (rd) parts of the horns are on top, with the cross sections through the left ventral (lv) and right ventral (rv) parts of the horns laterally and below the dorsal sectors.

Avtorsko zaščiteno gradivo

Downloaded From Vet-eBooks.com

2.3 Uterine structures in the cow

2.3.1 Non-pregnant uterus

When a linear ultrasound probe is positioned dorsally above the uterus and the sound beam is directed dorso-ventrally, a longitudinal section of the organ is obtained (Fig. 2.61). Rotating the probe slightly to the left and right brings the uterus with its horns into view. Its outline with the larger uterine curvature becomes clearly visible. The latter is a distinct narrow, hypoechoic line which separates the uterine wall from the usually somewhat more echoic surrounding tissue. The lesser curvature - the mesometrial edge of the uterus - is usually less obvious with a variable intensity. When the uterine tone is high, such as in estrus, it has, as with the larger curvature, a U-shaped, arched appearance. The dorsal and ventral sections of the same horn are at other times often so close to one another that they are separated by only a single, hyperechoic line, or diverge at a very acute angle.

The entire length of the spiraling uterine horn can usually only be depicted in a single image if the uterus is optimally positioned and the probe is directed at an acute angle in relation to the longitudinal axis of the cow. In addition, the ultrasound beam must be rotated slightly from dorsoventral to dorsolateral. In the majority of cases it is impossible to depict the entire curvature of a horn in a single image. Instead, by virtue of its curvature, the uterus can be sectioned at several places (Fig. 2.62). Using a linear scanner, between two and four sections through the uterine horn can often be visualized in a single image (TAVERNE et al. 1985). Also in the case of a pregnant uterus, its wall and the embryonic vesicle in its lumen will be sectioned at various levels. Only very rarely is it possible to depict the whole length of an embryonic vesicle (see chapter 2.3.2.5).

When using a suitable sector scanner, its greater maneuverability inside the rectum permits the operator to project a greater variety of sections through the uterus (Fig. 2.63 and 2.64). The fan shaped ultrasound plane can be rotated from the longitudinal axis of the animal, through various steps all the way to a perfectly transverse position. In this manner it is possible, with the sound waves directed dorsoventrally and transversely to the animal, to project a cross section through the uterus. In this plane of examination, a total of 4 transverse sections through the left and right uterine horns can be depicted simultaneously. These include 2 sections through the dorsal parts of the uterine horns and laterally below them 2 cross sections of the ventral parts of the uterine horns.

With the probe guided appropriately along a suitable path, the winding of the uterine horns from medial to lateral can be followed. Doing this creates the impression that the tips of the uterine horns curl more dorsocaudally during the luteal phase than during the days just before and just after estrus (PIERSON and GINTHER 1987). During the periovulatory period the horn ends are directed more horizontally in the caudolateral direction without rolling up in the dorsal direction. The lesser curvature describes a larger radius during this time than during diestrus. The spiraling shape of the uterus is therefor most pronounced during the phase of elevated progesterone concentrations.

Avtorsko zaščiteno gradivo

Downloaded From Vet-eBooks.com

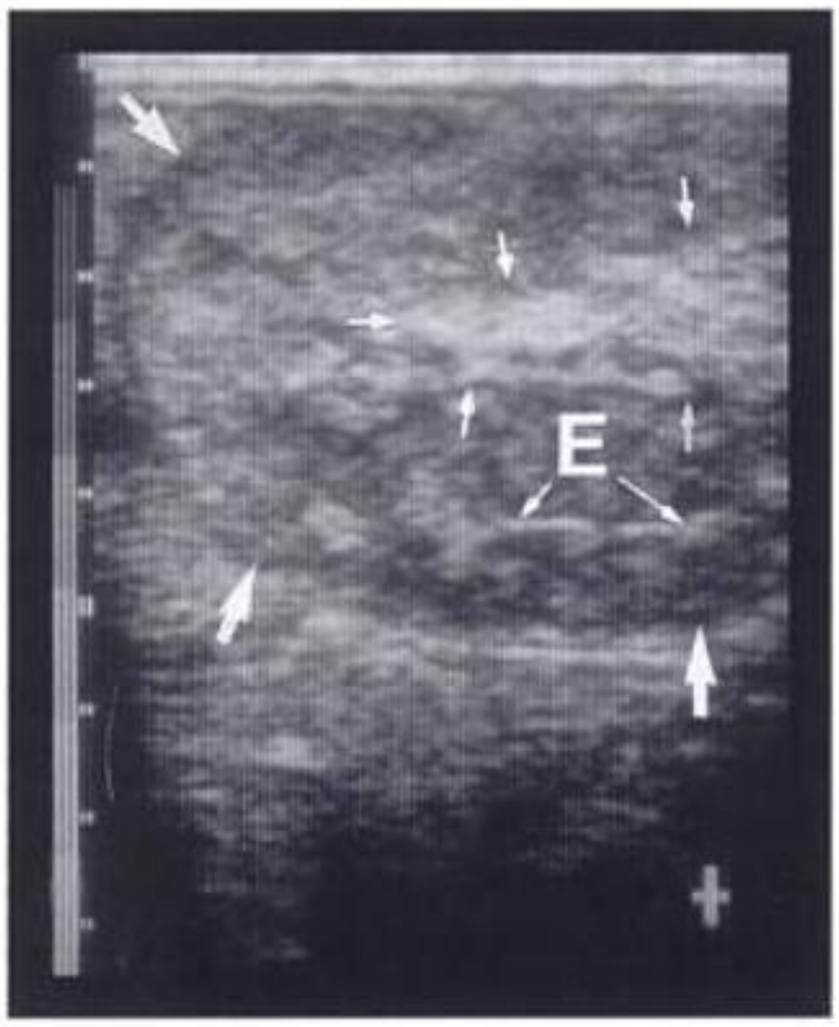


Fig. 2.65: Uterus of a cow during estrus. In the ventral part of the horn the hyperechoic line representing the appositioned surfaces of the endometrium (E). Large arrows indicate the greater curvature, small arrows the lesser curvature.

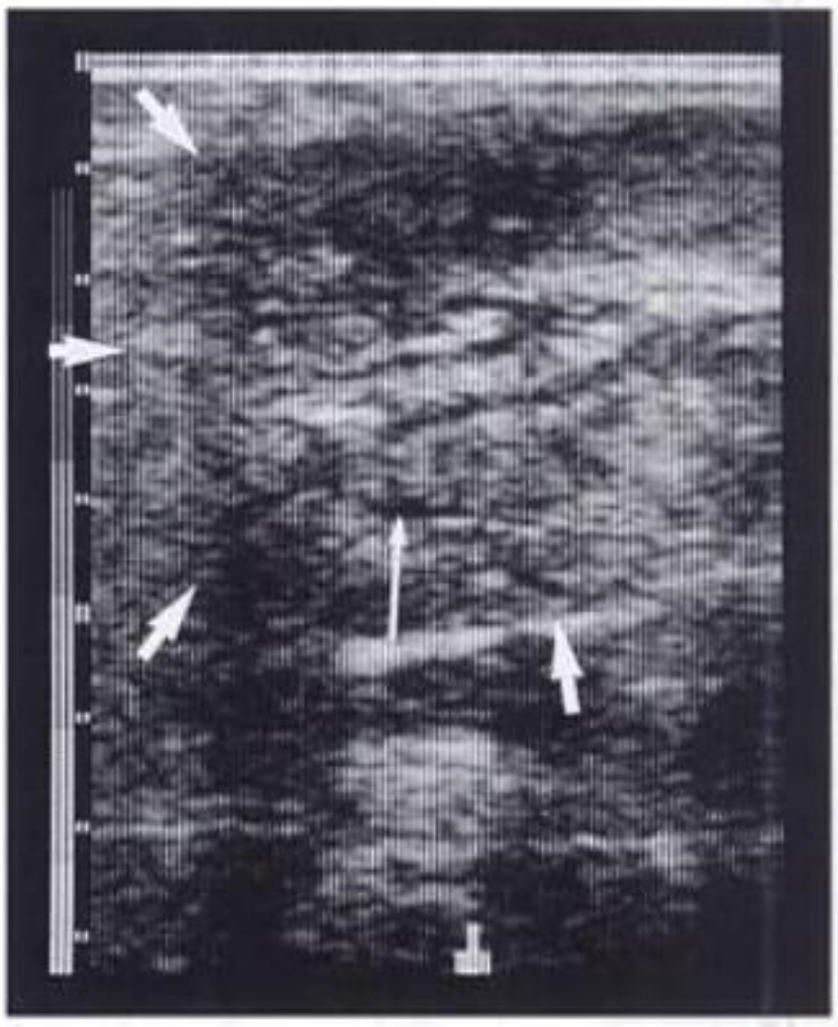


Fig. 2.66: Uterus of a cow during diestrus 8 days post ovulation. In the ventral sector of the horn a fluid accumulation can be recognized (small arrow). Large arrows demarcate the greater curvature.



Fig. 2.67: Sagittal section through a uterus during estrus. There is a few millimeter thick, hypoechoic area, representing estrous secretions (S), in the ventral part of the horn. Arrows demarcate the greater curvature.



Fig. 2.68: Sagittal section through a uterine horn during estrus. A prominent accumulation of secretions is present in the tip of the horn (arrows).

Avtorsko zaščiteno gradivo

Downloaded From Vet-eBooks.com

The section through the uterine wall contains granular, variably structured shades of echogenicity. In the center of the organ the appositioned surfaces of the luminal epithelium often produce a hyperechoic line (Fig. 2.65). This runs along the middle of the uterine section, from the tip of the horns up to and through the cervix. Large, coherent and anechoic fluid accumulations are not normally seen during diestrus. Depending on the stage of the cycle, smaller, thread like cavities a few millimeters thick can be found in the uterine lumen (Fig. 2.66 to 2.68). These are usually seen during estrus, but can also occur during diestrus. They are free of echoes and can be seen in various of uterine sections (PIERSON and GINTHER 1984 a). During estrus the amount of accumulated secretions in the uterine lumen varies considerably and may reach several centimeters (Fig. 2.68).

Avtorsko zaščiteno gradivo

Downloaded From Vet-eBooks.com

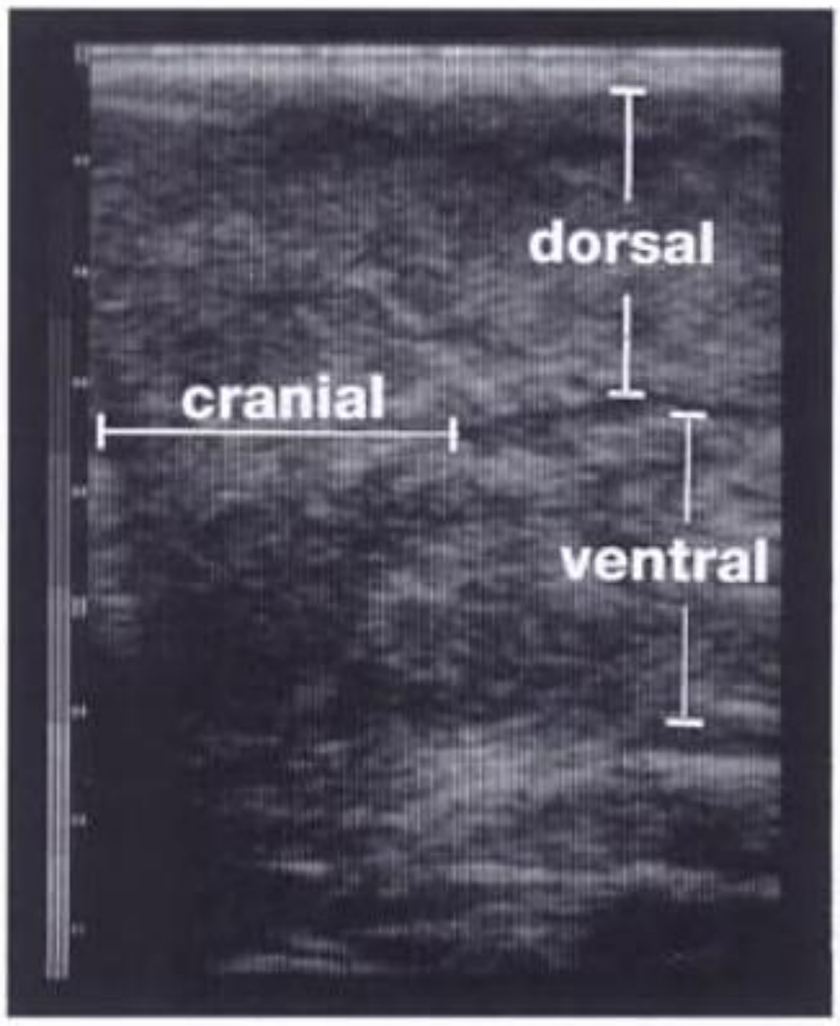


Fig. 2.69: Example of measuring the dorsal, cranial and ventral diameters of a uterine horn



Fig. 2.72: Example of an heterogenous uterine wall. Apart from the thin fluid accumulations there are areas of greater and lesser echogenicity in the uterine wall. Arrows demarcate the greater curvature.

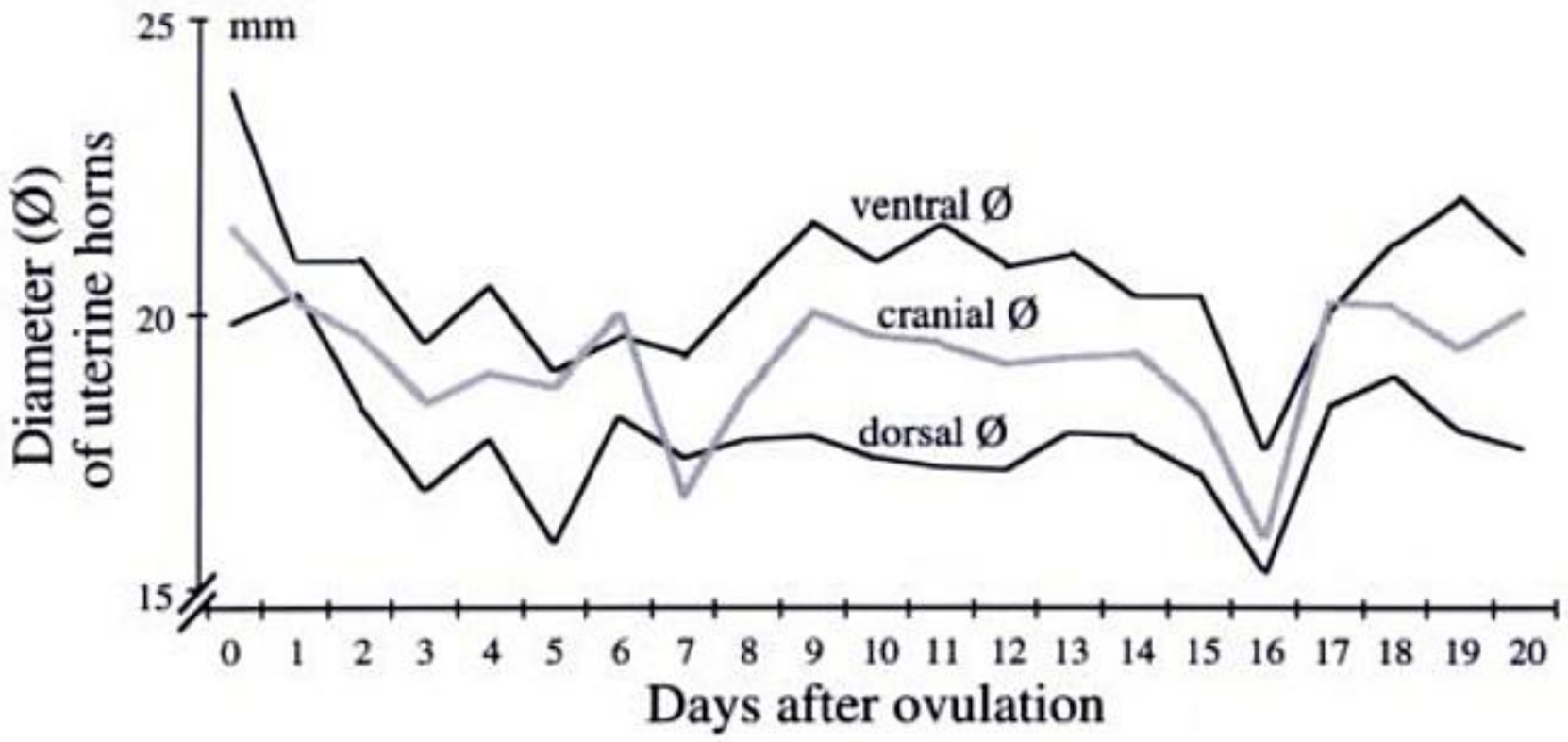


Fig. 2.70: Mean dorsal, cranial and ventral diameters of non-pregnant uterine horns during the estrous cycle in heifers.

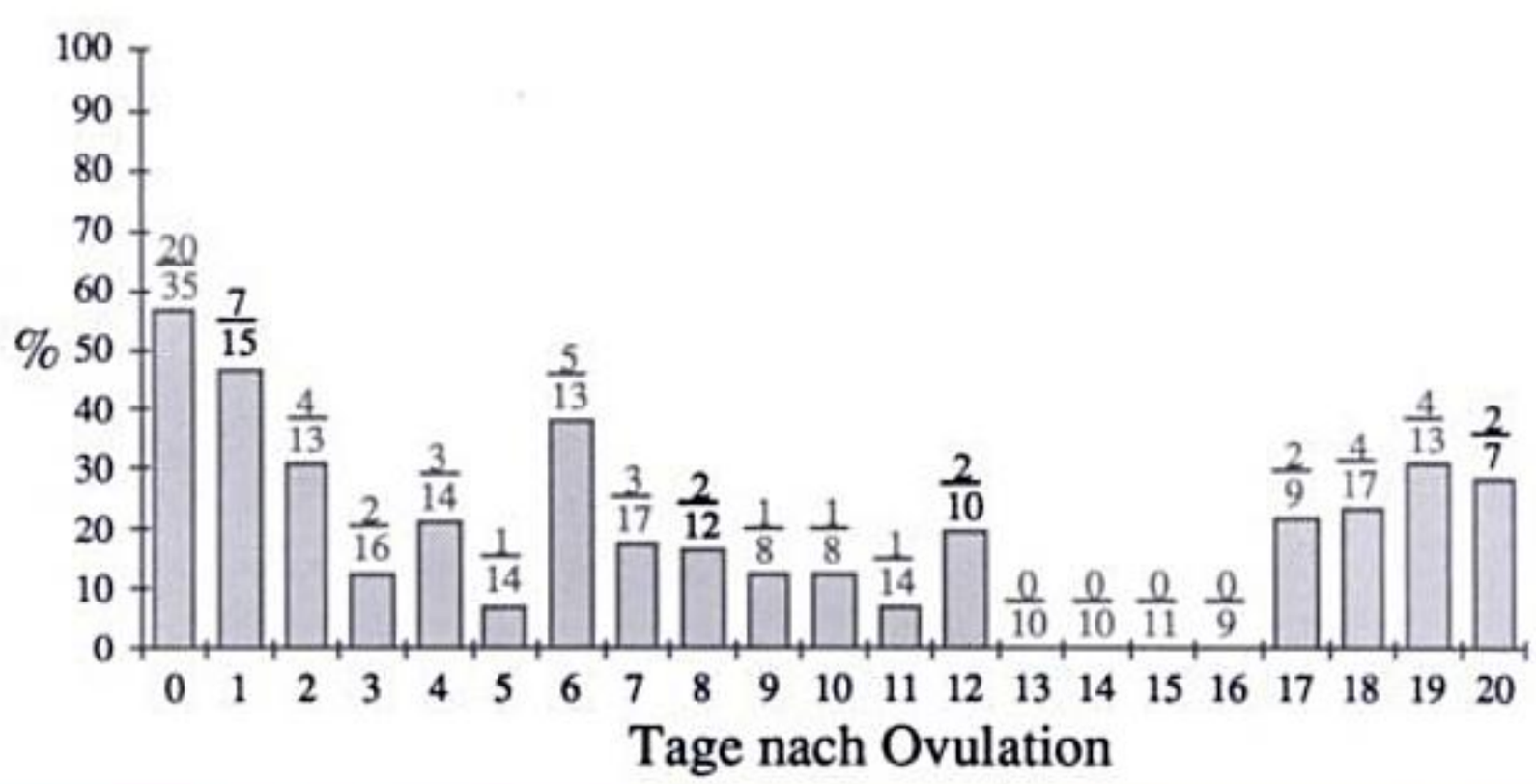


Fig. 2.71: The percentage of cows in which a sonographically detectable fluid accumulation could be found during the estrous cycle.

Avtorsko zaščiteno gradivo

Downloaded From Vet-eBooks.com

Several investigations were conducted to test whether any correlations between the stage of the cow's cycle and the ultrasonic image of her uterus existed. For this purpose the diameter of the uterine horns, intrauterine fluid accumulations and the sonographic appearance of the uterine wall were determined in a total of 51 estrous cycles of 12 heifers.

The thickness of the uterine horns could be monitored by measuring the changes in the dorsal, cranial and ventral diameters of the uterine horns (Fig. 2.69). All three diameters were largest at the time of estrus (Fig. 2.70). They decreased significantly during metestrus until the beginning of diestrus. The uterine horns then became thicker again to reach their widest diestrous diameter during the middle of cycle, between Days 9 and 14. On, or about Day 16 a substantial decrease in the uterine horn diameters occurred. The thickness of the horns increased again until the next estrus. Overall, a cycle dependent change in the thickness of the uterine horns could be demonstrated (VOLLMERHAUS 1957, PIERSON and GINTHER 1987). Throughout the cycle their thickest portion was the ventral, curved section of the horn. At the cranial and dorsal measuring sites the diameters were approximately 1 to 4 mm thinner.

In a large proportion of cows fluid accumulations are sonographically visible in the uterus at the time of estrus (PIERSON and GINTHER 1984 a). They are detected in about half the heifers on the day of estrus and in about one third of the heifers during the few days just prior or after estrus (Fig. 2.71). It is interesting that fluid accumulations can also occasionally be demonstrated during the early and mid luteal phase. The most frequent site of the fluid accumulation lies just distal to the larger curvature of the uterine horn in the part that winds caudolaterally. Fairly frequently, however, hypoechoic areas can also be found in other parts of the uterus. The size of the fluid accumulations can vary markedly in non-pregnant uteri. During estrus and diestrus fluid accumulations measuring 30 to 40 mm in length and 5 to 10 mm in width can occur.

The fact that fluid can also be found in the non-pregnant uterus is of considerable importance for the sonographic diagnosis of early pregnancy. Since secretions can be present in the uterus at any stage of the entire estrous cycle, even if no conception has taken place, the mere detection of a fluid accumulation should not be interpreted as a reliable sign of pregnancy. Pregnancy can only be diagnosed when embryonic components can be identified with certainty.

Particularly during proestrus, estrus and metestrus a layering of the uterine wall into a hypoechoic, adluminal zone and a more echoic peripheral zone is recognizable (Fig. 2.72). During this period one third to a half of all cows have a heterogeneously structured uterine wall. In about one half of those cows in which the structure of the uterine wall was examined ultrasonically during normal estrous cycles, a heterogenous structuring of the uterine wall could be recognized on the day of estrus. In the other half of the cows the uterine wall appeared to be homogeneously structured. During metestrus between 28 and 53 % of the cows still had heterogenous uterine walls. Laminated uterine walls could only be seen in a few cows during diestrus but in the majority of cases the uterine wall was homogeneously structured. During the days preceding the following estrus the percentage of heterogeneously structured uterine walls increased again to reach 50 %.

As a result of the edema of its more superficial layers and the accumulation of secretions, the inner areas of the uterine wall will become less echoic during the estrogen dominated stages of the estrous cycle. This leads to the layered image of the uterine wall. This seems to be a similar phenomenon to that observed in estrous mares where the edematous endometrium is distinct from the more dense tissue of the myometrium (GINTHER and PIERSON 1984, KÄHN and LEIDL 1985).

Avtorsko zaščiteno gradivo

Downloaded From Vet-eBooks.com

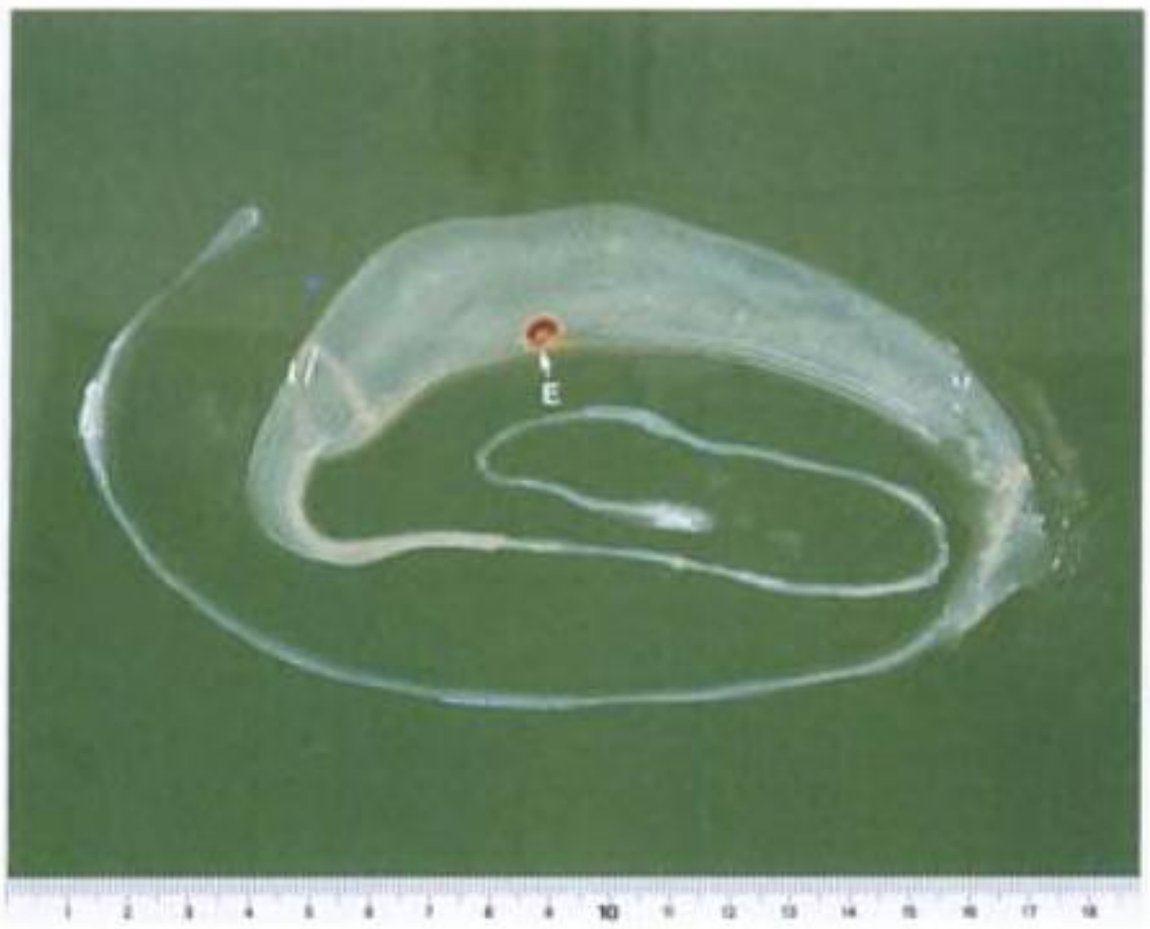


Fig. 2.73: Embryonic vesicle with embryo (E) from a cow on Day 26 of gestation (removed from the uterine lumen). The allantochorionic vesicle stretches thread like from the tip of one uterine horn to the other. In the pregnant horn the increase in embryonic fluid leads to an enlargement in the transverse diameter of the vesicle.



Fig. 2.74: Uterus on Day 12 of pregnancy. Hypoechoic sections (small arrows) through the embryonic vesicle are visible in several places. The outline of the uterine horn is demarcated by the larger arrows. Ultrasonogram produced with sector scanner at 5 MHz.

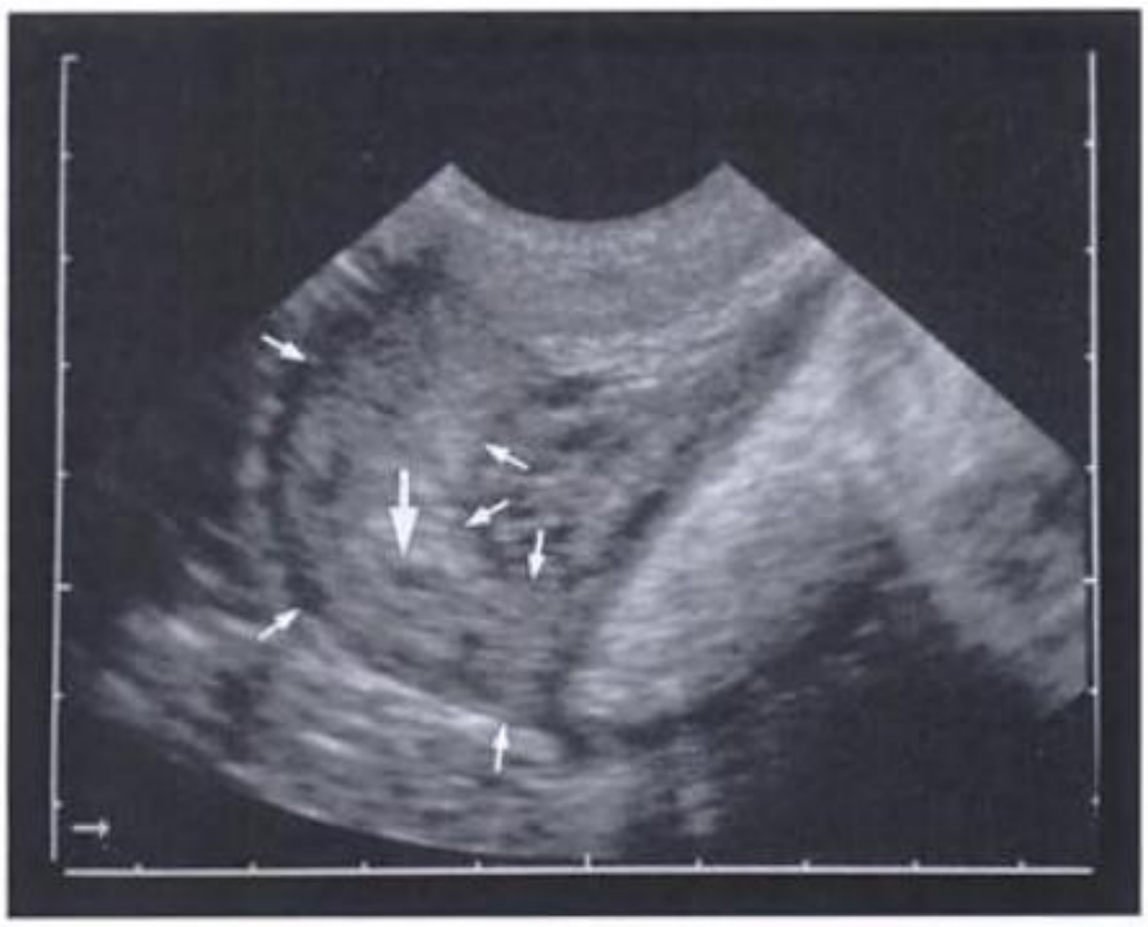


Fig. 2.75: Bovine uterus on Day 12 of pregnancy. A Hypoechoic section (large arrow) through the embryonic vesicle is visible in the ventral part of the uterine horn. The greater and lesser curvatures are demarcated by small arrows. Ultrasonogram produces with sector scanner at 5 MHz.

Avtorsko zaščiteno gradivo

Downloaded From Vet-eBooks.com

2.3.2 Pregnant uterus

From Day 15 of pregnancy the embryonic vesicle of the bovine will be a thin, thread like tube in the uterine lumen (BETTERIDGE et al. 1980). By Day 20 it will stretch from the tip of one uterine horn to the other and have a total length of up to 1 meter (WINTERS et al. 1942, CHAFFAUX et al. 1982). Until Day 25 the cross sectional diameter of the allantochorionic and amniotic vesicle is still so small that a fluid filled embryonic vesicle can only be detected by using higher frequency ultrasonography of 5 MHz or more (KÄHN 1985). From around Day 25 the amount of fluid in the allantochorionic vesicle increases rapidly so that also the embryonic vesicle's transverse diameter becomes considerably greater (Fig. 2.73).

2.3.2.1 Day 10 to 20 of pregnancy

If cows are examined sonographically every day after insemination a minute fluid accumulation may become apparent between Days 10 and 17 of the cycle (Fig. 2.74 and 2.75). The fluid will lie in the horn ipsilateral to the corpus luteum (CURRAN et al. 1986 a). It will appear as thin, anechoic areas that are round in shape in three quarters of all cows and measure 2 to 4 mm in size (PIERSON and GINTHER 1984 a). In approximately one third of the pregnant cows they will be elongated and are 2 mm thick and 3 to 7 mm long. The diameter of the embryonic vesicle appears to remain constant from Day 10 until Day 18, only its length increases. Between Days 17 and 20 of gestation, sometimes even earlier, hypoechoic sections through the embryonic vesicle are visible in various sectors of the pregnant horn of the uterus. In most cases these minute fluid accumulations are sections through the chorionic vesicle. At this stage it lies thread like in the uterine lumen and contains very little fluid (GREENSTEIN and FOLEY 1958). Around day 19 the embryonic vesicle will form a slight distention usually near the middle of the pregnant horn, in the same area where the fluid first became visible.

Sonographic imaging of the embryonic vesicle at this early stage is difficult and thus unreliable. For example experience was made that a fluid filled vesicle could be detected in some cows between Days 11 and 13, but not between Days 14 and 17, although the cows were later found to be pregnant. The maximum diameter of the fluid accumulation in early pregnancy before Day 20 reaches not more than 2 to 3 mm (BETTERIDGE et al. 1980). The largest diameter of the embryonic vesicle therefore lies at the lower limit of resolution achieved even by high performance ultrasound equipment. While it seems feasible that ultrasonography can be applied successfully for research purposes to study early pregnancy, it is not possible to use ultrasonography as a tool for the reliable pregnancy diagnosis before Day 20 (KASTELIC et al. 1989). From a differential diagnostic point of view the hypoechoic fluid accumulations cannot be distinguished reliably from similar images seen during estrus, diestrus or in certain pathological conditions.

Avtorsko zaščiteno gradivo

Downloaded From Vet-eBooks.com

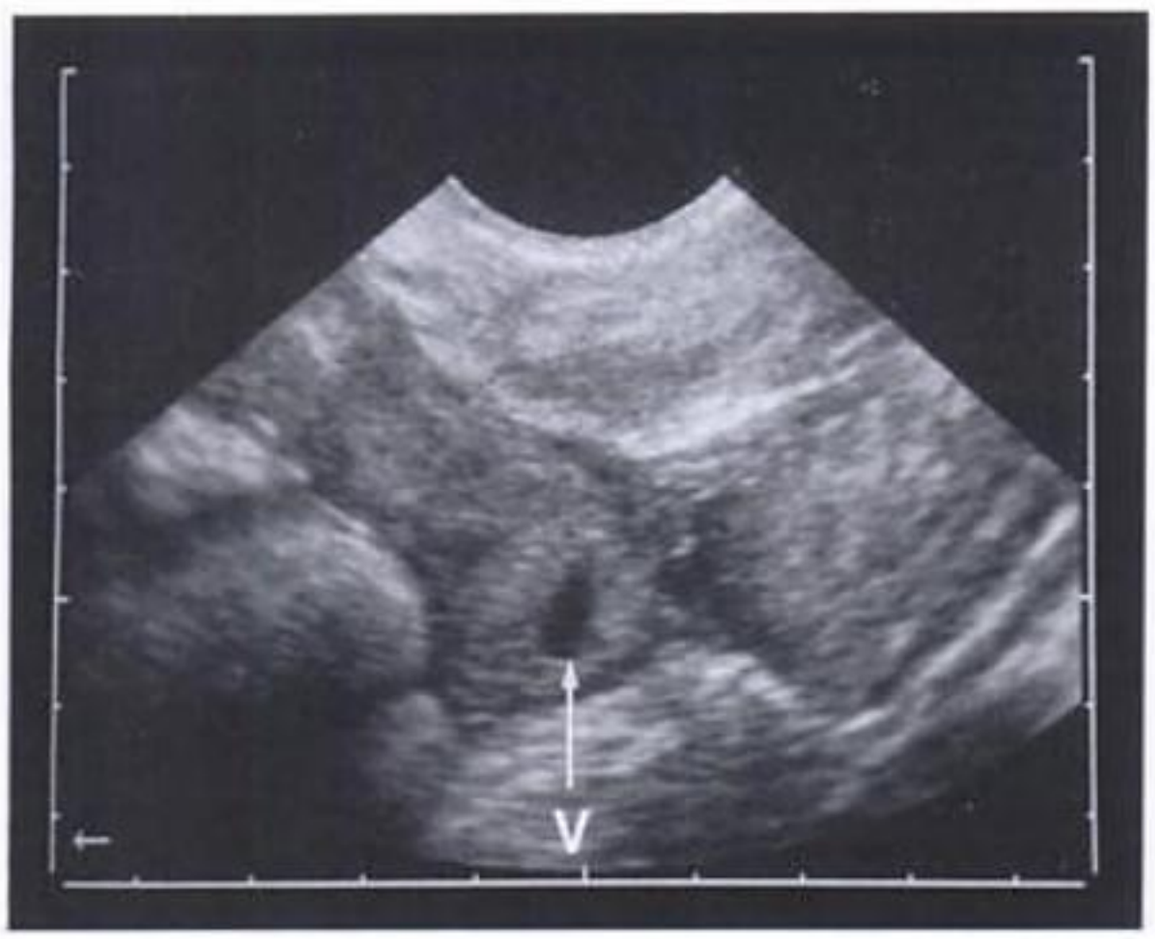


Fig. 2.76: Uterus on Day 21 of pregnancy. The hypoechoic area of the embryonic vesicle (V) has a size of 9.5 x 4 mm. Ultrasonogram produced with a sector scanner at 5 MHz.



Fig. 2.77: Uterus on Day 22 of pregnancy. The largest fluid collection inside the embryonic vesicle (V) is located in the ventral portion of the uterine horn. Arrows demarcate the greater curvature.

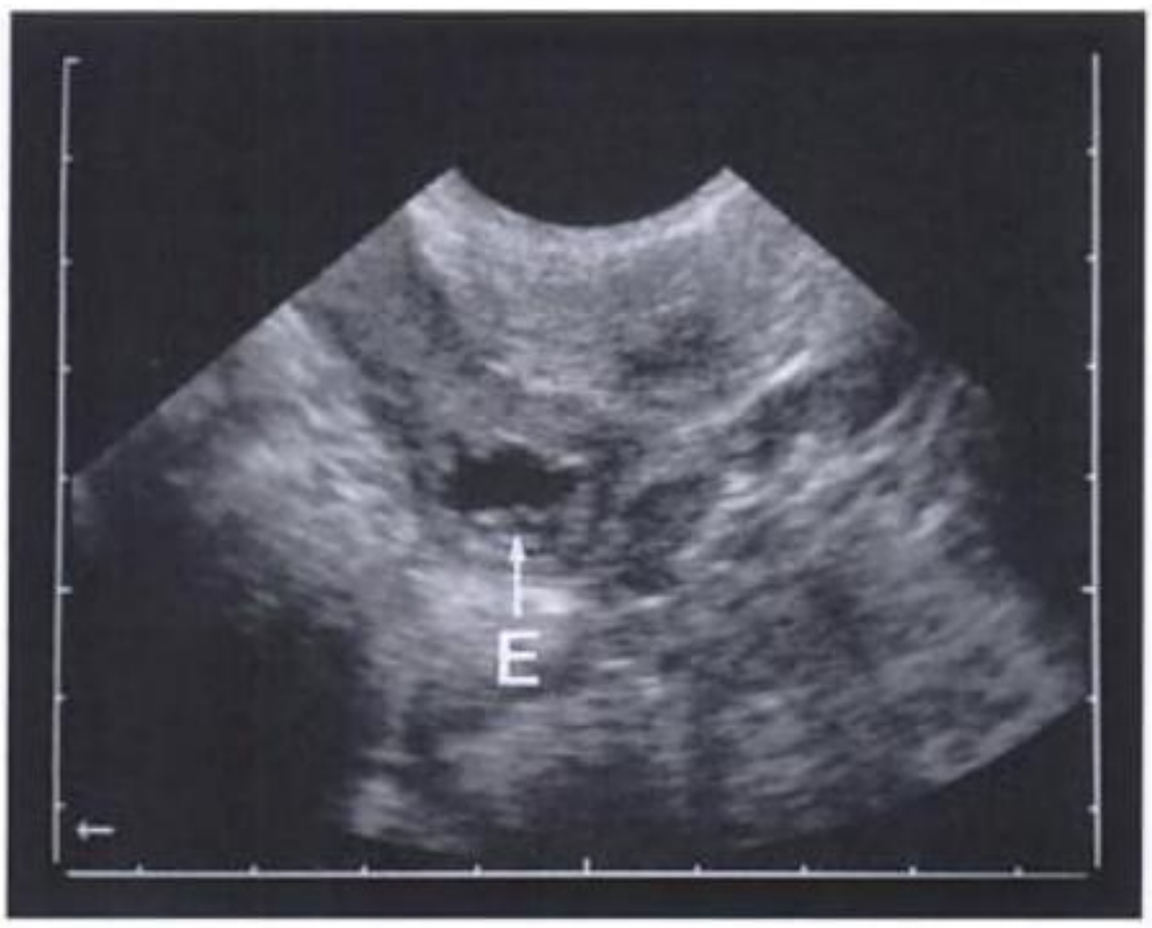


Fig. 2.78: Uterus on Day 23 of pregnancy. The embryo (E) lies at the floor of the vesicle. During real time scanning pulsation was detectable in the area of the developing heart. Ultrasonogram produced with sector scanner at 5 MHz.

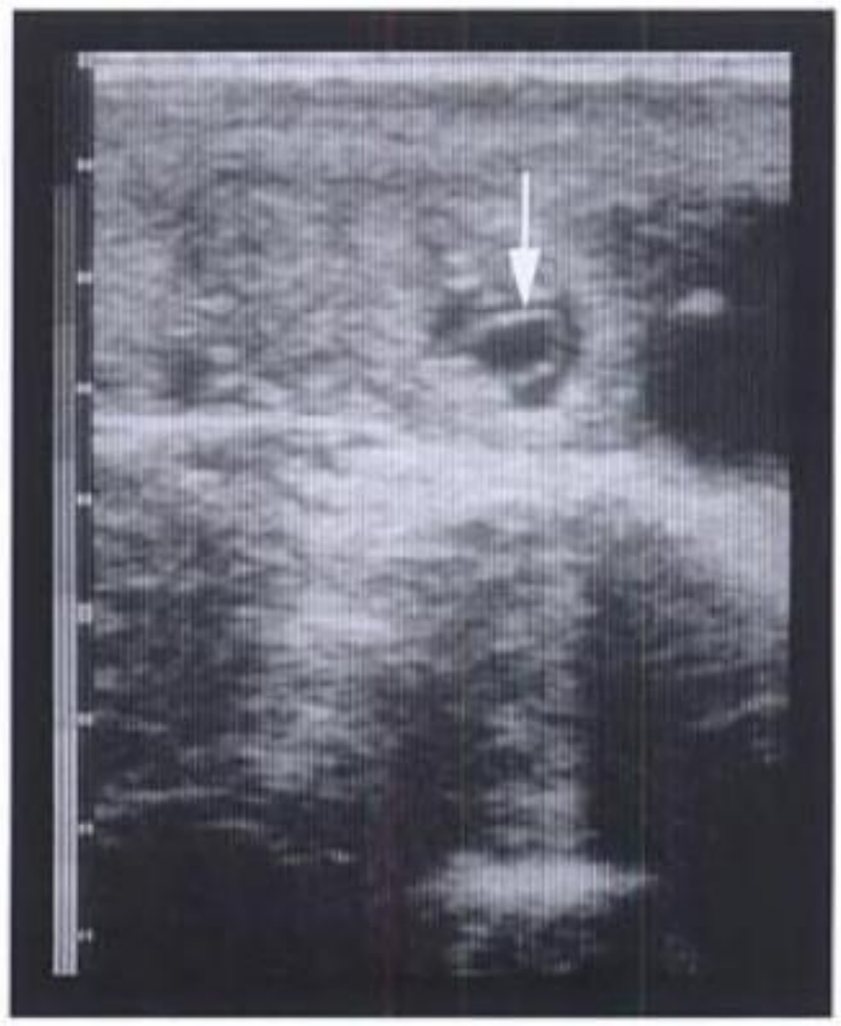


Fig. 2.79: Uterus on Day 24 of pregnancy. The allantoic membrane (arrow) floats inside the embryonic vesicle.

Avtorsko zaščiteno gradivo

Downloaded From Vet-eBooks.com

2.3.2.2 Day 21 to 24 of pregnancy

Between Days 21 and 24 of gestation the amount of fluid inside the embryonic vesicle has usually increased to such an extent that it becomes easier to visualize by ultrasonography (Fig. 2.76). At the site of its greatest expansion, usually in the area of the amnion, the embryonic vesicle reaches a diameter of between 3 and 5 mm and a length of about 1 cm on Day 22 of gestation (KÄHN 1985). The largest fluid accumulation is most frequently seen for the first time distal to the curvature of the uterine horn, in its free, winding section (Fig. 2.77). This is also the site where the embryo and its surrounding amnion become detectable for the first time.

Before Day 25 of pregnancy it can often be difficult to find the embryo itself. Sometimes its presence can be suspected, but it is difficult to differentiate it from other echoic structures. Rather frequently, though, it can be identified without doubt (Fig. 2.78). The length of the embryo between Days 21 and 24 is about 5 mm (CURRAN et al. 1986 a). Occasionally it is even possible at this time to see a heart beat in the form of flickering echoic points.

The non-pregnant status of a cow can, under certain circumstances, be diagnosed around Day 20 to 23 post insemination. In these cases one would base the negative pregnancy diagnosis on the small size of the corpus luteum (largest diameter ‹ 20 mm) and the absence of fluid in the uterus (KASTELIC et al. 1989). A positive pregnancy diagnosis can only be made with certainty once an embryo has been identified.

A thin, hyperechoic and towards the tip of the horn bulging membrane can sometimes be seen inside the embryonic fluid at about this stage of pregnancy (Fig. 2.79). Based on its position and the time of its appearance it is assumed that it represents the allantois (CURRAN et al. 1986 b). This thin, slightly floating membrane is only visible for a few days. According to experiences made thus far it is most frequently detectable on Days 23 to 26 of gestation. In some cases it may still be seen on Day 30 (Fig. 2.80). In the bovine, the allantoic vesicle undergoes particularly rapid growth in length around the 23rd day of pregnancy (SALISBURY et al. 1978). By Day 32 to 37 the allantois will line the entire inner surface of the chorion.

During this earliest phase of the sonographic pregnancy diagnosis particular attention must be paid to confirm that the observed fluid accumulation is intrauterine. There is always the pitfall of confusing the blood vessels that run on the surface of the uterus with fluid accumulations within the uterine lumen (TAVERNE et al. 1985). Finding the conceptus with certainty at this stage requires a thorough sonographic examination of the uterus. To establish an accurate diagnosis can sometimes take several minutes.

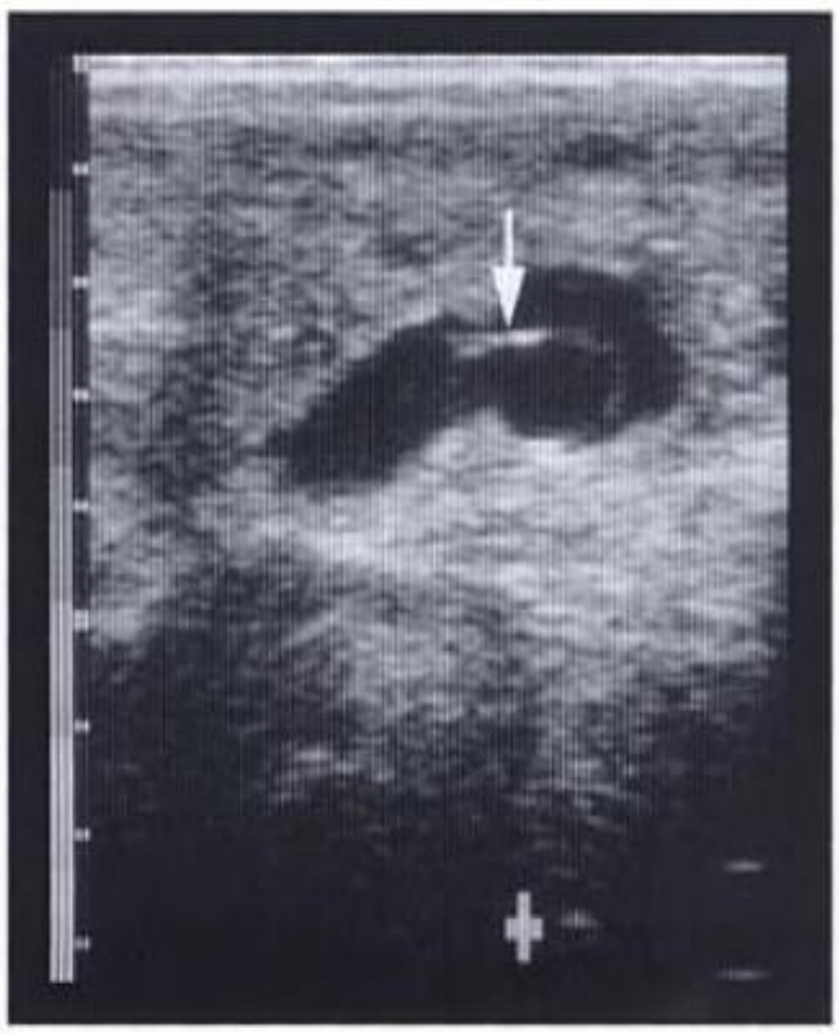


Fig. 2.80: Uterus on Day 28 of pregnancy. The membrane of the allantoic vesicle bulges towards the tip of the uterine horn. In the area where the sound waves impact vertically onto the allantoic membrane an intensive echo (arrow) becomes visible.

Avtorsko zaščiteno gradivo

Downloaded From Vet-eBooks.com

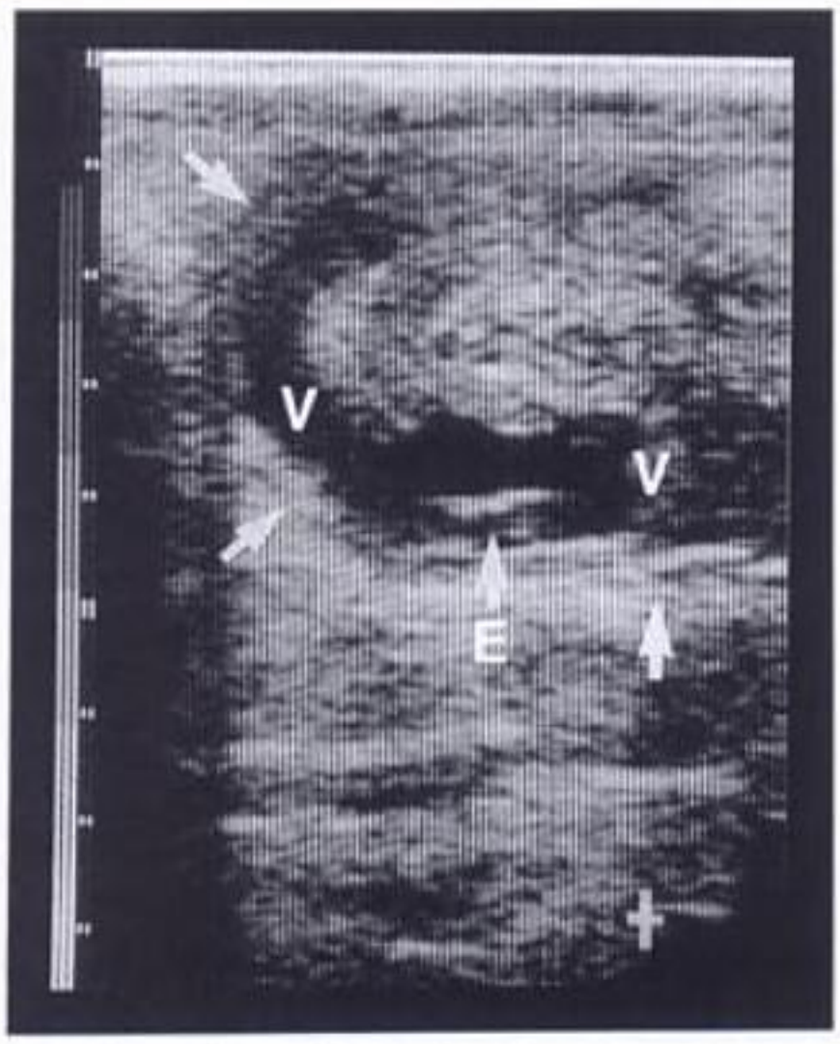


Fig. 2.81: Embryonic vesicle (V) and embryo (E) on Day 25 of pregnancy. The embryonic vesicle extends along the curvature (arrows) into the dorsal portion of the uterine horn.



Fig. 2.82: Embryonic vesicle on Day 26 of pregnancy. Two sections through the embryonic vesicle are visible. They appear to be separated by a portion of the echoic uterine wall.



Fig. 2.83: Nuclear magnetic resonance image of a uterus on Day 26 of pregnancy. In the pregnant horn three folds of the uterine wall protrude into its lumen laterally (small arrows) and one from dorsal to ventral (large arrow). Lateral to the horns are the ovaries (Ov).

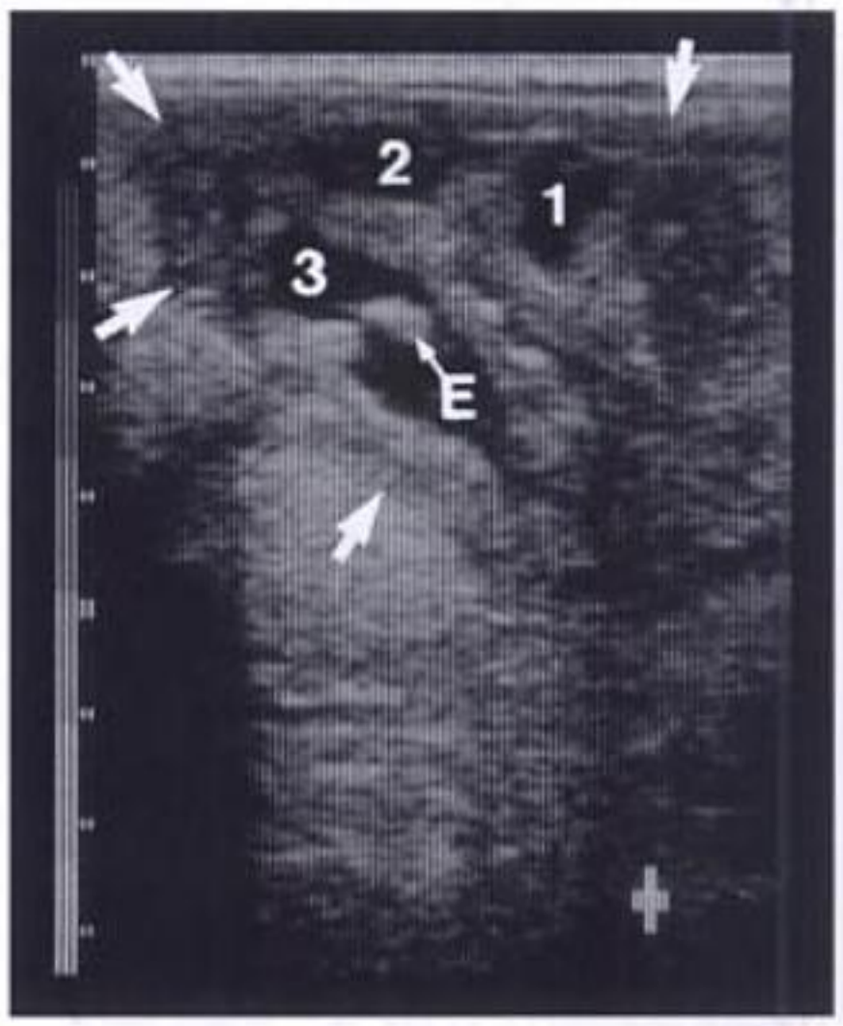


Fig. 2.84: Vesicle and embryo (E) on Day 29 of pregnancy. Portions of the uterine wall which lie in the scanning plane and the embryo divide the embryonic vesicle into pseudoampullar sectors (1, 2 and 3). Arrows demarcate the outline of the uterus.

Avtorsko zaščiteno gradivo

Downloaded From Vet-eBooks.com

2.3.2.3 Day 25 to 30 of pregnancy

On Day 25 of pregnancy the embryonic vesicle of the bovine reaches a diameter of 10 mm at the point of its largest expansion. By slight rotations of the ultrasound probe the course of the embryonic vesicle can be followed into much further areas of the free segment of the pregnant uterine horn at this stage. It also stretches through the curvature of the horn into the part where the two uterine horns are fused to form the uterine body (Fig. 2.81). Until Day 30 the diameter of the embryonic vesicle increases to 18 to 20 mm and is then also visible in the contralateral horn (CHAFFAUX et al. 1982, CURRAN et al. 1986 b). In the contralateral horn is much narrower with a diameter of 4 to 8 mm.

The course of the pregnant uterine horn - with its dorsal segment, the ventral bend and the caudally directed portion - is best demonstrated if the probe is positioned above the uterus with its sound plane oriented along the longitudinal axis of the cow's body and the beam directed dorsoventrally with a slight lateral deviation. This produces a sagittal section through the uterine horn which is characterized by the echoic, curved uterine wall surrounding the anechoic embryonic vesicle. It is usually not possible to position the sonographic plane in such a way that the embryonic vesicle is simultaneously visible in all parts of the horn. More often, only various segments of the embryonic vesicle will be depicted (Fig. 2.82 to 2.84). The fluid sac of the embryonic vesicle is interrupted in places by folds of the uterus which project into the lumen. This creates a pseudo-ampullar image (KÄHN et al. 1989). These folds and their spatial arrangement can be demonstrated very well on NMR scan pictures (Fig. 2.83). Typically, 2 to 3 anechoic sections through the chorionic vesicle are visible on a single ultrasound image at Day 25 of gestation (Fig. 2.82). More sections through the embryonic vesicle will become visible during the next few days so that 4 to 6 sections can often be seen by Day 30 (Fig. 2.84).

Avtorsko zaščiteno gradivo

Downloaded From Vet-eBooks.com



Fig. 2.85: Vesicle and embryo (E) on Day 26 of pregnancy. The embryo lies adjacent to the uterine wall.



Fig. 2.86: Vesicle and embryo (E) on Day 31 of pregnancy. The embryo is starting to move away from the uterine wall.

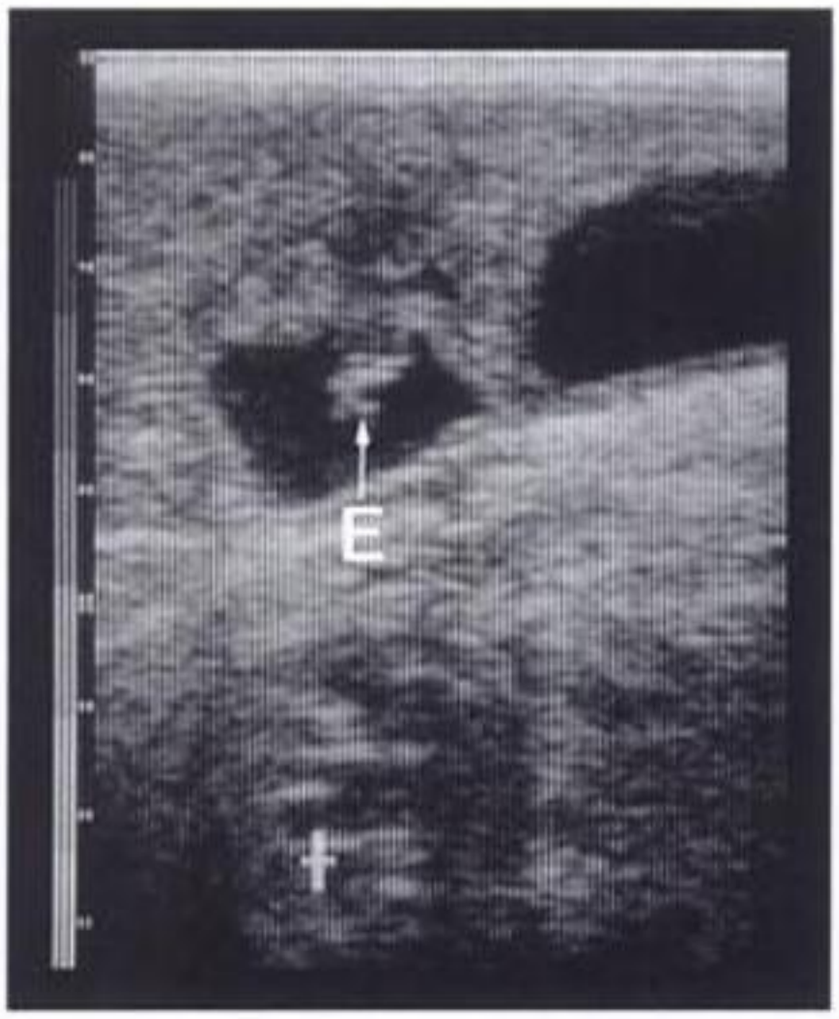


Fig. 2.87: Comparison of the sonographic pregnancy diagnosis at 5 MHz. Vesicle and embryo (E) on Day 32 of pregnancy.



Fig. 2.88: Comparison of the sonographic pregnancy diagnosis at 3.5 MHz. Vesicle with embryo (E) on Day 32 of pregnancy. The vesicle and the embryo are difficult to recognize.

Avtorsko zaščiteno gradivo

Downloaded From Vet-eBooks.com

The use of a high resolution scanner will ensure that the embryo can be detected in all cases of bovine pregnancy between Days 25 and 30 (PIERSON and GINTHER 1984 a). The embryo's echogenicity is a little more intense than that of the neighbouring endometrium (Fig. 2.85 to 2.87). Since the embryo lies very close to the uterine wall for the first month of pregnancy, it may prove difficult to find (Fig. 2.85). It projects from the wall into the anechoic uterine lumen and can be identified by the presence of a heart beat. The embryo starts to moves away from the wall during the next few days and by Day 30 it is completely surrounded by fluid (Fig. 2.86). To identify the embryo accurately its echo must be examined carefully to differentiate it from the reflections of other structures. Especially in the area where the sound waves impact vertically other structures may produce very intense echoes. Such areas include the sites where the allantoic membrane is exposed to vertically impacting sound waves which then generate very bright echoes. More ultrasound is returned from the reflective surface vertically oriented to the transducer, thereby creating the impression of a very intensely echoic structure (HASSLER 1984).

On average, the length of the embryo increases from 5 to 12 mm in the period from Days 25 to the 30 of pregnancy (PIERSON and GINTHER 1984 a, REEVES et al. 1984, CURRAN et al. 1986 b). If it is clearly visible its heart beat should also be detectable. The heart is the first organ of the bovine embryo that can be identified by ultrasonography. It can be detected only a few days after the very first cardiac contractions occur during the course of organogenesis. Around Day 20 the heart starts contracting rhythmically (SALISBURY et al. 1978, NODEN and DE LAHUNTA 1985 b)

The earliest time at which pregnancy can be diagnosed depends very much on the sound frequency and the quality of the scanner used (Fig. 2.87 and 2.88). Using a 5 MHz scanner it should be possible under practical conditions to demonstrate the embryonic vesicle with relative ease by Day 25. From this Day the absence of fluid from the uterus indicates with reasonable certainty that the cow is non-pregnant. If, in addition to the embryonic fluid, the embryo is visible a positive confirmation of pregnancy has been obtained. Under certain conditions the detection of an allantoic membrane a few days prior to the detection of the embryo is possible and may be taken as a positive confirmation of pregnancy.

While it is possible with a 5 MHz scanner under field conditions to deliver a reliable pregnancy diagnosis between Days 25 and 30, this is only possible at a later stage if lower frequency probes are used, due to their poorer resolution (TAVERNE et al. 1985, CHAFFAUX et al. 1986, HANZEN and DELSAUX 1987). With a frequency of 3 to 3.5 MHz, the demonstration of the embryonic vesicle and the embryo is usually delayed by about 5 days. At a frequency of 3 MHz the embryonic vesicle is visible after Day 25 and the embryo after Day 30 (TAINTURIER et al. 1983). Studies on the accuracy of ultrasonic pregnancy diagnoses indicated that at low frequencies of 3 or 3,5 MHz an accurate negative diagnosis could be made by Day 35 to 40 and a positive diagnosis not earlier than from Day 45 (TAVERNE et al. 1985, CHAFFAUX et al. 1986).

Avtorsko zaščiteno gradivo

Downloaded From Vet-eBooks.com



Fig. 2.89: Conceptus with embryo and amnion (2 arrows) on Day 33 of pregnancy. The amnion forms a thin membrane which surrounds the embryo. Ultrasonogram produced with sector scanner at 5 MHz.

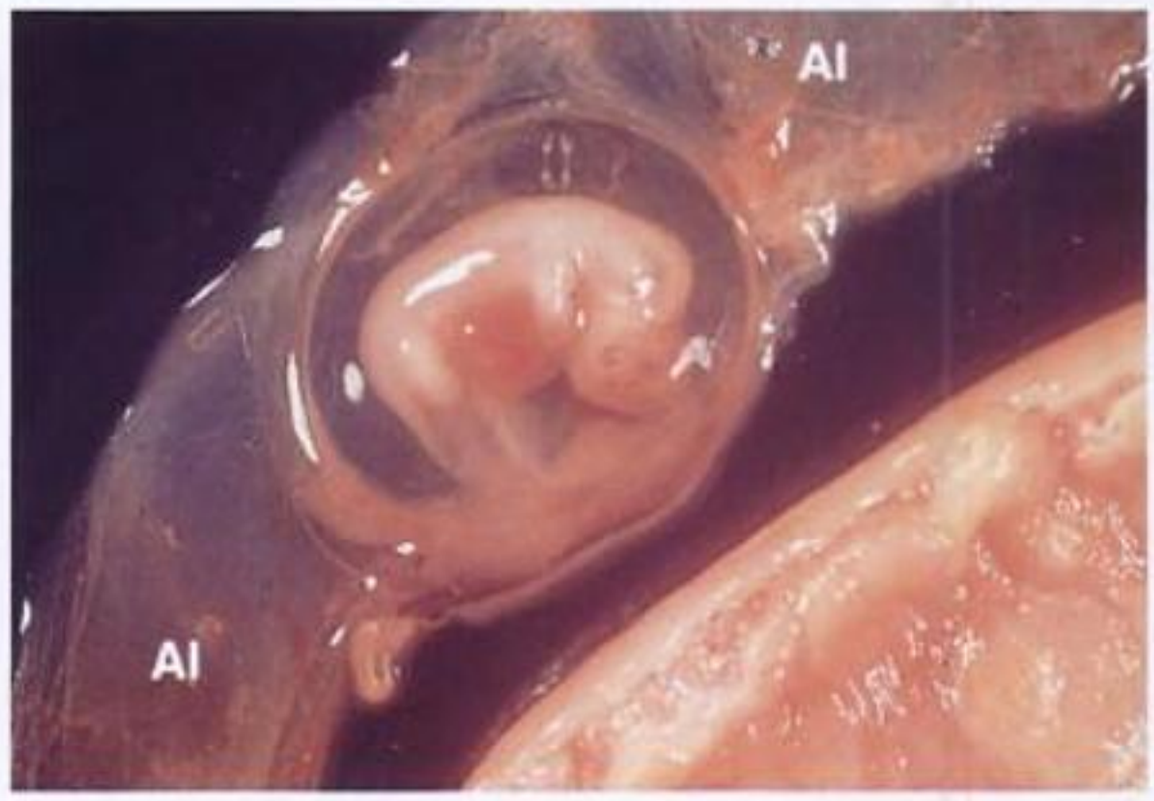


Fig. 2.90: Photograph of an embryo with surrounding amnion and adjoining allantochorion (Al) on Day 37 of pregnancy (specimen removed from the uterus).



Fig. 2.91: Conceptus with embryo and amnion (A) on Day 40 of pregnancy. The head of the embryo with the anechoic round area of the developing eye (arrow) lies towards the left. The crown-rump-length (CRL) is 20 mm. Ultrasonogram produced with sector scanner at 5 MHz.



Fig. 2.92: Ultrasonogram of a conceptus with embryo (E) and a single placentome (P) on Day 33 of pregnancy. The placentome protrudes bud-like into the lumen.

Avtorsko zaščiteno gradivo

Downloaded From Vet-eBooks.com

2.3.2.4 Day 31 to 40 of pregnancy

The crown-rump-length (CRL) of the embryo reaches 12 mm around Day 30, 15 mm by Day 35 and 20 mm by Day 40 (PIERSON and GINTHER 1984 a). Occasionally around Day 30, but usually around Day 35 the amniotic vesicle becomes apparent (Fig. 2.89 and 2.90). A few millimeters away from the embryo it forms a very thin, arched, hyperechoic line which surrounds the embryo.

Around Day 40 the mean diameter of the embryonic vesicle is about 2.5 cm and the CRL of the embryo about 2 cm (Fig. 2.91). The sizes of embryonic vesicles vary, however (MÜLLER et al. 1986). Sometimes the diameter varies between different sectors of the vesicle and there are also differences between individuals. Even during an examination the embryonic vesicle may undergo changes in diameter due to intestinal and uterine movements. It is thus not rare to find variable vesicle diameters when these are measured during a single ultrasound examination.

The placentomes also become visible for the first time between Days 30 and 40 (Fig. 2.92). On average, the first appearance of knob like protrusions can be expected around Day 35 (CURRAN 1986 b). The first signs of placentomes are usually noticeable in the area near the embryo.

Avtorsko zaščiteno gradivo

Downloaded From Vet-eBooks.com

2.3.2.5 Day 41 to 90 of pregnancy

From the first day of detection between Days 20 and 30 until Day 50 the embryo grows at a rate of approximately 1 mm per day (PIERSON and GINTHER 1984 a, KÄHN 1985). By Day 50 it would thus have a CRL of about 35 mm (Fig. 2.93). The cross sectional diameter of the placental vesicle also increases appreciably between Days 30 and 70 of pregnancy. It reaches 25 mm by Day 40, 35 to 40 mm by Day 50 and 50 to 60 mm by Day 70 (KÄHN 1985, CURRAN et al. 1986 b). The largest dilation of the uterus usually occurs in the area of the embryo, while the embryonic vesicle in the contralateral horn can be substantially narrower.

Around Day 40 a stage is reached when the sonographic examination of the pregnancy can be extended to include the demonstration of embryonic or fetal structures, respectively. From the diagnostic point of view the only organ that is available at this stage of pregnancy is the beating heart. In contrast, after Day 40 the outline of the fetus with its head, extremities and umbilical cord become visible (Fig. 2.94). From Day 35 to Day 45 the sonographically visible changes that transform the undifferentiated, primitive embryo into a fetus with a distinct body form, take place(WINTERS et al. 1942). At this time, first ossification centers can be noticed in the vertebrae, ribs and pelvic bones, on the upper and lower jaws, on the femur and humerus as well as on the radius, ulna and tibia.

Avtorsko zaščiteno gradivo

Downloaded From Vet-eBooks.com

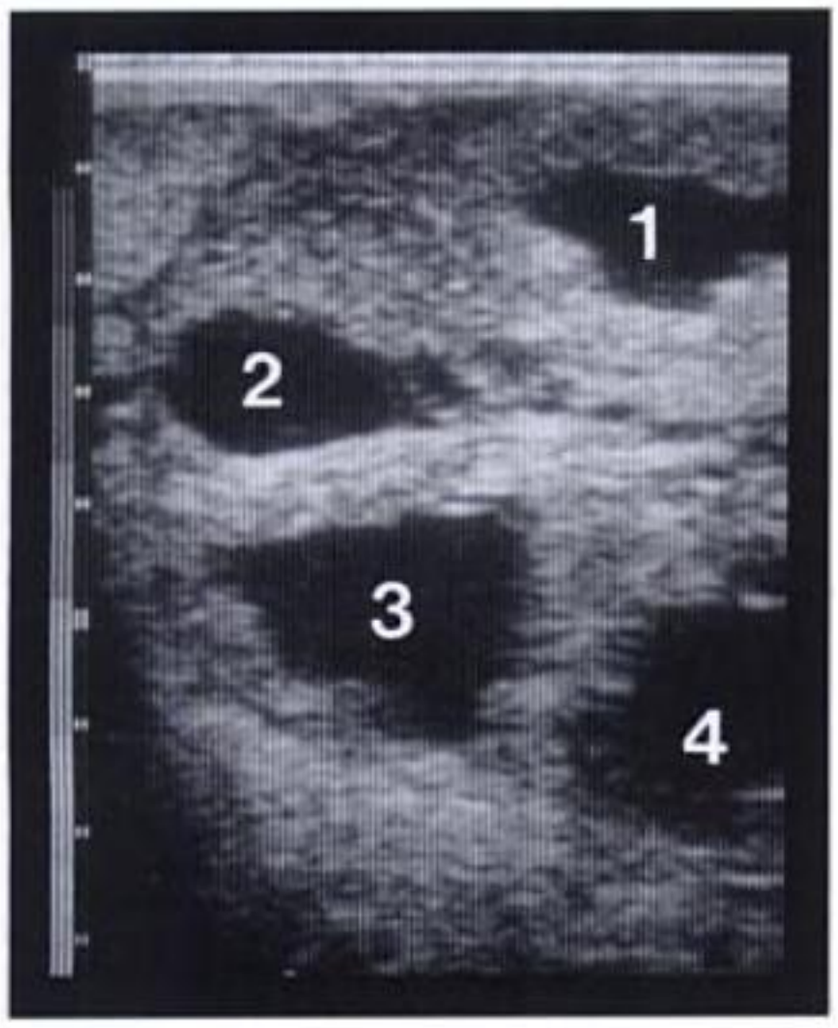


Fig. 2.95: Sagittal section through a pregnant uterine horn on Day 41 of pregnancy. The anechoic conceptual vesicle appears to be divided by folds of the uterine wall into 4 (1, 2, 3, 4) compartments.

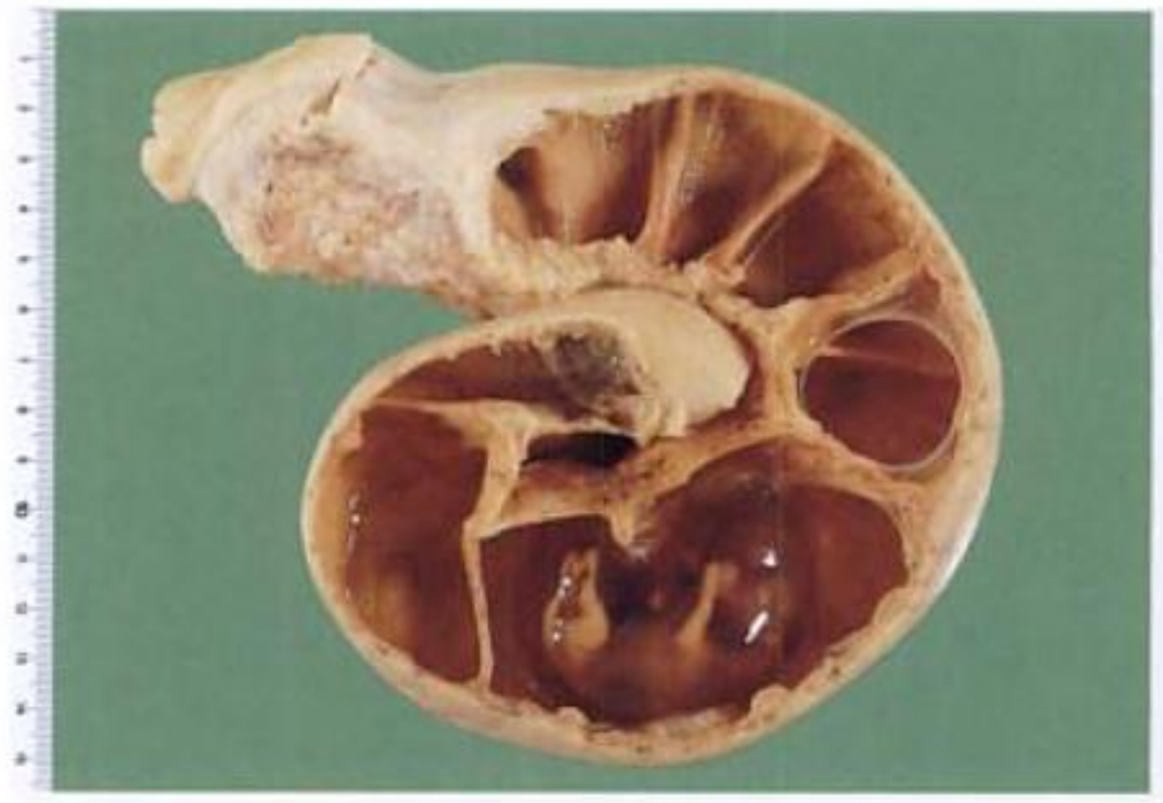


Fig. 2.96: Photograph of a sagittally opened uterine horn on Day 55 of pregnancy. The folds of the uterine wall lead to the compartmentalization of the pregnant uterine horn.

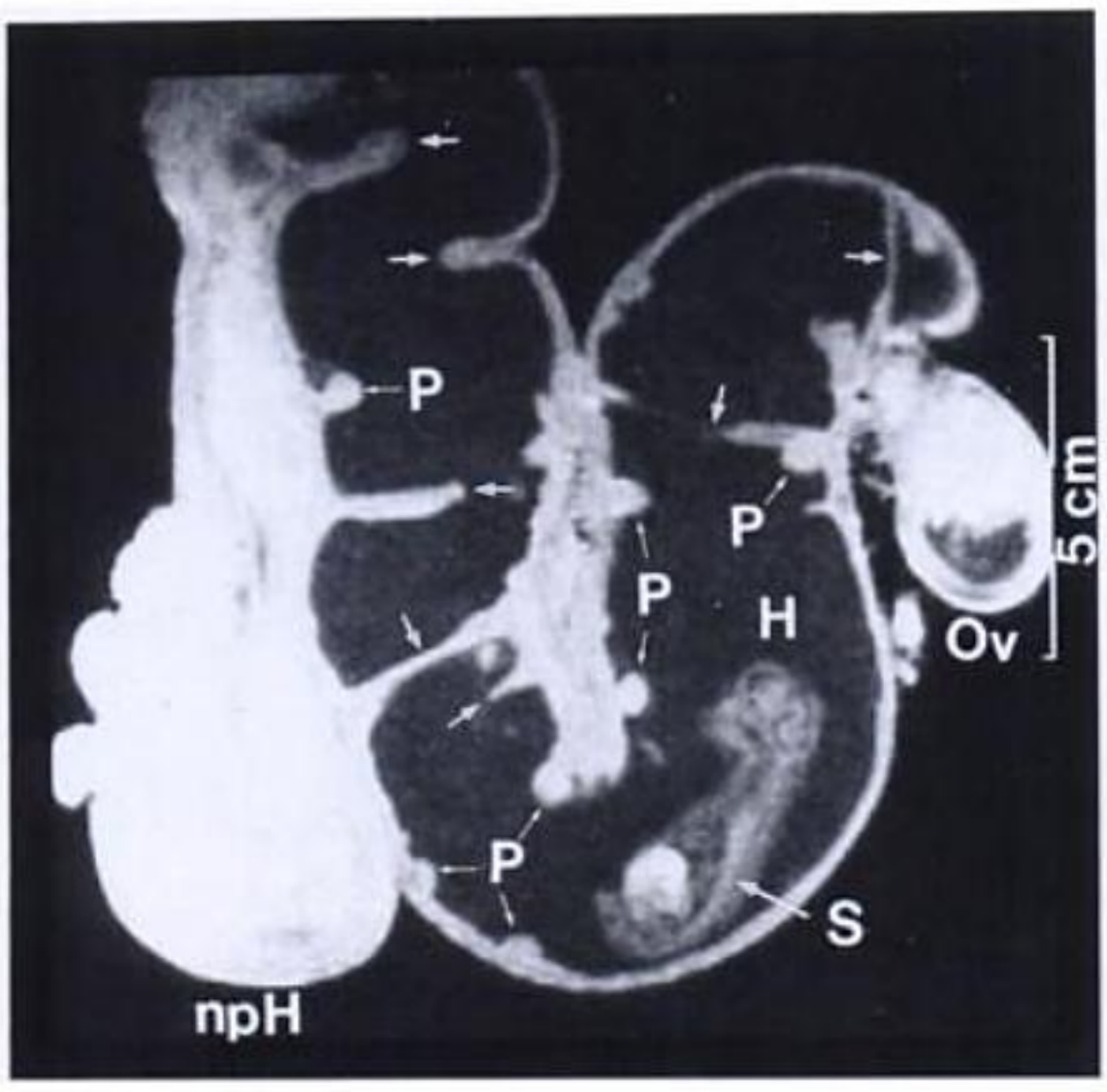


Fig. 2.97: Nuclear magnetic resonance image of a uterus on Day 55 of pregnancy. Inside the pregnant horn are folds (arrows) that reach vertically into the lumen, as well as placentomes (P). On the right is the ovary (Ov) with a Cl; on the left is the non-pregnant horn (nph). The head (H), spinal column (S) and the bright echo of the liver can be recognized.



Fig. 2.98: Photograph of a sagittally opened, pregnant uterine horn on Day 78 of pregnancy. The folds of the uterine wall straighten out as the pregnancy progresses.

Avtorsko zaščiteno gradivo

Downloaded From Vet-eBooks.com

The pseudo-ampullary appearance of the pregnant uterus is particularly pronounced during the 2nd month of pregnancy (Fig. 2.95). At this time numerous well developed uterine folds bulge into the lumen and divide the early pregnant uterus into compartments (KÄHN et al. 1989). In a sagittal section through the uterus the folds run virtually in straight lines between the larger and lesser curvatures of the pregnant horn. They are sickle shaped and project often 2 to 3 cm high into the uterine lumen (Fig. 2.96). They stand almost vertically to the outer surface of the uterus and are arranged transversely, in the form of circular folds, in relation to the longitudinal axis of the uterine lumen (Fig. 2.97). Their regular spacing and their prominent infolding form a pseudo-compartmentalization of the uterine horns.

As pregnancy continues these circular folds of the uterine wall gradually retract so that by Day 70 the compartmentalization becomes less prominent (Fig. 2.98).

If a linear scanner is used for the sonographic examination of the conceptus a 5 MHz probe will give good results until Week 6 of pregnancy. At this frequency the resolution is high enough to detect even small fluid accumulations as well as the still small embryonic structures. In addition, the scanning width of about 5 cm of the 5 MHz probe and its scanning depth of about 9 cm are adequate to rather completely depict the conceptus which is still quite small.

The lower frequency ultrasound with its deeper scanning depth has important advantages during the more advanced stages of pregnancy. As a result of the deeper field of view, larger parts of organs and wider segments of the pregnant uterus can be depicted. When a 5 MHz probe is used the CRL of a fetus may not be measurable after Day 60. Around this time the CRL reaches 6 cm which is the maximum scanning width of most 5 MHz linear probes (WHITE et al. 1985). If a lower frequency probe is selected the fetus may still be scanned in toto until Day 90.

Avtorsko zaščiteno gradivo

Downloaded From Vet-eBooks.com

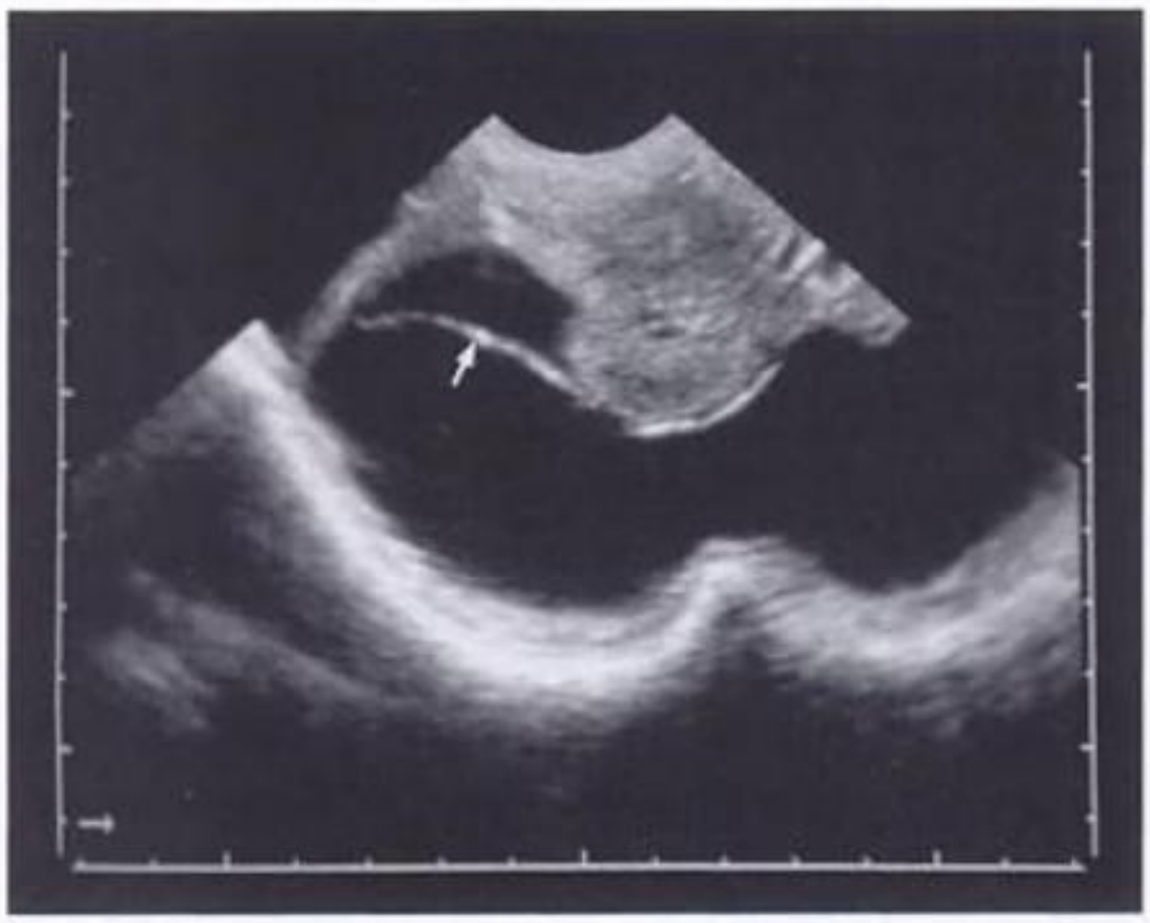


Fig. 2.99: Pregnant uterus with a placentome (P) on Day 102 of pregnancy. The hyperechoic membrane of the allantochorion (arrow) runs across the placentome.



Fig. 2.100: Placentome with its hyperechoic border in a pregnancy on Day 162.

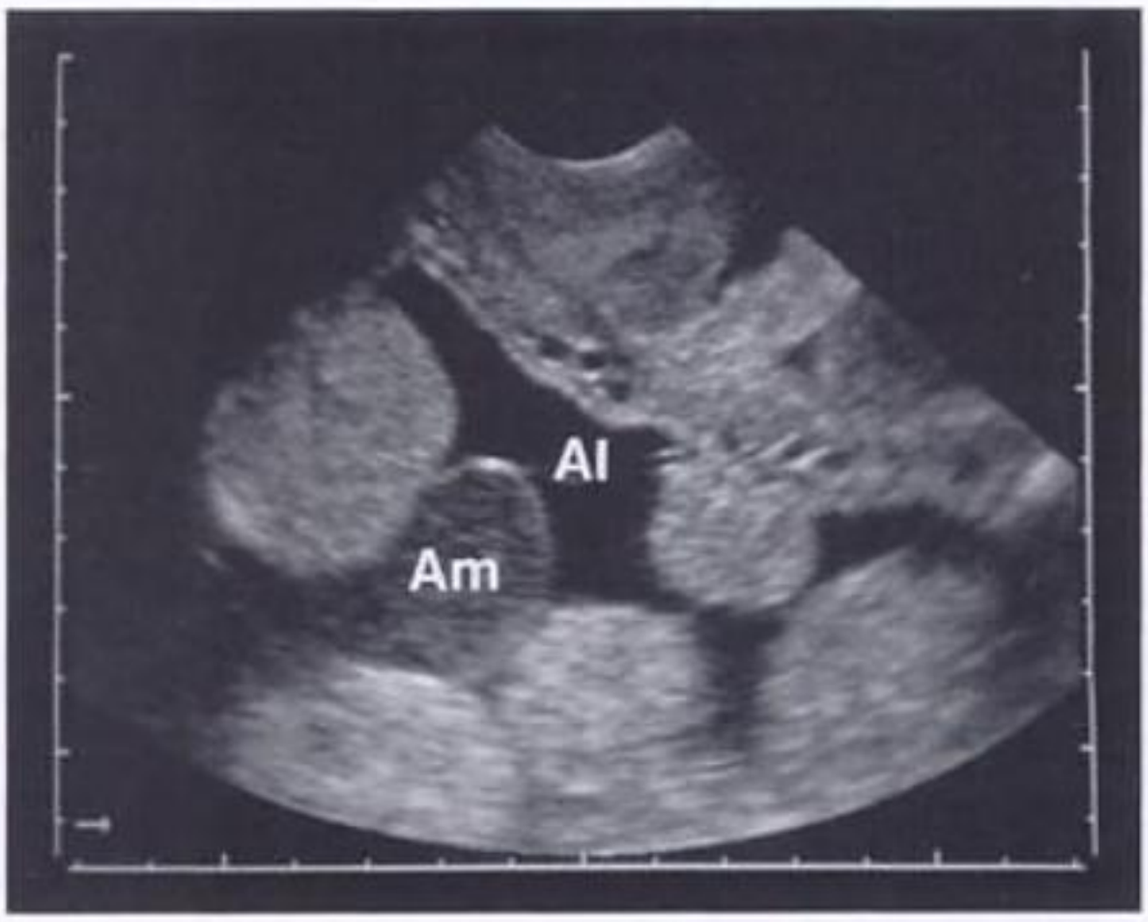


Fig. 2.101: Numerous, tightly packed placentomes in a uterus on Day 191 of pregnancy. Between the placentomes a section through the amniotic vesicle (Am) with its more echoic amniotic fluid can be seen. The allantoic fluid (Al) is much more hypoechoic.

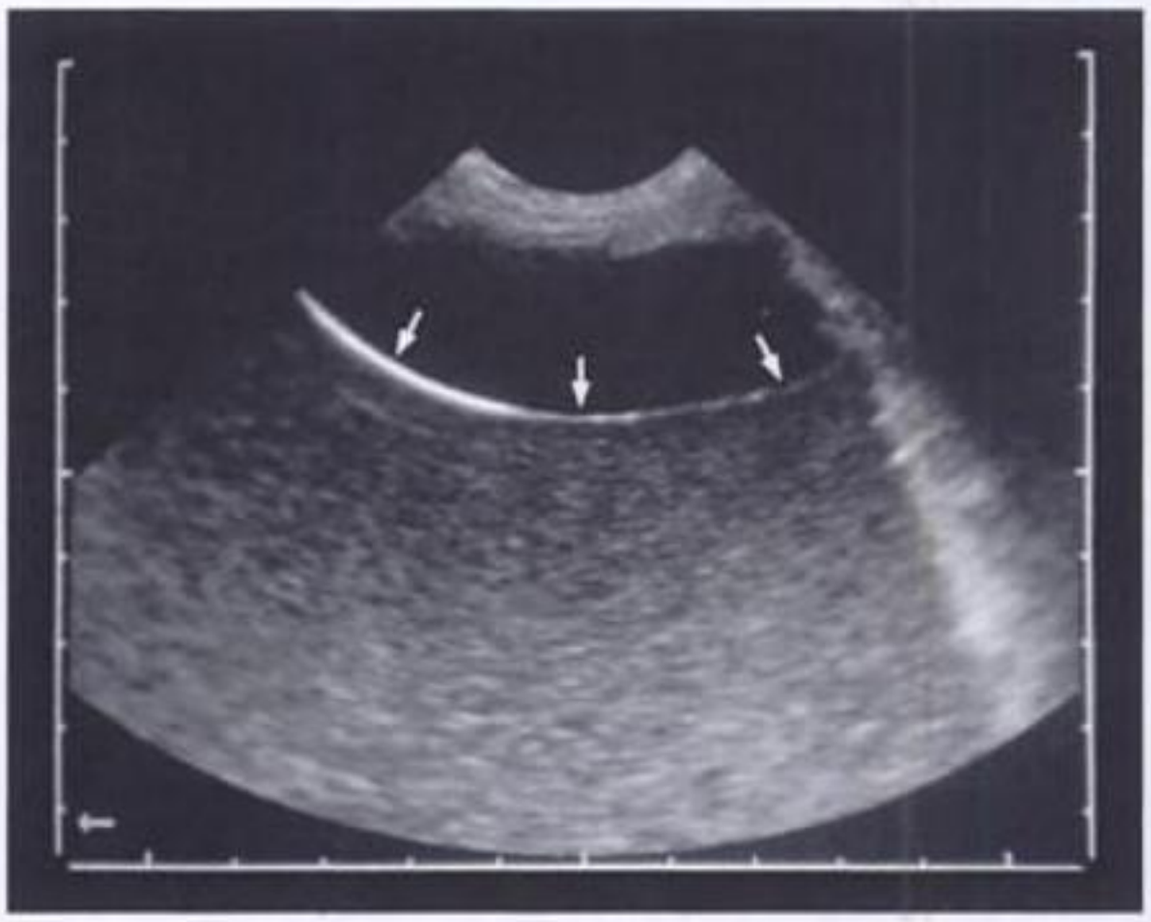


Fig. 2.102: Uterus with the hyperechoic amniotic membrane (arrows) which separates the echoic amniotic fluid from the hypoechoic allantoic fluid. Pregnancy on Day 191.

Avtorsko zaščiteno gradivo

Downloaded From Vet-eBooks.com

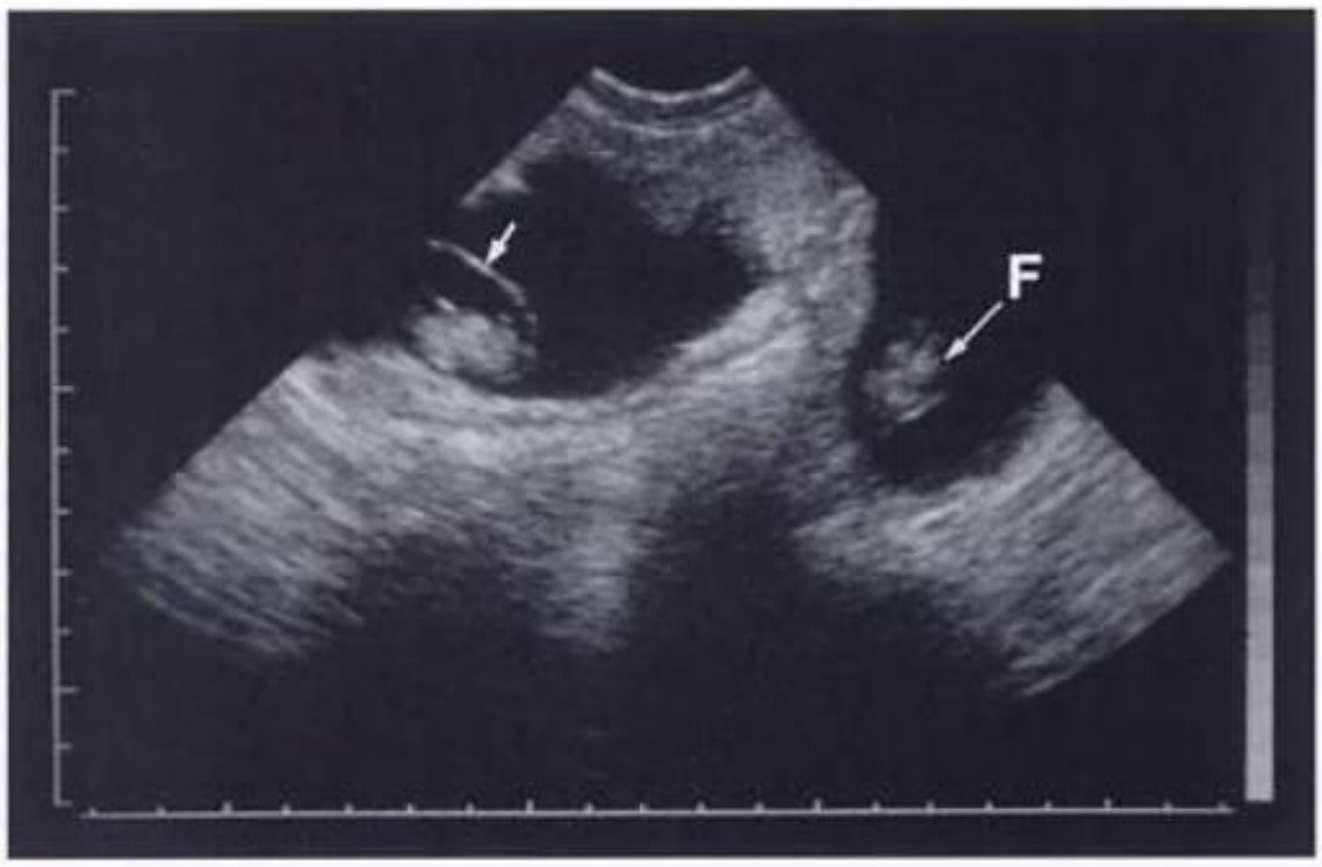


Fig. 2.103: Twins, which resulted from insemination and contralateral embryo transfer, in a cow on Day 41 of pregnancy. The transverse section through the uterus shows one fetus, surrounded by its amnion (arrow), in the left uterine horn and another fetus (F) in the right uterine horn.

Avtorsko zaščiteno gradivo

Downloaded From Vet-eBooks.com

2.3.2.7 Twin and multiple pregnancies

The sonographic diagnosis of a twin or multiple pregnancy can be justified if two or more embryos or fetuses were clearly visible. If two conceptuses can be depicted simultaneously on the monitor a sonographic diagnosis of a twin pregnancy is reliable (Fig. 2.103). If the two conceptuses lie in opposite uterine horns they can only be seen in one picture if the sound probe is turned into a virtually transverse position. A probe which allows multiple scanning planes during intrarectal applications is particularly suitable in such cases. So, for example, the use of a linear probe which is held lengthwise inside the rectum produces mostly sagittal sections through the uterus while transverse images through the organ are difficult to obtain. To diagnose a twin pregnancy the fetuses then have to be found one after the other. This can lead to diagnostic uncertainties, because it is not always clear during the course of an examination whether the second fetus that is found is not perhaps another view of the first one which has migrated back into the picture.

The second month of pregnancy appears to be the most suitable period for diagnosing twins. This period encompasses the stage at which from the embryos are first easily visible at around Day 28 to the stage when the advanced growth in the size of the fetuses prohibits them from being depicted simultaneously.

Avtorsko zaščiteno gradivo

Downloaded From Vet-eBooks.com

2.3.3 Uterine pathology

2.3.3.1 Embryonic death

First signs of an impending embryonic death are an undersized embryo and a reduced amount of embryonic fluid. The death of a conceptus can be reliably diagnosed once the embryonic heart beat has stopped.

In cases where embryonic death have been observed between Days 25 and 40 of pregnancy the heart beat persisted for several days after a retardation in growth had been detected (Fig. 2.104). Sometimes the heart beat did not cease until several days after first suspicions of an impending embryonic death, based on retarded embryonic growth, were raised (Fig. 2.105). Shortly before the heart comes to a complete standstill, one can often notice a markedly reduced pulse rate (KASTELIC et al. 1988). The normal embryo at this stage would have a heart rate of about 150 per minute (KÄHN 1989 b). As the resorption progresses the amount of embryonic fluid will decrease, while its echogenicity will increase. What started as floccular reflections at the beginning of the resorption will develop into a mass of snowy echoes. The embryo then looses its typical outline and becomes very indistinct.

2.3.3.2 Fetal mummification

In cases of pregnancy failure in the form of fetal mummification the uterine ultrasonograms usually contain very little conclusive information. Immediately below the uterine wall hyperechoic foci can be detected (Fig. 2.106). No fetal body parts have been identified in the mummies examined by transrectal ultrasonography thus far. The sound waves only penetrated a few centimeters into the fetus so that only a narrow, hyperechoic peripheral area could be identified. The tissues that lay deep to the fetus did not reflect any ultrasound echoes and remained anechoic (FISSORE et al. 1986). Obviously, the mummification process lead to tissue changes which caused an increased absorption of sound waves in the superficial tissue layers.

Between the surface of the mummified fetus and the uterine wall were no hypoechoic areas that could be seen as accumulations of fetal fluid.

2.3.3.3 Fetal maceration

Apart from the well known clinical features some sonographic signs of fetal maceration were seen in a case of this form of a pathological pregnancy. There was a very distinct difference between the echogenicity of the allantoic fluid and that of the amnion (Fig. 2.107). Due to its lack of reflections the allantoic fluid appeared virtually black, while hyperechoic, regularly distributed echoes whirled around inside the amniotic fluid. These were interpreted to have been caused by the increased cellular content of the amniotic fluid resulting from the disintegration of the fetal tissues.

Within the echoic amniotic fluid, fetal components were identifiable. The fetus and its organs were, however, much less distinct than in viable pregnancies. Due to the increased echogenicity of the amniotic fluid the fetal outlines contrasted less than normal. Structures within the fetus were only vaguely recognizable. This was assumed to have been the result of the onset of post-mortem changes. As a result of their hyperechoic echoes only bony parts could be differentiated from soft tissue components (FISSORE et al. 1986).

Avtorsko zaščiteno gradivo

Downloaded From Vet-eBooks.com

2.3.3.4 Postpartum uterus

After birth the most obvious sonographic structures in the uterine lumen are the caruncles (Fig. 2.108 to 2.110). Depending on the direction of the sonographic scanning, a variety of sections through the caruncles can be produced. Areas of differing echogenicity can be seen on the round or oval cross sections of caruncles. The most superficial layer is depicted as a hyperechoic layer. The deeper tissues of the placentome are relatively less echoic, resembling the image generated by loose tissue. From the site of its uterine attachment hyperechoic lines often radiate into the depth of the caruncle (Fig. 2.108).

The uterine lumen often appears to be virtually obliterated, even as early as the first day after calving with no larger accumulations of fluid recognizable (Fig. 2.108). In many cases, however, lochial secretions can be seen inside the uterine lumen (Fig. 2.109). They show the floccular echogenicities which are typical of fluids that contain cellular components. In such cases the caruncles protrude like mushrooms into the relatively hypoechoic uterine secretions. Even by two weeks post partum the normal postpartum uterus can still be distended by fluid several centimeters in diameter (OKANO and TOMIZUKA 1987). At this time a distinct reduction in the size of the caruncles can be demonstrated ultrasonically (Fig. 2.110). Smaller fluid accumulations can sometimes persist until the end of uterine involution.

When the uterine involution runs a pathological course in the form of a lochiometra the uterus can become extremely distended (Fig. 2.111). In such cases the placentomes often can not be seen. A hyperechoic area can sometimes be seen at the floor of the uterus. This is caused by the sedimentation of tissue breakdown-products and cellular elements in the lochial fluid.

Certain sonographic features of the postpartum uterus are also detectable in pathological situations such as endometritis. For example, the lochia can show the same echogenicity as is seen in many cases of endometritis (Fig. 2.112 to 2.115). The caruncles are then used as characteristic distinguishing features. The regressing caruncles usually remain detectable until the end of the postpartum period. Apart from this - and the usual clinical features - the diameter and the asymmetry in the size of the pregnant and non-pregnant uterine horns usually indicate a postpartum uterus.

Avtorsko zaščiteno gradivo

Downloaded From Vet-eBooks.com

2.3.3.5 Endometritis

Fluid accumulations which are detectable inside the lumen of a non-pregnant uterus can be indicative for chronic endometritis. The amount of the secretion can vary considerably (Fig. 2.112 and 2.113). In many cases a fluid filled lumen can only be detected in short segments of the uterus. In severe endometritis cases, however, both uterine horns can be distended to several centimeters along their entire length. In mild forms of endometritis no lumen may be evident ultrasonically.

Their echogenicity distinguishes the endometritic secretions from other uterine secretions as are seen during estrus or pregnancy (FISSORE et al. 1986). Anechoic fluids usually only occur under physiological conditions (Pierson and Ginther 1987). The fluid caused by inflammation contains floccular echoes. The echogenicity of the fluid can develop to snow-storm-like images and can become so severe that it appears nearly white. During observation periods of some minutes of extensive fluid accumulations it is usually possible to see turbulence within the fluid.

The value of transrectal ultrasonography in diagnosing endometritis in the cow must be judged with caution. Unless endometritis is accompanied by the accumulation of fluid inside the uterine lumen the use of ultrasonography will usually not detect pathological changes of endometritis. If the uterine lumen is, however, distended with fluid sonographic diagnosis may be possible.

A noteworthy phenomenon has been observed in cases of endometritis after intra-uterine treatment. After an iodine solution had been instilled into the uterine lumen the luminal surface of the endometrium became hyperechoic (Fig. 2.114). The hyperechogenicity developed immediately after the iodine infusion and persisted for a long time thereafter. The development of this increased echogenicity was also tested in excised uteri. In this manner it could be shown that the increased echogenicity did not originate from the iodine, but from the endometrium itself. After flushing the iodine solution out of the excised uteri the increased echogenicity persisted.

2.3.3.6 Pyometra

The most extreme form of endometritis, the pyometra, is sonographically characterized by a uterus which is considerably distended by an accumulation of fluid. The secretion inside the uterus contains uniformly and diffusely dispersed floccular reflections (Fig. 2.115). The echogenicity of the reflections depends on the consistency of the pyometra fluid. If the secretion is very thick and contains many cellular elements its echogenicity may be the same as that of the uterine wall, whereas a more liquid contents will appear much darker than the surrounding wall of the uterus.

The thickness of the uterine wall in the pyometra cases examined thus far varied considerably. Thick- and thin-walled pyometras can be found. Only when the wall is severely thickened can this be used to distinguish a pyometra from a pregnancy. The diagnosis of a pyometra on the basis of its ultrasonic image must be made with appropriate care. In advanced pregnancy the uterus is also distended and its fluid contents can be considerably echoic. For a reliable sonographic diagnosis of a pyometra an effort should be made to depict the entire course of the uterine lumen with its abnormal contents and to ensure that no fetal parts or structures can be found inside the fluid.

Avtorsko zaščiteno gradivo

Downloaded From Vet-eBooks.com

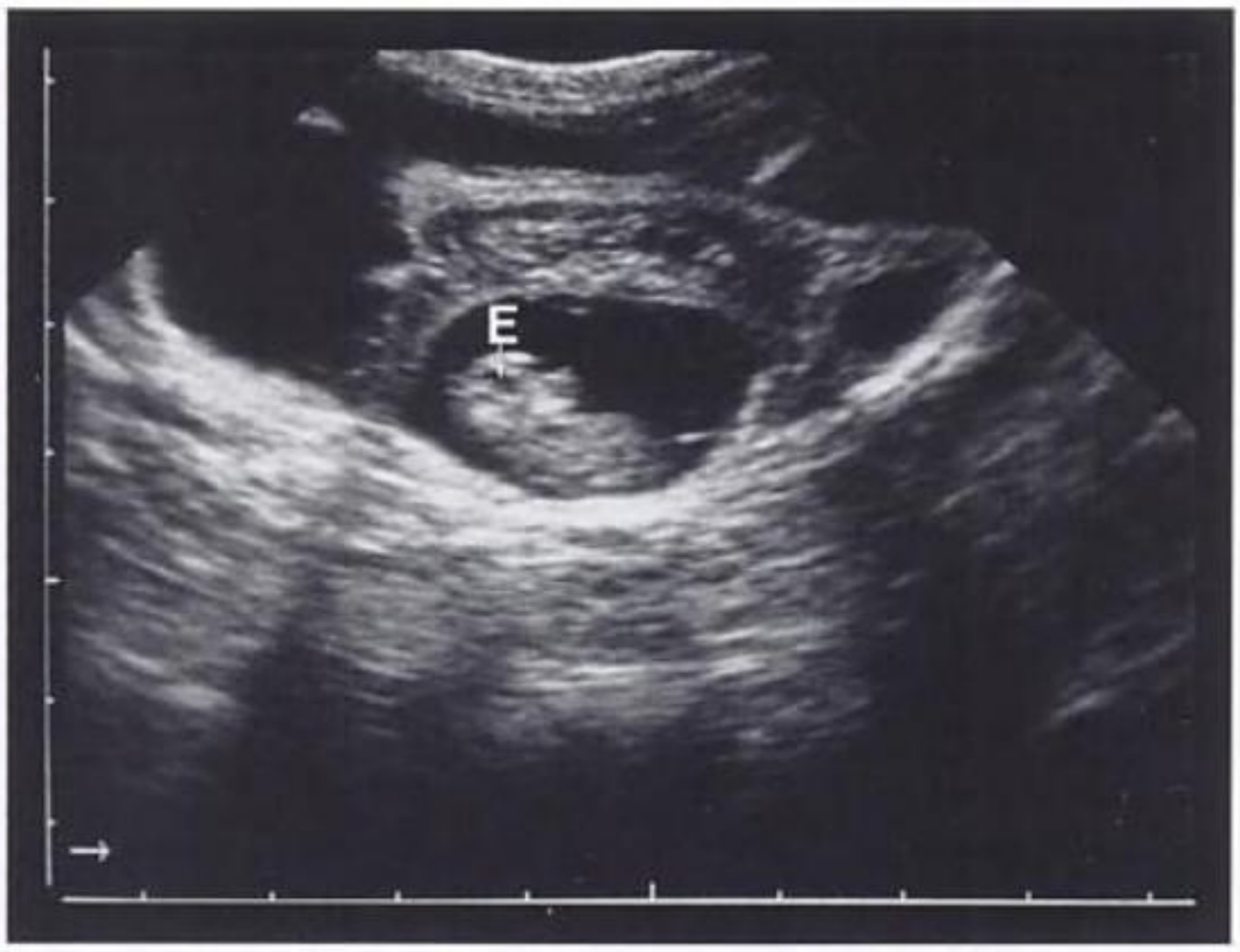


Fig. 2.117: Ventrodorsal sagittal section through a fetus on Day 48 of pregnancy. The head lies on the left. The hypoechoic developing eye (E) can be recognized.



Fig. 2.118: Transverse section through the head of a fetus at the level of the eyes on Day 102 of pregnancy. In the cranial aspects of the eyes the oval lenses (arrows) can be seen. Below the eyes is the spherical cerebral cranium (C).

Avtorsko zaščiteno gradivo

Downloaded From Vet-eBooks.com

2.4.1.1 Head

Next to the extremities, the head belongs to those body parts of the embryo that can be recognized relatively early. The obvious difference in impedance between its parts and that of the surrounding fetal fluids, its characteristic profile and a marked narrowing in the region of the neck allow for a clear differentiation between head and body from about the fifth week of pregnancy.

Apart from the facial skull the dark area of the developing eye within the head can be recognized on about Day 40 of pregnancy (Fig. 2.117). Initially, the embryonic eye is free of echoes and no ocular structures can be differentiated. From Day 70 of pregnancy echoic structures become visible within the eye (Fig. 2.118). These consist of arched, echoic lines which originate from the anterior and posterior walls of the lens. With a horizontal section through the head the eye balls have perfectly circular cross sections. In sagittal sections (in ophthalmology also referred to as vertical sections) they are slightly oval. With the sagittal beam the interpalpepral space becomes visible from about Month 6 of pregnancy (Fig. 2.119 and 2.120). At times the eyelids are clearly open and blinking movements of the lids can be observed. The relative echo enhancement by the hypoechoic eye ball makes the retrobulbar area appear more echoic than the neighbouring tissues at the same depth.

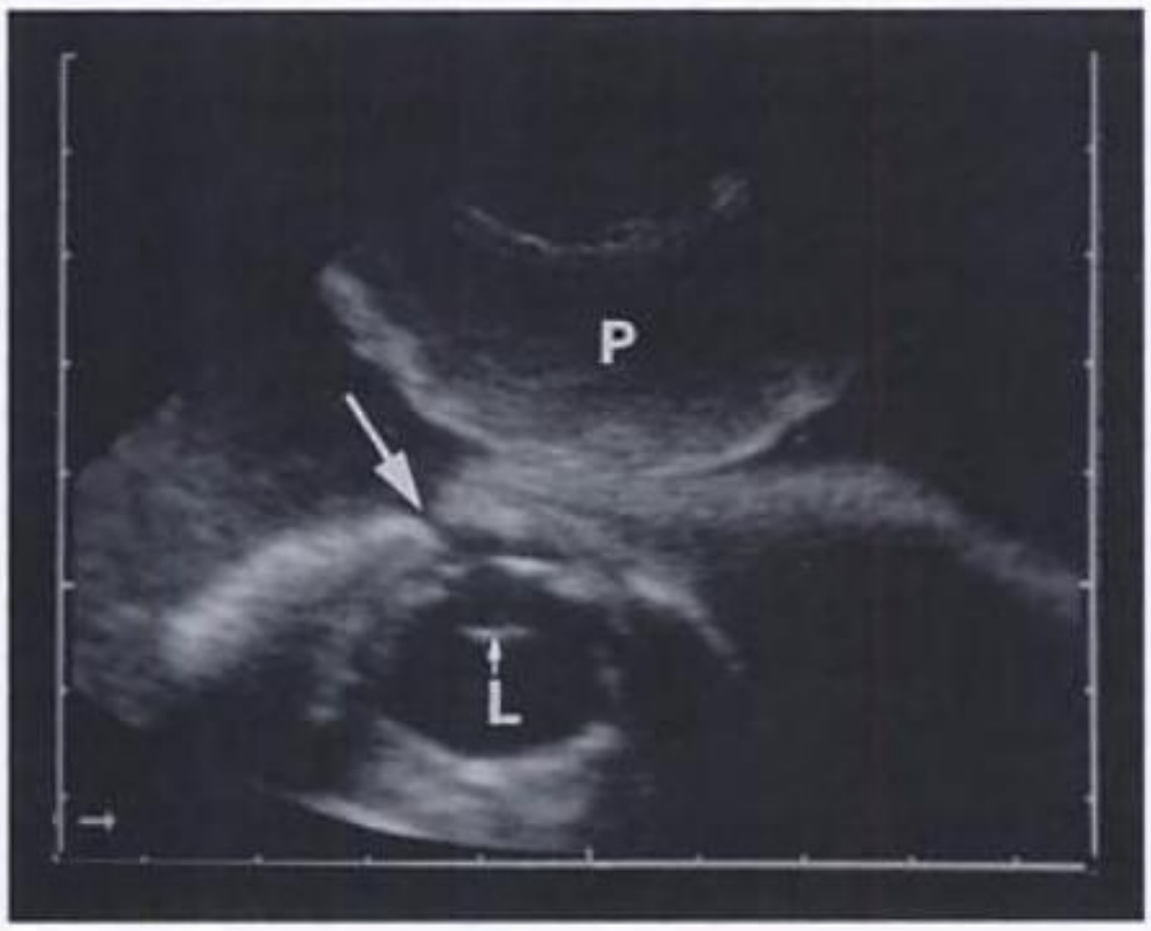


Fig. 2.119: Sagittal section through the eye of a fetus on Day 197 of pregnancy. The head lies dorsally against a placentome (P). The split (arrow) between the eye lids is open. The posterior curvature of the lens (L) can be seen.



Fig. 2.120: Sagittal section through the eye of a fetus on Day 205 of pregnancy. An eye lid projects from above the eye to the left. The retrobulbar area shows relative echo enhancement (E).

Avtorsko zaščiteno gradivo

Downloaded From Vet-eBooks.com



Fig. 2.121: Sagittal section through a fetus on Day 61 of pregnancy. In the head hyperechoic ossification centers can be seen in the mandible, maxilla and facial bones



Fig. 2.122: Horizontal section through the cranium on Day 84 with the cervical area on the right and the nose on the left. Cranially to the curved cerebral roof lies the sphenoid bone (S). Inside the brain are the two lateral ventricles (lv) with the falx cerebri between them



Fig. 2.123: Tangential sagittal section through a fetus on Day 127 of pregnancy. The fetus faces to the left. The eye with the lens (L) and the oval cerebral cranium are depicted.

Avtorsko zaščiteno gradivo

Downloaded From Vet-eBooks.com

The development of ossification centers provide the basis for the sonographic depiction of bones. Ossification centers that develop early on in the skull bones result in the depiction of hyperreflective structures in the head from the end of the second month of pregnancy (GJESDAL 1969). The first large hyperechoic structure is found in the region of the mouth (Fig. 2.121). It is found at the site of the mandible and depicts its characteristic future shape. At the end of Month 3 of pregnancy the ossification processes have progressed so far that individual skull bones can be recognized by their typical shapes (Fig. 2.122).

From Day 50 to 60 of pregnancy the bones of the cranium form a nearly closed, hyperechoic oval. A transverse section through the cranium shows a round cranial cavity (Fig. 2.118). A sagittal section through the cranium results in the depiction of an oval cranial cavity the longest diameter of which lies in the frontooccipital direction (Fig. 2.123). The cranial cavity can be seen in toto until Month 7. During the last two months of pregnancy the bones in the roof of the skull absorb so much ultrasound that the energy reflected from the bones at the base of the cranium is not sufficient for the production of an image on the monitor.

Avtorsko zaščiteno gradivo

Downloaded From Vet-eBooks.com



Fig. 2.124: Horizontal section through a fetus on Day 93 of pregnancy. The forehead points towards 1 o'clock, thorax and rump towards 7 o'clock. Inside the cranium the lateral ventricles (arrows), falx cerebri and the third ventricle can be seen.

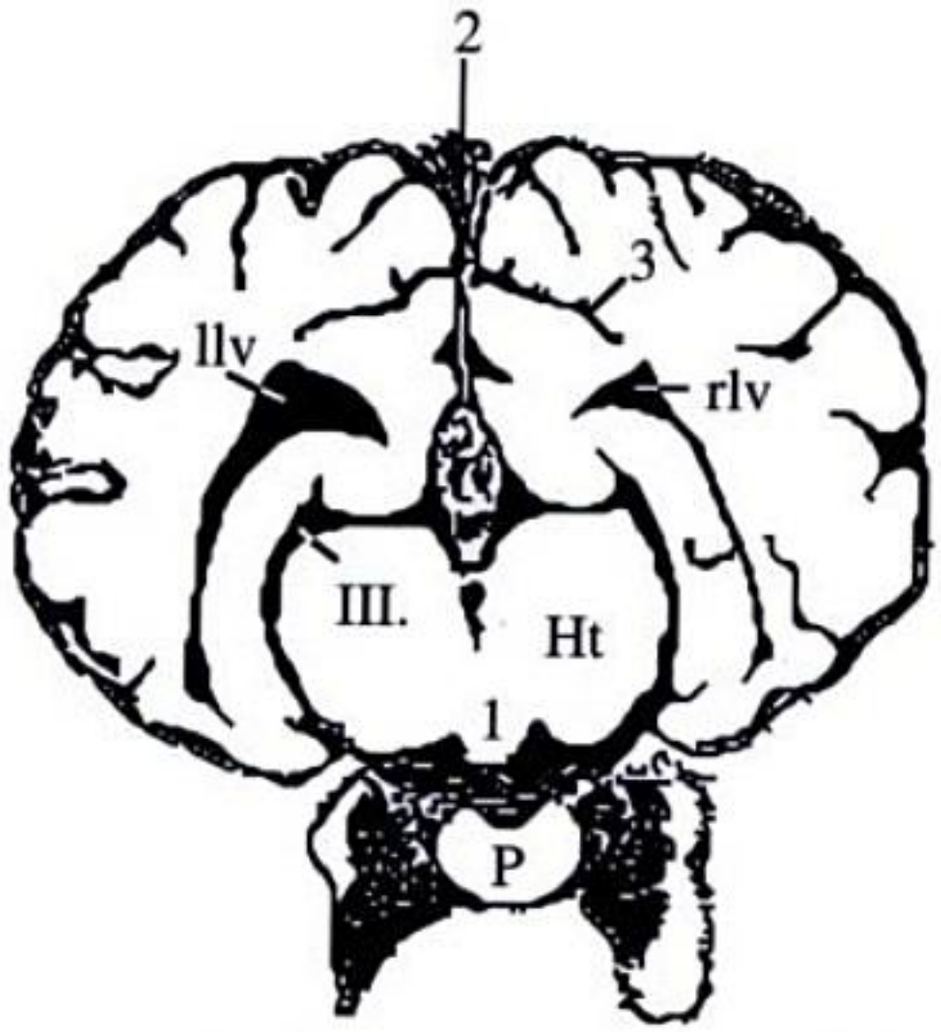


Fig. 2.125: Schematic presentation analogous to the scanning plane in Fig. 2.126. Cross section through the anterior brain at the level of the mamillary body and the pituitary (P). Ht hypothalamus, llv left lateral ventricle, rlv right lateral ventricle, 1 Corpus mamillare, 2 Falx cerebri, 3 Sulcus splenialis, III. third ventricle (adapted from SEIFERLE 1984).



Fig. 2.126: Transverse section through the cranium of a fetus on Day 147 of pregnancy at the level of the mamillary body and the pituitary analogous to the diagram in Fig. 2.125. The inner cavity is partitioned by the echoes of the ventricle and the Falx cerebri.

Avtorsko zaščiteno gradivo

Downloaded From Vet-eBooks.com



Fig. 2.128: Transverse section through the mouth and nose of a fetus on Day 161 of pregnancy. Starting from both edges of the hyperechoic hard palate (P) the developing teeth are producing long shadow artifacts. Above them are structures belonging to the nasal turbinates. Whisker hairs project away from the muzzle at 11 and 3 o'clock

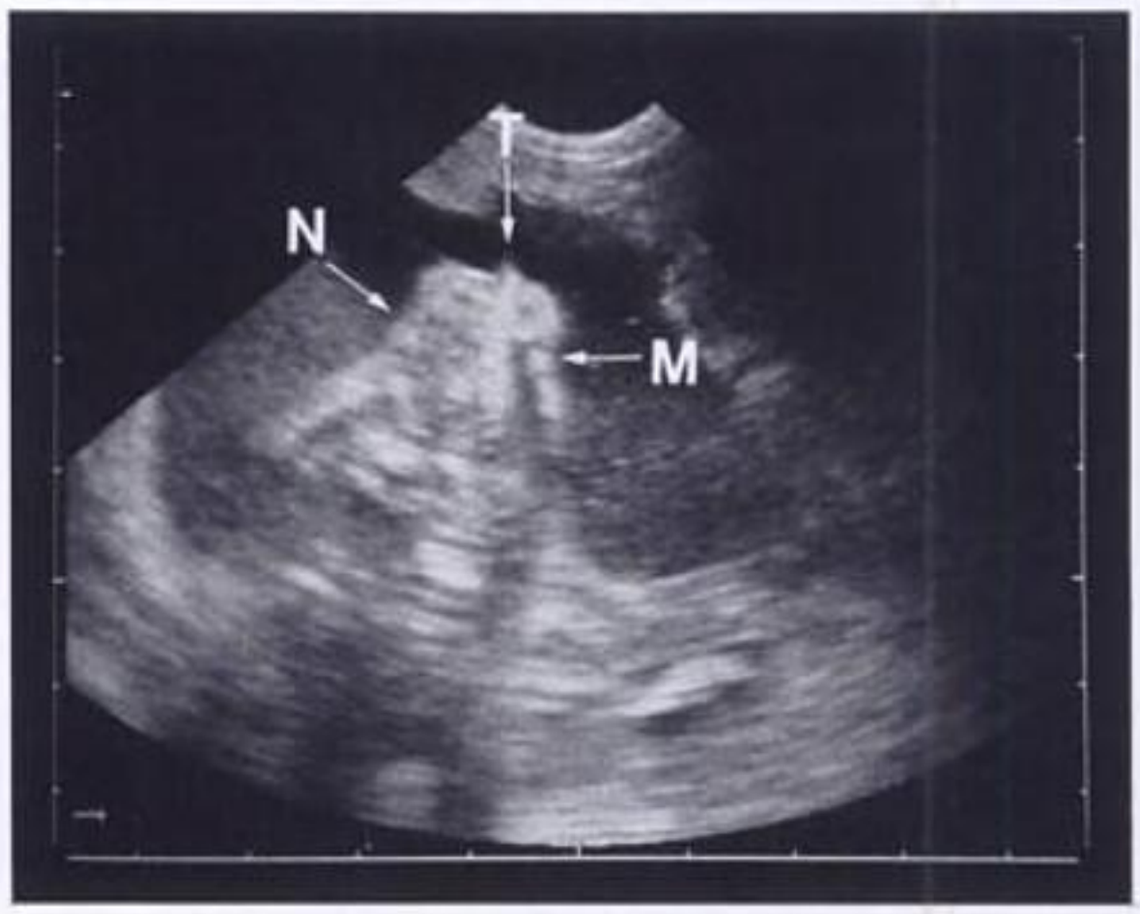


Fig. 2.129: Paramedian section through the facial skull of a fetus on Day 100 of pregnancy. The nose (N) points upwards. The maxilla lies on the left, the mandible (M) on the right. The tongue (T) projects from the mouth.

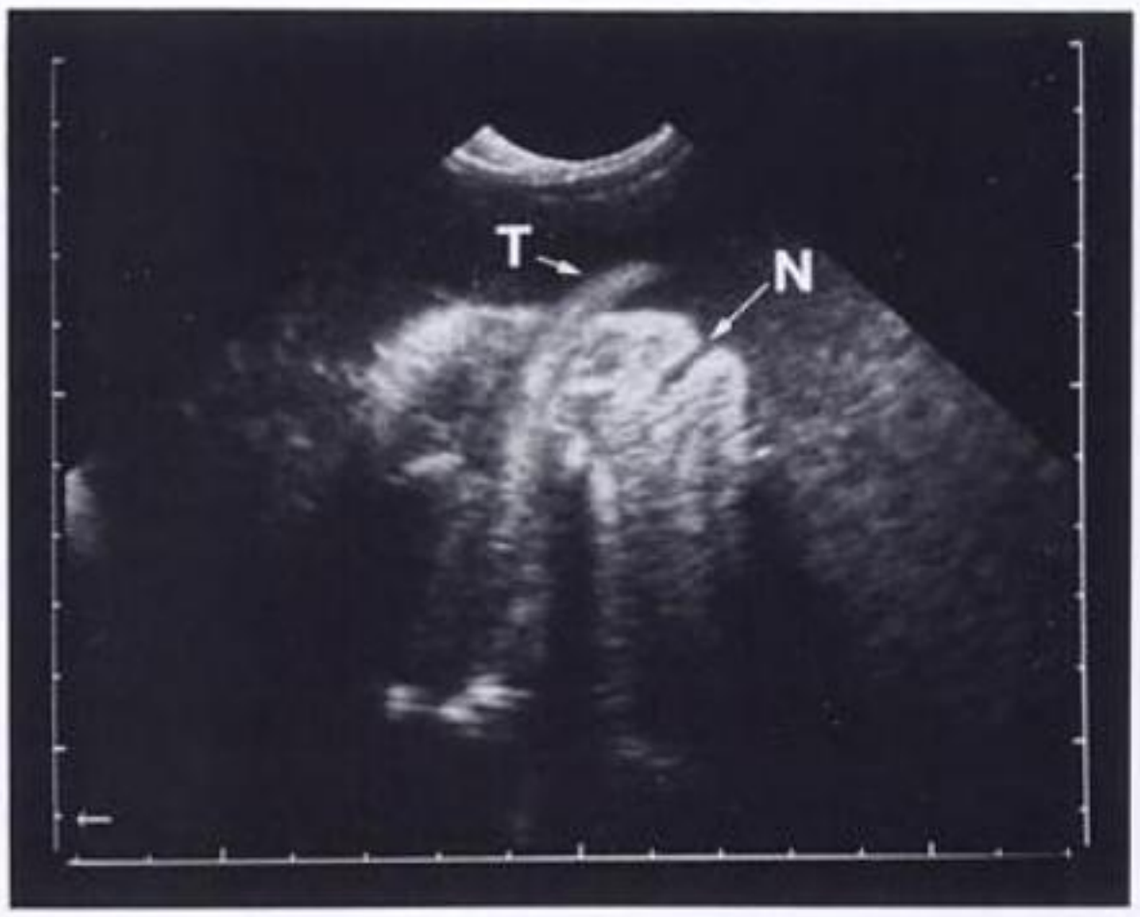


Fig. 2.130: Tangential sagittal section through the nose and mouth of a fetus on Day 185 of pregnancy. The mouth points upwards, the maxilla and nostrils (N) lie on the right and the mandible on the left. The tongue (T) sticks out of the mouth and is deflected in the direction of a nostril.

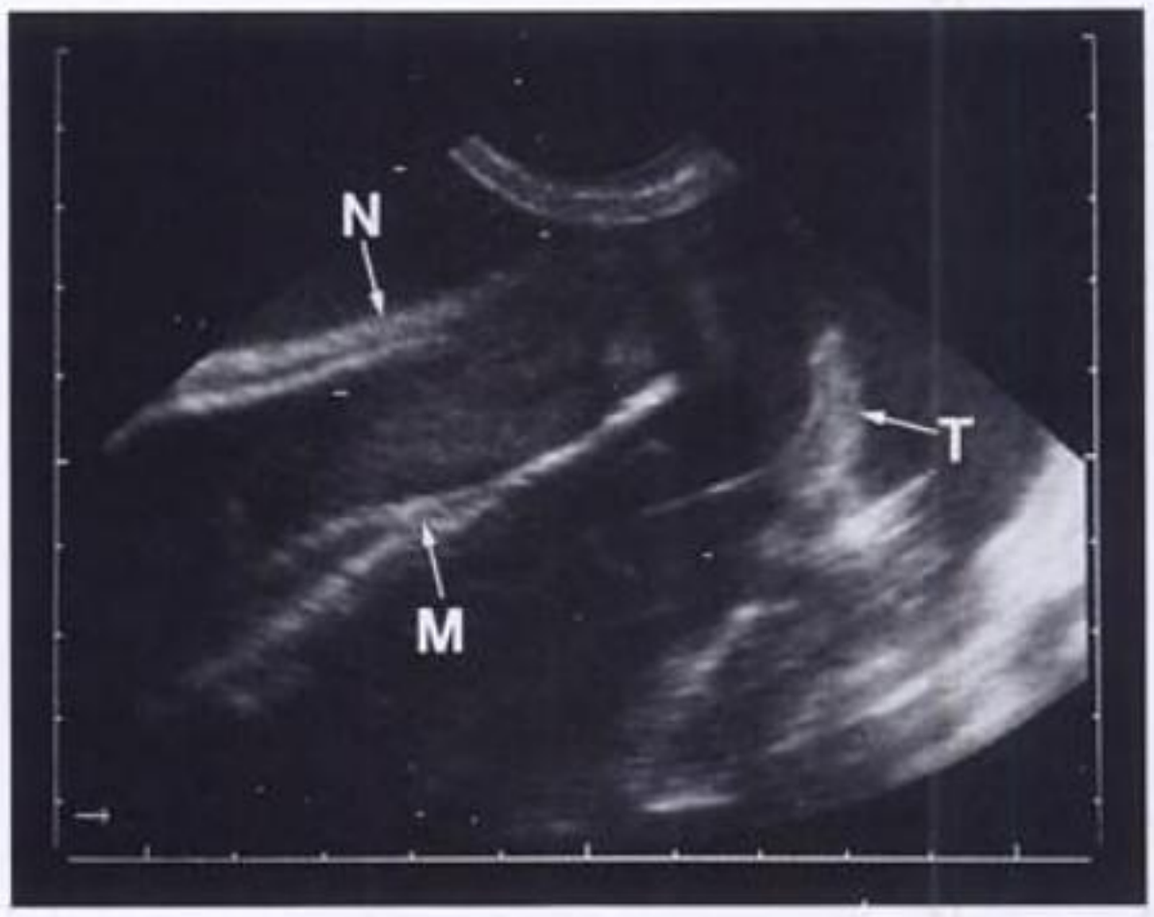


Fig. 2.131: Paramedian section through nose and mouth of a fetus on Day 184 of pregnancy. The nasal cavity is defined by the nasal bone (N) dorsally and the maxilla (M) ventrally. At 2 o'clock is the tongue (T), projecting from the mouth in the direction of the nasal entrance. The mouth is wide open.

Avtorsko zaščiteno gradivo

Downloaded From Vet-eBooks.com



Fig. 2.132: Image of an ear in a fetus on Day 199 of pregnancy. The tip of the ear points at 2 o'clock. The face lies to the left, off the image.

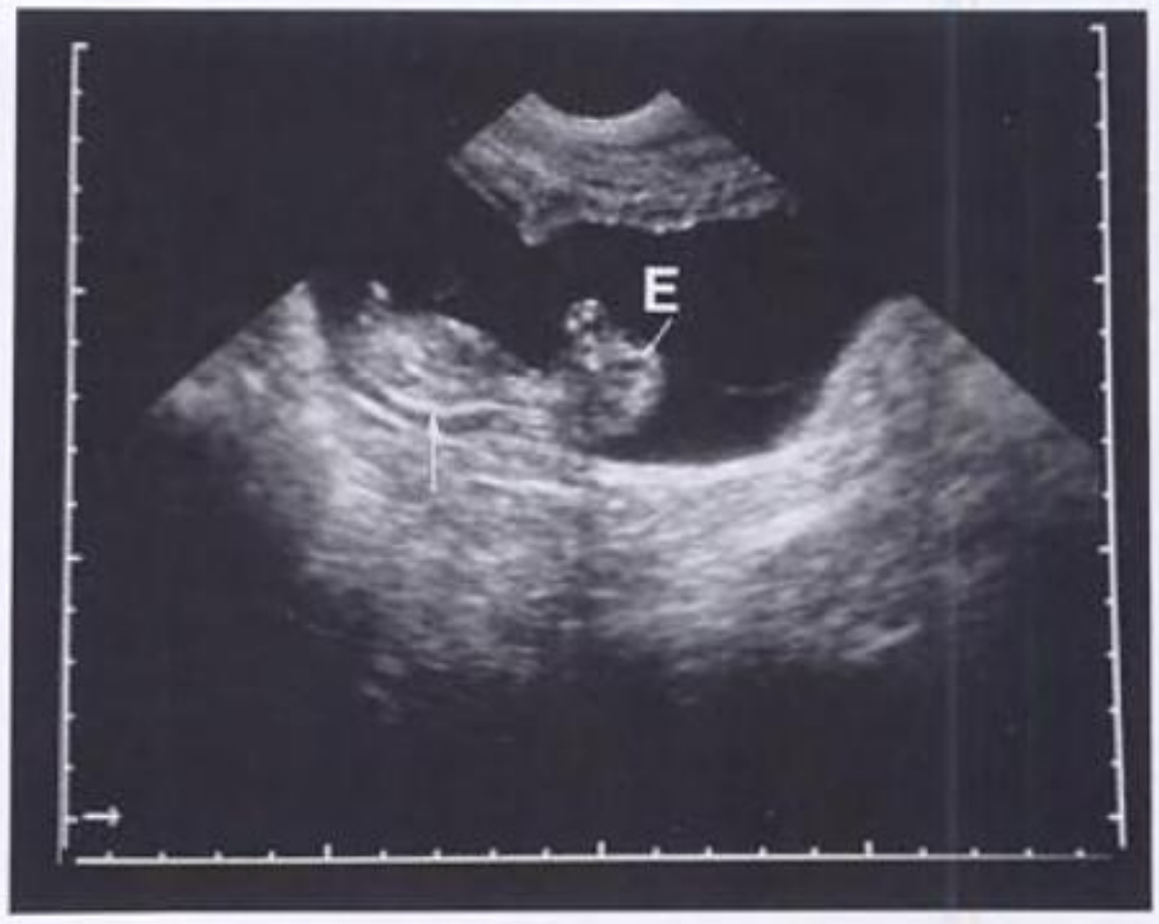


Fig. 2.133: Ventrodorsal sagittal section through a fetus on Day 61 of pregnancy. The head with the developing eye (E) lies on the right. In the areas of the maxilla and mandible bright ossification centers can be recognized. The spinal column (arrow) is hyperechoic.

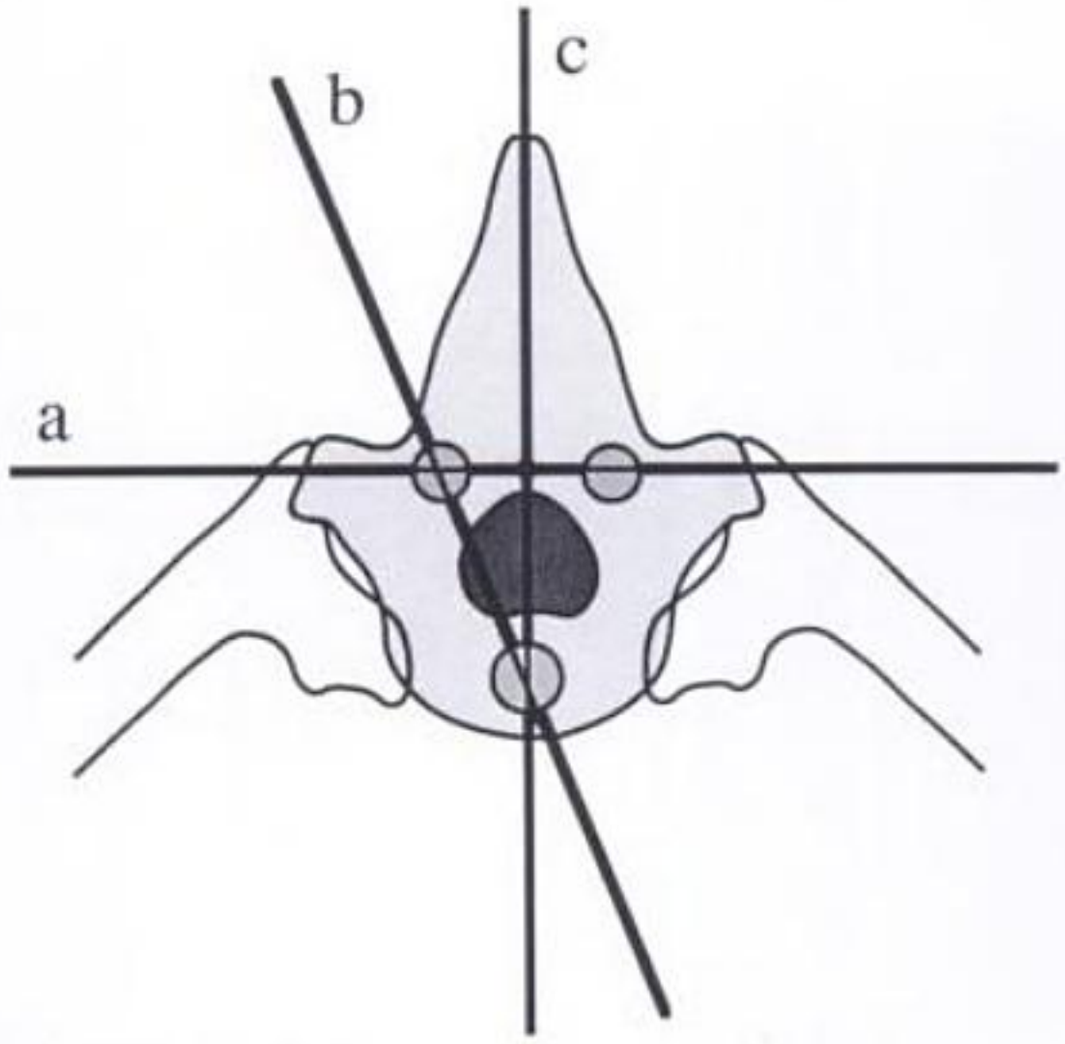


Fig. 2.134: Schematic presentation of the ultrasound examination of vertebrae. Depending on the angle at which the sound waves impact onto the vertebra different ossification centers may be depicted. a and b: double row of echoes; c: single row of echoes.

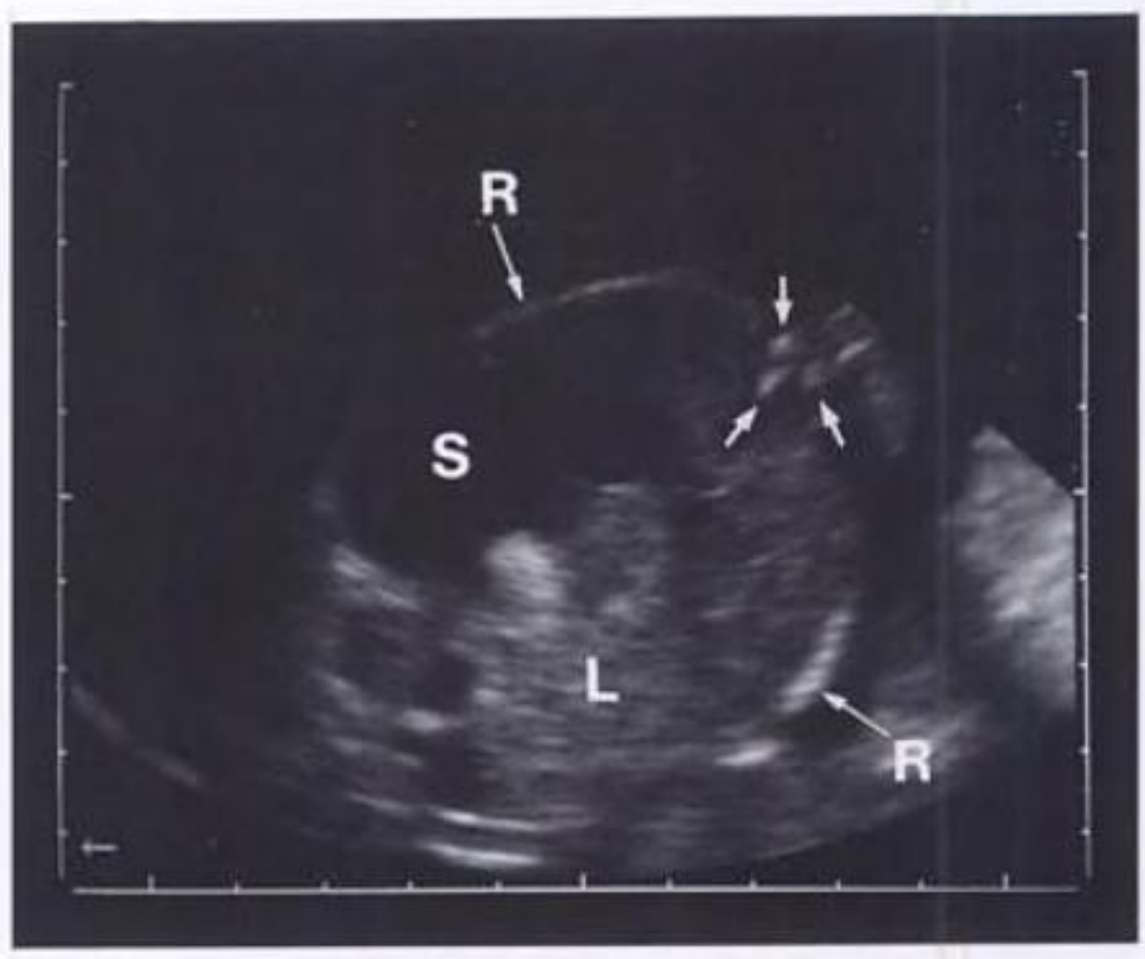


Fig. 2.135: Transverse section through the thorax at the level of the stomach and the liver in a fetus on Day 114 of pregnancy. Caudal view. Three ossification centers (arrows) of a thoracic vertebra can be seen. Two curved ribs (R) stretch around the trunk. The hypoechoic stomach (S) lies above with the live (L) underneath it.

Avtorsko zaščiteno gradivo

Downloaded From Vet-eBooks.com

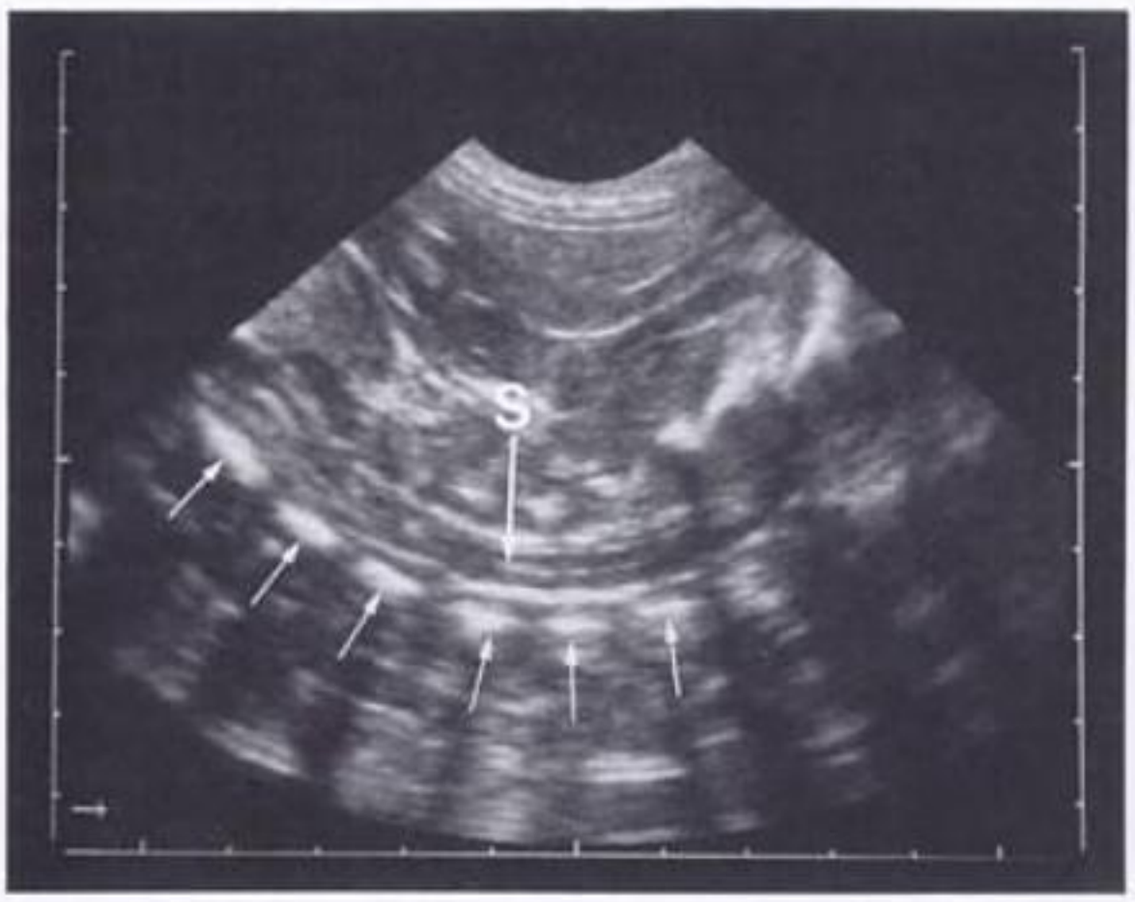


Fig. 2.136: Median section through the cervical spine on Day 161 of pregnancy. The spinal cord (S) and the vertebral bodies (arrows) below it are depicted. Shadow artifacts appear in the background of the vertebrae.

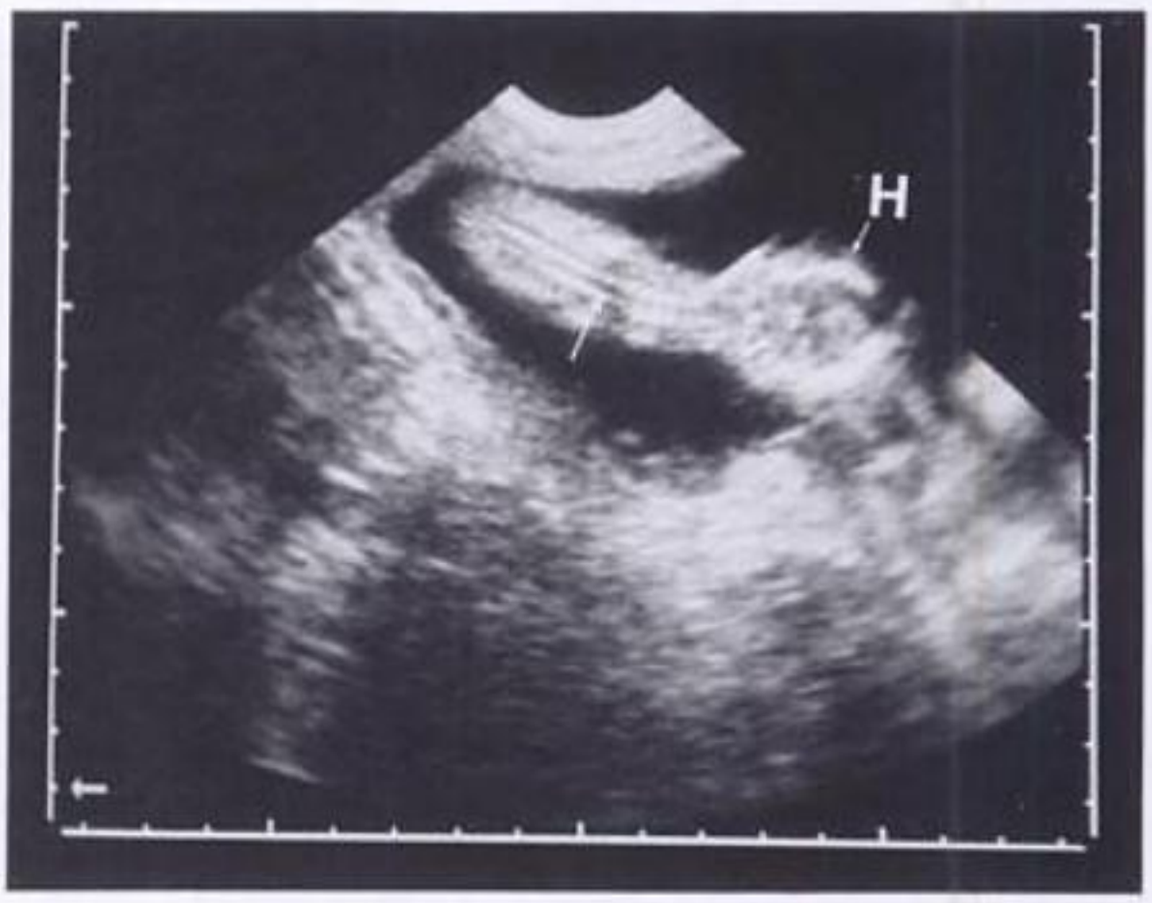


Fig. 2.137: Horizontal section through the head, neck and trunk of a fetus on Day 71 of pregnancy. The head (H) points to the right. A double row of echoic discs of the spinal column with a central, hypoechoic canal (arrow) runs through the middle of the neck and trunk.

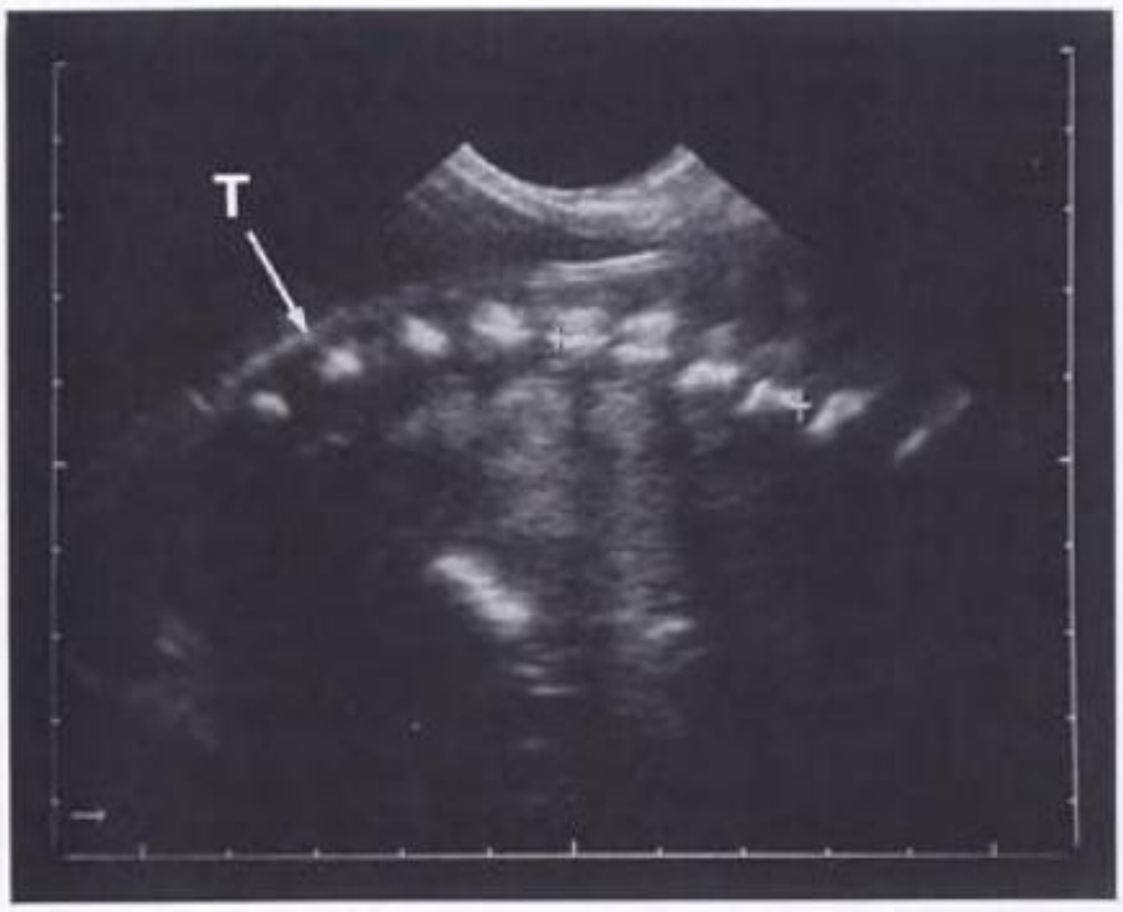


Fig. 2.138: Sacral and coccygeal vertebrae in a fetus on Day 165 of pregnancy. The sacral vertebrae lie on the right and are individually recognizable. The tail (T) stretches to the left.



Fig. 2.139: Ventrodorsal median section through the neck and anterior tip of the thorax in a fetus on Day 107 of pregnancy. The head (out of view) lies on the left, the cervical spine (CS) with the first few thoracic vertebrae ventrally. From the tip of the thorax the sternum (St) runs in the direction of 4 o'clock.

Avtorsko zaščiteno gradivo

Downloaded From Vet-eBooks.com

When the sectional plane lies exactly in the median it passes between the ossification centers of the left and right vertebral arches without producing any reflections, but it does strike the ossification center in the middle of the vertebral body (Fig. 2.136). After that only a row of disc shaped echoes can be seen. The same happens when the examination plane is moved to the paramedian or if it is rotated from the sagittal towards a more horizontal plane. In these cases the single row of echoes may originate either from the ossification centers in the vertebral arches or from those in the vertebral bodies.

Further rotation of the probe around the longitudinal axis produces the horizontal section with the sound beam directed latero-laterally. If the examination plane lies at the level of the vertebral arches, two parallel rows of echoes are again produced (Fig. 2.137). These represent the ossification centers of the left and right vertebral arches, respectively. Due to the natural curve of the spine a horizontal section through it will pass through individual vertebrae at different heights and therefore no rows of echoes from the same structure of the different vertebrae can be seen. Commonly therefore, for example, a short section of the thoracic spine may be seen as a double row of echoes, be continued caudally as a single row and form a double row again in the lumbar region.

On the exact horizontal section through the spinal column of the trunk one can sometimes see, apart from the reflections of the vertebral bodies, on both sides a further row of disc shaped echoes. These represent the sonographic images of the transverse processes. In this manner the horizontal section through the fetus can occasionally depict three parallel rows of echoes in the region of the spinal column.

The caudally extending tail of the fetus is characterized by the large number of lined up, disc shaped echoes of the vertebral bodies (Fig. 2.138). The image of the tail is very similar to that of the other parts of the spinal column. A double row of echoes or a clear spinal canal are, however, not evident. Not infrequently, movements of the tail can be observed.

Early on already, the vertebral echoes are very bright, and towards the end of pregnancy they can be described as hyperreflective. As the ossification of the vertebrae progresses, the typical image of shadowing becomes evident in their background(Fig. 2.136, 2.143, 2.144). From below the vertebrae hypoechoic shadows stretch into the depth of the image. The width of each shadow is approximately the same as that of the bony structure in the foreground. The shadowing effect is caused by the absorption of sound waves by the bony tissue which then causes very little sound to reach the tissues immediately behind the bone.

If areas behind the vertebral column are to be examined sonographically it is useful to move the probe to a point where the spinal column is no longer positioned in the path of the sound waves. In this manner the sound shadows, which originate behind the echoes of the vertebrae and run as parallel stripes through the entire image, can be avoided.

The spinal cord is best depicted on an exact median section (Fig. 2.136). This approach allows the sound waves to pass between the ossification centers of the vertebral arches on either side without generating any reflections. The spinal cord can then be examined without any shadows interfering with the image quality.

Avtorsko zaščiteno gradivo

Downloaded From Vet-eBooks.com



Fig. 2.140: Horizontal section through the neck of a fetus on Day 209 of pregnancy. The anechoic inner lumen of the trachea (T) is bordered by the two rows of transversely sectioned tracheal rings. The head (out of view) lies on the left.



Fig. 2.141: Horizontal section through the head-neck junction in a fetus on Day 183 of pregnancy. At the center the larynx (L), to the left a pulsating blood vessel (arrow).



Fig. 2.142: Horizontal section through a fetus on Day 70 of pregnancy. The head (H) lies on the right. The two hyperechoic rows of rib cross sections (arrows) produce a conical shape of the thorax.



Fig. 2.143: Horizontal section through the thorax on Day 126 of pregnancy. The thoracic inlet is positioned at 7 o'clock. From the rib cross sections shadows are cast across the heart (H). Lung tissue lies between the heart and the diaphragm (arrows). Hepatic veins can be seen branching from the caudal caval vein (V).

Avtorsko zaščiteno gradivo

Downloaded From Vet-eBooks.com

2.4.1.3 Neck

Apart from the typical image of the spine (Fig. 2.136 and 2.139) the trachea appears as a dominating structure on the sonogram of the neck (Fig. 2.140). Its longitudinal section features a prominent string of hyperechoic cartilaginous rings which surround the anechoic lumen of the tracheal tube. In comparison to the blood vessels that run in the cervical area the trachea has a much wider diameter. This is particularly evident on transverse sections through the neck which show the wide, hypoechoic tracheal pipe in about the middle of the neck just ventral to the spine. In the region of the head-neck junction the larynx can be seen (Fig. 2.141). Occasionally, swallowing movements can be observed here. On horizontal sections the common carotid artery can occasionally be traced on either side of the trachea and larynx. Its pronounced pulsation is striking.

2.4.1.4 Thorax

The ribs can be differentiated almost at the same time as the vertebrae. The ribs, thoracic vertebrae and sternum are all characterized by hyperreflective cross sectional images. The thoracic skeleton can be recognized by the strings of numerous hyperechoic disc shaped echoes and their typical topographic arrangement. On horizontal sections the rows of rib cross sections of both halves of the thorax form a cone (Fig. 2.142 and 2.143). The previously described phenomenon of shadow artifacts behind the spinal column can also be observed in the background of ribs and thoracic vertebrae. When the thorax is examined by longitudinal sections its image is obscured by parallel shadows (Fig. 2.143). This applies for horizontal sections with latero-lateral and sections with sagittal, dorsoventral beam directions. The distances between shadows correspond to the widths of the intercostal spaces. In advanced pregnancy the increased absorption of sound waves by the bones can seriously restrict the examination of organs lying behind the ribs. Under such circumstances it is possible to rotate the probe through 90 degree, thus allowing the examination of the thoracic contents through the intercostal spaces without any interference from the rib shadows.

The sternum does not produce the image of a single, coherent bone, but consists of a single row of discs (Fig. 2.139).

Avtorsko zaščiteno gradivo

Downloaded From Vet-eBooks.com

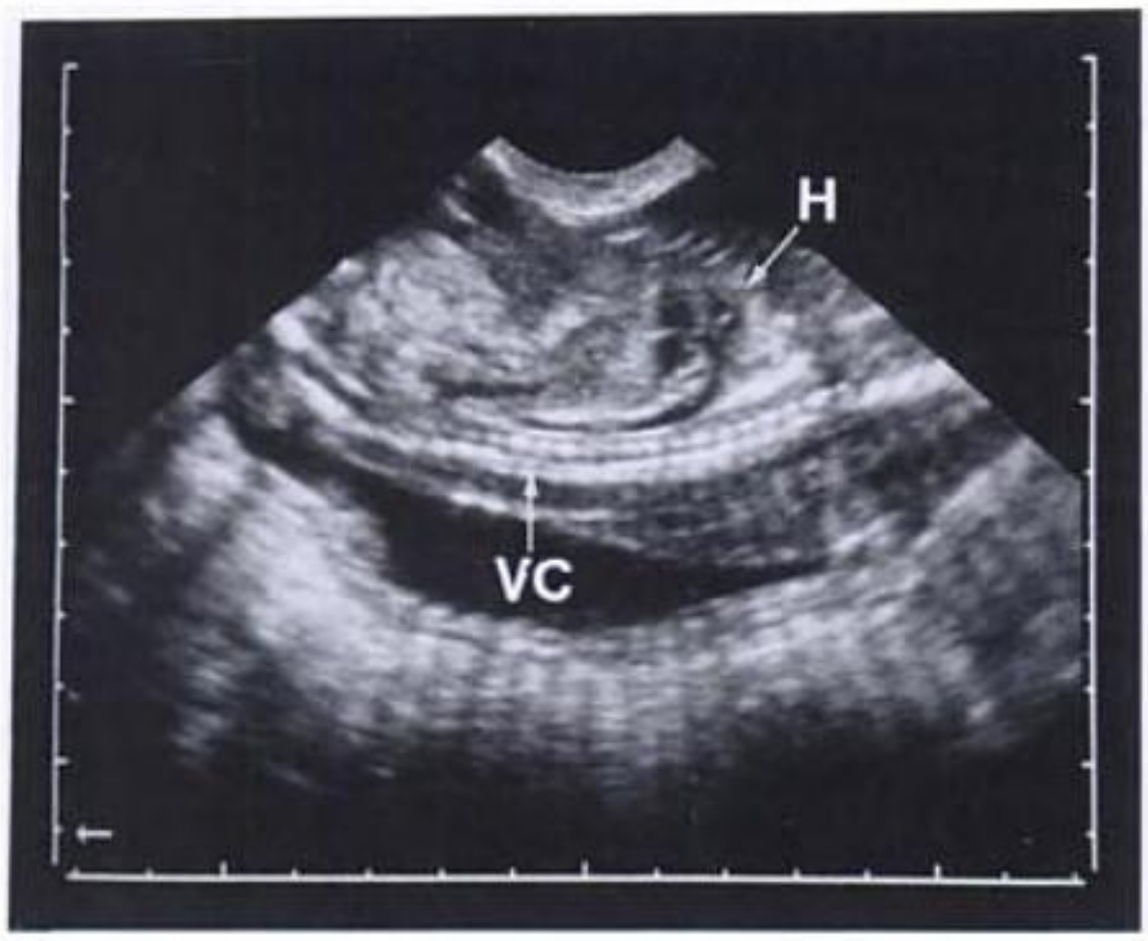


Fig. 2.144: Ventrodorsal sagittal section through a fetus on Day 91 of pregnancy. The neck is on the right. Heart chambers (H) and the aorta which runs ventrally of the vertebral column (VC) in a caudal direction can be identified.

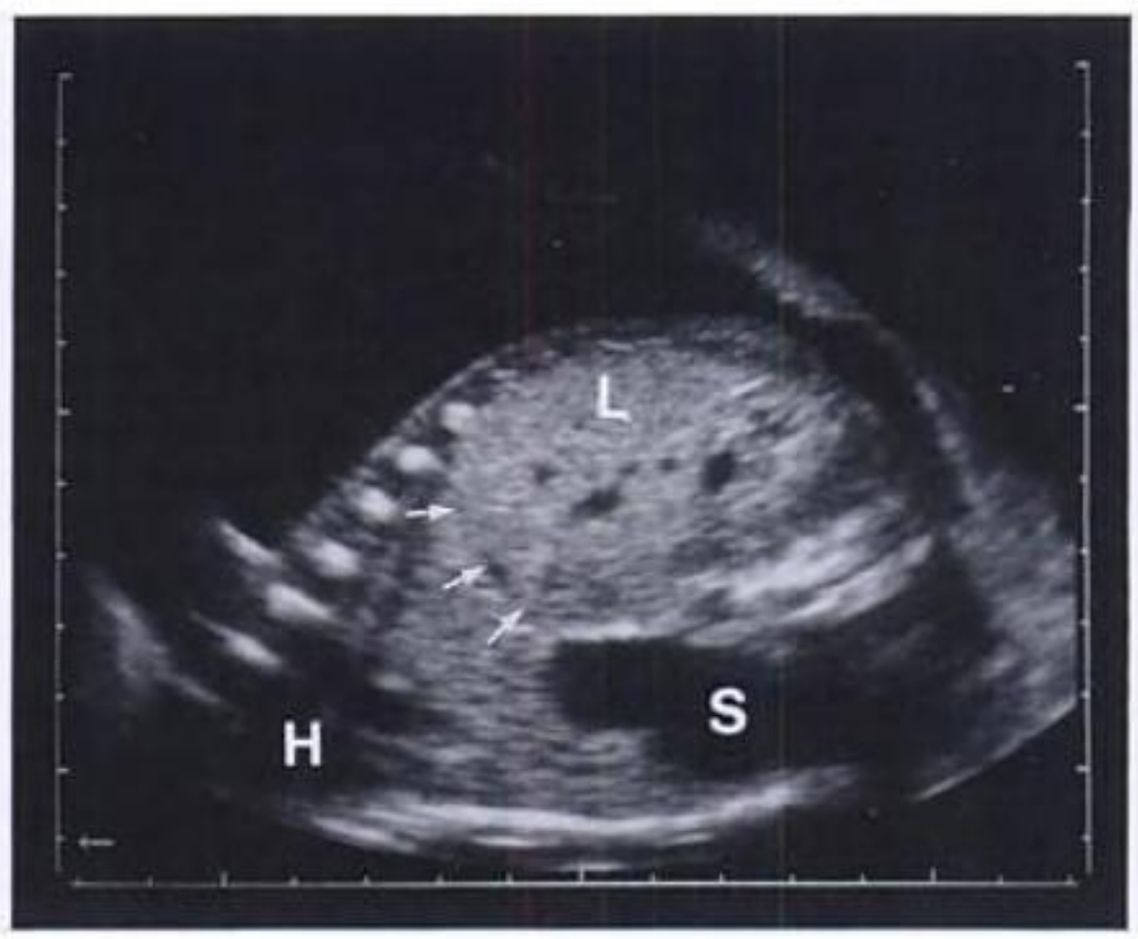


Fig. 2.145: Horizontal section through the thorax and abdomen of the fetus depicted in Fig. 2.143. The fetus is still lying in the same position on its left side. The heart (H) is on the left. Caudally to the dorsally positioned ribs is the liver (L) with several vessel cross sections. Cranially to the liver is the diaphragm (arrows) and below it is the stomach (S).



Fig. 2.146: Cross section through the omasum with its characteristic folds (arrows) in a fetus on Day 157 of pregnancy.

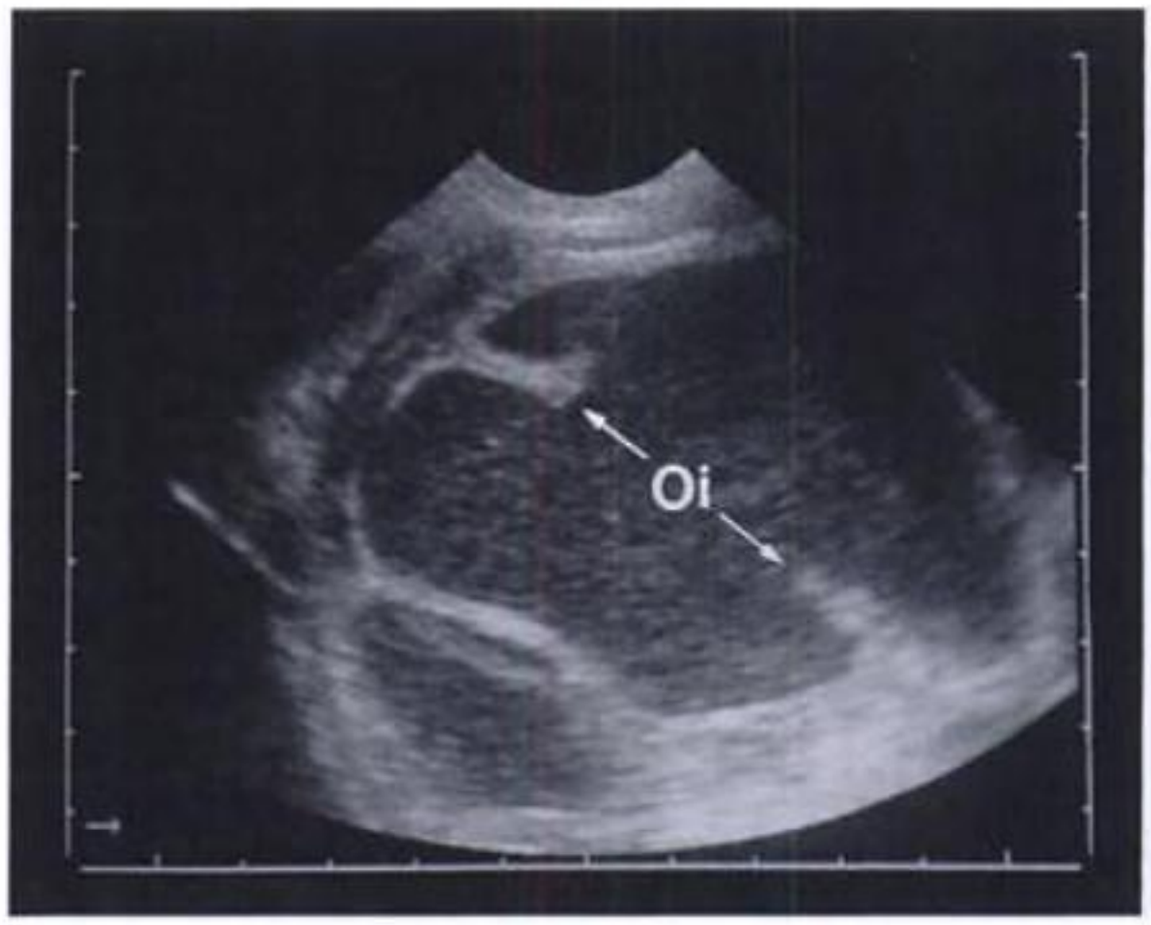


Fig. 2.147: Left paramedian section through the stomach of a fetus on Day 166 of pregnancy. The stomach contains snowy reflections which, during longer observation periods, will show obvious, turbulent movements. The dorsal and ventral sacs of the rumen communicate through the ostium intraruminale (Oi).

Avtorsko zaščiteno gradivo

Downloaded From Vet-eBooks.com

The cranial, apical sector of the thoracic cone is filled by the heart (Fig. 2.143 to 2.145). The latter is very striking with is obvious pulsation, its hypoechoic heart chambers which are surrounded by the echoic myocardial walls and subdivided by the bright septa and valves. The pulsation is clearly noticeable by the movements of the valves. In order to obtain a favorable image of the heart it is advisable to rotate the sound plane far enough until a window is found between the ribs that allows the sonographic examination to be performed without the interference of any rib shadows. This may be difficult and can be achieved if the fetus lies in the optimal position of having its front limbs in close proximity to the transducer. If the transducer can be positioned favorably it is sometimes possible to produce a 4-chamber section through the heart (Fig. 2.144). When an image of 2 or more chambers can be generated the functioning of the heart and its larger valves can be observed. By choosing the correct section through the thorax one can see the blood vessels leaving the heart.

The space between the heart and the diaphragm is filled by the echo of the lung. The lung echo is coarsely granular, very similar to that of the liver. The diaphragm itself cannot be illustrated sonographically. Its position can, however, be determined by subtle differences in the echogenicity between liver and lung (Fig. 2.143 and 2.145).

2.4.1.5 Abdomen

The developing stomach and the liver can be seen in the background of the last few ribs (Fig. 2.145). The liver can be recognized by its coarsely granular echo which is traversed by several large vessels in the center. The sonographically obvious stomach lies between the liver and the contralateral ribs. The stomach becomes ultrasonically visible shortly later than the heart and at about the same time (around Day 40 of pregnancy) as the developing eyes. It constitutes the largest anechoic area in the abdomen of the fetus, produces the typical image of a fluid filled, hollow organ and permits the identification of its typical shape and different anatomical regions (Fig. 2.146 and 2.147). As pregnancy progresses, the echogenicity of the stomach's contents will increase. At about Month 5 of pregnancy there will be already obvious echogenicity in the stomach. These will become more intense as time passes. Sometimes they will even develop into snow storm like reflections. If the stomach can then be observed over time one will often be able to observe turbulence within its fluid contents.

The position of the stomach can give an indication of the posture of the fetus. If the rumen lies dorsally next to the transducer the fetus will be lying on its right side; if the fetus lies on its left side the rumen will be on the side furthest from the transducer (Fig. 2.145 and 2.152). The description of the position of the fetus relative to that of the dam then depends on its presentation. In the case of a cranial presentation with the rumen found dorsally the fetus is in a left lateral position; where the presentation is caudal with the rumen still found dorsally the fetus is in a right lateral position. The same contrasts between presentation and position are valid for the ventrally situated rumen. In this case the cranial and caudal presentations imply a right and left lateral position, respectively.

In a median section through the fetus the abdominal aorta is seen as a hypoechoic band running just underneath the many bright echoes of the spinal column (Fig. 2.144). When observation periods over time are possible the aorta's pulsation can be seen. The wall of the vessel is hyperechoic.

Avtorsko zaščiteno gradivo

Downloaded From Vet-eBooks.com



Fig. 2.148: Section through the kidney of a fetus on Day 196 of pregnancy. Several renal lobes with cortical and medullary regions are visible.

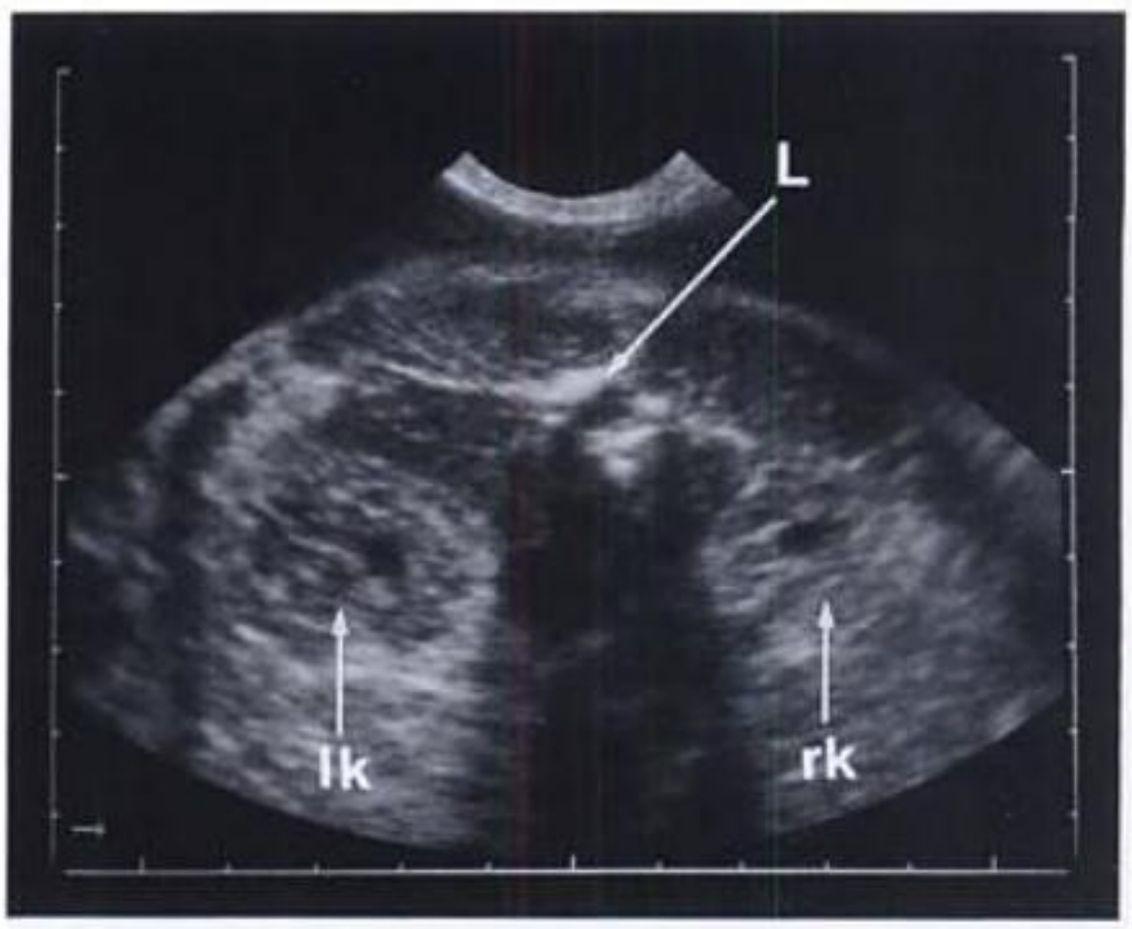


Fig. 2.149: Dorsoventral transverse section through the region of the lumbar vertebrae on Day 166 of pregnancy. Dorsally a lumbar vertebra (L) with both transverse processes. Above the latter the two Mm. longissimi. Below them: Left kidney (lk), right kidney (rk) and in between those the caudal caval vein and the abdominal aorta.

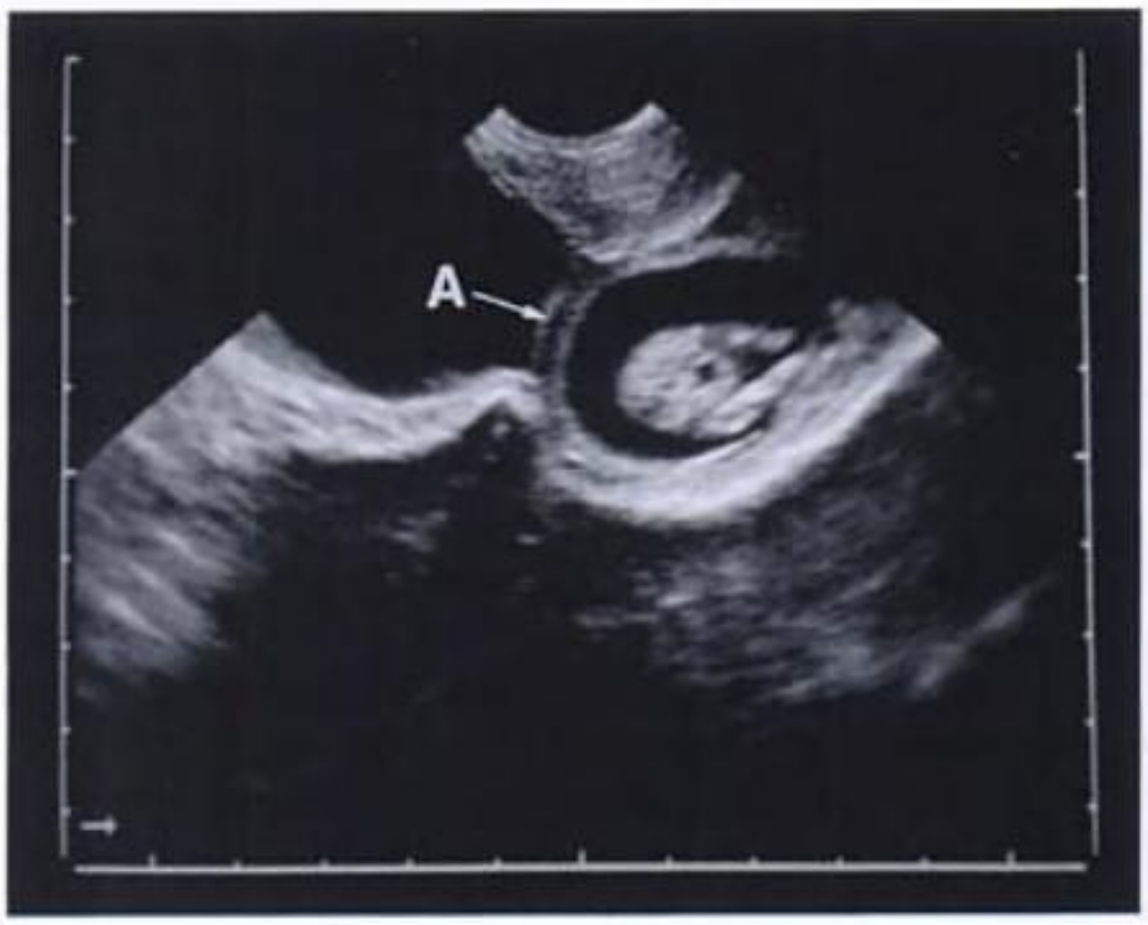


Fig. 2.150: Transverse section through the caudal abdomen of a fetus on Day 62 of pregnancy. The fetus lies on its side and is surrounded by its amnion (A). The two caudal limbs point to the right. Between the limbs is the small, anechoic urinary bladder.



Fig. 2.15: Transverse section through the caudal abdomen of a fetus on Day 86 of pregnancy. The scanning plane is tilted slightly to run from caudodorsal to cranioventral. The urinary bladder (U) with its dark lumen and echoic wall lies in the center. To the left of the bladder are pelvic bones (arrow).

Avtorsko zaščiteno gradivo

Downloaded From Vet-eBooks.com

The kidneys can also be depicted ultrasonographically. In the horizontal section they can be seen between the iliac bone and the last rib (Fig. 2.148). In a transverse section with the beam directed dorsoventrally they can be found at the level of the lumbar vertebrae, immediately ventral and lateral to the spine. With the transducer skillfully positioned, both kidneys can be shown on the same image (Fig. 2.149). They are relatively hypoechoic and present their typical anatomical structure, including multiple papilla divided by deep fissures. Better than in the transverse section, the longitudinal section permits the identification of numerous renal lobes which collectively form the kidney. On each of the renal lobes a more hyperechoic outer cortical and a less echoic central medullary region can be recognized.

The next smaller organ with an anechoic lumen beside the stomach is the urinary bladder. Finding the urinary bladder is sometimes difficult - even with a well exposed pelvis. Although it is sometimes visible at an early stage of pregnancy (Fig. 2.150), its accurate identification may prove very difficult. The degree of filling of the bladder appears to vary. The urinary bladder presents with its anechoic, fluid filled lumen and lies in the midline of the ventral abdomen, just at the pelvic inlet (Fig. 2.151). On either side of the bladder the umbilical arteries which run in the direction of the umbilicus, can be found. These can be relatively thick and must be differentiated from the urinary bladder. The difficulty in finding the fetal urinary bladder by ultrasonography may be caused by presumed ability of the fetus to regularly empty the bladder from an early stage of pregnancy on. Shortly after urination it may thus be very difficult to recognize the fetal bladder.

Avtorsko zaščiteno gradivo

Downloaded From Vet-eBooks.com



Fig. 2.152: Horizontal section through the thorax, abdomen and pelvis of a fetus on Day 95 of pregnancy. The apex **of the** thorax points towards 8 o'clock, the stomach (S) lies ventrally. The two halves of the bony pelvis, with hyperechoic ischial and ileal bones (arrows), form a cone, the apex of which is directed towards 2 o'clock.

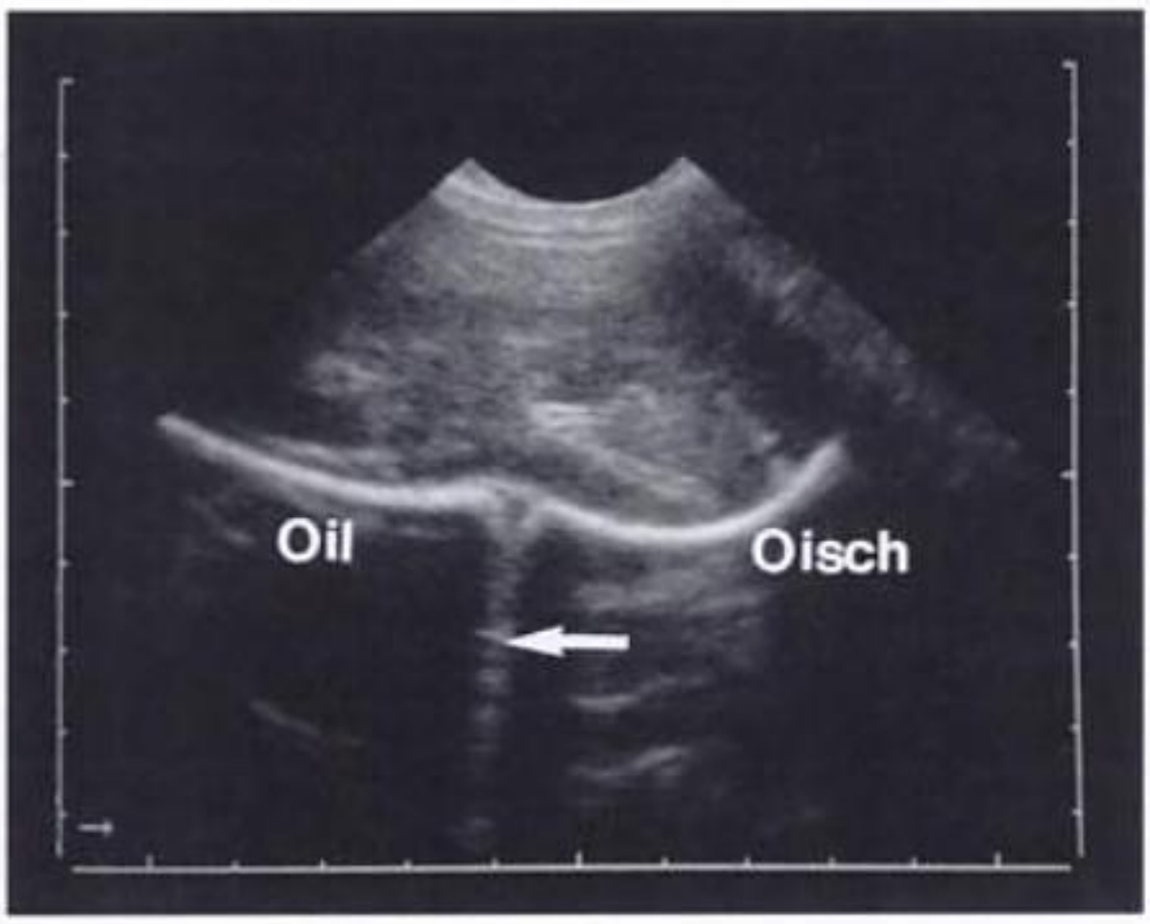


Fig. 2.153: Oblique horizontal section through the pelvis of a fetus on Day 211 of pregnancy. The connection between the ileal (O il) and ischial (O isch) bones, in the area of the acetabulum, is not yet ossified. Ultrasound penetrates this point (arrow).

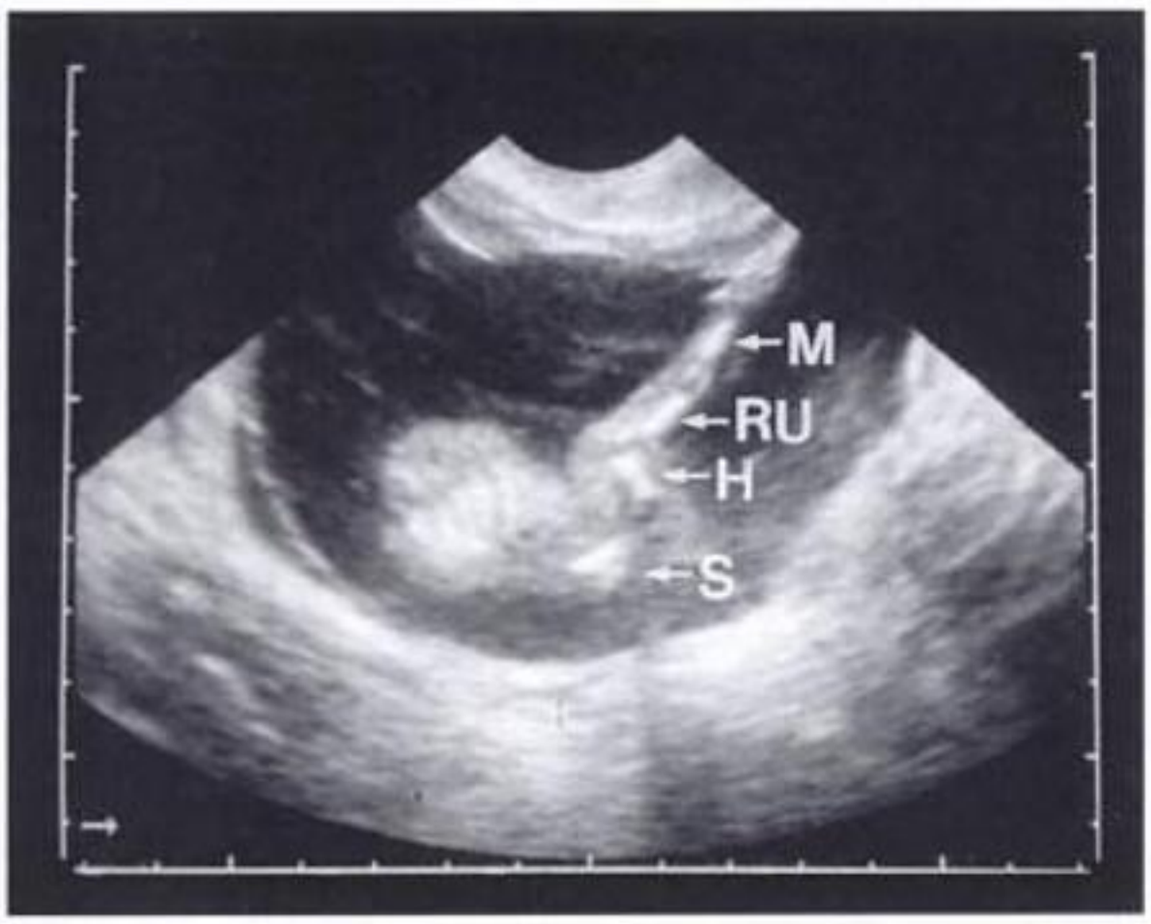


Fig. 2.154: Tangential sagittal section through the front limb of a fetus on Day 75 of pregnancy. The back of the fetus lies ventrally and the head on the right (off the image). The front leg with scapula (S), humerus (H), radius and ulna (RU) and metacarpus (M) is visible.

Avtorsko zaščiteno gradivo

Downloaded From Vet-eBooks.com

2.4.1.6 Pelvis

During early pregnancy both halves of the bony pelvis can be depicted simultaneously on a horizontal section (Fig. 2.152). On each side the ilium and ischium can be seen. They present as four rod shaped, hyperechoic structures. In horizontal section the ischium is slightly shorter than the ilium. The 2 bones lie one behind the other, parallel to the longitudinal axis of the body and form, with their counterparts on the other side, the blunted cone shape of the bony pelvis. The latter narrows slightly towards its caudal opening. When the ultrasound beam is directed latero-laterally, the demonstration of both halves of the pelvis is only possible in the first half of pregnancy. Thereafter, the nearer half of the bony pelvis absorbs so much ultrasound that the other half cannot be seen (Fig. 2.153). At this stage only the ilium and ischium nearest to the transducer can still be depicted.

The pelvic region can be recognized towards the end of the second month of pregnancy when its ossification centers become visible. The iliac and ischiac bones can then be seen as individual structures around week 11 to 12 of pregnancy. The bones of the pelvis are well suited to aid the search for the genitalia, the urinary bladder and the hind limb.

2.4.1.7 Front limb

The sonographic visualization of the extremities is based on the depiction of their bony and cartilaginous components. Due to the large difference in impedance between bony tissue and the surrounding soft tissues the former are easy to recognize by their intensive reflections.

On the front limb the larger long bones, such as humerus, radius, ulna and metacarpus can be identified for the first time around weeks 10 to 12 of pregnancy (Fig. 2.154). At this stage the ossification process has obviously progressed far enough to produce continuous, rod shaped echoes in the regions of the diaphyses. After this time the length measurements of the bones are taken between the two ends of their hyperechoic diaphyses. Prior to this the measurements are taken from the edge of each limb segment to its point of angulation. They therefore reflect not only the length of the main bone, but include the joint and soft tissue components of each segment. At the end of the 4th month of pregnancy it is still possible to depict the full thickness of the long bones of the front limb. Due to the advanced perichondrial ossification at about Month 5 it is only possible to see those sides of the bone cortex of the humerus, radius and ulna, as well as metacarpus and phalanxes that are nearest to the transducer (Fig. 2.155). The sound reflection from, and absorption on the compact bone are so strong that the background is no longer accessible. It remains black.

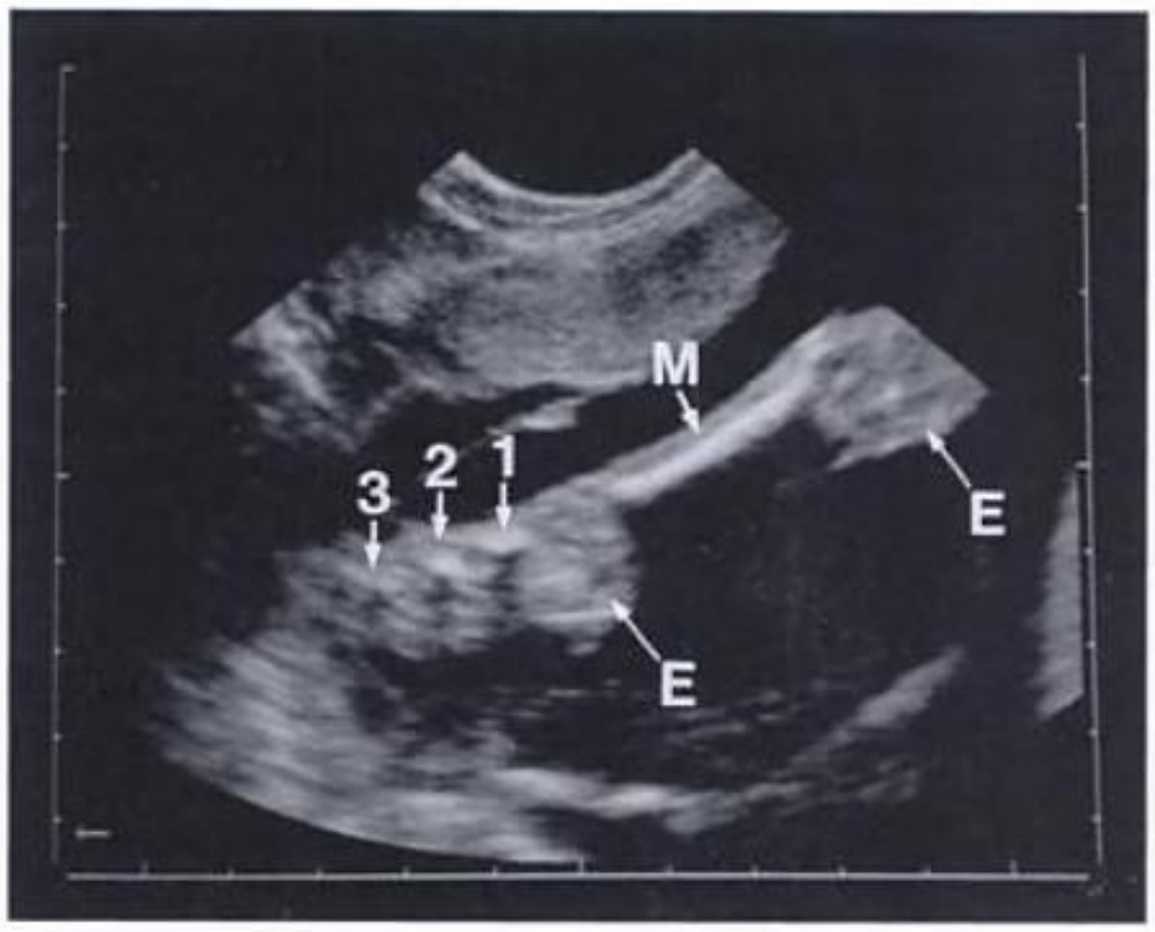


Fig. 2.155: Sagittal section through a front foot on Day 135 of pregnancy. The cortices of the metacarpus (M), proximal (1), middle (2) and distal (3) phalanxes are so well ossified that only the foreground is visible. The two cartilaginous epiphyses (E) of the metacarpus can be seen clearly.

Avtorsko zaščiteno gradivo

Downloaded From Vet-eBooks.com

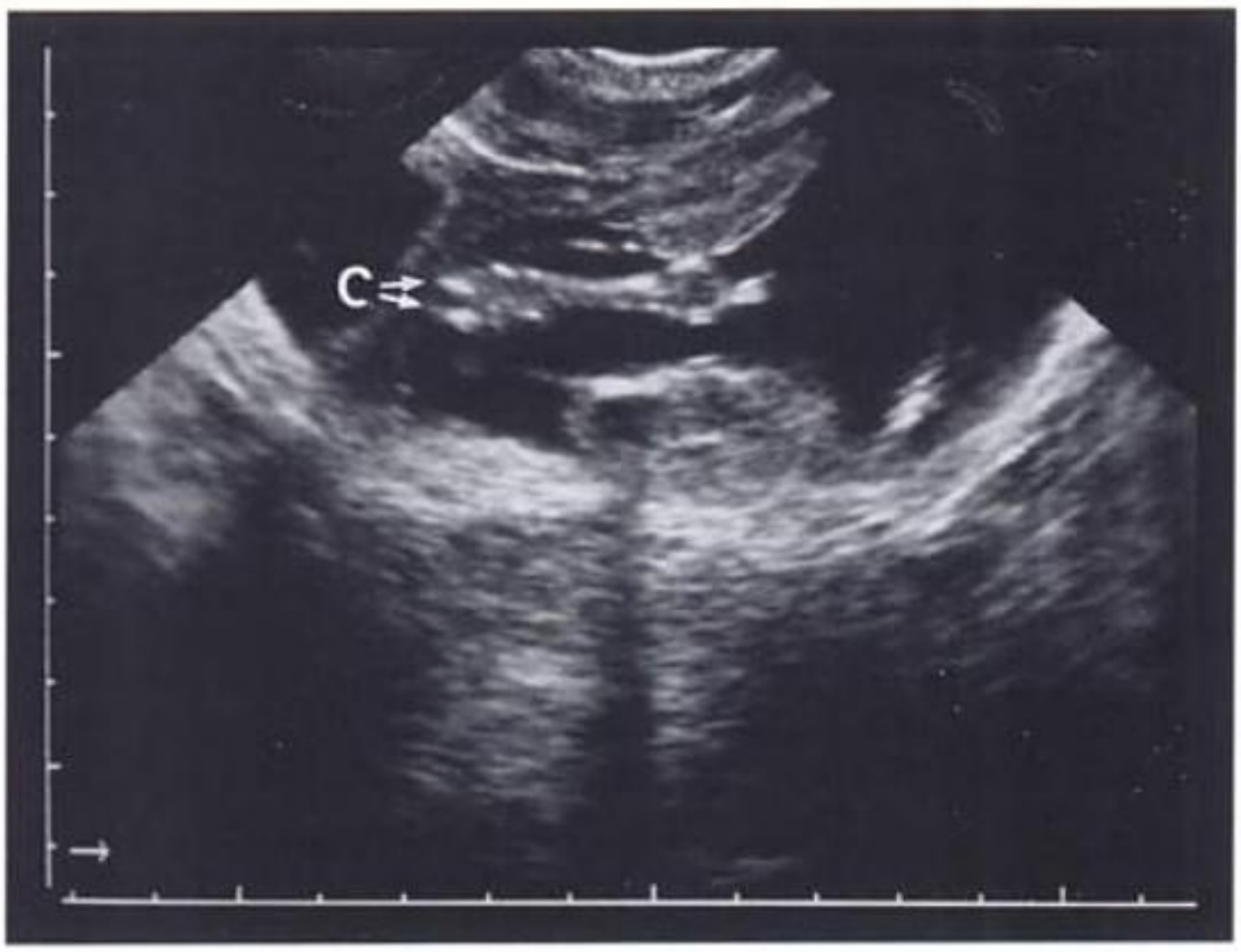


Fig.2.156: Transverse section through the front foot of a fetus on Day 97 of pregnancy. The two hyperechoic claws (C) point to the left. To the right of the claws are the two bright spots of the dewclaws. The front limb is epicted up to its carpal joint.



Fig. 2.157: Palmar view of the claws of both front feet in a fetus on Day 164 of pregnancy. In the centers of the claws (lc) of the left foot lie the hyperechoic digital bones. The image of the right claws (rc) shows only the hooves.

Avtorsko zaščiteno gradivo

Downloaded From Vet-eBooks.com

Apart from the bony parts, the horny parts at the tip of the extremities can also be shown. Main and dewclaws can be seen (Fig. 2.156). The horny wall of the main hooves can be recognized from Month 4 (Fig. 2.157). Its echogenicity increases over the following months and the hoof wall as well as distal phalangeal bone can be identified.

2.4.1.8 Hind limb

The chronological order in which the bones of the hind limb can be depicted are very similar to that seen in the front limb. Although individual ossification centers can be detected by Day 60, specific long bones such as femur, tibia and metatarsus can only be identified reliably starting Week 10 of pregnancy. A few weeks later the entire thickness of the diaphysis of the bone can be illustrated (Fig. 2.158). The diaphyses of the femur, tibia and metatarsus produce very bright echoes. During Month 5 the ossification is so pronounced that only those walls of the diaphyses that are nearest to the transducer can be depicted (Fig. 2.159).

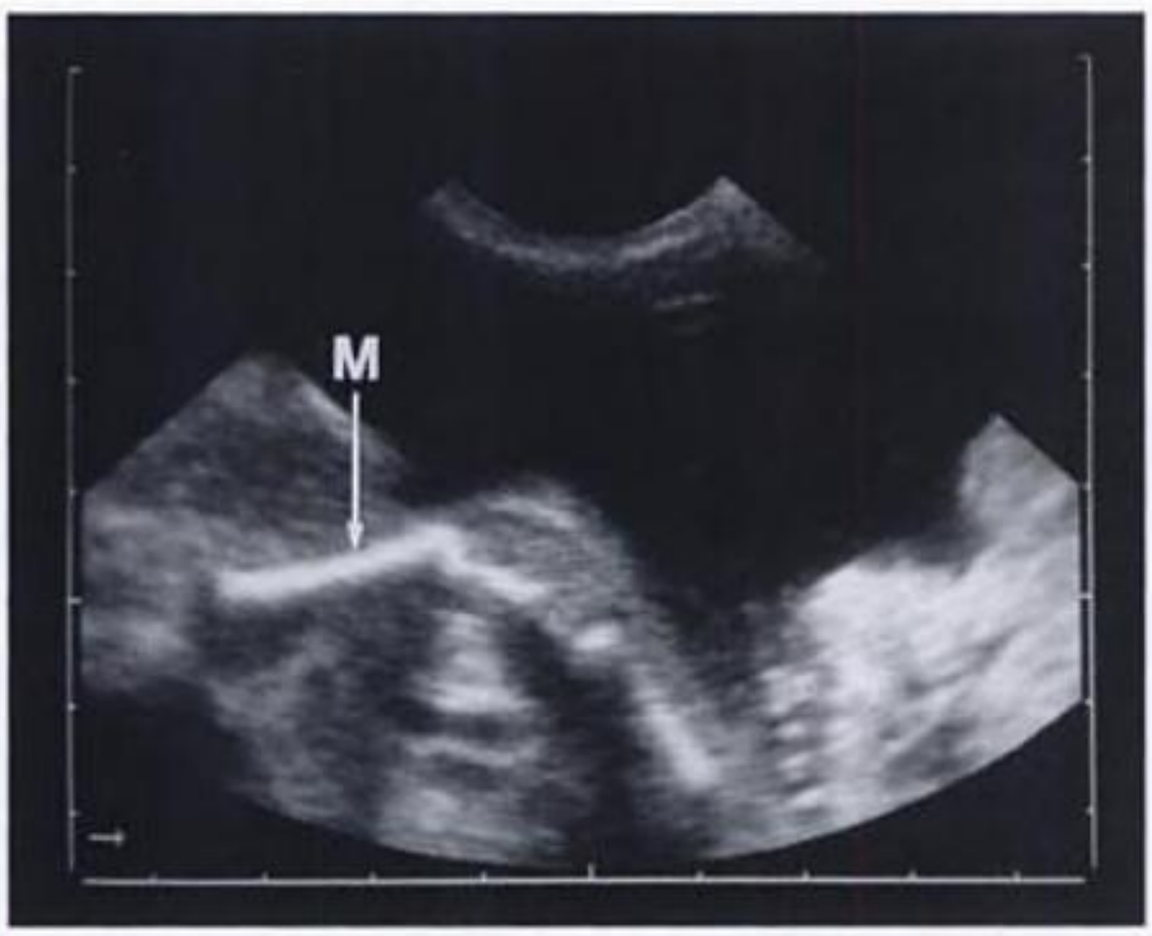


Fig. 2.158: Plantodorsal sagittal section through the hind limb of a fetus on Day 110 of pregnancy. The tarsal joint lies on top and is flexed. The bright diaphysis of the metatarsus (M) points to 8 o'clock, the tibia to 5 o'clock.

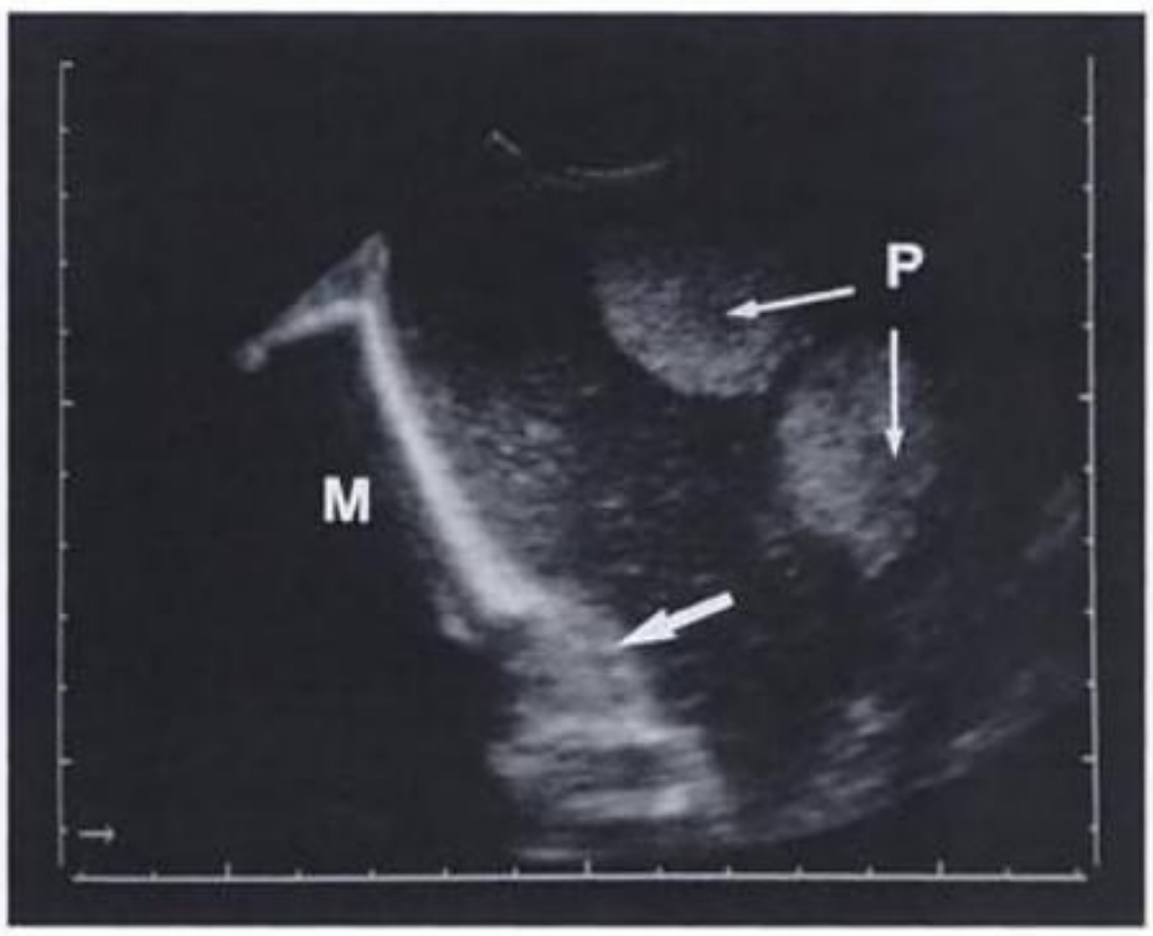


Fig. 2.159: Longitudinal section through the metatarsus (M) of a fetus on Day 171 of pregnancy. One side of the bony diaphysis produces a hyperechoic reflection. Distal to the diaphysis lies a cartilaginous epiphysis (arrow). There are two placentomes (P) in the right half of the picture.

Avtorsko zaščiteno gradivo

Downloaded From Vet-eBooks.com

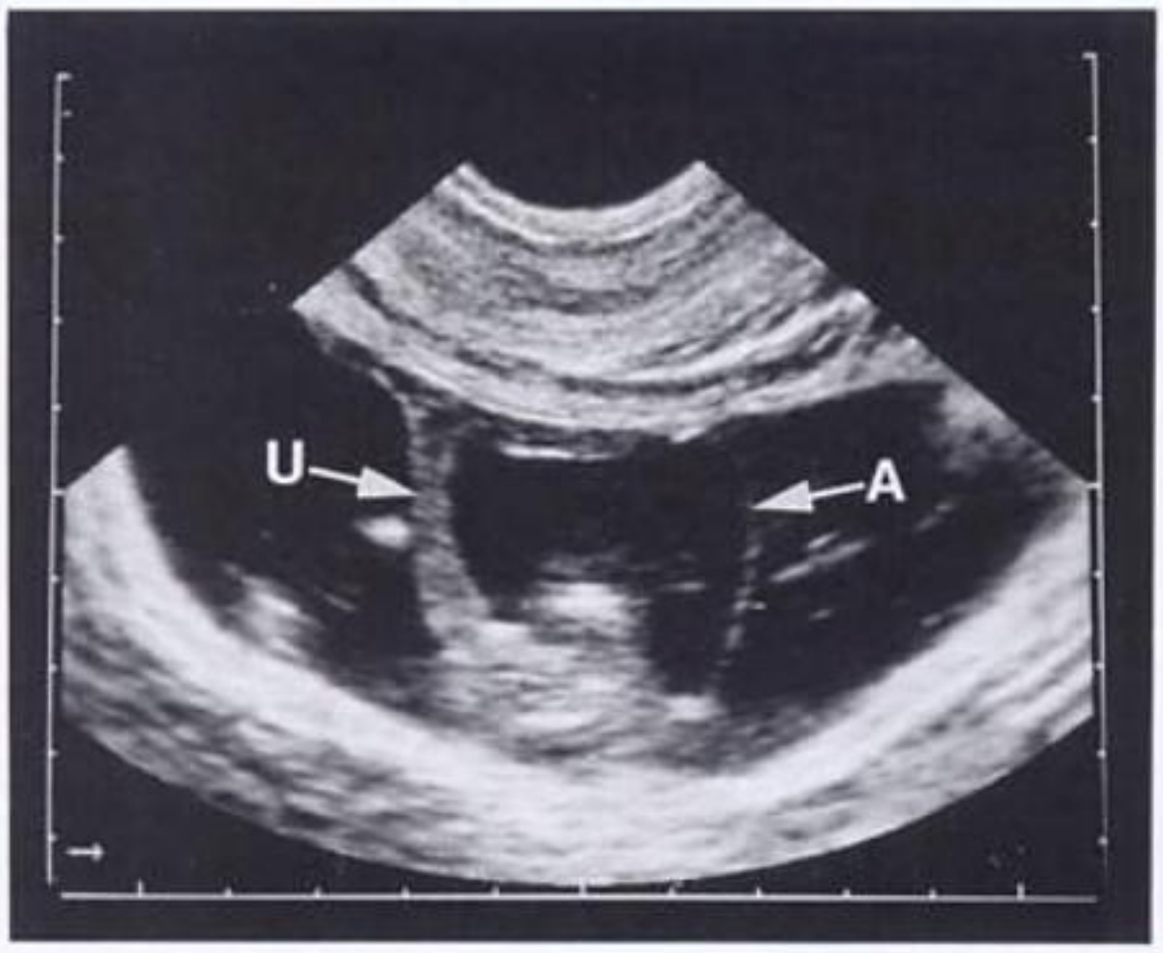


Fig. 2.160: Uterus with fetus in its amnion (A) on Day 63 of pregnancy. The umbilical cord (U) runs dorsally from the fetus to the antimesometrial edge of the uterus.



Fig. 2.161: Transverse section through the umbilicus of a fetus on Day 110 of pregnancy. The 4 lumina of the umbilical arteries and veins can be recognized.



Fig. 2.162: Longitudinal section through the insertion of the umbilical cord (arrow) in a fetus on Day 110 of pregnancy. The hypoechoic lumina of two umbilical vessels are separated by the vessel walls.

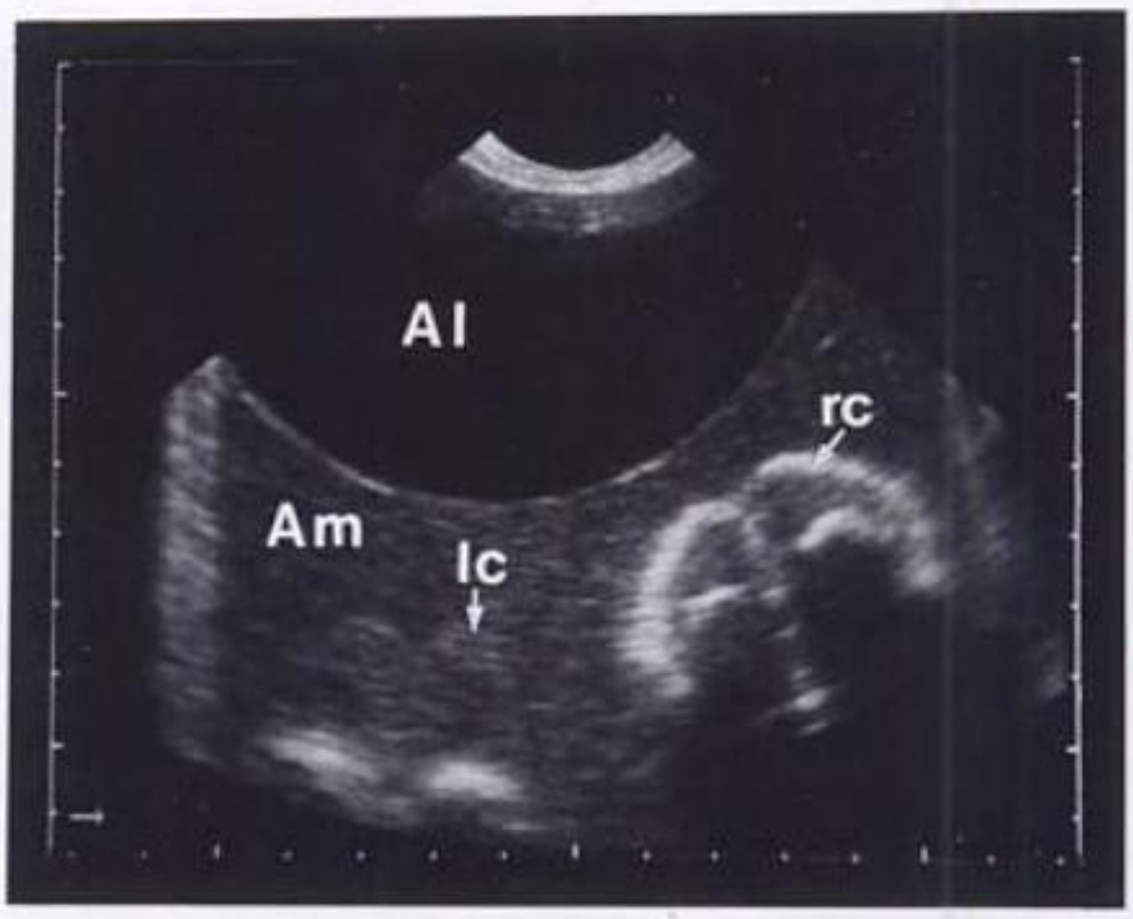


Fig.2.163: The hypoechoic allantoic fluid (Al) and the snowy amniotic fluid (Am) are separated by the amniotic membrane. Inside the amniotic fluid lie the left (lc) and right (rc) claws of a fetus on Day 206 of pregnancy. Palmar view.

Avtorsko zaščiteno gradivo

Downloaded From Vet-eBooks.com

2.4.1.9 Umbilical cord, amnion and allantois

The umbilical cord can be seen early on the ultrasound monitor. At the time when the outline of the embryo becomes visible and the head and neck can be differentiated the umbilical cord can also be identified. It runs from the embryo in a dorsal direction to the site of its division at the antimesometrial wall of the uterus (Fig. 2.160). From Month 3 of pregnancy the two umbilical arteries and veins can be seen inside the umbilical cord. They are particularly impressive when seen in a cross section through the umbilical cord (Fig. 2.161). In this view the four vessels are arranged in a square. Where the umbilical cord enters into the abdomen the two umbilical arteries can be traced caudally in the direction of the urinary bladder. The umbilical vein can be traced cranially to the liver.

In a longitudinal section through the umbilical cord only two vessels can be seen (Fig. 2.162). If the section runs tangentially through the umbilical cord one will not necessarily see a vessel lumen. In this case the umbilical cord appears solid and may be confused with the more caudally situated scrotum.

The amnion can be recognized as a very thin hyperechoic membrane by Day 30 of pregnancy (see Chapter 2.3.2.4). Without significantly changing its thickness it remains visible until the end of pregnancy. The fluid contained inside the amnion is hypoechoic, almost black, for the first few months of pregnancy. First reflections appear at about the end of the 2nd month of pregnancy. They rapidly become denser and soon create the image of a snow storm. The echoes become so intense during the third trimester of pregnancy that the term "snow storm appearance" seems justified (Fig. 2.163). Echoic particles also appear inside the allantoic fluid during the course of pregnancy.

Avtorsko zaščiteno gradivo

Downloaded From Vet-eBooks.com



Fig. 2.164: Median section through a male fetus at the level of the pelvis on Day 92 of pregnancy. The spine stretches from 10 o'clock to 12 o'clock. The scrotum (arrows) points towards 4 o'clock. Ultrasonogram produced in waterbath.



Fig. 2.165: Section through the same fetus analogous to the examination plane in Fig. 2.164. On the ventral abdomen are the scrotum and genital tubercle.

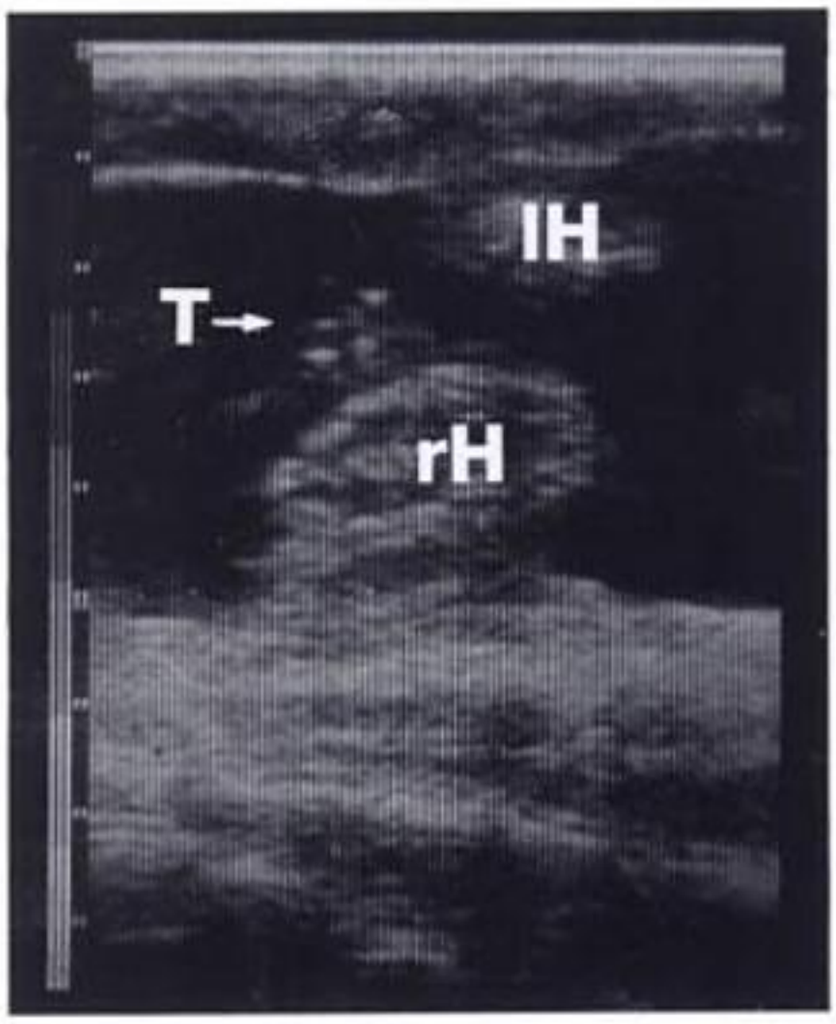


Fig. 2.166: Horizontal section through a female fetus at the level of the mammary glands on Day 101 of pregnancy. Between the left (lH) and the right (rH) hind extremities lie the four bright echoes of the cross sections of the teats (T). Ultrasonogram produced in a waterbath.

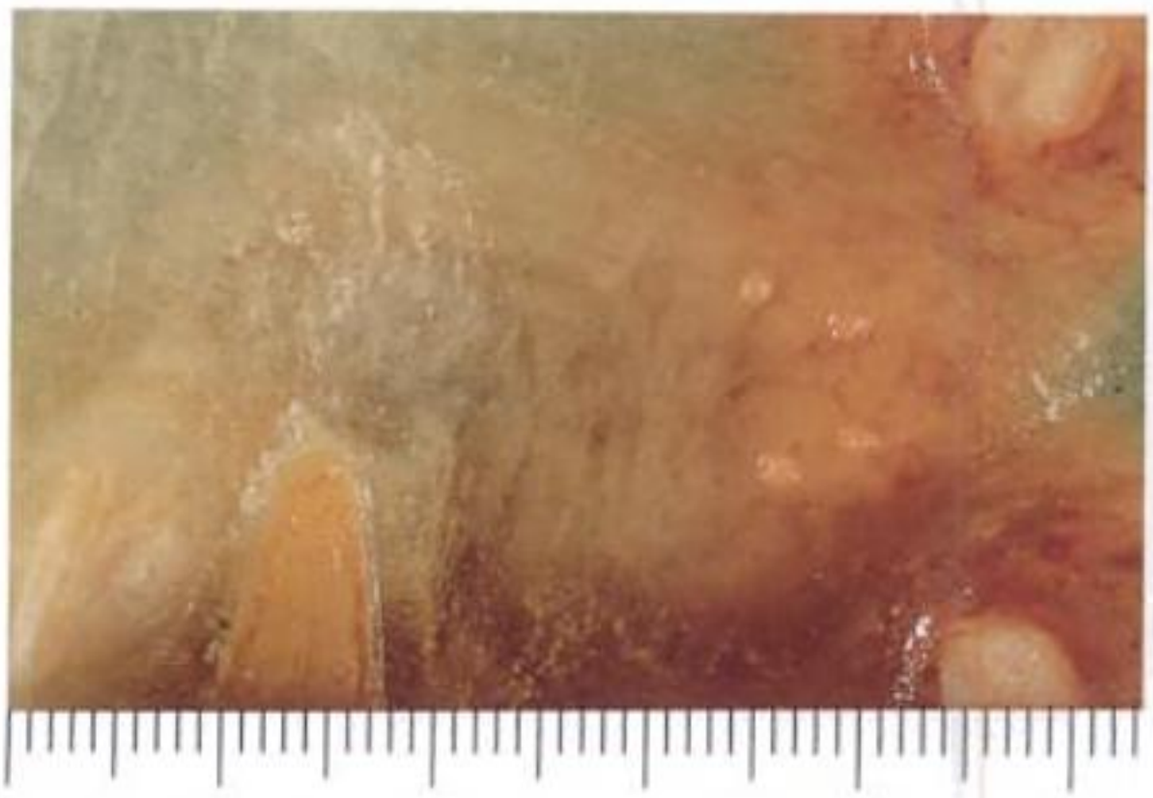


Fig. 2.167: Section through the same fetus analogous to the scanning plane in Fig. 2.166.

Avtorsko zaščiteno gradivo

Downloaded From Vet-eBooks.com

2.4.2 Sex determination in the bovine fetus

2.4.2.1 Scrotum, teats and genital tubercle

The scrotum of the male fetus can be depicted by ultrasonography (Fig. 2.164 and 2.165). Based on experience to date it seems possible to determine fetal sex by the detection of the scrotum from the Month 3 of pregnancy. First fetal sex determinations may be possible between Days 50 and 60, but the scrotum cannot, however, be identified with certainty at this stage. After Day 60 the scrotum can then be identified more clearly (Fig. 2.168 to 2.171). In positive cases the male gender can now be diagnosed with certainty (MÜLLER and WITTKOWSKI 1986).

In female fetuses the developing teats can be depicted (Fig. 2.166 and 2.167). As a result of their intense echogenicity the teats become evident as four hyperreflective dots which are arranged in a square. They are best identified on horizontal sections.

Another way of determining the fetal sex is based on the determination of the relative position of the genital tubercle (Curran et al. 1989). The genital tubercle will give rise to the penis and prepuce in the case of males and to the vulva and clitoris in the case of females. Initially the genital tubercle will be positioned between the hind legs in both sexes, but between the Day 40 and 60 of pregnancy it will migrate towards the umbilicus in male fetuses and towards the tail root in female fetuses. The genital tubercle will present as a bilobular, ovoid structure, a few millimeters in size and of intense echogenicity. On the basis of the relative position of the genital tubercle it becomes possible to predict the fetal sex from about Day 55 of pregnancy.

Avtorsko zaščiteno gradivo

Downloaded From Vet-eBooks.com



Fig. 2.168: Laterolateral transverse section through the pelvis of a fetus on Day 86 of pregnancy. The upper portions of both hind extremities point to the right. Between them lies the scrotum (s). The base of the tail can be seen at about 9 o'clock (arrow).

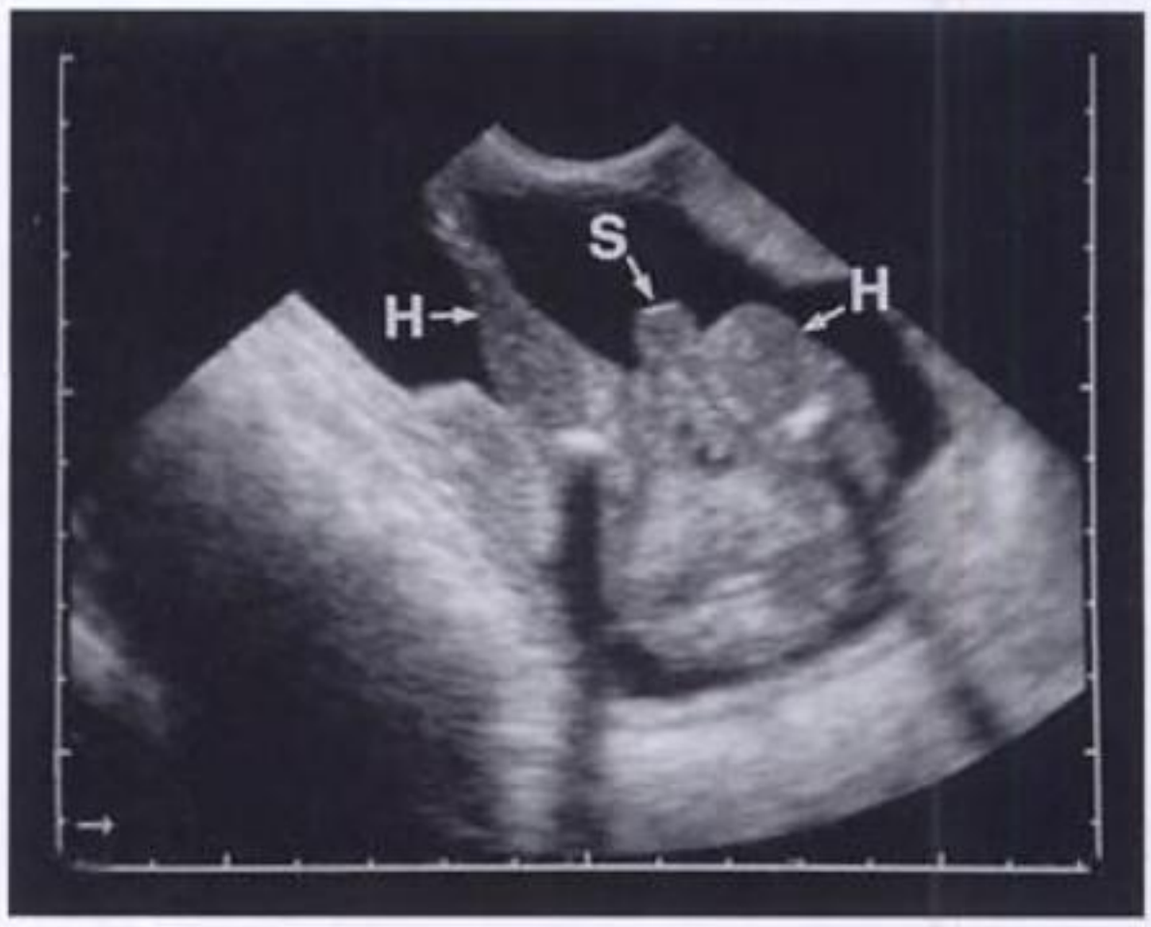


Fig. 2.169: Transverse section through the pelvis of a fetus on Day 99 of pregnancy. The fetus lies on its back. Between the two hind limbs (H) the scrotum (S) is pointing towards 12 o'clock.



Fig. 2.170: Horizontal section distal to the pelvis through the knee joint of a fetus on Day 129 of pregnancy. Inside the transversely imaged scrotum (S) the two hypoechoic testicular structures can be seen. To the left of the scrotum is an oval cross section through the muscles of the upper thigh.



Fig. 2.171: Median section through the scrotum of a fetus on Day 170 of pregnancy. The head of the fetus lay on the right. Inside the scrotum the testicle (arrow) can be seen. Below the scrotum the umbilical cord (U) with 2 vessels can be recognized.

Avtorsko zaščiteno gradivo

Downloaded From Vet-eBooks.com

Depending on the position of the fetus and the orientation of the probe the fetal scrotum can be detected between the hind legs on median, transverse or horizontal sections (Fig. 2.168 to 2.171). The biggest threat of misdiagnosing the presence of a scrotum comes from structures in the vicinity of the scrotum. In this context the umbilical cord and any parts of the tail that may have been drawn in between the hind limbs should be mentioned first. In order to avoid confusing the scrotum with the base of the umbilical cord, attempts should always be made to demonstrate, apart from the suspected scrotum, the umbilical cord. Only if the course of the umbilical cord can be followed all the way to its origin on the abdominal wall, and if, in addition, to it the scrotum can be identified as a separate structure a definitive diagnosis can be made.

From Month 4 of pregnancy ultrasonograms may reveal testicular structures inside the scrotum (Fig. 2.171) which are less echoic than the scrotum proper. Testicular descent starts during the 3rd month in the bovine fetus and is completed in the 5th month of pregnancy (HULLINGER and WENSING 1985, SCHUMMER and VOLLMERHAUS 1987).

According to experiences made thus far the positive recognition of the female sex by depicting the developing teats appears to be rather difficult during the early stages of pregnancy. The teats are occasionally confused with other echoic spots in the region of the pelvis. Structures often misdiagnosed as teats include the hyperechoic images of transverse sections through pelvic bones or the femur. The determination of fetal sex using the position of the genital tubercle appears to yield more accurate results in the female fetus.

The period from 55 to 60 days of pregnancy seems to be particularly well suited for the determination of the position of the genital tubercle, and thus the sex of the fetus (CURRAN et al. 1989). If the sex is to be determined by detecting the scrotum or the teats the period between Days 70 and 120 seems to be better suited for the examination. If both criteria, position of the genital tubercle as well as the depiction of either scrotum or teats, are used in conjunction a relatively high accuracy in the determination of the sex of the fetus can be attained between Days 55 and 120 (WIDEMAN et al. 1989). It must be emphasized that much operator experience is needed, and that the sex of the fetus cannot be determined in every case during a single sonographic examination. Occasionally, only follow-up examinations allow the sex of the fetus to be determined accurately.

Avtorsko zaščiteno gradivo

Downloaded From Vet-eBooks.com

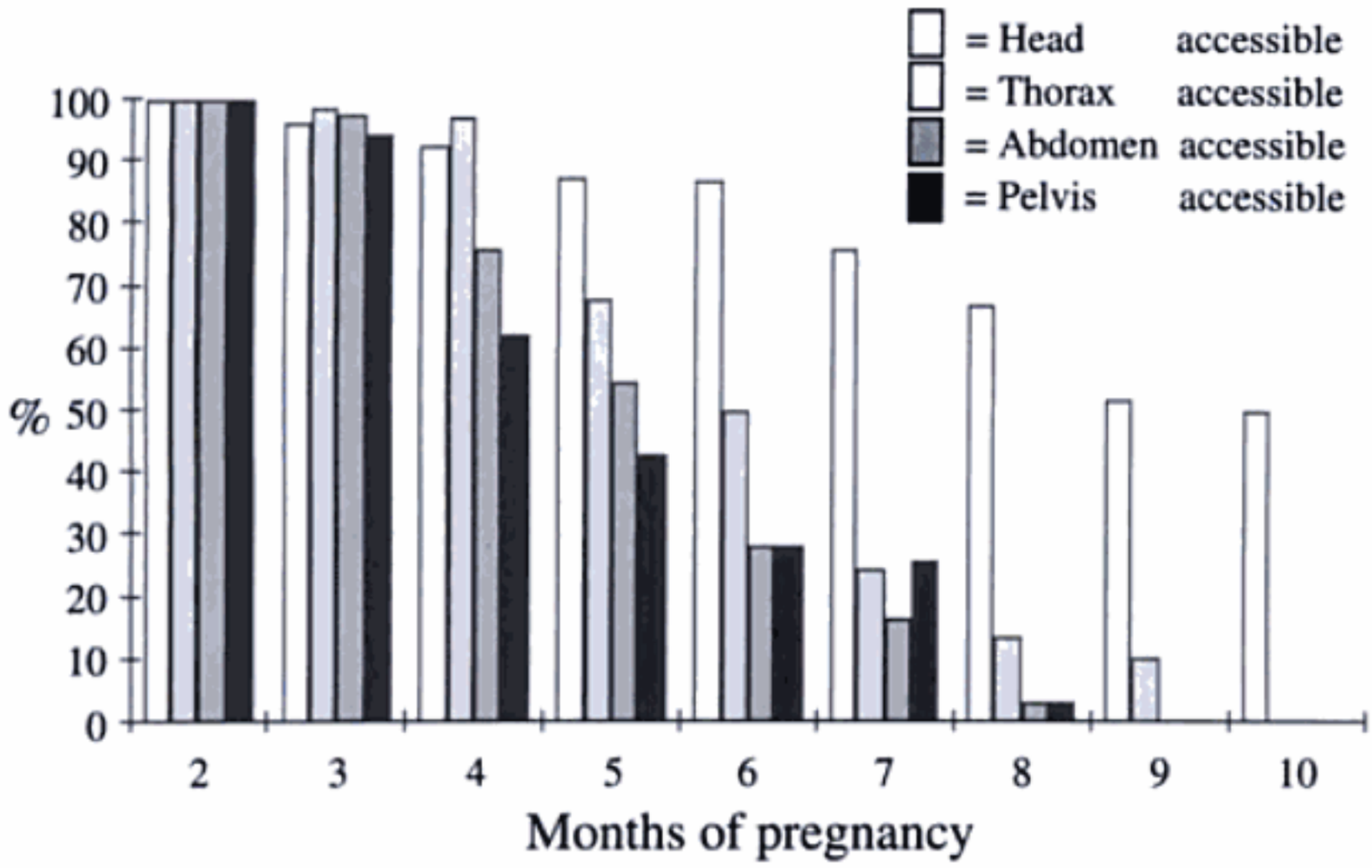


Fig. 2.172: Frequency with which fetal body parts were accessible by transrectal ultrasonography during pregnancy in heifers (adapted from Kähn 1989 b).

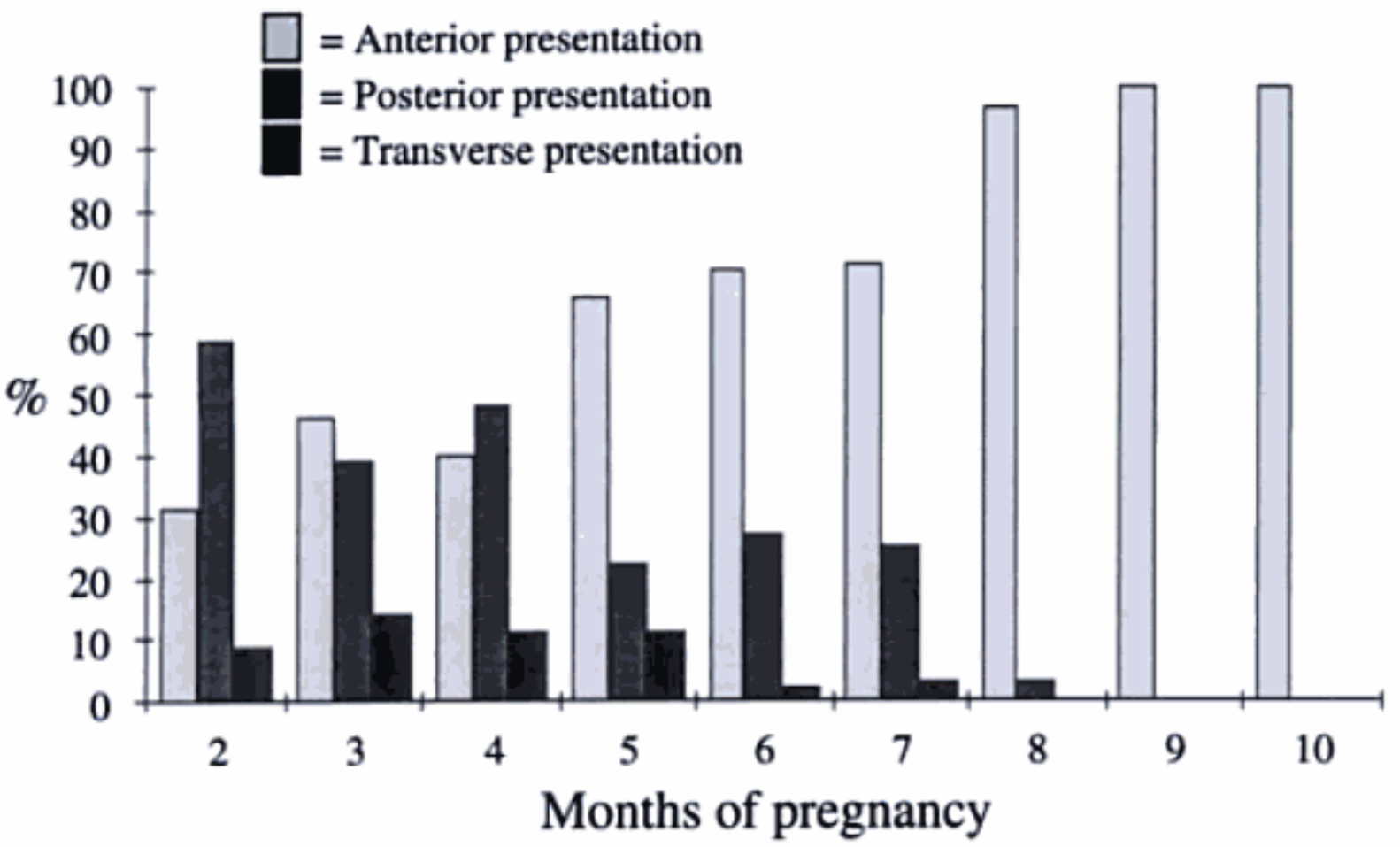


Fig. 2.173: The intra-uterine presentations of bovine fetuses during pregnancy (adapted from Kähn 1989 b).

Avtorsko zaščiteno gradivo

Downloaded From Vet-eBooks.com

2.4.3 Accessibility of bovine fetuses for transrectal sonography and their intra-uterine presentations during pregnancy

2.4.3.1 Accessibility of fetal body parts

The specific intra-uterine positioning of the fetus during the course of pregnancy has a direct effect on the ability to depict fetal body parts by ultrasonography. This means that the accessibility of certain structures is limited by the typical intra-uterine presentations of the fetus at the different stages of pregnancy and by their growth rates. Due to these factors, for example, the scrotum and developing teats, the thoracic and lumbar vertebrae, the ribs, the size of the stomach or the length of the limb bones often cannot be accessed for sonographic fetometry during the last trimester of pregnancy.

During one study the fetuses of 19 pregnant cows were ultrasonically examined 485 times at intervals of a few days from the 2nd to the 10th months of pregnancy (KÄHN 1989 b). During the second month of pregnancy the entire fetus could be depicted regularly at every examination (Fig. 2.172). In the third month the head, thorax, abdomen and pelvis were within reach of the penetration depth of the ultrasound waves in 95 % of cases. During the following months the accessibility of the individual body parts decreased. In Month 5 the thorax, abdomen and pelvis could still be depicted in one half of the cases. In these cases the cardiac activity could also be demonstrated ultrasonically. The trunk of the fetuses could only be seen in 25 % of cases in the 6th and 7th months of pregnancy and was only visible in isolated cases from the 8th month. The head was the body component that could be depicted in 87 % of ultrasonograms during the entire length of pregnancy.

If certain body parts are reachable by transrectal sonography their prominent organs can also be examined and surveyed regularly on the ultrasound monitor.

2.4.3.2 Fetal intra-uterine presentations

The frequency with which the various body parts of bovine fetuses can be reached by sonography is significantly determined by their position within the dam's uterus. Until the end of the fourth month anterior and posterior presentations of the fetus occur with equal frequency (Fig. 2.173). From Month 5 the anterior presentations occur more frequently. Between the fifth and seventh months of pregnancy about 25 % of fetuses are still in posterior presentation. The final positioning into an anterior presentation appears to be achieved predominantly during the transition from the 7th to the 8th month, by Days 220 of pregnancy. Thereafter posterior presentation can only be observed in isolated cases.

Avtorsko zaščiteno gradivo

Downloaded From Vet-eBooks.com



Fig. 2.174: Example of measuring the largest diameter of the eye. Sagittal section through the skull of a fetus on Day 157 of pregnancy.

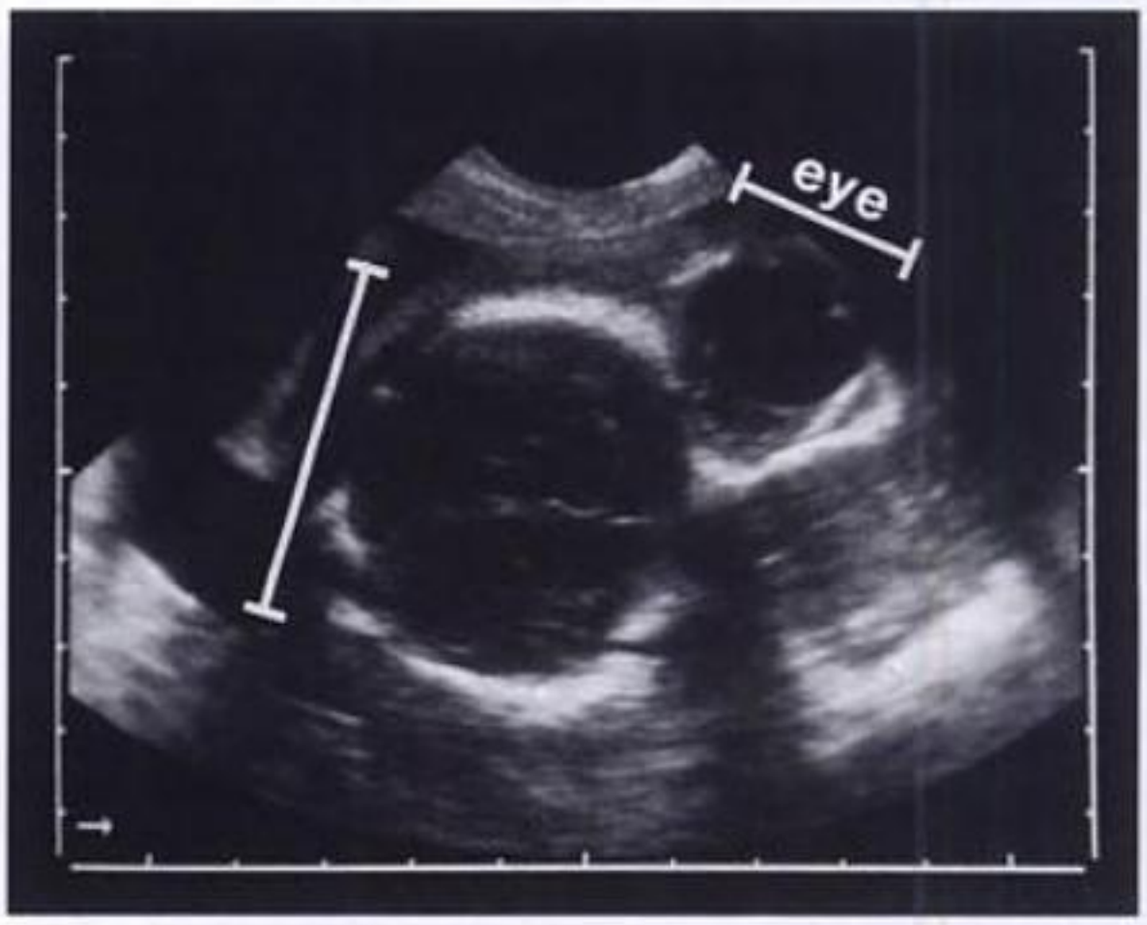


Fig. 2.175: Example of measuring the largest diameters of the cerebral cranium and the eye. Sagittal section through the skull of a fetus on Day 141 of pregnancy.

Avtorsko zaščiteno gradivo

Downloaded From Vet-eBooks.com

2.4.4 Sonographic fetometry in cattle

The size and stage of development of a bovine fetus can be determined in vivo by using intra-uterine sonographic survey, that is ultrasonic fetometry (WHITE et al. 1985, KÄHN 1989 b). There are numerous useful applications of fetometry in veterinary practice. Where disturbances set in during a pregnancy the extent of their affect on the fetus can be assessed by fetal sonography. Where doubts exist with regard to the time of impregnation in pregnant cows fetal sonographic measurements can be used to establish the real age of the calf with reasonable accuracy.

In order to obtain conclusive results it is important to conduct the fetometric survey as precisely as possible. Before any measurements of any fetal parts are taken the probe should be rotated and swiveled gently until the largest possible section of the organ is depicted on the monitor. Measurements of all sizes are taken along a straight line between two points. In this manner, for example, the crown-rump-length (CRL) is determined along the direct line between the crown and the ischium, and not along the curvature of the neck and back.

2.4.4.1 Eye and braincase

The eye is the organ that is most frequently available for fetometry by transrectal sonography during all stages of pregnancy. By optimally positioning the ultrasound probe a section which shows the largest diameter of the eye should be obtained (Fig. 2.174 and 2.175). In doing so it is not always possible to determine the exact direction of the section through the organ. This means that transverse, sagittal and horizontal sections, as well as transitional sections between these, may end up being chosen for assessment. In order to obtain the highest possible degree of accuracy the largest diameter should be measured between the two furthest removed points on the border between the anechoic eyeball and the hyperechoic, surrounding orbit in all cases. The largest diameter increases from around 4 mm on Day 60, to 10 mm on Day 90 and to 30 mm at the end of pregnancy (Fig. 2.187 and Tab. 2.1).

Apart from the eye the cranial cavity is another structure of the head that is easy to find and to identify. It is thus well suited for fetometric assessment. The bones of the roof of the skull and the basal parts of the cranium form an oval shape which surrounds the brain and is sharply contrasted against the hypoechoic brain cortex. This clear border is used for the determination of the largest inner diameter of the cranial cavity (Fig. 2.175). The largest distance between the outer surfaces of the cranial bones is seen as the outer diameter of the brain cavity. The cranial cavity can be biometrically evaluated until the end of the 7th month of pregnancy. During the last two months of pregnancy so much ultrasound is absorbed by the bones of the cranial roof that it becomes impossible to depict a complete section through the cranial cavity and thus to obtain its largest diameter. On Day 60 the largest inner diameter of the cranial cavity is 10 mm and the largest outer diameter is 17 mm on average (Fig. 2.188 and Tab. 2.1). Both parameters increase linearly over the following months to reach 63 to 76 mm and 80 to 96 mm, respectively, during the seventh month of pregnancy.

Avtorsko zaščiteno gradivo

Downloaded From Vet-eBooks.com

2.4.4.2 Heart frequency, crown-rump-length, diameters of stomach, trunk, scrotum and umbilical cord

The movements of the heart can first be seen very early at the end of the first month of pregnancy. Due to the relative ease with which the thorax can be depicted through the following few months the cardiac action can be monitored without much difficulty (see Chapter 2.4.1.4 and Fig. 2.181). In fetuses which lie in anterior presentation the heart can often be monitored even during the last month of pregnancy.

The heart rate of young fetuses is very high, occasionally reaching a value of 180 to 204 beats per minute during the third month of pregnancy (CURRAN et al. 1986 b). The mean heart rate decreases as pregnancy progresses and lies around 160 beats per minute at Day 60, 150 around Day 90 and 130 to 140 between the fifth and ninth months of pregnancy (Fig. 2.176 and Tab. 2.1). Generally, the variations in the heart rate are considerable. In fetuses examined repeatedly at weekly intervals it was possible, in many of them, to detect significantly different heart rates at successive examination times.

The crown-rump-length (CRL) of bovine fetuses can only be determined over a relatively short period. Due to the limited size of the image of most ultrasound scanners it is hardly ever possible to still depict fetuses in toto once they have reached a length of more than 10 cm. The CRL (measured between the occipital bone and the first vertebra of the tail) reaches 12 cm towards the end of the third month of pregnancy (Fig. 2.187 and Tab. 2.1). The daily increase in CRL is about 1.4 mm at the beginning of the second month and increases to 2.5 to 3 mm during the third month. The determination of the CRL is one of the most accurate means of deciding on the age of a fetus (HACKELÖER 1984, WHITE et al. 1985).

The anechoic lumen of the stomach can be reliably recognized and surveyed towards the end of the second month of pregnancy (Fig. 2.177, 2.187 and Tab. 2.1). At this time the largest diameter of the stomach lies around 8 mm. It increases linearly during the following months. The stomach can regularly be depicted in its totality and its diameter determined until the sixth month, thereafter only in individual cases.

The scrotum can also be evaluated fetometrically. From Day 60 it forms an echoic structure which projects from the abdominal wall. The scrotal width can be determined on a transverse section through the pelvic region. From the fourth month of pregnancy an exact transverse section through the scrotum can be recognized on the basis that both testes are depicted next to each other (Fig. 2.178). The largest width of the scrotum increases linearly until the seventh month of pregnancy and reaches an average of 30 mm (Fig. 2.188 and Tab. 2.1).

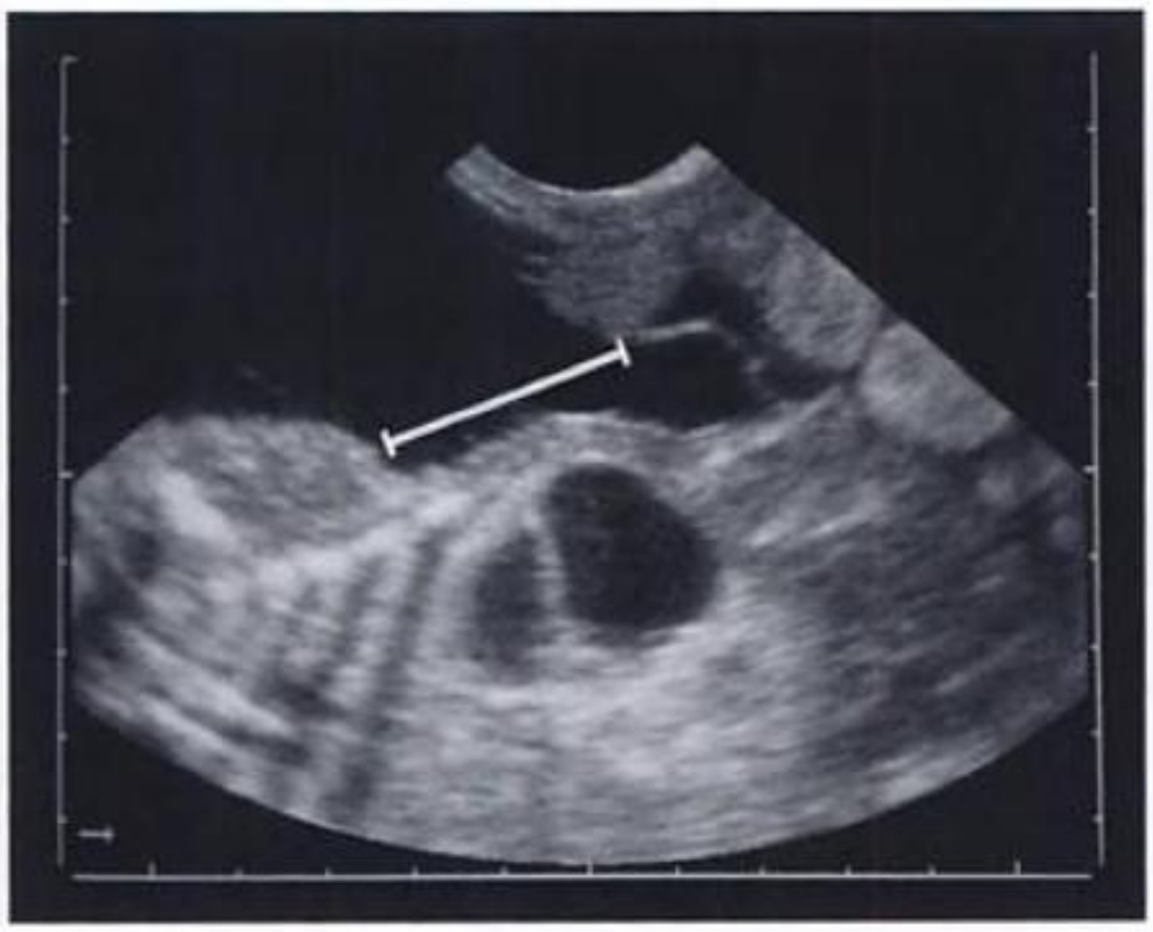


Fig. 2.177: Measuring the largest diameter of the stomach. Horizontal section through the abdomen of a fetus on Day 107 of pregnancy.

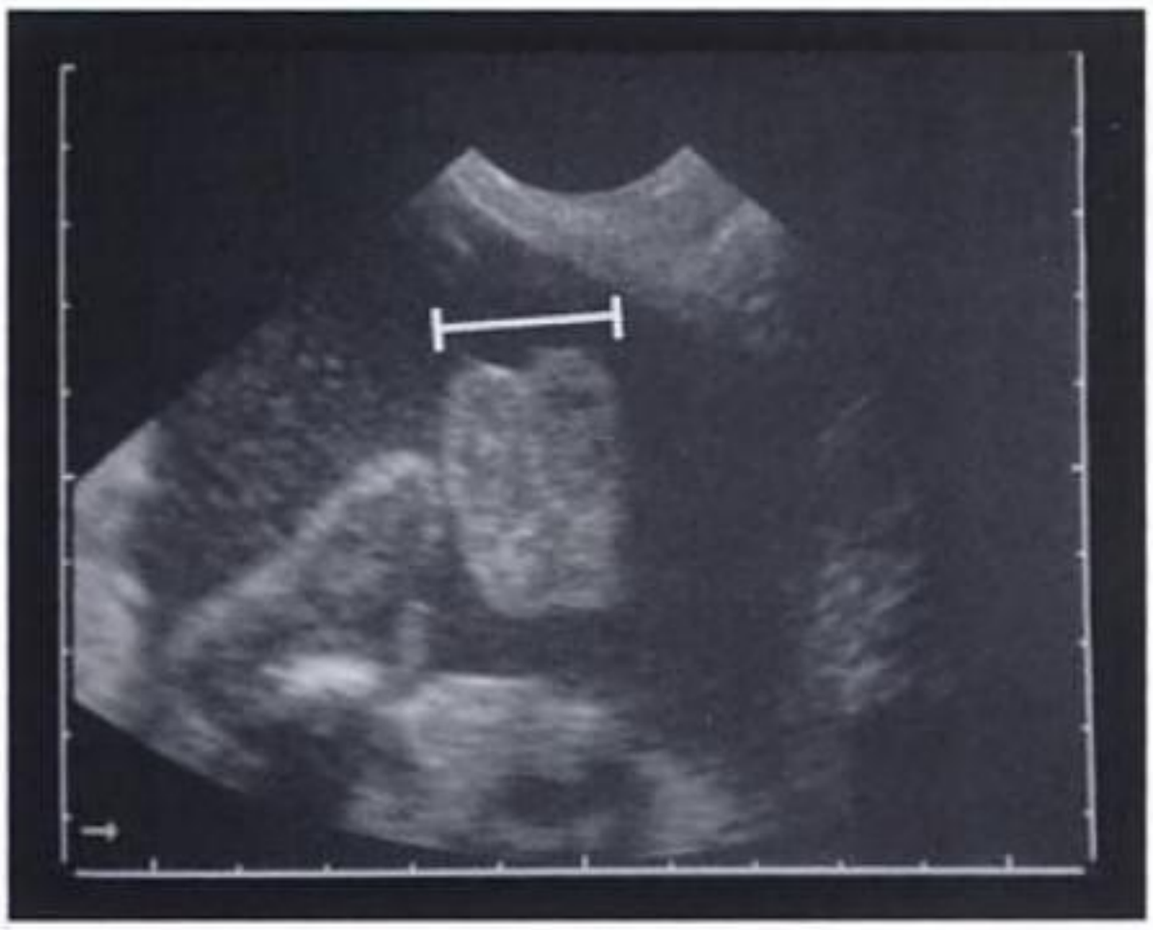


Fig. 2.178: Measuring the width of the scrotum. Transverse section through the pelvic region of a fetus on Day 151 of pregnancy.

Avtorsko zaščiteno gradivo

Downloaded From Vet-eBooks.com



Fig. 2.179: Measuring the trunk diameter on a transverse section through the abdomen of a fetus on Day 81 of pregnancy. At about 11 o'clock is the anechoic stomach and at 2 o'clock a cross section through the umbilical cord.



Fig. 2.180: Measuring the largest trunk diameter on a transverse section through a fetus on Day 62 of pregnancy. The cervical spine and the cone shaped thorax are hyperechoic.



Fig. 2.181: Example of observing the pulsating heart in the apex of the thorax as well as measuring the length of 4 ribs and their associated intercostal spaces. Horizontal section through the thorax of a fetus on Day 166 of pregnancy.



Fig. 2.182: Measuring the length of 6 lumbar vertebrae and their associated intervertebral spaces. Horizontal section through the thorax and abdomen of a fetus on Day 92 of pregnancy. Ultrasonogram of an excised fetus in a waterbath.

Avtorsko zaščiteno gradivo

Downloaded From Vet-eBooks.com



Fig. 2.183: Measuring the length of the diaphysis of a fetal metacarpus (M) on a section through a fore limb showing also the first, second and third phalanxes (1, 2, 3) on Day 125 of pregnancy.

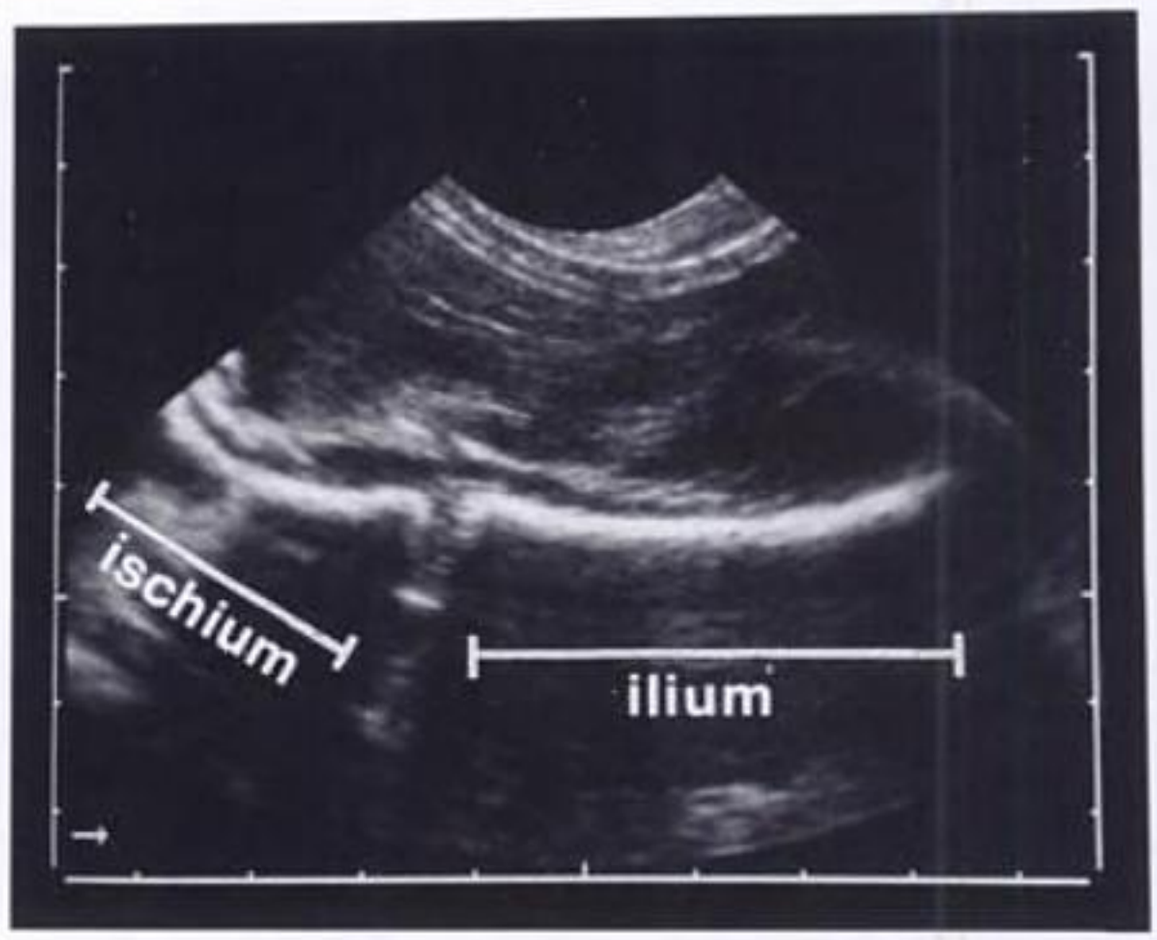


Fig. 2.184: Measuring the lengths of the ilium and ischium in a sagittal section through the pelvis of a fetus on Day 189 of pregnancy.



Fig. 2.185: Measuring the length of a femur in a horizontal section through the pelvic portion of a fetus on Day 104 of pregnancy.

Avtorsko zaščiteno gradivo

Downloaded From Vet-eBooks.com

2.4.4.4 Front and hind limbs

The fetometry of the limb bones involves the measuring of the lengths of their hyperechoic regions. These regions represent the ossified sections of their diaphyses (Fig. 2.183, 2.185, 2.186). The ossification centers are characterized by their very intense reflections. Their echoic parts end relatively abruptly at the transitions to the cartilaginous components of the bones. When measuring the length of bones the ultrasound beam should impact vertically onto the bone. In the front limb the ossified parts of the scapula, humerus, radius and ulna, as well as metacarpus can be evaluated by fetometry. Since the radius and ulna are difficult to differentiate ultrasonically, their echoes are usually seen as a single one. The bones of the pelvic limb that are available for fetometric purposes are the ilium, ischium, femur, tibia and metatarsus (Fig. 2.184 to 2.186 and Tab. 2.1).

The long bones of front and hind limb have approximately the same length and show similar growth rates (Fig. 2.187, 2.188 and Tab. 2.1). The ossified diaphyses of scapula, humerus, radius and ulna, metacarpus, femur, tibia, and metatarsus have an average length of 12 to 16 mm on Day 90 and grow to 55 to 65 mm in length by Day 180.

Among the bones of the front limb the metacarpus is the easiest to reach by ultrasonography and can, in cases of anterior presentation, still be depicted in advanced pregnancy (Fig. 2.183). When the metacarpal bones lie close to the maternal pelvis, the optimal rotation of the ultrasound probe will often allow them to be brought into the optimal plane relative to the sound beam and thus greatly facilitate the taking of reliable measurements. Generally, all bones of the front and hind limbs can be evaluated fetometrically until about the seventh month of pregnancy. After this stage they are too large to be depicted completely on a single ultrasound image.

The optimal approach for the fetometric age determination of bovine fetuses depends on the stage of the pregnancy and on the accessibility of the fetal body parts. When the head can be reached the biometry of the eye and the skull cavity should be considered reliable parameters. The eyes and skull cavity can be measured very accurately and are usually accessible throughout the course of the pregnancy. Apart from these there are numerous suitable body parts that can be used during the first half of pregnancy. The accuracy of the fetal age estimation can be enhanced by the combined assessment of as many measurements as possible.

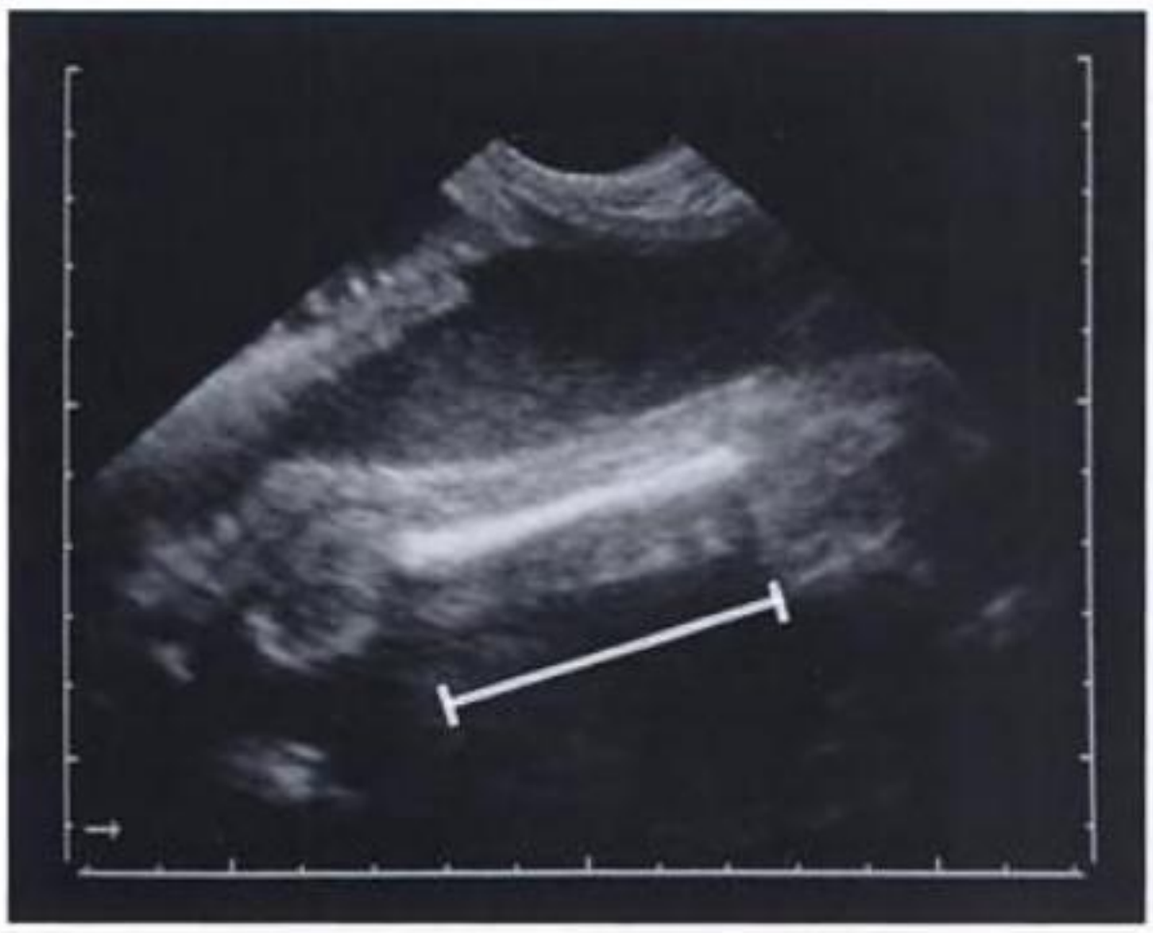


Fig. 2.186: Measuring the length of the diaphysis of the metatarsus in a section through the metacarpus of a fetus on Day 175 of pregnancy.

Avtorsko zaščiteno gradivo

Downloaded From Vet-eBooks.com

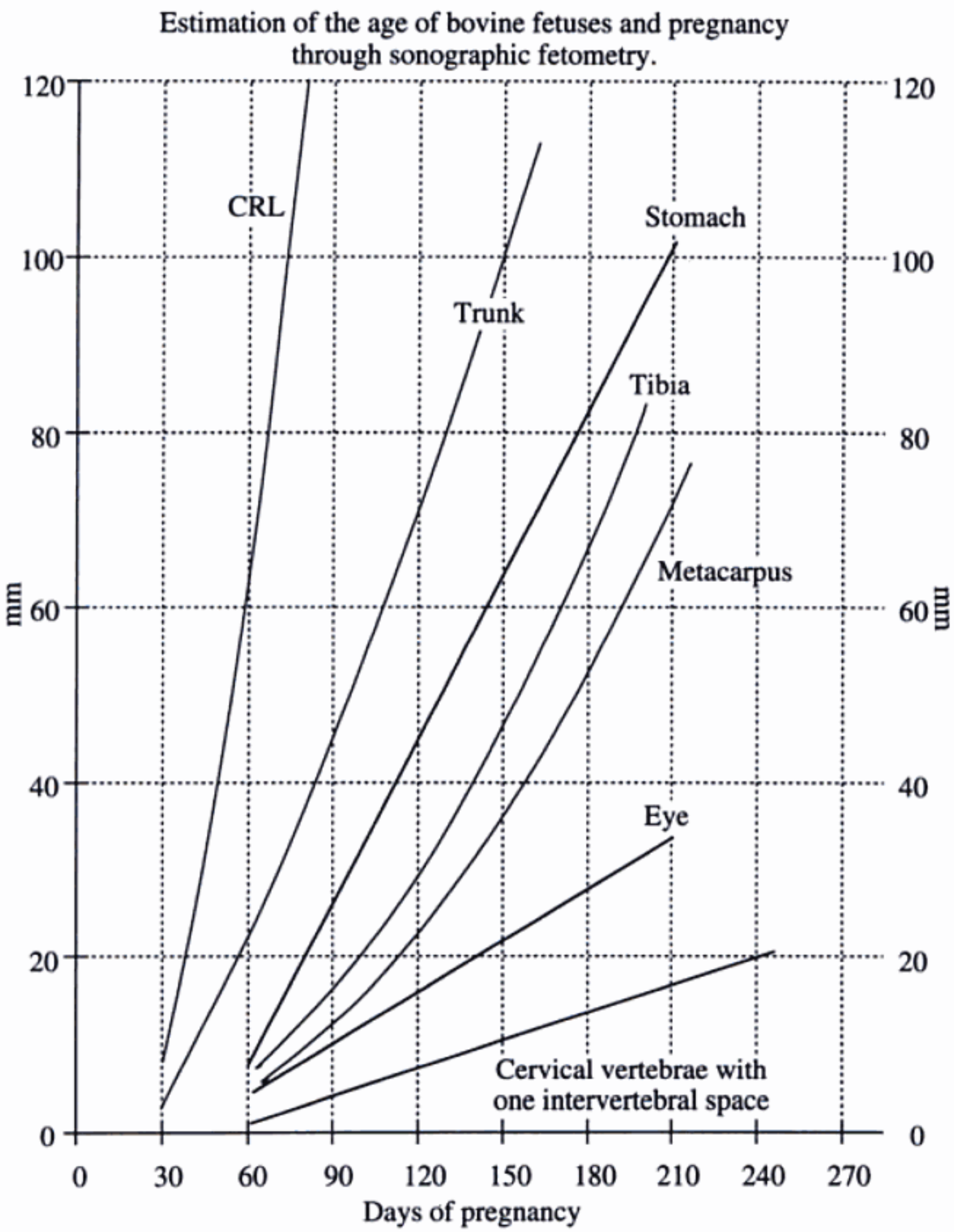


Fig. 2.187: Regressions of the growth rates of the crown-rump-length (CRL), the largest diameters of the trunk, stomach and eye, the lengths of tibia and metacarpus, as well as that of one cervical vertebra with its intervertebral space in bovine fetuses during pregnancy.

Avtorsko zaščiteno gradivo

Downloaded From Vet-eBooks.com

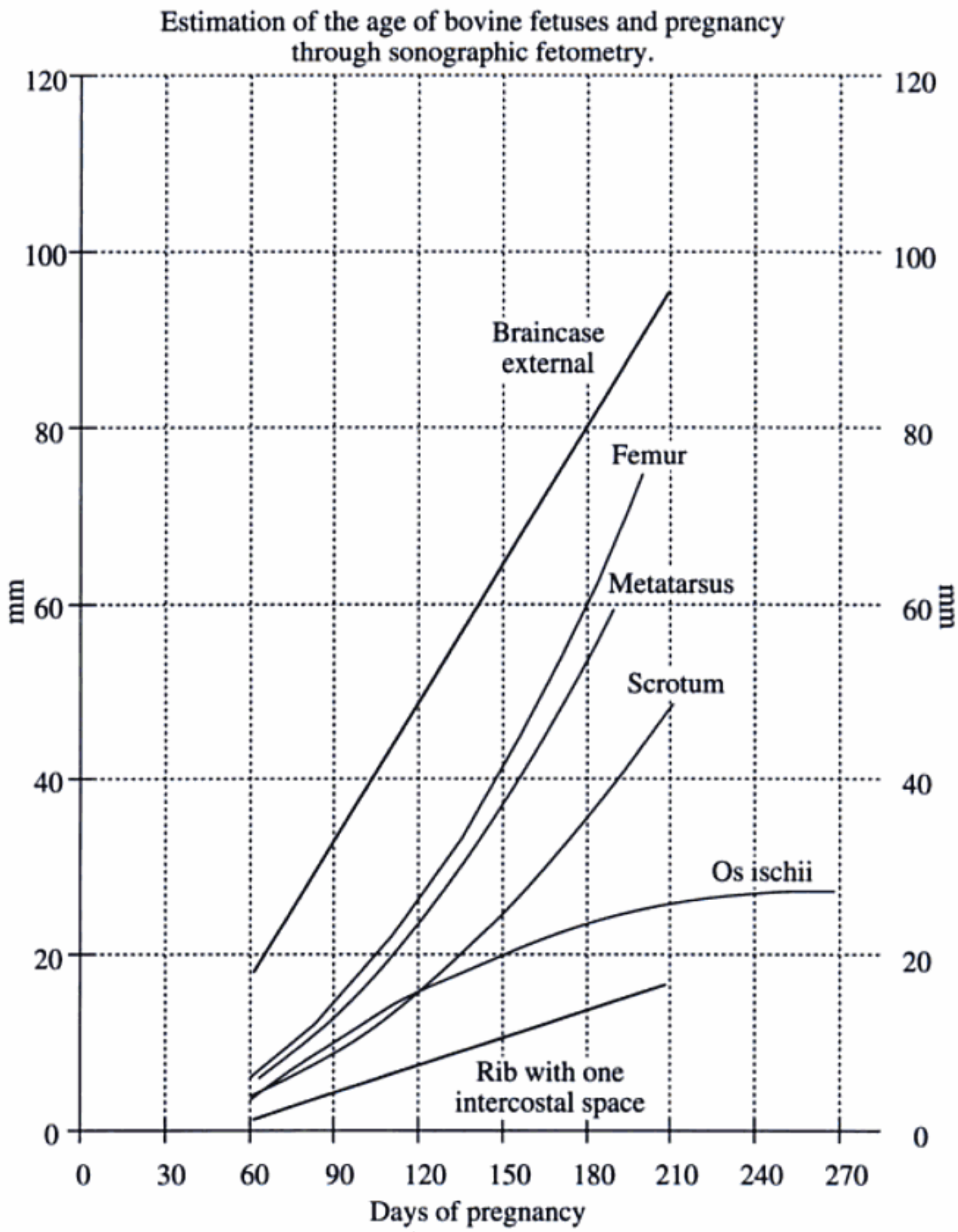


Fig. 2.188: Regressions of the growth rates of the external diameter of the braincase, the length of the femur, metatarsus and ischiac bone, the cross sectional diameter of the scrotum, as well as one rib cross section with its corresponding intercostal space in bovine fetuses during pregnancy.

Avtorsko zaščiteno gradivo

Downloaded From Vet-eBooks.com

References to chapter 2

ANDRESEN, P., R. DEHNING und A. SCHNEIDEGGER (1986): Ein Beitrag zum Granulosazelltumor beim Rind. Prakt. Tierarzt 4, 307–309.

BETTERIDGE, K. J., M. D. EAGLESOME, G. C. B. RANDALL and D. MITCHELL (1980): Collection, description and transfer of embryos from cattle 10–16 days after oestrus. J. Reprod. Fert. 59, 205–216.

CHAFFAUX, S., F. VALON et J. MARTINEZ (1982): Evolution de l'image échographique du produit de conception chez la vache. Bull. Acad. vét. Fr. 55, 213–221.

CHAFFAUX, S., G. N. S. REDDY, F. VALON and M. THIBIER (1986): Transrectal real-time ultrasound scanning for diagnosing pregnancy and for monitoring embryonic mortality in dairy cattle. Anim. Reprod. Sci. 10, 193–200.

CHOUDARY, J. B., J. T. GIER and G. B. MARIAN (1968): Cyclic changes in bovine vesicular follicles. J. Anim. Sci. 27, 468–741.

CURRAN, S., R. A. PIERSON and O. J. GINTHER (1986 a): Ultrasonographic appearance of the bovine conceptus from days 10 through 20. J. Am. vet. med. Ass. 189, 1289–1294.

CURRAN, S., R. A. PIERSON and O. J. GINTHER (1986 b): Ultrasonographic appearance of the bovine conceptus from days 20 through 60. J. Am. vet. med. Ass. 189, 1295–1302.

CURRAN, S., J. P. KASTELIC and O. J. GINTHER (1989): Determining sex of the bovine fetus by ultrasonic assessment of the relative location of the genital tubercle. Anim. Reprod. Sci. 19, 217–227.

DOBRINSKI, W. und H. KREMER (1982): Verschiedene Arten von B-Bild-Geräten und einige ihrer technischen Eigenschaften. In: Sonographische Diagnostik innerer Erkrankungen pp. 8–25. Hrsg.: H. Kremer. Verlag Urban & Schwarzenberg, München, Wien, Baltimore.

DRIANCOURT, M. A., D. ANDRIEU et W. W. THATCHER (1988): Suivi de la croissance folliculaire par échographie au cours de cycles naturels et stimulés chez la vache. Recl. Méd. vét. Éc. Alfort 164, 109–114.

FISSORE, R. A., A. J. EDMONDSON, R. L. PASHEN and R. H. BONDURANT (1986): The use of ultrasonography for the study of the bovine reproductive tract. II. Non-pregnant, pregnant and pathological conditions of the uterus. Anim. Reprod. Sci. 12, 167–177.

GINTHER, O. J. and R. A. PIERSON (1984): Ultrasonic anatomy and pathology of the equine uterus. Theriogenology 21, 505–516.

GINTHER, O. J., L. KNOPF and J. P. KASTELIC (1989 a): Temporal associations among ovarian events in cattle during oestrous cycles with two and three follicular waves. J. Reprod. Fert. 87, 223–230.

GINTHER, O. J., L. KNOPF and J. P. KASTELIC (1989 b): Ovarian follicular dynamics in heifers during early pregnancy. Biol. Reprod. 41, 247–254.

GJESDAL, F. (1969): Age determination of bovine foetuses. Acta vet. scand. 10, 197–218.

GREENSTEIN, J. S. and R. C. FOLEY (1958): Early embryology of the cow. I. Gastrula and primitive streak stages. J. Dairy Sci. 41, 409–421.

HACKELÖER, B.-J. (1984): Ultraschall-Untersuchungen im I. Trimester. In: Die Ultraschalldiagnostik in der Schwangerschaft 3. Aufl., pp. 47–58. Hrsg.: H.-J. Holländer. Verlag Urban & Schwarzenberg, München, Wien, Baltimore.

HANZEN, C. and B. DELSAUX (1987): Use of transrectal B-mode ultrasound imaging in bovine pregnancy diagnosis. Vet. Rec. 121, 200–202.

HASSLER, D. (1984): Physik und Technik der Ultraschalldiagnostik. In: Die Ultraschalldiagnostik in der Schwangerschaft 3. Aufl., pp. 3–37. Hrsg.: H.-J. Holländer. Verlag Urban & Schwarzenberg, München, Wien, Baltimore.

HOLLÄNDER, H.-J. (1984): Untersuchungen im II. und III. Trimester. Anatomie und Biometrie des Fetus. In: Die Ultraschalldiagnostik in der Schwangerschaft 3. Aufl., pp. 59–80. Hrsg.: H.-J. Holländer. Verlag Urban & Schwarzenberg, München, Wien, Baltimore.

HULLINGER, R. L. and C. J. G. WENSING (1985): Descent of the testis in the fetal calf. Acta anat. 121, 63–68.

IRELAND, J. J. (1987): Control of follicular growth and development. J. Reprod. Fert., Suppl. 34, 39–54.

IRELAND, J. J., D. B. COULSON and R. L. MURPHREE (1979): Follicular development during four stages of the estrous cycle of beef cattle. J. Anim. Sci. 49, 1261–1269.

KÄHN, W. (1985): Zur Trächtigkeitsdiagnose beim Rind mittels Ultraschall. Tierärztl. Umsch. 40, 472–477.

KÄHN, W. (1986): Vorkommen und Wachstumsdynamik von Gelbkörpern mit Hohlraum während des Ovarialzyklus bei Rindern und deren Hormonprofile. Dtsch. tierärztl. Wschr. 93, 475–480.

KÄHN, W. (1989 a): Gelbkörper mit und ohne Hohlraum bei Rindern. Ihr Vorkommen und ihre Entwicklung im Zyklus und während der Frühgravidität. Tierärztl. Prax., Suppl. 4, 1–6.

KÄHN, W. (1989 b): Sonographic fetometry in the bovine. Theriogenology 31, 1105–1121.

KÄHN, W. (1989 c): Die Entwicklung von Follikeln beim Rind; Veränderungen ihrer Anzahl und Größe während des Ovarialzyklus. Berl. Münch. tierärztl. Wschr. 102, 44–49.

KÄHN, W. (1990): Sonographic imaging of the bovine fetus. Theriogenology 33, 385–396.

KÄHN, W. und W. LEIDL (1985): Sonographische Befunde am Uterus von Stuten mit Ultraschall bei einer Fequenz von 5 Megahertz (MHz). Pferdeheilkunde 1, 239–246.

KÄHN, W. und W. LEIDL (1986): Die Anwendung der Echographie zur Diagnose der Ovarfunktion beim Rind. Tierärztl. Umsch. 41, 3–12.

KÄHN, W. und W. LEIDL (1987): Echographische Befunde an Ovarien von Stuten. Tierärztl. Umsch. 42, 257–266.

KÄHN, W. und W. LEIDL (1988): Auswirkungen einer HCG-Stimulation bei Rindern mit einem zystischen oder einem kompakten Gelbkörper: Progesteronprofile, Ovulationsinduktion und Ausbildung eines 2. Gelbkörpers. Tierärztl. Umsch. 43, 430–439.

KÄHN, W., W. LEIDL und R. RIENMÜLLER (1989): Die Kammerung des Rinderuterus während der Frühgravidität. Ein Vergleich morphologischer, sonographischer und kernspintomographischer Befunde. J. vet. Med. A 36, 641–652.

KASTELIC, J. P., S. CURRAN, R. A. PIERSON and O. J. GINTHER (1988): Ultrasonic evaluation of the bovine conceptus. Theriogenology 29, 39–54.

KASTELIC, J. P., S. CURRAN and O. J. GINTHER (1989): Accuracy of ultrasonography for pregnancy diagnosis on days 10 to 22 in heifers. Theriogenology 31, 813–820.

KITO, S., K. OKUDA, K. MIYAZAWA and K. SATO (1986): Study on the appearance of the cavity in the corpus luteum of cows by using ultrasonic scanning. Theriogenology 25, 325–333.

LEIDL, W., U. BRAUN, K. OKUDA, R. STOLLA und D. SCHAMS (1983): Klassifizierung der Ovarzysten des Rindes. Wien. tierärztl. Mschr. 70, 208–213.

MATTON, P., V. ADELAKOUN, Y. COUTURE and J. J. DUFOUR (1981): Growth and replacement of the bovine ovarian follicles during the estrous cycle. J. Anim. Sci. 52, 813–820.

MÜLLER, E. and G. WITTKOWSKI (1986): Visualization of male and female characteristics of bovine fetuses by real-time ultrasonics. Theriogenology 25, 571–574.

MÜLLER, E., D. RATH, E. KLUG und H. MERKT (1986): Die Anwendbarkeit der Sonographie zur Diagnostik am weiblichen Genitale des Rindes. Berl. Münch. tierärztl. Wschr. 99, 311–318.

NICKEL, R., A. SCHUMMER, K.-H. WILLE und H. WILKENS (1984): Beckengürtel. In: Lehrbuch der Anatomie der Haustiere, Band I, pp. 83–91. Von: R. Nickel, A. Schummer und E. Seiferle. Verlag Paul Parey, Berlin und Hamburg.

NODEN, D. M. and A. DE LAHUNTA (1985 a): Trunk muscles and connective tissues. In: The Embryology of Domestic Animals pp.

Avtorsko zaščiteno gradivo

Downloaded From Vet-eBooks.com

140–155. Eds.: D. M. Noden and A. de Lahunta. Verlag Williams & Wilkins, Baltimore, London, Los Angeles, Sydney.
NODEN, D. M. and A. DE LAHUNTA (1985 b): Cardiovascular system II: heart. In: The Embryology of Domestic Animals pp. 231–256. Eds.: D. M. Noden and A. de Lahunta. Verlag Williams & Wilkins, Baltimore, London, Los Angeles, Sydney.
OKANO, A. and T. TOMIZUKA (1987): Ultrasonic observation of postpartum uterine involution in the cow. Theriogenology 27, 369–376.
OKUDA, K. (1982): Morphologische und endokrinologische Untersuchungen am Corpus luteum periodicum und graviditatis des Rindes. Vet. med. Diss., München.
PIERSON, R. A. and O. J. GINTHER (1984 a): Ultrasonography for detection of pregnancy and study of embryonic development in heifers. Theriogenology 22, 225–233.
PIERSON, R. A. and O. J. GINTHER (1984 b): Ultrasonography of the bovine ovary. Theriogenology 21, 495–504.
PIERSON, R. A. and O. J. GINTHER (1986): Ovarian follicular populations during early pregnancy in heifers. Theriogenology 26, 649–659.
PIERSON, R. A. and O. J. GINTHER (1987): Ultrasonographic appearance of the bovine uterus during the estrous cycle. J. Am. vet. med. Ass. 190, 995–1001.
QUIRK, S. M., G. J. HICKEY and J. E. FORTUNE (1986): Growth and regression of ovarian follicles during the follicular phase of the oestrous cycle in heifers undergoing spontaneous and $PGF_{2\alpha}$-induced luteolysis. J. Reprod. Fert. 77, 211–219.
REEVES, J. J., N. W. RANTANEN and M. HAUSER (1984): Transrectal real-time ultrasound scanning of the cow reproductive tract. Theriogenology 21, 485–494.
SALISBURY, G. W., N. L. VANDEMARK and J. R. LODGE (1978): Gestation. In: Physiology of Reproduction and Artificial Insemination of Cattle 2nd ed., pp. 130–162. Eds.: G. W. Salisbury, N. L. VanDemark and J. R. Lodge. Verlag W. H. Freeman and Co., San Francisco.
SCHNEEBELI, J. (1984): Untersuchungen über das Vorkommen von Interöstrusfollikeln beim Rind. Schweiz. Arch. Tierheilk. 126, 221–229.
SCHUMMER, A. und B. VOLLMERHAUS (1987): Hüllen des Hodens und des Samenstrangs. Harn- und Geschlechtsapparat. In: Lehrbuch der Anatomie der Haustiere II, 6. Aufl., pp. 333–339. Von: R. Nickel, A. Schummer und E. Seiferle. Verlag Paul Parey, Berlin und Hamburg.
SEIFERLE, E. (1984): Harte Hirn- und Rückenmarkshaut. Hüllen des Zentralnervensystems. In: Lehrbuch der Anatomie der Haustiere, Band IV, pp. 171–174. Von: R. Nickel, A. Schummer und E. Seiferle. Verlag Paul Parey, Berlin und Hamburg.
SIROIS, J. and J. E. FORTUNE (1988): Ovarian follicular dynamics during the estrous cycle in heifers monitored by real-time ultrasonography. Biol. Reprod. 39, 308–317.
STAIGMILLER, R. B. and B. G. ENGLAND (1982): Folliculogenesis in the bovine. Theriogenology 17, 43–52.
TAINTURIER, D., F. ANDRE, M. CHAARI, K. W. SARDIANA, J. L. LE NET ET L. LIJOUR (1983): Intérêt de l'échotomographie pour le contrôle de la reproduction d'un grand troupeau de vaches laitières. Revue Méd. vét. 134, 419–424.
TAVERNE, M. A. M., O. SZENCI, J. SZÉTAG and A. PIROS (1985): Pregnancy diagnosis in cows with linear-array real-time ultrasound scanning: a preliminary note. The Veterinary Quarterly 7, 264–270.
VOLLMERHAUS, B. (1957): Untersuchungen über die normalen zyklischen Veränderungen der Uterusschleimhaut des Rindes. Zentbl. Vet. Med. 4, 18–50.
WHITE, R. A. S. and W. R. ALLEN (1985): Use of ultrasound echography for the differential diagnosis of a granulosa cell tumour in a mare. Equine vet. J. 17, 401–402.
WHITE, I. R., A. J. F. RUSSEL, I. A. WRIGHT and T. K. WHYTE (1985): Real-time ultrasonic scanning in the diagnosis of pregnancy and the estimation of gestational age in cattle. Vet. Rec. 117, 5–8.
WIDEMANN, D., C. G. DORN and D. C. KRAEMER (1989): Sex detection of the bovine fetus using linear array real-time ultrasonography. Theriogenology 31, 272.
WINTERS, L. M., W. W. GREEN and R. E. COMSTOCK (1942): Prenatal development of the bovine. Univ. Minn. Agric. Exper. Sta., Techn. Bul. 151, 1–44.

Avtorsko zaščiteno gradivo

Downloaded From Vet-eBooks.com

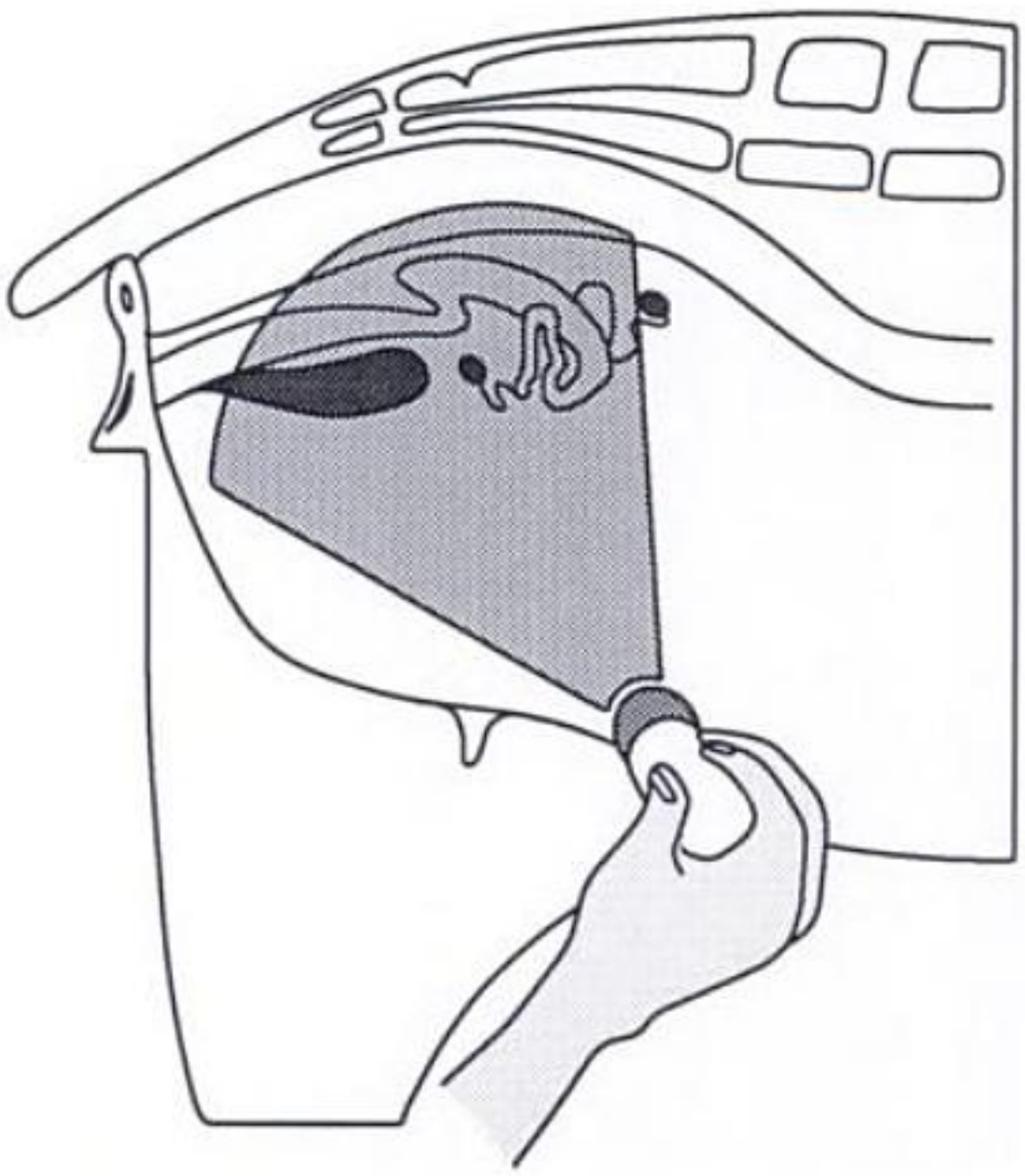


Fig. 3.1: Schematic presentation of the transcutaneous ultrasound examination of a ewe. The probe is applied in the hairless area cranial in front of the udder.

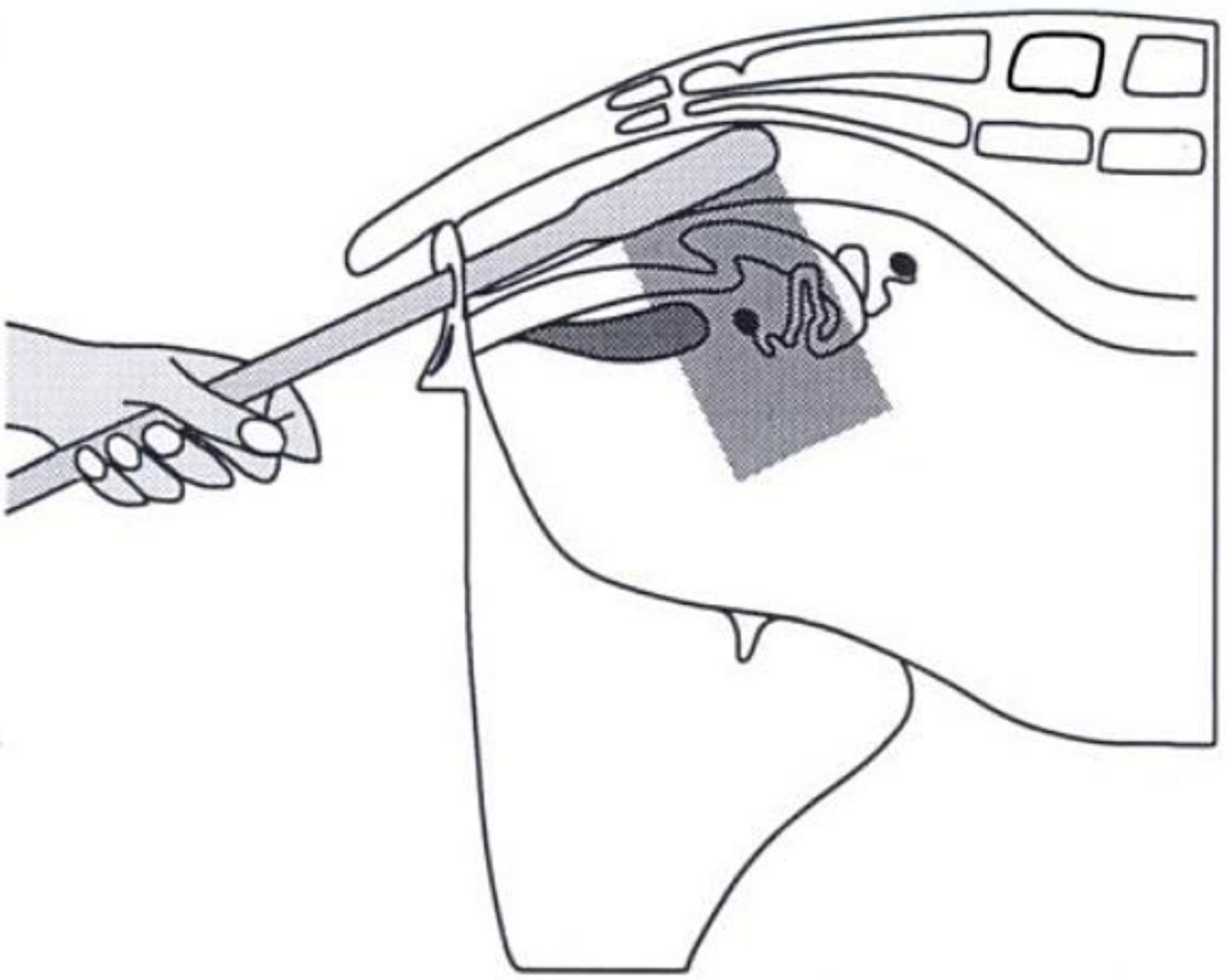


Fig. 3.2: Schematic presentation of the transrectal ultrasound examination of a sheep. The probe is advanced about 15 cm into the rectum until the urinary bladder becomes visible.

Avtorsko zaščiteno gradivo

Downloaded From Vet-eBooks.com

3 Ultrasonography in sheep and goats

For many years various ultrasound techniques have been used to diagnose pregnancy in sheep and goats. The A - mode and Doppler techniques used in the past are considered non-imaging systems (LINDAHL 1969). Neither technique is able to produce an image of the conceptus, but rather illustrates its presence by detection of a characteristic pattern of amplitudes or through an audible or optically detectable frequency modulation. Today, the imaging ultrasound technique, the real time B - mode ultrasonography, is used in small ruminants (FOWLER and WILKINS 1980, TAINTURIER et al. 1983 a and b). In countries where intensive sheep farming is practiced the sonographic examination of these animals for pregnancy detection and the determination of fetal numbers is applied routinely (FOWLER and WILKINS 1984, WHITE et al. 1984, DAVEY 1986). The imaging sonography is superior to the non-imaging methods, because it is more accurate and enables the operator to detect the number and viability of the fetuses (BUCKRELL 1988, JARDON 1988).

3.1 Technique of ultrasonography in sheep and goats

The ultrasound examination of sheep and goats can be performed in two different ways. The internal genitalia can be depicted by applying the ultrasound probe to the ventral abdomen - the transcutaneous ultrasonography - or by introducing the probe into the rectum - the transrectal ultrasonography (Fig. 3.1 and 3.2). Both methods have been shown to be useful in sheep and goats (FOWLER and WILKINS 1985, KASPAR 1988, KASPAR 1989). The choice of which technique to use depends on the diagnosis that is to be made, the type of the available ultrasound probe, as well as the working conditions during the examination of large flocks. Based on current experience the transrectal examination is more accurate than the transcutaneous method until Day 35 of pregnancy. Between Days 35 and 70 both methods appear to be equally accurate. The transcutaneous approach is preferred during the second half of pregnancy, because it allows a larger portion of the pregnant uterus to be visualized and it is much more practical.

Generally, scanners with sector, linear and convex probes at frequencies of 3.5 to 5.0 MHz can be used for both approaches. In practice the frequency of 5 MHz is versatile. Linear probes appear better suited for the transrectal examinations, whereas sector probes are preferred for transcutaneous examinations.

3.1.1 Transcutaneous sonography

For transcutaneous sonography the probe is applied to the groin area immediately cranial to the udder (Fig. 3.1). In the majority of sheep and goat breeds this area is relatively free of wool or hair, allowing for good coupling of the probe without prior clipping of the hair in the area. In addition, the non-pregnant and early pregnant uteri are best visualized from this site. Only during the last trimester does the pregnant uterus extend so far forward that the probe has to be moved cranially in order to permit a complete examination of the fetuses. In these cases some wool or hair needs to be removed before the examination can be performed. In order to accurately count the number of fetuses after Day 100 of pregnancy an area of 20 to 40 cm around the udder must be clipped and both sides of the abdomen have to be scanned. For a simple pregnancy diagnosis, in other words a mere distinction between pregnant and non-pregnant, the probe can be positioned just cranial to the udder and no clipping of hair or wool is required - even in late pregnancy (FOWLER and WILKINS 1985).

The transcutaneous ultrasonography can be performed while the ewe is standing, sitting or lying down. Practical experience has shown that the examination

Avtorsko zaščiteno gradivo

Downloaded From Vet-eBooks.com

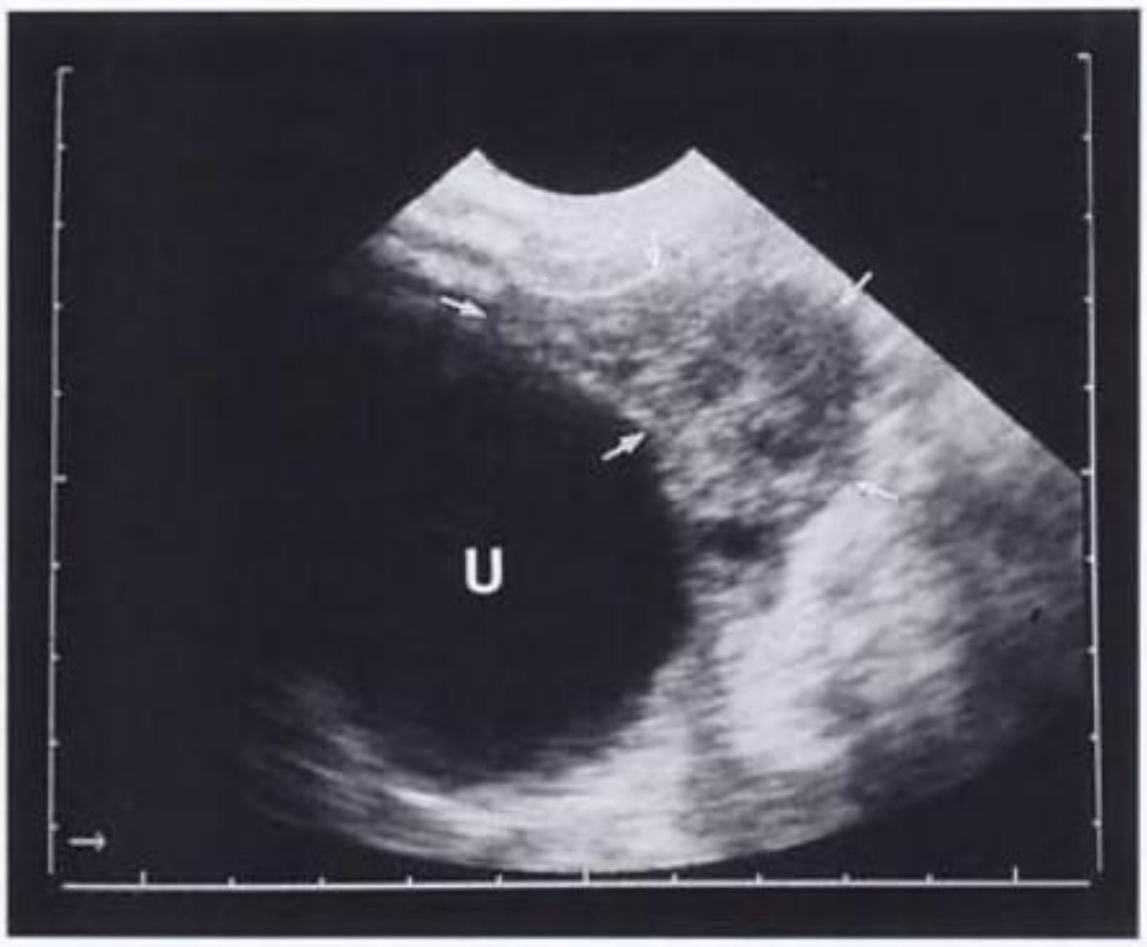


Fig. 3.3: Transcutaneous image of the urinary bladder (U) and the non-pregnant uterus (arrows) of a ewe in a sagittal section with ventrodorsally directed beam.



Fig. 3.4: Transrectal image of the urinary bladder (U) and the non-pregnant uterus (arrows indicate the greater curvature) in a nanny goat in a sagittal section with dorsoventrally directed beam.

Avtorsko zaščiteno gradivo

Downloaded From Vet-eBooks.com

should start on the right hand side of the animal. In most cases the full rumen pushes the pregnant uterus to the right side where it is found with greater reliability and speed. The transcutaneous sonographic examination is greatly facilitated if a helper, standing on the left side of the sheep, bends over the animal and pulls up its right hind leg.

The probe is applied to the hairless area in front of the udder, immediately cranial to the sebum filled inguinal gland. The sound waves are directed dorsally and slightly caudomedially. The probe is then pressed moderately against the abdomen in the direction of the urinary bladder. When large flocks are examined working conditions should be optimized as far as possible. It has proven most useful to chase the sheep on to a 80 to 100 cm high ramp where a standing examiner can scan the sheep without too much discomfort. The number of sheep that can be scanned in a given period of time depends on the experience of the examiner, the predominant stage of pregnancy of the sheep in the flock and the prevailing working conditions. Where the purpose of the examination is merely to distinguish between pregnant and non-pregnant sheep up to 100 ewes can be scanned in one hour (DE BOIS and TAVERNE 1984). If the number of fetuses in each pregnant ewe must also be determined the examination speed will be slower and may take up to 1 to 2 min. per ewe in some cases.

The above mentioned information on sonographic examinations of sheep relate to small to medium sized flocks (‹ 500 sheep). More intense experience on large flocks in prominent sheep farming countries has shown that the diagnostic accuracy and the speed of the examination can both be enhanced by the introduction of improved techniques. Such techniques include, for example, the use of clamps that allow the ewe to be placed in a special position for the examination. In this regard it has been shown that fetal numbers can most accurately be determined when the ewe is in dorsal recumbency or in a hanging position (FOWLER and WILKINS 1985).

In order to obtain the best possible image quality it is necessary to apply a coupling gel between the skin surface and the ultrasound probe. When scanning standing animals the gel is applied onto the scanning surface of the probe before the latter is placed against the skin. When the animal is scanned in the recumbent position the gel is distributed onto the skin surface. In preparation for the scanning exercise it is very useful to starve the animals by removing their feed for 12 hours during the preceding night. This precaution often helps to obtain a better image quality and thus leads to increased speed and accuracy during the examination (BUCKRELL 1988).

In order to ensure accurate results during the pregnancy diagnosis a systematic approach is essential. First, the urinary bladder should be found and depicted. It is easily recognized by its anechoic lumen and typical shape (Fig. 3.3). The non-pregnant uterus appears in the area of the apex of the bladder. The non-pregnant uterine horns are usually found cranially and ventrally, sometimes also laterally, to the urinary bladder. Also in the presence of a pregnancy, the uterus can be found in the vicinity of the apex of the bladder. Depending on the stage of pregnancy one would then follow the expanded pregnant uterus in a cranial direction.

3.1.2 Transrectal sonography

A prerequisite for the transrectal sonography is the availability of a probe that can be introduced into the rectum and whose scanning surface can be rotated ventrally and laterally. Probes with outer dimensions of 10 cm length, 3 cm height and 2 cm width can be introduced without any difficulty into the rectums of sheep and goats (KASPAR 1988).

Prior to a transrectal sonographic examination the animal must be properly restrained. This will help to

Avtorsko zaščiteno gradivo

Downloaded From Vet-eBooks.com



Fig. 3.5: Waterbath image of an excised ovary of a ewe. The two corpora lutea show the moderate echogenicity of luteal tissue. The ovarian parenchyma is more echoic.



Fig. 3.6: Photograph of the same ovary sectioned through the scanning plane in Fig. 3.5 and showing the 2 corpora lutea. A small cavity is present in the center of the left corpus luteum.



Fig. 3.7: Transrectal image of a follicle (diameter = 7 mm) on the ovary of a nanny goat. The ovary lies ventral to the non-pregnant uterus. Small arrows demarcate the outline of the ovary, large arrows that of the uterus.

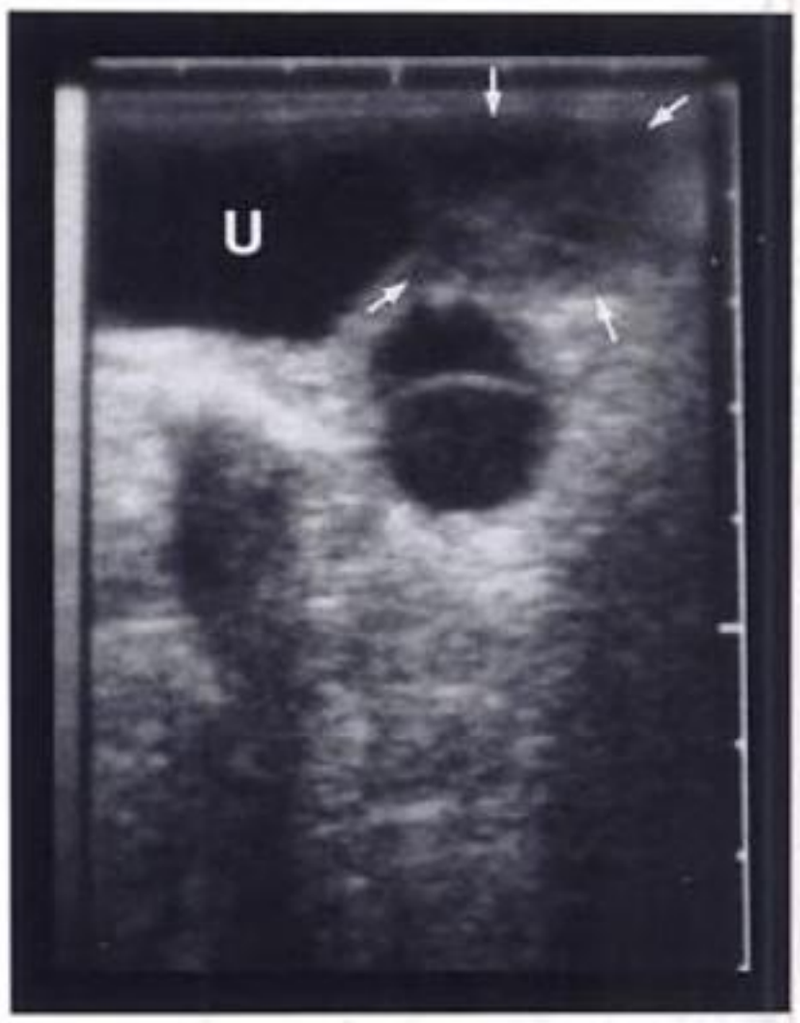


Fig. 3.8: Transrectal image of two large vesicles on the ovary of a ewe with suspected cystic follicular degeneration. The ovary lies cranioventrally of the urinary bladder (U) and ventrally of the non-pregnant uterus (arrows).

Avtorsko zaščiteno gradivo

Downloaded From Vet-eBooks.com

avoid injuries that may result from the animal's defensive struggling. Advancing and steering the probe inside the rectum of a sheep or goat is achieved from the outside (Fig. 3.2). If the ultrasound probe is attached to a sufficiently stiff cable the latter can be used to advance the probe into the rectum and then to further manipulate it there. Where the cable of the probe is flexible a pipe or rod can be used to stiffen the connection to the probe (Fig. 4.3).

The ultrasound probe is first lubricated and then introduced through the anus into the rectum. It is then pushed cranially for about 15 cm where the urinary bladder should become visible. Removal of the feces from the rectum or the application of a coupling gel before the introduction of the probe into the rectum are not necessary for the transrectal sonography in sheep and goats. Once the bladder has been identified, the probe - with the sound beam directed ventrally - is advanced slowly while it is also swiveled laterally through 45 degrees in both directions until the uterus comes into view (Fig. 3.4). Occasionally, feces that lie between the probe and the gut wall may obscure the image. By moving the probe back and forth a little, or by reintroducing it, this hindrance can be removed. When sheep in their second or third trimester of pregnancy are scanned it may be helpful to elevate their abdominal wall a little in order to better visualize parts of the pregnant uterus. Transrectal sonographic examinations take a little more time to perform than the transcutaneous ones. When many animals are to be checked an examination time of 1 to 2 minutes per animal should be expected (BUCKRELL et al. 1986). Provided the probe is handled skillfully inside the rectum serious injuries do not occur. Irritation of the rectal mucosa may lead to mild hemorrhage which is generally harmless.

3.2 Ovarian structures in sheep and goats

3.2.1 Follicles and corpora lutea

Based on the findings of examinations on excised ovaries in a waterbath, follicles and corpora lutea of the small ruminants produce echo patterns similar to those observed in cattle (see chapter 2.2). Corpora lutea produce reflections very typical of the low density of luteal tissue (Fig. 3.5 and 3.6). A cavity of a few millimeters can be seen at the centers of many corpora lutea. Follicles are characterized by the presence of anechoic fluid in their antrum.

A routine diagnostic visualization of the ovaries by means of ultrasonography is not yet possible at all stages of the cycle in sheep and goats (BUCKRELL 1988). Follicles and corpora lutea of sheep and goats can be so small that they cannot reliably be detected by the use of currently employed ultrasonographic equipment. In sheep with unknown cyclic activity, for example, most follicles have a diameter of only a few millimeters which is below the resolution capacity at which reliable inter-

Avtorsko zaščiteno gradivo

Downloaded From Vet-eBooks.com



Fig. 3.9: Ovary of a ewe after superovulatory treatment. On the left of the ovary several corpora lutea (arrows) and on the right 3 follicles (diameters between 5 to 6 mm). (Ultrasonogram from Nov. 22, 15:00. The sheep was treated as follows: Nov. 9, PGF2α; Nov. 19-22, FSH bid and Nov. 21, 18:00, PGF2α. Estrus occurred on Nov. 23).



Fig. 3.10: Ovary (cranial to the urinary bladder, U) in a ewe on the day of estrus after superovulatory treatment. Eight to ten follicles with diameters of 4 to 8 mm can be seen on the ovary. (Ultrasonogram from Nov. 23, 18:00. The sheep was treated as follows: Nov. 9: PGF2α; Nov. 19: ECG sid and Nov. 21, 18:00, PGF2α).

Avtorsko zaščiteno gradivo

Downloaded From Vet-eBooks.com

pretations of the image can still be made. At times follicles of 5 mm diameter or more can be identified on the ovaries of proestrous ewes (Fig. 3.7). Large, anechoic vesicles can also be found on the ovaries of animals suffering from the relatively rare condition of cystic degeneration of follicles (Fig. 3.8). The cavities inside hollow corpora lutea of sheep and goats can be confused with small follicles. The reason for this is that the echoic wall of the hollow corpora lutea may be as thin as 1 to 2 mm and thus frequently overlooked.

Based on the as yet limited experiences it can be concluded that transrectal ultrasonography may be useful in assessing ovarian features in specific ovine and caprine cases, for example determining follicular development after superovulatory treatment. Studies on goats have shown that the ovaries with their developing follicles could only be identified in some animals during the first few days of superovulatory treatment (DORN et al. 1989). Only prior to ovulation, when some of the follicles reached an inner diameter of up to 10 mm, could the ovaries be found with certainty.

In studies conducted by the author the follicular development in superovulated sheep was observed. By transrectal sonography the ovaries were reliably detectable - if they had responded to the hormonal therapy with follicular activity. The image resulting from many adjacent, anechoic follicles was so typical that the ovaries could be identified without difficulty. The largest follicles of sheep had a diameter of 5 to 6 mm on the day of prostaglandin treatment and 6 to 8 mm on the day of ovulation (Fig. 3.9 and 3.10). Ultrasonography made it possible to assess whether a ewe had responded with the development of multiple follicles to the hormonal treatment. The exact number of follicles could only be estimated. Some of the sheep were examined by transcutaneous endoscopy after they had been examined by transrectal ultrasonography. This revealed that the sonographic examination enabled the investigator to correctly establish the tendency in follicle numbers, but that counting the exact number of follicles was impossible.

Occasionally, and only with difficulty, could ovaries be identified that had not, or only inadequately, responded to the superovulatory treatment by the development of multiple follicles.

Avtorsko zaščiteno gradivo

Downloaded From Vet-eBooks.com



Fig. 3.11: Sagittal section through the non-pregnant uterus of a ewe. The greater curvature of the uterus is marked by arrows. Transrectal ultrasonogram.



Fig. 3.12: Sagittal section through the uterus of a ewe on the day of estrus following superovulatory treatment. Multiple, small fluid collections (arrows) are visible inside the lumen of the uterus. Transrectal ultrasonogram.

Avtorsko zaščiteno gradivo

Downloaded From Vet-eBooks.com

3.3 Uterine structures in sheep and goats

Generally, the findings on the non-pregnant uterus as well as the uterus and conceptus during pregnancy are similar in sheep and goats (TAINTURIER et al. 1983 a and b).

3.3.1 Non-pregnant uterus

The non-pregnant uterus of sheep and goats can be found inside the pelvis in the vicinity of the apex of the urinary bladder. It can be depicted by transrectal, as well as transcutaneous sonography (Fig. 3.3 and 3.4).

During a transrectal examination, a sagittal section through the uterus is produced if the probe is held dorsally above the uterus, and its scanning plane is directed ventrally and parallel to the longitudinal axis of the body (Fig. 3.11). The cranial border of the uterus, in the form of its larger curvature, can be seen as a convex structure. The lesser curvature of the non-pregnant uterus can only be recognized with difficulty. On section the uterine wall produces a homogenous, coarsely granular echo. The uterine lumen or any fluid accumulations inside the uterus can usually not be detected in the normal, non-pregnant uterus. Only during proestrus and estrus of ewes treated for superovulation did the uterus regularly contain fluid accumulations (Fig. 3.12).

Avtorsko zaščiteno gradivo

Downloaded From Vet-eBooks.com

3.3.2 Pregnant uterus

3.3.2.1 Before Day 20 of pregnancy

The earliest indication of the presence of a pregnancy is the demonstration of embryonic fluid inside the uterus. The trophoblast of the ewe and goat begins to elongate considerably from the Day 11 of pregnancy (KING et al. 1982). By Day 13 to 14 the embryonic vesicle lies as a 10 cm long tube in the uterine horn ipsilateral to the corpus luteum of pregnancy. By Day 16 to 18 it extends into the contralateral horn (ROWSON and MOOR 1966). Around Day 20 of pregnancy the narrow embryonic vesicle extends from the tip of the pregnant horn to the tip of the contralateral horn of the uterus.

Transrectal sonography occasionally allows the visualization of anechoic sections through the embryonic vesicle between Days 14 and 19 of pregnancy (BUCKRELL 1988). During this period the demonstration of an anechoic lumen is, however, unreliable and cannot be used to positively diagnose pregnancy. The chorionic and amniotic vesicles contain so little fluid at this stage that the embryonic vesicle of only a few millimeters can only sporadically be visualized (Fig. 3.13). Small fluid accumulations in the uterus can also originate from causes other than pregnancy.

Prior to Day 20 transrectal sonography may be useful as a research tool to study, for example, embryonic death; it does not constitute a practical means of reliably diagnosing pregnancy at this stage.

3.3.2.2 Day 20 to 40 of pregnancy

From Day 20 to 25 of pregnancy the demonstration of embryonic fluid is regularly possible in sheep and goats examined by transrectal sonography (BUCKRELL 1988). At this stage of pregnancy anechoic embryonic fluid accumulations occur inside the lumen of the early pregnant uterus - frequently even in several places which appear as a series of vesicles (Fig. 3.14). They can usually be found immediately cranial or cranioventrally to the urinary bladder (BUCKRELL et al. 1986, GEARHART et al. 1988). The amount of embryonic fluid increases rather rapidly over the following few days so that ever larger portions of the embryonic vesicle become visible. The largest cross sections through the vesicle increase from around 10 mm on Day 20, to 15 mm on Day 25 and to 20 mm on Day 30 (Fig. 3.14 to 3.16).

It is often not possible to see the connections between locules of embryonic fluid which would demonstrate that they are all parts of a single embryonic vesicle. More often, an image consisting of apparently

Avtorsko zaščiteno gradivo

Downloaded From Vet-eBooks.com



Fig. 3.16: Uterus of a ewe on Day 29 of pregnancy. Three anechoic sections through embryonic vesicles are visible. Transrectal ultrasonogram.

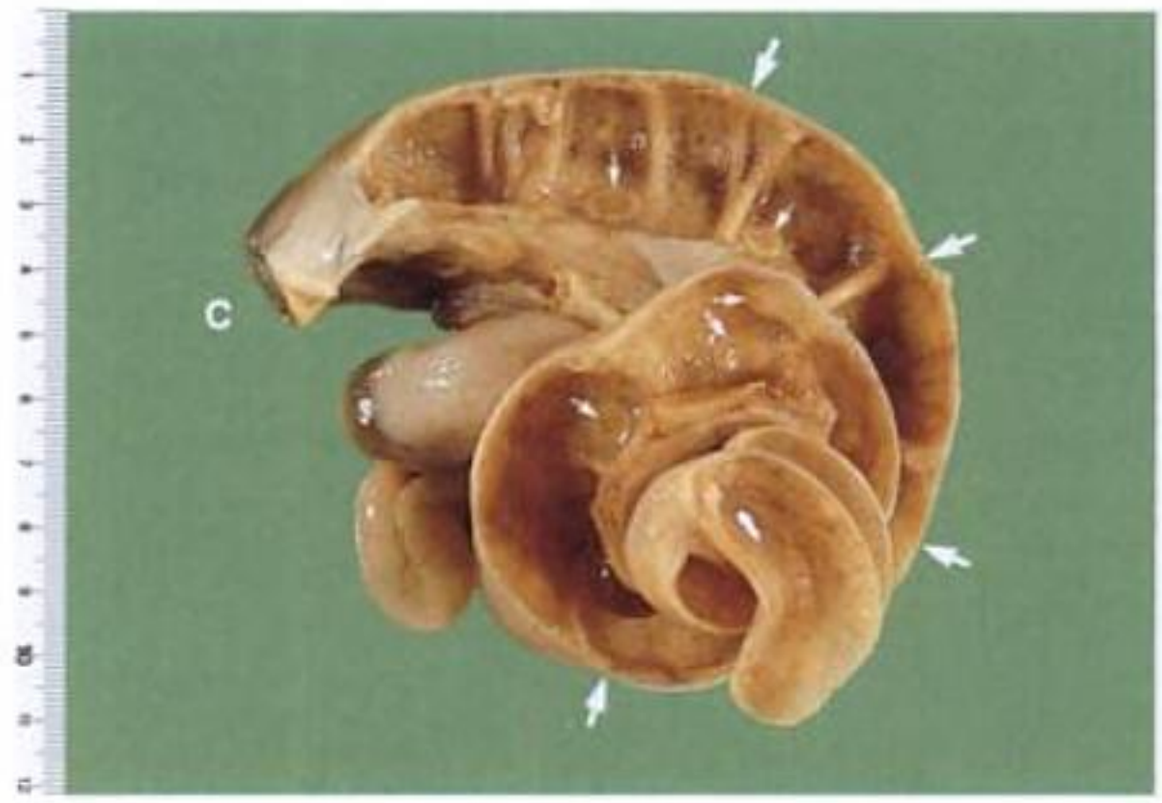


Fig. 3.17: Photograph after a sagittal section through the right uterine horn of a ewe on Day 29 of pregnancy. The uterine lumen is partitioned into several compartments by vertical folds of the uterine wall. Bowl shaped caruncles (small arrows) are recognizable. The greater curvature is marked by large arrows, the cervix (C; partly cut off) lies on the left.

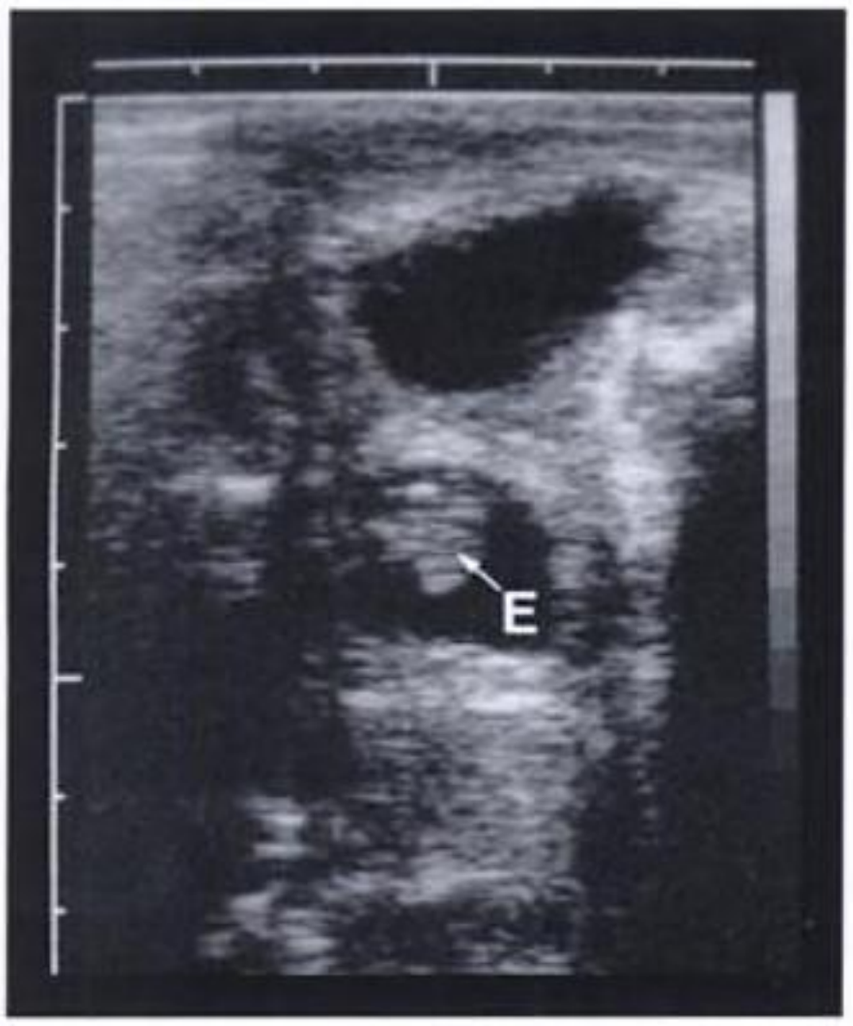


Fig. 3.18: Uterus of a nanny goat on Day 24 of pregnancy. The echoic embryo (E) lies, surrounded by anechoic embryonic fluid, in the ventral section of the uterine horn. Transrectal ultrasonogram.



Fig. 3.19: Uterus of a nanny goat on Day 25. The uterus lies cranial to the urinary bladder (U). In the ventral section of the uterine horn 2 placentomes can be seen as button like protrusions. Transrectal ultrasonogram.

Avtorsko zaščiteno gradivo

Downloaded From Vet-eBooks.com



Fig. 3.24: Transrectal horizontal section through an ovine fetus on Day 60 of pregnancy. In the apex of the thorax (arrows) lies the heart, to the left of that the moderately echoic liver (L) with cross sections through some large hepatic blood vessels.



Fig. 3.25: Transcutaneous horizontal section through the skull of an ovine fetus on Day 65 of pregnancy. One eye (arrow) with its lens lies at the top, the other eye (arrow) at the bottom. To the right of the latter lies the hyperechoic oval of the cranial cavity. The biparietal diameter (BPD) measures 23.5 mm.

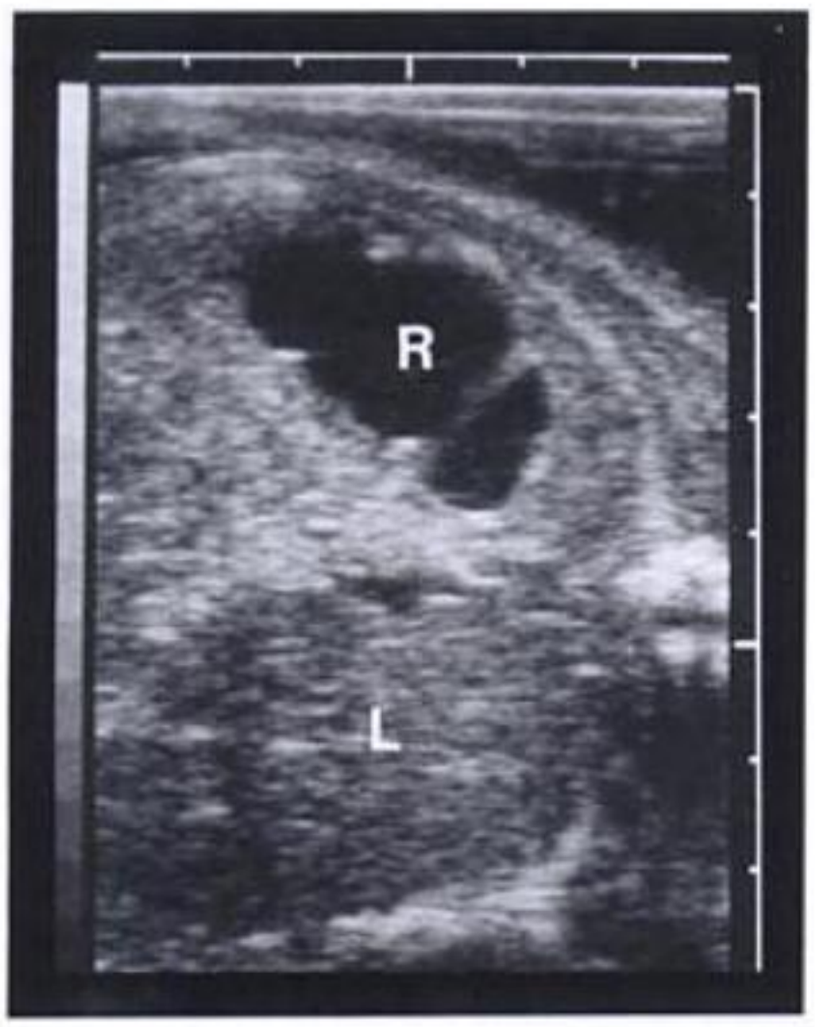


Fig. 3.26: Transrectal horizontal section through the abdomen of an ovine fetus on Day 96 of pregnancy. The hypoechoic lumen of the rumen (R) lies at the top, the liver (L) at the bottom, an echoic vertebra on the right.

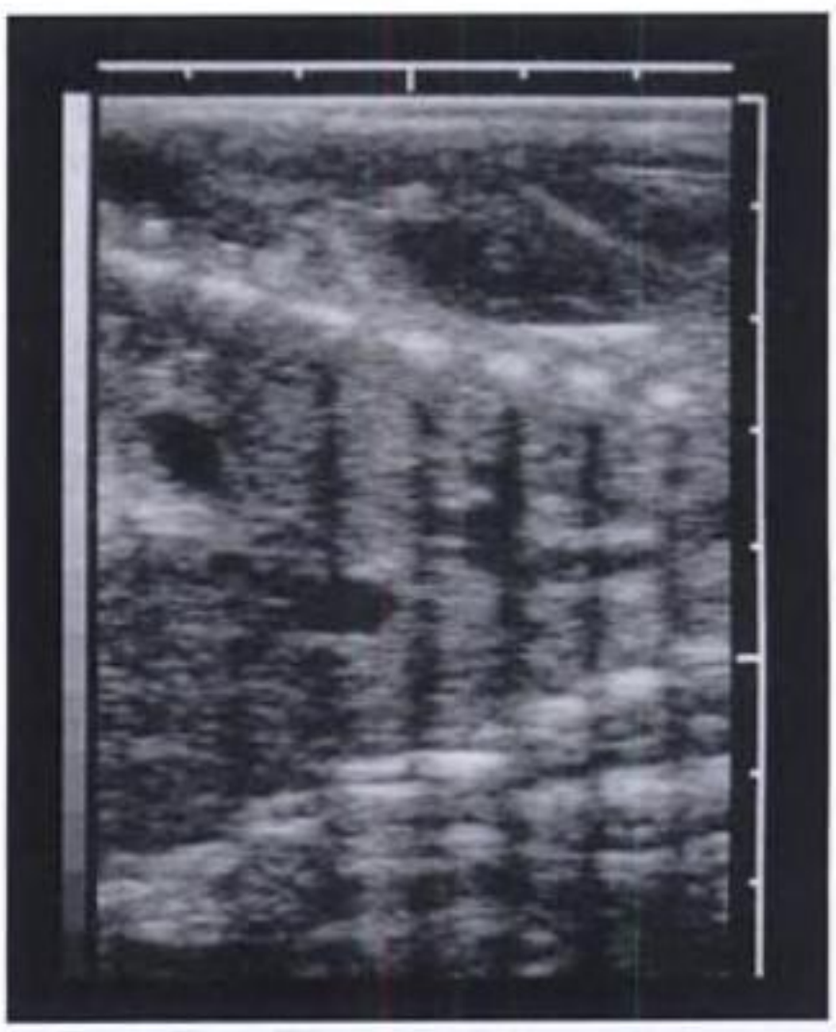


Fig. 3.27: Transrectal horizontal section through the thorax of an ovine fetus on Day 96 of pregnancy. Shadow artifacts originate from the conically arranged rib cross sections and run into the depth of the image.

Avtorsko zaščiteno gradivo

Downloaded From Vet-eBooks.com

During the second and third trimesters of pregnancy numerous organs of ovine and caprine fetuses can be depicted sonographically (DE BOIS and TAVERNE 1984). In general, the different organs and body parts produce images similar to those described for bovine fetuses (Chapter 2.4). The cranial cavity and eyes, heart, stomach, kidneys and umbilical cord can be depicted with particular clarity (Fig. 3.24 to 3.30). As a result of their intense echogenicity the bony parts, such as the skull, spinal column, ribs and the extremities, can be identified without difficulty. The fetuses show intensive mobility at this stage, resulting in frequent positional changes (SCHEERBOOM and TAVERNE 1985).

By taking fetal measurements the age of a pregnancy can be estimated or, in the case of a known service date, the developmental status of the conceptuses can be assessed. Next to many other body parts, the biparietal diameter (BPD) of ovine and caprine fetuses is particularly well suited for fetometric evaluation (Fig. 3.25). The biparietal diameter of ovine and caprine fetuses increases nearly linearly during the course of pregnancy (HAIBEL and PERKINS 1989, HAIBEL et al. 1989). On average, the biparietal diameter grows from 7.5 to 10 mm on Day 40, to 23 to 26 mm around Day 70 and to 40 to 45 mm at about Day 100.

Avtorsko zaščiteno gradivo

Downloaded From Vet-eBooks.com



Fig. 3.31: Transrectal ultrasonogram of three placentomes of a nanny goat on Day 63 of pregnancy. Depending on the direction of the sectional plane the cup-shape of the placentomes will produce a variety of images.

Avtorsko zaščiteno gradivo

Downloaded From Vet-eBooks.com

3.3.3 Uterine pathology

Pathological conditions of the uterus, such as pyometra, hydrometra and mucometra, and in cases of abnormal pregnancies, such as embryonic deaths, fetal mummification, hydrallantois and hydramnion can all be diagnosed by ultrasonography (BUCKRELL 1988, GEARHART et al. 1988).

Pyometra in the ewe is characterized by an intrauterine fluid accumulation which contains obvious reflections (Fig. 3.32). The echogenicity of the fluid depends on the relative amount of cellular material in the secretion. A snow-storm-like image is typical.

The term hydrometra in goats signifies the accumulation of large amounts of sterile fluid inside the uterus in the presence of a persistent corpus luteum and the failure of the doe to cycle (PIETERSE and TAVERNE 1986). The ultrasound image in a case of hydrometra is characterized by the large, hypoechoic fluid accumulations inside the uterus (Fig. 3.33). Frequently, several closely adjacent fluid filled cavities separated by sections of thin uterine wall can be seen. This image originates from the coiling and kinking of the uterine horns which are filled with secretions and portions of which form tightly appositioned locules. No fetal echoes or placentomes are present. Treatment with PGF2α usually leads to the prompt emptying of the uterus, but small amounts of sonographically detectable fluid may remain for some time (Fig. 3.34).

Early cases of hydrometra, where the amount of fluid is rather small, can be confused with pregnancy during sonographic examinations. In doubtful cases the doe should be reexamined at least 40 days after the last service date. At this time a fetus should be detectable in a pregnant doe and an accurate diagnosis can be established (PIETERSE and TAVERNE 1986).

Dropsy of the fetal membranes includes those conditions in which there is a pathological increase in the amount of fetal fluids, as in hydrallantois and hydramnion. In a case of hydrallantois the sonographic examination will reveal a uterus that is filled to the extreme with anechoic fluid (Fig. 3.35). As is the case in hydrometra, hyperechoic sections of the thin uterine wall will traverse the allantoic fluid. In order to differentiate between hydrallantois and hydramnion on one hand and disturbances in non-pregnant animals (pyo- and hydrometra) on the other one should look for fetal structures. Typically, in cases of dropsy of the fetal membranes, placentomes and/or fetuses can be depicted whereas these are not present in cases of pyo- and hydrometra.

Avtorsko zaščiteno gradivo

Downloaded From Vet-eBooks.com

References to chapter 3

BUCKRELL, B. C. (1988): Applications of ultrasonography in reproduction in sheep and goats. Theriogenology 29, 71–84.

BUCKRELL, B. C., B. N. BONNETT and W. H. JOHNSON (1986): The use of real-time ultrasound rectally for early pregnancy diagnosis in sheep. Theriogenology 25, 665–673.

DAVEY, C. G. (1986): An evaluation of pregnancy testing in sheep using a real-time ultrasound scanner. Aust. vet. J. 63, 347–348.

DEAS, D. W. (1977): Pregnancy diagnosis in the ewe by an ultrasonic rectal probe. Vet. Rec. 101, 113–115.

DE BOIS, C. H. W. en M. A. M. TAVERNE (1984): Drachtigheidsonderzoek bij het schaap D. M. V. twee-dimensionele echografie. Vlaams diergeneesk. Tijdschr. 53, 240–252.

DORN, C. G., B. A. WOLFE, E. BESSOUDO and D. C. KRAEMER (1989): Follicular detection in goats by ultrasonography. Theriogenology 31, 185.

EVANS, H. E. and W. O. SACK (1973): Prenatal development of domestic and laboratory mammals: Growth curves, external features and selected references. Zentbl. Vet. Med. Reihe C 2, 11–45.

FOWLER, D. G. and J. F. WILKINS (1980): The identification of single and multiple bearing ewes by ultrasonic imaging. Proc. Aust. Soc. Anim. Prod. 13, 492.

FOWLER, D. G. and J. F. WILKINS (1984): Diagnosis of pregnancy and number of foetuses in sheep by real-time ultrasonic imaging. I. Effects of number of foetuses, stage of gestation, operator and breed of ewe on accuracy of diagnosis. Livestock Production Science 11, 437–450.

FOWLER, D. G. and J. F. WILKINS (1985): Developing a field technique for determining litter number during pregnancy in sheep. Miscellaneous Bulletin 10, Dep. of Agriculture New South Wales.

GEARHART, M. A., W. E. WINGFIELD, A. P. KNIGHT, J. A. SMITH, D. A. DARGATZ, J. A. BOON and C. A. STOKES (1988): Real-time ultrasonography for determining pregnancy status and viable fetal numbers in ewes. Theriogenology 30, 323–337.

HAIBEL, G. K. and N. R. PERKINS (1989): Real-time ultrasonic biparietal diameter of second trimester Suffolk and Finn sheep fetuses and prediction of gestational age. Theriogenology 32, 863–869.

HAIBEL, G. K., N. R. PERKINS and G. M. LIDL (1989): Breed differences in biparietal diameters of second trimester Toggenburg, Nubian and Angora goat fetuses. Theriogenology 32, 827–834.

JARDON, C. (1988): Utilisation actuelle du diagnostic de gestation, en élevage, chez la brebis. Recl. Méd. vét. Éc. Alfort 164, 135–140.

KASPAR, B. (1988): Beitrag zur Sonographie in der gynäkologischen Diagnostik, insbesondere zur Feststellung der Gravidität bei Schaf und Ziege. Tagungsbericht »Krankheiten der kleinen Wiederkäuer« der DVG, Gießen 10.6.1988.

KASPAR, B. (1989): Ultraschalluntersuchung bei Ziegen: Eine zuverlässige Methode zur Trächtigkeitsfeststellung. Der Ziegenzüchter 5, 8–12.

KING, G. J., B. A. ATKINSON and H. A. ROBERTSON (1982): Implantation and early placentation in domestic ungulates. J. Reprod. Fert., Suppl. 31, 17–30.

LANGFORD, G. A., J. N. B. SHRESTHA, P. S. FISER, L. AINSWORTH, D. P. HEANEY and G. J. MARCUS (1984): Improved diagnostic accuracy by repetitive ultrasonic pregnancy testing in sheep. Theriogenology 21, 691–698.

LINDAHL, I. L. (1969): Comparison of ultrasonic techniques for the detection of pregnancy in ewes. J. Reprod. Fert. 18, 117–120.

LINDAHL, I. L. (1971): Pregnancy diagnosis in the ewe by intrarectal Doppler. J. Anim. Sci. 32, 922–925.

LOGUE, D. N., J. T. HALL, S. MCROBERTS and A. WATERHOUSE (1987): Real-time ultrasonic scanning in sheep: The results of the first year of its application on farms in south-west Scotland. Vet. Rec. 121, 146–149.

OTT, R. S., W. F. BRAUN, T. F. LOCK, M. A. MEMON and J. L. STOWATER (1981): A comparison of intrarectal Doppler and rectal abdominal palpation for pregnancy testing in goats. J. Am. vet. med. Ass. 178, 730–731.

OWENS, J. L. and J. R. ARMSTRONG (1985): Diagnosis of foetal number in prolific sheep. Proc. N. Z. Soc. Anim. Prod. 45, 155–157.

PIETERSE, M. C. and M. A. M. TAVERNE (1986): Hydrometra in goats: Diagnosis with real-time ultrasound and treatment with prostaglandins or oxytocin. Theriogenology 26, 813–821.

RIERA, G. S. (1984): Some similarities and differences in female and goat reproduction. Proc. 10th Int. Congr. Anim. Reprod. & A. I. IV, VII–1–VII–4.

ROWSON, L. E. A. and R. M. MOOR (1966): Development of the sheep conceptus during the first fourteen days. J. Anat. 100, 777–785.

RÜSCH, P., M. BERCHTOLD und L. EGGER (1981): Das Echolotverfahren zum Trächtigkeitsnachweis beim Schaf im Vergleich zur Ultraschall-Doppler-Technik. Tierärztl. Umsch. 36, 180–188.

SCHEERBOOM, J. E. M. and M. A. M. TAVERNE (1985): A study of the pregnant uterus of the ewe and the goat using real-time ultrasound scanning and electromyography. Vet. Res. Com. 9, 45–56.

SCHEIBE, K. M., G. EMELING und L. MARSHALL (1986): Vergleichende Untersuchung zur Trächtigkeitsdiagnose beim Schaf. Mh. Vet. Med. 41, 158–164.

TAINTURIER, D., L. LIJOUR, M. CHAARI, K. W. SARDJANA et B. DENIS (1983 a): Diagnostic de la gestation chez la brebis par échotomographie. Revue Méd. vét. 134, 523–526.

TAINTURIER, D., L. LIJOUR, M. CHAARI, K. W. SARDJANA et J. L. LE NET (1983b): Diagnostic de la gestation chez la chèvre par échotomographie. Revue Méd. vét. 134, 597–599.

TAVERNE, M. A. M., M. C. LAVOIR, R. VAN OORD and G. C. VAN DER WEYDEN (1985): Accuracy of pregnancy diagnosis and prediction of foetal numbers in sheep with linear-array real-time ultrasound scanning. The Veterinary Quartely 7, 256–263.

TRAPP, M. J. and A. L. SLYTER (1983): Pregnancy diagnosis in the ewe. J. Anim. Sci. 57, 1–5.

WATT, B. R., G. A. ANDERSON and I. P. CAMPBELL (1984): A comparison of six methods used for detecting pregnancy in sheep. Aust. vet. J. 61, 377–382.

WHITE, I. R., A. J. F. RUSSEL and D. G. FOWLER (1984): Real-time ultrasonic scanning in the diagnosis of pregnancy and the determination of fetal numbers in sheep. Vet. Rec. 115, 140– 143.

Avtorsko zaščiteno gradivo

Downloaded From Vet-eBooks.com



Fig. 4.1: Transcutaneous ultrasound examination in a pig. The probe is applied just above the last three mammary glands.



Fig. 4.2: Transrectal ultrasound examination in a pig. The probe is directed from the outside by a guide rod (see Fig. 4.3), introduced into the rectum and rotated back and forth over the uterus and the ovaries.



Fig. 4.3: For transrectal ultrasound examinations in pigs the linear probe and its cable can be stiffened by a metal or plastic rod.

Avtorsko zaščiteno gradivo

Downloaded From Vet-eBooks.com

4 Ultrasonography in pigs

In pigs pregnancy diagnosis by ultrasound techniques have been utilized for many years. As in sheep and goats the non-imaging techniques, such as the ultrasound-Doppler (FRASER et al. 1971, ISAKOV 1974) and A-mode techniques (LINDAHL et al. 1975, O'REILLY 1976, PEJSAK and WIERZCHOS 1981, BALKE and ELMORE 1982) were used for this purpose.

In recent years the imaging ultrasonography has been used more frequently to diagnose pregnancies (INABA et al. 1983, BOTERO et al. 1984, IRIE et al. 1984, CARTEE et al. 1985, TAVERNE et al. 1985, TAINTURIER and MOYSAN 1985, JACKSON 1986).

4.1 Technique of ultrasonography in pigs

The imaging ultrasound technique can be used in the pig by applying the probe to the skin of the ventral abdomen (transcutaneous sonography) or by introducing the probe into the rectum (transrectal sonography) (CARTEE et al. 1985, FRAUNHOLZ et al. 1989).

4.1.1 Transcutaneous sonography

For the transcutaneous sonographic scanning of the sow the probe is held against the skin surface of the ventral abdomen, just dorsal to the last three mammary complexes, in the area from the attachments of the mammary glands to 15 cm further dorsally (Fig. 4.1). The probe is held in such a way that the sound plane lies level and impacts perpendicularly onto the abdominal wall and an area of about 20 by 15 cm is scanned. Imaging the pregnant uterus is achieved fastest if the horizontally oriented scanning plane is rotated up and down through the abdomen. Should the uterus not be detected initially, the same procedure is repeated after moving the probe several centimeters in a cranial or caudal direction. In order to depict the left and right components of the uterus and ovaries of pigs both sides of the abdomen must be scanned. In doing this it is often possible to find both halves of the uterus, but it is often not possible to differentiate between the left and the right uterine horns. The full stomach and spiral colon often push the uterus towards the right side of the abdomen where it is then usually easier to find.

Restraining methods or sedation of sows are usually unnecessary during either the transcutaneous or the transrectal scanning procedures. It is also not necessary to remove the hair in the area where the ultrasound probe is held against the skin. The sows should be tied up or held in a tight chute during the examination. Offering them some feed may distract and calm them.

4.1.2 Transrectal sonography

During the transrectal sonographic examination of sows the probe is best manipulated from outside the rectum after advancing it into the rectum and then rotated over the uterus (Fig. 4.2). Manipulating the probe with one hand inside the rectum is often difficult and can stress the animals considerably. In order to be able to manipulate the ultrasound probe from the outside, the probe and its connecting cable must be stiffened. For this purpose the probe and the cable are tied to a 80 cm long guide-rod made from a non-twisting material, such as metal or plastic (Fig. 4.3). The rod encloses the cable and the probe on 3 sides, leaving only the scanning surface open. With the aid of this rod the probe can then be advanced and withdrawn or rotated in the desired direction inside the rectum (FRAUNHOLZ et al. 1989).

Avtorsko zaščiteno gradivo

Downloaded From Vet-eBooks.com

Prior to the transrectal examination as much of the feces as possible should be manually removed from the rectum, then the probe introduced and pushed forward along the rectal floor. If the probe becomes trapped in a rectal fold it may be helpful to initially guide it into the rectum for a short distance by enclosing it in a hand. Depending on the size of the sow that is to be examined, its reproductive status and the organ that is targeted the probe is advanced to a depth of about 30 to 40 cm. The dimensions of the probe used for this examination should not exceed a width or height of 2 to 3 cm and a length of 10 cm. Provided the procedure is conducted skillfully there is no need to be afraid of serious injuries during the examination.

4.2 Ovarian structures in pigs

Using transrectal examinations it is frequently possible to sonographically depict the porcine ovaries (FRAUNHOLZ 1988). The ovaries can also be scanned by transcutaneous ultrasonography (MADEC et al. 1988, WEITZE et al. 1989). The ovaries of both, non-pregnant and pregnant sows can be depicted. Based on current experience, it may sometimes be difficult and take time to find the ovaries on both sides of the body. In addition, when sows are scanned transcutaneously, it is necessary to change sides.

In general, follicles, corpora lutea and ovarian cysts can be sonographically depicted. The exact identification and counting of the different functional structures on the ovary requires practice and may often be possible only to a limited extent.

4.2.1 Follicles and corpora lutea

Follicles are characterized by the anechoic follicular fluid. Normally there are numerous follicles with diameters between 1 and 6 mm on the ovaries of sows at all stages of the estrous cycle (SCHNURRBUSCH et al. 1981). A few days prior to ovulation larger follicles become visible, so that during proestrus and estrus several follicles with diameters of 5 to 11 mm can be found (Fig. 4.6). Confusion can be caused by the presence of hemorrhagic corpora lutea and the larger blood vessels in the vicinity of the ovaries. Cross sections through blood vessels need to be sonographically differentiated from follicles.

Usually most estrous follicles in the pig reach ovulation. Only occasionally do large follicles and corpora lutea occur simultaneously. This may happen during the cycle as well as in pregnancy.

Corpora lutea produce the echo typical of luteal tissue (Fig. 4.4 and 4.5). Their sonographic cross section is hypoechoic. The surrounding ovarian stroma is a little brighter. They are more difficult to recognize than follicles. Since they lie very close together on the ovaries their numbers can usually only be estimated (Fig 4.7). Luteinized and hemorrhagic corpora lutea can occur simultaneously (MADEC et al. 1988). The size of cyclic corpora lutea varies between 5 and 10 mm (SCHNURRBUSCH et al. 1981, MADEC et al. 1988). Corpora lutea of pregnancy can be 1 to 2 mm larger.

Avtorsko zaščiteno gradivo

Downloaded From Vet-eBooks.com

4.3 Uterine structures in pigs

4.3.1 Non-pregnant uterus

The non-pregnant uterus of the pig is difficult to recognize with certainty. The uterine wall produces a finely granular, homogenous echo pattern (Fig. 4.12). Due to the tortuous nature of the uterine horns their ultrasound images usually consist of several cross sections through the horns. As long as the uterus contains no fluid it may be difficult to reliably identify it amongst the loops of intestine.

Occasionally the cervix can be seen (Fig. 4.13). The cervical mucosa appears as an echoic line which follows a winding or even zigzag course. This image is caused by the typical pulvini cervicalis of the pig's cervix. If the cervical canal is slightly open and contains some fluid a curvy, poorly echoic band, surrounded by the more echoic cervical wall will be visualized.

4.3.2 Pregnant uterus

4.3.2.1 Before Day 20 of pregnancy

The earliest sonographic indication for the presence of pregnancy is the detection of embryonic fluid inside the uterus. On the ultrasound image the fluid contents of the early conceptus will appear as anechoic areas inside the uterine lumen, and they will be surrounded by the echoic uterine wall. If conception has taken place, one may occasionally see the first signs of fluid accumulations between Days 12 and 14 post insemination. Depending on the position of the uterine horns, the direction of the sonographic plane and the number of conceptuses, varying numbers of dark sections through embryonic fluid may be detectable (BOTERO et al. 1984, CARTEE et al. 1985, FRAUNHOLZ et al. 1989). Between Days 15 and 20 these anechoic areas reach diameters of 10 to 20 mm (Fig. 4.14). At the end of the third week of pregnancy echoic structures become evident inside the anechoic fluid. These echoes originate from the embryos and their surrounding amniotic membranes.

The application of ultrasonography for pregnancy diagnoses before Day 20 of pregnancy is not practical. False diagnoses cannot be avoided at this stage, because it may be impossible to detect any embryonic fluid in the uterus of pregnant sows at this time (INABA et al. 1983).

4.3.2.2 Day 20 to 115 of pregnancy

The embryos usually become recognizable around Day 20 of pregnancy (Fig. 4.15) and their heart beats detectable a few days later (BOTERO et al. 1984, CARTEE et al. 1985, FRAUNHOLZ et al. 1989).

Avtorsko zaščiteno gradivo

Downloaded From Vet-eBooks.com



Fig. 4.16: Uterus of a sow on Day 26 of pregnancy. The embryo is surrounded by its amniotic sac (arrow). Its crown-rump-length (CRL) measures 22 mm. Transrectal ultrasonogram.



Fig. 4.17: Uterus of a sow on Day 27 of pregnancy. A hyperechoic placental membrane (arrows) is drifting inside the anechoic placental fluid. Transrectal ultrasonogram.

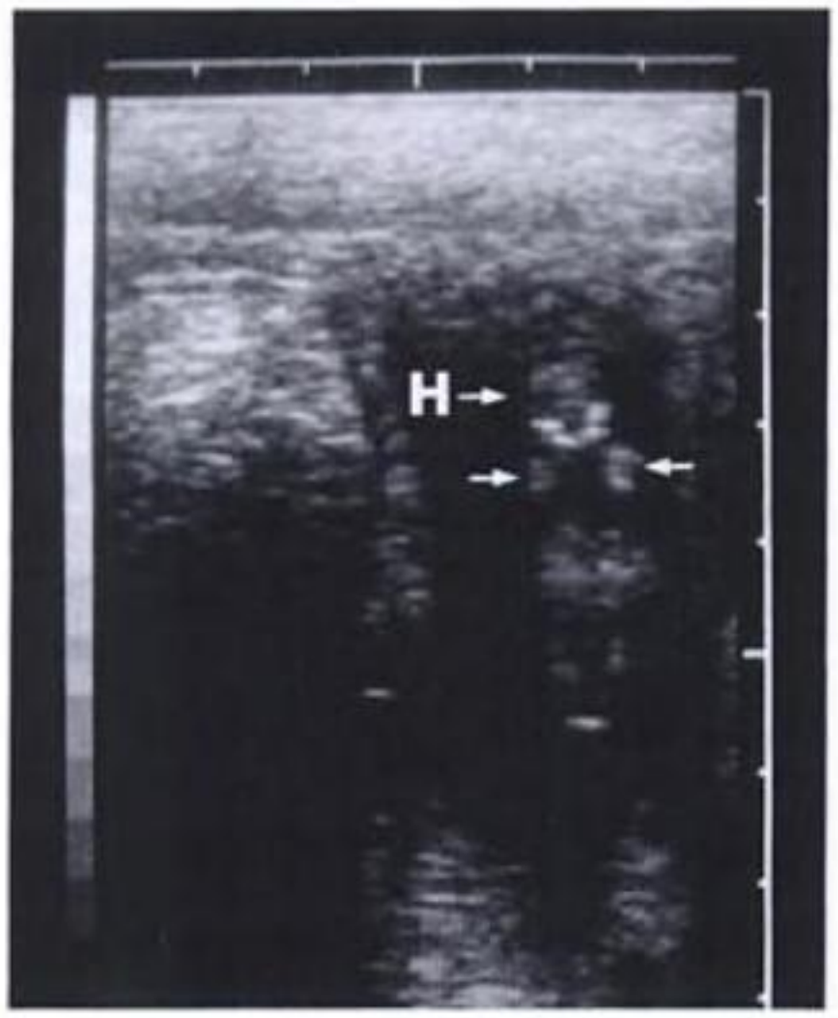


Fig. 4.18: Uterus of a sow on Day 35 of pregnancy. The CRL of the fetus measures 31 mm. The head (H) with both eyes, front extremities (arrows) and the trunk can be identified. Transcutaneous ultrasonogram.



Fig. 4.19: Horizontal section through the thorax of a porcine fetus on Day 65 of pregnancy. The hyperechoic discs of the rib cross sections form a cone. The heart (marked by the crosses) lies in the apex of the cone. Transcutaneous ultrasonogram.

Avtorsko zaščiteno gradivo

Downloaded From Vet-eBooks.com

The crown-rump-length (CRL) of the embryos measures approximately 8 to 10 mm around Day 20, 20 mm around Day 28 and 30 to 35 mm around Day 35 (Fig. 4.16 and 4.18). Their trunk diameter increases from approximately 10 to 20 mm between Days 25 and 35 (MARTINAT-BOTTE et al. 1988).

During this period hyperechoic portions of the fetal membranes can be seen drifting in the embryonic fluid (Fig. 4.17). During the further course of the pregnancy the embryos show a very rapid increase in size (Fig. 4.19). They reach a CRL of 50 mm around Day 40 and 100 mm around Day 50 (ULLREY et al. 1965, EVANS and SACK 1973).

Around Day 30 the contours of the embryos become evident and the head, abdomen and the extremities can be differentiated. In the weeks that follow several developing internal organs can be identified. The hypoechoic areas of the orbit and stomach, the pulsating heart and the echoic reflections of the rib cross sections and the vertebrae are particularly striking (Fig. 4.19 to 4.21).

Avtorsko zaščiteno gradivo

Downloaded From Vet-eBooks.com

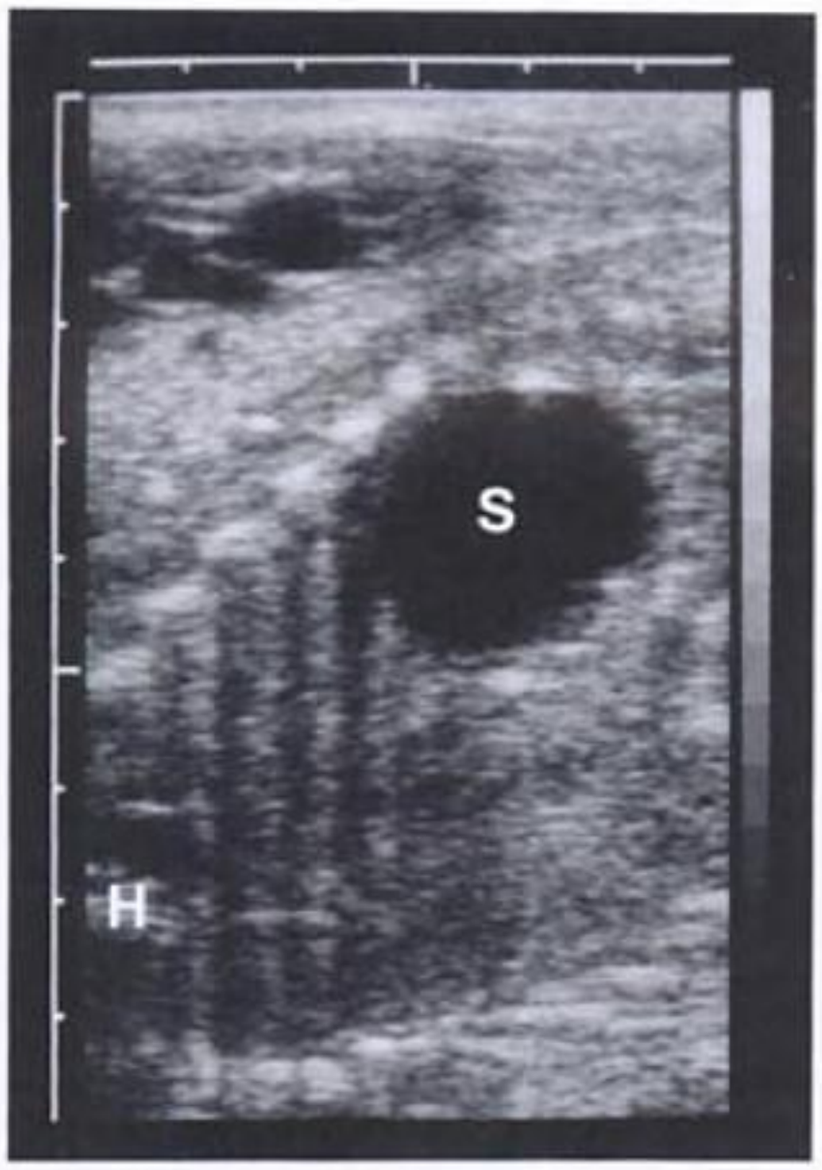


Fig. 4.20: Horizontal section through the thorax of a porcine fetus on Day 93 of pregnancy. Behind the hyperechoic rib cross sections lie the stomach (S) and the heart (H). Transrectal ultrasonogram.

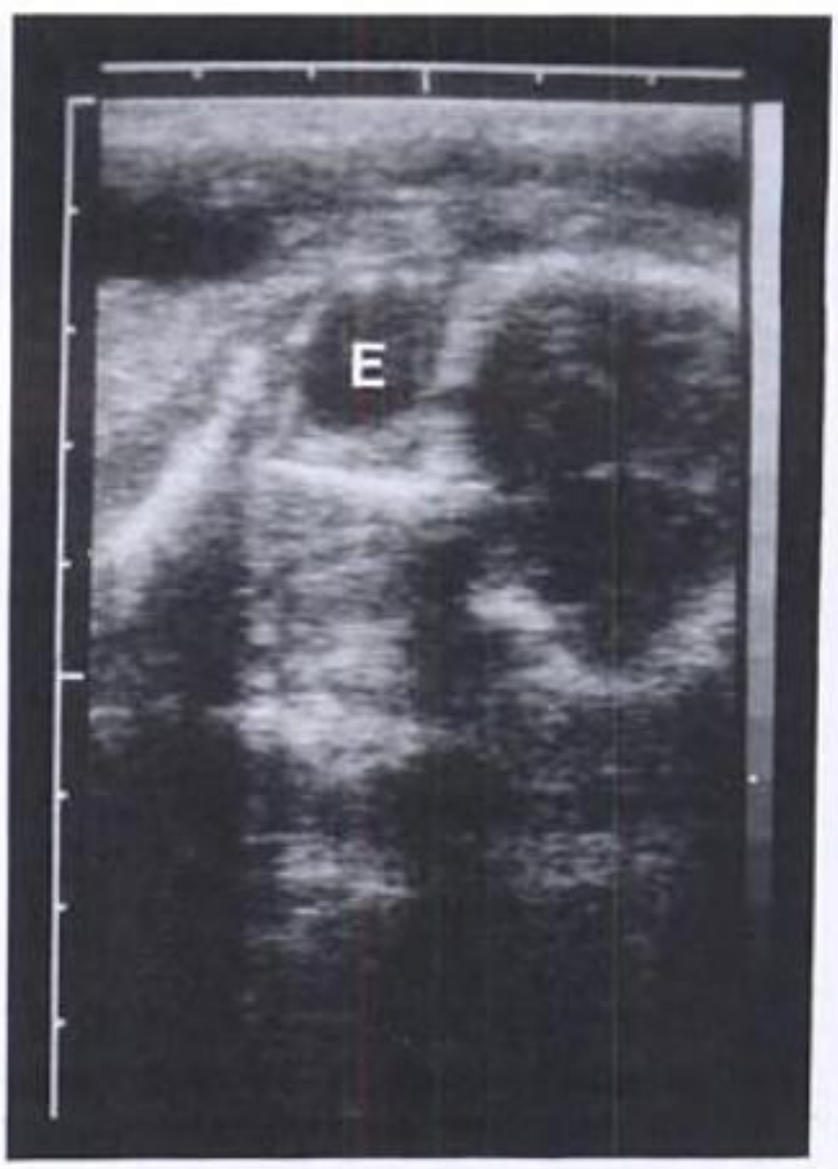


Fig. 4.21: Transrectal ultrasonogram of the head in a porcine fetus on Day 99 of pregnancy. The nose points to the left, the eye (E) lies dorsally and to its right is the oval cerebral cranium. Transrectal ultrasonogram.

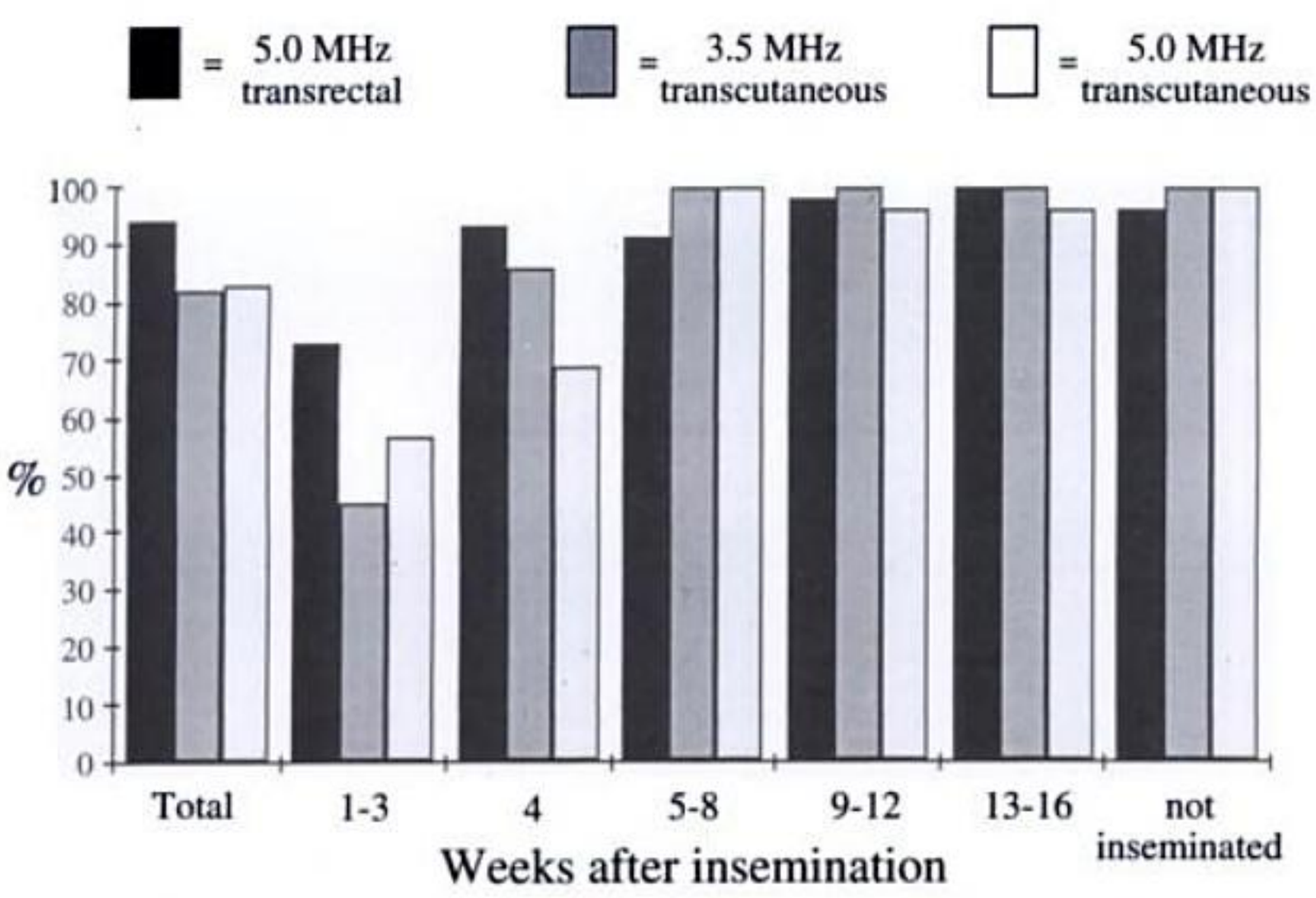


Fig. 4.22: The accuracy (= number of correct diagnoses/number of diagnoses made) of transrectal (5 MHz) and transcutaneous (3.5 and 5 MHz) ultrasonography for pregnancy diagnosis in pigs (adapted from FRAUNHOLZ et al. 1989).

Avtorsko zaščiteno gradivo

Downloaded From Vet-eBooks.com

References to chapter 4

BALKE, J. M. E. and R. G. ELMORE (1982): Pregnancy diagnosis in swine: A comparison of the technique of rectal palpation and ultrasound. Theriogenology 17, 231–236.

BOTERO, O., F. MARTINAT-BOTTÉ et. F. CHEVALIER (1984): Diagnostic précoce de gestation par échographie d'ultrasons. Journées Rech. Porcine en France. 16, 181–188.

BOTERO, O., F. MARTINAT-BOTTÉ and F. BARITEAU (1986): Use of ultrasound scanning in swine for detection of pregnancy and some pathological conditions. Theriogenology 26, 267–278.

CARTEE, R. E., T. A. POWE and R. L. AYER (1985): Ultrasonographic detection of pregnancy in sows. Mod. vet. Pract. 66, 23–26.

EBBERT, W. (1984): Die zystöse Degeneration des Ovars als Teil des Anöstruskomplexes beim Schwein. Vet. med. Diss., Gießen.

EVANS, H. E. and W. O. SACK (1973): Prenatal development of domestic and laboratory mammals: Growth curves, external features and selected references. Zentbl. Vet. Med. Reihe C 2, 11–45.

FRASER, A. F., V. NAGARATNAM and R. B. CALLICOTT (1971): The comprehensive use of doppler ultrasound in farm animal reproduction. Vet. Rec. 88, 202–205.

FRAUNHOLZ, J. (1988): Zur transrektalen und transkutanen Sonographie in der gynäkologischen Diagnostik beim Schwein. Vet. med. Diss., München.

FRAUNHOLZ, J., W. KÄHN und W. LEIDL (1989): Ein Vergleich zwischen der transrektalen und transkutanen Sonographie zur Trächtigkeitsdiagnose beim Schwein. Mh. Vet. Med. 44, 425–430.

INABA, T., Y. NAKAZIMA, N. MATSUI and T. IMORI (1983): Early pregnancy diagnosis in sows by ultrasonic linear electronic scanning. Theriogenology 20, 97–101.

IRIE, M., K. OHMOTO and S. KUMAGA (1984): Diagnosis of pregnancy in pigs by real time ultrasonic B-mode scan. Jap. J. zootechn. Sci. 55, 381–388.

ISAKOV, D. (1974): Application de la technique ultrasonique (Doppler) pour un diagnostic précoce de gravidité des truies. Schweiz. Arch. Tierheilk. 116, 245–258.

JACKSON, G. H. (1986): Pregnancy diagnosis in the sow using real-time ultrasonic scanning. Vet. Rec. 119, 90–91.

LINDAHL, I. L., J. P. TOTSCH, P. A. MARTIN and P. J. DZIUK (1975): Early diagnosis of pregnancy in sows by ultrasonic amplitude-depth analysis. J. Anim. Sci. 40, 220–222.

MADEC, F., F. MARTINAT-BOTTÉ, Y. FORGERIT, M. LE DENMAT et J.-C. VAUDELET (1988): Utilisation de l'échotomographie en élevage porcin. Recl. Méd. vét. Éc. Alfort 164, 127–133.

MARRABLE, A. W. and R. R. ASHDOWN (1967): Quantitative observations on pig embryos of known ages. J. agric. Sci., Camb. 69, 443–447.

MARTINAT-BOTTÉ, F., F. BARITEAU, M. LEPERCQ, Y. FORGERIT et TERQUI (1988): L'échographie d'ultrasons. Outil de diagnostic de gestation chez la truie. Recl. Méd. vét. Éc. Alfort 164, 119–126.

O'REILLY, P. J. (1976): Pregnancy diagnosis in pigs by ultrasonic amplitude depth analysis. A field evaluation. Ir. vet. J. 30, 165–167.

PEJSAK, Z. and E. WIERZCHOŚ (1981): An early diagnosis of pregnancy in sows by means of ultrasonics. Medycyna wet. 37, 139–141.

SCHNURRBUSCH, U., J. BERGFELD, K.-P. BRÜSSOW und U. KALTOFEN (1981): Schema zur Ovarbeurteilung beim Schwein. Mh. Vet. Med. 36, 811–815.

TAINTURIER, D. et. F. MOYSAN (1985): Diagnostic de la gestation par échotomographie chez la truie. Revue Méd. vét. 136, 289–293.

TAVERNE, M. A. M., L. OVING, M. VAN LIESHOUT and A. H. WILLEMSE (1985): Pregnancy diagnosis in pigs: a field study comparing linear-array real-time ultrasound scanning and amplitude depth analysis. The Veterinary Quarterly 7, 271–276.

ULLREY, D. E., J. I. SPRAGUE, D. E. BECKER and E. R. MILLER (1965): Growth of the swine fetus. J. Anim. Sci. 24, 116–118.

VANDEPLASSCHE, M., J. SPINCEMAILLE und R. BOUTERS (1971): Die zystöse Eierstocksdegeneration bei der Sau. Dtsch. tierärztl. Wschr. 78, 91–93.

WEITZE, K. F., O. HABECK, T. WILLMEN and D. RATH (1989): Detection of ovulation in the sow using transcutaneous sonography. Zuchthygiene 24, 40–42.

Avtorsko zaščiteno gradivo

Downloaded From Vet-eBooks.com

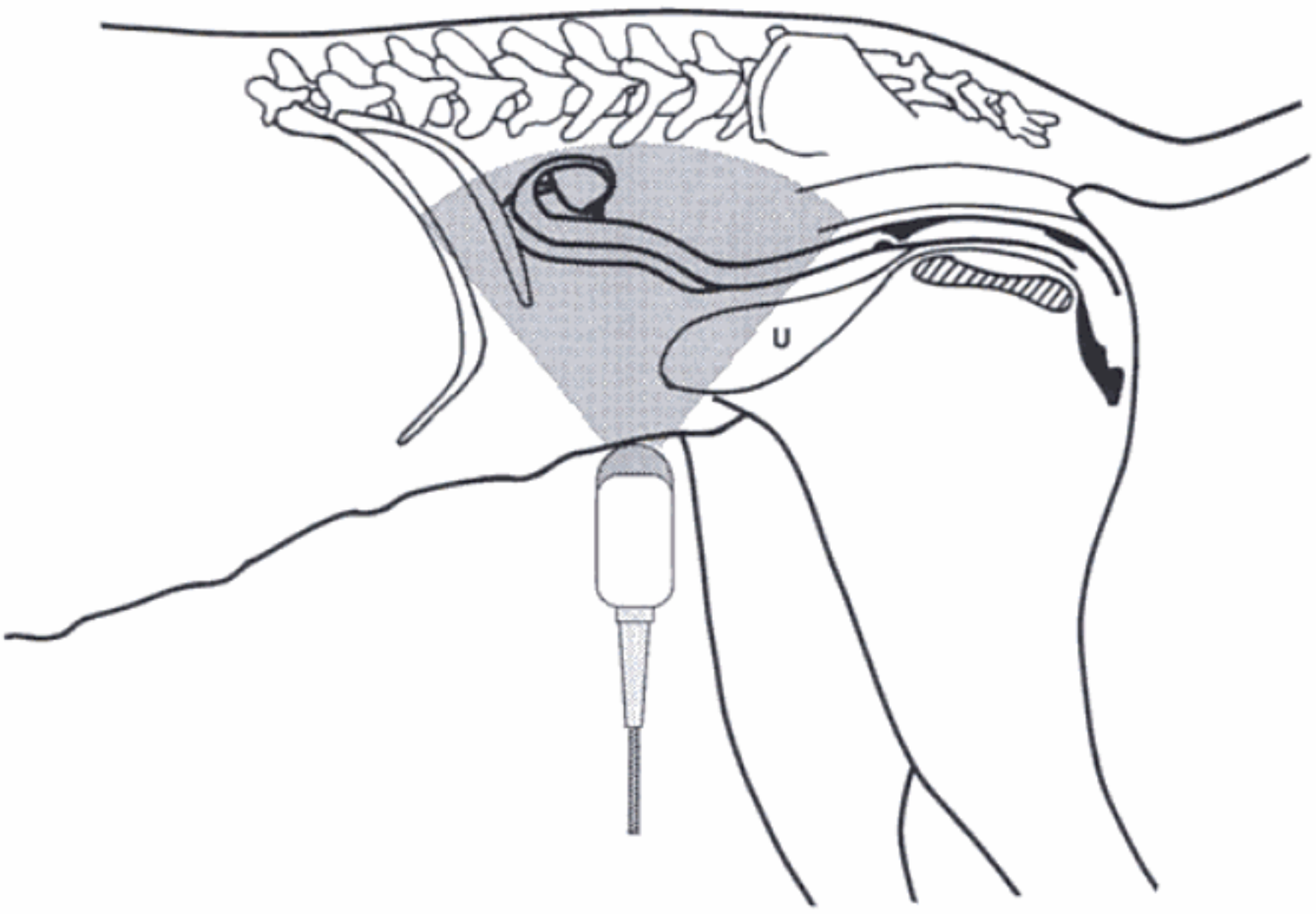


Fig. 5.1: Sonography in a standing bitch using a sector scanner. The uterus lies dorsal to the urinary bladder (U).

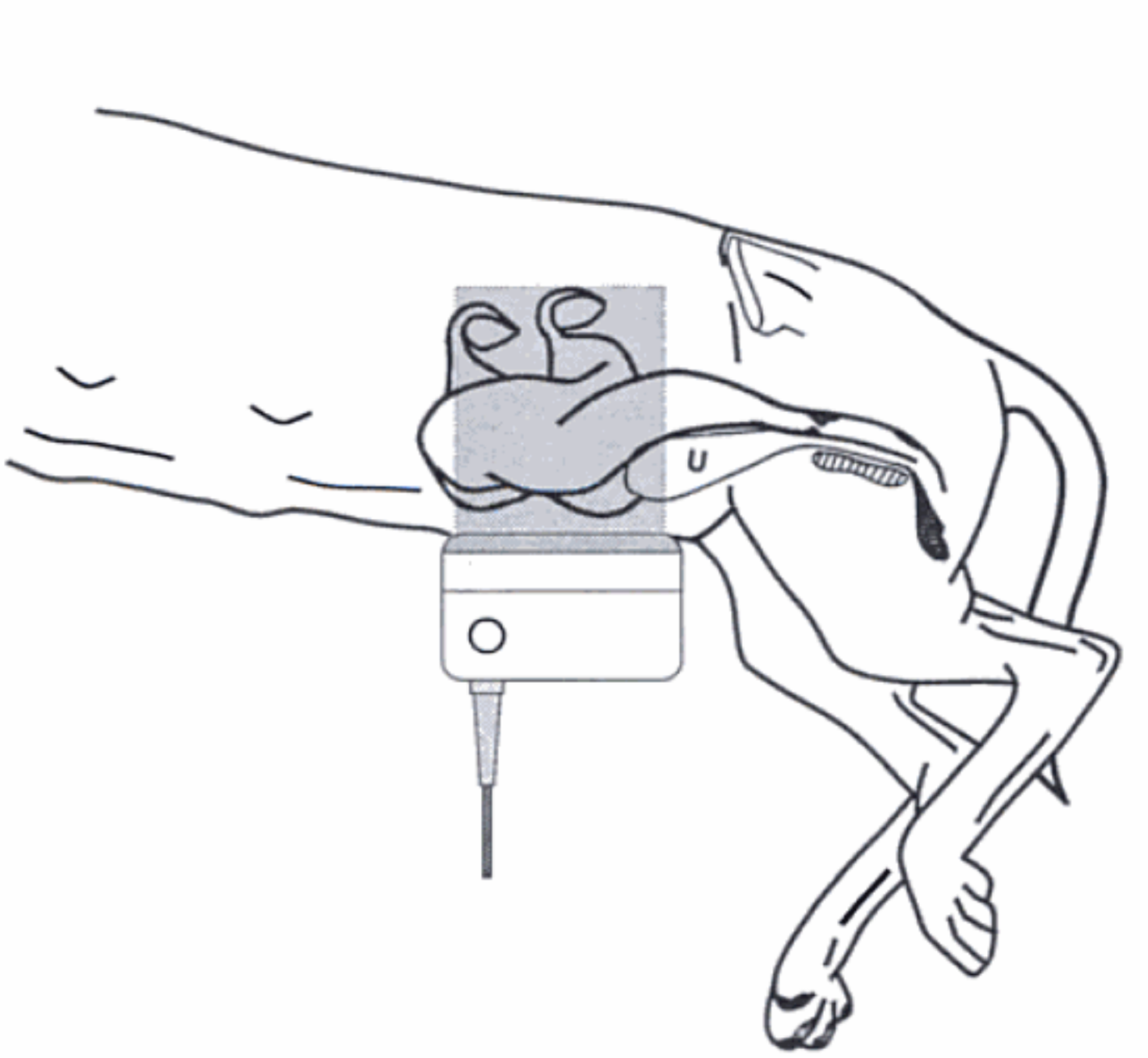


Fig. 5.2: Sonography in a pregnant bitch in lateral recumbency using a linear scanner. The uterus, in the tubular stage, lies cranial to the urinary bladder (U).

Avtorsko zaščiteno gradivo

Downloaded From Vet-eBooks.com

5 Ultrasonography in dogs and cats

The application of sonography during reproductive and obstetric examinations is enjoying increasing popularity in small animal practice. Imaging ultrasonography frequently offers a suitable alternative to radiological examinations. It can thus contribute to a reduction in the technical efforts and safety risks that are associated with radiographic examinations. In addition, sonography makes early pregnancy detection possible and usually permits an assessment of the viability of the conceptuses. Also in its application to diagnose other pathological conditions of the genital tract ultrasonography can be considered equally, or even more effective than other diagnostic techniques (PFOFFENBARGER and FEENEY 1986).

5.1 Technique of ultrasonography in dogs and cats

For reproductive and obstetric examinations in dogs and cats transcutaneous sonography is used. The ultrasound probe is positioned externally against the abdominal wall (Fig. 5.1 and 5.2). A transrectal approach, using small rectal probes adapted from human medicine, appears feasible in larger bitches, but has not been tested adequately in veterinary practice.

Linear, sector and convex scanners are all suitable for transcutaneous sonography in dogs and cats. The use of 5 MHz scanners in small animals presents a useful compromise between image quality and scanning depth.

Of critical importance for optimal image quality is the air-free coupling between the probe and the patient's skin because hair is very disruptive. Before dogs and cats are to be scanned a 5 to 8 cm path should be clipped between the two rows of mammary glands, extending from the pubis to cranial of the umbilicus. Even in dogs with few hairs clipping will improve the image quality. Although one could omit the clipping of dogs with a sparse coat, this may have disadvantages. If the hair was not removed prior to the examination, in order to achieve high image quality, the probe has to be pressed more firmly against the skin and more coupling gel needs to be applied. The excessive coupling gel is then more difficult to remove after the examination. It is also much more difficult to handle probes with large contact surfaces, mostly linear probes, on unclipped dogs. Based on current experience dog owners tolerate the clipping of hair between their dogs' mammary glands quite well. Obese animals, even if their hair is clipped, tend to provide unsatisfactory ultrasound images (TAVERNE et al. 1985). In lactating bitches as well as those with inflammatory or neoplastic changes in the mammary gland the approach through the linea alba may be difficult. In such animals it will be beneficial to position the probe above the mammary glands.

The sonographic examination can be performed on the standing or recumbent bitch without sedation (Fig. 5.1 and 5.2). Larger dogs should be examined while they are standing. In this position the uterus will lie closest to the ventral abdominal wall, it cannot easily escape to a more lateral position and is thus easiest to reach. Also, animals that are sick or in late pregnancy experience the least amount of stress and discomfort in this position. Small dogs and cats are easily examined in lateral or dorsal recumbency (GÜNZEL and LÜNING 1983). In pregnant females in dorsal recumbency it should be borne in mind that the pressure of the fetuses onto the larger abdominal vessels can interfere with circulation. Forced respiration or panting can seriously affect the stillness of the image and thus make its interpretation much more difficult. Temporarily closing either the mouth or the nostrils of the dog can reduce the disturbing effect of respiratory movements, or momentarily remove them.

Avtorsko zaščiteno gradivo

Downloaded From Vet-eBooks.com

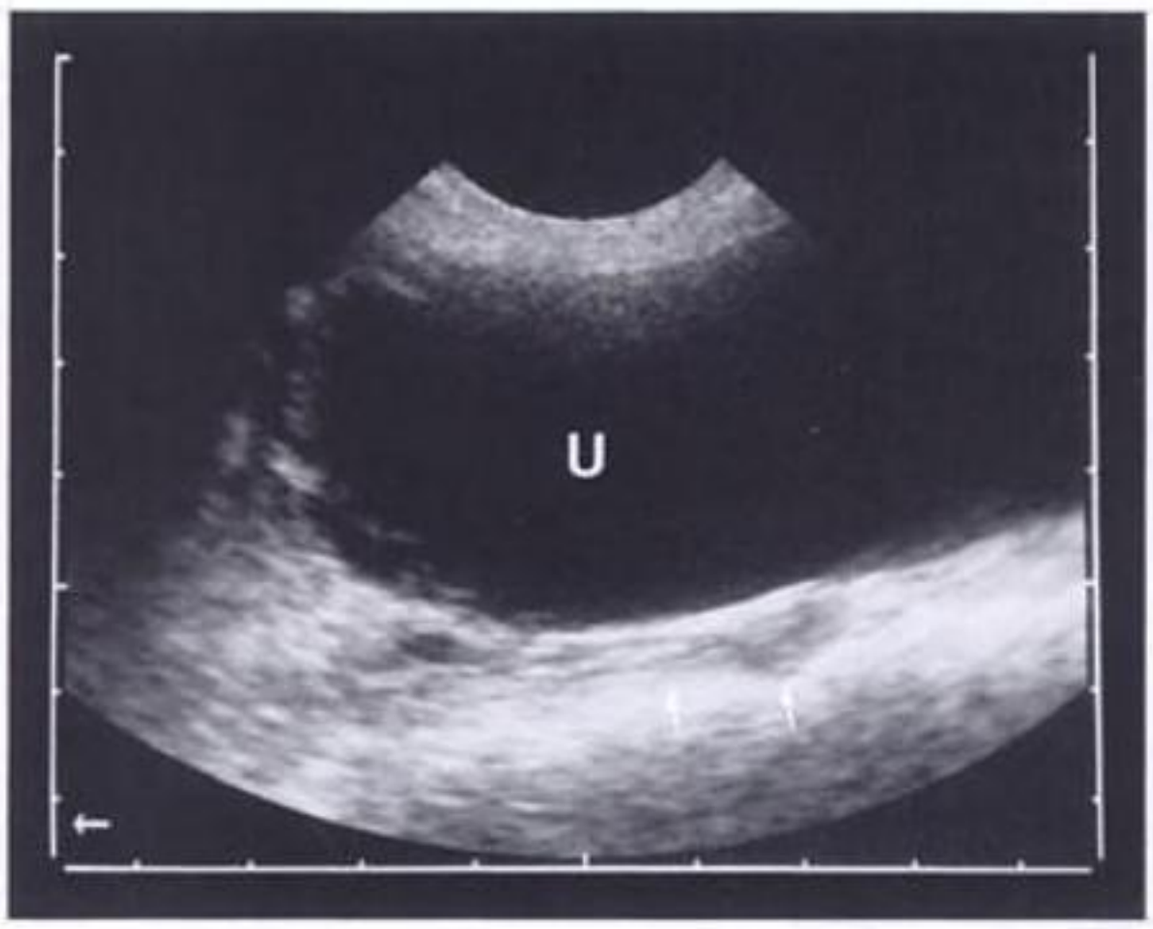


Fig. 5.3: Urinary bladder (U) and non-pregnant uterus at the level of the cervix (arrows) in a bitch. Using transcutaneous sonography with the beam directed ventrodorsally with the probe applied to the ventral abdomen, the anechoic urinary bladder will be imaged close to the transducer and the uterus will lie in the depth of the image.

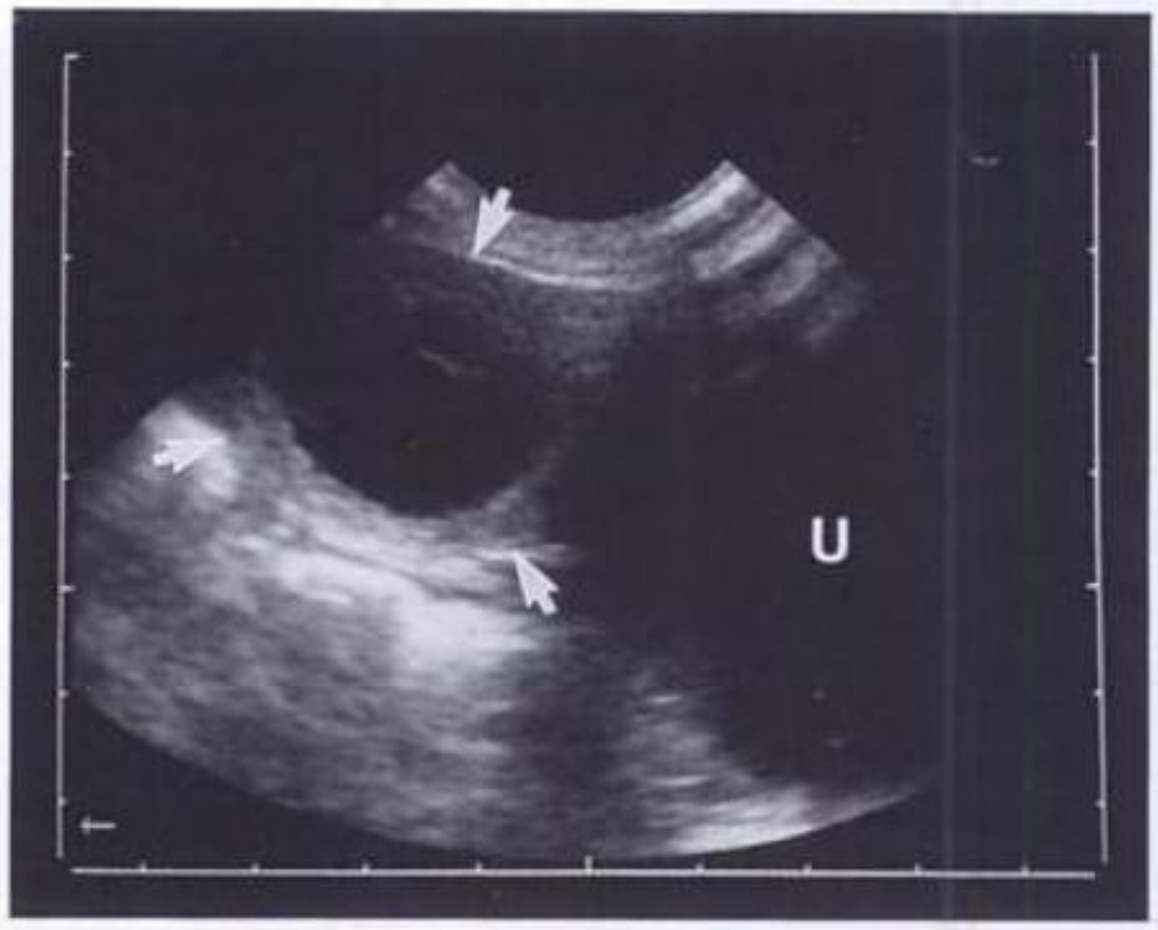


Fig. 5.4: Transcutaneous view of the urinary bladder (U) and the uterus in a bitch examined with a sector scanner on Day 28 of pregnancy. Cranial to the bladder is a conceptus (arrows).

Avtorsko zaščiteno gradivo

Downloaded From Vet-eBooks.com

In order to produce an image of the uterus the probe is positioned between the two rows of mammary glands. Its beam is directed ventro-dorsally and it is placed directly in front of the pubic bone. Following this technique it must be remembered that the image closest to the probe originate from the ventral part of the abdomen, while the portion of the image furthest removed from the probe corresponds to the tissues in the dorsal abdomen. In contrast to the situation as it is seen during transrectal scanning of cows and mares the images seen in the transcutaneous examination appear to be upside-down. During transrectal sonographic examinations the uterus usually lies close to the probe and the urinary bladder somewhat deeper. In contrast, during the transcutaneous sonographic examination of the dog and cat the urinary bladder will be closest to the transducer with the uterus in the depth of the image (Fig. 5.3). A systematic approach is essential if a thorough examination is to be obtained. The sonographic examination of the internal genitalia should proceed from caudal to cranial. First, the urinary bladder is identified inside the pelvis. It produces the typical image of a hollow, hypoechoic organ and serves as the reference point for the examination. A full urinary bladder is preferred for ultrasound examinations. The bladder is easier to find when it is full and it acts as an acoustic window, because its fluid contents will cause the relative amplification of the ultrasound passing through it and this facilitates the imaging of structures behind it. Dorsal to the urinary bladder lies the rectum. In transverse section it produces a round cross section with the surface closest to the transducer producing a bright and convex image. Due to the absorption of the sound waves by the rectal contents, an acoustic shadow usually originates behind the rectum and runs into the depth of the image.

One should attempt to find the pregnant or pathological uterus in the area of the fundus of the urinary bladder (Fig. 5.4). Using the bladder as reference point this is usually possible by moving the scanning plane from side to side. In cats, and occasionally in dogs, in dorsal recumbency the uterine horns can lie far laterally. They can then be moved into the image by moderate finger pressure onto the abdominal wall.

Avtorsko zaščiteno gradivo

Downloaded From Vet-eBooks.com

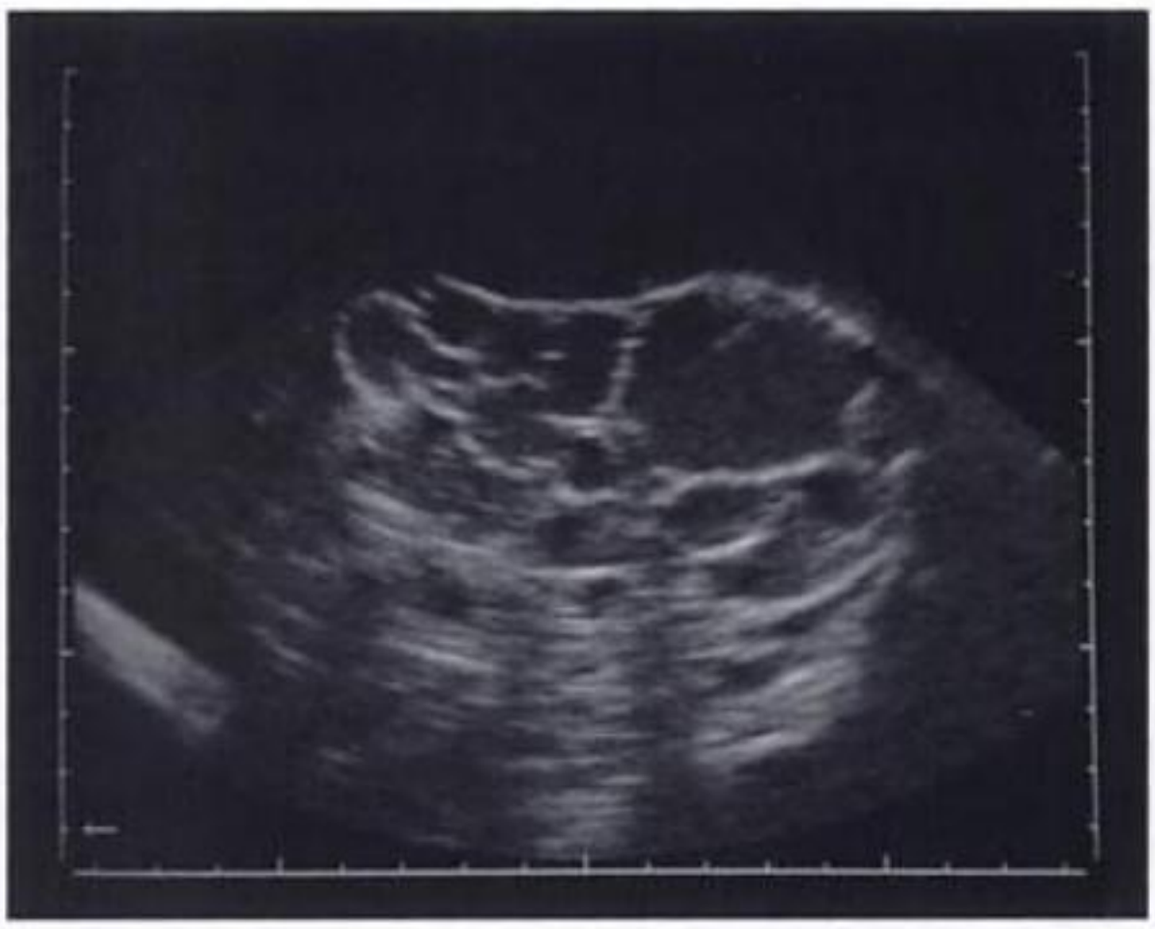


Fig. 5.5: Sonogram of a canine ovary with cystic disorder. The ovary measures 10 by 8 by 7 cm and contains numerous vesicular structures of varying sizes.



Fig. 5.6: Photograph of the sectioned ovary from Fig. 5.5 after the bitch was ovariectomized.



Fig. 5.7: Sonogram of an ovarian tumor in a cat. The enlarged ovary (arrows) exhibits the heterogenous echogenicity of mixed tumor tissue.

Avtorsko zaščiteno gradivo

Downloaded From Vet-eBooks.com

5.2 Ovarian structures in dogs and cats

With currently available ultrasound equipment, diagnostic ultrasonography of the canine and feline ovary is largely limited to the detection of pathological conditions. Follicles and corpora lutea which are normally only a few millimeters in diameters are too small to be detected reliably by conventional ultrasonography (SCHMIDT et al. 1986, PYCZAK 1990).

5.2.1 Ovarian tumors and cysts

Some pathological changes on the ovaries of dogs and cats are sonographically recognizable. Suitable indications for the use of sonography include ovarian tumors and cysts (PFOFFENBARGER and FEENEY 1986, SCHMIDT et al. 1986).

Cystic ovaries in the bitch can produce ultrasonograms which appear honeycombed in structure and contain numerous anechoic cavities (Fig. 5.5 and 5.6). The cysts vary in size, are fluid filled and separated from one another by thin, echoic walls. Some cysts may have a polygonal shape.

In one case of an ovarian tumor in a cat the enlarged ovary of heterogenous echogenicity was striking (Fig. 5.7). Large parts of the ovarian tumor were made up of hypoechoic, solid tissue. In places anechoic, fluid-filled structures were embedded in the tumor.

Avtorsko zaščiteno gradivo

Downloaded From Vet-eBooks.com

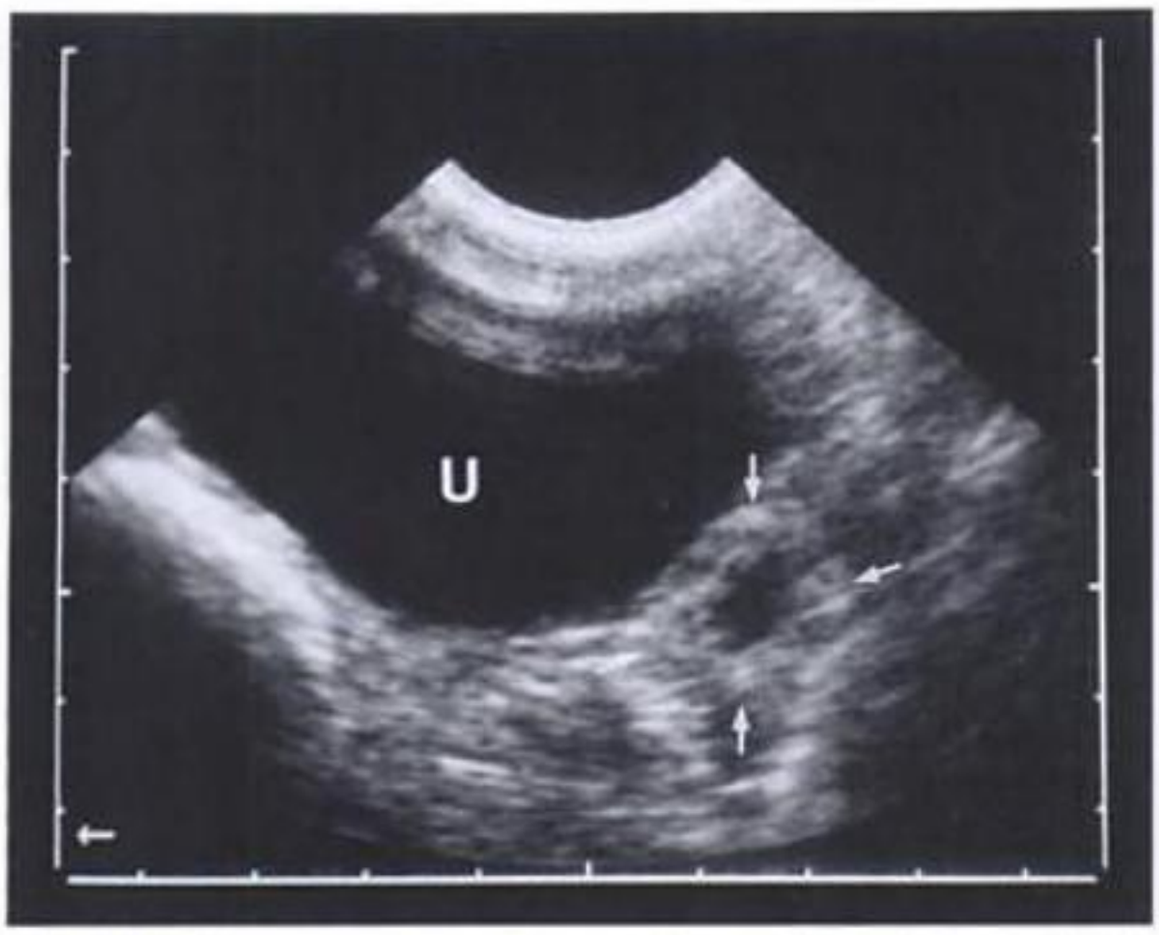


Fig. 5.8: Uterus of a bitch around Day 18 of pregnancy. The uterine wall in the vicinity of the conceptus (arrows) appears thickened and surrounds a small anechoic fluid accumulation craniodorsally (to the right in this picture) of the urinary bladder (U).

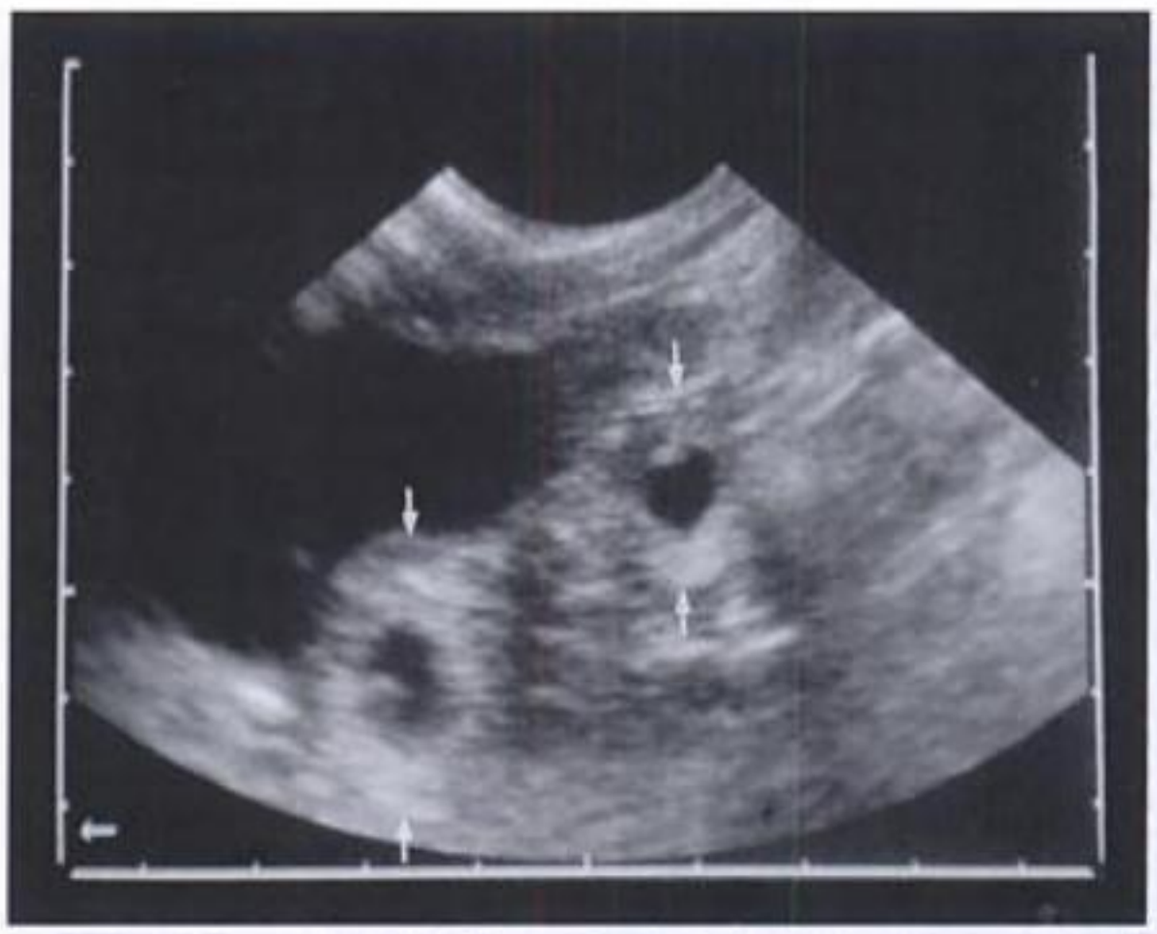


Fig. 5.9: Uterus of a bitch around Day 22 of pregnancy. Two conceptuses (arrows) lie dorsally and cranially (to the right and below in the picture) of the urinary bladder. The uterine wall surrounds anechoic fluid in which embryonic structures can be seen.



Fig. 5.10: Photograph of the excised uterus of a cat around Day 21 of pregnancy. Five spherical bulges, each containing an embryo, are present.

Avtorsko zaščiteno gradivo

Downloaded From Vet-eBooks.com

5.3 Uterine structures in dogs and cats

Important indications for sonographic examinations of dogs and cats include pregnancy diagnoses and the recognition of pathological changes of the uterus. The non pregnant, inconspicuous uterus of the dog and cat cannot reliably be depicted with the image quality of currently employed ultrasound equipment (INABA et al. 1984, SCHMIDT et al. 1986). Occasionally its sonographic image may be recognizable, but then it is difficult to distinguish with confidence between the uterine horns and the surrounding intestinal loops (DAVIDSON et al. 1986). One exception is the postpartum uterus immediately after parturition. It can be recognized on the basis of its size and the identification of its characteristic placental zones.

The sonographic features of the pregnant uterus of the dog and cat are largely the same. For that reason they will be discussed together in the following section. Particular mention will be made where important differences between the species occur.

5.3.1 Pregnant uterus

5.3.1.1 Before Day 20 of pregnancy

If high resolution ultrasound is used it may occasionally be possible to detect signs of pregnancy on the ultrasonograms of the dog and cat before Day 20 of pregnancy (Fig. 5.8). The sonographic basis for pregnancy diagnosis, however, difficult and relatively inaccurate at this stage, and is therefore not considered worthwhile in general practice (MAILHAC et al. 1980, H et al. 1986). It has been reported that hypoechoic areas of a few millimeters in diameter could be found in the regions of the developing conceptuses as early as the second week of pregnancy (BOULET 1982, CARTEE and ROWLES 1984). It is still being debated as to whether these areas represent the trophoblasts themselves or whether they are areas of edematous swellings (HOLST and PHEMISTER 1971). Also in the cat it was reported that 2 to 3 mm anechoic areas of embryonic fluid could be seen in the uterine lumen by Day 11 to 14 of pregnancy and that the echoes of the developing embryos were detectable between Days 15 and 20 (DAVIDSON et al. 1986).

5.3.1.2 Day 20 to 30 of pregnancy

From Day 20 of gestation 1 it becomes possible, under practical conditions, to diagnose a pregnancy by sonography in the bitch and the queen (MAILHAC et al. 1980, LAIBLIN et al. 1982, MAILHAC 1982, SHILLE and GONTAREK 1985, FLÜCKIGER et al. 1988).

The conceptuses which are filled with hypoechoic embryonic fluid can be seen on the ultrasound monitor (Legrand et al. 1982). They are surrounded by the echoic uterine wall (Fig. 5.9). The development of ampullae is characteristic for the stage between Days 20 and 30. At this time the ampullae of the bitch are ovoid in shape. On a longitudinal view they produce an oval image and a circular one in a transverse view. In the cat the ampullae are spherical at this stage (Fig. 5.10). When the ampullae first become visible they often do not contain any internal embryonic echoes. Usually the more caudally positioned ampullae (nearer the urinary bladder) are easier to find than those that lie in the cranial abdomen.

---

[1] In this chapter all the data on the stage of pregnancy were based on the day of parturition, as far as this was known. Day 0 = Day of partus minus 63. For the dog this approach provides the most accurate estimation of the exact gestational age under practical conditions. If it was impossible to backdate, the day of the first service or insemination was taken as Day 0.

Avtorsko zaščiteno gradivo

Downloaded From Vet-eBooks.com

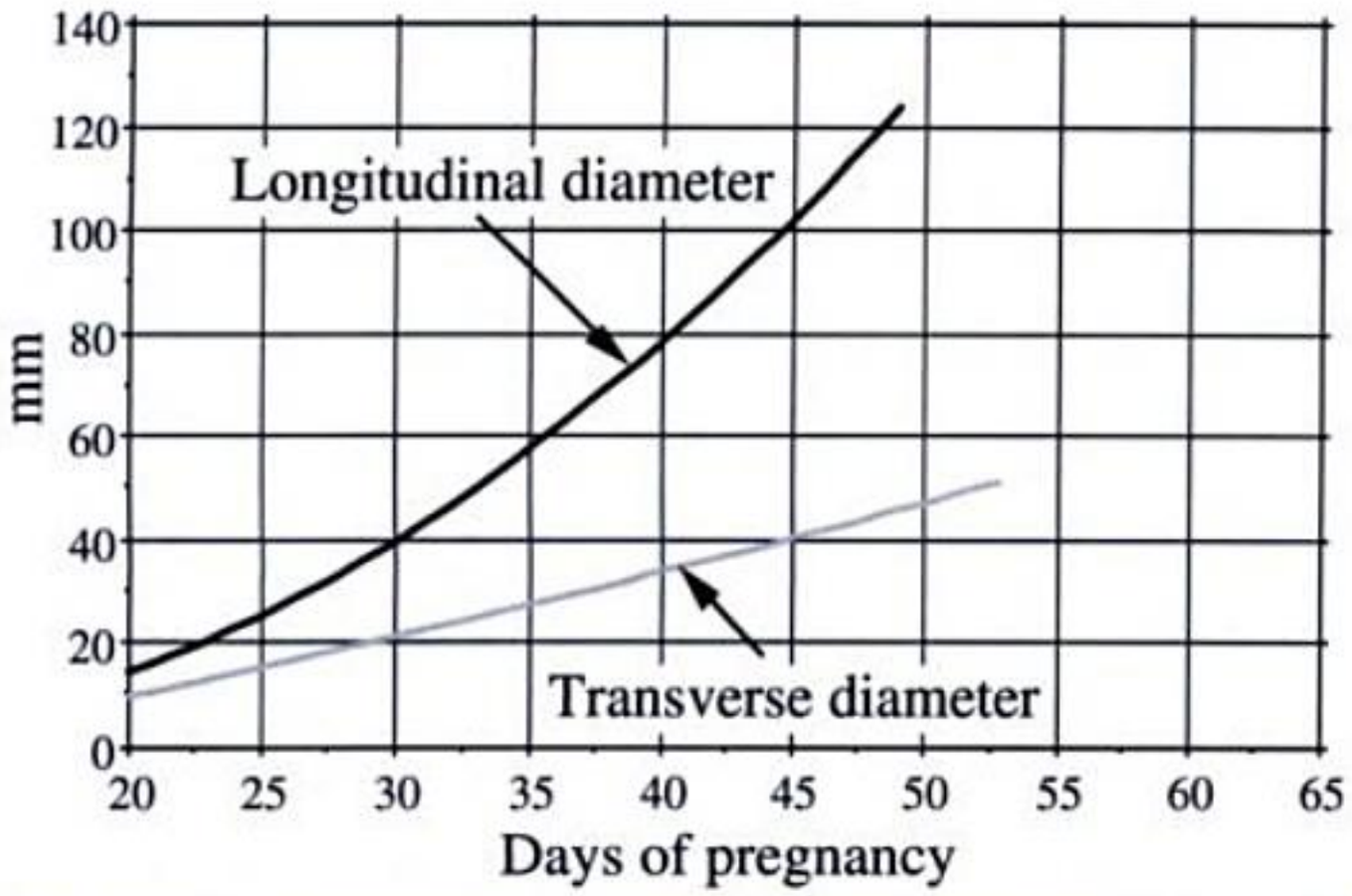


Fig. 5.11: The increases in the longitudinal and transverse diameters of embryonic and fetal vesicles during pregnancy in bitches (regressions; adapted from PYCZAK 1990).



Fig. 5.12: Transverse section through a bitch's urinary bladder with two blood vessels (arrows) running dorsally to it. Cross sections through blood vessels can be confused with conceptuses. Examination in three dimensions makes the differentiation easier by revealing the longitudinal course of blood vessels; see Fig. 5.13.

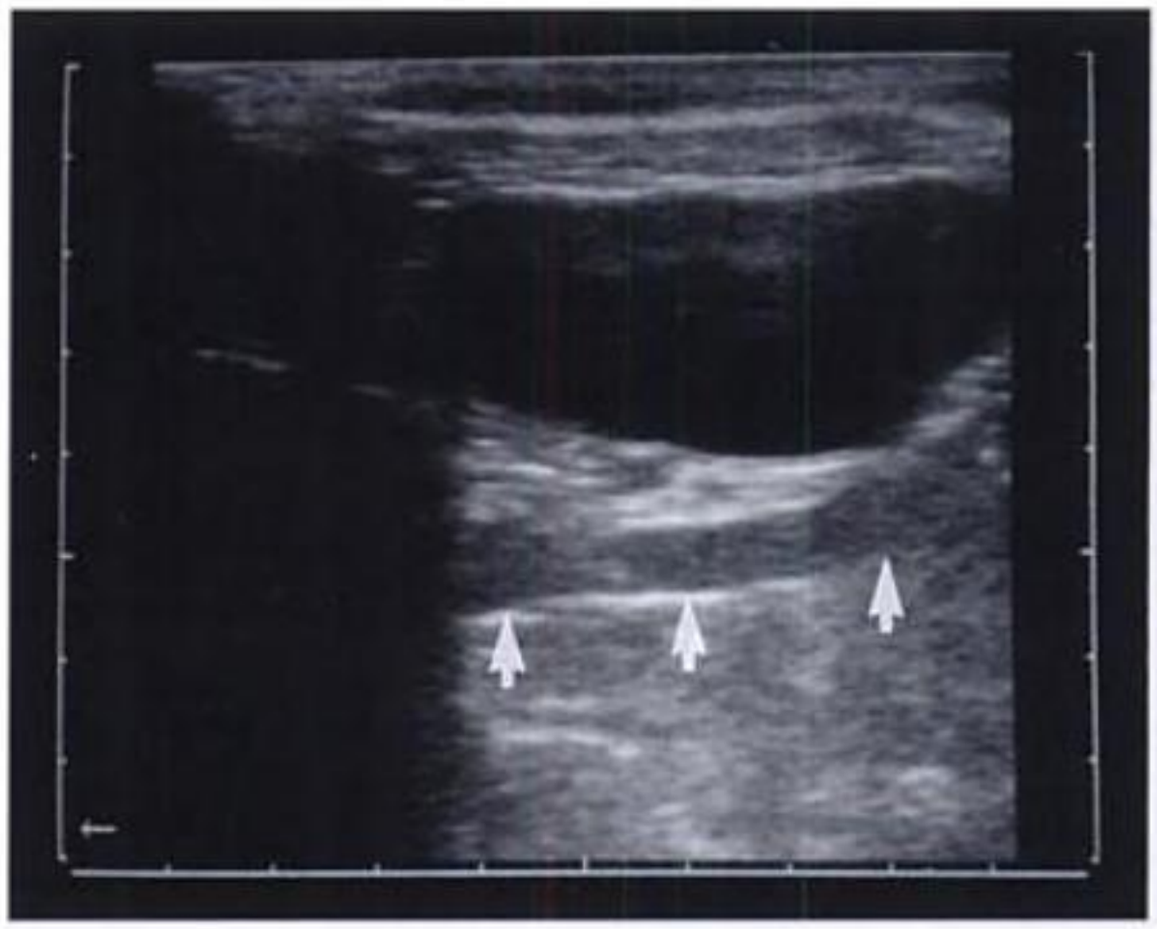


Fig. 5.13: Longitudinal section through a bitch's urinary bladder with a blood vessel (arrows) dorsally to it (see also Fig. 5.12).

Avtorsko zaščiteno gradivo

Downloaded From Vet-eBooks.com

On Day 20 the conceptuses have an inner diameter of 10 to 20 mm. In bitches they grow to a mean size of 20 by 40 mm by about Day 30 (Fig. 5.11). These sizes are meant to serve as guidelines and may vary considerably between bitches of different breeds. The conceptuses of cats have approximately the same sizes as those of bitches (MAILHAC et al. 1980).

Under practice conditions a reliable pregnancy diagnosis using 5 MHz ultrasound is possible in most cases from Day 25 of gestation (TAVERNE et al. 1985, FLÜCKIGER et al. 1988, PYCZAK 1990). Although it appears possible at an earlier stage in some cases it must be remembered that the breeding date in dogs can differ considerably from the ovulation date and it is thus difficult to accurately establish gestational age in dogs. Matings performed several days prior to ovulation can result in pregnancies. When examined ultrasonographically the conceptuses in such cases will be less developed and will not have attained the size expected based on the breeding date. This can lead to false negative diagnoses in cases where the pregnancy diagnosis is performed very early. Use of the lower frequency of 3.5 MHz or less may mean the time of the earliest possible pregnancy diagnosis can be delayed by a few days (GÜNZEL and LÜNING 1983).

In order to avoid misdiagnoses, other fluid filled bodies must be differentiated from conceptuses. In particular, blood vessels and loops of intestine that run in the vicinity of the urinary bladder must be considered. The cross sections through larger blood vessels adjacent to the uterus can appear very similar to young conceptuses (Fig. 5.12). Questionable images should be depicted in 3 dimensions in order to identify them correctly. Rotation of the transducer will reveal the longitudinal shape of a blood vessel (Fig. 5.13) and the spherical shape of a conceptus (Fig. 5.14). The pulsation of a blood vessel and the peristaltic movements in a gut loop will also aid the differentiation.

Avtorsko zaščiteno gradivo

Downloaded From Vet-eBooks.com

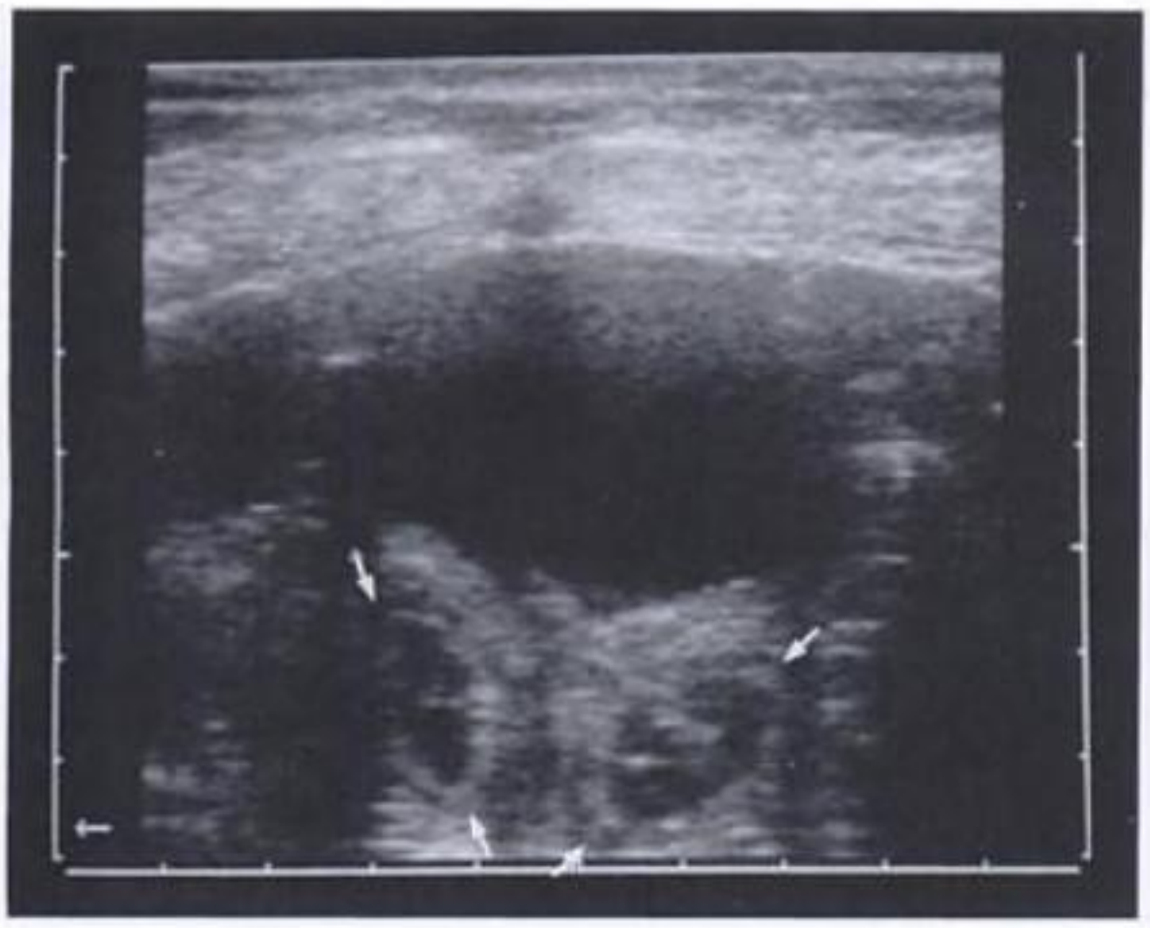


Fig. 5.14: Uterus of a bitch around Day 24 of pregnancy. Membranes of the yolk sacs can be seen inside the two embryonic vesicles (arrows) which lie dorsal to the urinary bladder (below the urinary bladder in the picture) .

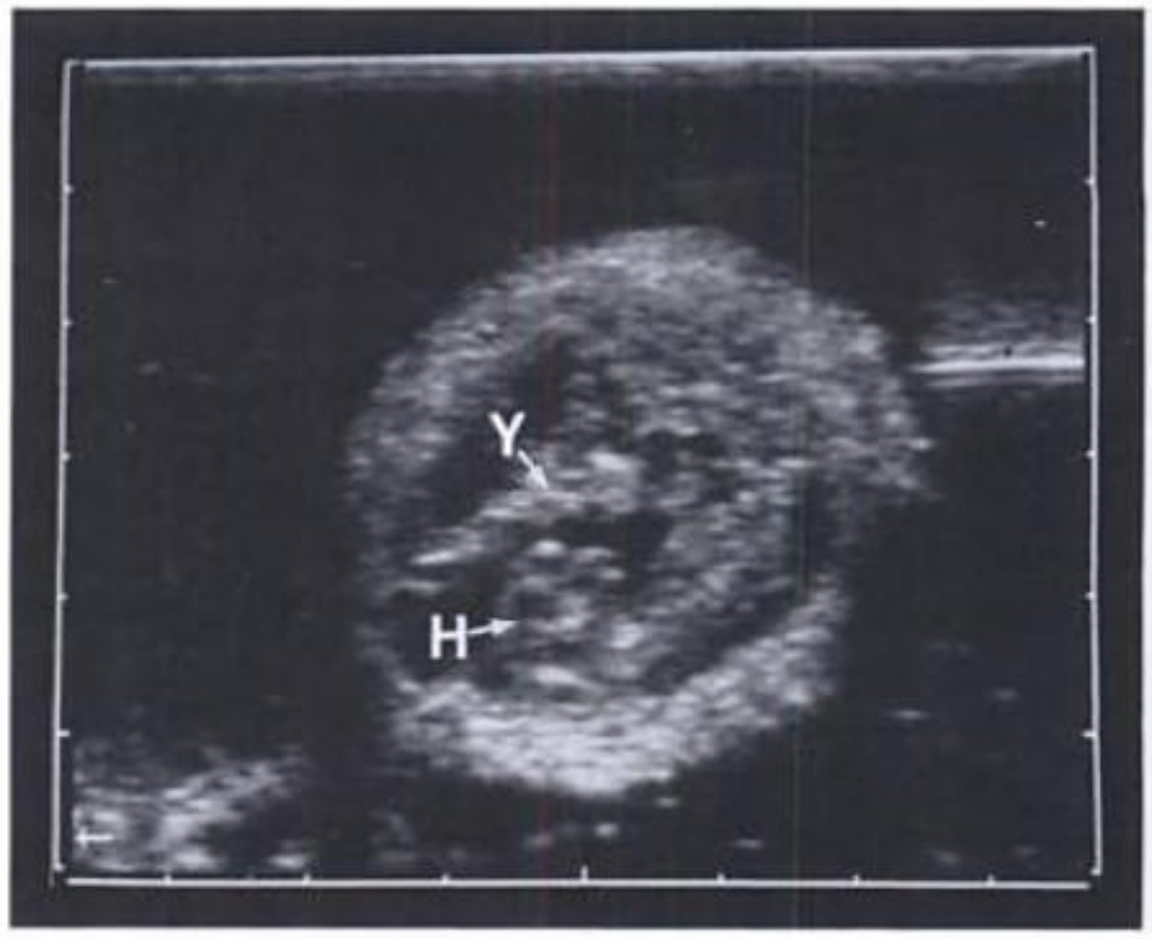


Fig. 5.15: Conceptus of a bitch around Day 27 of pregnancy. A longitudinal section of the embryo with its head (H) and its yolk sac (Y) can be seen inside the vesicle. Ultrasonogram produced in a waterbath.

Avtorsko zaščiteno gradivo

Downloaded From Vet-eBooks.com

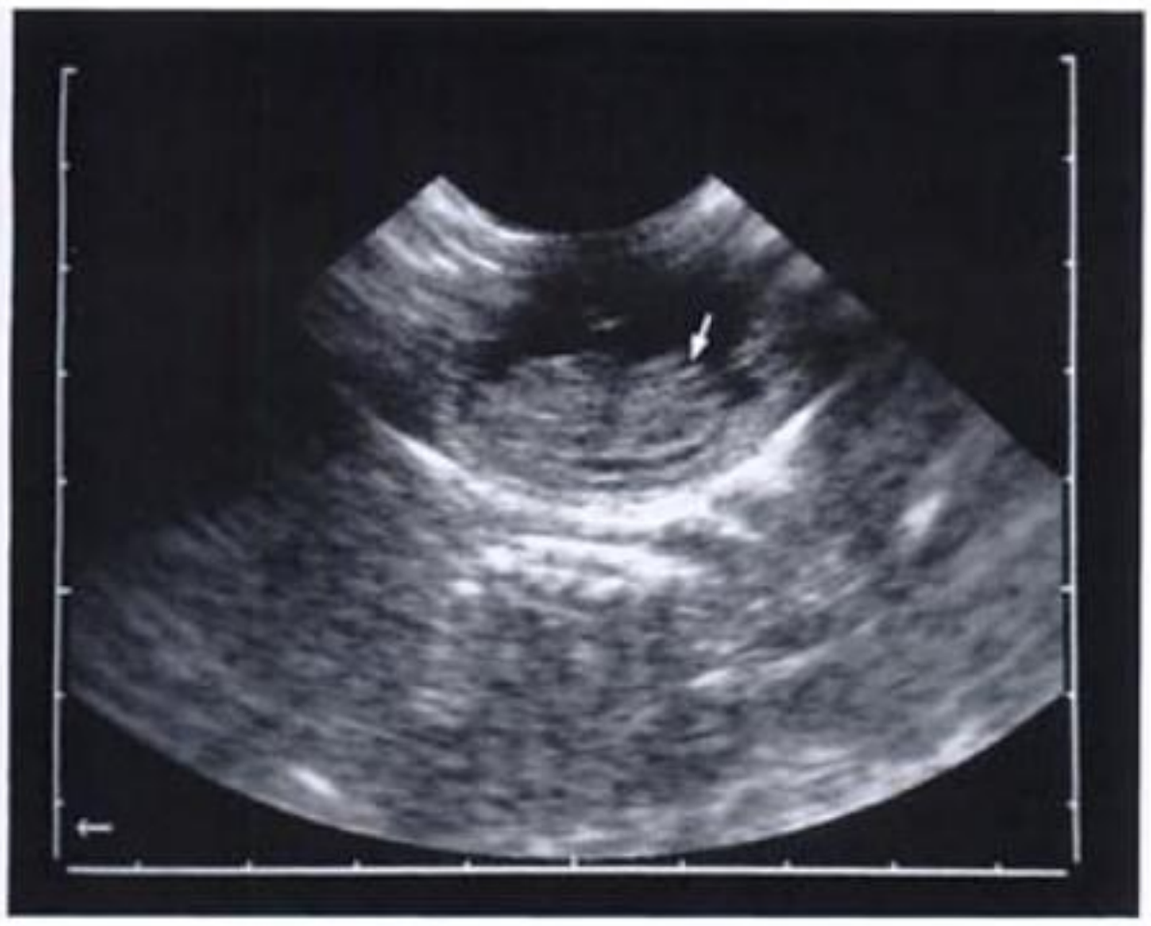


Fig. 5.16: Feline conceptus around Day 25 of pregnancy. The embryo, in longitudinal section, lies with its head (arrow) towards the right inside the vesicle. Measuring the crown-rump-length (CRL) is possible.

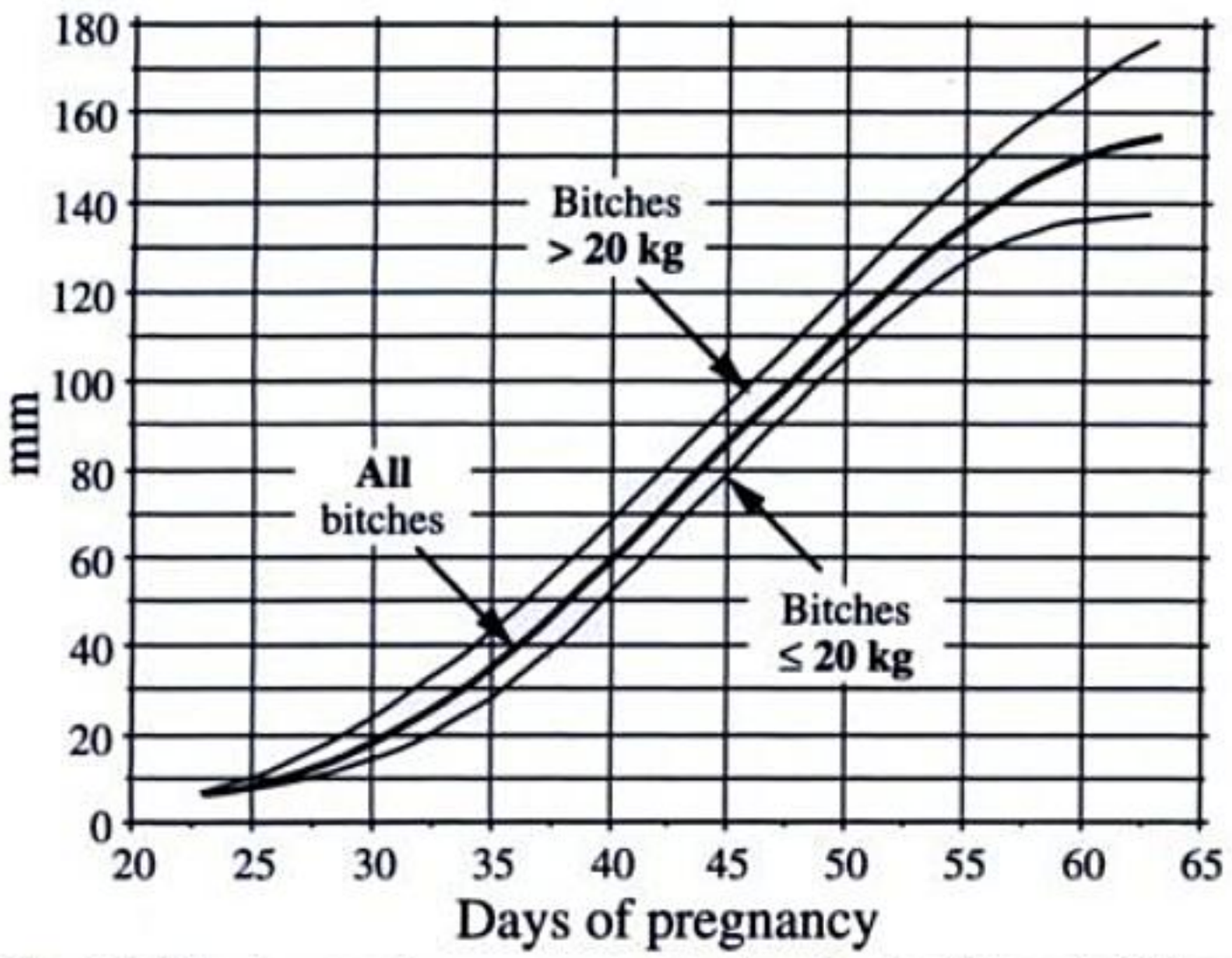


Fig. 5.17: The increase in crown-rump-lengths of canine fetuses in bitches of different body weights (regressions; adapted from PYCZAK 1990).

Avtorsko zaščiteno gradivo

Downloaded From Vet-eBooks.com

Days 25 and 30. In dogs and cats one can now start to measure the crown-rump-length of the fetuses (Fig. 5.16 and 5.17). Canine fetuses will have a CRL of between 20 and 25 mm at about Day 30 (CARTEE and ROWLES 1984). Feline fetuses will also reach a size of 20-25 mm between Days 25 and 30 (DAVIDSON et al. 1986).

5.3.1.3 Day 31 to 50 of pregnancy

At around Day 30 the fetal vesicles start to elongate and become more ovoid and elongated, both in the bitch and cat (PYCZAK 1990). The ampullary shape of the uterus starts to diminish from Day 35 -40 and changes to a more tubular shape (Fig. 5.18). This will bring about noticeable changes in the sonographic features of the pregnant uterus. From now on it will be difficult, if not impossible, to follow the string of neighbouring conceptuses on a longitudinal section of a single uterine horn. Due to the strong coiling of the uterine horns the conceptuses of both horns can now lie next to one another in unpredictable ways. Also the expansion of the individual fetal vesicles shows that their ampullary shape is disappearing (Fig. 5.19). The anechoic fluid collections around individual fetuses increases more rapidly in the longitudinal direction as compared to the cross section (Fig. 5.11). By Day 35 to 40 they reach inner transverse diameters of 25 to 35 mm and inner longitudinal diameters of 60 to 80 mm (SHILLE and GONTAREK 1985).



Fig. 5.18: Photograph of the excised uterus of a bitch around Day 35 of pregnancy. At about this time the ampullar appearance of the uterus precedes the tubular stage.

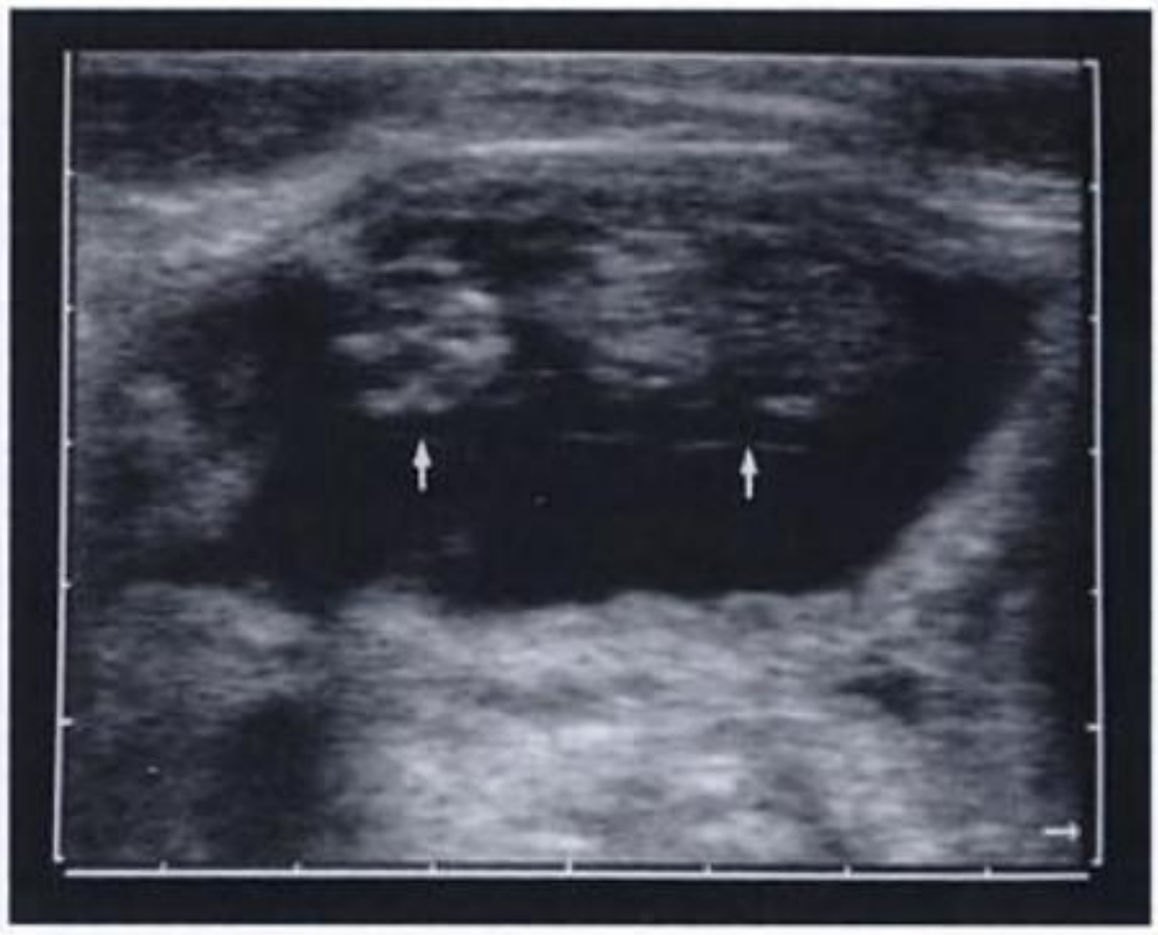


Fig. 5.19: Uterus of a bitch around Day 34 of pregnancy. The fetus, surrounded by the amniotic membrane (arrows) lies with its head towards the right inside the fetal vesicle. The conceptuses assume an oval shape at this stage.

Avtorsko zaščiteno gradivo

Downloaded From Vet-eBooks.com

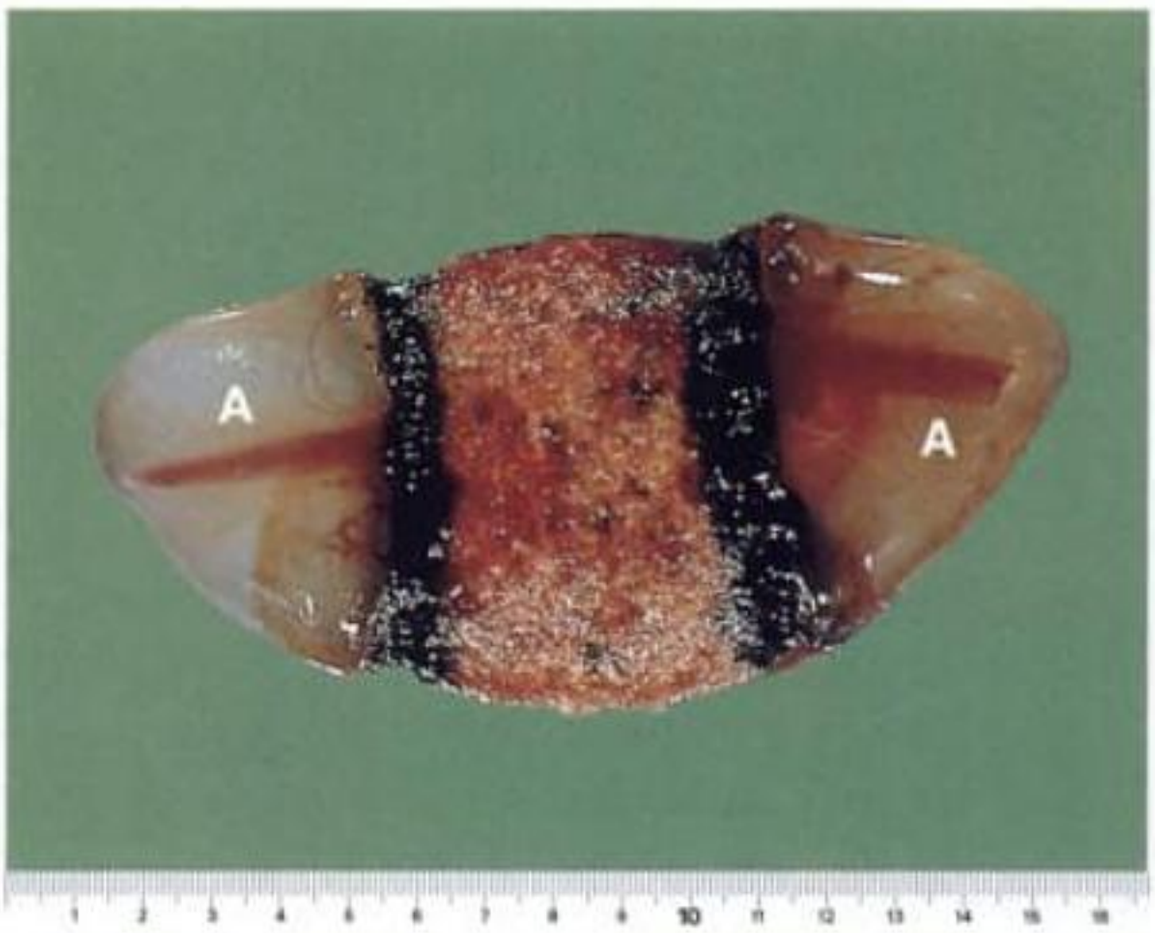


Fig. 5.20: Photograph of a conceptus that was removed from the uterus of a bitch at around Day 41 of pregnancy. The fetus, enveloped by its allantoic sac (A), is surrounded by the fetal component of the zonary placenta.



Fig. 5.21: Conceptus of a bitch around Day 35 of pregnancy. The fetus lies with its head towards the left within the zonary placenta. The edges of the placenta are curled on their margins (arrows) to result in their bowl-like shapes. Ultrasonogram produced in a waterbath.



Fig. 5.22: Conceptus of a bitch in week 5 of pregnancy. Enclosed in the zonary placenta (arrows) is the fetus (sagittal section) with its head towards the right; below it lies the yolk sac (Y).

Avtorsko zaščiteno gradivo

Downloaded From Vet-eBooks.com

Along with the longitudinal expansion of the fetal sacs the zonary placenta become apparent (Fig. 5.20). In the middle of the vesicle the zonary placenta forms a cylinder surrounding the embryo or fetus. It is seen as a finely granular structure of moderate echogenicity (Fig. 5.21). While the placenta occupies virtually the entire surface area of the fetal membranes during the early ampullary stage it now only covers the central area of each conceptus after Day 30. Through their elongation the vesicles' ends remain free of placenta. In these areas the uterine wall appears thin. Over almost its whole width the zonary placenta lies closely adherent to the endometrium. Only near their edges the zonary placenta curl away from the endometrium and project slightly into the uterine lumen. On longitudinal ultrasound images of the uterine horns the zonary placenta with their bowl-shaped edges can be recognized. The placenta is thicker than the uterine wall.

The fetuses are suspended inside their surrounding zonary placenta (Fig. 5.22). The yolk sac also lies within the zonary placenta. It is well developed in the dog and remains present until the end of pregnancy. On longitudinal sections through the uterus it can be seen as an extended, echoic tube. It extends over almost the entire length of the conceptus and thus reaches beyond the ends of the placental bands.

From Day 30 of gestation the contours of the fetuses become discernible (Fig. 5.22). The head and rump can be distinguished and the limbs are visible as echoic buds. If it is possible to observe individual fetuses for some time one will already be able to see some active fetal movements (GÜNZEL and LÜNING 1983, CARTEE and ROWLES 1984).

From Day 35 to 40 organogenesis in canine and feline fetuses has progressed so far that one can recognize developing organs inside their bodies. Inside the

Avtorsko zaščiteno gradivo

Downloaded From Vet-eBooks.com

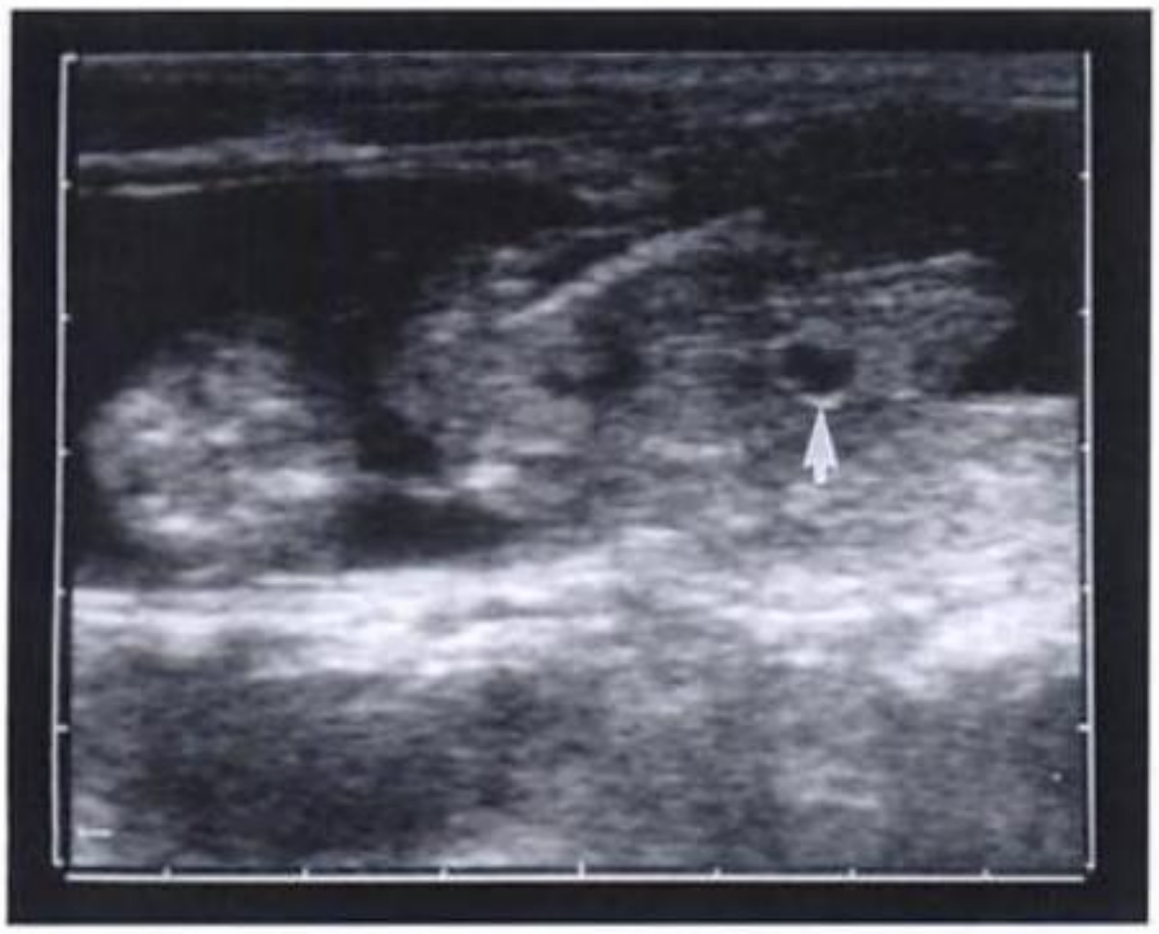


Fig. 5.23: Horizontal section through a fetus of a bitch around Day 41 of pregnancy. The head lies on the left. Caudally to the hyperechoic rib cross sections of the left thoracic wall lies the anechoic lumen of the stomach (arrow).



Fig. 5.24: Horizontal section through a canine fetus around Day 46 of pregnancy. The curved echo of the diaphragm outlines that of the liver. The anechoic area in the caudal abdomen represents the urinary bladder. Ultrasonogram produced in a waterbath.

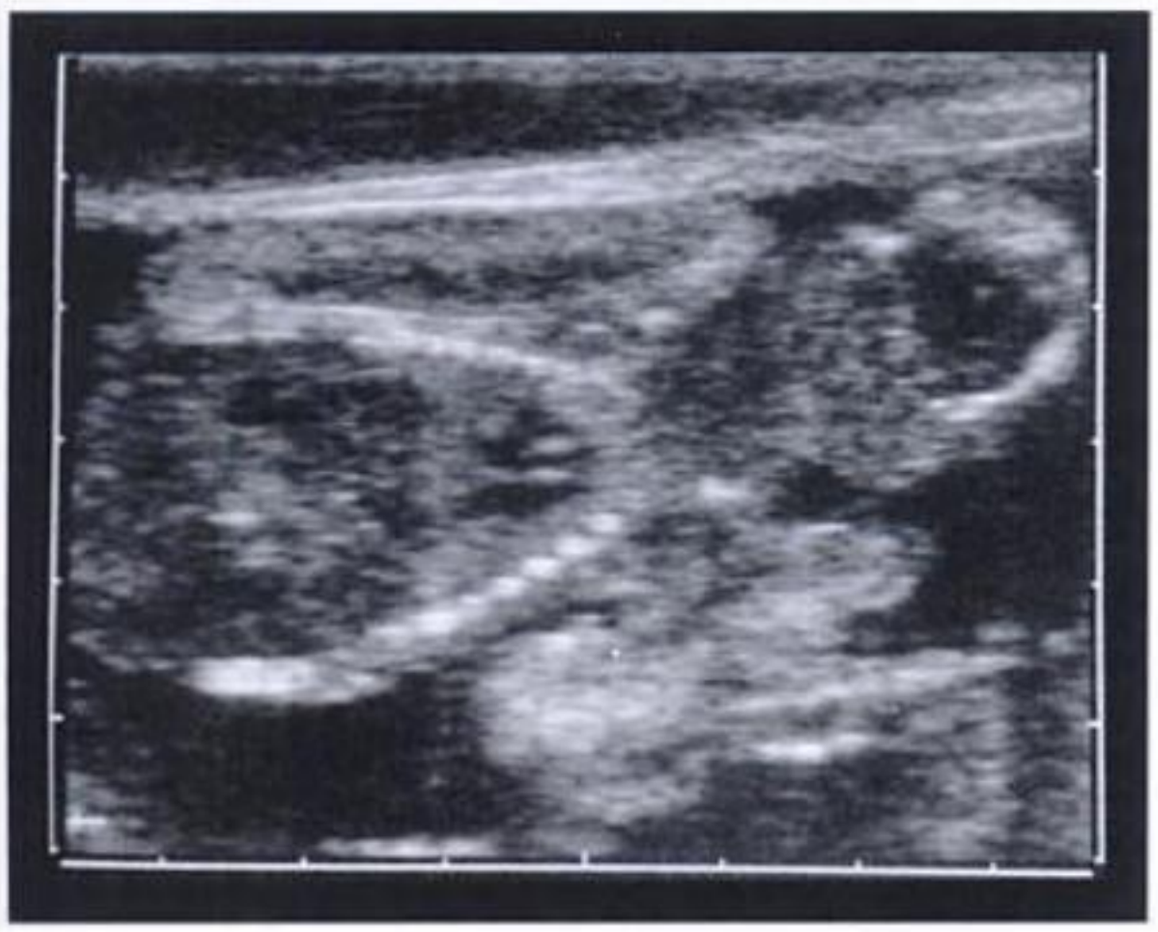


Fig. 5.25: Horizontal section through a canine fetus around Day 46 of gestation. The hyperechoic rib cross sections of the two halves of the thorax form a cone shaped pattern. Anechoic heart chambers can be seen in the apex of the thorax.

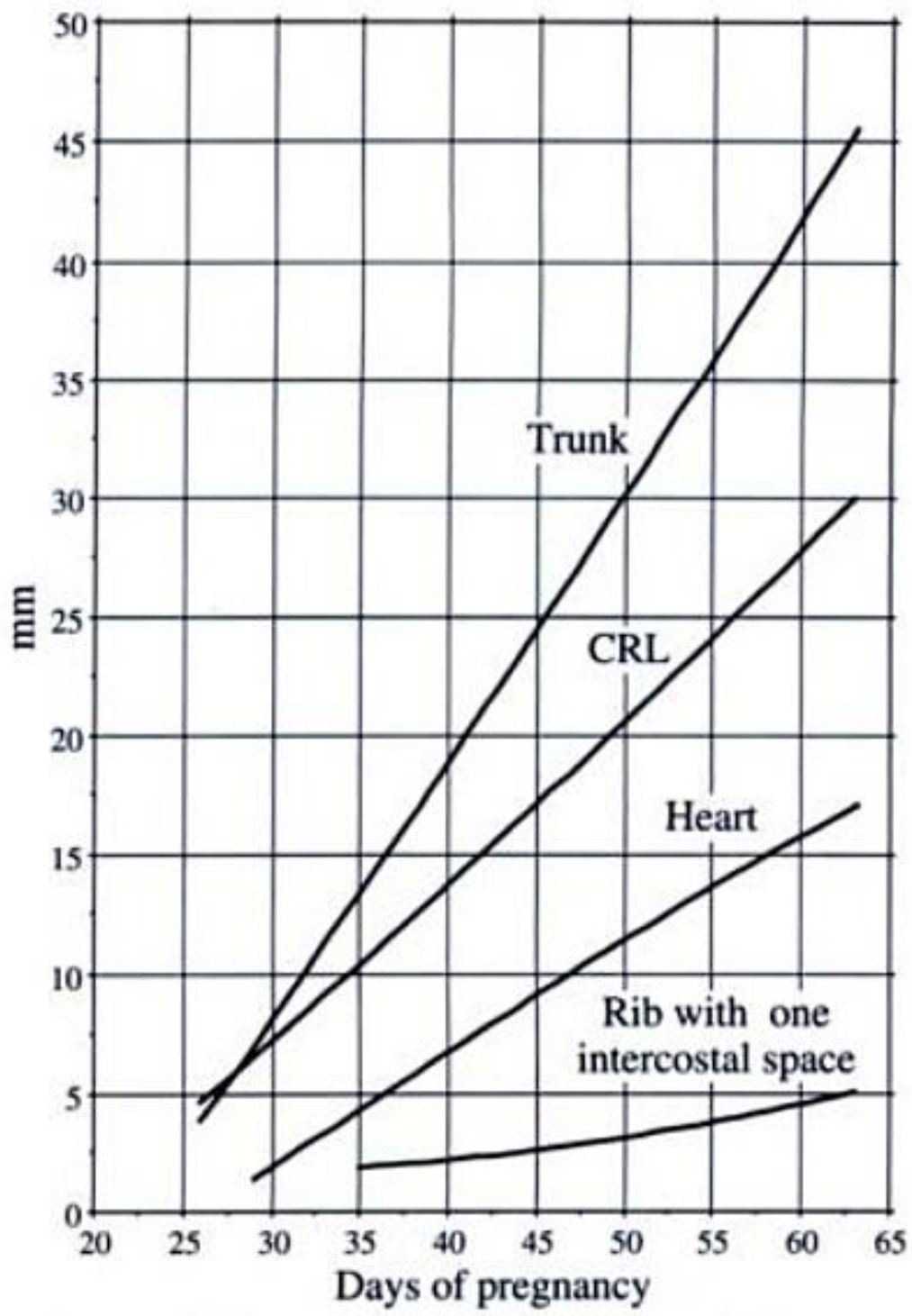


Fig. 5.26: The increases in trunk, biparietal and cardiac diameters as well as the length of one rib cross section and one intercostal space in canine fetuses during pregnancy (regressions; adapted from PYCZAK 1990).

Avtorsko zaščiteno gradivo

Downloaded From Vet-eBooks.com

abdomen the large dark area of the stomach is easily identified (BONDESTAM et al. 1983, INABA et al. 1984, NOMURA 1984). The liquid gastric contents are largely anechoic (Fig. 5.23). Next to it lies the moderately echoic area of the liver. The next, smaller anechoic area in the caudal abdomen is that of the urinary bladder (Fig. 5.24). The onset of mineralization of the bones increases their echogenicity from Day 35 to 45. The facial bones (Fig. 5.19, 5.21, 5.22) and the discs of the vertebrae and rib cross sections (Fig. 5.25) are the first to become visible. Initially the sound absorption by the developing bones is so minor that no echo shadows are created in their backgrounds.

Both body halves need to be scanned very carefully if the litter size of a bitch is to be determined by ultrasonography. Counting the number of fetuses and assigning each fetus to a specific uterine horn is difficult on a sagittal examination plane. The transverse section is more suitable to ensure an optimal orientation and a clear distinction between the uterine horns. By tipping the transducer from the left to the right side and back it is possible to view both sides virtually simultaneously. If the transverse view is maintained and the transducer is rotated from cranial to caudal, the number of fetuses can be counted most accurately. By continuously, yet slowly, moving the transducer one fetus after the next will come into view. Even with this procedure errors occur. The number of expected pups can only be determined with reasonable accuracy in small litters (BONDESTAM et al. 1984). In general, the accuracy of the fetal count decreases with increasing litter size (BONDESTAM et al. 1983, SHILLE and GONTAREK 1985, TOAL et al. 1986).

In dogs it is also possible to assess the development of the conceptuses and the gestational age by fetometry (Fig. 5.26). Thus far data have been collected for the following parameters: Crown-rump-length and biparietal, abdominal and cardiac diameters, as well as the size of one rib cross section with one intercostal space (CARTEE and ROWLES 1984, PYCZAK 1990). The ultrasonographically measured crown-rump-lengths largely correspond to those obtained after removal of the fetuses from the uterus (EVANS and SACK 1973). The established values represent average sizes for different breeds of dogs. They are intended as guide line values and can vary considerably with the breed of the individual bitch. Separating the data for large (› 20 kg) and small (20 kg) bitches shows distinct differences with regard to the growth in length of the fetuses. For example, the length of fetuses of large breeds will be about 70 mm on the Day 40 of gestation which is 15 mm more than the corresponding value of 55 mm for small dogs. As the use of ultrasonography spreads, it is anticipated that more exact data on the fetal growth of dogs and cats of the various breeds will become available. Fetal diagnostics, and with them the determination of gestational age, will then become a great deal more refined in dogs.

Very little data is available on the crown-rump-length of feline fetuses (CHRISTIANSEN and SCHMIDT 1982). They have a mean length of about 3.5 cm on Day 35, 6.5 cm on Day 40, 8.0 cm on Day 45, 10 cm on Day 50 and 11.5 cm on Day 55.

Avtorsko zaščiteno gradivo

Downloaded From Vet-eBooks.com



Fig. 5.30: Embryonic death in a bitch around Day 22 of pregnancy. The pear shape of the conceptus to the right of the urinary bladder is evident.

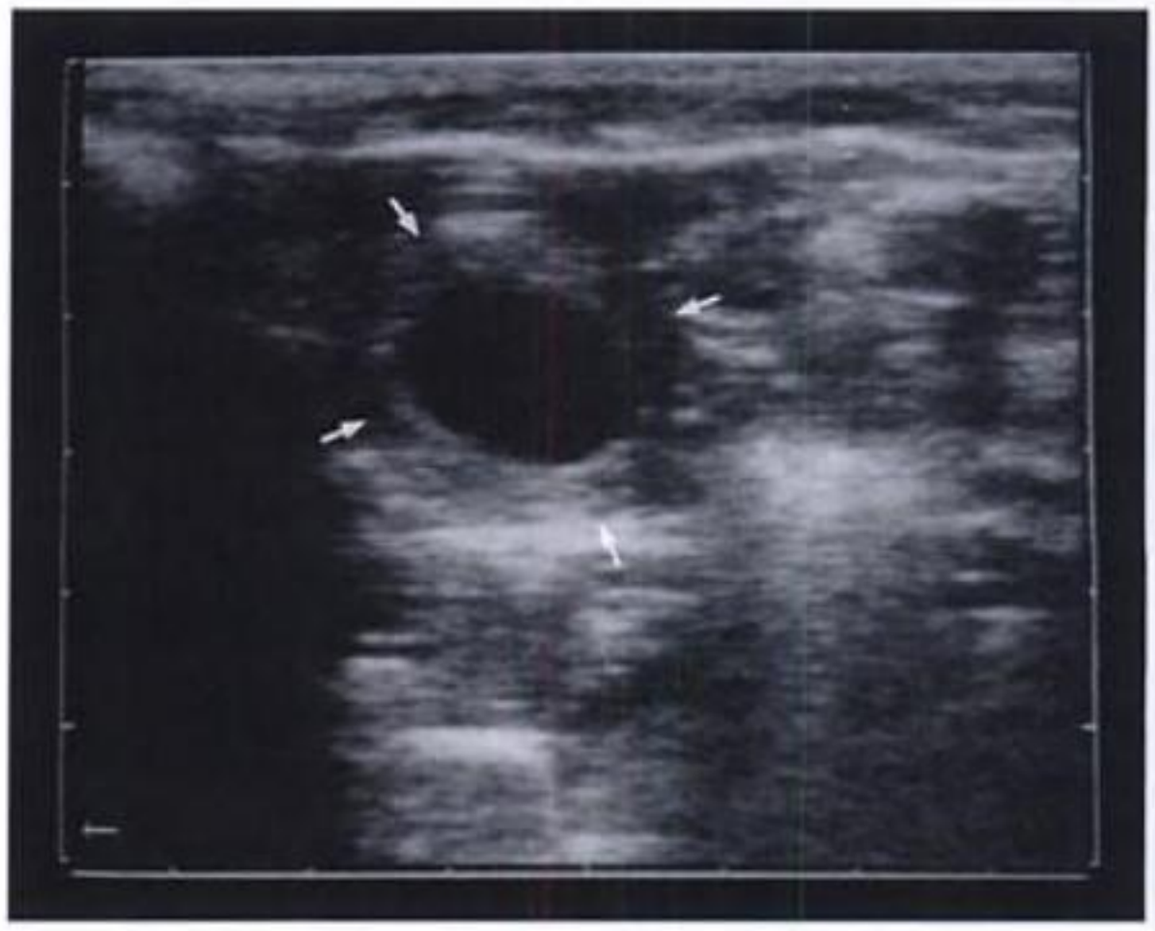


Fig. 5.31: Embryonic death in a bitch around Day 26 of pregnancy. No embryonic structures could be found inside the embryonic vesicle (arrows). Four other conceptuses did contain embryonic echoes; four live pups were born.

Avtorsko zaščiteno gradivo

Downloaded From Vet-eBooks.com

5.3.2 Uterine pathology

5.3.2.1 Embryonic death

Occasionally an embryonic mortality can be sonographically observed in a bitch (TAVERNE et al. 1985). The resulting resorptions may involve individual conceptuses or the entire litter. Ultrasound examination during the ampullary stage of early gestation reveals that the conceptuses usually have a spherical to ovoid shape. In some cases of embryonic resorptions it was noticed that some embryonic vesicles developed different shapes. Some of them were obviously more flat, appeared flaccid and they became irregular in shape, occasionally developing pointed ends (Fig. 5.30). Such vesicles were also smaller than the neighboring, live ones or was to be expected based on the mating date.

Apart from the above, conceptuses at Day 25 to 35 have been seen to contain no or only small internal embryonic echoes (Fig. 5.31). When such abnormally shaped or sized conceptuses as well as conceptuses without internal embryonic echoes were followed during the further course of the pregnancy they were seen to become progressively smaller until they eventually disappeared. In those cases where an embryonic death had been diagnosed in most cases it only affected single conceptuses; the remainder of the litter continued to develop uneventfully.

Avtorsko zaščiteno gradivo

Downloaded From Vet-eBooks.com



Fig. 5.32: Pyometra in a bitch. The uterine lumen is dilated to several centimeters. Due to the very tortuous nature of the uterine horns the ultrasound beam hit several wall sections (arrows). The uterus appears partitioned.



Fig. 5.33: Photograph of an excised pyometra of a bitch. The uterus shows pseudoampullar dilations.

Avtorsko zaščiteno gradivo

Downloaded From Vet-eBooks.com

5.3.2.2 Pyometra, endometritis, cystic glandular hyperplasia

An important indication for ultrasonography in bitches and cats is the detection of pathological conditions of the uterus. These include pyometra, endometritis and cystic glandular hyperplasia and their transitional forms.

The recognition of markedly fluid-filled pyometras in bitches and cats is easy (SCHMIDT et al. 1986, PYCZAK 1990). In well developed pyometras the accumulated fluid leads to severe distention of the uterus (Fig. 5.32). Frequently, the uterus does not produce an image of a long, fluid filled tube, but rather shows thin sections of uterine wall appearing inside the fluid at irregular intervals and creating a compartmentalized image of the uterus. This image originates from the severe twisting in the uterine horns, sections of which, sometimes completely kinked, come to lie close together. The echogenicity of the pyometra exudate varies between almost anechoic and moderately echoic (KOMAREK 1986, PFOFFENBARGER and FEENEY 1986). It primarily depends on the degree of cellularity of the exudate. From a differential diagnostic point of view the pyometra must be differentiated from the hemometra. The ultrasonogram is not of much help when making the differentiation. The clinical examination has to provide the conclusive decision in these cases (SCHMIDT et al. 1986).

Pyometras with ampullary dilations of the uterine horns can also be found. These pseudoampullae can be single or multiple and uni- or bilateral (Fig. 5.33). Pyometras with these ampullary dilations can be confused with early pregnancies (PYCZAK 1990). When attempting to differentiate between the two the presence of embryonic or fetal echoes inside the fluid will support a positive pregnancy diagnosis.

Avtorsko zaščiteno gradivo

Downloaded From Vet-eBooks.com

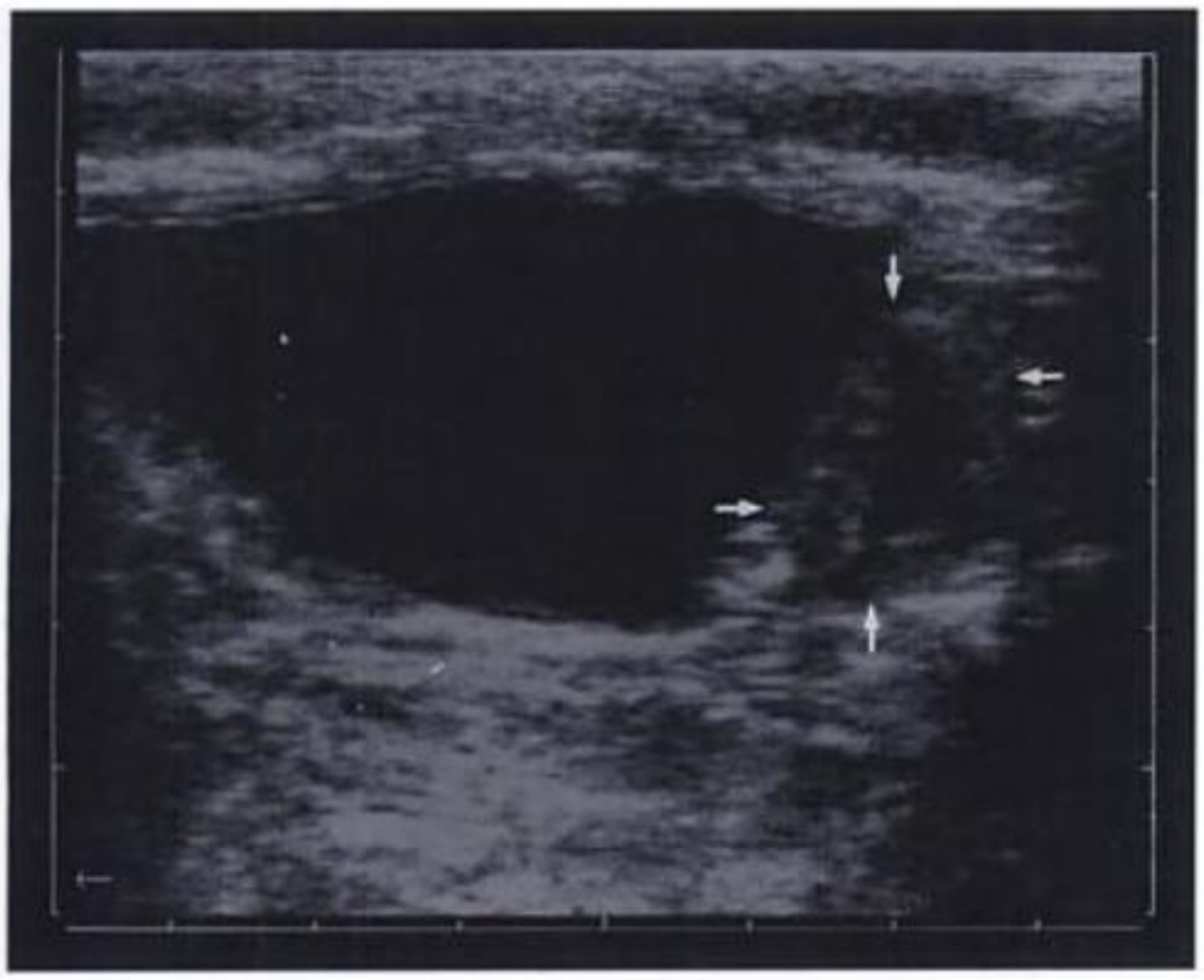


Fig. 5.34: Transverse section through the pelvic area of a bitch suffering from endometritis. A cross section through a uterine horn (arrows) is seen next to the urinary bladder. The horn has a thickened wall and contains a small amount of exudate.

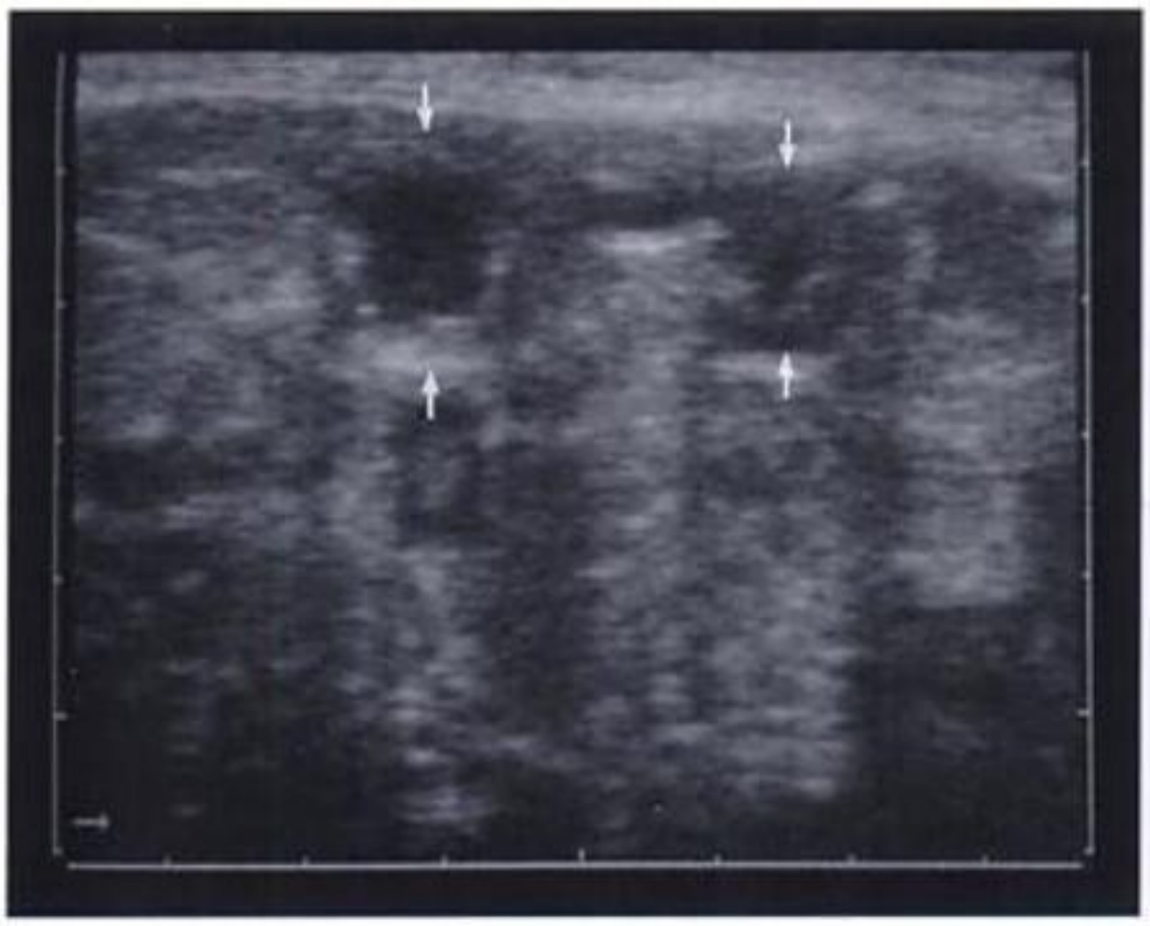


Fig. 5.35: Ultrasonogram of a bitch showing gut loops (arrows) filled with watery contents. The fluid filled intestine must be differentiated from a uterus affected by inflammatory changes.



Fig. 5.36: Cystic glandular hyperplasia of the endometrium. A longitudinal section through one uterine horn (arrows) shows moderate, hypoechoic changes in its wall.

Avtorsko zaščiteno gradivo

Downloaded From Vet-eBooks.com

References to chapter 5

BONDESTAM, S., I. ALITALO and M. KÄRKKÄINEN (1983): Real-time ultrasound pregnancy diagnosis in the bitch. J. small Anim. Pract. 24, 145–151.

BONDESTAM, S., M. KÄRKKÄINEN, I. ALITALO and M. FORSS (1984): Evaluating the accuracy of canine pregnancy diagnosis and litter size using real-time ultrasound. Acta vet. scand. 25, 327–332.

BOULET, D. (1982): Application de l'échographie au diagnostic de gestation chez la chienne Braque de Weimar. Bull. Acad. vét. Fr. 55, 229–232.

CARTEE, R. E. and T. ROWLES (1984): Preliminary study of the ultrasonographic diagnosis of pregnancy and fetal development in the dog. Am. J. vet. Res. 45, 1259–1265.

CHRISTIANSEN, J. og M. SCHMIDT (1982): Aldersbestemmelse af fostre hos hund og kat. Nord. Vet. Med. 34, 354–361.

DAVIDSON, A. P., T. G. NYLAND and T. TSUTSUI (1986): Pregnancy diagnosis with ultrasound in the domestic cat. Vet. Radiol. 27, 109–114.

EVANS, H. E. and W. O. SACK (1973): Prenatal development of domestic and laboratory mammals: Growth curves, external features and selected references. Zentbl. Vet. Med. Reihe C 2, 11–45.

FLÜCKIGER, M., P. KRAMERS, U. HIRT, K. HUTER-WISSLER und S. ARNOLD (1988): Früherfassung der Trächtigkeit bei der Hündin. J. vet. Med. A 35, 450–454.

GÜNZEL, A.-R. und I. LÜNING (1983): Zur echographischen Trächtigkeitserkennung mit dem VETOSCAN Ultraschallgerät – Möglichkeiten und Grenzen des Einsatzes bei der Hündin. Dtsch. tierärztl. Wschr. 90, 440–443.

HOLST, P. A. and R. D. PHEMISTER (1971): The prenatal development of the dog: Preimplantation events. Biol. Reprod. 5, 194–206.

INABA, T. N. MATSUI, R. SHIMIZU and T. IMORI (1984): Use of echography in bitches for detection of ovulation and pregnancy. Vet. Rec. 115, 276–277.

JOHNSTON, S. D., F. O. SMITH, N. C. BAILIE, G. R. JOHNSTON and D. A. FEENEY (1983): Prenatal indicators of puppy viability at term. Comp. on Continuing Education 5, 1013–1026.

KOMAREK, J. V. (1986): Die sonographische Diagnose einer Pyometra beim Hund. Kleintier-Prax. 31, 297–298.

LAIBLIN, C., S. SCHMIDT und J. W. DUDENHAUSEN (1982): Erste Erfahrungen mit dem ADR-Real-Time-Scanner zur Trächtigkeitsdiagnose bei Schaf, Schwein, Hund und Katze. Berl. Münch. tierärzl. Wschr. 95, 473–476.

LEGRAND, J. J., B. CARLIER, I. BERTRAND et P. F. VIARD (1982): Images échographiques de l'anatomie abdominale des carnivores domestiques. Bull. Acad. vét. Fr. 55, 223–228.

MAILHAC, J. M. (1982): Diagnostic de gestation chez la chatte par échographie. Bull. Acad. vét. Fr. 55, 233–236.

MAILHAC, J. M., S. CHAFFAUX, J. J. LEGRAND, B. CARLIER et F. HEITZ (1980): Diagnostic de la gestation chez la chatte: utilisation de l'échographie. Recl. Méd. vét. Éc. Alfort 156, 899–907.

NOMURA, K. (1984): Pregnancy diagnosis by a real-time ultrasound scanner in bitches. J. Jap. vet. med. Ass. 37, 140–144.

POFFENBARGER, E. M. and D. A. FEENEY (1986): Use of gray-scale ultrasonography in the diagnosis of reproductive disease in the bitch: 18 cases (1981–1984). J. Am. vet. med. Ass. 189, 90–95.

PYCZAK, T. (1990): Einsatzmöglichkeiten der Sonographie in der gynäkologischen und geburtshilflichen Diagnostik bei Hund und Katze. Vet. med. Diss., München.

SCHMIDT, S., D. SCHRAG und B. GIESE (1986): Ultraschalldiagnostik in der Gynäkologie beim Kleintier. Tierärztl. Prax. 14, 123–141.

SHILLE, V. M. and J. GONTAREK (1985): The use of ultrasonography for pregnancy diagnosis in the bitch. J. Am. vet. med. Ass. 187, 1021–1025.

TAVERNE, M. A. M., A. C. OKKENS and R. VAN OORD (1985): Pregnancy diagnosis in the dog: a comparison between abdominal palpation and linear-array real-time echography. The Veterinary Quarterly 7, 249–255.

TOAL, R. L., M. A. WALKER and G. A. HENRY (1986): A comparison of real-time ultrasound, palpation and radiography in pregnancy detection and litter size determination in the bitch. Vet. Radiol. 27, 102–108.

Avtorsko zaščiteno gradivo

Downloaded From Vet-eBooks.com

Subject index

Numbers indicate text pages, *italic numbers* indicate figures with a certain subject. **Letters** before the numbers indicate the species: **E** = Equine, **B** = Bovine, **OC** = Ovine and Caprine, **P** = Porcine, **CF** = Canine and Feline.

A
Abortion **E** 71,
Accessibility **E** 65, *1.90*, **B** 173,
Allantochorion **E** 51, **B** 119f, *2.73*, *2.99*, **OC** *3.28*,
Allantoic
— fluid **E** 49f, 75, **B** 133, *2.101f*, 167, *2.163*,
— sac **E** 49f, *1.63*, **B** *2.73*, 121, *2.80*,
Allantois **E** 49, *1.61f*, *1.74*, **B** 121, *2.79f*, 133, 167, *2.163*, **CF** *5.20*,
Amnion **E** 77, **B** *2.9f*, 121, 127, *2.89f*, 133, 167, *2.163*, **OC** 201, *3.20*, *3.28*, **P** 219,
Amniotic
— fluid **E** 75, **B** 133, *2.101f*, 167, *2.163*,
— sac **OC** 197, **P** *4.16*,
A mode ultrasound see ultrasound, A mode
Ampullae **CF** 233, *5.8f*, 239,
Anestrus **E** 41,
Aorta, abdominal see fetus, aorta, abdominal
Artifact 15, 85,
Artery, carotid see fetus, artery, carotid
— umbilical see fetus, artery, umbilical

B
Biparietal diameter **OC** 203, *3.25*, **CF** 243,
Blastocyst **E** 43,
Brain see fetus, brain

C
Caruncle **B** 139, *2.108f*, **OC** *3.17*, 205,
Catheter, ballooned 47, *1.60*,
Cervical rings **B** 85, *2.8*,
Cervix **E** 13, 43, **B** 85, *2.8*, 115, **P** 219, *4.13*, **CF** *5.3*,
Cesarian section **CF** 245,
Chorion **E** 53, **B** 119f, **OC** 197,
Clipping **E** 13, **OC** 187, **CF** 227,
Clitoris see fetus, clitoris
Colon **E** 13, *1.7*, **P** 213,
Conceptus **E** 43f, *1.52f*, 69, 79, **B** 119f, *2.73f*,
— mobility **E** 45, 55, 79,
— growth **E** 45f, *1.55*, **B** 123f,
Convex scanner 83, 187, 227,
Corpus
— albicans **B** 97,
— hemorrhagicum **E** 29f, *1.27f*, **P** 215,
— luteum **E** 25f, *1.21f*, **B** *2.5*, 95f, *2.25f*, 109, *2.54*, **OC** 191, *3.5f*, **P** 215, *4.4f*,
— — accessory **E** 31f,
— — growth **B** 97, 103f, *2.43f*,
— — of pregnancy **E** 27, 31, *1.29f*, **B** 97, *2.33*, *2.37*, 101f, *2.42f*, **P** *4.7*,
— — persisting **OC** 209,
— — regressing **E** 25, *1.22f*, **B** *2.32*,
— — shape **E** 25, **B** 95,
— — size **B** 97, 103f, *2.43f*,
— — with cavity **B** *2.11f*, 91, 95f, *2.27f*, 109, *2.57f*, **OC** 191, *3.6*,
— — — growth **B** 103f, *2.43f*,
— — — incidence **B** 103f, *2.41f*,
Cotyledon **OC** *3.28*,
Coupling gel 11, 189,
Crown rump length, embryonic or fetal **E** 49f, *1.69*, **B** 125f, 177, *2.187*, **OC** 201f, **P** 221, *4.16*, **CF** 239, *5.17*, 243,
Cumulus oophorus 89,
Cyst
— ovarian see follicular, ovarian cyst
— endometrial see endometrial cysts
Cystadenoma **E** 39, *1.41f*,
Cystic corpus luteum see corpus luteum with cavity
Cystic glandular hyperplasia **CF** 249f, *5.36*,

D
Diaphragm see fetus, diaphragm
Diaphysis 163f, *2.159*, 181,
Diestrus **B** 93, 103, 113f,
— follicle see follicle, diestrus
Doppler ultrasound see ultrasound, Doppler
Double ovulation see ovulation, double ovulation

E
Ear see fetus, ear
ECG **OC** *3.10*,
Echo- see ultrasound
Echography see sonography
Ectoderm **E** *1.61*,
Ejaculate **E** 43, *1.51*,
Embryo **E** *1.58f*, 49f, *1.116*, **B** *2.9f*, *2.73*, 121, *2.78*, *2.81*, *2.84*, *125f*, **OC** 199f, *3.18*, *3.20f*, **P** 219f, *4.15f*, **CF** 237f, *5.15f*,
— ascent **E** 49f, *1.62f*,
— growth **E** 49f, **B** 121, 125f, **P** 221,
— transfer **B** *2.103*,
Embryonic death **E** 45f, 55, *1.77*, 69, *1.95f*, 75, **B** 137, *2.104f*, **OC** 201, 207, *5.29*, **CF** 247, *5.30f*,
Endoderm **P***1.61*,
Endometrial
— folds **E** 41, *1.50*, 69, *1.101*, *1.103*, 73f, **B** 123, *2.83*, 131, *2.95f*, **OC** 199, *3.17*,
— cysts **E** 45, 53f, *1.75*, 75, 79, *1.113f*,
Endometritis **E** 43, 75f, **B** 139f, *2.112f*, **CF** 249f, *5.34*,
Endometrium **P***1.6*, 41, *1.47f*, 69, 73, *1.105f*, **B** 115f, *2.65*, 141,
Epiphysis *2.155*,
Estrus **E** 19, 33, 41, **B** 93f, 113f,
— secretion **B** 115f, *2.67f*, *2.71*,
Extremity, front, hind see fetus, extremity
Eye see fetus, eye

Downloaded From Vet-eBooks.com

F
Falx cerebri see fetus, falx cerebri
Femur see fetus, femur
Fertility **B** 101f,
Fetal
— death see embryonic death
— maceration **B** 137, *2.107,*
— mummification **B** 137, *2.106,* **OC** 209,
— puncture **E** 57f,
Fetometry **E** 65f, *1.91f,* **B** 175f, *2.174f,* **OC** 203, **CF** 243,
Fetus **E** 51, *1.69f,* 61f, *1.84f,* **B** 143f, *2.117f,* **OC** 201f, *3.22f,* **P** 221, **CF** 241f, *5.21f,*
— abdomen **E** 65, *1.90,* **B** 159, *2.145f,* 173, *2.172,*
— age determination **E** 65f, *1.91f,* **B** 175f, *2.187f,* **OC** 203,
— aorta, abdominal **B** 159, *2.144,*
— artery, carotid **B** 157,
— artery, umbilical **E** 63, *1.89,* **B** 161, 167, *2.161,*
— brain **B** 149,
— — case **E** 61, *1.84,* 65, *1.91f,* **B** *2.118,* 147f, *2.122f,* 175, *2.175,* **OC** 203, *3.25,* **P** *4.21,*
— cerebral ventricle **B** *2.122,* 149, *2.124f,*
— claw **B** 165, *2.156f, 2.163,*
— clitoris **B** 169,
— corpus mamillare **B** *2.125f,*
— diaphragm **B** *2.143,* 159, *2.145,* **CF** *5.24,*
— ear **B** 151, *2.132,*
— extremity, front **B** 129, *2.93,* 163, *2.154f,* 181, **OC** *3.23,* 203, **P** 221, *4.18,*
— extremity, hind **B** 129, *2.93,* 165, *2.158f,* 181, **OC** *3.23,* 203, **P** 221,
— eye (s) **E** *1.69f,* 61, *1.84,* 65, *1.91f,* **B** 145, *2.117f,* 175, *2.174f,* **OC** 203, *3.25,* **P** 221, *4.21,*
— — lashes **B** 145, *2.120,*
— — lid **B** 145, *2.119f,* 151,
— — lens **E** 61, *1.84,* **B** 145, *2.118f,*
— falx cerebri **B** *2.122,* 149, *2.124f,*
— femur **B** 165, 181, *2.185,*
— genital tubercle **E** 63, **B** 169f, *2.165,*
— growth **B** *Table 2.1, 2.187f,*
— head **E** *1.69f,* 65, *1.90,* **B** 129, *2.93f,* 145, 173, *2.172,* **OC** *3.23,* **P** 221, *4.18, 4.21,* **CF** 241, *5.22,*
— heart **E** 61, *1.86,* **B** *2.143f,* 159, **OC** *3.24,* **P** 221, *4.19f,* **CF** *5.25,*
— — chamber **E** 61, *1.86,* **B** 159, *2.144,*
— — rate **E** 61, *1.87,* 69, **B** 137, 177, *2.176,*
— — valves **E** 61, **B** 159,
— humerus **B** 163, *2.154,* 181,
— hypothalamus **B** *2.125,*
— ilium **B** 163, *2.152f,* 181, *2.184,*
— intercostal space **B** 157, 179,
— intestine **OC** *3.29,*
— ischium **B** 163, *2.152f,* 181, *2.184,*
— kidney **B** 161, *2.148f,*
— larynx **B** 157, *2.141,*
— liver **E** 63, *1.88,* **B** 159, *2.145,* **OC** *3.24, 3.26, 3.29,* **CF** 243,
— lung **B** 159, **OC** *3.29,*
— mandible **B** 147, *2.121, 2.129f,*
— maxilla **B** *2.121,* 149f, *2.129f,*
— metacarpus **B** 163, *2.154f,* 181, *2.183,*
— metatarsus **B** 165, *2.158f,* 181, *2.186,*
— mouth **B** 149, *2.127f,*
— nasal bone **B** 151, *2.131,*
— neck **E** 61, *1.85,* **B** *2.140f,*
— nose **B** 149f, *2.128f,*
— omasus **B** *2.146,*
— ossification **B** 129, *2.94,* 147, 153f, *2.134f,* **CF** 243,
— ostium intraruminale **B** *2.147,*
— palate **B** 149, *2.127f,*
— pelvis **E** 65, **B** 163, *2.152f,* 173, *2.172,*
— penis **B** 169,
— phalanx **B** 163, *2.155, 2.183,*
— pituitary **B** *2.125f,*
— plexus choriodei **B** 149,
— position of **B** 173,
— prepuce **B** 169,
— radius **B** 163, *2.154,* 181,
— rib **E** 61, *1.86, 1.91,* 67, *1.93,* **B** 157, 179, *2.181,* **OC** 203, *3.27,* **P** 221, *4.19f,* **CF** 243, *5.25,*
— rumen **B** *2.147,* **OC** *3.26,*
— scapula **B** *2.154,* 181,
— sphenoide bone **B** *2.122,*
— spinal cord **E** *1.85,* **B** 153f, *2.136,*
— stomach **E** 63, *1.88, 1.91,* 67, **B** 159, *2.145f,* 177, **OC** *3.29,* **P** 221, *4.20,* **CF** 243, *5.23,*
— tail **E** 61, **B** 155, *2.138,*
— trunk **E** *1.88,* 65, *1.91,* 67, *1.94,* **B** 173, 179, *2.179f,* **P** 221, **CF** 243,
— umbilical cord **E** 51, *1.67, 1.70,* 63, 77, **B** 129, *2.94,* 167, *2.160f,* 179,
— urinary bladder **B** 161, *2.150f,* 167, **CF** 243, *5.24,*
— scrotum **E** 63, **B** 169f, *2.164f,* 177,
— sternum **B** *2.139,* 157,
— sulcus splenialis **B** *2.125f,*
— teats **B** 169f, *2.166f,*
— teeth **B** 149, *2.127f,*
— testis **E** 63, **B** 171, *2.170f,*
— thorax **E** 61, *1.86,* 65f, *1.90,* **B** 157, *2.142f,* 173, *2.172,* **OC** *3.24,*
P *4.19f,*
— tibia **B** 165, *2.158,* 181,
— tongue **B** 151, *2.129f,*
— trachea **B** 157, *2.140,*
— ulna **B** 163, *2.154,* 181,
— vein, caudal caval **E** *1.88,* **B** *2.143,*
— vein, umbilical **E** 63, *1.89,* **B** 167, *2.161,*
— vertebrae **E** 61, *1.85,* **B** 153f, *2.134f,* 179, *2.182,* **P** 221, **CF** 243,
— vertebral
— — arch **B** 153f,
— — body **B** 153f, *2.136,*
— — column **E** 61, **B** 153f, *2.133f,* **OC** 203, *3.29f,*
— vulva **B** 169,
Fixation **OC** 189, **P** 213, **CF** 227,
Foal heat **E** 71f, *1.104,*
Follicle **E** 15f, *1.9f,* **B** 89f, *2.13f,* **OC** 191f, **OC** 191, *3.7, 3.9f,* **P** 215, *4.6,*
— anovulatoric **E** 33f, *1.33f,*
— diestrus **B** 93, *2.18f,*
— dominant **E** 19, *1.12,* **B** 93, *2.21,*
— during pregnancy **E** 33, **B** 93,
— estrus **E** *1.9f,* 19, *1.22f,* **B** *2.13f,* 93f, *2.24,* **OC** 191f, **P** 215,
— growth **E** 19, *1.12,* **B** 93, *2.21,*
— hemorrhage **E** 27, *1.24,* 35, *1.35,*
— hemorrhagic **E** 33f, *1.35,*
— luteinizing **E** 33, *1.33f,*
— metestrus **B** 93, *2.17,*
— preovulatory **E** 19,
— proestrus **B** 93, *2.32,*

Avtorsko zaščiteno gradivo
Downloaded From Vet-eBooks.com

— puncture **E** 23, *1.18f,*
— shape **E** 19, *1.14f,* **B** 89,
— size **E** 19, *1.12,* **B** 91f, 2.12f,
Follicular
— antrum **E** 17, 21, **B** 89f,
— cyst see also ovarian cyst **B** 107f, *2.49f,* **P** 217, *4.8f,*
— fluid **E** 17, 21, **B** 89f,
— luteal cyst **B** 107f, *2.51,*
— thecal cyst **B** 107f, *2.49f,*
— wall **E** 15, 17, 21, **B** 89f, *2.13, 2.19,*
— wave **B** 93, *2.22f,*
Frontal section 149,
FSH **OC** *3.9,*

G
Genital tubercle see fetus, genital tubercle
Granulosa cell tumor **E** 37, *1.37f,* **B** 111, *2.59f,*
Growth retardation **B** 137,
Gut see intestine

H
HCG 105,
Heart see also fetus, heart
— activity, embryonic **E** 49, 69, 79, **B** 121, 125, 137, **OC** 199, **CF** 237,
Heat see estrus
Hind extremity see fetus, extremity, hind
Horizontal section 67, 143, *2.116,*
Humerus see fetus, humerus
Hydrallantois **E** 71, *1.99,* **OC** 209, *3.35,*
Hydramnion **E** 71, *1.99,* **OC** 209,
Hydrometra **OC** 207f, *3.33f,*
Hymen, persistent **E** 77, *1.111,*

I
Ilium see fetus, ilium
Impedance *1.7,*
Implantation **E** 45, 51, 79,
Inguinal gland **OC** 189,
Intestine see also Fetus, intestine **CF** 235, 251, *5.35,*
— wall **E** *1.7,*
Iodine solution **B** 141, *2.114,*
Ischium see fetus, ischium

J

K
Kidney see fetus, kidney

L
Larynx see fetus, larynx
Leucocytes **E** *1.109,*
Linear scanner *1.2,* 83f, *2.1f,* 187, 227,
Liver see fetus, liver
Lochia **E** 71f, *1.100f,* **B** 139, *2.109f,*
Lochiometra **E** 71, *1.102,* **B** *2.111,*
Longitudinal section 143,
Lung see fetus, lung
Luteal tissue 25, 95f, 105f,
Luteinization **E** 27, 33, *1.33f,*
Luteolysis **E** 25, **B** 97,

M
Maceration see fetal, maceration
Mandible see fetus, mandible
Maxilla see fetus, maxilla
Median section 143, *2.116,*
Mesoderm **E** *1.61,*
Metacarpus see fetus, metacarpus
Metatarsus see fetus, metatarsus
Metestrus **B** 91f, *2.17,* 117,
Mucometra **E** 77, *1.111,* **OC** 209,
Multiple pregnancy **OC** 199, 207,
Mummification see fetal mummification
Myometrium **E** 41, *1.47f,* **B** 117,

N
Neck see fetus, neck
Nose see fetus, nose
Nuclear magnetic resonance imaging 123, *2.83, 2.97, 3.29,*

O
Obstetrical examination **CF** 245,
Ossification see fetus, ossification
Ovarian
— hematoma **E** 35, *1.36,*
— tumor **E** 37f, *1.37f,* **B** 111, *2.59f,* **CF** 231, *5.7,*
— cyst **E** 39, *1.43f,* **B** 107f, *2.49f,* **OC** 191, *3.8,* **P** 217, *4.8f,* **CF** 231, *5.5f,*
Ovariectomy **E** 37,
Ovary **E** 15, **B** 85, 89f, *2.11f,* **OC** 191f, *3.5f,* **P** 215f, *4.4f,* **CF** 231, *5.5f,*
Ovulation **E** 19f, *1.16f,* 27, **B** 91f, **OC** 193, **P** 215,
— double ovulation **E** 19, *1.13,* 31, 53, 55,

P
Palate see fetus, palate
Paramedian section 143,
Parturition **E** 61,
Pelvis see also fetus, pelvis **B** 85, *2.6f,*
Penetration depth 87, 131, 173,
Penis see fetus, penis
PGF see prostaglandin
Placenta **CF** 241, *5.22f,*
Placentation **E** 45, 51, **CF** 245, *5.29,*
Placentome **B** 127, *2.92, 2.97f,* 133, **OC** 199, *3.19,* 205, *3.29f,*
Plexus choriodei see fetus, plexus choriodei
PMSG see ECG
Position see also fetus, position 159
Posterior presentation 159, 173, *2.173,*
Postpartum period **B** 139, *2.108f,*
Prepuce see fetus, prepuce
Proestrus **B** 93, 117,
Progesterone **E** 33, **B** 105f,
Prostaglandin **OC** 193, *3.9f,* 209, *3.34,*
Pregnancy
— age determination **E** 65f, *1.91f,* **B** 175f, *2.187f,* **OC** 203,
— diagnosis, sonographic
— — accurracy **E** 43f, **B** 125, **OC** 187, 207, **P** 223, *4.22,*
— — time of **E** 45f, **B** 125, **OC** 201f, 205f, **P** 223, **CF** 235,
— disorder **E** 71, *1.98f,* **B** 137, *2.104f,* **OC** 209, **CF** 245, *5.28,*
Presentation, anterior 159, 173, *2.173,*
Puncture
— device **E** 57, *1.80,*
— of fetus see fetal, puncture

Avtorsko zaščiteno gradivo

Downloaded From Vet-eBooks.com

— of follicles see follicle, puncture
Pyometra **E** 77, *1.109f,* **B** 141, *2.115,* **OC** 207f, *3.32,* **CF** 249f, *5.32f,*

Q

R
Radius see fetus, radius
Reflection 69, *1.97,* 73f,
— reverberation 85, *2.7,*
— specular reflection 45, 79,
— surface 15, 125,
Rectal examination **E** 11, 79, **B** 83,
Rectum **E** 11, **B** 83, **CF** 229,
Resolution 87f, *2.9f,*
Resorption see embryonic death
Reverberation see reflection, reverberation
Rumen see fetus, rumen

S
Sagittal section 13, *2.2,* 143, *2.116,*
Sector scanner *1.3,* 83f, *2.3f,* 113, *2.62f,* 143, 187, 227,
Sex determination **E** 63, **B** 169,
Scanning width **B** 131,
Scapula see fetus, scapula
Scrotum see fetus, scrotum
Shadowing see ultrasound shadows
Sonography, technique of
— transcutaneous **E** 13, 65, **OC** 187f, *3.2,* 207, **P** 213, *4.1,* 223, **CF** 227f, *5.1f,*
— transrectal **E** 11, *1.1,* 65, *1.90,* **B** 83f, *2.1f,* **OC** 187f, *3.2,* 207, **P** 213f, *4.2,* 223,
— transvaginal **E** 23, *1.18,* 57f, *1.80f,*
Sound see ultrasound
Specular reflection see reflection, specular reflection
Spinal cord see fetus, spinal cord
Spoke wheel pattern **E** 41, *1.48f,*
Sternum see fetus, sternum
Stomach see fetus, stomach
Superovulation **B** 91f, *2.19f,* 101, *2.39,* **OC** 193, *3.9f,*

T
Tail see fetus, tail
Testicular descent **E** 63, **B** 171,
Testis see fetus, testis
Thorax see fetus, thorax
Tibia see fetus, tibia
Tongue see fetus, tongue
Trachea see fetus, trachea
Transverse position *2.173,*
Transverse section 83, *2.3f,* 113, *2.63f, 2.103,* 143, *2.116,*
Trophoblast **OC** 197,
Twin pregnancy **E** 31, 45, 51f, *1.71f,* 79, **B** 135, *2.103,* **OC** *3.21f,* 207,
— treatment **E** 55,

U
Ulna see fetus, ulna
Ultrasound
— absorption 11, 65, 137, 147, 155, 163,
— A mode 187, 207, 213,
— Doppler 187, 207, 213,
— enhancement 15f, *1.8f,*
— examination see sonography
— frequency 17, 25, 43, 51, 87f, *2.9f,* 125, *2.87f,* 131, 187, 201, 223,
— gel see coupling gel
— impact *1.8f,* 15f
— reflection *1.7,* 15, 163,
— shadows 15f, *1.8f, 1.39,* 61, 155f, *3.27,*
— wave 15, 87,
Umbilical cord see fetus, umbilical cord
Urinary bladder see also fetus, Urinary bladder **E** 11, *1.2, 1.3,* 77, *1.110,* **B** 85, *2.5f, 2.13,* **OC** 189, *3.3, 3.8,* **CF** 229, *5.3f,*
Urine **E** 11, *1.2, 1.3,* 77,
Urometra **E** 77, *1.112,*
Uterus **E** 41f, **B** 113f, **OC** *3.3f,* 195f, **P** 219f, *4.12f,* **CF** *5.3f, 233f,*
— infusion **E** 75, *1.108,*
— non-pregnant **E** 41f, *1.47f,* **B** *2.2f,* 113f, *2.61f,* **OC** *3.3f,* 195, *3.11f,* **P** 219, *4.12f,* **CF** *5.3,* 233,
— — during anestrus **E** 41,
— — during diestrus **E** 41, *1.47,* **B** 113f, *2.61, 2.66,*
— — during estrus **E** 41, *1.48f,* 71, **B** 113f, *2.62, 2.65, 2.67f,* **OC** 195, *3.12,*
— — during postpartum period **E** 71f, *1.100f,* **B** 139, *2.108f,* **CF** 245, *5.29,*
— pregnant **E** 43f, *1.52f,* **B** *2.38,* 119f, 2.73f, **OC** 197f, *3.13f,* **P** 219, *4.14f,* **CF** 233, *5.8f,*
Uterine
— body **E** 13, *1.5,* 45, **B** 85,
— compartments **B** 123, 131, *2.95f,* **OC** 199, *3.16f,*
— curvature
— — large **B** *2.2,* 113, *2.61, 2.65f, 2.75,* **OC** *3.4,* 195,
— — small **B** 113, *2.61, 2.65, 2.75,* **OC** 195,
— horn **E** 13, *1.4f, 1.47f,* 45, **B** 85, 113f, *2.61f, 2.69f,* **OC** 197,
— lumen **E** 43, 75, **B** 115, 121, 131, *2.95f,* **OC** 195,
— wall **E** 45, *1.58,* 79, **B** 115f, *2.61f,* 131, *2.95f,* **OC** 195,

V
Vagina **E** 77, **B** 85,
Vein, umbilical see fetus, vein, umbilical
Vertebral column see fetus, vertebral column
Vertical section **B** 145,
Vestibulum **B** 85,

W

X

Y
Yolk sac **E** 49f, *1.61f, 1.74,* **CF** 237, *5.15,* 241, *5.22,*

Z
Zonary placenta see placenta

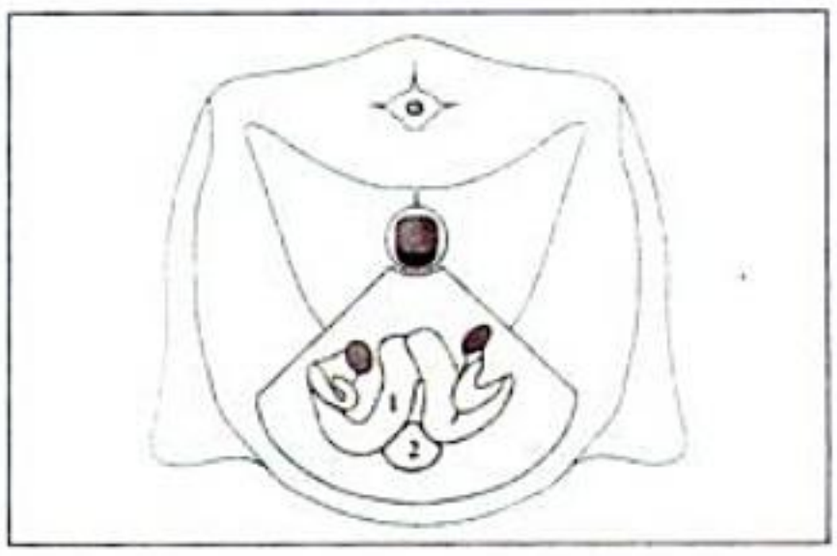
Avtorsko zaščiteno gradivo

Downloaded From Vet-eBooks.com

Veterinary Reproductive Ultrasonography covers all of the most important domestic large and small animals and is a comprehensive and uniquely illustrated account of veterinary gynecologic examination and reproduction. Commencing with the common indications for ultrasonography, gynecologic and obstetric examination, the book moves on to interpret ultrasonographic findings. The pregnant and non-pregnant uterus, pathologic changes of the uterus and other abnormal ultrasonographic findings are described and explained.

This comprehensive guide to horse, cattle, sheep, goat, swine, dog and cat gynecologic examination and reproduction explains technique as well as interpretation. Its extensive illustration provides quick access and answers.

Veterinary Reproductive Ultrasonography, with its nearly 400 top-quality illustrations and descriptive legends, is the definitive guide to reproductive problems facing the busy practitioner in day-to-day practice.





ISBN 3-89993-005-3

Avtorsko zaščiteno gradivo

Downloaded From Vet-eBooks.com